Bor- und Kohlenstoff-basierte Liganden im Spannungsfeld von Donor- und Akzeptorfunktionalität

Kumulative Dissertation

verfasst von
Leon Maser, M.Sc.
aus Friedberg

dem
Fachbereich Chemie
der
Philipps-Universität Marburg
Hochschulkennziffer 1180
vorgelegt

zur Erlangung des akademischen Grades
Doktor der Naturwissenschaften (Dr. rer. nat.)

Marburg, 2019

Eingereicht am 03.09.2019
Prüfung abgelegt am 23.10.2019

Erstgutachter: Dr. Robert Langer
Zweitgutachterin: Prof. Dr. Stefanie Dehnen

Für meinen Vater

Danksagung

Ich möchte mich zuerst bei Herrn Dr. Robert Langer bedanken; ich durfte ein sehr interessantes Forschungsgebiet mit extrem viel Freiraum erkunden. Ich weiß dieses Vertrauen sehr zu schätzen - trotzdem erinnere ich mich nicht an einen Tag, an dem seine Tür nicht für eine Frage oder Diskussion offenstand.

Ein großes "Dankeschön!" gebührt auch Frau Prof. Stefanie Dehnen, deren Vorlesungen über anorganische Chemie für mein initiales Interesse an diesem Fach verantwortlich sind. Auch ihre stete Unterstützung hat mir beim Verfassen dieser Arbeit sehr geholfen.

Nicht zu vergessen ist natürlich der ganze Arbeitskreis Dehnen und insbesondere die Nachwuchsgruppen und deren Leiter*innen Dr. Johanna Heine, Dr. Gunnar Werncke und neuerdings Dr. Frank Tambornino. Ihr habt für ein immer angenehmes Arbeitsklima gesorgt. Ich möchte mich natürlich besonders bei all jenen bedanken, die in der Nachwuchsgruppe Langer tätig waren. Allen voran Dr. Lisa Vondung, die eine super Laborpartnerin gewesen ist, mir viel über quantenchemische Rechnungen beigebracht und mich zu meiner ersten GRC motiviert hat. Natürlich auch die früheren Mitarbeiter des AKs, Felix, Nina und Weiqin, gefolgt von Max, Maik A., Lukas, Maik G., Andi und Christian. Besonders viele Kaffeepausen habe ich mit Maik G. und Andi verbracht, aber auch mein neuester Kollege Yinwu sorgt immer für gute Stimmung. Jan gebührt ein besonderer Dank dafür, dass er mich seit dem Kindergarten immer mit einem offenen Ohr begleitet. Nicht zu vergessen auch seine Frau Dr. Susi! Mit euch beiden destilliert es sich doch am besten. Bei Angelika, Benedikt und Lisa möchte ich mich für das Korrekturlesen bedanken.

Weiterhin danke ich den Mitarbeitern der Service-Abteilungen des Fachbereichs für alle durchgeführten Messungen und Analysen sowie die ständige Hilfsbereitschaft. Auf keinen Fall vergessen möchte ich Reuti, der im Prinzip eine Service-Abteilung für Server- und Clusterfragen aller Art alleine betreibt.

Auch außerhalb der Uni haben einige Menschen zur Durchführung meiner Dissertation beigetragen - vielleicht den größten Teil. Meinen lieben Eltern gebührt eine Menge Dank dafür, dass sie mich in allem meinem Tun stets unterstützen. Bei meiner Verlobten, Angelika, will ich mich dafür bedanken, dass sie seit über zehn Jahren an meiner Seite ist und, besonders während ich diese Arbeit verfasste, mein Seelenheil behütet hat.

Erklärung

Ich versichere hiermit, dass weder an der Philipps-Universität Marburg noch an einer anderen in- oder ausländischen Hochschule der Versuch einer Promotion erfolgt ist. Des Weiteren versichere ich, dass die vorliegende Promotionsschrift mit dem Titel:

Bor- und Kohlenstoff-basierte Liganden
im Spannungsfeld von Donor- und Akzeptorfunktionalität

selbstständig verfasst und weder in der vorliegenden noch ähnlicher Form als Prüfungsleistung vorgelegt wurde. Es wurden keine anderen als die angegebenen Hilfsmittel und Quellen benutzt. Sämtliche Stellen der Arbeit, die verwendeten Werken im Wortlaut oder dem Sinn nach entnommen sind, wurden entsprechend kenntlich gemacht.

Marburg, den 18. November 2019

_____

Leon Maser

Die vorliegende Dissertation wurde im Zeitraum von April 2016 bis August 2019 unter der Betreuung von Dr. Robert Langer und Prof. Dr. Stefanie Dehnen in der Nachwuchsgruppe Langer am Fachbereich Chemie der Philipps-Universität Marburg angefertigt.

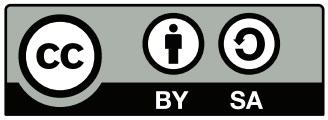

Inhaltsverzeichnis

Abkürzungsverzeichnis

$2e^{-}$-2z	Zwei-Elektronen-Zwei-Zentren
CDP	Carbodiphosphoran
DFT	Dichtefunktionaltheorie
EDA	*Energy Decomposition Analysis*
ETS	*Extended Transition State (Method)*
HEP	*Huynh Electronic Parameter*
HOMO	*Highest Occupied Molecular Orbital*
IR	Infrarot
$^{i}Pr_2$-bimy	1,3-Diisopropylbenzimidazolin-2-yliden
LEP	*Lever Electronic Parameter*
LUMO	*Lowest Unoccupied Molecular Orbital*
LiHMDS	Lithium-bis(trimethylsilyl)amid
NBO	*Natural Bond Orbital*
NHC	N-heterocyclisches Carben
NMR	*Nuclear Magnetic Resonance*
NPA	*Natural Population Analysis*
PA	Protonenaffinität
QTAIM	*Quantum Theory of Atoms in Molecules*
TEP	*Tolman Electronic Parameter*
bcp	*bond critical point*
ccp	*cage critical point*
dppm	Bis(diphenylphosphino)methan
na	*nuclear attractor*
rcp	*ring critical point*

1 Einleitung

Die Komplexchemie als Konzept zur Erklärung des Aufbaus von Molekülen mit zentralem Metallatom ist bereits vor über 120 Jahren eingeführt worden.[1] Grundlegend war die Unterscheidung zwischen Oxidationsstufe des Metalls und dessen Koordinationszahl sowie der Aufbau von Koordinationspolyedern. Anfangs wurden besonders einfache Kohlenstoff-, Stickstoff- und Sauerstoff-basierte Liganden (z.B. CN^-, NH_3, H_2O) sowie die Halogenide in Komplexen untersucht. Koordinationsverbindungen, in denen eine Bindung zwischen einem Bor-Atom oder -Ligand und einem Metallatom gebildet wird, sind hingegen erst seit Beginn der Sechzigerjahre bekannt.[2]
Im Laufe der Zeit sind neue Liganden und Donorgruppen in Erscheinung getreten, die aufgrund ihrer auffälligen Eigenschaften besonderes Interesse erweckt haben. Im Folgenden soll auf einige dieser Liganden eingegangen, ihre Eigenschaften diskutiert und deren Bedeutung erklärt werden.

1.1 Kohlenstoff-basierte Liganden

1.1.1 Kohlenstoffmonoxid

Einer der wohl bekanntesten einfachen Kohlenstoff-basierten Liganden ist das Kohlenstoffmonoxid. Das unter Standardbedingungen als Gas vorliegende, stark toxische Molekül ist der Menschheit schon seit Jahrtausenden bekannt, wurde aber erst Anfang des 19. Jahrhunderts gezielt synthetisiert und korrekt identifiziert.[3] Die erste Metall-Carbonyl-Verbindung, $[Pt(CO)_2Cl_2]$, wurde bereits 1868 durch Schützenberger isoliert.[4] Doch erst die Synthese von $[Ni(CO)_4]$ 1890 durch Mond als hochtoxische, farblose Flüssigkeit mit niedrigem Siedepunkt von 43 °C führte dazu, dass die Besonderheiten von CO als Ligand erkannt und auch wenig später industriell zur Darstellung von hochreinem Nickel genutzt wurden.[5]
Als diatomarer Verbindung stehen dem Kohlenmonoxid-Molekül nur vierzehn Elektronen bzw. zehn Valenzelektronen zur Verfügung, die in Form von mesomeren Grenzstrukturen lokalisiert werden können (Abb. 1).

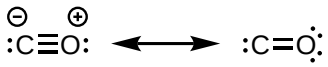

Abbildung 1: Mögliche Grenzstrukturen des Kohlenstoffmonoxid-Moleküls.

Experimentellen Beobachtungen wird am ehesten die Grenzstrukturformel gerecht, die durch eine formale Dreifachbindung zwischen Sauerstoff und Kohlenstoff gekennzeichnet ist. Als neutraler Ligand bindet das Kohlenstoffmonoxid-Molekül über das Kohlenstoff-Atom und kann sowohl als σ-Donor als auch π-Akzeptor fungieren (Abb. 2). Die Koordination erfolgt meist terminal, in mehrkernigen Verbindungen kann auch eine Kantenverknüpfung oder Überkappung einer Dreiecksfläche erfolgen (μ-CO-κC oder μ_3-CO-κC). Seltener erfolgt eine Verbrückung über Kohlenstoff und Sauerstoff (μ-CO-1κC,2κO).

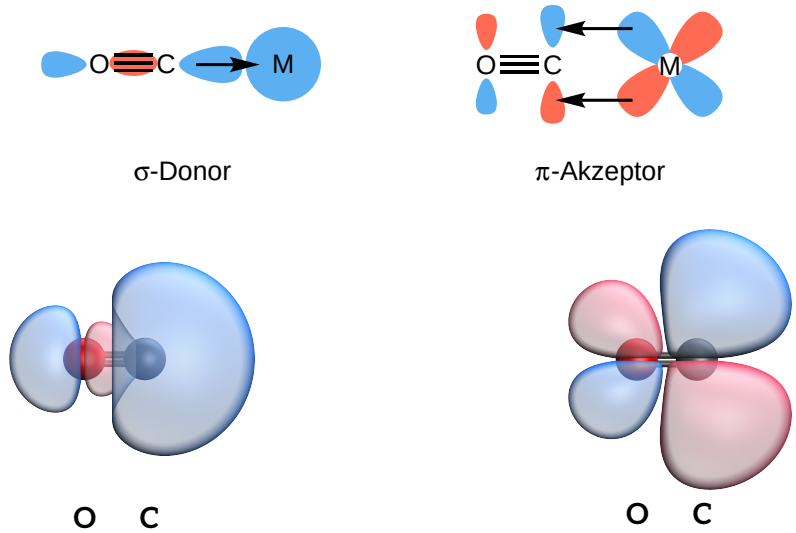

Abbildung 2: Oben: schematische Darstellung der Donor- und Akzeptor-Wechselwirkungen. Unten: HOMO (links) und eines der zwei entarteten LUMOs (rechts) von Kohlenstoffmonoxid (G16, B97D/def2-TZVPP, Iso-Wert 0.05).

Das *highest occupied molecular orbital* (HOMO) ist stark am Kohlenstoff-Atom lokalisiert und kann von dort aus σ-donierend wirken. Dahingegen sind die *lowest unoccupied molecular orbitals* (LUMO und LUMO+1) zwar auch stärker am Kohlenstoff-Atom lokalisiert, durch die Knotenebene entlang der C–O-Bindung jedoch in der passenden Symmetrie, um π-Elektronendichte akzeptieren zu können. Fälle, in denen CO als reiner σ-Donor auftritt, sind auch bekannt.[6] Obwohl es sich bei dem HOMO-1 und HOMO-2 um besetzte Orbitale in π-Symmetrie handelt, fungieren diese aufgrund der zu tiefen energetischen Lage praktisch nicht donierend.
Besonders von den Übergangsmetallen der mittleren Gruppen sind neutrale binäre Carbonylverbindungen bekannt,[7] im Periodensystem anfangend mit $[V(CO)_6]$ und endend mit $[Ni(CO)_4]$. Die sehr frühen und die sehr späten Übergangsmetalle zeigen eine wesentlich geringere Stabilität und sind entweder, wie im Fall der Gruppe 4, nur als substituierte Derivate $[M(CO)_{7-n}L_n]$ (M = Ti, Zr, Hf) isolierbar oder in Form von geladenen Komplexen bekannt.[8] So können in kationischen Verbindungen sehr frühe oder späte Übergangsmetallcarbonyle beobachtet werden,[9–11] wohingegen die anionischen Verbindungen[12] z.B. als Collman's Reagenz ($Na_2[Fe(CO)_4]$) in der organischen Synthese Anwendung finden.[13]
Bei Kohlenmonoxid handelt es sich um einen bemerkenswerten Liganden. Dies zeigt die Vielzahl an bekannten Verbindungen, die einen oder mehrere CO-Liganden tragen, deutlich. Zwar ist das Kohlenmonoxid-Molekül nicht hoch reaktiv, trotzdem kann es aber teilweise schon durch eine einfache Reaktion von reinem Kohlenmonoxid und elementarem Übergangsmetall zur Koordination unter Ausbildung stabiler Bindungen gebracht werden. Der Grund hierfür liegt in dem für die Koordination an viele Übergangsmetalle energetisch günstigen Lage von HOMO und LUMO. Diese führt zu einer Synergie aus σ-Donierung, die die Elektronendichte am Metallzentrum erhöht, was wiederum die π-Rückbindung vom Me-

tall zum Kohlenmonoxid begünstigt. Aufgrund ihres relativen Elektronenreichtums können vor allem Übergangsmetalle niedriger Oxidationsstufen starke π-Rückbindungen ausbilden. Diese besondere Kombination aus starken σ-Donor- und π-Akzeptor-Eigenschaften hebt Kohlenmonoxid von anderen Liganden ab.[14]
Nicht koordiniertes Kohlenmonoxid kann aus vielen Gleichgewichtsreaktionen einfach entfernt werden, um die Reaktion in die gewünschte Richtung zu lenken. Im Gegensatz zu anderen labilen Liganden ist kein komplizierter Aufreinigungsschritt notwendig, da es unter Standardbedingungen als Gas vorliegt. Metallcarbonyle stellen deshalb ideale Präkursorverbindungen dar.
Während Kohlenmonoxid als nicht beteiligter Ligand (engl. *spectator ligand*) durchaus auch in katalytischen Anwendungen zu finden ist, fehlt jedoch die Möglichkeit durch Substitution mit funktionellen Gruppen einen fest koordinierten, mehrzähnigen Liganden zu erzeugen. Dies würde das genaue Einstellen von sterischen und elektronischen Eigenschaften ermöglichen, was sich besonders für die Anwendung in Katalysatoren als sehr vorteilhaft erwiesen hat. Eine Veränderung des Donor-Charakters von koordiniertem Kohlenmonoxid ist nur begrenzt möglich. Die bekanntesten Reaktionen von CO-Liganden verändern diese drastisch oder führen direkt zur Abspaltung vom Zentralatom. Neben der Hieber'schen Basenreaktion, bei der ein nukleophiler Angriff durch OH^- auf ein CO zu dessen Eliminierung als CO_2 führt, ist bei Einsatz von Lithium-Alkylverbindungen die Bildung von Fischer-Carbenen zu beobachten, die als reaktive Liganden zu Folgechemie neigen.

1.1.2 N-heterocyclische Carbene

Die nach Ernst Otto Fischer benannten Fischer-Carbene sind die ersten in Übergangsmetallkomplexen isolierten Carbene.[15] Es handelt sich Kohlenstoff(+II)-Verbindungen, die einem Übergangsmetall ein Elektronenpaar dativ zur Verfügung stellen. Im Allgemeinen sind Fischer-Carbene sehr reaktive Verbindungen, die deshalb zunächst noch als nicht in freier Form isolierbar galten. Nach den ersten Untersuchungen durch Wanzlick zeigte sich jedoch bald, dass die als N-heterocyclisch bezeichneten Carbene (NHCs) eine Ausnahme bilden.[16] Wie der Name verrät, handelt es sich um meist fünfgliedrige zyklische Verbindungen, in denen ein Kohlenstoffatom in der formalen Oxidationsstufe +II durch zwei benachbarte Stickstoff-Atome stabilisiert wird. Es ergibt sich ein dem Kohlenmonoxid sehr stark ähnelndes Bindungsverhalten mit σ-Donor- und π-Akzeptor-Eigenschaften, das auch anhand der Molekülorbitale nachvollzogen werden kann (Abb. 4). Diese Analogie deutet bereits darauf hin, dass es sich um gute Liganden für Übergangsmetallkomplexe handeln sollte. Tatsächlich konnten bereits Ende der Sechzigerjahre erste NHC-basierte Übergangsmetallkomplexe isoliert werden.[17,18] Es sollte jedoch noch bis 1990 dauern, bis das erste NHC von A. J. Arduengo III. bei DuPont durch Substitution mit Adamantyl-Gruppen in stabiler, freier Form isoliert werden konnte (Abb. 3).[19]

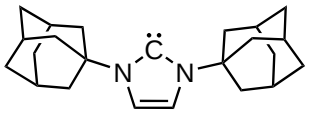

Abbildung 3: Erstes frei isoliertes N-heterocyclisches Carben.[19]

Im Vergleich zu dem oben diskutierten Kohlenmonoxid als Ligand handelt es sich bei NHCs im Allgemeinen um leicht stärkere σ-Donoren, wohingegen die π-Rückbindungsfähigkeiten etwas schwächer ausgeprägt sind. Im Gegensatz zu CO bieten sich bei NHCs eine Vielzahl an Möglichkeiten zur Modifikation an. So kann die Ringgröße der NHCs unterschiedlich gewählt, die Sättigung des Kohlenstoffgerüstes variiert und funktionelle Gruppen sowohl im Rückgrat als auch als Substituenten an den Stickstoffatomen angebracht werden.
Diese vielfältigen Möglichkeiten machen NHCs universell einsetzbar und förderten das Interesse an diese Verbindungsklasse immens.[20,21]

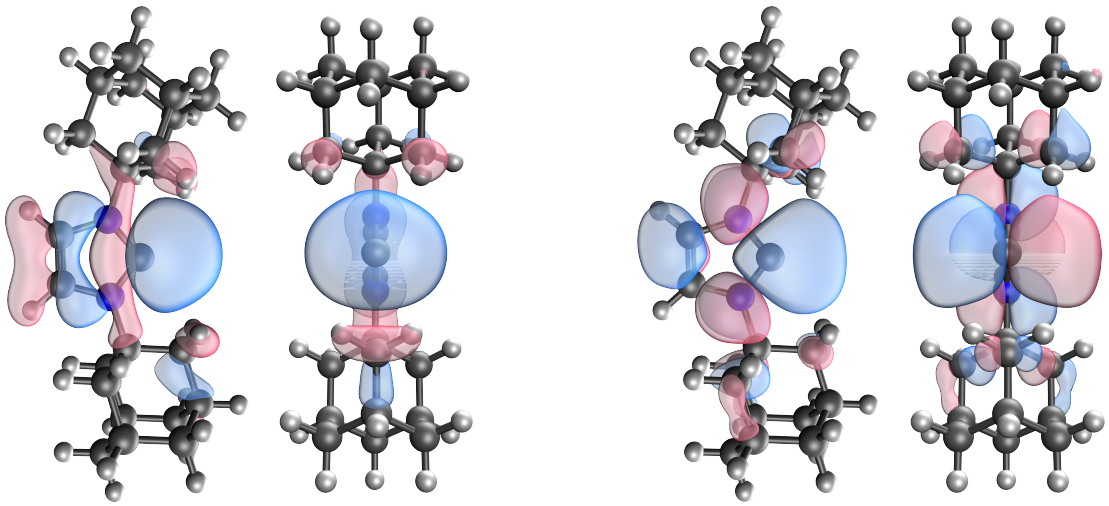

Abbildung 4: Für den σ-donierenden Charakter verantwortliches HOMO (links) und den π-akzeptierenden Charakter verantwortliches LUMO+3 (rechts) des Adamantyl-NHC (G16, B97D/def2-TZVPP, Iso-Wert 0.05).

Anwendung in der Katalyse

Im Gegensatz zu Kohlenmonoxid können bei NHCs durch Substitution der organischen Reste eine Vielzahl an Verbindungen hergestellt werden, die sich in ihren sterischen und elektronischen Eigenschaften unterscheiden. Zudem sind NHC-basierte Liganden weniger labil als Kohlenmonoxid-Liganden. Das macht diese Ligandenklasse, in Verbindung mit den gut abstimmbaren Donor-Eigenschaften, für die Verwendung in Katalysatoren hochinteressant.[22,23]
Das wohl beste Beispiel hierfür sind die Grubbs-Katalysatoren der zweiten Generation, die mit

großem Erfolg in der Olefinmetathese eingesetzt werden und für ihren Entwickler Robert H. Grubbs 2005 zu einem Nobelpreis führten.[24,25]

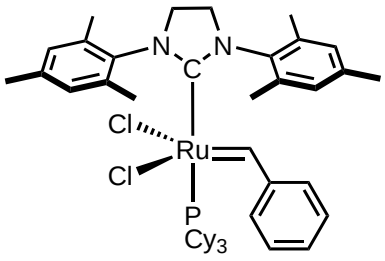

Abbildung 5: Olefinmetathese-Katalysator der zweiten Generation.[24]

Die Erfolge der NHCs in der katalytischen Olefinmetathese sind nicht zuletzt auch auf den kinetischen *trans*-Effekt[26] und thermodynamischen *trans*-Einfluss[27,28] des NHC-Liganden zurückzuführen. Versuche der genauen Quantifizierung des *trans*-Effekts bzw. -Einflusses wurden bereits häufiger vorgenommen, sind aber aufgrund der vielen Variablen nur begrenzt zu verallgemeinern.[29–32]
Es ist trotzdem zu erwarten, dass Liganden, die sowohl starke σ- als auch starke π-Donoren sind, einen deutlicheren Einfluss auf den *trans*-ständigen Liganden haben sollten. Eine Ligandenklasse, die entsprechende Donor-Eigenschaften zeigen kann, wird durch die Carbodiphosphorane (CDPs) gebildet. Tonner *et al.* veröffentlichten 2008 eine quantenchemische Studie, in der sie den Vergleich von NHC und CDP im Kontext der Olefinmetathese-Katalysatoren vornehmen (Abb. 6).[33]

Abbildung 6: Quantenchemisch verglichene NHC- und CDP-basierte Modellsysteme.[33]

Die Autoren kommen darin zu dem Schluss, dass CDP-basierte Liganden in den Grubbs-Systemen zu vergleichbaren, wenn nicht sogar besseren Aktivitäten führen sollten. Aufgrund des Austauschs von π-akzeptierendem NHC mit einem π-donierenden CDP ist zu erwarten, dass sich der *trans*-Einfluss stark ändert. Als Folge dessen ist es möglich, dass sich neue Reaktivitäten des komplexen Katalysatorsystems eröffnen.[34]

1.1.3 Carbodiphosphorane

Das erste - und wohl meistuntersuchte - CDP, Hexaphenylcarbodiphosphoran, wurde 1961 von Ramirez *et al.* erstmals synthetisiert.[35] Die bald folgenden röntgenographischen Untersuchungen zeigten eine gewinkelte Struktur, die typischerweise in ähnlicher Form auch in

Verbindungen beibehalten wird.[36] Vor kurzem konnte jedoch auch eine lineare Form kristallisiert werden.[37] Die korrekte Klassifizierung dieser Verbindung, welche Grenzstruktur für das Molekül die passendste ist und wie diese zu zeichnen ist, unterlag einer gewissen Kontroverse (Abb. 7).[38–48]

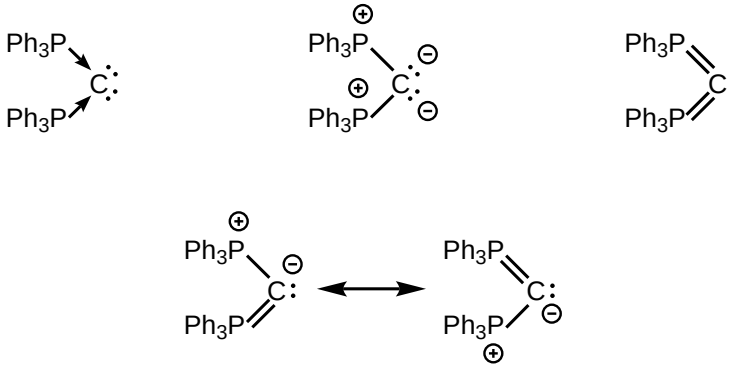

Abbildung 7: Einige der gängigsten Notationen von Hexaphenylcarbodiphosphoran. Eine umfangreichere Übersicht ist in [49] zu finden.

Die Beschreibung des zentralen Kohlenstoffatoms erfolgt basierend auf theoretischen Untersuchungen der Bindungsverhältnisse in Carbodiphosphoranen häufig durch die Grenzstruktur, die ein zentrales Kohlenstoffatom in der formalen Oxidationsstufe ±0 enthält, welches durch zwei dativ bindende Phosphine stabilisiert wird (Abb. 7, oben links). Als solches verfügt das Hexaphenylcarbodiphosphoran über zwei freie Elektronenpaare, die durch die zwei höchst liegenden besetzten Molekülorbitale repräsentiert werden (Abb. 9). Die Formen der Molekülorbitale deuten auf starken σ- und π-Charakter am Kohlenstoff-Atom hin, wie bereits bei CO und NHCs diskutiert. Da beide Orbitale besetzt sind, stellt die Klasse der CDPs σ- und π-Donoren dar.

Bereits kurz nach der ursprünglichen Synthese wurden erste Übergangsmetallkomplexe isoliert[50,51] und über die Jahre umfangreiche Untersuchungen der Donoreigenschaften vorgenommen.[49,52–54] Diese zeigen, dass prinzipiell drei Arten von Additionsverbindungen gebildet werden können (Abb. 8).

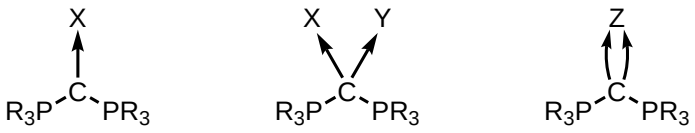

Abbildung 8: Additionsverbindungen von CDPs mit elektrophilen Substraten X.

Einfache Addukte, in dem das CDP als σ-Donor an ein Substrat koordiniert, liegen häufiger vor als Diaddukte. Bei letzteren bilden die zwei Elektronenpaare des CDP zu zwei getrennten Substraten jeweils eine Bindung aus. In einer dritten Variante werden beide freien Elektronenpaare an ein Substrat doniert; hier fungiert das CDP σ- und π-donierend.

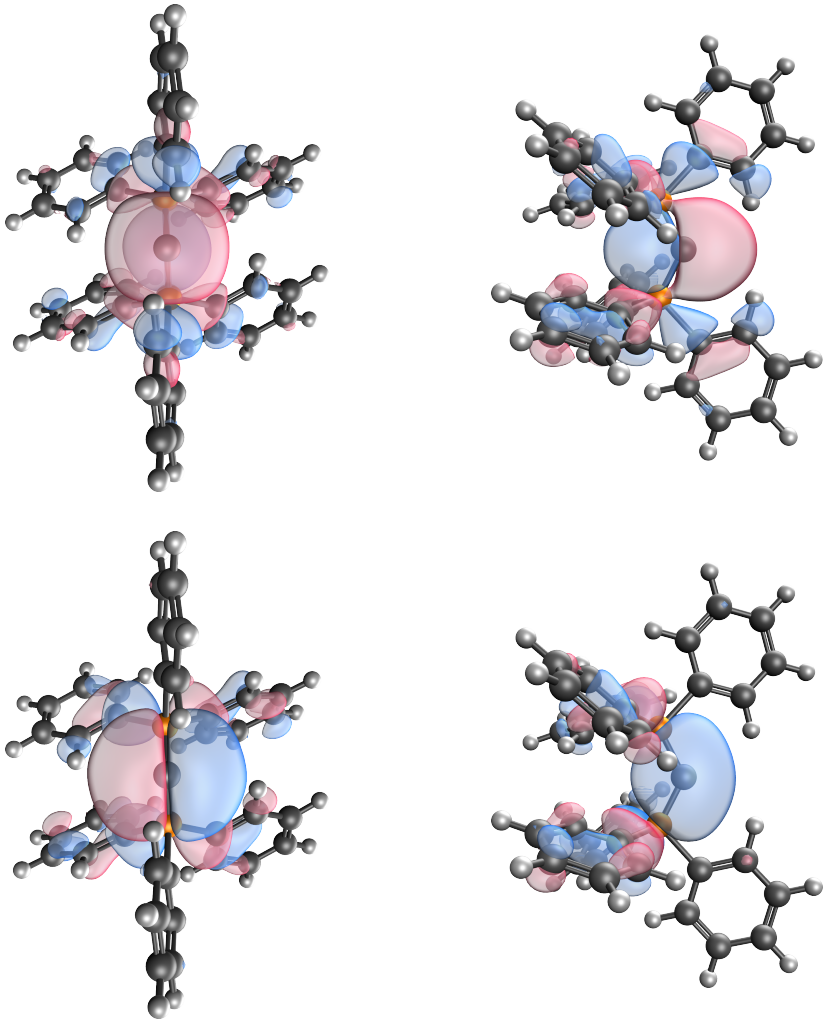

Abbildung 9: Für den σ-donierenden Charakter verantwortliches HOMO-1 (oben) und den π-donierenden Charakter verantwortliches HOMO (unten) des Hexaphenylcarbodiphosphorans (G16, B97D/def2-TZVPP, Iso-Wert 0.05).

Eine Justierung und Abstimmung der elektronischen und sterischen Eigenschaften kann bei CDPs durch Variation der Substituenten an den stabilisierenden Phosphinen vorgenommen werden. Dies ermöglicht die individuelle Anpassung an verschiedenste Einsatzzwecke.

1.2 Bor-basierte Liganden

Während, wie eingangs erwähnt, von den Elementen der zweiten Periode besonders Kohlenstoff-, Stickstoff- und Sauerstoff-basierte Liganden weit verbreitet sind, finden Bor-basierte Liganden noch relativ wenig Anwendung. Es existieren zwar einige lange bekannte Verbindungsklassen von Übergangsmetallen mit Bor, bei diesen liegen jedoch keine klassischen Zwei-Elektronen-Zwei-Zentren-Bindungen ($2e^{-}$-2z) zwischen Metall und Bor vor.[55] Die am häufigsten vertretene Klasse ist die der Boride, bei denen es sich um Festphasen handelt.[56] Es

folgen Metalla(hetero)borane und schließlich η-gebundene Bor-haltige Heterocyclen. In diesen Verbindungsklassen lässt sich die Tendenz zur Bildung von Clustern mit Mehrzentrenbindungen beobachten; dies mag ein Grund für die relativ späte strukturelle Charakterisierung von Komplexen mit $2e^{-}$-2z-Bindungen sein. Obwohl schon Anfang der Siebzigerjahre untersucht,[2] konnte der röntgenographische Nachweis solcher Verbindungen erst 1990 durch die Gruppen von Baker und Merola erbracht werden.[57,58] Seit diesen Veröffentlichungen ist das Interesse an der Entwicklung und Nutzung Bor-basierter Liganden stark angestiegen und bleibt bis heute ein wichtiges Forschungsgebiet.[55,59–61]
Nach dem aktuellen Stand der Forschung lassen sich die Bor-basierten Liganden in drei prinzipielle Gruppen einteilen: Borane, Boryle und Borylene.
Bei den Boranen handelt es sich um die wohl typischsten Vertreter, bei denen ein leeres p_z-Orbital am Bor vorliegt und die somit Lewis-sauren Charakter aufweisen.
Die Boryle wurden bereits in den Sechzigerjahren intensiver untersucht. Exakte Identifizierungen wurden zu diesem Zeitpunkt jedoch nicht durchgeführt und so konnten erst zu Beginn der Neunzigerjahre entsprechende Komplexe isoliert werden.[57] Die erste Synthese eines freien Boryl-Anions erfolgte 2006 von Yamashita und Nozaki, quasi als NHC-Analogon.[62] Das zentrale Bor-Atom liegt hier gebunden durch zwei Stickstoff-Atome vor, wie im klassischen Motiv der NHCs. Durch die negative Ladung am Bor-Atom wird das p_z-Orbital nun halb besetzt. Die sterisch sehr anspruchsvollen 2,6-Diisopropylphenyl-Gruppen sorgen für eine effektive Abschirmung. Die vielfältigen Einsatzmöglichkeiten des neuen Liganden demonstrierten die Autoren durch die Implementierung in einen PBP-Pinzetten-Liganden.[63]
Der letzte und jüngste Vertreter, die Borylene, sind hingegen wie Borane wieder neutrale Verbindungen. Da das p_z-Orbital im Gegensatz zu diesen jedoch voll besetzt ist, handelt es sich um σ-Donoren, die wie Kohlenmonoxid auch als π-Akzeptoren wirken können. Dieses Verhalten zeigt eine klare Verwandtschaft mit Kohlenmonoxid und NHCs. Aus diesem Grund soll im Folgenden genauer auf sie eingegangen werden.

1.2.1 Borylene

In Borylenen liegt das Bor-Atom anders als bei Boranen (+III) und Borylen (+II) in der formalen Oxidationsstufe +I vor. Erste isolierte Beispiele von verbrückenden[64,65] oder terminalen[66,67] Borylen-Liganden kamen Mitte der Neunzigerjahre aus der Gruppe von Braunschweig. Ihr Potential, als starke σ-Donor-Liganden mit π-Rückbindungsanteil zu fungieren, wurde hier bereits erkannt. In fast 25 Jahren hat das Feld der Borylen-basierten Liganden eine stetig wachsende Vielfalt an Komplexen generiert.[68,69]
Die archetypische Verbindung Bormonofluorid ist isoelektronisch zu Kohlenmonoxid und diesem somit am nächsten verwandt. Wie auch im Fall von CO können verschiedene Mesomeriestrukturen verfasst werden, die jedoch alle die Oktettregel verletzen und/oder die Zuordnung von Formalladungen erfordern (Abb. 10).

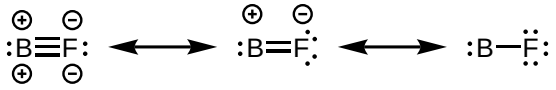

Abbildung 10: Drei mögliche Grenzstrukturen für das Bormonofluorid-Molekül.[70]

Ganz anders als beim Kohlenmonoxid handelt es sich bei freiem Bormonofluorid um eine sehr instabile Verbindung, die bereits bei -196 °C zu einem nicht weiter identifizierten, grünen Polymer abreagiert.[71] Aus diesem Grund wurden Bormonofluorid- oder Borylen-basierte Verbindungen häufig lediglich quantenchemisch untersucht. Als Resultat wurden im Vergleich zu Kohlenmonoxid bessere σ-Donoreigenschaften bei ähnlichen oder sogar noch stärker ausgeprägten π-Akzeptor-Eigenschaften vorhergesagt.[14,72] Bei dem Vergleich der Bindungssituationen der isoelektronischen Moleküle N_2, CO und BF wird der Trend in den Ligandeneigenschaften über die Bindungsordnung erklärt.[70]

Abbildung 11: HOMO (links) und eines der zwei entarteten LUMOs (rechts) von Bormonofluorid (G16, B97D/def2-TZVPP, Iso-Wert 0.05).

So sind in dem symmetrischen Distickstoff-Molekül N_2 beide Atome je zur Hälfte an allen Molekülorbitalen beteiligt und diese dementsprechend gleichmäßig verteilt. Dies spiegelt sich in der hohen Bindungsordnung von 3.0 wieder. Im Fall des Kohlenmonoxid-Moleküls CO führt die Elektronegativitätsdifferenz zu einer Beeinflussung des π-Anteils der Bindung. Dementsprechend wird eine etwas niedrigere Bindungsordnung von 2.6 erhalten. Dieser Effekt ist für das Bormonofluorid-Molekül BF noch wesentlich stärker ausgeprägt, für das sich eine theoretische Bindungsordnung von 1.4 ableiten lässt. Damit einhergehend werden die Molekülorbitale stärker an den Atomen lokalisiert. HOMO und LUMO sind hauptsächlich Bor-zentriert und führen so zu den stärker ausgeprägten Donor- und Akzeptoreigenschaften (Abb. 11).

Während es nicht möglich ist, Bormonofluorid unter für Experimentatoren geeigneten Bedingungen zu verwenden, wurde 2011 von Bertrand eine Borylen-Variante isoliert, die durch zwei cyclische (Alkyl)(amino)carbene stabilisiert wird.[73] Wenig später wurde ein Komplex dargestellt, indem eine solche Donorgruppe L_2BH, die als Liganden-stabilisiertes Borylen bezeichnet werden könnte, erst synthetisiert und in einem Folgeschritt mit [(thf)$Cr(CO)_5$] zum entsprechenden Chrom-Komplex umgesetzt wurde.[74]

Tatsächlich konnte 2019 ein Komplex isoliert werden, in dem ein Bormonofluorid terminal an ein Eisen-Atom gebunden ist (Abb. 12). Die Synthese erfolgte durch Drance *et al.* nicht von freiem BF aus, sondern durch eine Redox-Reaktion von Bortrifluorid mit einem Eisen(-II)-Präkursor.[75]

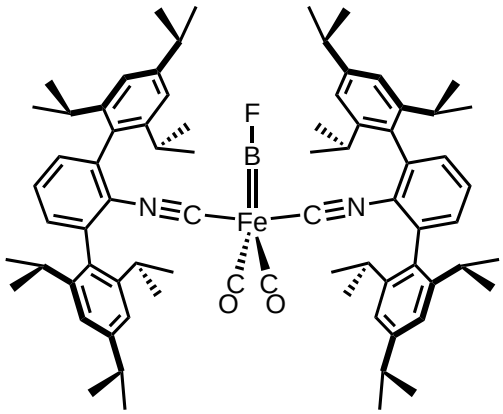

Abbildung 12: Struktur des ersten Übergangsmetallkomplexes mit terminal koordinierender BF-Einheit.[75]

Von Figueroa und Mitarbeitern konnten die analogen CO- und N_2-haltigen Komplexe ebenfalls isoliert werden. Die experimentellen Beobachtungen sowie die quantenchemischen Analysen der drei Komplexe bestätigen den prognostizierten Trend der Donorstärke.

1.3 Analogien zu Stickstoff-basierten Liganden

Stickstoff-basierte Donorgruppen sind in der homogenen Katalyse stark vertreten. Insbesondere Liganden mit einem Amin-basierten Donor im Rückgrat zeigen gute Eigenschaften als Hydrierungskatalysatoren,[76–79] wie auch Erfolge aus der eigenen Gruppe zeigen konnten.[80] In den meisten Fällen wird ein mehrzähniger Ligand verwendet, der das Stickstoff-Atom in der für die jeweilige Reaktion am günstigsten Position fixiert. Sehr häufig handelt es sich bei den mehrzähnigen Systemen um Pinzetten-Liganden.[81,82] Aufgrund des Chelat-Effektes wirken diese stabilisierend und führen dazu, dass die Dissoziation des Liganden und somit der Stickstoff-basierten Donorgruppe thermodynamisch ungünstiger wird. Eine Veränderung des Donor-Charakters wird bei der sogenannten bifunktionalen bzw. kooperativen Katalyse beobachtet. So können auf sekundären Aminen basierte Donorgruppen als Protonen-Relais agieren und ein Proton auf ein Substrat übertragen oder, im Laufe eines katalytischen Zyklus nach erfolgter Deprotonierung, wieder reprotoniert werden (Schema 1).[83–85]

Bor-Verbindungen des Typs L_2BH wurden schon im Titel ihrer ersten Publikation als Amin-Analoga identifiziert.[73] Es ist also anzunehmen, dass eine ähnliche Reaktivität prinzipiell möglich ist. Gleiches gilt für Carbodiphosphorane selbst nicht, aber für deren protonierte Derivate.

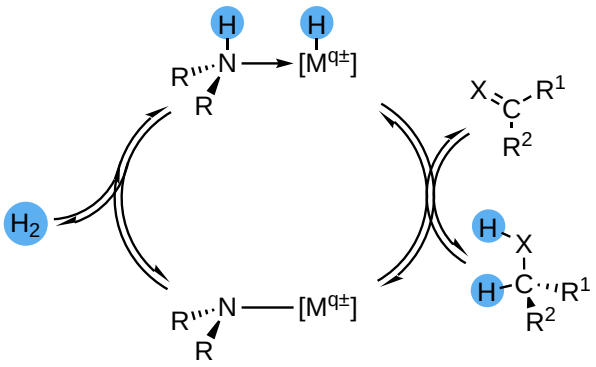

Schema 1: Sekundäre Amine als Donorgruppen in kooperativer Katalyse.

Die Protonenaffinitäten dieser Verbindungen wurden bereits untersucht.[39,40,86] Sie liegen in einem Bereich, der für sekundäre Amine nicht ungewöhnlich ist und somit Parallelen in den Reaktivitäten andeutet.

1.4 Metall-Ligand-Interaktionen

1.4.1 Klassifizierung

Häufig werden in Metallkomplexen die Interaktionen zwischen Zentralatom und Liganden nicht ausführlich beschrieben, sondern nur eine Koordinationszahl und formale Oxidationsstufe zugewiesen. Diese Methodik mag für einfachere Koordinationsverbindungen ausreichend sein, sie führt jedoch zu Problemen, sobald von einem bestehenden Komplex aus Rückschlüsse auf dessen Bestandteile gezogen werden sollen. So können die koordinativen Bindungen auf verschiedene Arten zustande gekommen sein.
Eine Variante, die eine übersichtliche Grundlage zur genaueren Beschreibung der Metall-Ligand-Interaktionen ermöglicht, wurde zum Beispiel durch Green 1995 veröffentlicht.[87] In dem Übersichtsartikel zu der *covalent bond classification* beschreibt er drei Funktionen, durch die die Interaktionen zwischen Zentralatom und eines daran bindenden Atoms spezifiziert werden können. Die Einordnung der Liganden in drei Kategorien erfolgt formal durch Spaltung der Ligand-Metall-Bindung unter Bildung der neutralen Liganden. Es wird zwischen dem kovalent bindenden X-Typ-Liganden, dem als Elektronenpaar-Donor fungierenden L-Typ-Liganden und dem Elektronenpaar akzeptierenden Z-Typ-Liganden unterschieden (Abb. 13).

Dem Formalismus folgend finden sich die meisten Liganden als X- oder L-Typ eingeordnet. Zu den typischen Liganden des X-Typs gehören Anionen wie beispielsweise die Halogenide oder Hydrid, während Elektronenpaar donierenden, Lewis-basischen Liganden wie Kohlenmonoxid, NHCs und Phosphinen der L-Typ zugewiesen ist. Die wenigsten Vertreter finden sich in der Kategorie der Z-Typ-Liganden. Ein großer Teil hiervon wird durch Bor(+III)-Verbindungen

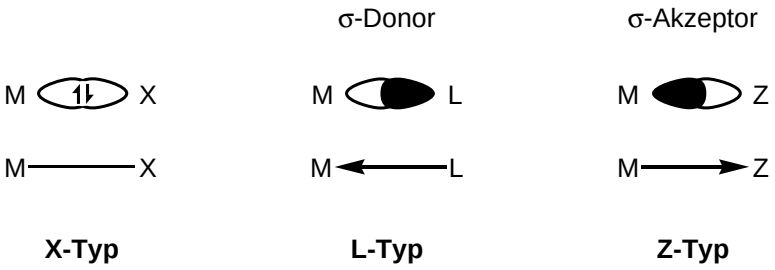

Abbildung 13: Beispielhafte Darstellung der drei definierten Klassen an Bindungsinteraktionen anhand von σ-Wechselwirkungen.[87]

wie BH_3, BR_3 und den Bortrihalogeniden gestellt.
Bei genauerer Betrachtung der oben beschriebenen Bor-basierten Ligandenklassen der Borane, Boryle und Borylene lässt sich erkennen, dass diese durch die *covalent bond classification* in unterschiedliche Kategorien eingeteilt werden. So können Borane aufgrund ihres Lewis-aziden Charakters als Z-Typ-Liganden, Boryle als einfach anionische Verbindungen als X-Typ-Liganden und Borylene durch den relativen Elektronenreichtum als L-Typ-Liganden eingeordnet werden (Abb. 14).

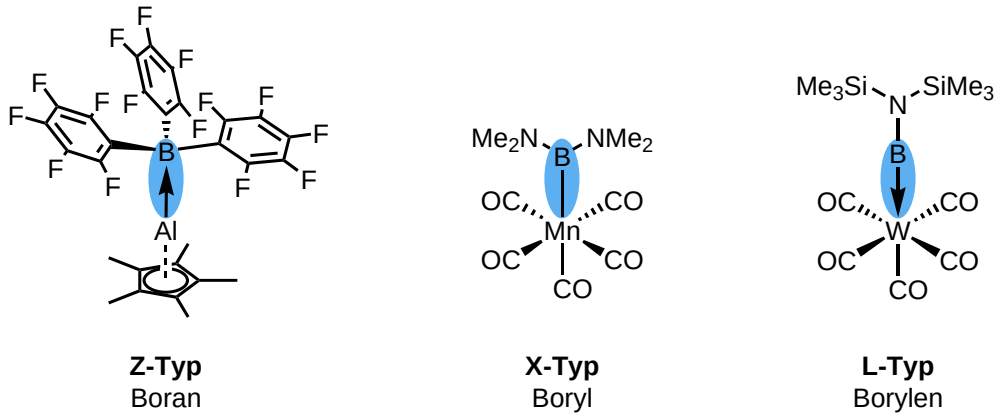

Abbildung 14: Beispiele für Bor-Liganden des Z-,[88] X-[57] und L-Typs.[66,67]

In vielen Komplexen haben Bindungen zumindest teilweise dativen Charakter. In dieser Dissertation werden, zur besseren Übersichtlichkeit und wie in der Koordinationschemie üblich, einfache Striche verwendet. Pfeile anstelle der klassischen Bindungsstriche werden nur dann gezeichnet, wenn explizit auf eine besondere Bindungssituation hingewiesen werden soll.

1.4.2 Pinzetten-Liganden als Plattform

Unter den so genannten Pinzetten-Liganden versteht man tridentate Liganden, die in einer Ebene meridional an ein zentrales Metallatom koordinieren. Die sich so ergebenden Pinzetten-Komplexe zeichnen sich durch ein rigides Ligandengerüst und einer damit verbundenen hohen thermischen Stabilität aus. Diese beruht auf dem Chelat-Effekt, ein Zusammenspiel aus

Entropiegewinn, Löslichkeit und Ringbildung. Weitere Vorteile von Pinzetten-Liganden sind die gut einstellbaren sterischen und elektronischen Eigenschaften, die sich häufig einfach über die Substituenten der Donoratome kontrollieren lassen (Abb. 15).[89] Durch rigide Pinzetten-Liganden kann in quadratisch-planaren Komplexen eine Umlagerung zu einer tetraedrischen Koordinationsgeometrie verhindert werden. Während die zentrale Donorgruppe aufgrund ihres *trans*-Einflusses direkt die Reaktivität des Komplexes oder die eines *trans*-ständigen Substrates beeinflusst, ist es zudem möglich, die terminalen Donorgruppen so zu modifizieren, dass sich eine Hemilabilität ergibt.

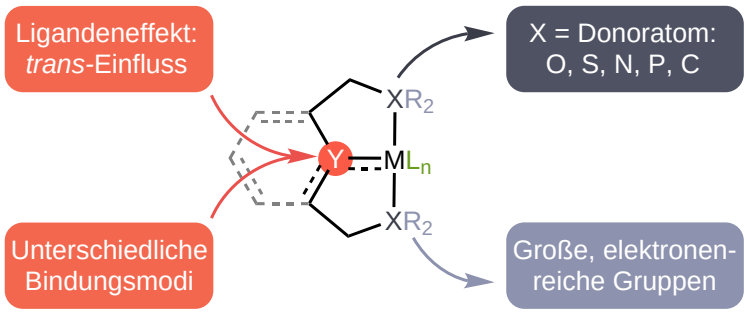

Abbildung 15: Schematischer Aufbau von Pinzetten-Liganden in Übergangsmetallkomplexen.

Obwohl die ersten - damals noch nicht als solche bezeichneten - Pinzetten-Liganden bereits 1976 von Moulton und Shaw[90] synthetisiert wurden, sollte es noch über zwanzig Jahre dauern, bis durch Milstein die erste erfolgreiche Anwendung eines Palladium-Pinzetten-Komplexes zur Katalyse der Heck-Reaktion publiziert wurde.[91]
Eine gängige Nomenklatur für Verbindungen diesen Typs ist es, wie bereits von Moulton und Shaw eingeführt, die chemischen Symbole der Donor-Atome aneinanderzureihen. So handelt es sich bei den gezeigten Beispiel-Komplexen um renommierte Vertreter der Aryl-basierten PCP-,[92] Amin-basierten PNP-[93] und Boryl-basierten PBP-Pinzetten-Liganden[63] (Abb. 16).

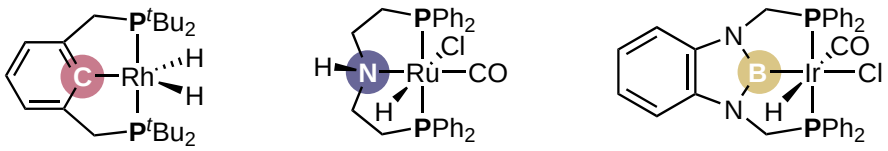

Abbildung 16: Aryl-basierter PCP-, Amin-basierter PNP- und Boryl-basierter PBP-Pinzetten-Komplex.[63,92,93]

Während es sich bei den PCP-Liganden um die häufigste Form der Pinzetten-Liganden handelt, ist besonders in den homogenkatalytischen Anwendungen die PNP-Form extrem erfolgreich vertreten. Durch Pinzetten-Liganden lassen sich außerdem auch schwache Donoren, die als monodentate Liganden nur schlecht koordinieren oder schnell selbst von koordinierenden Lösungsmitteln verdrängt werden würden, zur Koordination bringen. Die Stabilisierung erfolgt

hier, da durch die weiteren Donoratome des Liganden eine räumliche Nähe des schwachen Donors zu dem Metallzentrum erzwungen wird. Besonders stark ist dieser Effekt für den mittleren Donor des Pinzetten-Liganden ausgeprägt.
Hierdurch eröffnet sich die Möglichkeit der Stabilisierung und Untersuchung ungewöhnlicher, oder als monodentate Liganden hoch reaktiver, Gruppen durch Verankerung im Zentrum eines Pinzetten-Liganden. Es bietet sich daher an, die vorgestellten Donorgruppen der Typen L_2BH und L_2C bzw. $[L_2CH]^+$ durch Einbringen in eine Pinzetten-Plattform zu stabilisieren. Während die Synthese NHC-basierter Pinzetten-Liganden durch die entsprechenden Imidazolium-Salze bereits gut untersucht ist, stellen besonders Bor-Verbindungen des Typs L_2BH eine größere Herausforderung dar.[94]
Im Fall der CDP-basierten Pinzetten-Liganden sind aktuell drei Beispiele literaturbekannt. Hierbei handelt es sich um einen CCC-Pinzetten-Liganden, durch C-H-Aktivierung der *ortho*-Position zweier Phenylringe von Hexaphenylcarbodiphosphoran gebildet,[95–97] einen PCP-Pinzetten-Liganden, der durch Templatsynthese erhalten werden konnte,[98–101] und einen NCN-Pinzetten-Liganden, der Ende 2018 durch Zhao, Frenking und Zhu publiziert wurde (Abb. 17).[102]

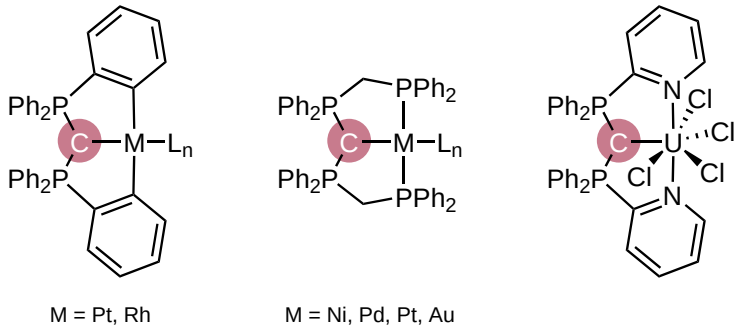

Abbildung 17: Bekannte Komplexe CDP-basierter Pinzetten-Liganden.[95–102]

Prinzipiell auf stabilisiertem Borylen basierende, also die Gruppe L_2BH enthaltende Pinzetten-Komplexe konnten erstmals 2016 in unserer Arbeitsgruppe durch Vondung isoliert werden (Abb. 18).[103–105] Der Pinzetten-Ligand bildet sich in der Koordinationssphäre des zentralen Eisen-Atoms durch Umlagerung eines Boran-Liganden.

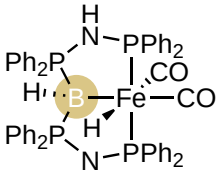

Abbildung 18: Erster Pinzetten-Komplex mit L_2BH-Einheit im Rückgrat.[103,104]

1.4.3 Experimentelle Quantifizierung von Metall-Ligand-Interaktionen

Eine experimentelle Quantifizierung der Donorstärke von Liganden kann auf verschiedenen Wegen stattfinden. Im Allgemeinen wird zuerst ein gut untersuchter, einfacher Präkursor-Komplex mit dem zu untersuchenden Liganden zur Reaktion gebracht. Anschließend wird eine spektroskopisch einfach untersuchbare Eigenschaft gemessen und in den Vergleich mit Messwerten anderer Liganden und/oder des Präkursor-Komplexes gestellt. Hieraus resultiert ein Ligandenparameter, der zum Abschätzen und Bewerten von Trends katalogisiert werden kann. Im Folgenden werden die bekanntesten Ligandenparameter kurz erklärt.

Tolman Electronic Parameter

Ursprünglich für Phosphine entwickelt, stellt der *Tolman Electronic Parameter* (TEP) mittlerweile den wohl bekanntesten der modernen Ligandenparameter dar.[106] Die Synthese erfolgte durch Reaktion des Phosphins mit Nickeltetracarbonyl (Schema 2).

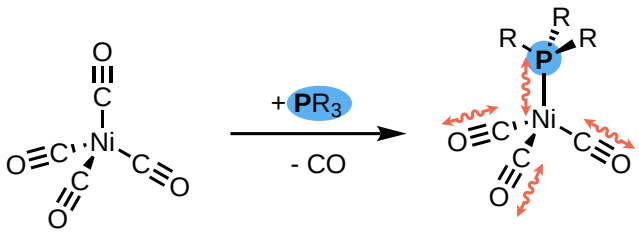

Schema 2: Synthese der Verbindungen zur Bestimmung des TEP und gemessene Schwingungen.

Der TEP wird nach Isolation der Komplexverbindung durch IR-spektroskopische Messung der A_1-Schwingungsmode der Carbonyl-Liganden bestimmt. Die Begründung der Korrelation der Frequenz der C–O-Schwingungen mit der Donorstärke liegt in den Orbitalwechselwirkungen des Metalls mit den π-akzeptierenden CO-Liganden, wie weiter oben bereits diskutiert (siehe Abb. 2). In Kombination mit den sterischen Einflüssen, definiert über den Kegelwinkel, konnte Tolman Rückschlüsse auf Eigenschaften und Reaktivitäten von einer großen Anzahl an Phosphinen ziehen. Der TEP kann ebenso einfach für NHCs bestimmt werden und ermöglicht so den direkten Vergleich von Phosphinen und NHC-Liganden.[107–109] Auch für CDP-basierte Liganden sind in der Zwischenzeit Untersuchungen zur Bestimmung des TEP erfolgt.[110]
Die hohe Toxizität des verwendeten $[Ni(CO)_4]$ kann durch analoge Komplexe anderer Metalle vermieden werden. So wurde von der Gruppe um Crabtree eine Alternative unter Verwendung von Rhodium(+I) oder Iridium(+I) entwickelt, die später durch die Gruppe von Nolan weiter modifiziert wurde.[111,112] Die neueren Methoden werden aber dadurch komplizierter, dass die Synthesen der Analyt-Komplexe nicht in einem Schritt zu vollziehen sind.

Lever Electronic Parameter

Über das Redox-Potential von Ruthenium(+III/+II)-[113] oder Rhenium(+III/+II)-[114] Redoxpaaren ist es möglich, eine elektrochemische Parametrisierung von Liganden vorzunehmen. Hierzu wird ein Komplex der Form $[ML_6]$ erzeugt und dessen elektrochemisches Potential gemessen (Schema 3). Der Beitrag des zu messenden Liganden ist dementsprechend ein Sechstel des Gesamtpotentials. Um eine Aussage über die Donorstärke eines Liganden zu treffen und diese in σ- und π-Anteile zu zerlegen, wird ein quantenmechanischer Ansatz mittels Störungstheorie genutzt.[115]

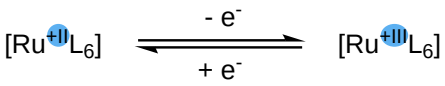

Schema 3: Redoxpaar zur Messung des elektrochemischen Potentials.[113]

Huynh Electronic Parameter

Eine weitere Methode, Donorstärken verschiedener Liganden zu messen, wurde von Huynh entwickelt. Hier erfolgt die Bestimmung der Ligandenstärke mittels einer ^{13}C NMR-Sonde. Ausgehend von einem quadratisch-planaren Palladium(+II)-Komplex mit zwei *trans*-ständigen Bromido-Liganden, dem zu untersuchenden Liganden und dem NHC-Liganden 1,3-Diisopropylbenzimidazolin-2-yliden (^{i}Pr$_2$-bimy) wird hierzu die chemische Verschiebung des Carben-Kohlenstoffatoms von ^{i}Pr$_2$-bimy gemessen. Als Ausgangsmaterial wird eine dimere Palladium-Spezies mit verbrückenden Bromo-Liganden und endständigen NHC-Liganden verwendet, die unter Zugabe des zu messenden Donorliganden in zwei Monomere zerfällt (Schema 4).[116,117]

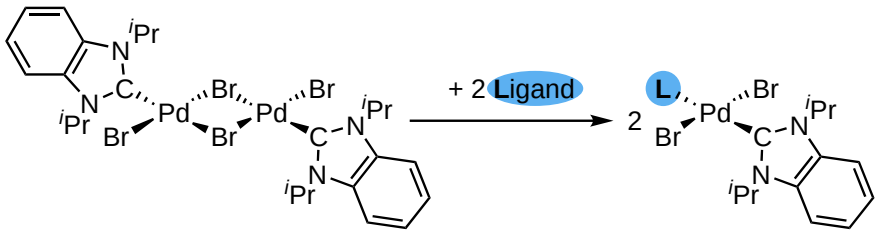

Schema 4: Synthese der Analyt-Komplexe zur Bestimmung des ^{13}C NMR-basierten HEP.[116]

Der originale *Huynh Electronic Parameter* (HEP) erfuhr seitdem zwei Weiterentwicklungen. Zum einen wurden Gold(+I)-Komplexe genutzt, um besonders starke Donoren und NHC-basierte Liganden zu untersuchen.[118] Zum anderen wurde das System auch für die Erfassung von bidentaten Liganden mit zwei gleichen Donorgruppen eingesetzt.[119]

1.4.4 Quantenchemische Quantifizierung von Metall-Ligand-Interaktionen

Quantentheorie der Atome in Molekülen

Die Quantentheorie der Atome in Molekülen (*quantum theory of atoms in molecules*, QTAIM) wurde von Richard F. W. BADER in den Achtzigerjahren entwickelt und schlägt eine Brücke zwischen abstrakten Konzepten wie Lewis- und Valenzstrichformeln[120] und der physikalisch zu messenden Elektronendichte $\rho(\vec{r})$.[121–123] Zur Zeit der Entwicklung der Theorie wurde primär die aus quantenchemischen Rechnungen erhaltene Wellenfunktion Ψ genutzt, um $\rho(\vec{r})$ zu ermitteln (Gl. (1.1)).

$$\rho(\vec{r}) = N\int \Psi^*(\vec{Q})\Psi(\vec{Q})\mathrm{d}\tau' \tag{1.1}$$

N = Anzahl der Elektronen
$\vec{Q}$ = Gesamtmenge der Koordinaten aller Elektronen
τ' = Spinkoordinaten aller Elektronen und Raumkoordinaten von N-1 Elektronen

Es war bereits bekannt, dass auch Röntgenbeugungsexperimente einen Zugang zu $\rho(\vec{r})$ bieten, jedoch können erst durch die stete Weiterentwicklung der Röntgendiffraktometer hochaufgelöste Elektronendichtekarten erstellt werden. Hierzu werden die aus Röntgenbeugungsexperimenten ermittelten Strukturfaktoren und die Zellparameter genutzt (Gl. (1.2)).

$$\rho(\vec{r}) = \frac{1}{V}\sum_h\sum_k\sum_l F(hkl)\mathrm{e}^{-2\pi i\vec{h}\cdot\vec{r}} \tag{1.2}$$

V = Volumen der Elementarzelle
h, k, l = Miller-Indizes
F = Strukturfaktor
$\vec{h} = \begin{pmatrix} h/a \\ k/b \\ l/c \end{pmatrix}$ mit a, b, c = Elementarzelldimensionen

Die experimentell oder auf quantenchemischem Wege erhaltene Elektronendichte $\rho(\vec{r})$ wird beim QTAIM-Ansatz topologisch analysiert. Atomkerne bilden lokale Maxima der Elektronendichte, von denen aus diese in alle Richtungen abnimmt. Sobald ein oder mehrere Atome in räumlicher Nähe zueinander sind, bilden sich so genannte Nullflussflächen. An diesen entspricht der Gradient der Elektronendichte $\nabla\rho(\vec{r})$, also die erste Ableitung, gleich null (Gl. (1.3)).

$$\nabla\rho(\vec{r}) = \vec{i}\frac{\partial\rho}{\partial x} + \vec{j}\frac{\partial\rho}{\partial y} + \vec{k}\frac{\partial\rho}{\partial z} \tag{1.3}$$

$\vec{i}, \vec{j}, \vec{k}$ = Einheitsvektoren

Die Nullflussflächen bilden Bassins, die im Normalfall je ein Atom enthalten. Durch Integration der Elektronendichte des zugehörigen Bassins können atomare Eigenschaften, wie z.B. die

Gesamtladung q_i eines Atoms ermittelt werden (Gl. (1.4)).

$$q_i = Z_i - \int_{\Omega} \rho(\vec{r}) \mathrm{d}\vec{r} \tag{1.4}$$

q_i = Gesamtladung des Atoms
Ω = Bassin
Z_i = Kernladung

Für eine weitere Differenzierung der lokalen Minima und Maxima der Elektronendichteverteilung wird die zweite Ableitung, die Laplace-Funktion $\Delta\rho(\vec{r})$ herangezogen (Gl. (1.5)).

$$\Delta\rho(\vec{r}) = \nabla^2\rho(\vec{r}) = \frac{\partial^2\rho(\vec{r})}{\partial x^2} + \frac{\partial^2\rho(\vec{r})}{\partial y^2} + \frac{\partial^2\rho(\vec{r})}{\partial z^2} = \lambda_1 + \lambda_2 + \lambda_3 \tag{1.5}$$

$\lambda_1, \lambda_2, \lambda_3$ = Eigenwerte der Hesse-Matrix

Die Summe der Vorzeichen der einzelnen Terme der Laplace-Funktion (Gl. (1.5)) gibt Auskunft über die kritischen Punkte. Hierbei handelt es sich um spezielle Punkte, bei denen die nach der Diagonalisierung der Hesse-Matrix erhaltenen Eigenwerte λ_1, λ_2 und λ_3 alle ungleich null sind. Es kommt zur Unterscheidung zwischen vier Fällen. Nimmt $\rho(\vec{r})$ in alle drei Raumrichtungen ab, ist die Summe der Vorzeichen der Eigenwerte -3 und es handelt sich um einen atomkritischen Punkt (*nuclear attractor*, na). Ist die Summe der Vorzeichen -1, nimmt $\rho(\vec{r})$ in zwei Richtungen ab und in eine zu, es liegt ein bindungskritischer Punkt (*bond critical point*, bcp) vor. Bei einer Vorzeichensumme von +1 handelt es sich um einen ringkritischen Punkt (*ring critical point*, rcp) und sind alle Vorzeichen positiv (+3) um einen käfigkritischen Punkt (*cage critical point*, ccp). Bei einem rcp nimmt $\rho(\vec{r})$ in einer Richtung zu, bei einem cpp in alle.
$\Delta\rho(\vec{r})$ lässt sich, wie schon $\rho(\vec{r})$ und $\nabla\rho(\vec{r})$, auch als topologische Karte darstellen. Dies ist eine viel verwendete Darstellung, da $\Delta\rho(\vec{r})$ Auskunft über Bereiche der Anreicherung (negatives Vorzeichen) oder einen Abfluss (positives Vorzeichen) von $\rho(\vec{r})$ gibt. Im Vergleich von $\rho(\vec{r})$, $\nabla\rho(\vec{r})$ und $\Delta\rho(\vec{r})$ in Form zweidimensionaler Karten am Beispiel von Bormonofluorid lässt sich unschwer erkennen, dass der Informationsgehalt von $\Delta\rho(\vec{r})$ zwar bereits deutlich über dem von $\rho(\vec{r})$ liegt, aber erst das Eintragen des Bindungspfades und der kritischen Punkte macht den Vergleich mit klassischen Strichformeln möglich (Abb. 19).
Die Verbindung zwischen zwei Atomen, die der maximalen Elektronendichte folgt, wird als Bindungspfad bezeichnet.[124] Im Gegensatz zu den chemischen Bindungen, die z.B. in Lewis-Strichformeln gemalt werden, handelt es sich weder notwendigerweise um die kürzeste Strecke zwischen zwei Atomen noch muss hier eine Bindung im klassischen Sinne vorliegen.[125] Vielmehr zeigt ein Bindungspfad eine Interaktion zwischen Atomen an, die auf der physikalischen Elektronendichte basiert. Als Kriterium für die tatsächliche Stabilität einer Bindung wird die Gesamtenergiedichte *H* des bcp herangezogen. Auch Rückschlüsse auf die vorliegende Bindungsart können anhand des bcp gezogen werden.

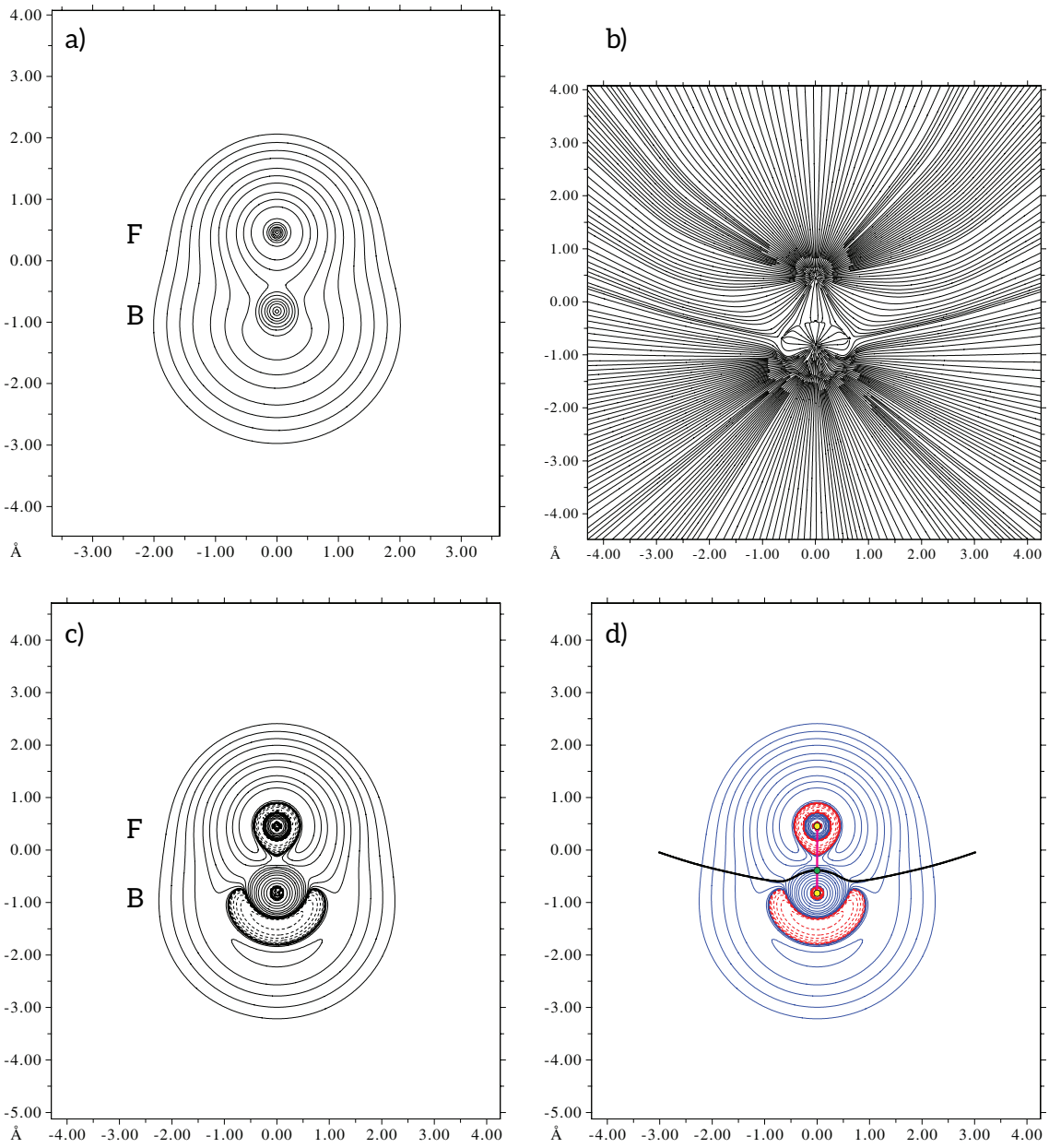

Abbildung 19: Bormonofluorid (G16, B97D/def2-TZVPP) als Modell für verschiedene Darstellungsarten: **a)** $\rho(\vec{r})$ als topologische Karte **b)** $\nabla\rho(\vec{r})$ als Gradientenlinienkarte **c)** $\Delta\rho(\vec{r})$ als topologische Karte (positives Vorzeichen mit durchgezogener, negatives mit gestrichelter Linie) **d)** $\Delta\rho(\vec{r})$ als topologische Karte (positives Vorzeichen blau, negatives rot) mit bindungs- (grün) und atomkritischen (gelb) Punkten sowie Bindungspfad (magenta) und Nullflussfläche (schwarz).

Eine wichtige Größe ist hierbei die räumliche Form der Bindung, die über die Elliptizität ε anhand der zwei negativen Eigenwerte λ_i und λ_j des bcp mit $\lambda_i \leq \lambda_j$ beschrieben wird (Gl. (1.6)).

$$\varepsilon = \frac{\lambda_i}{\lambda_j} - 1 \tag{1.6}$$

σ-Einfachbindungen sind im Idealfall zylindrisch und demensprechend gilt ε = 0. Eine Abweichung von null deutet auf eine Mehrfachbindung oder Mehrzentrenbindung hin. Auch das Vorzeichen von $\Delta\rho(\vec{r})$ am bcp kann Auskunft über die vorliegende Bindungsart geben. Kovalente Bindungen weisen aufgrund der relativ hohen Ladungsdichte entlang des Bindungspfades typischerweise ein negatives Vorzeichen auf, wohingegen ionische Bindungen durch die stärkere Lokalisierung von $\rho(\vec{r})$ an den Atomkernen für $\Delta\rho(\vec{r})$ am bcp positive Vorzeichen generieren. Besonders bei schwachen Interaktionen ist diese Art der Identifikation nicht immer zuverlässig, da sich $\rho(\vec{r})$ nur marginal ändert. Die Lage eines bcp entlang des Bindungspfades gibt zusätzlich Auskunft über die Polarisierung der Bindung. Eine kovalente, nicht polarisierte Bindung sollte den bcp auf halbem Wege zwischen den Atomen aufweisen, bei Elektronegativitätsdifferenzen wandert der Punkt zu dem elektronenärmeren Bindungspartner.
Die Analyse nach Bader bietet sich aufgrund der Vielzahl an Informationen, die über Bindungen erhalten werden können, besonders dafür an, die meist dativen Bindungen zwischen Donor und Metallatom in Übergangsmetallkomplexen genauer zu untersuchen.

Energie-Dekompositions-Analyse

Die Energie-Dekompositions-Analyse (*energy decomposition analysis*, EDA oder auch *extended transition state (method)*, ETS) wurde bereits in den Siebzigern von Morokuma und Ziegler und Rauk entwickelt.[126–129] Die Methode wird stetig weiterentwickelt und kann Einblick in viele Bindungsinteraktionen geben.[130,131]
In der EDA wird aus den zwei Fragmenten A und B das Molekül A–B mit der Energie E_{AB} und der relaxierten Wellenfunktion Ψ_{AB} gebildet. Im Zuge der Analyse wird die Entstehung dieser Wellenfunktion schrittweise aus der Interaktion der Fragmente A^0 und B^0, jeweils in den Grundzuständen Ψ^0_{A} und Ψ^0_{B} der Energien E^0_{A} und E^0_{B}, untersucht. Zuerst erfolgt eine Verformung einhergehend mit einer elektronischen Anregung der Fragmente A^0 und B^0 aus den Grundzuständen in die Zustände Ψ_{A} und Ψ_{B} mit den zugehörigen Energien E_{A} und E_{B}, so wie sie im Molekül AB vorliegen. Die Gesamtenergie, die für diese Zustandsveränderung notwendig ist, ist die Präparationsenergie E_{prep} (Gl. (1.7)).

$$\Delta E_{\mathrm{prep}} = E_{\mathrm{A}} - E^0_{\mathrm{A}} + E_{\mathrm{B}} - E^0_{\mathrm{B}} \tag{1.7}$$

Die Gesamtwechselwirkungsenergie E_{int}, der wesentliche Bestandteil der EDA, wird als Differenz der Energien der Fragmente in ihren angeregten Zuständen und der Energie des Moleküls formuliert (Gl. (1.8)).

$$\Delta E_{\mathrm{int}} = E_{\mathrm{AB}} - E_{\mathrm{A}} - E_{\mathrm{B}} \tag{1.8}$$

Die Bindungsdissoziationsenergie D_{e} wird dementsprechend aus der Summe von ΔE_{prep} und

ΔE_{int} erhalten (Gl. (1.9)).

$$-D_{\text{e}} = \Delta E_{\text{int}} + \Delta E_{\text{prep}} \tag{1.9}$$

Für das Zustandekommen einer Bindung ist in der EDA als erstes eine Annäherung der Fragmente A und B aus unendlicher Entfernung notwendig. Die Elektronendichte der Fragmente erfährt hier noch keine Veränderung und dementsprechend resultiert ein Molekül-Präkursor mit der Wellenfunktion $\Psi_{\text{A}}\Psi_{\text{B}}$. Die zugehörige Energie E^0_{AB} entspricht der quasiklassischen Coulomb-Wechselwirkung ΔE_{elstat} (Gl. (1.10)).

$$\Delta E_{\text{elstat}} = \sum_{\alpha\in\text{A}}\sum_{\beta\in\text{B}} \frac{Z_\alpha Z_\beta}{R_{\alpha\beta}} + \int V_{\text{B}}(r)\rho_{\text{A}}(r)\text{d}r + \int V_{\text{A}}(r)\rho_{\text{B}}(r)\text{d}r + \iint \frac{\rho_{\text{A}}(r_1)\rho_{\text{B}}(r_2)}{r_{12}}\text{d}r_1\text{d}r_2 \tag{1.10}$$

Da die Wellenfunktion $\Psi_{\text{A}}\Psi_{\text{B}}$ gegen das Pauli-Prinzip verstößt, wird diese antisymmetrisiert und renormalisiert, was zu dem Zwischenzustand Ψ^0 mit der Energie E^0 führt (Gl. (1.11)).

$$\Psi^0 = \text{N}\hat{\text{A}}\{\Psi_{\text{A}}\Psi_{\text{B}}\} \tag{1.11}$$

Die Energiedifferenz zwischen den Zuständen wird als Pauli-Repulsion ΔE_{Pauli} bezeichnet (Gl. (1.12)).

$$\Delta E_{\text{Pauli}} = E^0_{\text{AB}} - E^0 \tag{1.12}$$

Die Relaxation aus dem Zwischenzustand in den finalen Zustand Ψ_{AB} des Moleküls AB erfolgt durch das Wechselwirken der Orbitale der Fragmente miteinander. Es gibt somit den kovalenten Anteil der Bindung wieder und wird als Orbitalinteraktion ΔE_{orb} bezeichnet (Gl. (1.13)).

$$\Delta E_{\text{orb}} = E_{\text{AB}} - E^0_{\text{AB}} \tag{1.13}$$

Dementsprechend ist es auch möglich, ΔE_{orb} in Beiträge von Orbitalen der verschiedenen irreduziblen Darstellungen Γ der Punktgruppe des betrachteten Moleküls AB zu zerlegen (Gl. (1.14)).

$$\Delta E_{\text{orb}} = \sum_{\Gamma} \Delta E_{\Gamma} \tag{1.14}$$

Die aus den einzelnen Schritten erhaltenen Energiebeiträge der elektrostatischen Wechselwirkung, der Pauli-Repulsion und der Orbitalwechselwirkung machen die Gesamtheit der Interaktionsenergie aus (Gl. (1.15)).

$$\Delta E_{\text{int}} = \Delta E_{\text{elstat}} + \Delta E_{\text{Pauli}} + \Delta E_{\text{orb}} \tag{1.15}$$

In Übergangsmetallkomplexen kann die Bindungsstärke der Donor-Metall-Bindung durch die

EDA untersucht werden. Dies ist hilfreich, um den Vergleich von Donorstärken verschiedener Liganden im Bezug auf ein identisches Metallzentrum zu vereinfachen. Zusätzlich bietet sich die Möglichkeit, die Orbitalwechselwirkung in σ- und π-Anteile aufzuspalten. Im Hinblick auf die Donor- und Akzeptorfunktionalitäten der verschiedenen Liganden steht damit ein praktisches Werkzeug zur Verfügung.

2 Motivation & Projektumfang

Während Stickstoff-basierte Donorgruppen, insbesondere integriert in zwei- oder dreizähnige Liganden, in der Homogenkatalyse viel und vor allem erfolgreiche Anwendung finden, waren zu Beginn dieser Arbeit weder Carbodiphosphoran- noch Borylen-basierte Liganden in katalytischen Anwendungen bekannt. Erste Ergebnisse kamen hierzu aus der eigenen Arbeitsgruppe von Lisa Vondung, die erste Untersuchungen zu einem Pinzetten-Komplex mit L_2BH-basierter Donorgruppe durchführte.[132] Aufgrund der vorhergesagten - und zum Teil auch demonstrierten - großen Donorstärke, sollten sich genau diese funktionellen Gruppen gut eignen, um sehr elektronenreiche Übergangsmetallkomplexe darzustellen. Diese könnten dann die Aktivierung von Substraten mit sehr stabilen Bindungen ermöglichen. Genauso besteht die Möglichkeit, unter Verwendung außergewöhnlicher Donorgruppen, bislang unbekannte Reaktivitäten zu beobachten.

Ein konkretes Beispiel für die Anwendbarkeit von Amin-analogen Donorgruppen in Übergangsmetallkomplexen mit der Möglichkeit der kooperativen Katalyse ist die Entwicklung einer nachhaltigen Alternative für das Haber-Bosch-Verfahren. In der jüngeren Vergangenheit hat sich angedeutet, dass Amin-basierte PNP-Pinzettenliganden hier einen homogenkatalytischen Weg eröffnen könnten.[133] Daher ist das Interesse sehr hoch, die Forschung auf diesem Gebiet voranzutreiben.[134,135] Ebenso ist vorstellbar, dass eine Inkorporation von molekularem Stickstoff in organische Moleküle mit den richtigen Katalysatoren direkt und ohne den Umweg über Ammoniak möglich ist.[136]

Im Zuge dieser Forschungsarbeit sollte das Reaktionsverhalten von Bor- oder Kohlenstoff-basierten Donorgruppen der Formen L_2BH, L_2C und $[L_2CH]^+$ im Hinblick auf Analogien und Unterschiede zu den bekannten Amin-basierten Gruppen untersucht werden. Da anzunehmen war, dass die Gruppen entsprechend hohe Empfindlichkeiten zeigen, sollten die intrinsischen Eigenschaften von Pinzetten-Liganden sowohl zur Stabilisierung der Donoren wie auch resultierender Komplexe genutzt werden.

Zum Beginn der Untersuchungen lagen nur für zwei CDP-basierte Pinzetten-Liganden Berichte in der Literatur vor. Wie bereits in der Einleitung erwähnt, entsteht der CDP-basierte CCC-Pinzetten-Ligand *in situ* unter C–H-Aktivierung und ist als solcher nur bedingt attraktiv. Nicht alle Übergangsmetalle sind für C–H-Aktivierungen geeignet und ein Abspalten des Liganden mit abschließender Isolierung in freier Form ist nicht erfolgversprechend. Der zweite literaturbekannte Pinzetten-Ligand hingegen zeigte viele Charakteristika, die ihn für Untersuchungen interessant machten. Es handelt sich um einen PCP-Pinzetten-Liganden, was, in Anbetracht der großen Erfolge der Amin-basierten PNP-Pinzetten-Liganden, sehr positiv zu bewerten ist. Die terminalen Phosphingruppen eignen sich sehr gut als Donorgruppen, sind in Form von Diphenylphospin-Derivaten jedoch gleichzeitig sehr unempfindlich. Zudem besteht bei Phosphin-basierten Donorgruppen im Allgemeinen immer die Möglichkeit, Modifikatio-

nen vorzunehmen und die organischen Substituenten auszutauschen, um so Einfluss auf die sterischen und elektronischen Eigenschaften zu nehmen. Auch die Isolation des Liganden in Salzform wurde bereits berichtet und bot so einen idealen Startpunkt für die Synthese neuer Komplexe.

Im Bereich der Borylene bzw. deren stabilisierter Derivate boten sich die Ergebnisse aus der eigenen Gruppe für weitere Untersuchungen an. Der in unserer Gruppe zuerst synthetisierte Pinzetten-Komplex mit einer $(R_3P)_2BH$-Gruppe als zentraler Donoreinheit schien einen adäquaten Ausgangspunkt zu bieten. Aufgrund des ungewöhnlichen Entstehens des Pinzetten-Liganden sollte eine alternative Möglichkeit der Darstellung ermittelt werden, die dessen Isolation in freier Form ermöglicht.

Um die Vergleichbarkeit der Donorgruppen zu gewährleisten, sollte ein System gefunden werden, in dem strukturell möglichst ähnliche Komplexe für die drei verschiedenen Donorgruppen erzeugt und isoliert werden können. Anhand dieser Komplexe sollte im Anschluss eine extensive Untersuchung der Bindungssituation und Reaktivität durchgeführt werden, um Gemeinsamkeiten und Unterschiede der Donorgruppen zu identifizieren (Schema 5).

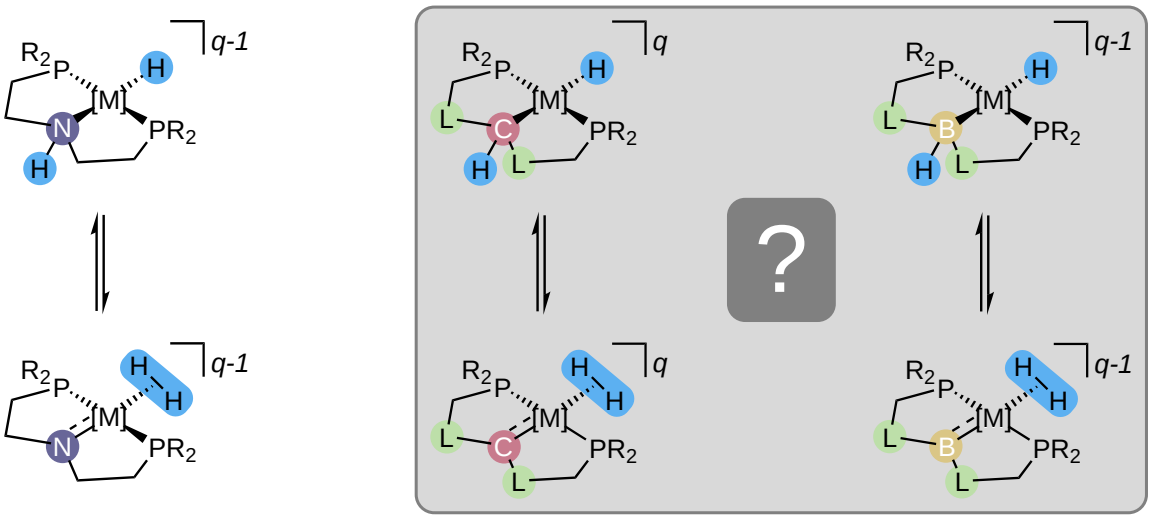

Schema 5: Mögliche Reaktionsmuster von formal isoelektronischen Donorgruppen basierend auf R_2NH, $[L_2CH]^+$ und L_2BH sowie deprotonierte Varianten im Vergleich. L = σ-Donor / π-Akzeptor.

3 Kumulativer Teil

Der Inhalt dieser kumulativen Dissertation wird aus fünf bereits veröffentlichten Artikeln gebildet, die in der unten gezeigten, chronologischen Reihenfolge behandelt werden. Der erste Artikel enthält Teile meiner Arbeit, zu Artikel drei haben alle Autoren gleichermaßen beigesteuert, die Artikel zwei, vier und fünf sind maßgeblich von meinen Ergebnissen getragen.

1. *Donor ligands based on tricoordinate boron formed by B–H-activation of bis(phosphine)-boronium salts*
   Grätz, M.; Bäcker, A.; Vondung, L.; Maser, L.; Reincke, A.; Langer, R.
   Chemical Communications **2017**, *53*, 7230–7233.
   DOI: 10.1039/C7CC02335A.

2. *Carbodiphosphorane-based nickel pincer complexes and their (de)protonated analogues: dimerisation, ligand tautomers and proton affinities*
   Maser, L.; Herritsch, J.; Langer, R.
   Dalton Transactions **2018**, *47*(31), 10544-10552.
   DOI: 10.1039/C7DT04930G.

3. *The ABC in pincer chemistry – From amine- to borylene- and carbon-based pincer-ligands*
   Maser, L.; Vondung, L.; Langer, R.
   Polyhedron **2018**, *143*, 28–42.
   DOI: 10.1016/j.poly.2017.09.009.

4. *Quantifying the donor strength of ligand-stabilized main group fragments*
   Maser, L.; Schneider, C.; Vondung, L.; Alig, L.; Langer, R.
   Journal of the American Chemical Society **2019**, *141*(18), 7596-7604.
   DOI: 10.1021/jacs.9b02598.

5. *Comparing the acidity of $(R_3P)_2BH$-based donor groups in iridium pincer complexes*
   Maser, L.; Schneider, C; Alig, L; Langer, R.
   Inorganics **2019**, *7*(5), 61.
   DOI: 10.3390/inorganics7050061.

3.1 Donor ligands based on tricoordinate boron formed by B–H-activation of bis(phosphine)boronium salts

Maik Grätz, Andreas Bäcker, Lisa Vondung, Leon Maser, Arian Reincke, Robert Langer, *Chemical Communications* **2017**, *53*, 7230–7233.

Beschreibung und Inhalt

Es werden Ergebnisse zu Phosphan-stabilisierten, Bor-basierten Donorgruppen aus früheren Arbeiten der Gruppe wieder aufgegriffen. So konnten Vondung *et al.* in vorangegangenen Arbeiten die Bildung eines PBP-Pinzetten-Liganden in der Koordinationssphäre eines Eisen-Komplexes aus einem Phosphino-Boran und weiterem Phosphin beobachten und die zentrale L_2BH-Donorgruppe als Liganden-stabilisiertes Borylen oder Boryl-Anion identifizieren.[103,104] In diesem Artikel wird die Synthese eines Bis(phosphino)boroniumsalzes beschrieben, das als Präkursor für die Synthese von PBP-Pinzetten-Komlexen eingesetzt werden kann. Durch Reaktion mit einem geeigneten Metallpräkursor wird unter B–H-Bindungsaktivierung ein Komplex gebildet, in dem der PBP-Pinzetten-Ligand entsprechend tridentat meridional an das entsprechende Metallatom gebunden ist.

Die Synthese des Bis(phosphino)boroniumsalzes erfolgte durch Reaktion von zwei Äquivalenten Bis(diphenylphosphino)methan (dppm) mit einem Äquivalent des Monobromoboran-Dimethylsulfid-Addukts (Schema 6).

Die Reaktivität des resultierenden Bis(phosphino)boroniumsalzes wurde gegenüber Nickel- und Palladiumpräkursoren untersucht. Mit Bis(cycloocta-1,5-dien)nickel und $[Pd(PPh_3)_4]$ wurden Produktgemische erhalten und es zeigte sich, dass eine Spaltung der Phosphor-Bor-Bindung erfolgt. Der Einsatz von $[Ni(CO)_4]$ resultiert in einer bidentaten κ*P,P'*-Koordination des Liganden unter Verdrängung zweier CO-Liganden, es erfolgt also keine Aktivierung der B–H-Bindung. Diese konnte durch Verwendung von $[Pd(MeCN)_2Cl_2]$ erreicht werden und der resultierende kationische Komplex der Form $[\{(dppm)_2BH\}PdCl]X$ ($X = Cl^-, Br^-$) wurde röntgenographisch untersucht.

Die quadratisch-planare Koordination deutet auf Palladium in der formalen Oxidationsstufe +II hin. Um eine Abgrenzung zu häufig beobachteten Z-Typ- und selteneren X-Typ-Liganden zu schaffen, wurde ein Vergleich mit entsprechenden literaturbekannten Komplexen durchgeführt.[137,138] Unter Zuhilfenahme quantenchemischer Methoden, wie der NBO- und QTAIM-Analysen, konnte weiter gezeigt werden, dass sich der Pinzetten-Ligand in dem synthetisierten Komplex klar von den bereits bekannten unterscheidet. Eine Klassifizierung als Elektronenpaar-donierender L-Typ-Ligand ist somit gerechtfertigt und komplettiert die Reihe der synthesechemisch zugänglichen Ligandenklassen nach der *covalent bond classification* von Bor-basierten Pinzetten-Liganden in Palladiumkomplexen.

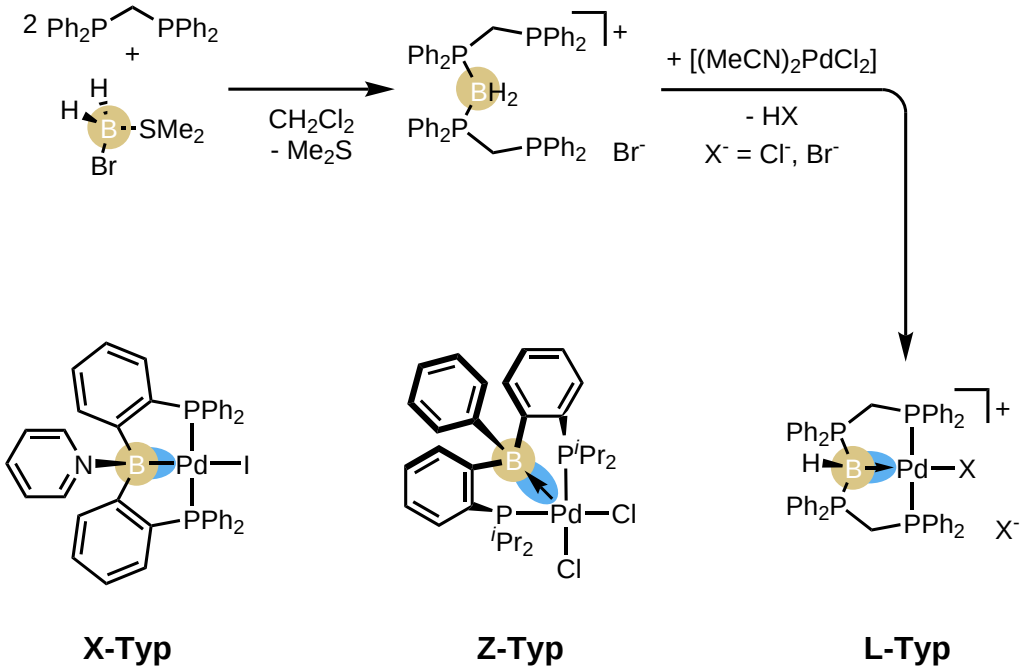

Schema 6: Synthese des Bis(phosphino)boroniumsalzes und anschließende Umsetzung zum Palladiumkomplex, indem die L_2BH-Einheit, im Vergleich mit bekannten X- und Z-Typ-Liganden, L-Typ-Ligandeneigenschaften zeigt.[137,138]

Eigener Anteil

Die erstmalige Synthese des Bis(phosphino)boroniumsalzes wurde von mir durchgeführt, ebenso wie die Analytik in Form von IR- und NMR-Spektroskopie und den massenpektrometrischen Untersuchungen. Außerdem erfolgte die Strukturaufklärung *via* Einkristallröntgenstrukturanalyse durch mich. Die weiteren synthesechemischen Arbeiten wurden mit meiner Unterstützung von Maik Grätz, Andreas Bäcker und Arian Reincke im Zuge ihrer jeweiligen Diplom-, Master- oder Vertiefungsarbeit vorgenommen. Zusammen mit Lisa Vondung wurden die DFT-Rechnungen im Bereich der bereits literaturbekannten, zum Vergleich herangezogenen Palladiumkomplexe ausgeführt und ausgewertet. Die Projektidee kam von Robert Langer, der dieses Projekt auch koordinierte.

3.2 Carbodiphosphorane-based nickel pincer complexes and their (de)protonated analogues: dimerisation, ligand tautomers and proton affinities

Leon Maser, Jan Herritsch, Robert Langer, *Dalton Transactions* **2018**, *47*(31), 10544-10552.

Beschreibung und Inhalt

Die Reaktivität von Carbodiphosphoran-basierten Donorgruppen in Pinzetten-Liganden war bislang weitgehend unbekannt. Es handelt sich jedoch um ein wichtiges, zu Amin- (R_2NH) und Bor-basierten Donorgruppen des Typs L_2BH formal isoelektronisches Analogon. Der Nickel-Komplex des Carbodiphosphoran-basierten PCP-Pinzetten-Liganden [{(dppm)$_2$C}NiCl]Cl wurde für die Untersuchung der Reaktivität im Bezug auf Säuren und Basen sowie das bessere Verständnis der Bindungssituation herangezogen.
Bei Umsetzung von [{(dppm)$_2$C}NiCl]Cl mit einem Äquivalent Tetrafluoroborsäure zeigt sich, dass die Protonierung am Carbodiphosphoran-Kohlenstoff erfolgt (Schema 7).

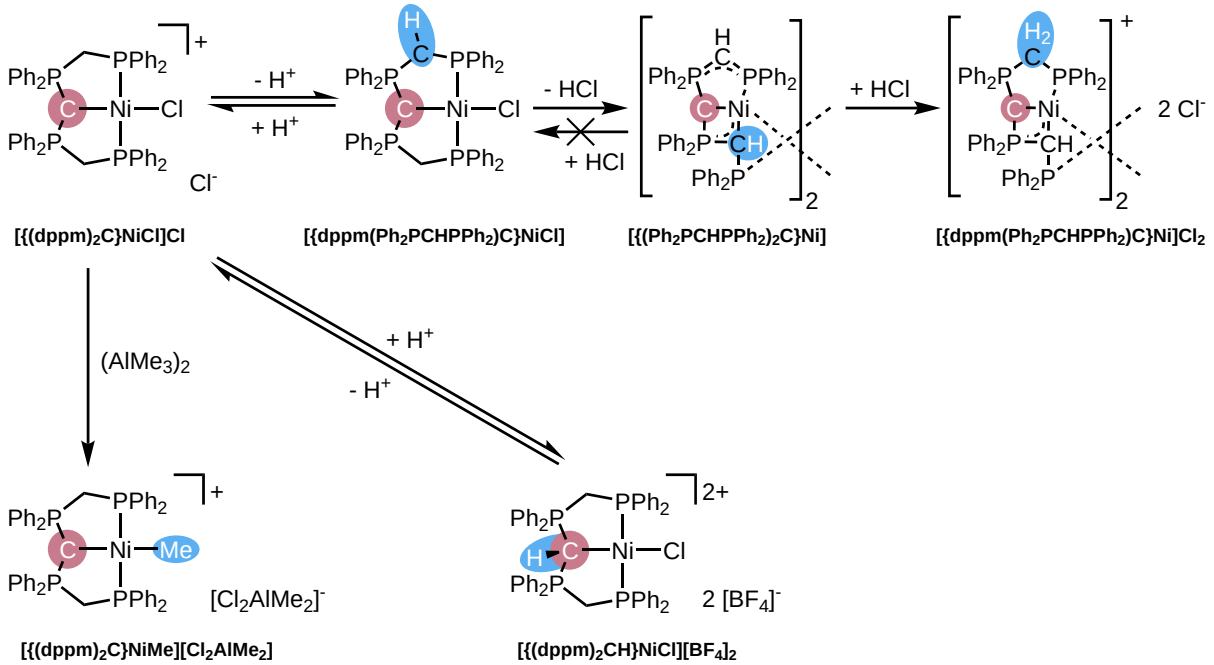

Schema 7: (De)protonierungsreaktionen von [{(dppm)$_2$C}NiCl]Cl und Reaktivität gegenüber $(AlMe_3)_2$.

Der dikationische Komplex $[\{(dppm)_2CH\}NiCl]^{2+}$ konnte mit Tetrafluoroborat $[BF_4]^-$ als schwach koordinierendem Anion isoliert werden.
Die Deprotonierungsversuche ausgehend von [{(dppm)$_2$C}NiCl]Cl erfolgten anfangs mit Methyllithium. Hierbei zeigte sich, dass die Deprotonierung einer der CH_2-Gruppen in Konkurrenz mit der Substitution des Chlorido-Liganden am Nickel-Atom steht. Durch die Wahl einer geeigneten, nicht-nukleophilen Base wie Lithiumbis(trimethylsilyl)amid kann die quantitative

Deprotonierung erreicht und der Komplex [{dppm($Ph_2PCHPPh_2$)}C)NiCl] isoliert werden. Der Ligandenaustausch von Chlorido- gegen Methyl-Liganden ist hingegen durch Trimethylaluminium zu bewerkstelligen und ein Komplex der Zusammensetzung [($dppm_2CH$)NiMe][Me_2AlCl_2] wird erhalten.
Der deprotonierte, neutrale Komplex [{dppm($Ph_2PCHPPh_2$)C}NiCl] zeigt bei weiterer Umsetzung mit Base interessante Folgechemie. So wird nicht einfach, wie erwartet, auch die zweite CH_2-Brücke im Rückgrat deprotoniert, sondern es erfolgt im gleichen Zuge eine Dimerisierung durch Koordination einer CH-Einheit, die einen Phosphin-Liganden verdrängt. Dieses Phosphin koordiniert nun an ein zweites Nickel-Atom und führt so zu einer Verbrückung zweier Komplexe unter Eliminierung des Chlorido-Liganden als Lithiumchlorid. Das erhaltene Dimer [($Ph_2PCHPPh_2$)$_2$C)Ni]$_2$ reagiert jedoch bei Zugabe eines Äquivalents HCl nicht wieder zu [{dppm($Ph_2PCHPPh_2$)C}NiCl]. Stattdessen bleibt die dimere Struktur erhalten und [{dppm($Ph_2PCHPPh_2$)C}Ni]$_2$$Cl_2$ entsteht. Die Struktur entspricht einem dikationischen Dimer, in dem die nicht koordinierenden CH-Einheiten zu CH_2 reprotoniert wurden.

Quantenchemische Untersuchungen an Modellkomplexen zeigen, dass die π-Donoreigenschaften des CDPs in dem untersuchten System nicht zum Tragen kommen. Sowohl im Falle von [($dmpm_2$C)NiCl]$^+$ als auch dem deprotonierten [{dmpm($Me_2PCHPMe_2$)C}NiCl] handelt es sich bei dem HOMO um eine doppelte π-antibindende Darstellung zwischen CDP-Kohlenstoff, Nickel-Atom und Chlorido-Liganden. Durch die Protonierung des CDP-Kohlenstoffatoms in [({dmpm}$_2$CH)NiCl]$^+$ entfällt deren π-antibindende Wechselwirkung zum Nickel-Atom.
Die Beobachtung, dass die Interaktion zwischen CDP-Kohlenstoff und zentralem Nickel-Atom weder durch Protonierung noch durch Deprotonierung einer oder beider der CH_2-Brücken wesentlich beeinflusst wird, spiegelt sich auch in der QTAIM-Analyse und den Partialladungen der *natural population analysis* wider. Ein Vergleich der Gibbs-Enthalpien des freien Liganden in verschiedenen Protonierungszuständen sowie monomerer und dimerer Modellverbindungen zeigt, dass die gebundenen Liganden nicht in deren thermodynamisch günstigsten Zuständen vorliegen. Zudem liegt die dimere Modellverbindung [{dmpm($Me_2PCHPMe_2$)C}Ni]$_2$$Cl_2$ um 15 kJ·mol^{-1} niedriger als das monomere Isomer [{dmpm($Me_2PCHPMe_2$)C}NiCl], wodurch die experimentell beobachtete höhere Stabilität der Verbindung [{dppm($Ph_2PCHPPh_2$)C}Ni]$_2$$Cl_2$ gegenüber Luft im Vergleich zum monomeren Komplex [{dppm($Ph_2PCHPPh_2$)C}NiCl] zu erklären ist.
Um die beobachtete Reaktivität von [{($dppm)_2$C}NiCl]Cl zu [{($dppm)_2$CH}NiCl][BF_4]$_2$ und umgekehrt besser in Relation zu den eingangs erwähnten Amin- und Borylen-basierten Donorgruppen zu vergleichen, wurde die Protonenaffinität (PA) grundsätzlich experimentell zugänglicher Modellverbindungen quantenchemisch bestimmt (Abb. 20).

Der erhaltene Wert von 1108 kJ·mol^{-1} für den Amid-basierten Komplex liegt deutlich über dem für den Carbodiphosphoran-basierten Komplex mit 807 kJ·mol^{-1}. Dies macht den Carbodiphosphoran-basierten Liganden als potentiell kooperativen Liganden interessant. Katalyti-

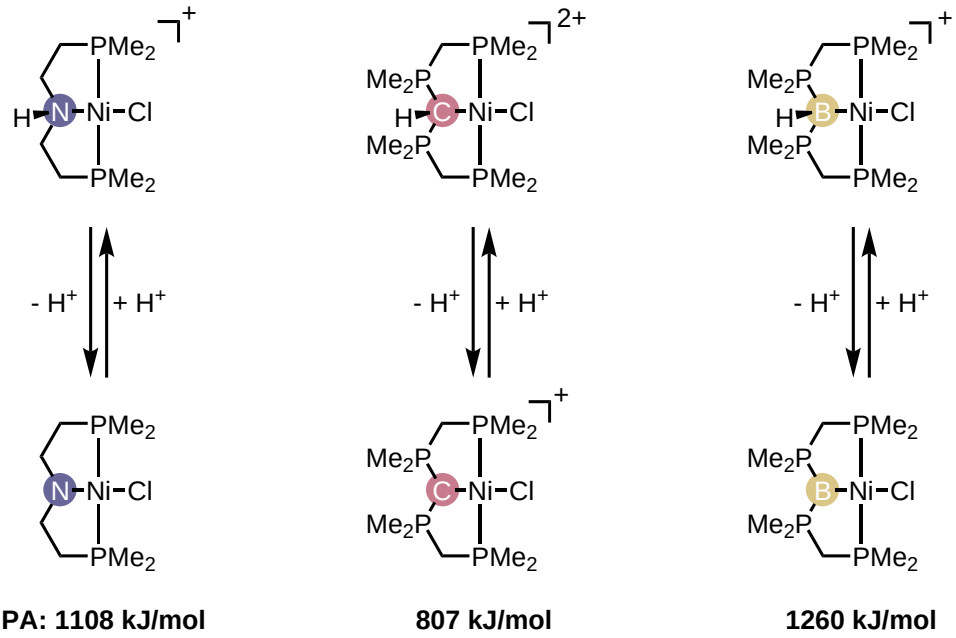

Abbildung 20: Protonenaffinitäten formal isoelektronischer Donorgruppen in Nickel-Pinzetten-Komplexen (G09, B97D/def2TZVPP).

sche Reaktionen, die ein sogenanntes *proton shuttle* benötigen, könnten durch eine Donorgruppe mit niedriger Basizität beschleunigt werden. Die PA des Bor-basierten Donors zeigt mit 1260 kJ·mol^{-1}, dass $([R_3P)_2B]^-$ im Vergleich zu $[R_2N]^-$ und $(R_3P)_2C$ im Modellkomplex eine stärkere Base darstellt. Im weiteren Vergleich mittels QTAIM lässt sich erkennen, dass der Laplace der Elektronendichte im Bereich der Donor-Wasserstoff-Bindung nicht mit den berechneten PAs korreliert. Es wird jedoch deutlich, dass die Phosphor-Bor-Interaktionen gut als dative Bindungen, ausgehend von den Phosphor-Atomen, beschrieben werden können.

Eigener Anteil

Die experimentellen Arbeiten zur Methylierung des Startkomplexes $[\{(dppm)_2C\}NiCl]Cl$ zu $[\{(dppm)_2CH\}NiMe][Me_2AlCl_2]$ wurden von Jan Herritsch im Zuge eines von mir betreuten Vertiefungspraktikums durchgeführt, inklusive der Analytik mit Ausnahme der Röntgenkristallstrukturanalyse. Die quantenchemischen Berechnungen der Protonenaffinitäten für die verschiedenen Donorgruppen fanden ebenfalls im Zuge des Vertiefungspraktikums unter meiner Betreuung statt.

Die Diffraktionsexperimente an den Einkristallen der Komplexe $[\{(Ph_2PCHPPh_2)_2C\}Ni]_2$ und $[\{dppm(Ph_2PCHPPh_2)C\}Ni]_2Cl_2$ führte ich selbst durch, die Messungen der Einkristalle von $[\{(dppm)_2CH\}NiCl][BF_4]_2$, $[\{dppm(Ph_2PCHPPh_2)C\}NiCl]$ und $[\{(dppm)_2CH\}NiMe][Me_2AlCl_2]$ wurden von Robert Langer vorgenommen. Die Strukturlösung und -verfeinerung wurde von mir durchgeführt. Die analytischen Daten (IR- und NMR-Spektroskopie, Massenspektrometrie) wurden von mir gesammelt und interpretiert. Die weiteren quantenchemischen Untersu-

chungen wurden mit Robert Langer geplant und von mir durchgeführt. Die Ergebnisse wurden von mir ausgewertet.
Die Planung und Koordination des Projektes erfolgte in Zusammenarbeit mit Robert Langer, ebenso wie das Verfassen des Manuskriptes.

3.3 The ABC in pincer chemistry – From Amine- to Borylene- and Carbon-based pincer-ligands

Leon Maser, Lisa Vondung, Robert Langer, *Polyhedron* **2018**, *143*, 28–42.

Beschreibung und Inhalt

Dieser Übersichtsartikel dient dem Vergleich von Pinzetten-Liganden, in denen ein Stickstoff-, Kohlenstoff- oder Bor-Atom als zentraler Donor Verwendung findet. Im Speziellen werden formal isoelektronische Alkyl- ($[R_2CH]^-$), Amin- (R_2NH), ligandenstabilisierte Borylen- (L_2BH) und protonierte Carbodiphosphoran-basierte ($[L_2CH]^+$) Donorgruppen im Hinblick auf die gezeigten Reaktivitäten betrachtet (Abb. 21).

Während sekundäre Amine in Pinzetten-Liganden breite Anwendung finden, können durch Inkorporation als zentraler Donor auch hoch reaktive Gruppen stabilisiert werden. Die Reaktivitäten von Alkyl- und Amin-basierten Pinzetten-Komplexen sind vergleichsweise gut untersucht, die der formal isoelektronischen Borylen- und protonierten CDP-basierten Komplexe jedoch noch nicht.

Bei den Amin-basierten Ligandengerüsten liegt das Stickstoff-Atom meist in einer trigonal-pyramidalen oder pseudo-tetraedrischen Geometrie vor. Es handelt sich um reine σ-Donoren mit mittlerer Ligandenfeldaufspaltung. Neben der Funktion als Ligand für ein zentrales Metallatom agiert das Stickstoff-Atom in katalytischen Reaktionen häufig als sogenanntes *proton relay* oder *proton shuttle*. Es wird also das am als Donor fungierendem Stickstoff-Atom anfangs gebundene Proton auf ein Substrat übertragen. Im Zuge des Katalysezyklus wird das Stickstoff-Atom z.B. durch heterolytische Diwasserstoffspaltung wieder protoniert. Diese Art der Katalyse wird im Allgemeinen als *cooperative* oder *bifunctional catalysis* bezeichnet, der Pinzetten-Ligand als *cooperative ligand*.

Alkyl-basierte Liganden zeigen verwandte Reaktionsmuster, sind allerdings weniger C–H-azide und zeigen dementsprechend eher α- oder β-Hydrideliminierungen als einen Protonenübertrag. Auch diese Reaktionen können reversibel sein und sind damit für katalytische Anwendungen interessant.
Den Amin-basierten Pinzetten-Komplexen sehr ähnliche Reaktivitäten zeigen die protonierten CDP-basierten Pinzetten-Liganden. Eine Deprotonierung des zentralen Kohlenstoffatoms erfolgt mit vergleichbar niedrigem Energieaufwand, die Azidität ist entsprechend höher als die vergleichbarer Amin-Pinzetten-Komplexe. Das freie Elektronenpaar, das durch die Deprotonierung formal am Kohlenstoff-Atom entsteht, kann entweder über die P–C–P-Bindung im Rückgrat delokalisiert werden oder als π-Donor zum zentralen Metallatom koordinieren. Die

niedrigere Protonenaffinität der Carbodiphosphoran-basierten Pinzetten-Komplexe macht diese potentiell zu interessanten *cooperative ligands* in der *cooperative catalysis*. Während die heterolytische Spaltung von Substraten ungünstiger verläuft, ist zu erwarten, dass der Übertrag von Protonen begünstigt ist.

Die Bor-basierten Liganden werden in drei verschiedenen Varianten diskutiert. So können Boryl- und Carboran-basierte Pinzetten-Liganden zum Beispiel in (De)hydrierungsreaktionen oder Suzuki-Kupplungen verwendet werden. Die hochreaktive Klasse der Borylene kann durch das Pinzettenliganden-Rückgrat mittels Basen stabilisiert werden und zeigt sehr starke σ-donierende Eigenschaften. Im Gegensatz zu den Amin- und protonierten CDP-Liganden scheint hier keine Deprotonierung möglich.

Zusammenfassend lässt sich erkennen, dass die durch L_2BH oder $[L_2CH]^+$ gebildeten zentralen Donorgruppen in Pinzetten-Liganden eine interessante Ergänzung zu den bereits gut untersuchten Amin-basierten Pinzetten-Komplexen bieten. Die Reaktivitäten unterscheiden sich in beiden Fällen deutlich von denen der Amine und eröffnen weitere Möglichkeiten in der Homogenkatalyse.

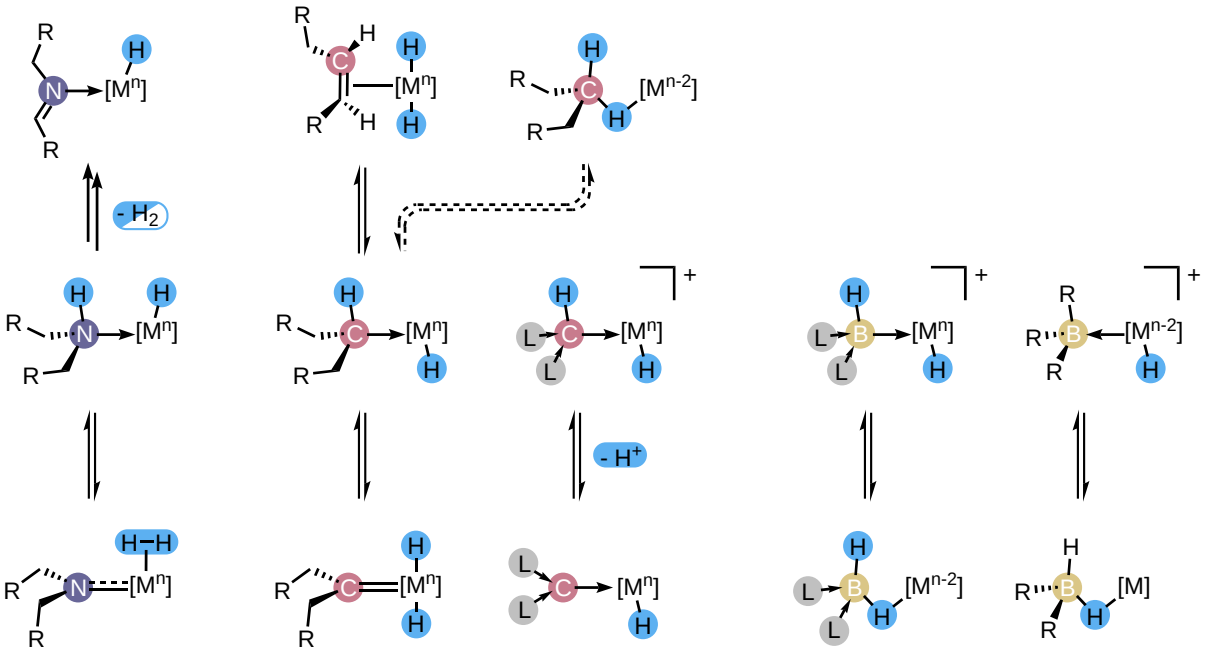

Abbildung 21: Von isoelektronischen Donorgruppen gezeigte Reaktionsmuster.

Eigener Anteil

Lisa Vondung verfasste den Teil des Übersichtsartikels, der sich mit Bor-basierten Donorgruppen beschäftigt, Robert Langer die Inhalte zu den Alkyl- und Amin-basierten Donorgruppen.

Die Beiträge zu den Carbodiphosphoran-basierten Donorgruppen wurden von mir beigesteuert. Die Einleitung, der Vergleich und die Zusammenfassung wurden von allen Autoren gemeinsam erarbeitet.

3.4 Quantifying the donor strength of ligand-stabilized main group fragments

Beschreibung und Inhalt

In dieser Publikation werden anhand strukturell sehr ähnlicher Iridium(+III)-Komplexe eine Reihe an Untersuchungen durchgeführt, die die starken Donoreigenschaften der Bor- ($(R_3P)_2BH$) und CDP-basierten ($(R_3P)_2C$, $[(R_3P)_2CH]^+$) Pinzetten-Liganden belegen, Ausblicke auf die höheren Homologen ebenjener ermöglichen und schlussendlich zu einem neuen Ligandenparameter führen.

Die Basis der Untersuchungen bilden experimentelle Ergebnisse zur Synthese von Iridium(+III)-Komplexen, die - bis auf die zentrale Donorgruppe des Pinzetten-Liganden - einen isostrukturellen Aufbau um das zentrale Iridium-Atom zeigen. Hierzu wird ein Iridium(+I)-Präkursor mit einem Vorläufermolekül der Pinzetten-Liganden, das mindestens ein Proton am zentralen Haftatom trägt, zur Reaktion gebracht (Abb. 22).

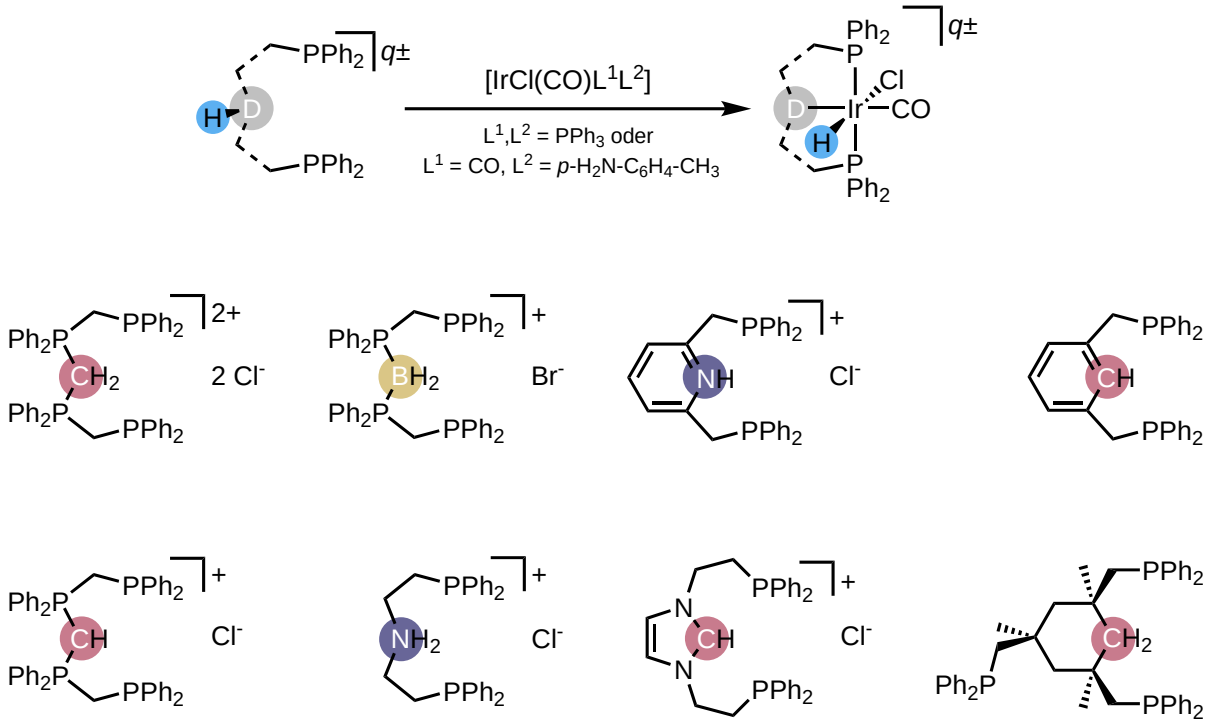

Abbildung 22: Oben: Oxidative Addition der Präkursoren zu Iridium(+III)-Komplexen. Unten: Übersicht der verwendeten Liganden-Vorläufermoleküle.

Die so erhaltenen Iridium(+III)-Komplexe weisen einen Carbonyl-Liganden in *trans*-Position zu der zu untersuchenden Donorgruppe auf. Durch IR-spektroskopische Messungen kann die Wellenzahl $\tilde{\nu}_{CO}$ der Streckschwingung der C–O-Bindung bestimmt werden, die durch stärkere π-Rückbindung geschwächt wird. Dies wiederum gibt Aufschluss über die Elektronendichte am Iridium, welche bei ansonsten gleichbleibender Koordination hauptsächlich durch den

trans-ständigen Donor beeinflusst wird. Die Streckschwingung kann also, ähnlich wie bei dem TEP als qualitatives Maß für die Donorstärke verwendet werden (Abb. 23). Die Wellenzahl der C–O-Streckschwingung lässt sich zusätzlich parallel *in silico* mit quantenmechanischen Methoden errechnen.

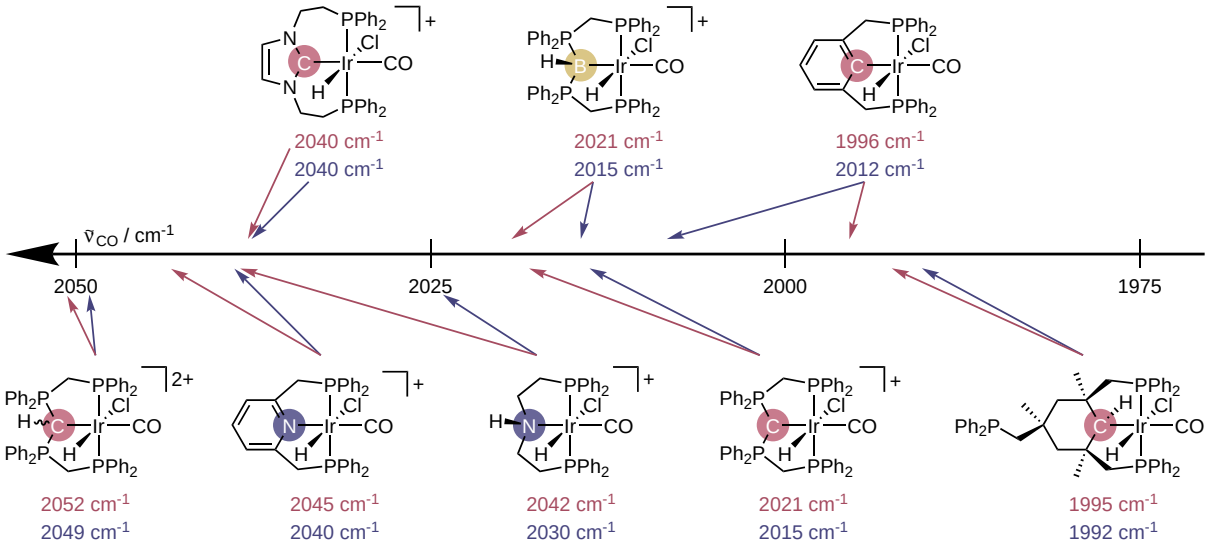

Abbildung 23: Übersicht über die experimentellen (blau) und berechneten (rot) $\tilde{\nu}_{CO}$ der synthetisierten Iridium-Komplexe.

Der Vergleich der Werte aus Theorie und Experiment zeigt eine gute Übereinstimmung. Motiviert hierdurch wurden die DFT-Berechnungen auf nicht experimentell dargestellte Iridium-Pinzetten-Komplexe mit bekannten zentralen Donorgruppen ausgeweitet. Dabei wurden auch die schwereren Homologen der dargestellten Pinzetten-Liganden mit $(R_3P)_2BH$-, $(R_3P)_2C$- und $[(R_3P)_2CH]^+$-Donorgruppen zusätzlich untersucht (Abb. 24).

Der Ligandenparameter zeigt, dass die schwereren Homologen ähnlich gute Liganden wie die leichtesten Vertreter der jeweiligen Gruppe sein sollten. Aus der Betrachtung der Molekülorbitale geht hervor, dass mit steigender Ordnungszahl eine Abnahme des Orbitalüberlapps zwischen Donoratom und Metallatom einhergeht, was mit der steigenden Wellenzahl der C–O-Streckschwingung übereinstimmt. Eine genaue Aussage zur Donorstärke ist aufgrund dessen schwer zu treffen. Die Ligandenvarianten, die kein Wasserstoffatom am zentralen Donor tragen, sind mit den schwersten Homologen nicht stabil und zeigen einen Bindungsbruch zwischen Donor- und Phosphoratom. Der Überblick über alle untersuchten Komplexe lässt vermuten, dass die Ladung des Liganden den größten Einfluss auf die Donorstärke nimmt. So sind kationische Liganden bei hohen Wellenzahlen (> 2050 cm^{-1}) einzuordnen, neutrale Liganden im Bereich von 2050 bis 2000 cm^{-1} und anionische Liganden ab ungefähr 2010 cm^{-1}. Um einen tieferen Einblick in die Bindungssituation zwischen den untersuchten Donorgruppen und dem Iridium-Atom zu erhalten, wurden Modellsysteme der Komplexe entwickelt, bei denen die zentrale Donorgruppe getrennt von den terminalen Phosphingruppen vorliegt. Die

resultierende, monodentate Koordination an das Iridium-Atom lässt sich so quantenchemisch *via* EDA untersuchen und in die einzelnen Beiträge aufteilen. Es lässt sich erkennen, dass es sich bei der Bor-basierten Donorgruppe $(R_3P)_2BH$ um den stärksten σ-Donor handelt, da der CDP-basierte Ligand noch einen kleinen π-Anteil in der Bindung zeigt. Die Summe der Wechselwirkungen, die in der EDA bestimmt wurden, die Interaktionsenergie E_{Int}, korreliert zudem sehr gut mit den berechneten und gemessenen $\tilde{\nu}_{CO}$ und legitimiert den neuen Ligandenparameter weiter.

Eigener Anteil

Die Carben-, Pyridin- und Aryl-basierten Iridium-Pinzettenkomplexe wurden von mir synthetisiert und analysiert, ebenso wie Reproduktionsansätze der CDP- und Bor-basierten Komplexe. Die analytischen Daten aus IR- und NMR-Spektroskopie, Massenspektrometrie und Elementaranalyse wurden von mir gesammelt, ausgewertet und interpretiert. Die Strukturlösung und -verfeinerung der Diffraktionsexperimente an Einkristallen wurde zum Teil von Robert Langer und zum Teil von mir durchgeführt. Die quantenchemischen Untersuchungen wurden in Zusammenarbeit mit Robert Langer geplant und von mir vorgenommen. Unterstützung erhielt ich von Lisa Vondung, die die EDA-Rechnungen ausführte. Robert Langer koordinierte das Projekt, die Planung einzelner Teile erfolgte in Absprache mit mir. Das Manuskript wurde in Kooperation mit Robert Langer verfasst.

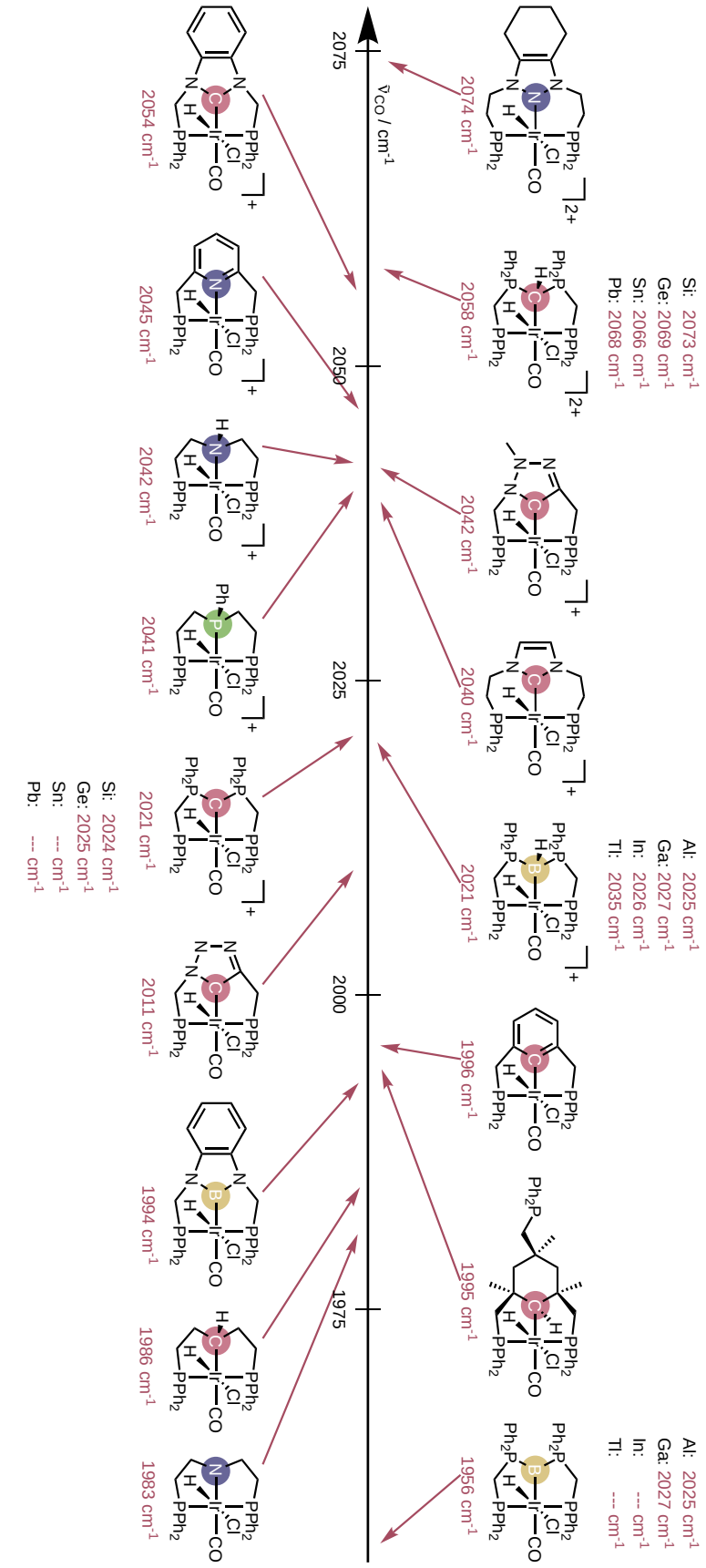

Abbildung 24: Übersicht über die berechneten $\tilde{\nu}_{CO}$ aller Iridium-Komplexe (G16, B97D/def2TZVPP).

3.5 Comparing the acidity of $(R_3P)_2BH$-based donor groups in iridium pincer complexes

Beschreibung und Inhalt

In diesem Artikel wird die Reaktivität von Iridium-Komplexen basierend auf Donorgruppen der Typen R_2NH, $(R_3P)_2BH$ und $[(R_3P)_2CH]^+$ gegenüber Basen direkt verglichen. Die Pinzetten-Komplexe der allgemeinen Formel $[(PEHP)IrCl(CO)H]^q$ (q = +1, +2) besitzen alle ein an das zentrale Donoratom E (N, B, C) gebundenes Wasserstoffatom. Hierdurch ergeben sich zwei primäre Reaktionswege gegenüber Basen. Zum einen die Deprotonierung des Donoratoms E, die zu einer Änderung der Ladung des Komplexes von Δq = -1 führt, und zum anderen die reduktive Eliminierung von HCl, durch die sich die Ladung des Komplexes nicht ändert, jedoch die Oxidationsstufe des zentralen Iridium-Atoms.

Der Amin-basierte Pinzetten-Komplex reagiert mit einem Äquivalent Base unter Verlust des hydridischen Wasserstoffatoms, wie durch ^{1}H NMR-Spektroskopie nachverfolgbar ist. Anhand der analytischen Daten kann davon ausgegangen werden, dass unter reduktiver Eliminierung von HCl ein symmetrischer Iridium(+I)-Komplex der Formel $[(\{Ph_2P(CH_2)_2\}_2NH)Ir(CO)]$ entsteht (Schema 8).

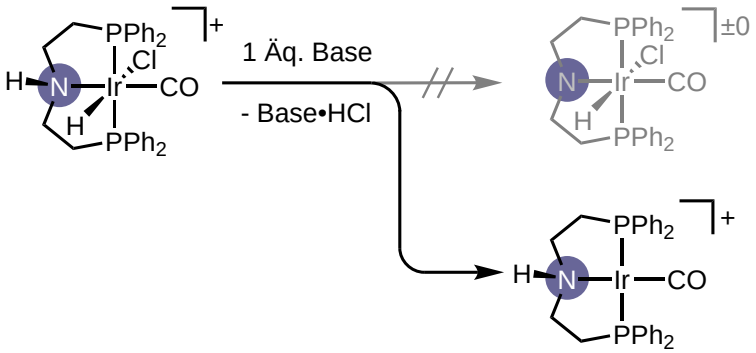

Schema 8: Reduktive Eliminierung (beobachtet) und Ligandendeprotonierung (nicht beobachtet) des Amin-basierten Iridium-Pinzetten-Komplexes [(PNHP)IrCl(CO)H]Cl.

Weitere Zugabe von Base führt zu einem Produktgemisch, welches nicht eindeutig identifiziert werden konnte.

Der auf protoniertem CDP $[(R_3P)_2CH]^+$ basierte Komplex $[\{(dppm)_2CH\}IrHCl(CO)]^{2+}$ liegt von Anfang an schon als Gemisch der *cis*- und *trans*-Isomere im Verhältnis von etwa 1:1 vor. Ein kleiner Teil (ca. 6 %) ist bereits ohne Base als deprotonierter Komplex $[\{(dppm)_2C\}IrHCl(CO)]^+$ zu beobachten. 2D-NMR-Experimente zeigen, dass sowohl ein dynamisches Gleichgewicht zwischen *trans*-$[\{(dppm)_2CH\}IrHCl(CO)]^{2+}$ und $[\{(dppm)_2C\}IrHCl(CO)]^+$ existiert, als auch ein Isomerisierungsprozess von *cis*- und *trans*-Komplex stattfindet. Da der deprotonierte Komplex nur in geringem Maße vorlag und sowohl durch Deprotonierung des *cis*- als auch des *trans*-Komplexes entstehen sollte, wurde die Reaktivität gegenüber Base mit dem Gemisch bestimmt. Im Gegensatz zu dem Amin-basierten Komplex findet hier eine Deprotonierung im Liganden-

rückgrat statt und nur [{(dppm)$_2$C}IrHCl(CO)]Cl verbleibt (Schema 9).

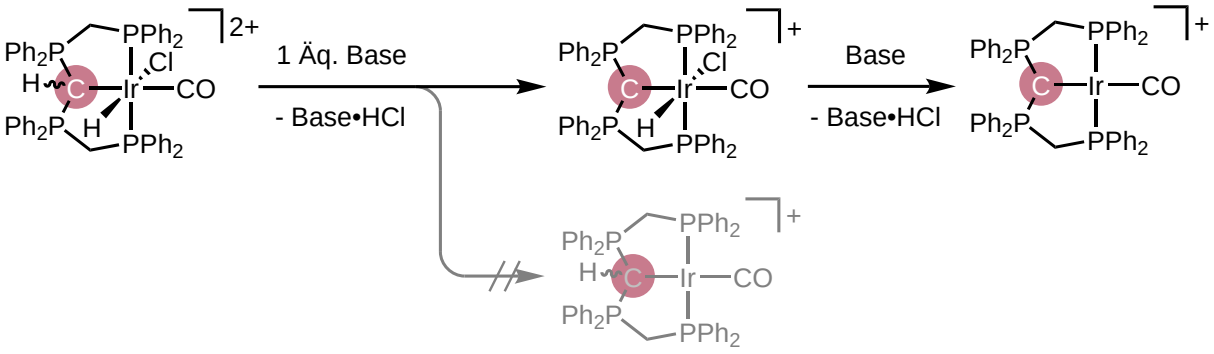

Schema 9: Beobachtete Deprotonierung des Ligandenrückgrates und anschließende reduktive Eliminierung sowie direkte reduktive Eliminierung von HCl des Komplexes [{(dppm)$_2$CH}IrHCl(CO)]Cl$_2$.

Weitere Zugabe eines Überschusses an 1,8-Diazabicyclo[5.4.0]undec-7-en als Base führt zu einer reduktiven Eliminierung von HCl, wie NMR-spektroskopisch und massenspektrometrisch zu beobachten war.
Im Falle von [{(dppm)$_2$BH}IrHCl(CO)]$^+$ mit (R$_3$P)$_2$BH als zentraler Donoreinheit zeigt sich eine analoge Reaktivität, wie bereits bei dem Amin-basierten Komplex beobachtet (Schema 10).

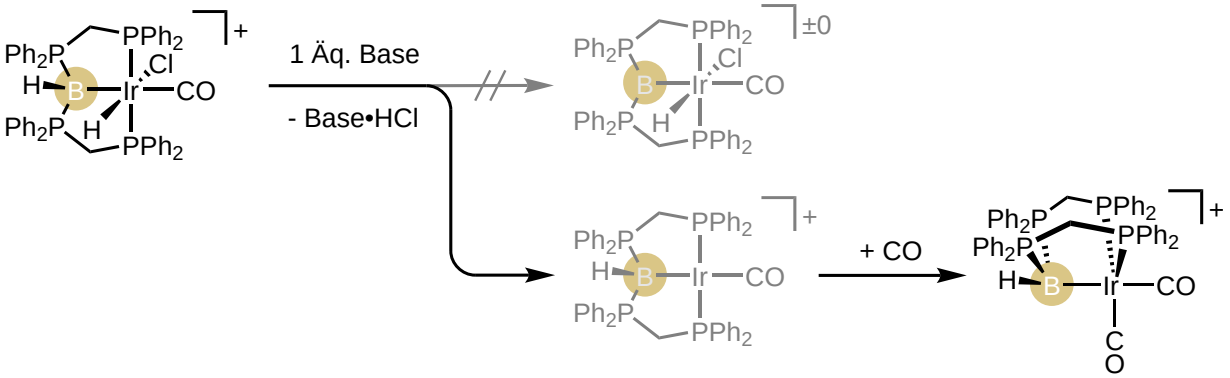

Schema 10: Reaktion von [{(dppm)$_2$BH}IrHCl(CO)]$^+$ unter Bildung eines trigonal-pyramidal koordinierten Iridium(+I)-Komplexes.

Das ^{1}H NMR-Spektrum zeigt nach der Reaktion kein Hydrid-Signal mehr und das ^{1}H{^{11}B} NMR-Spektrum bestätigt, dass weiterhin ein Wasserstoffatom am Bor-Atom gebunden bleibt. Nach Aufreinigung konnte ein für die Röntgenstrukturanalyse geeigneter Einkristall erhalten werden, der im Gegensatz zu den im Vorangehenden erhaltenen Produkten der reduktiven Eliminierung eine trigonal-bipyramidale Struktur aufweist. Es können zwei Carbonylliganden identifiziert werden, was im Einklang mit den Ergebnissen der IR-spektroskopischen Untersuchungen steht. Im Vergleich zu literaturbekannten Iridium(+I)-Komplexen trigonal-bipyramidaler Koordination mit zwei *cis*-ständigen Carbonylliganden ist die Wellenzahl der C–O-Streckschwingungen relativ niedrig, was wieder als Indikator für die starke Donorstärke des ligandenstabilisierten Borylens gesehen werden kann.

Mit Hilfe von DFT-Rechnungen wurden, ausgehend von den protonierten Komplexen, die Protonenaffinitäten (PA) für die entweder am zentralen Donoratom oder am Iridium-Atom deprotonierten Komplexe bestimmt. Die Ergebnisse spiegeln die beobachteten Reaktivitäten wider, von CDP- über Amin- zu Bor-basiertem Donor nehmen die berechneten PA beider Pfade zu und es findet ein Wechsel der präferierten Reaktivität statt. Die PA des am Kohlenstoff-Atom deprotonierten CDP-basierten Komplexes (PA = 864 $kJ \cdot mol^{-1}$) liegt um 36 $kJ \cdot mol^{-1}$ niedriger als die des am Iridium-Atom deprotonierten (PA = 900 $kJ \cdot mol^{-1}$). Die Stickstoff-basierten Komplexe liegen energetisch sehr ähnlich (PA [(PN^HP)IrCl(CO)] = 1129 $kJ \cdot mol^{-1}$, PA [(PNP)IrCl(CO)H] = 1126 $kJ \cdot mol^{-1}$) und könnten damit prinzipiell beide entstehen. Die experimentell beobachtete, quantitativ erfolgende reduktive Eliminierung muss also aus anderen Gründen, wie z.B. einer kinetischen Bevorzugung, stattfinden. Die größte Differenz und PA zeigen die Bor-basierten Komplexe (PA [(PB^HP)IrCl(CO)] = 1175 $kJ \cdot mol^{-1}$, PA [(PBP)IrCl(CO)H] = 1257 $kJ \cdot mol^{-1}$). Zum einen spiegelt das die beobachtete Reaktivität wider, zum anderen verdeutlicht es die hohe Basizität des Bor-Atoms, die Einfluss auf die Donorstärke des Liganden nimmt.

Eigener Anteil

Im Zuge dieses Projekts überprüfte ich in Reproduktionsexperimenten vorläufige Ergebnisse von Lukas Alig und Christian Schneider aus deren Masterarbeiten und vervollständigte die Analytik mit IR- und NMR-Spektren sowie massenspektrometrischen Untersuchungen. Die quantenchemischen Analysen sind nach Absprache mit Robert Langer von mir geplant und durchgeführt worden, das Manuskript wurde in Zusammenarbeit verfasst.

4 Zusammenfassung

In dieser Arbeit sollten auf Bor oder Kohlenstoff basierende Donorgruppen in den Formen $(R_3P)_2BH$, $(R_3P)_2C$ und $[(R_3P)_2CH]^+$ untersucht werden. Mit Hilfe von stabilisierenden Pinzetten-Liganden waren Übergangsmetallkomplexe dieser Gruppen zu isolieren. Ein tieferer Einblick in die Bindungssituationen der Donorgruppen mit Schwerpunkt auf der Donor-Metall-Interaktion sollte erarbeitet werden. Im Anschluss waren die allgemeinen Reaktionsmuster der Übergangsmetallkomplexe, besonders im Hinblick auf (De)protonierungsreaktionen, zu ermitteln und zu erklären. Ein besonderes Augenmerk war auf die Parallelen mit Amin-basierten Pinzetten-Liganden und deren Komplexe zu legen.

Ein zu dem bereits bekannten CDP-basierten Pinzetten-Liganden quasi isostruktureller Ligandenpräkursor mit zentraler $(R_3P)_2BH$-Einheit konnte über die Reaktion eines Borans mit zwei Äquivalenten dppm erreicht werden. Ausgehend von diesem Boroniumsalz wurde ein Pinzetten-Komplex mit einem Palladium-Atom als Zentrum dargestellt. Durch Vergleich struktureller, spektroskopischer und quantenchemischer Daten mit als X- und Z-Typ identifizierten, Bor-basierten Liganden konnte eine Zuordnung der Gruppe $(R_3P)_2BH$ als L-Typ-Donoreinheit sichergestellt werden.
Beginnend mit dem literaturbekannten CDP-basierten Nickel-Pinzetten-Komplex wurden die Reaktivitäten gegenüber Säuren und Basen im Detail untersucht. Durch Base erfolgte erst eine Deprotonierung einer CH_2-Brücke des Rückgrats, bei weiterer Zugabe von Base fand jedoch eine Dimerisierung statt, die nicht direkt reversibel war. Die Stabilität der isolierten Komplexe wurde anhand quantenmechanischer Modellkomplexe aufgeklärt. Wurde der Startkomplex aber mit einer Säure mit schwach koordinierendem Anion versetzt, ließ sich eine Protonierung des CDP-Kohlenstoffatoms erreichen. Röntgenbeugungsdaten der erhaltenen monomeren Komplexe zeigten nur kleine Unterschiede der Bindungslänge des CDP-Kohlenstoffatoms zum zentralen Nickel-Atom. Durch DFT-Rechnungen und QTAIM-Analyse ließ sich zeigen, dass die Eigenschaft der CDPs, auch als π-Donor zu fungieren, hier vernachlässigbar war. Die berechnete Protonenaffinität des CDP-basierten Modellkomplexes war im Vergleich zum Amid-Modellkomplex deutlich niedriger und deutete eine gute Eignung als Ligand in der kooperativen Katalyse an.

Durch Übertragen der Ligandensysteme auf einen Iridium(+III)-basierten Komplex gelang es, die Liganden in einer vergleichbaren Umgebung zu untersuchen (Schema 11). Umsetzungen mit Base zeigten, dass sich von protonierten CDP-Donoren einfach wieder ein Proton entfernen lässt, wohingegen im Falle von Aminen und $(R_3P)_2BH$ als Donor-Gruppen die reduktive Eliminierung am Metallzentrum vorrangig stattfindet. Die Reaktivitäten wurden auch in den berechneten Protonenaffinitäten widergespiegelt und bestätigten die an Nickel-Modellsystemen vorangegangenen Untersuchungen.

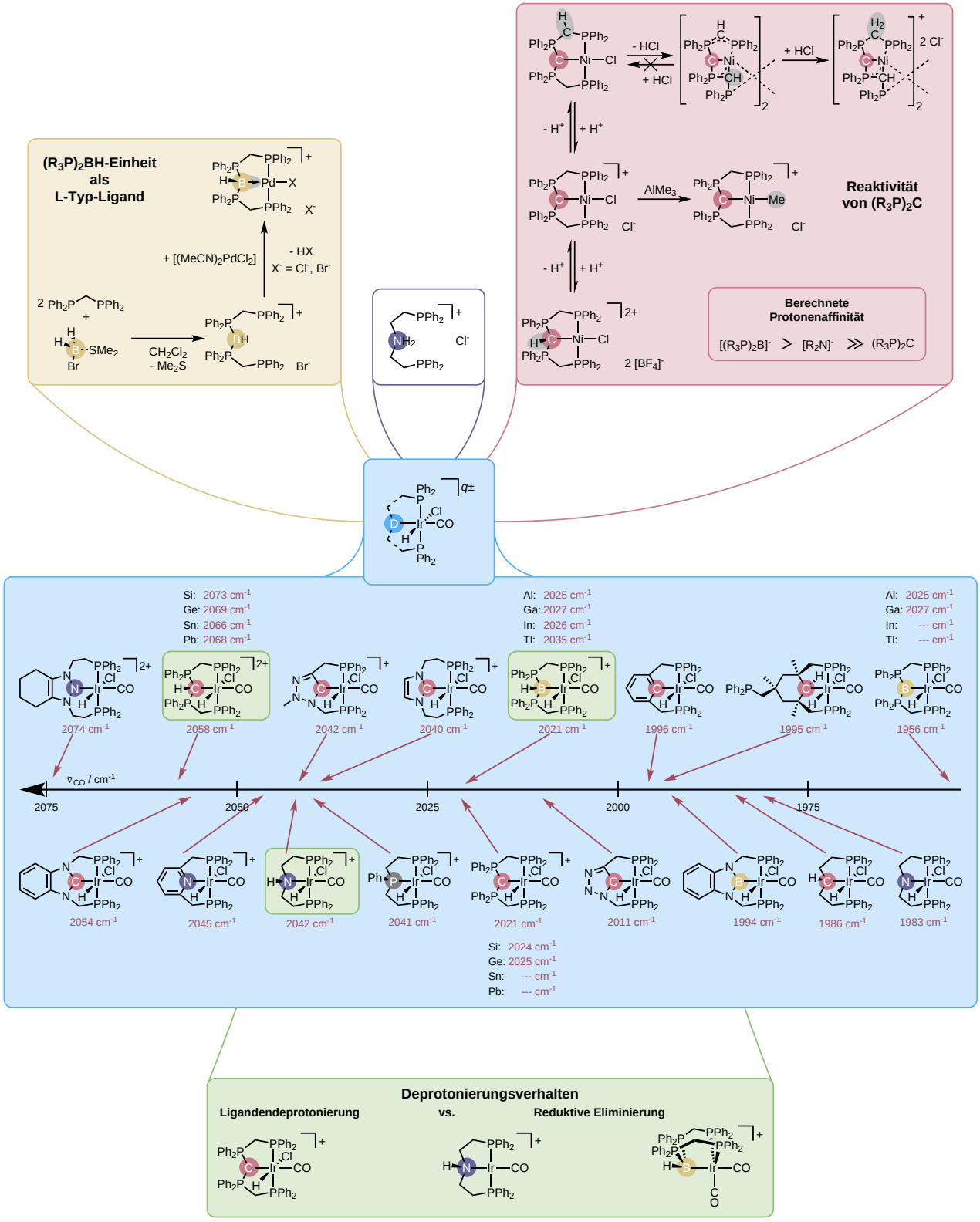

Schema 11: Zusammenfassung und Zusammenhänge der im Rahmen dieser Arbeit durchgeführten Untersuchungen.

Die verwendete Synthese der Iridium-Komplexe zeigte sich als vielseitig einsetzbar und ermöglichte es, die Donorstärken weiterer Gruppen mit in die Vergleiche einzubeziehen. Während sich Donoren der Form $[(R_3P)_2CH]^+$ als relativ schwach erwiesen, ist insbesondere der Donor basierend auf $(R_3P)_2BH$ als außergewöhnlich stark für einen neutralen Donor einzuordnen. Die CDP-basierte Donoreinheit zeigte absolut eine dazu nahezu identische Donorstärke. Nach weiteren Untersuchungen mittels EDA war aber aufgrund eines geringen π-Bindungsanteils die Donorstärke zu relativieren und der Bor-basierte Ligand als stärkster neutraler, reiner σ-Donor der isolierten Komplexe anzusehen.
Da sich die Korrelation zwischen den experimentell ermittelten und berechneten Frequenzen der C–O-Streckschwingung als sehr gut erwies, konnte eine Erweiterung der untersuchten Donorgruppen durch rein quantenchemisch untersuchte Komplexe durchgeführt werden. So war es möglich, die Donorstärke der deprotonierten Variante des Bor-basierten Donors, $[(R_3P)_2B]^-$ zu bestimmen, die schweren Homologen der $(R_2P)_2C$-, $[(R_3P)_2CH]^+$-, $(R_3P)_2BH$- und $[(R_3P)_2B]^-$-basierten Donorgruppen zu untersuchen und die beobachteten Trends zu bestätigen.

Zusammenfassend ist in dieser Arbeit ein experimenteller Vergleich der Reaktivitäten formal isoelektronischer Donorgruppen durchgeführt und mit quantenchemischen Analysen untermauert worden. Es konnte ein neuer Ligandenparameter vorgestellt werden, der erstmals den direkten Vergleich von zentralen Donorgruppen in einem Pinzetten-Liganden-Gerüst mit anionischer, neutraler oder kationischer Ladung ermöglicht.

5 Summary

In this work, donor groups based on boron or carbon in the form of $(R_3P)_2BH$, $(R_3P)_2C$ and $[(R_3P)_2CH]^+$ were to be investigated. In transition metal complexes that were to be isolated with the donor groups of interest stabilized in pincer ligands, insight in the bonding situation of the different donor groups with emphasis on the donor-metal interactions was to be gained. The general reaction behaviour, especially in (de)protonation reactions, was to be determined and explained. Special attention was to be paid to the parallels towards amine-based ligands and pincer complexes.

A virtually isostructural analogue of the CDP-based pincer ligand precursor was synthesized with a central $(R_3P)_2BH$-group by reaction of a borane with two equivalents of dppm. Starting with this boronium salt, a palladium-based pincer complex was isolated. By comparing structural, spectroscopic, and quantum chemical data with boron-based ligands identified as X- and Z-type, an assignment of the $(R_3P)_2BH$-group as an L-type donor was secured.
Starting with the CDP-based nickel pincer complex from literature, the reactivities towards acids and bases were investigated in detail. Through base, first the deprotonation of one CH_2-group in the backbone takes place, followed upon further addition of base by a not directly reversible dimerization process. The stability of the isolated complexes is clarified by quantum chemical means with the help of model complexes. If the starting compound is reacted with an acid containing a weakly coordinating anion instead, the protonation of the CDP-carbon atom can be achieved. X-ray data of the different isolated monomeric complexes only show minute differences in the bond lengths of the CDP-carbon atom to the nickel atom. By DFT calculations and QTAIM analysis, it can be demonstrated that the ability of the $(R_3P)_2C$-group to also act as π-donor is negligible in the present case. The calculated proton affinity of the CDP-based model complex is, in comparison to the amide-based model complex, notedly lower and hints at a good suitability for cooperative catalysis.

By transferring the ligand systems to an iridium(+III)-based scaffold, it was possible to investigate the ligands in a comparable environment (scheme 12). Reactions with base show that protonated CDP-based $[(R_3P)_2CH]^+$ donor groups are readily deprotonated, whereas amines and boron-based $(R_3P)BH$-groups as donors primarily lead to reductive elimination on the metal centre. The reactivities are reflected by calculated proton affinities and confirm the preceding investigations with the nickel model systems.

The employed synthesis of the iridium complexes proved to be versatile and enabled the addition of further pincer ligands for donor strength comparison. While donors based on the $[(R_3P)_2CH]^+$-group were shown to be relatively weak, particularly the donor group based on $(R_3P)_2BH$ is exceptionally strong for a neutral ligand. The CDP-based donor group is shown to be almost identical in donor ability. After further investigations by EDA, the donor strength in regards to the σ-contribution is lower due to partial π-interaction and thus, the ligand based

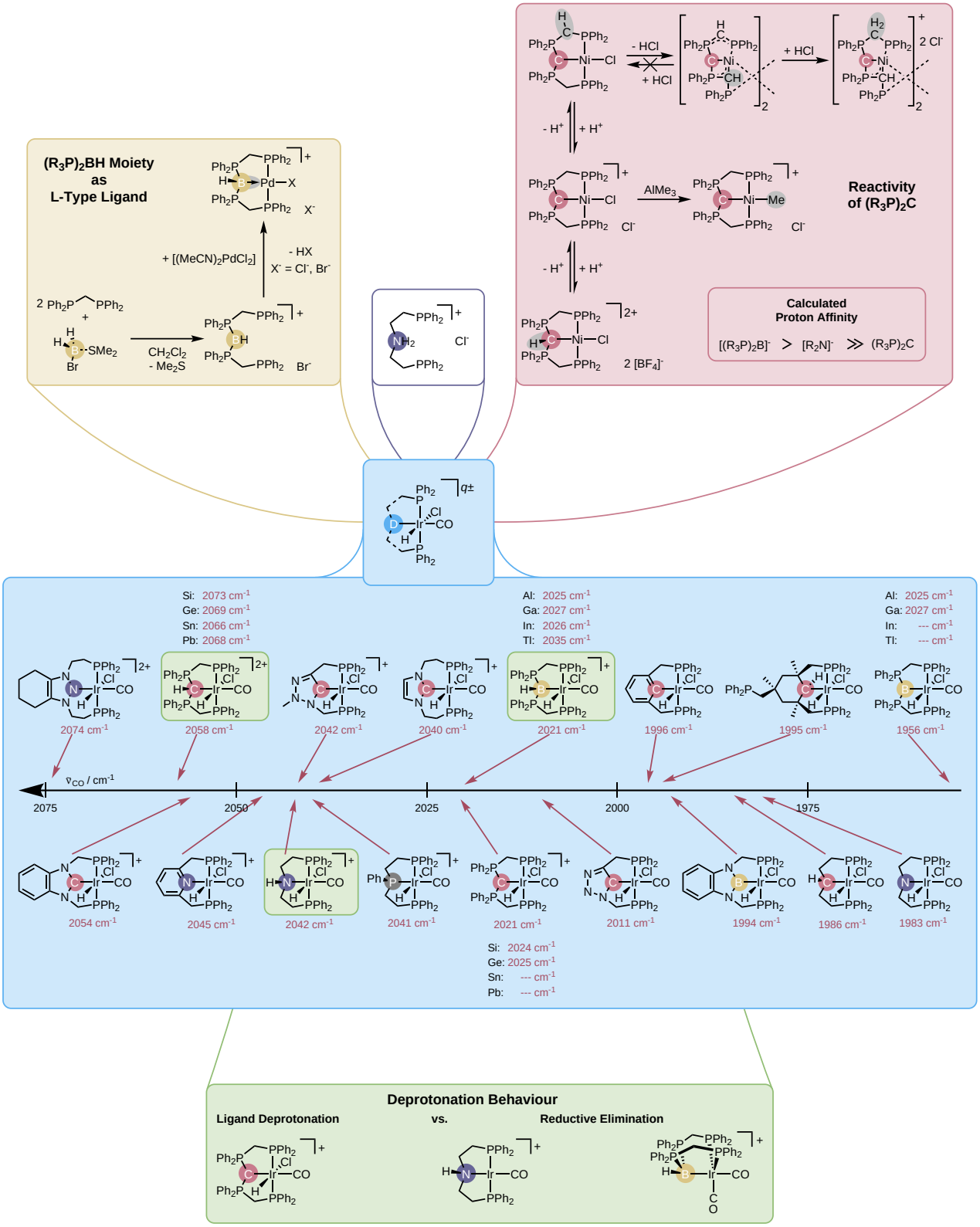

Scheme 12: Summary and connections of the investigations conducted over the time of this thesis.

on boron is to be regarded as the strongest neutral, solely σ-donating donor of all isolated complexes.
Owing to the very good correlation of calculated and experimentally measured C–O-stretching frequencies, donor groups solely investigated by quantum chemical methods were added to the comparison. Thus it was possible to determine the donor strength of the boron-based ligands deprotonated analogue, the $[(R_2P)_2B]^-$ moiety as well as the heavy homologues of the $(R_2P)_2C$, $[(R_3P)_2CH]^+$, $(R_3P)_2BH$ and $[(R_3P)_2B]^-$ donors and further confirm the observed trends.

Summing up, in this dissertation, an experimental comparison of the reactivities of formally isoelectronic donor groups was carried out and fortified by quantum chemical analyses. Additionally, a new ligand parameter, allowing the direct comparison of the central donor groups in pincer ligand scaffolds with anionic, neutral, and cationic charges, is presented.

Literaturverzeichnis

[1] A. Werner, *Z. anorg. allg. Chem.* **1893**, *3*, 267–330.

[2] G. Schmid, *Angew. Chem. Int. Ed.* **1970**, *9*, 819–830.

[3] G. H. Neild, *Nephrol. Dial. Transplant.* **1996**, *11*, 1885–1889.

[4] P. Schützenberger, *Ann. Chim. Phys.* **1868**, *15*, 100–106.

[5] L. Mond, C. Langer, F. Quincke, *J. Chem. Soc. Trans.* **1890**, *57*, 749–753.

[6] F. Aubke, C. Wang, *Coord. Chem. Rev.* **1994**, *137*, 483–524.

[7] F. Calderazzo in *Encycl. Inorg. Bioinorg. Chem.* John Wiley & Sons, Ltd, Chichester, UK, **2011**.

[8] M. Zhou, L. Andrews, C. W. Bauschlicher, *Chem. Rev.* **2001**, *101*, 1931–1961.

[9] L. Weber, *Angew. Chem. Int. Ed.* **1994**, *33*, 1077–1078.

[10] X. Xing, J. Wang, H. Xie, Z. Liu, Z. Qin, L. Zhao, Z. Tang, *Rapid Commun. Mass Spectrom.* **2013**, *27*, 1403–1409.

[11] A. D. Brathwaite, J. A. Maner, M. A. Duncan, *Inorg. Chem.* **2014**, *53*, 1166–1169.

[12] J. E. Ellis, *Organometallics* **2003**, *22*, 3322–3338.

[13] J. P. Collman, *Acc. Chem. Res.* **1975**, *8*, 342–347.

[14] U. Radius, F. M. Bickelhaupt, A. W. Ehlers, N. Goldberg, R. Hoffmann, *Inorg. Chem.* **2002**, *37*, 1080–1090.

[15] E. O. Fischer, A. Maasböl, *Angew. Chem.* **1964**, *76*, 645–645.

[16] H. W. Wanzlick, *Angew. Chem. Int. Ed.* **1962**, *1*, 75–80.

[17] K. Öfele, *J. Organomet. Chem.* **1968**, *12*, 42–43.

[18] H.-W. Wanzlick, H.-J. Schönherr, *Angew. Chem. Int. Ed.* **1968**, *7*, 141–142.

[19] A. J. Arduengo, R. L. Harlow, M. Kline, *J. Am. Chem. Soc.* **1991**, *113*, 361–363.

[20] W. A. Herrmann, C. Köcher, *Angew. Chem. Int. Ed.* **1997**, *36*, 2162–2187.

[21] M. N. Hopkinson, C. Richter, M. Schedler, F. Glorius, *Nature* **2014**, *510*, 485–496.

[22] W. A. Herrmann, *Angew. Chem. Int. Ed.* **2002**, *41*, 1290–1309.

[23] J. M. B. P. H. Dixneuf, A. F. L. S. Hegedus, P. H. P. Knochel, G. V. K. S. Murai, *Focus Catal.* **2012**, *2012*, 8.

[24] T. M. Trnka, R. H. Grubbs, *Acc. Chem. Res.* **2001**, *34*, 18–29.

[25] M. S. Sanford, J. A. Love, R. H. Grubbs, *J. Am. Chem. Soc.* **2001**, *123*, 6543–6554.

[26] A. Pidcock, R. E. Richards, L. M. Venanzi, *J. Chem. Soc. A* **1966**, 1707–1710.

[27] G. B. Kauffman, *J. Chem. Educ.* **1977**, *54*, 86.

[28] F. Basolo, R. G. Pearson in, *Bd. 4*, 1, **1962**, 381–453.

[29] B. J. Coe, S. J. Glenwright, *Coord. Chem. Rev.* **2000**, *203*, 5–80.

[30] B. Pinter, V. Van Speybroeck, M. Waroquier, P. Geerlings, F. De Proft, *Phys. Chem. Chem. Phys.* **2013**, *15*, 17354.

[31] R. F. See, D. Kozina, *J. Coord. Chem.* **2013**, *66*, 490–500.

[32] A. C. Tsipis, *Dalt. Trans.* **2019**, *48*, 1814–1822.

[33] R. Tonner, G. Frenking, *Chem. Commun.* **2008**, *1*, 1584–1586.

[34] D. J. Nelson, S. Manzini, C. A. Urbina-Blanco, S. P. Nolan, *Chem. Commun.* **2014**, *50*, 10355–10375.

[35] F. Ramirez, N. B. Desai, B. Hansen, N. McKelvie, *J. Am. Chem. Soc.* **1961**, *83*, 3539–3540.

[36] A. T. Vincent, P. J. Wheatley, *J. Chem. Soc. Dalt. Trans.* **1972**, *5*, 617–621.

[37] P. J. Quinlivan, G. Parkin, *Inorg. Chem.* **2017**, *56*, 5493–5497.

[38] H. Schmidbaur, *Angew. Chem. Int. Ed.* **2007**, *46*, 2984–2985.

[39] R. Tonner, F. Öxler, B. Neumüller, W. Petz, G. Frenking, *Angew. Chem.* **2006**, *118*, 8206–8211.

[40] R. Tonner, F. Öxler, B. Neumüller, W. Petz, G. Frenking, *Angew. Chem. Int. Ed.* **2006**, *45*, 8038–8042.

[41] G. Frenking, B. Neumüller, W. Petz, R. Tonner, F. Öxler, *Angew. Chem. Int. Ed.* **2007**, *46*, 2986–2987.

[42] G. Frenking, B. Neumüller, W. Petz, R. Tonner, F. Öxler, *Angew. Chem.* **2007**, *119*, 3044–3045.

[43] D. Himmel, I. Krossing, A. Schnepf, *Angew. Chem.* **2014**, *126*, 378–382.

[44] D. Himmel, I. Krossing, A. Schnepf, *Angew. Chem. Int. Ed.* **2014**, *53*, 370–374.

[45] G. Frenking, *Angew. Chem. Int. Ed.* **2014**, *53*, 6040–6046.

[46] G. Frenking, *Angew. Chem.* **2014**, *126*, 6152–6158.

[47] D. Himmel, I. Krossing, A. Schnepf, *Angew. Chem.* **2014**, *126*, 6159–6160.

[48] D. Himmel, I. Krossing, A. Schnepf, *Angew. Chem. Int. Ed.* **2014**, *53*, 6047–6048.

[49] W. Petz, *Coord. Chem. Rev.* **2015**, *291*, 1–27.

[50] W. C. Kaska, D. K. Mitchell, R. Reichelderfer, *J. Organomet. Chem.* **1973**, *47*, 391–402.

[51] W. C. Kaska, D. K. Mitchell, R. F. Reichelderfer, W. D. Korte, *J. Am. Chem. Soc.* **1974**, *96*, 2847–2854.

[52] W. Petz, C. Kutschera, S. Tschan, F. Weller, B. Neumüller, *Z. Anorg. Allg. Chem.* **2003**, *629*, 1235–1244.

[53] W. Petz, G. Frenking, *Carbodiphosphoranes and Related Ligands*, **2010**, 49–92.

[54] G. Frenking, R. Tonner, S. Klein, N. Takagi, T. Shimizu, A. Krapp, K. K. Pandey, P. Parameswaran, *Chem. Soc. Rev.* **2014**, *43*, 5106–5139.

[55] H. Braunschweig, M. Colling, *Coord. Chem. Rev.* **2001**, *223*, 1–51.

[56] G. Akopov, M. T. Yeung, R. B. Kaner, *Adv. Mater.* **2017**, *29*, 1604506.

[57] R. T. Baker, D. W. Ovenall, J. C. Calabrese, S. A. Westcott, N. J. Taylor, I. D. Williams, T. B. Marder, *J. Am. Chem. Soc.* **1990**, *112*, 9399–9400.

[58] J. R. Knorr, J. S. Merola, *Organometallics* **1990**, *9*, 3008–3010.

[59] H. Braunschweig, *Angew. Chem. Int. Ed.* **1998**, *37*, 1786–1801.

[60] H. Braunschweig, C. Kollann, D. Rais, *Angew. Chem. Int. Ed.* **2006**, *45*, 5254–5274.

[61] J. T. Goettel, H. Braunschweig, *Coord. Chem. Rev.* **2019**, *380*, 184–200.

[62] Y. Segawa, M. Yamashita, K. Nozaki, *Science* **2006**, *314*, 113–115.

[63] Y. Segawa, M. Yamashita, K. Nozaki, *Organometallics* **2009**, *28*, 6234–6242.

[64] H. Braunschweig, T. Wagner, *Angew. Chem. Int. Ed.* **1995**, *34*, 825–826.

[65] H. Braunschweig, T. Wagner, *Angew. Chem.* **1995**, *107*, 904–905.

[66] H. Braunschweig, C. Kollann, U. Englert, *Angew. Chem. Int. Ed.* **1998**, *37*, 3179–3180.

[67] H. Braunschweig, C. Kollann, U. Englert, *Angew. Chem.* **1998**, *110*, 3355–3357.

[68] H. Braunschweig, M. Colling, *Eur. J. Inorg. Chem.* **2003**, *2003*, 393–403.

[69] H. Braunschweig, R. D. Dewhurst, V. H. Gessner, *Chem. Soc. Rev.* **2013**, *42*, 3197–3208.

[70] R. J. Martinie, J. J. Bultema, M. N. Vander Wal, B. J. Burkhart, D. A. Vander Griend, R. L. DeKock, *J. Chem. Educ.* **2011**, *88*, 1094–1097.

[71] P. L. Timms, *J. Am. Chem. Soc.* **1967**, *89*, 1629–1632.

[72] A. W. Ehlers, E. J. Baerends, F. M. Bickelhaupt, U. Radius, *Chem. Eur. J.* **1998**, *4*, 210–221.

[73] R. Kinjo, B. Donnadieu, M. A. Celik, G. Frenking, G. Bertrand, *Science* **2011**, *333*, 610–613.

[74] L. Kong, Y. Li, R. Ganguly, D. Vidovic, R. Kinjo, *Angew. Chem. Int. Ed.* **2014**, *53*, 9280–9283.

[75] M. J. Drance, J. D. Sears, A. M. Mrse, C. E. Moore, A. L. Rheingold, M. L. Neidig, J. S. Figueroa, *Science* **2019**, *363*, 1203–1205.

[76] W. Kuriyama, T. Matsumoto, O. Ogata, Y. Ino, K. Aoki, S. Tanaka, K. Ishida, T. Kobayashi, N. Sayo, T. Saito, *Org. Process Res. Dev.* **2012**, *16*, 166–171.

[77] R. Noyori, T. Ohkuma, *Angew. Chem. Int. Ed.* **2001**, *40*, 40–73.

[78] S. Werkmeister, K. Junge, B. Wendt, E. Alberico, H. Jiao, W. Baumann, H. Junge, F. Gallou, M. Beller, *Angew. Chem. Int. Ed.* **2014**, *53*, 8722–8726.

[79] S. Chakraborty, H. Dai, P. Bhattacharya, N. T. Fairweather, M. S. Gibson, J. A. Krause, H. Guan, *J. Am. Chem. Soc.* **2014**, *136*, 7869–7872.

[80] F. Schneck, M. Assmann, M. Balmer, K. Harms, R. Langer, *Organometallics* **2016**, *35*, 1931–1943.

[81] D. Benito-Garagorri, K. Kirchner, *Acc. Chem. Res.* **2008**, *41*, 201–213.

[82] C. Gunanathan, D. Milstein, *Chem. Rev.* **2014**, *114*, 12024–12087.

[83] P. A. Dub, T. Ikariya, *ACS Catal.* **2012**, *2*, 1718–1741.

[84] J. I. van der Vlugt, *Eur. J. Inorg. Chem.* **2012**, *2012*, 363–375.

[85] S. Schneider, J. Meiners, B. Askevold, *Eur. J. Inorg. Chem.* **2012**, *2012*, 412–429.

[86] R. Tonner, G. Frenking, *Chem. Eur. J.* **2008**, *14*, 3273–3289.

[87] M. Green, *J. Organomet. Chem.* **1995**, *500*, 127–148.

[88] J. D. Gorden, A. Voigt, C. L. B. Macdonald, J. S. Silverman, A. H. Cowley, *J. Am. Chem. Soc.* **2000**, *122*, 950–951.

[89] E. Peris, R. H. Crabtree, *Chem. Soc. Rev.* **2018**, *47*, 1959–1968.

[90] C. J. Moulton, B. L. Shaw, *J. Chem. Soc. Dalt. Trans.* **1976**, 1020–1024.

[91] M. Ohff, A. Ohff, M. E. van der Boom, D. Milstein, *J. Am. Chem. Soc.* **1997**, *119*, 11687–11688.

[92] M. Gupta, C. Hagen, R. J. Flesher, W. C. Kaska, C. M. Jensen, *Chem. Commun.* **1996**, *28*, 2083–2084.

[93] M. Nielsen, A. Kammer, D. Cozzula, H. Junge, S. Gladiali, M. Beller, *Angew. Chem. Int. Ed.* **2011**, *50*, 9593–9597.

[94] L. Benhamou, E. Chardon, G. Lavigne, S. Bellemin-Laponnaz, V. César, *Chem. Rev.* **2011**, *111*, 2705–2733.

[95] W. Petz, B. Neumüller, *Polyhedron* **2011**, *30*, 1779–1784.

[96] K. Kubo, N. D. Jones, M. J. Ferguson, R. McDonald, R. G. Cavell, *J. Am. Chem. Soc.* **2005**, *127*, 5314–5315.

[97] K. Kubo, H. Okitsu, H. Miwa, S. Kume, R. G. Cavell, T. Mizuta, *Organometallics* **2017**, *36*, 266–274.

[98] C. Reitsamer, W. Schuh, H. Kopacka, K. Wurst, E. P. Ellmerer, P. Peringer, *Organometallics* **2011**, *30*, 4220–4223.

[99] S. Stallinger, C. Reitsamer, W. Schuh, H. Kopacka, K. Wurst, P. Peringer, *Chem. Commun.* **2007**, *012*, 510–512.

[100] C. Reitsamer, S. Stallinger, W. Schuh, H. Kopacka, K. Wurst, D. Obendorf, P. Peringer, *Dalt. Trans.* **2012**, *41*, 3503.

[101] C. Reitsamer, W. Schuhe, H. Kopacka, K. Wurst, P. Peringer, *Organometallics* **2009**, *28*, 6617–6620.

[102] W. Su, S. Pan, X. Sun, S. Wang, L. Zhao, G. Frenking, C. Zhu, *Nat. Commun.* **2018**, *9*, 4997.

[103] L. Vondung, N. Frank, M. Fritz, L. Alig, R. Langer, *Angew. Chem.* **2016**, *128*, 14665–14670.

[104] L. Vondung, N. Frank, M. Fritz, L. Alig, R. Langer, *Angew. Chem. Int. Ed.* **2016**, *55*, 14450–14454.

[105] M. Grätz, A. Bäcker, L. Vondung, L. Maser, A. Reincke, R. Langer, *Chem. Commun.* **2017**, *53*, 7230–7233.

[106] C. A. Tolman, *Chem. Rev.* **1977**, *77*, 313–348.

[107] R. Dorta, E. D. Stevens, C. D. Hoff, S. P. Nolan, *J. Am. Chem. Soc.* **2003**, *125*, 10490–10491.

[108] R. Dorta, E. D. Stevens, N. M. Scott, C. Costabile, L. Cavallo, C. D. Hoff, S. P. Nolan, *J. Am. Chem. Soc.* **2005**, *127*, 2485–2495.

[109] D. G. Gusev, E. Peris, *Dalt. Trans.* **2013**, *42*, 7359.

[110] R. Tonner, G. Frenking, *Organometallics* **2009**, *28*, 3901–3905.

[111] A. Chianese, X. Li, M. Janzen, J. Faller, R. Crabtree, *Organometallics* **2003**, *22*, 1663–1667.

[112] R. A. Kelly III, H. Clavier, S. Giudice, N. M. Scott, E. D. Stevens, J. Bordner, I. Samardjiev, C. D. Hoff, L. Cavallo, S. P. Nolan, *Organometallics* **2008**, *27*, 202–210.

[113] A. B. P. Lever, *Inorg. Chem.* **1990**, *29*, 1271–1285.

[114] A. B. P. Lever, *Inorg. Chem.* **1991**, *30*, 1980–1985.

[115] S. S. Fielder, M. C. Osborne, A. B. P. Lever, W. J. Pietro, *J. Am. Chem. Soc.* **1995**, *117*, 6990–6993.

[116] H. V. Huynh, Y. Han, R. Jothibasu, J. A. Yang, *Organometallics* **2009**, *28*, 5395–5404.

[117] Q. Teng, H. V. Huynh, *Dalt. Trans.* **2017**, *46*, 614–627.

[118] S. Guo, H. Sivaram, D. Yuan, H. V. Huynh, *Organometallics* **2013**, *32*, 3685–3696.

[119] Q. Teng, H. V. Huynh, *Inorg. Chem.* **2014**, *53*, 10964–10973.

[120] G. N. Lewis, *J. Am. Chem. Soc.* **1916**, *38*, 762–785.

[121] R. F. W. Bader, *Acc. Chem. Res.* **1985**, *18*, 9–15.

[122] R. F. W. Bader, *Atoms in Molecules: A Quantum Theory*, Clarendon Press, Oxford, **1994**.

[123] P. Popelier, *Atoms in Molecules: An Introduction*, Pearson Education Limited, Harlow, **2000**.

[124] R. F. Bader, *J. Phys. Chem. A* **1998**, *102*, 7314–7323.

[125] R. F. Bader, *J. Phys. Chem. A* **2009**, *113*, 10391–10396.

[126] K. Morokuma, *J. Chem. Phys.* **1971**, *55*, 1236–1244.

[127] K. Kitaura, K. Morokuma, *Int. J. Quantum Chem.* **1976**, *10*, 325–340.

[128] T. Ziegler, A. Rauk, *Theor. Chim. Acta* **1977**, *46*, 1–10.

[129] T. Ziegler, A. Rauk, *Inorg. Chem.* **1979**, *18*, 1755–1759.

[130] M. V. Hopffgarten, G. Frenking, *Wiley Interdiscip. Rev. Comput. Mol. Sci.* **2012**, *2*, 43–62.

[131] L. Zhao, M. von Hopffgarten, D. M. Andrada, G. Frenking, *Wiley Interdiscip. Rev. Comput. Mol. Sci.* **2018**, *8*, e1345.

[132] L. Vondung, Dissertation, Philipps-Universität Marburg, **2017**.

[133] B. Askevold, J. T. Nieto, S. Tussupbayev, M. Diefenbach, E. Herdtweck, M. C. Holthausen, S. Schneider, *Nat. Chem.* **2011**, *3*, 532–537.

[134] Y. Tanabe, Y. Nishibayashi, *Coord. Chem. Rev.* **2013**, *257*, 2551–2564.

[135] K. C. MacLeod, P. L. Holland, *Nat. Chem.* **2013**, *5*, 559–565.

[136] *Nitrogen Fixation*, (Hrsg.: Y. Nishibayashi), Springer International Publishing, Cham, **2017**.

[137] S. Bontemps, M. Sircoglou, G. Bouhadir, H. Puschmann, J. A. K. Howard, P. W. Dyer, K. Miqueu, D. Bourissou, *Chem. - A Eur. J.* **2008**, *14*, 731–740.

[138] D. Schuhknecht, F. Ritter, M. E. Tauchert, *Chem. Commun.* **2016**, *52*, 11823–11826.

[139] Autodesk Inventor Professional 2018, Autodesk, Inc. San Rafael, CA, **2018**.

[140] L. Maser, J. Herritsch, R. Langer, *Dalt. Trans.* **2018**, *47*, 10544–10552.

[141] L. Maser, L. Vondung, R. Langer, *Polyhedron* **2018**, *143*, 28–42.

[142] L. Maser, C. Schneider, L. Vondung, L. Alig, R. Langer, *J. Am. Chem. Soc.* **2019**, *141*, 7596–7604.

[143] L. Maser, C. Schneider, L. Alig, R. Langer, *Inorganics* **2019**, *7*, 61.

Anhang

Konstruktionen

Im Zuge dieser Dissertation wurden mehrere Konstruktionen angefertigt, von denen sich zwei als besonders nützlich erwiesen. Diese werden im Folgenden erläutert und die Konstruktionsskizzen für eine mögliche Reproduktion hinterlegt. Die Anfertigung der Konstruktionen sowie der Zeichnungen erfolgte mit Hilfe des Programms *Autodesk® Inventor® Professional 2018*, einer 3D CAD Software für Produktentwicklungen mit der Studenten-Lizenz.[139]

Heizblock für Schlenk- und NMR-Rohre

Dieser Heizblock wurde für die Verwendung mit den *Heidolph MR Hei-Tec* Magnetrührern entworfen. Eine Verwendung auf anderen Heizrührern sollte jedoch problemlos möglich sein, solange der Durchmesser der Rührfläche 147 mm nicht überschreitet und die Temperaturregelung über einen Sensor in der Heizplatte oder extern über einen Temperaturfühler der Mindestlänge 60 mm und Maximaldurchmesser 3.2 mm erfolgt.
Der Heizblock ist aus einem einzigen Werkstück gefertigt. Als Material wurde aufgrund der guten Kombination von Temperaturleitfähigkeit, Kosten und Haltbarkeit Aluminium gewählt. Das gleichzeitige Erwärmen von jeweils bis zu sieben Schlenk-Rohren mit einem Durchmesser von 25 mm und NMR-Rohren mit einem Durchmesser von 5 mm ist möglich. In der Mitte des Heizblocks befindet sich eine Aufnahme für die *Heidolph* Pt-1000 Temperatursonde. In der Unterseite befindet sich eine 3 mm tiefe, runde Vertiefung, damit der Heizblock nicht von der Rührplatte des Magnetrührers rutschen kann.

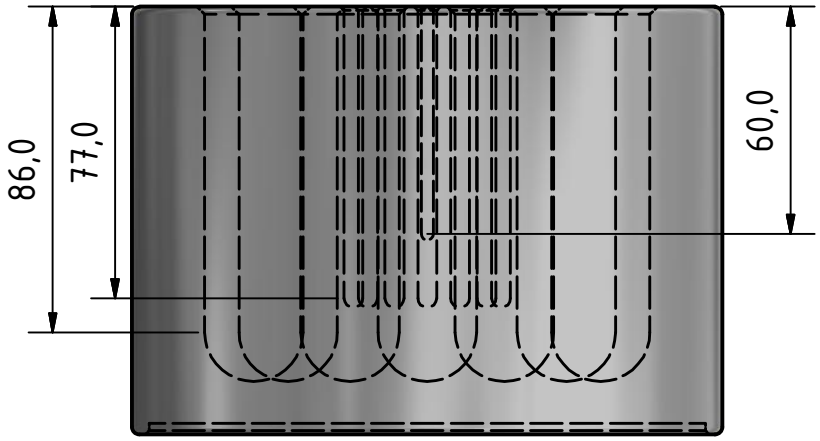

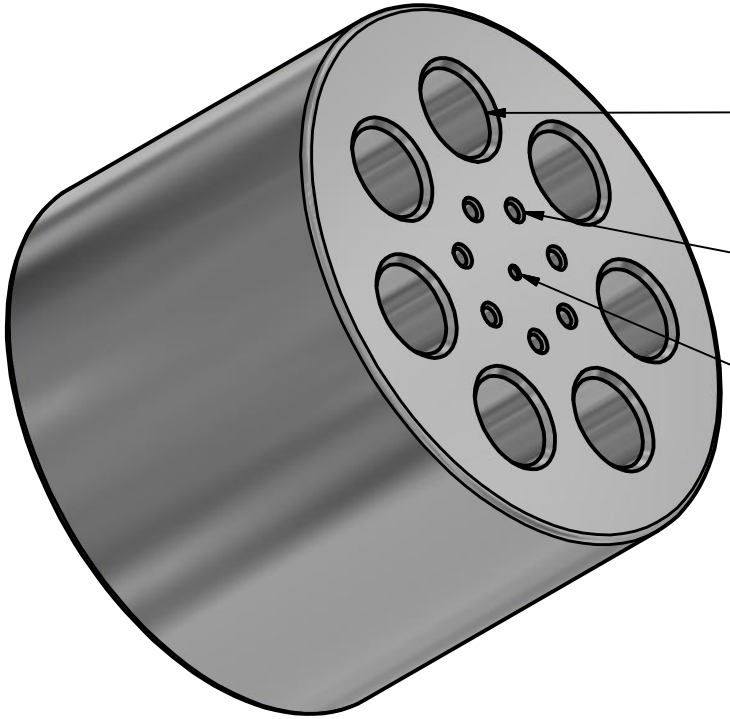

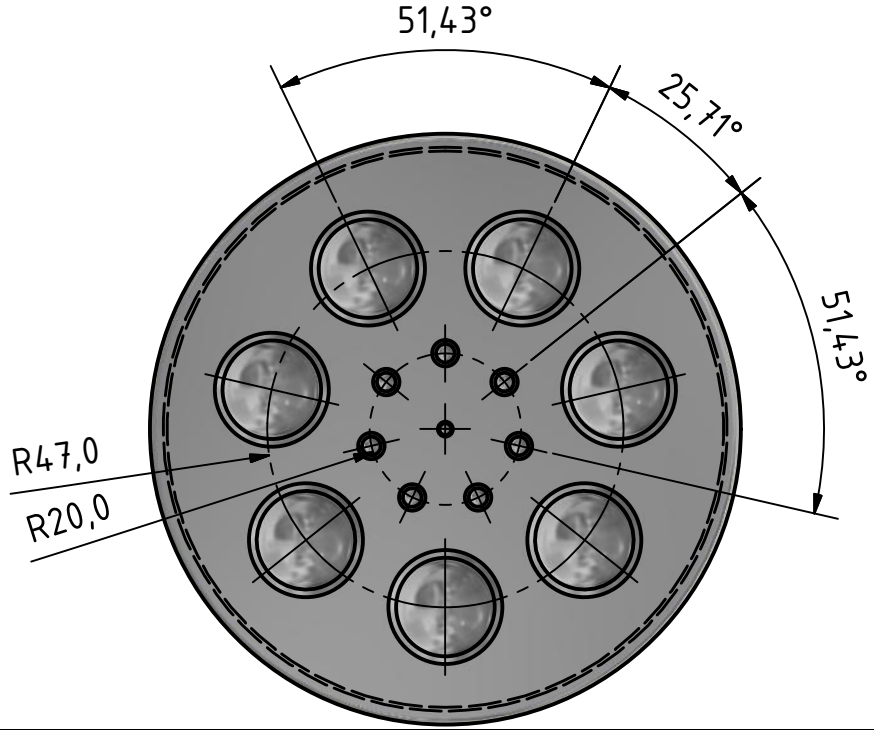

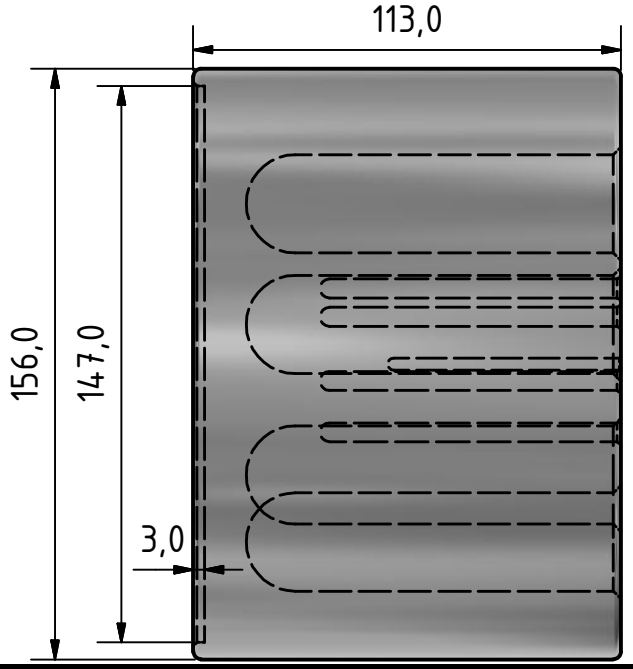

Heizblock für Heidolph MR
Hei-Tec Magnetrührer

Material: Aluminium

Angaben in mm
Maßstab 1:2

Leon Maser

12.11.2018

Abfüllhilfe für Elementaranalyse-Proben

Diese Abfüllhilfe für CHN-Analysen ist für die Verwendung mit Zinn-Kapseln eines Durchmessers von 3 mm und einer Höhe von 6 mm konzipiert. Die Probenanfertigung erfolgt typischerweise in der Glovebox. Die Abfüllhilfe besteht aus drei Hauptteilen, die jeweils aus mehreren Einzelteilen zusammengefügt werden:

A Stempel

- **A-1** Griff, Kunststoff
- **A-2** Stift, plan, Edelstahl

B Trichter

- **B-1** Trichter, Aluminium
- **B-2** Stift, eine Seite angefast, Edelstahl, x2

C Unterteil

- **C-1** Lochplatte, Edelstahl
- **C-2** Stützplatte, Edelstahl
- **C-3** Unterteil, Kunststoff

Der Stempel **A** besteht aus dem Griff **A-1**, der fest mit dem Edelstahlstift **A2** verbunden ist.
Der Trichter **B-1** ist ebenfalls fest mit den Edelstahlstiften **B-2**, mit der angefasten Seite nach unten, verbunden. Die Flügel an **B-1** verhindern das Wegrollen und ermöglichen einen besseren Griff.
Das Unterteil **C** besteht aus dem Kunststoff-Unterteil **C-3**, in das die Stützplatte **C-2** lose gelegt wird; die Lochplatte **C-1** kann nun seitlich oberhalb der Stützplatte eingeschoben werden. Die große Bohrung im Kunststoffteil **C-3** dient zwei Zwecken. Zum einen wird das Gewicht des gesamten Unterteils **C** auf unter 60 g reduziert, die Höchstabwiegekapazität einer der verwendeten Feinwaagen; zum anderen kann hier der Stempel verwahrt werden, so dass die komplette Abfüllhilfe an einem Stück verwahrt werden kann (Trichter **B** in Lochplatte).

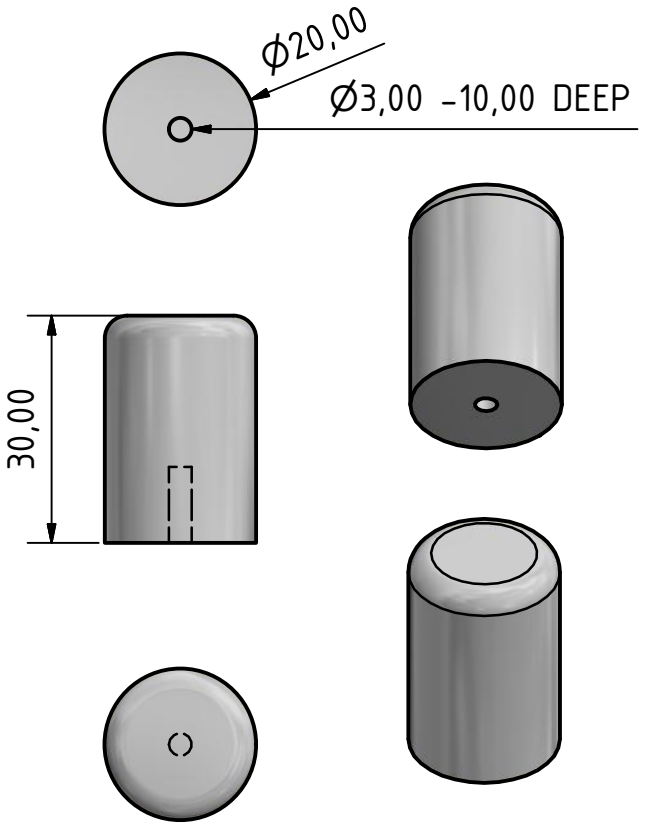

Griff A-1

Material:
Kunststoff

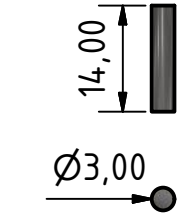

Stift A-2

Material: Edelstahl

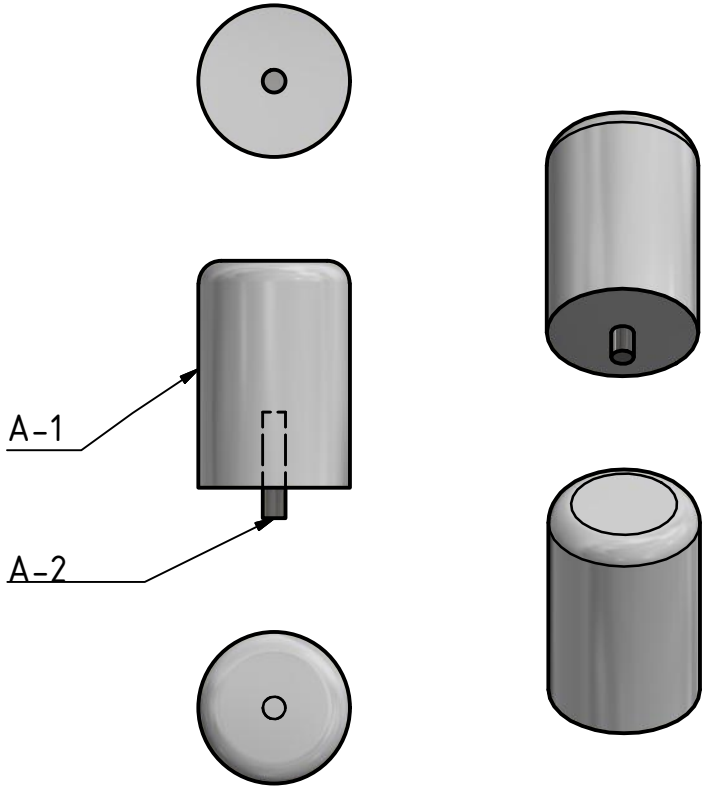

Stempel A, zusammengesetzt

Angaben in mm
Maßstab 1:1

Leon Maser

07.11.2018

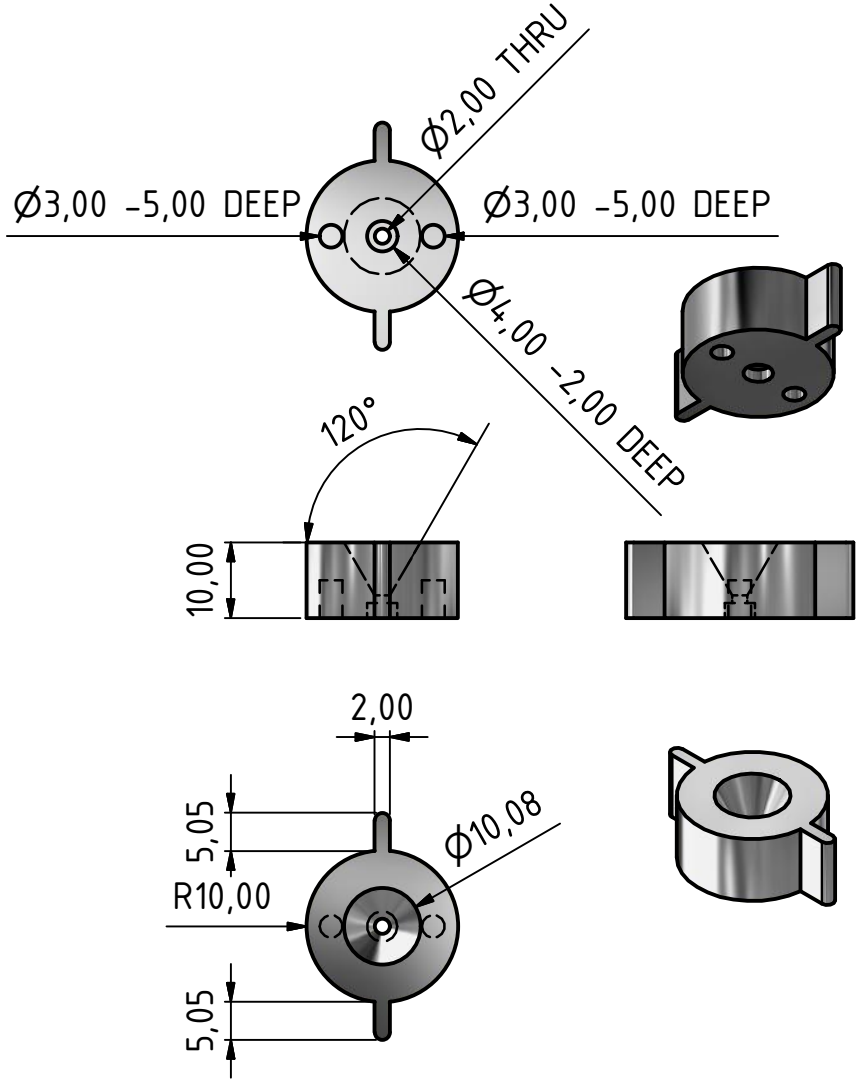

Trichter B-1

Material: Aluminium

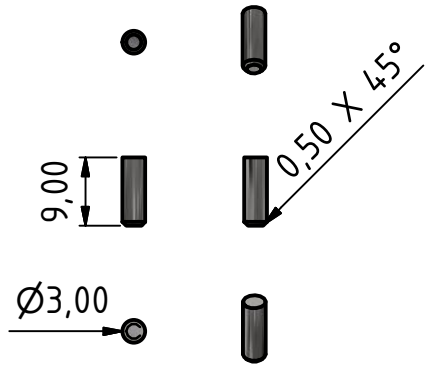

Stift B-2

Material: Edelstahl

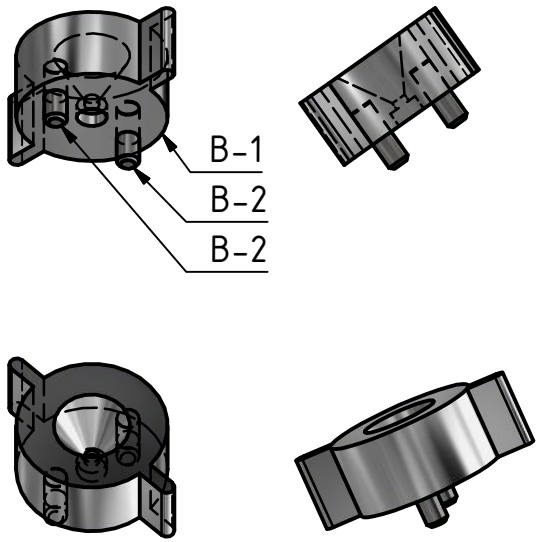

Trichter B,
zusammengesetzt

Angaben in mm
Maßstab 1:1

Leon Maser

07.11.2018

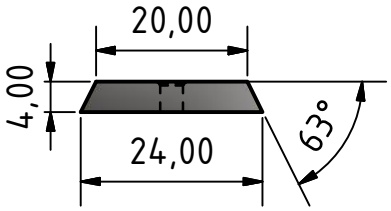

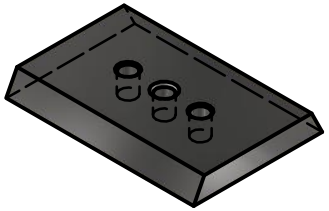

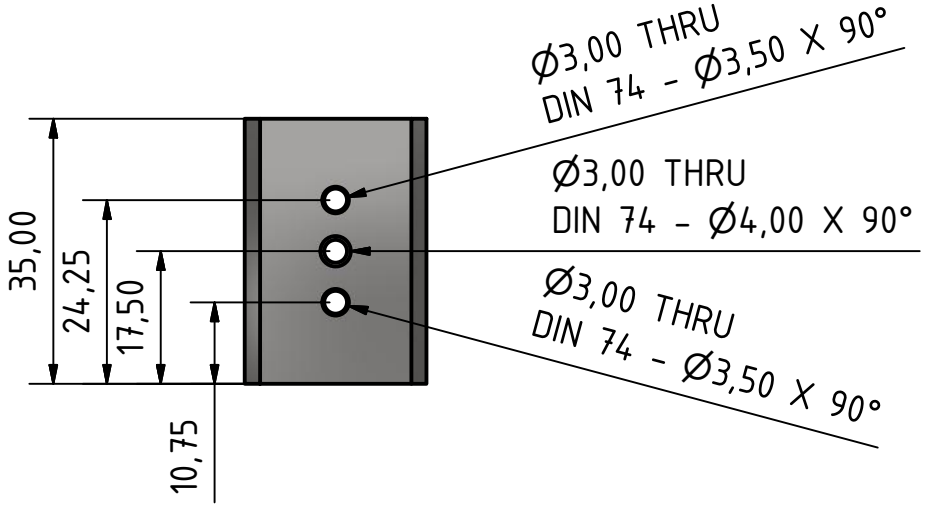

Lochplatte C-1 für CHN-Abfüllhilfe

Material: Edelstahl

Angaben in mm
Maßstab 1:1

Leon Maser

07.11.2018

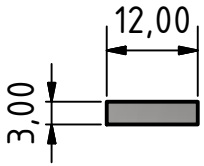

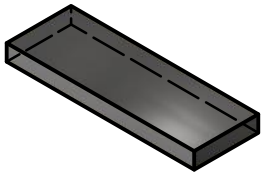

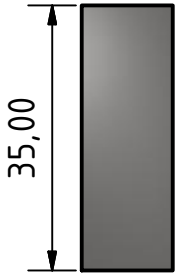

Stützplatte C-2 für CHN-Abfüllhilfe

Material: Edelstahl

Angaben in mm
Maßstab 1:1

Leon Maser

07.11.2018

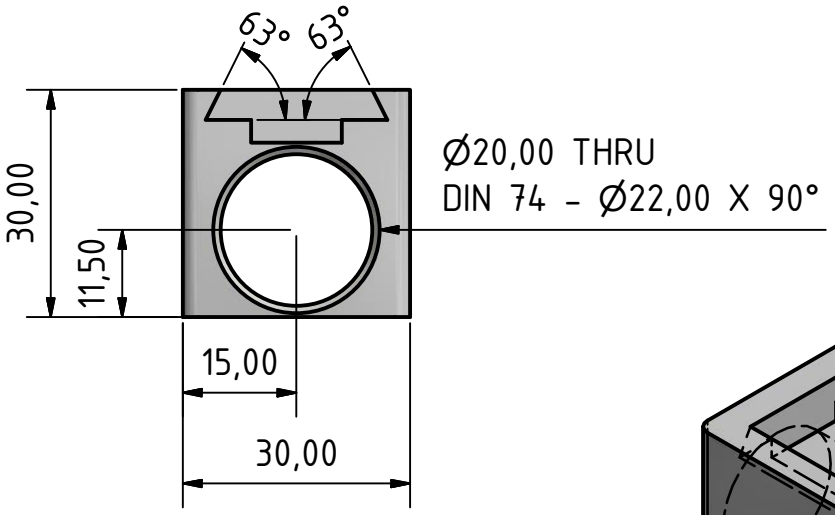

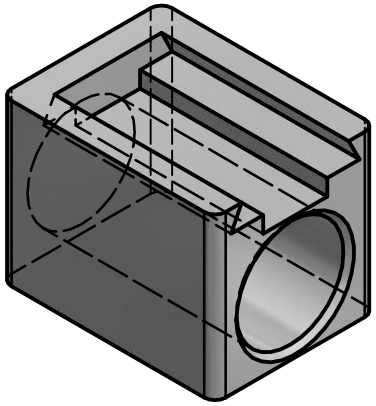

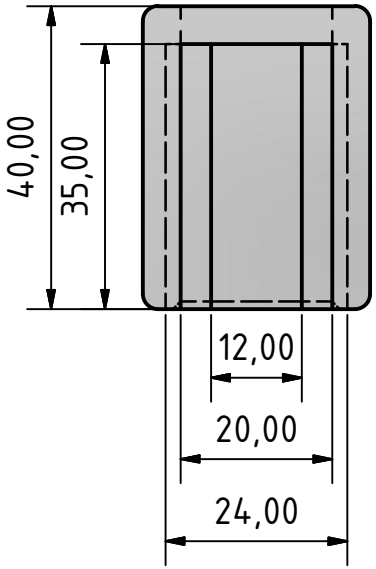

Unterteil C-3 für CHN-Abfüllhilfe

Material: Kunststoff

Angaben in mm
Maßstab 1:1

Leon Maser

07.11.2018

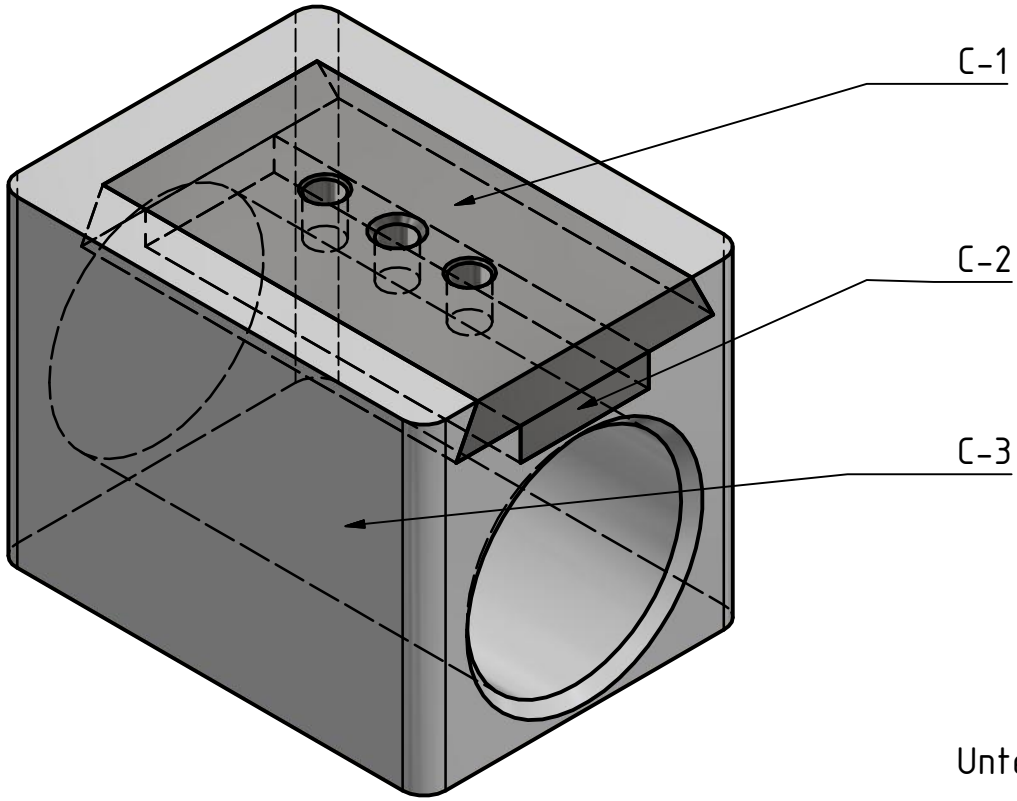

Unterteil C für CHN-Abfüllhilfe

Maßstab 2:1

Leon Maser

07.11.2018

Zum Vorbereiten einer Probe wird der Zinn-Kapsel mit der Öffnung nach oben in das mittlere der drei Löcher der Lochplatte **C-1** gestellt. Der Trichter **B** kann nun, geführt durch die Stifte **B-2**, exakt über der Öffnung der Kapsel positioniert werden und ermöglicht das einfache Befüllen. Nach Befüllen wird der Trichter **B** wieder entfernt und der obere Rand der Kapsel im aus der Lochplatte **C-1** stehenden Bereich entweder (Methode a) mit einer Zange zusammengepresst und so kaltpressverschweißt oder (Methode b) mit einer Pinzette zusammengedrückt und mit dem Stempel **A** in dem mittleren Loch der Platte unter Druck kaltpressverschweißt. Im Fall (a) kann die Kapsel direkt nach oben entnommen werden, im Fall (b) wird die Lochplatte **C-1** seitlich aus dem Unterteil **C** hinausgeschoben, so dass die komprimierte Kapsel mit Hilfe des Stempels **A** nach unten entfernt werden kann. Methode a empfiehlt sich für flüssige Substanzen, während Methode b bei festen Substanzen den Fehler durch noch enthaltenes Inertgas minimieren kann.

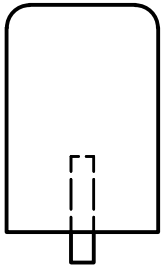

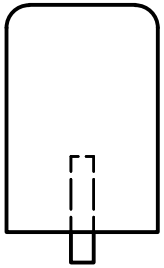

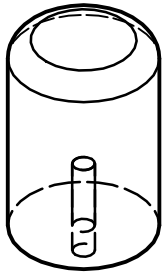

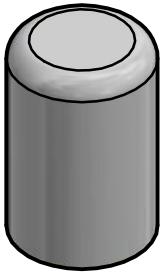

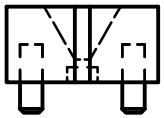

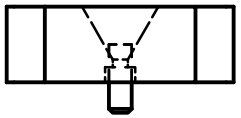

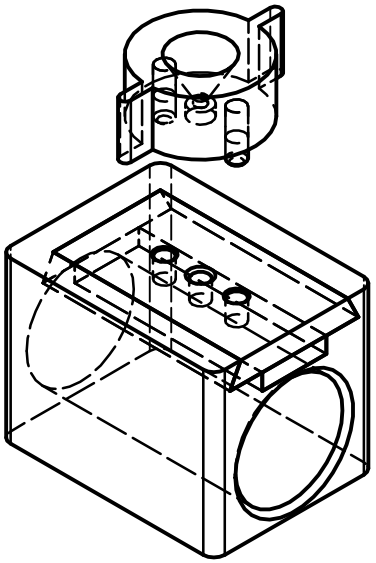

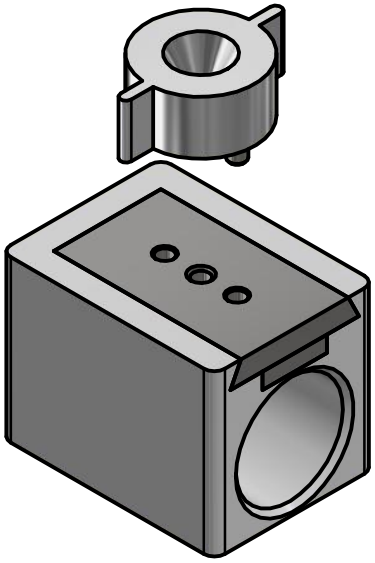

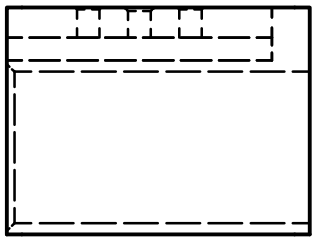

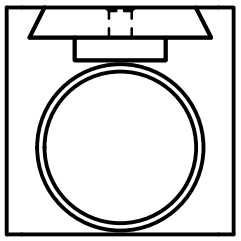

Elementaranalyse-Abfüllhilfe
komplett

Maßstab 1:1

Leon Maser

07.11.2018

Bash-Skripte

Während der quantenchemischen Rechnungen wurden einige Skripten verfasst, die mir das Arbeiten auf dem Marburger Rechencluster MaRC2 immens vereinfachten. Ich möchte diese der Nachwelt nicht vorenthalten, garantiere jedoch nicht für deren einwandfreie Funktion. Sie wurden für Gaussian09 verfasst und angepasst, um auch mit Gaussian16 verwendet werden zu können.

Gaussian Projektskript

Dieses Skript ermöglicht das Bearbeiten verschiedener Projekte mit jeweiligen Standard-Konfigurationen. Aus *.xyz-Dateien werden die entsprechenden Eingabe-Dateien für eine Voroptimierung der Geometrie, eine Optimierung mit größerem Basissatz und anschließender Frequenzrechnung erstellt und als verkettete Jobs abgeschickt.

```
#!/bin/bash

#Hier definition der zu bearbeitenden projekte
clear
cd ~/bin

if [ ! -f workdirectories.lst ];
  then
    echo "Seems you're running this for the first time..."
    echo "You will have to add a directory for me to work on!"
    echo "Here, i'll list 'em for you:"
    cd
    while true; do
      for i in $(ls -d */); do echo ${i%%/}; done
      read -p "Input directory to add!" ausgesucht2
      if [ ! -d ${ausgesucht2} ] ;
        then
          echo "Invalid choice!"
          read -p "Exit? (Y)es" yn
          case $yn in
            [Yy]* )  exit;;
            * ) echo "Try again!";;
          esac
      else
        cd ~/bin
        echo "${ausgesucht2}" > workdirectories.lst
        break
      fi
    done
fi
```

```
31
32 #auswahl des Projektordners aus liste oder zufügen eines neuen
33 echo "Which projekt to work on?"
34 while true; do
35   readarray -t projektordner < workdirectories.lst
36   counter=0
37   for x in ${projektordner[@]}; do
38     echo "(${counter}) $x"
39     counter=$[counter + 1]
40   done
41   echo "(${counter}) Add new directory"
42   read -p "Please enter option number!" ausgesucht
43   if [ "$ausgesucht" -gt "$counter" ] ;
44     then echo "Invalid choice!"
45   elif [ "$ausgesucht" -eq "$counter" ] ;
46     then
47       echo "Please select a directory!"
48       cd
49       while true; do
50         for i in $(ls -d */); do echo ${i%%/}; done
51         read -p "Input directory to add!" ausgesucht2
52         if [ ! -d ${ausgesucht2} ] ;
53           then
54             echo "Invalid choice!"
55             read -p "Exit? (Y)es" yn
56             case $yn in
57               [Yy]* )  exit;;
58               * ) echo "Try again!";;
59             esac
60         else
61           cd ~/bin
62           echo "${ausgesucht2}" >> workdirectories.lst
63           break
64         fi
65       done
66   else
67     break
68   fi
69 done
70
71 #Gehe in Projektordner
72 cd
73 if  [ ! -d ${projektordner[$ausgesucht]} ] ;
74   then
75     echo "Project folder does not exist!"
76     echo "Please delete it from ~/bin/workdirectories.lst!"
77     exit
78 fi
```

```
79
80 cd ~/${projektordner[$ausgesucht]}
81
82 #Lese config file ein oder erstelle sie
83 if [ -f config ] ;
84   then
85     funktional=$(grep "Standard functional:" "config"|awk '{print $3}')
86     basissatz=$(grep "Standard basis set:" "config"|awk '{print $4}')
87     memory=$(grep "Memory:" "config"|awk '{print $2}')
88     prozessoren=$(grep "Cores:" "config"|awk '{print $2}')
89     zeit=$(grep "Runtime:" "config"|awk '{print $2}')
90     echo "Settings to be used:"
91     echo "Standard functional: $funktional"
92     echo "Standard basis set: $basissatz"
93     echo "Memory: $memory"
94     echo "Cores: $prozessoren"
95     echo "Runtime: $zeit"
96 else
97   echo "Config file not found!"
98   while true; do
99     read -p "Do you wish to create one? (Y)es/(N)o?" yn
100       case $yn in
101         [Yy]* ) echo -e "Configuring config file now. \n Please choose your standard
      settings!";
102           read -p "Which functional do you want to use?"  funktional
103           read -p "Which basis set do you want to use?" basissatz
104           read -p "How much memory (MB) should be allocated per core?" memory
105           read -p "How many cores to use?" prozessoren
106           read -p "How many hours per job?" zeit
107           echo -e "Standard settings for this project:\n" > config
108           echo "Standard functional: $funktional" >> config
109           echo "Standard basis set: $basissatz" >> config
110           echo "Memory: $memory" >> config
111           echo "Cores: $prozessoren" >> config
112           echo "Runtime: $zeit" >> config
113           break;;
114         [Nn]* ) echo "Without a config, no cookies!"; exit;;
115         * ) echo "Please answer yes or no.";;
116       esac
117   done
118 fi
119
120 #suche nach .xyz-files im projektordner
121 xyz_files=$(ls *.xyz 2> /dev/null | wc -l)
122 if [ **"$xyz_files" = "0"** ]
123   then
124     echo "No xyz-file(s) found, exiting."
125     exit
```

```
126 fi
127
128 #konvertiere xyz-files in gültige input files
129 #ergibt files à la geo1_def2SVP_${xyzname}.in sowie alte files
130 #später bennenung: a-... ; davor also nen suchlauf nach schon benannten directories
131 dos2unix *.xyz
132 for i in *.xyz; do
133   xyzname=$(basename "$i" .xyz)
134
135   # neuen folder für die inputs und das saubere original
136   mkdir $xyzname
137   mv $i ./$xyzname
138   cd $xyzname
139   #Standard-Input Geometrieoptimierung MIT KLEINEM BASISSATZ
140   echo "%mem=$((memory * 10))MB" >> geo1_def2SVP_${xyzname}.in
141   echo "%chk=${xyzname}.chk" >> geo1_def2SVP_${xyzname}.in
142   echo "#p ${funktional}/Def2SVP" >> geo1_def2SVP_${xyzname}.in
143   echo "opt(tight,maxcycle=200)" >> geo1_def2SVP_${xyzname}.in
144   echo "scf(tight,maxcycle=200)" >> geo1_def2SVP_${xyzname}.in
145   echo "gfinput gfoldprint iop(6/7=3)" >> geo1_def2SVP_${xyzname}.in
146   echo "nosymm" >> geo1_def2SVP_${xyzname}.in
147   echo "" >> geo1_def2SVP_${xyzname}.in
148   echo "First geometry-optimization of ${xyzname} with def2SVP basis set" >>
        geo1_def2SVP_${xyzname}.in
149   echo "" >> geo1_def2SVP_${xyzname}.in
150   read -p "Charge and multiplicity of ${xyzname}? (charge, multiplicity)" chmu
151   echo "$chmu" >> geo1_def2SVP_${xyzname}.in
152   #Reinschieben von xyz-koordinaten
153   awk 'NF > 3' $i >> geo1_def2SVP_${xyzname}.in
154   echo "" >> geo1_def2SVP_${xyzname}.in
155   awk 'NF > 3' $i >> clean_${xyzname}.xyz
156
157   #Standard-Input Geometrieoptimierung MIT STANDARD BASISSATZ
158   echo "%mem=$((memory * 10))MB" >> geo2_${basissatz}_${xyzname}.in
159   echo "%chk=${xyzname}.chk" >> geo2_${basissatz}_${xyzname}.in
160   echo "#p ${funktional}/${basissatz}" >> geo2_${basissatz}_${xyzname}.in
161   echo "Geom=AllCheck" >> geo2_${basissatz}_${xyzname}.in
162   echo "opt(tight,maxcycle=200)" >> geo2_${basissatz}_${xyzname}.in
163   echo "scf(tight,maxcycle=200)" >> geo2_${basissatz}_${xyzname}.in
164   echo "gfinput gfoldprint iop(6/7=3)" >> geo2_${basissatz}_${xyzname}.in
165   echo "nosymm" >> geo2_${basissatz}_${xyzname}.in
166   echo "" >> geo2_${basissatz}_${xyzname}.in
167   echo "Second geometry-optimization of ${xyzname} with ${basissatz} basis set" >>
        geo2_${basissatz}_${xyzname}.in
168   echo "" >> geo2_${basissatz}_${xyzname}.in
169   echo "$chmu" >> geo2_${basissatz}_${xyzname}.in
170   echo "" >> geo2_${basissatz}_${xyzname}.in
171
```

```
172   #Standard-Input Frequenzrechnung MIT STANDARD BASISSATZ
173   echo "%mem=$((memory * 10))MB" >> freq1_${basissatz}_${xyzname}.in
174   echo "%chk=${xyzname}.chk" >> freq1_${basissatz}_${xyzname}.in
175   echo "#p ${funktional}/${basissatz}" >> freq1_${basissatz}_${xyzname}.in
176   echo "Geom=AllCheck" >> freq1_${basissatz}_${xyzname}.in
177   echo "freq gfinput gfoldprint iop(6/7=3)" >> freq1_${basissatz}_${xyzname}.in
178   echo "" >> freq1_${basissatz}_${xyzname}.in
179   echo "Frequency calculation of ${xyzname} with ${basissatz} basis set" >> freq1_${
        basissatz}_${xyzname}.in
180   echo "" >> freq1_${basissatz}_${xyzname}.in
181
182   # cleanup
183   rm $i
184
185   #Submitten der jobs als Kette
186   subg16 -c -m 4000 -p 16 -t 48 -y -Y geo1_def2SVP_${xyzname}.in > Job_1.id
187   ID=$(cat Job_1.id | awk '{print $1}')
188   subg16 -c -m $memory -p $prozessoren -t $zeit -y -Y -j $ID geo2_${basissatz}_${
        xyzname}.in > Job_2.id
189   ID=$(cat Job_2.id | awk '{print $1}')
190   subg16 -c -m $memory -p $prozessoren -t $zeit -y -Y -j $ID freq1_${basissatz}_${
        xyzname}.in  > Job_3.id
191   cd ~/${projektordner[$ausgesucht]}
192
193 done
```

Gaussian Auswertungsskript

Dieses Skript erkennt die Art der durchgeführten Rechnung einer entsprechenden Ausgabe-Datei, vorausgesetzt, es handelt sich nur um einen Jobtypen. Entsprechend der erkannten Rechnungsart werden Optionen zum weiteren Vorgehen angeboten; hierzu zählen Frequenzrechnungen nach Geometrieoptimierungen, Korrekturen negativer Moden und die Ausgabe von für weitere Analysen benötigter Dateien.

```
1  #!/bin/bash
2  clear
3
4  shortname=$(basename "$1" .out)
5  shortname=$(basename "$shortname" .in)
6  shortname=$(basename "$shortname" .)
7
8
9  #This Script automatically detects the type of a gaussian09 calculation and offers
       the user different choices for further analysis of the results
10 #Usage is as follows:
11 #Auto.sh your_calculation_name_here
```

```
12 #No suffix is needed for "your_calculation_name_here"
13 #This script has ONLY been testet on calculations containing a single type
       instruction set
14
15 #Functions ======================================================================
16 function check_inputfile {
17 testin=0
18 testin=$(ls -t -r ${shortname}.in 2> /dev/null | wc -l)
19 if [ "$testin" != "0" ]; then
20   echo "Input file found."
21 else
22   echo "No Input file found."
23 fi
24 }
25
26 function check_outputfile {
27 testout=0
28 testout=$(ls -t -r ${shortname}.out 2> /dev/null | wc -l)
29 if [ "$testout" != "0" ]; then
30   echo "Output file found."
31 else
32   echo "No Output file found."
33 fi
34 }
35
36 function get_calculation_type {
37 typ=0
38 if [ "$testin" = "1" ]; then
39   if grep -q "opt(" "${shortname}.in"; then
40     echo "${shortname} is a geometry optimization calculation."
41     typ="geo"
42   elif grep -q "freq " "${shortname}.in"; then
43     echo "${shortname} is a frequency calculation."
44     typ="freq"
45   elif grep -q "nboread" "${shortname}.in"; then
46     echo "${shortname} is a nbo-analysis calculation."
47     typ="nbo"
48   elif grep -q "nbo6read" "${shortname}.in"; then
49     echo "${shortname} is a NBO6-analysis calculation."
50     typ="nbo"
51   elif grep -q "put=wf" "${shortname}.in"; then
52     echo "${shortname} is a *.wfx/wfn-creation calculation."
53     typ="wf"
54   fi
55 else
56   if grep -q "opt(" "${shortname}.out"; then
57     echo "${shortname} is a geometry optimization calculation."
58     typ="geo"
```

```
59    elif grep -q "freq " "${shortname}.in"; then
60      echo "${shortname} is a frequency calculation."
61      typ="freq"
62    elif grep -q "nboread" "${shortname}.in"; then
63      echo "${shortname} is a nbo-analysis calculation."
64      typ="nbo"
65    elif grep -q "nbo6read" "${shortname}.in"; then
66      echo "${shortname} is a NBO6-analysis calculation."
67      typ="nbo"
68    elif grep -q "put=wf" "${shortname}.in"; then
69      echo "${shortname} is a *.wfx/wfn-creation calculation."
70      typ="wf"
71    else
72      echo "ERROR: could not determine calculation type!"
73      typ="unknown"
74    fi
75  fi
76  }
77
78  function check_termination {
79  term=0
80  if [ "$testout" = "1" ]; then
81    if grep -q "Normal termination of Gaussian" "${shortname}.out"; then
82      echo "Calculation was terminated normally."
83      term=1
84    else
85      echo "Calculation was aborted."
86    fi
87  else
88    echo "Cannot determine termination of calculation since no output is available"
89  fi
90  }
91
92  function get_base_and_functional {
93  if [ "$testout" = "1" ]; then
94    fuba=$(grep -m 1 "#p" ${shortname}.out | awk '{print $2}' )
95    basissatz=$(basename $fuba)
96    funktional=$(dirname $fuba)
97  elif [ "$testin" = "1" ]; then
98    fuba=$(head -n 3 ${shortname}.in | tail -1 | awk '{print $2}' )
99    basissatz=$(basename $fuba)
100   funktional=$(dirname $fuba)
101 else
102   echo "Neither input- nor output-file found!"
103   echo "This should not happen!"
104 fi
105 echo "Current functional and basis set: ${funktional}/${basissatz}"
106 }
```

```
107
108 function submit_job_with_choices {
109 while true; do
110   read -p "Should it be submitted? (Y)es/(N)o? " yn
111   case $yn in
112     [Yy]* ) while true; do
113             echo "Please choose a setting:"
114             echo "(1) 8 CPU's, 1 hour - test queue"
115             echo "(2) 16 CPU's, 1 day - short queue"
116             echo "(3) 32 CPU's, 2 days - long queue"
117             echo "(4) 32 CPU's, 10 days - longest calculation possible"
118             echo "(A) Abort"
119             read -p "Choose next step! " yn
120             case $yn in
121               1 ) subg16 -c -m 4200 -p 8 -t 1 "$newfile"; exit;;
122               2 ) subg16 -c -m 4200 -p 16 -t 24 "$newfile"; exit;;
123               3 ) subg16 -c -m 4200 -p 32 -t 48 "$newfile"; exit;;
124               4 ) subg16 -c -m 4200 -p 32 -t 240 "$newfile"; exit;;
125               [Aa] ) echo "Aborting."; break;;
126               * ) echo "Please choose an option!";;
127             esac
128           done
129           break;;
130     [Nn]* ) echo "Not submitting new input."; break;;
131     * ) echo "Please answer yes or no!";;
132   esac
133 done
134  }
135
136 function add_output_coordinates_to_newfile {
137 if grep -q "Distance matrix (angstroms):" "${shortname}.out"; then
138   echo "$(sed -n -e '/Largest change from initial coordinates is atom/,/Distance
      matrix (angstroms):/ p' ${shortname}.out | tail -n +11 | head -n -2 | awk '{
      print $2"\t"$4"\t"$5"\t"$6}')"
139   echo "$(sed -n -e '/Largest change from initial coordinates is atom/,/Distance
      matrix (angstroms):/ p' ${shortname}.out | tail -n +11| head -n -2 | awk '{print
       $2"\t"$4"\t"$5"\t"$6}')" >> "$newfile"
140 elif grep -q "Standard orientation:" "${shortname}.out"; then
141   echo "$(sed -n -e '/Standard orientation:/,/Rotational constants (GHZ):/ p' ${
      shortname}.out | tail -n +6 | head -n -2 | awk '{print $2"\t"$4"\t"$5"\t"$6}')"
142   echo "$(sed -n -e '/Standard orientation:/,/Rotational constants (GHZ):/ p' ${
      shortname}.out | tail -n +6 | head -n -2 | awk '{print $2"\t"$4"\t"$5"\t"$6}')"
      >> "$newfile"
143 else
144   echo "$(sed -n -e '/Largest change from initial coordinates is atom/,/Rotational
      constants (GHZ):/ p' ${shortname}.out | tail -n +16 | head -n -2 | awk '{print
      $2"\t"$4"\t"$5"\t"$6}')"
145   echo "$(sed -n -e '/Largest change from initial coordinates is atom/,/Rotational
```

```
    constants (GHZ):/ p' ${shortname}.out | tail -n +16 | head -n -2 | awk '{print
    $2"\t"$4"\t"$5"\t"$6}')" >> "$newfile"
146 fi
147
148 #In principle, multi-calculation jobs can be used as well. It has to be known which
    job is the last geometry optimization:
149 #if grep -q "Link1:  Proceeding to internal job step number  2" "${shortname}.out";
    then
150 # sed -n -e '/Link1:  Proceeding to internal job step number  2/,$p' ${shortname}.
    out | sed -n -e '/Standard orientation:/,/Rotational constants (GHZ):/ p' | tail
     -n +6 | head -n -2 | awk '{print $2"\t"$4"\t"$5"\t"$6}' >> "$newfile"
151 #else
152 # sed -n -e '/Standard orientation:/,/Rotational constants (GHZ):/ p' ${shortname}.
    out| tail -n +6 | head -n -2 | awk '{print $2"\t"$4"\t"$5"\t"$6}' >> "$newfile"
153 #fi
154
155 }
156
157 function add_error_output_coordinates_to_newfile {
158 echo "$(grep -A 1000 "Input orientation" ${shortname}.out | tail -1000 | sed -n -e
    '/Input orientation:/,/Rotational constants (GHZ):/ p' | tail -n +6 | head -n -2
     | awk '{print $2"\t"$4"\t"$5"\t"$6}')" >> "$newfile"
159 }
160
161 function prepare_xyz-file {
162 echo "Preparing xyz-file."
163 while true; do
164   read -p "Please name the xyz-file! " name
165   name=$(basename "$name" .xyz)
166   newfile="${name}.xyz"
167   if [ ! -f "$newfile" ];
168     then
169       if [ "$term" = "1" ]; then
170         add_output_coordinates_to_newfile
171       elif [ "$term" = "0" ]; then
172         add_error_output_coordinates_to_newfile
173       fi
174       awk 'FNR==NR { a[$1]=$2; next } $1 in a { $1=a[$1] }'1 > olex_${newfile} ~/bin
    /element-conversion.txt "$newfile"
175       echo "$newfile has been written!"; exit;
176     else
177       echo "Name already taken, please pick another!"
178   fi
179 done
180 }
181
182 #Main Script ====================================================================
183
```

```
184 #Preparations
185 check_inputfile         #switches $testin
186 check_outputfile        #switches $testout
187 get_calculation_type      #sets $typ
188 check_termination        #switches $term
189 get_base_and_functional     #sets $basissatz, $funktional
190
191 #Weiteres Vorgehen in abhängigkeit vom Rechnungstyp
192 if [ "$typ" = "geo" ]; then
193   #Wenn alles vohanden und erfolgreich, dann:
194   if [ "$testin" = "1" ] && [ "$testout" = "1" ] && [ "$term" = "1" ]; then
195     while true; do
196       echo "Available options:"
197       echo "(1) Make frequency calculation"
198       echo "(2) Make xyz-file"
199       echo "(Q) Exit"
200       read -p "Choose next step! " yn
201       case $yn in
202         1 ) echo "Writing new frequency calculation."
203             newfile="freq_${shortname}.in"
204             #finden der ladung und multiplizität
205             lamu=$(grep "Charge = " ${shortname}.out| awk '{print $3, $6}')
206             #einlesen des memorys, checkpunktfiles und funktional/basissatz aus der
    angegebenen frequenzrechnung
207             zeile1bis3=$(head -n 3 ${shortname}.in)
208             #Standard-Input Frequenzrechnung MIT STANDARD BASISSATZ
209             echo "$zeile1bis3" >"$newfile"
210             echo "freq gfinput gfoldprint iop(6/7=3)" >> "$newfile"
211             echo "" >> "$newfile"
212             echo "Frequency calculation of ${shortname} with previous basis set" >>
    "$newfile"
213             echo "" >> "$newfile"
214             echo "$lamu" >> "$newfile"
215             add_output_coordinates_to_newfile
216             echo "" >> "$newfile"
217             echo "New frequency calculation $newfile written."
218             submit_job_with_choices;;
219         2 ) prepare_xyz-file;;
220         [Qq] ) echo "Quitting."; exit;;
221         * ) echo "Please choose an option!";;
222       esac
223     done
224   #Rechnung abgebrochen:
225   elif [ "$testin" = "1" ] && [ "$testout" = "1" ] && [ "$term" = "0" ]; then
226     while true; do
227       echo "Available options:"
228       echo "(1) Make new geometry optimization"
229       echo "(2) Make frequency calculation"
```

```
230       echo "(3) Make xyz-file"
231       echo "(Q) Exit"
232       read -p "Choose next step! " yn
233       case $yn in
234         1 ) while true; do
235             echo "Current functional and basis set: ${funktional}/${basissatz}"
236             echo "(1) Keep current setting"
237             echo "(2) Change functional and/or basis set manually"
238             echo "(3) Use def2TZVPP as basis set"
239             echo "(Q) Exit"
240             read -p "Choose next step! " yn
241             case $yn in
242               1 ) break;;
243               2 ) while true; do
244                   read -p "Input new functional or (S)kip! " nfu
245                   case $nfu in
246                     [Ss]* ) break;;
247                     * ) while true; do
248                           echo "New functional: $nfu"
249                           read -p "Correct? (Y)es/(N)o? " yn
250                           case $yn in
251                             [Yy]* )   funktional=$nfu
252                                   break;;
253                             [Nn]* )  break;;
254                             * ) echo "Please answer yes or no.";;
255                           esac
256                       done
257                   esac
258                 done
259                 while true; do
260                   read -p "Input new basis set or (S)kip! " nbs
261                   case $nbs in
262                     [Ss]* ) break;;
263                     * ) while true; do
264                           echo "New basis set: $nbs"
265                           read -p "Correct? (Y)es/(N)o? " yn
266                           case $yn in
267                             [Yy]* )   basissatz=$nbs
268                                   break;;
269                             [Nn]* )  break;;
270                             * ) echo "Please answer yes or no.";;
271                           esac
272                       done
273                   esac
274                 done
275                 break;;
276               3 ) basissatz="def2TZVPP"
277                 break;;
```

```
278             [Qq] ) echo "Quitting."; exit;;
279             * ) echo "Please choose an option!";;
280           esac
281         done
282         echo "Will utilize $funktional and $basissatz"
283         #Ladung und Multiplizität
284         lamu=$(grep -m 1 "Charge = " ${shortname}.out | awk '{print $3, $6}')
285         #einlesen des checkpunktfiles und funktional/basissatz aus der angegebenen
     frequenzrechnung
286         zeile1und2=$(head -n 2 ${shortname}.in)
287         #Input Geometrieoptimierung MIT ANDEREM FUNKTIONAL & BASISSATZ
288         newfile="new_${shortname}.in"
289         echo "$zeile1und2" >"$newfile"
290         echo "#p ${funktional}/${basissatz}" >> "$newfile"
291         echo "opt(tight,maxcycle=200)" >> "$newfile"
292         echo "scf(tight,maxcycle=200)" >> "$newfile"
293         echo "gfinput gfoldprint iop(6/7=3)" >> "$newfile"
294         echo "nosymm" >> "$newfile"
295         echo "" >> "$newfile"
296         echo "Geometry-optimization of ${shortname} after addition of negative
    frequency" >> "$newfile"
297         echo "" >> "$newfile"
298         echo "$lamu" >> "$newfile"
299         add_error_output_coordinates_to_newfile
300         echo "" >> "$newfile"
301         echo "New geometry optimization $newfile written."
302         submit_job_with_choices;;
303       2 ) echo "Writing new frequency calculation."
304           newfile="freq_${shortname}.in"
305           #finden der ladung und multiplizität
306           lamu=$(grep "Charge = " ${shortname}.out| awk '{print $3, $6}')
307           #einlesen des memorys, checkpunktfiles und funktional/basissatz aus der
    angegebenen frequenzrechnung
308           zeile1bis3=$(head -n 3 ${shortname}.in)
309           #Standard-Input Frequenzrechnung MIT STANDARD BASISSATZ
310           echo "$zeile1bis3" >"$newfile"
311           echo "freq gfinput gfoldprint iop(6/7=3)" >> "$newfile"
312           echo "" >> "$newfile"
313           echo "Frequency calculation of ${shortname} with previous basis set" >>
    "$newfile"
314           echo "" >> "$newfile"
315           echo "$lamu" >> "$newfile"
316           add_output_coordinates_to_newfile
317           echo "" >> "$newfile"
318           echo "New frequency calculation $newfile written."
319           submit_job_with_choices;;
320       3 ) prepare_xyz-file;;
321       [Qq] ) echo "Quitting."; exit;;
```

```
322         * ) echo "Please choose an option!";;
323       esac
324     done
325   #Nur Output vorhanden:
326   elif [ "$testout" = "1" ] && [ "$testin" = "0" ]; then
327       while true; do
328       echo "Available options:"
329       echo "(1) Make xyz-file"
330       echo "(Q) Exit"
331       read -p "Choose next step! " yn
332       case $yn in
333         1 ) prepare_xyz-file;;
334         [Qq] ) echo "Quitting."; exit;;
335         * ) echo "Please choose an option!";;
336       esac
337     done
338   #nur Input vorhanden:
339   elif [ "$testout" = "0" ] && [ "$testin" = "1" ]; then
340     echo "Only input file found! Exiting."
341     exit
342   #Irgendwas anderes
343   else
344     echo "An error occured. Quitting!"
345     exit
346   exit
347   fi
348 elif [ "$typ" = "freq" ]; then
349   #Check auf negative frequenzen
350   nfreq=0
351   if grep -q "imaginary" "${shortname}.out"; then nfreq=1
352     echo "Imaginary modes found!"
353   else
354     echo "No imaginary modes found!"
355   fi
356   #Wenn alles vohanden und erfolgreich und keine neg frequenzen, dann:
357   if [ "$testin" = "1" ] && [ "$testout" = "1" ] && [ "$term" = "1" ] && [ "$nfreq"
       = "0" ]; then
358     while true; do
359       echo "Available options:"
360       echo "(1) Analysis by nbo and creation of wfx- and fchk-files + summary-file"
361       echo "(2) Geometry optimization with new basis set"
362             echo "(Q) Exit"
363       read -p "Choose next step! " yn
364       case $yn in
365         1 ) #job höchster nummer finden und diese ausgeben
366             files=$(ls -t -r Job* 2> /dev/null | wc -l)
367             if [ "$files" != "0" ]
368               then
```

```
369               basename $(ls Job* | tail -1 | cut -c 5-) .id >> highest.tmp
370               counter=$(<"highest.tmp")
371               rm highest.tmp
372             else
373               counter=1
374           fi
375           echo "The new calculations will start with the Job-ID $counter."
376
377           #einlesen des checkpunktfiles und funktional/basissatz aus der
    angegebenen frequenzrechnung
378           zeile2und3=$(head -n 3 ${shortname}.in | tail -2)
379           #ladung und multiplizität
380           lamu=$(grep "Charge = " ${shortname}.out | awk '{print $3, $6}')
381           #koordinaten
382           koordinaten=$(sed -n -e '/Standard orientation:/,/Rotational constants (
    GHZ):/ p' ${shortname}.out | tail -n +6 | head -n -2 | awk '{print $2, $4, $5,
    $6}')
383           #check auf energies.sh
384           if [ -f energies.txt ]; then
385             echo "Energy summary of same name found, skipping."
386           else
387             energies.sh ${shortname}.out
388           fi
389           #check auf fchk
390           checkpoint=$(basename $(head -n 2 ${shortname}.in | tail -1 | cut -c 6-)
     .chk)
391           if [ -f ${checkpoint}.fchk ]; then
392             echo "fchk-file of same name found, skipping."
393           else
394             formchk -v g16 -v g16 ${checkpoint}.chk
395           fi
396           #check auf wfx
397           if [ -f ${shortname}.wfx ]; then
398             echo "wfx-file of same name found, skipping."
399           else
400             #Standard-Input wfx-File MIT STANDARD BASISSATZ
401             echo "%mem=16000MB" > wfx_${shortname}.in
402             echo "$zeile2und3" >> wfx_${shortname}.in
403             echo "pseudo=read" >> wfx_${shortname}.in
404             echo "density=current" >> wfx_${shortname}.in
405             echo "punch=archive" >> wfx_${shortname}.in
406             echo "output=wfx" >> wfx_${shortname}.in
407             echo "" >> wfx_${shortname}.in
408             echo "wfx-file calculation ${shortname} with ${basissatz} basis set"
    >> wfx_${shortname}.in
409             echo "" >> wfx_${shortname}.in
410             echo "$lamu" >> wfx_${shortname}.in
411             echo "$koordinaten" >> wfx_${shortname}.in
```

```
412             echo "" >> wfx_${shortname}.in
413             echo "" >> wfx_${shortname}.in
414             echo "${shortname}.wfx" >> wfx_${shortname}.in
415             echo "" >> wfx_${shortname}.in
416             echo "New wfx calculation wfx_${shortname}.in written."
417             #Submitten des jobs
418             while true; do
419               read -p "Should it be submitted? (Y)es/(N)o? " yn
420               case $yn in
421                 [Yy]* )   if [ -f Job_${counter}.id ]; then
422                         lauf=$(cat Job_${counter}.id | awk '{print $1}')
423                         qstat | tail -n +3 |awk '{print $1 >> "temp.lst"}'
424                         if grep -q "${lauf}" "temp.lst"; then
425                           ID=$( cat Job_${counter}.id | awk '{print $1}')
426                           counter=$[counter + 1]
427                           subg16 -c -m 4000 -p 16 -t 8 -y -Y -f -j $ID wfx_${
    shortname}.in > Job_${counter}.id
428                         else
429                           counter=$[counter + 1]
430                           subg16 -c -m 4000 -p 16 -t 8 -y -Y -f wfx_${shortname}.
    in > Job_${counter}.id
431                         fi
432                         rm temp.lst
433                       else
434                         subg16 -c -m 4000 -p 16 -t 8 -y -Y -f wfx_${shortname}.in
    > Job_${counter}.id
435                       fi
436                       break;;
437                 [Nn]* ) echo "Not submitting wfx-calculation."; break;;
438                 * ) echo "Please answer yes or no!";;
439               esac
440             done
441           fi
442
443           #check auf nbo
444           if [ -f nbo_${shortname}.out ]
445             then
446               echo "nbo-file of same name found, skipping."
447             else
448               #Standard-Input Populationsanalyse MIT STANDARD BASISSATZ
449               echo "%mem=40000MB" > nbo_${shortname}.in
450               echo "$zeile2und3" >> nbo_${shortname}.in
451               echo "scf(tight,maxcycle=200) gfinput gfoldprint" >> nbo_${shortname
    }.in
452               echo "POP(full, nbo6read)" >> nbo_${shortname}.in
453               echo "density=current" >> nbo_${shortname}.in
454               echo "" >> nbo_${shortname}.in
455               echo "Population analysis calculation of ${shortname} with ${
```

```
    basissatz} basis set" >> nbo_${shortname}.in
456                 echo "" >> nbo_${shortname}.in
457                 echo "$lamu" >> nbo_${shortname}.in
458                 echo "$koordinaten" >> nbo_${shortname}.in
459                 echo "" >> nbo_${shortname}.in
460                 echo '$NBO' "BNDIDX FILE=nbo-visualisation PLOT NBOSUM MULORB" '$END
    ' >> nbo_${shortname}.in
461                 echo "" >> nbo_${shortname}.in
462                 echo "New nbo calculation nbo_${shortname}.in written."
463                 #Submitten des jobs
464                 while true; do
465                   read -p "Should it be submitted? (Y)es/(N)o? " yn
466                   case $yn in
467                     [Yy]* )    if [ -f Job_${counter}.id ]; then
468                                  lauf=$(cat Job_${counter}.id | awk '{print $1}')
469                                  qstat | tail -n +3 |awk '{print $1 >> "temp.lst"}'
470                                  if grep -q "${lauf}" "temp.lst"
471                                    then
472                                      ID=$(cat Job_${counter}.id | awk '{print $1}')
473                                      counter=$[counter + 1]
474                                      subg16 -c -m 4000 -p 32 -t 48 -y -Y -f -j $ID nbo_${
    shortname}.in > Job_${counter}.id
475                                  else
476                                    counter=$[counter + 1]
477                                    subg16 -c -m 4000 -p 32 -t 48 -y -Y -f nbo_${
    shortname}.in > Job_${counter}.id
478                                fi
479                                rm temp.lst
480                              else
481                                subg16 -c -m 4000 -p 32 -t 48 -y -Y -f nbo_${shortname}.
    in > Job_${counter}.id
482                              fi
483                              break;;
484                     [Nn]* ) echo "Not submitting nbo-calculation."; break;;
485                     * ) echo "Please answer yes or no!";;
486                   esac
487                 done
488           fi
489           exit;;
490       2 )
491           while true; do
492             echo "Current functional and basis set: ${funktional}/${basissatz}"
493             echo "(1) Keep current setting"
494             echo "(2) Change functional and/or basis set manually"
495             echo "(3) Use def2TZVPP as basis set"
496             echo "(Q) Exit"
497             read -p "Choose next step! " yn
498             case $yn in
```

```
499                 1 ) break;;
500                 2 ) while true; do
501                     read -p "Input new functional or (S)kip! " nfu
502                     case $nfu in
503                       [Ss]* ) break;;
504                       * ) while true; do
505                         echo "New functional: $nfu"
506                         read -p "Correct? (Y)es/(N)o? " yn
507                         case $yn in
508                           [Yy]* )   funktional=$nfu
509                                 break 2;;
510                           [Nn]* )   break 2;;
511                           * )     echo "Please answer yes or no.";;
512                         esac
513                       done
514                     esac
515                   done
516                   while true; do
517                     read -p "Input new basis set or (S)kip! " nbs
518                     case $nbs in
519                       [Ss]* ) break;;
520                       * ) while true; do
521                         echo "New basis set: $nbs"
522                         read -p "Correct? (Y)es/(N)o? " yn
523                         case $yn in
524                           [Yy]* ) basissatz=$nbs
525                               break 2;;
526                           [Nn]* ) break 2;;
527                           * )   echo "Please answer yes or no.";;
528                         esac
529                       done
530                     esac
531                   done
532                   break;;
533                 3 ) basissatz="def2TZVPP"
534                   break;;
535                 [Qq] ) echo "Quitting."; exit;;
536                 * ) echo "Please choose an option!";;
537               esac
538             done
539             echo "Will utilize $funktional and $basissatz"
540             #Ladung und Multiplizität
541             lamu=$(grep -m 1 "Charge = " ${shortname}.out | awk '{print $3, $6}')
542             #einlesen des checkpunktfiles und funktional/basissatz aus der
    angegebenen frequenzrechnung
543             zeile1und2=$(head -n 2 ${shortname}.in)
544             #Input Geometrieoptimierung MIT ANDEREM FUNKTIONAL & BASISSATZ
545             newfile="new_${shortname}.in"
```

```
546             echo "$zeile1und2" >"$newfile"
547             echo "#p ${funktional}/${basissatz}" >> "$newfile"
548             echo "opt(tight,maxcycle=200)" >> "$newfile"
549             echo "scf(tight,maxcycle=200)" >> "$newfile"
550             echo "gfinput gfoldprint iop(6/7=3)" >> "$newfile"
551             echo "nosymm" >> "$newfile"
552             echo "" >> "$newfile"
553             echo "Geometry-optimization of ${shortname} after addition of negative
    frequency" >> "$newfile"
554             echo "" >> "$newfile"
555             echo "$lamu" >> "$newfile"
556             add_output_coordinates_to_newfile
557             echo "" >> "$newfile"
558             echo "New geometry optimization $newfile written."
559             submit_job_with_choices;;
560         [Qq] ) echo "Quitting."; exit;;
561         * ) echo "Please choose an option!";;
562       esac
563     done
564   fi
565   #Wenn alles vohanden und erfolgreich, aber neg frequenzen, dann:
566   if [ "$testin" = "1" ] && [ "$testout" = "1" ] && [ "$term" = "1" ] && [ "$nfreq"
      = "1" ]; then
567     while true; do
568       echo "Available options:"
569       echo "(1) Deflect imaginary modes and create new geometry optimization"
570       echo "(2) Create xyz-files"
571       echo "(Q) Exit"
572       read -p "Choose next step! " yn
573       case $yn in
574         1 )   #Ladung und Multiplizität
575             lamu=$(grep -m 1 "Charge = " ${shortname}.out | awk '{print $3, $6}')
576             #einlesen des checkpunktfiles und funktional/basissatz aus der
    angegebenen frequenzrechnung
577             zeile1bis3=$(head -n 3 ${shortname}.in)
578             #finden der Standard-xyz-koordinaten aus fertigem frequenz.out und
    aufteilen in atomnummer und koordinaten
579             if grep -q "Link1:  Proceeding to internal job step number  2" "${
    shortname}.out"; then
580               sed -n -e '/Link1:  Proceeding to internal job step number  2/,$p' ${
    shortname}.out | sed -n -e '/Standard orientation:/,/Rotational constants (GHZ)
    :/ p' | tail -n +6 | head -n -2 | awk '{print $4"\n"$5"\n"$6 >> "coordinates.lst
    "; print $2 >> "atoms.lst"}'
581             else
582               sed -n -e '/Standard orientation:/,/Rotational constants (GHZ):/ p' ${
    shortname}.out| tail -n +6 | head -n -2 | awk '{print $4"\n"$5"\n"$6 >> "
    coordinates.lst"; print $2 >> "atoms.lst"}'
583             fi
```

```
584
585         #Vektoren erster negativer Frequenz
586         sed -n -e '/imaginary frequencies (negative Signs)/,/                    4
                    5                        6/ p' ${shortname}.out | tail -n
    +15 | head -n -1 | awk '{print $3"\n"$4"\n"$5 >> "vectors.lst"}'
587
588         readarray -t atome < atoms.lst
589         readarray -t koordinaten < coordinates.lst
590         readarray -t vektoren < vectors.lst
591
592         #Berechnung der neuen Atomkoordinaten
593         s=0
594         for i in ${koordinaten[@]}; do
595           e=${koordinaten[$s]}
596           r=${vektoren[$s]}
597           summe[$s]=$(bc -l <<< "$e+$r")
598           ((s++))
599         done
600
601         #Standard-Input Geometrieoptimierung MIT STANDARD BASISSATZ
602         newfile="newgeo_${shortname}.in"
603         echo "$zeile1bis3" >"$newfile"
604         echo "opt(tight,maxcycle=200)" >> "$newfile"
605         echo "scf(tight,maxcycle=200)" >> "$newfile"
606         echo "gfinput gfoldprint iop(6/7=3)" >> "$newfile"
607         echo "nosymm" >> "$newfile"
608         echo "" >> "$newfile"
609         echo "Geometry-optimization of ${shortname} after addition of negative
    frequency" >> "$newfile"
610         echo "" >> "$newfile"
611         echo "$lamu" >> "$newfile"
612
613         #Einfügen der neuen Atomkoordinaten
614         s=0
615         for i in ${atome[@]}; do
616           f=$s
617           g=$f; ((g++))
618           h=$g; ((h++))
619           printf "%-10s %-20s %-20s %-20s %-20s\n" ${i} ${summe[$f]} ${summe[$g
    ]} ${summe[$h]} >> "$newfile"
620           s=$((s+3))
621         done
622         echo "" >> "$newfile"
623
624         #Clean-Up
625         rm atoms.lst
626         rm coordinates.lst
627         rm vectors.lst
```

```
628             echo "New geometry optimization $newfile written."
629
630             submit_job_with_choices
631
632             break;;
633         2) prepare_xyz-file;;
634         [Qq] ) echo "Quitting."; exit;;
635         * ) echo "Please choose an option!";;
636       esac
637     done
638   #Nur Output vorhanden, aber okay und keine negativen frequenzen:
639   elif [ "$testout" = "1" ] && [ "$testin" = "0" ] && [ "$term" = "1" ] && [ "$nfreq
      " = "0" ]; then
640     while true; do
641       echo "Available options:"
642       echo "(1) Bond analysis by nbo and wfx"
643       echo "(2) Geometry optimization with new basis set"
644       echo "(Q) Exit"
645       read -p "Choose next step! " yn
646       case $yn in
647         1 ) echo "Not yet implemented. Quitting."; exit;;
648         2 ) echo "Not yet implemented. Quitting."; exit;;
649         [Qq] ) echo "Quitting."; exit;;
650         * ) echo "Please choose an option!";;
651       esac
652     done
653   #nur Input vorhanden:
654   elif [ "$testout" = "0" ] && [ "$testin" = "1" ]; then
655       echo "Only input file found! Exiting."
656       exit
657   #Irgendwas anderes
658   else
659       echo "An error occured. Quitting!"
660       exit
661     exit
662   fi
663 elif [ "$typ" = "unknown" ]; then
664   #Check auf negative frequenzen
665   nfreq=0
666   if grep -q "imaginary" "${shortname}.out"; then nfreq=1
667     echo "Imaginary modes found!"
668   else
669     echo "No imaginary modes found!"
670   fi
671   while true; do
672     echo "Calculation type unknown! Use at your own risk!"
673     echo "Available options:"
674     echo "(1) Make frequency calculation"
```

```
675     echo "(2) Make xyz-file"
676     echo "(3) Find and deflect imaginary frequencies"
677     echo "(4) Bond analysis by nbo and wfx"
678     echo "(5) Geometry optimization with new basis set"
679     echo "(Q) Exit"
680     read -p "Choose next step! " yn
681     case $yn in
682       1 ) echo "Not yet implemented. Quitting."; exit;;
683       2 ) echo "Not yet implemented. Quitting."; exit;;
684       3 ) echo "Not yet implemented. Quitting."; exit;;
685       4 ) echo "Not yet implemented. Quitting."; exit;;
686       5 ) echo "Not yet implemented. Quitting."; exit;;
687       [Qq] ) echo "Quitting."; exit;;
688       * ) echo "Please choose an option!";;
689     esac
690   done
691 else
692   echo "An error occured!"
693   printf "Calculation Type: %s\nInputfile: %s\nOutputfile: %s\nTermination: %s\
        nNegative Frequencies:%s\n" "$typ" "$testin" "$testout" "$term" "$nfreq"
694   exit
695 fi
```

Wissenschaftliche Publikationen

ARTIKEL

Inorganics

März 2019 Comparing the Acidity of $(R_3P)_2BH$-Based Donor Groups in Iridium Pincer Complexes

L. Maser, C. Schneider, L. Alig, R. Langer, *Inorganics* **2019**, *7*(5), 61.
DOI: 10.3390/inorganics7050061

Journal of the American Chemical Society

April 2019 Quantifying the Donor Strength of Ligand-Stabilized Main Group Fragments

L. Maser, C. Schneider, L. Vondung, L. Alig, R. Langer, *J. Am. Chem. Soc.* **2019**, *141*(18), 7596–7604.
DOI: 10.1021/jacs.9b02598

Dalton Transactions

Februar 2018 Carbodiphosphorane-based nickel pincer complexes and their (de)protonated analogues: dimerisation, ligand tautomers and proton affinities

L. Maser, J. Herritsch, R. Langer, *Dalt. Trans.* **2018**, *47*(31), 10544-105552.
DOI: 10.1039/C7DT04930G

Polyhedron

September 2017 The ABC in pincer chemistry – From amine- to borylene- and carbon-based pincer-ligands

L. Maser, L. Vondung, R. Langer, *Polyhedron* **2018**, *143*, 28–42.
DOI: 10.1016/j.poly.2017.09.009

Chemical Communications

März 2017 Donor ligands based on trivalent boron formed by B-H-activation of bis(phosphine)boronium salts

M. Grätz, A. Bäcker, L. Vondung, L. Maser, A. Reincke, R. Langer, *Chem. Commun.* **2017**, *53*, 7230–7233.
DOI: 10.1039/C7CC02335A

Journal of Organometallic Chemistry

August 2015 Synthesis and Reactivity of Iron(II) Hydride Complexes Containing Diphenylphosphine Ligands

L. Maser, K. Flosdorf, R. Langer, *J. Organomet. Chem.* **2015**, 791, 6–12.
DOI: 10.1016/j.jorganchem.2015.04.030

European Journal of Inorganic Chemistry

Januar 2015 Substitutional Lability of Diphosphine Ligands in Tetrahedral Iron(II) Chloro Complexes

R. Langer, F. Bönisch, L. Maser, C. Pietzonka, L. Vondung, T. P. Zimmermann, *Eur. J. Inorg. Chem.* **2014**, *2015*, 141–148.
DOI: 10.1002/ejic.201402859

30. Oktober 2019

Nachdrucke der diskutierten Publikationen

Die Nachdrucke der im kumulativen Part diskutierten Publikationen sind in der gleichen Reihenfolge wiedergegeben und mit der Genehmigung der jeweiligen Verlage nachgedruckt:
Publikation **1**[105] und **2**[140] mit Genehmigung der *Royal Society of Chemistry*, **3**[141] mit Genehmigung von *Elsevier*, **4**[142] mit Genehmigung von *ACS Publications* (Copyright *American Chemical Society*), **5**[143] mit Genehmigung von *MDPI*.
Die *supporting informations* der Artikel sind ebenfalls nachgedruckt, die Teile mit den xyz-Koordinaten der optimierten Strukturen für quantenchemische Methoden wurden jedoch aus Platzgründen weggelassen. Das Gleiche gilt für die *crystallographic information files*. Beide sind in digitaler Form bei den Original-Publikationen und erstere in der elektronischen Version dieser Dissertation zu finden.

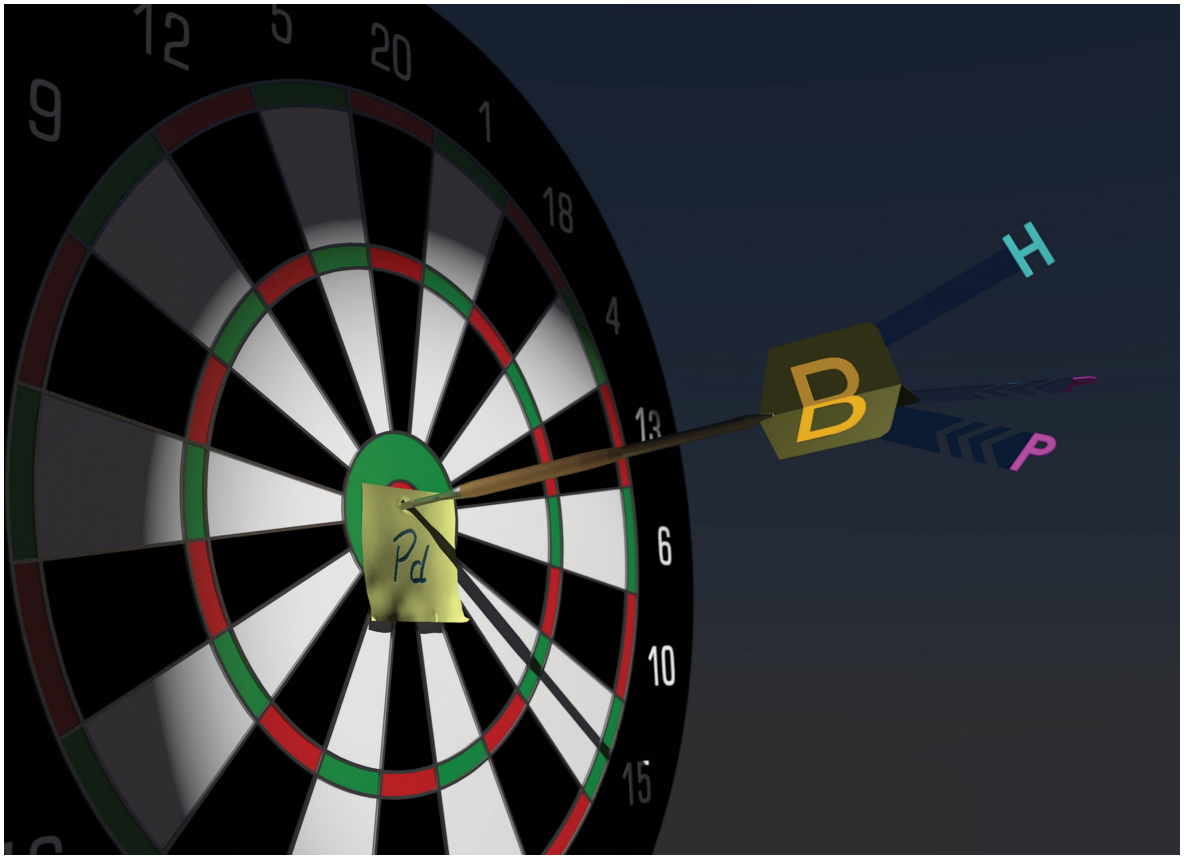

Showcasing research from the group of Robert Langer at the Department of Chemistry, Philipps-University Marburg, Germany

Donor ligands based on tricoordinate boron formed by B–H-activation of bis(phosphine)boronium salts

A novel method for the preparation of PBP-pincer complexes from bis(phosphine)boronium salts is reported. The central $(R_3P)_2HB$-moiety in a palladium complex is demonstrated to be an L-type ligand, therewith completing a series of pincer-type complexes with Z-, X- and L-type boron-based ligands.

As featured in:

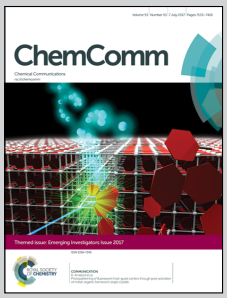

See Robert Langer *et al.*, *Chem. Commun.*, 2017, **53**, 7230.

ROYAL SOCIETY OF CHEMISTRY

rsc.li/chemcomm

Registered charity number: 207890

ChemComm

COMMUNICATION

View Article Online
View Journal | View Issue

Cite this: *Chem. Commun.*, 2017, **53**, 7230

Received 27th March 2017,
Accepted 27th April 2017

DOI: 10.1039/c7cc02335a

rsc.li/chemcomm

Donor ligands based on tricoordinate boron formed by B–H-activation of bis(phosphine)boronium salts†‡

Maik Grätz,[a] Andreas Bäcker,[a] Lisa Vondung,[a] Leon Maser,[a] Arian Reincke[a] and Robert Langer *[ab]

We report a novel method for the preparation of PBP-pincer complexes from bis(phosphine)boronium salts. The central $(R_3P)_2HB$-moiety in a palladium complex is demonstrated to be a L-type ligand, therewith completing a series of pincer-type complexes with Z-, X- and L-type boron-based ligands, respectively.

Tricoordinate boron compounds are typically Lewis acids with a vacant p_z-orbital, whose dimerization is often prevented by π-donating substituents such alkoxides or amides. The interaction of such boron-species with electron rich metal complexes is usually described by a dative bond from the central metal atom to the electron deficient BR_3-ligand.[1–18] According to the covalent bond classification these σ-accepting ligands are referred to as Z-type ligands.[19]

The utilization of at least two π-accepting substituents at the boron atom allows for the stabilization of trigonal planar compounds with an occupied p_z-orbital, which are formally construed as boron(I) compounds.[20,21] Examples for these kinds of nucleophilic boron compounds vary from tricyanoborate dianions[22–24] over dicyanoboryl anions[25] to ligand stabilized borylenes.[26–30] Quantum chemical investigations of the latter indicate that species like L_2HB: are sufficiently stabilized by cyclic alkyl amino carbenes (CAAC) and N-heterocyclic carbenes (NHC), but for ligands like carbon monoxide or phosphines the B–L-bond dissociation energy has been calculated to be rather low to expect easily accessible stable compounds.[31] However, experimental studies have shown that nucleophilic boron compounds are reacting with transition metal precursors such as [(L)MCl] (M = Cu, Au; L = phosphine, carbene)[25,32] and $[Cr(CO)_5(thf)]$.[32] Furthermore, quantum chemical investigations predict that reactive borylenes such as $(R_3P)_2HB$: can be stabilized as ligands in gold complexes.[31]

In this context, we recently observed the formation of an iron PBP-complex containing a central $(R_3P)_2HB$-group coordinated to the iron atom.[33,34] Analysis of structural and spectroscopic properties of this compound in combination with a detailed bonding analysis and reactivity studies indicated a L-type donor interaction of the tricoordinate boron-group to the central iron atom. The arm-(de)protonation of this complex results in overall dianionic, anionic and neutral pincer-type ligands without significant change of the bonding situation. However, this iron complex is formed in an odd rearrangement that exclusively occurred in the reported case.

Due to the unexpected "Umpolung" of the ligand properties in combination with the unusual reactivity, we were interested to investigate further transition metals with this pincer-type ligand. Herein we report the formation of such PBP-type pincer complexes by B–H-activation of bis(phosphine)boronium salts. Our study shows that in the case of nucleophilic metal complexes P–B-bond cleavage can be competitive. The obtained palladium(II) complex reported herein nicely illustrates the different coordination modes, ranging from $(R_3P)_2HB$-groups to LR_2B-ligands and typical BR_3-based Z-type ligands (Scheme 1).

Based on the finding that a bis(phosphine)boronium ligand is involved in the reversible B–H-reductive elimination,[34] we supposed that PBP-pincer complexes should generally be accessible by oxidative addition of $(R_3P)_2BH_2$-cations to an unsaturated metal fragment. Starting from the readily available

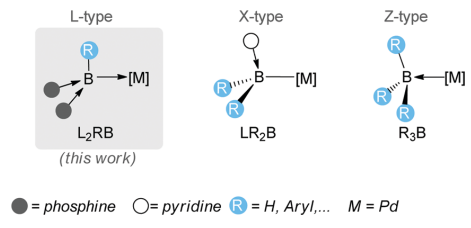

Scheme 1 Comparison of different classes of boron-based ligands.

[a] *Department of Chemistry, Philipps-Universität Marburg, Hans-Meerwein-Str., 35032 Marburg, Germany. E-mail: robert.langer@chemie.uni-marburg.de*
[b] *Lehn Institute of Functional Material (LIFM), Sun Yat-Sen University Guangzhou (SYSU), Xingang Road West, Guangzhou 510275, P. R. China*

† Dedicated to Dieter Fenske on occasion of his 75th birthday.

‡ Electronic supplementary information (ESI) available. CCDC 1540277–1540279. For ESI and crystallographic data in CIF or other electronic format see DOI: 10.1039/c7cc02335a

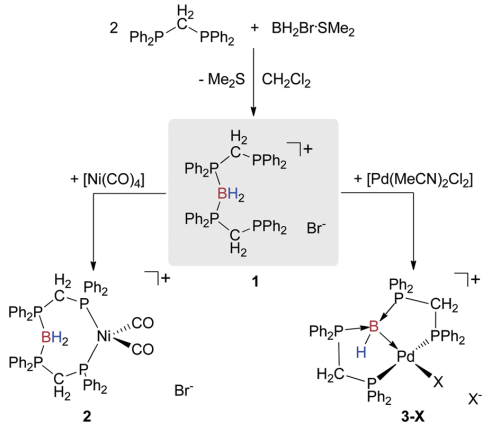

Scheme 2 Synthesis of the bis(phosphine)boronium salt **1** from dppm and its reactivity towards nickel and palladium precursors (X = Cl, Br).

1,1-bis(diphenylphosphino)methane (dppm), we attempted a possible synthesis by the reaction with 0.5 equivalents of $BH_2Br{\cdot}SMe_2$, leading to the formation of a single reaction product according to $^{31}P\{^1H\}$ and $^{11}B\{^1H\}$ NMR spectra (Scheme 2). The appearance of a broad resonance at 8.8 ppm and a doublet resonance at −22.7 ppm ($^2J_{PP}$ = 66.1 Hz) in the $^{31}P\{^1H\}$ NMR spectrum indicates that one phosphorus atom of each dppm unit is bound to boron. The broad resonance at −33.1 ppm in the $^{11}B\{^1H\}$ NMR spectrum is in agreement with previously reported bis(phosphine)boronium cations.[35–39] Upon ^{11}B-decoupling of the ^1H NMR spectrum, a triplet resonance at 2.69 ppm ($^2J_{HP}$ = 20.4 Hz) with an integral of two is observed, which is assigned to the BH_2-group. Finally, we confirmed the formation of the bis(phosphine)-boronium salt **1** by X-ray diffraction of suitable single crystals.[40]

Next, we investigated the reactivity of **1** towards different nickel and palladium precursors. The reaction with one equivalent of $[Ni(cod)_2]$ at −78 °C resulted in an orange solution, which subsequently turned darker with continued stirring. The $^{31}P\{^1H\}$ NMR spectra at ambient temperature showed several singlet resonances, indicating that P–B-bond cleavage occurred in a rather unselective reaction. In one case, it was possible to grow suitable crystals for X-ray diffraction from the reaction mixture, which were identified as $[(dppm)_3Ni_3Br_2]$.[40] However, the yield of these crystals was very low and their formation was not completely reproducible. Nonetheless, the formation of such species provides further evidence that P–B-bond cleavage is the preferred reaction pathway with $[Ni(cod)_2]$. The reaction with $[Ni(CO)_4]$ leads to a single reaction product without decomposition of the pre-ligand (Scheme 2), as judged by the appearance of a doublet resonance at 20.8 ppm ($^2J_{PP}$ = 33.3 Hz) and a broad resonance at 7.5 ppm. In agreement with the observation of a two-proton-resonance at 4.28 ppm for the BH_2-group, the single crystal X-ray diffraction analysis confirmed the formation of the cationic dicarbonyl complex **2** with an unreacted BH_2-moiety (Fig. 1). The P–B-bond distances (1.918–1.920 Å) in the eight-membered ring formed by the pre-ligand and a $Ni(CO)_2$-fragment

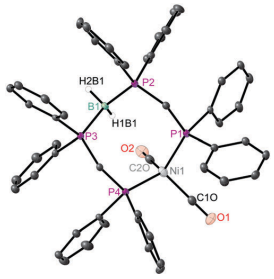

Fig. 1 Molecular structure of the cation in **2** in the solid state (ellipsoids are drawn at 30% probability, carbon-bound hydrogen atoms are omitted); selected distances (Å) and angles (°): Ni1–C2O 1.786(4), Ni1–C1O 1.788(4), Ni1–P4 2.2028(9), Ni1–P1 2.2143(9), B1–P2 1.918(4), B1–P3 1.920(4); P4–Ni1–P1 113.24(3), P2–B1–P3 118.3(2).

are slightly shorter than the distances in **1** (1.927–1.942 Å). With 2.203–2.214 Å the Ni–P-bond distances in **2** are marginally shorter than in related nickel(0)-dicarbonyl complexes with wide bite-angle diphosphine ligands.[41,42]

The reaction of **1** with palladium precursors turned out to be non-uniform as well. With $[Pd(PPh_3)_4]$, the formation of precipitate is observed and various products are detected in the $^{31}P\{^1H\}$ NMR spectrum, including the palladium(I)-complex $[(dppm)PdBr]_2$.[43] In a similar manner as with $[Ni(cod)_2]$, P–B-bond-cleavage seems to be the preferred reaction pathway. In contrast, the reaction of **1** with $[Pd(MeCN)_2Cl_2]$ leads to the formation of a precipitate, while the $^{31}P\{^1H\}$ NMR spectrum of the supernatant solution lacks any resonances. The $^{31}P\{^1H\}$ NMR spectrum of the precipitate dissolved in DMSO exhibits a doublet of doublets resonance at 81.8 ppm and a broad resonance at 59.3 ppm, indicating the formation of a novel PBP-type pincer complex $[(HB\{dppm\}_2)PdCl]^+$ (**3-Cl**).§ In addition, a triplet resonance at 84.4 ppm of low intensity is observed (ratio 9 : 1) that is assigned to the palladium-bound phosphorus atoms of the corresponding bromido complex $[(HB\{dppm\}_2)PdBr]^+$ (**3-Br**). Meanwhile, the $^{11}B\{^1H\}$ NMR spectrum exhibits only one broad resonance at −24.5 ppm, whose chemical shift is in agreement with previously reported ligand-stabilized borylenes bound to a transition metal.[25,32,44] To confirm the identities of **3**, we tried to grow suitable single crystals for X-ray diffraction, but all attempts resulted in precipitation and the crystallization of minor quantities of [**3-Br**]Br (Fig. 2).

The cationic palladium complex **3-Br** exhibits a direct Pd–B-bond (2.114–2.129 Å)[40] to the central $(R_3P)_2HB$-group of the newly formed pincer-ligand. Pd–Br- and Pd–P-distances are in agreement with other square planar palladium(II)–phosphine complexes ($\sum Pd_\alpha$ = 360.42°).[45–48]

Tricoordinate boron compounds bound to a transition metal are usually interpreted as σ-accepting Z-type ligands, which in the present case would result in the formulation of palladium(0) that, in turn, is expected to be non-square planar. However, the square planar coordination geometry and the detected bond length in **3-Br**, as well as the spectroscopic data are in agreement with a palladium(II) complex containing a boron-based donor

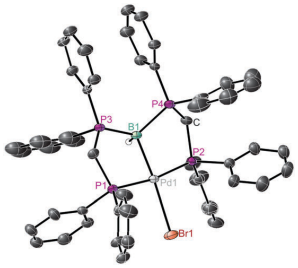

Fig. 2 Molecular structure of the cation in **3-Br** in the solid state (ellipsoids are drawn at 30% probability, carbon-bound hydrogen atoms are omitted). Selected distances (Å) and angles (°): Pd1–B1 2.129(11), Pd1–Br1 2.561(6), Pd1–P1 2.3031(15), Pd1–P2 2.3041(15), P3–B1 1.929(12), 2.005(12); P2–Pd1–P1 170.98(5), B1–Pd1–Br1 168.3(3).

ligand. To get further insight, we performed quantum chemical investigations for the methyl-substituted complexes using density functional theory (DFT). Analysis of the frontier molecular orbitals in $\mathbf{3^{Me}}$**-Cl** reveals that two B–Pd–Cl interactions are relevant for the description of the Pd–B-bond. The HOMO−2 involves a bonding interaction between boron and palladium, which appears to have π-type symmetry (Fig. 3). The HOMO−8 in $\mathbf{3^{Me}}$**-Cl** includes two bonding interactions, Pd–B and Pd–Cl, with a σ-type symmetry. The neutral palladium(II) complex [(κ^{2}P,P′-HB{dmpm}$_2$)PdBrCl] ($\mathbf{4^{Me}}$**-Cl/Br**) with a dissociated B–H-group was found to be an energetic minimum as well ($\Delta E_{3^{Me}-4^{Me}}$ = +80 kJ mol^{-1}). In agreement with previous quantum chemical investigations on phosphine-stabilized borylenes,[31] the boron atom in the dissociated $(PR_3)_2HB$-moiety exhibits a trigonal planar environment with a HOMO of π-type symmetry. The occupied p_z-orbital at the boron atom in $\mathbf{4^{Me}}$**-Cl/Br**, which is stabilized by π-back bonding to the phosphine substituents, clearly indicates the Lewis-base nature of the dissociated ligand. Natural population analysis revealed a negative charge of −0.85*e* at the boron atom in $\mathbf{3^{Me}}$**-Cl**, which is in agreement with an overall charge transfer of 0.26*e* relative to $\mathbf{4^{Me}}$**-Cl/Br**. This view is further supported by a topological analysis of the electron density within the Quantum Theory of Atoms in Molecules (QTAIM) framework. The Laplacian of the electron density shows that electron density is donated from the boron atom towards the bond critical point (bcp) of the boron palladium bond (Fig. 4).

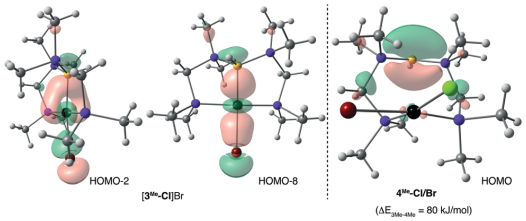

Fig. 3 HOMO−2 and HOMO−8 of complex $\mathbf{3^{Me}}$**-Cl**; HOMO of complex $\mathbf{4^{Me}}$**-Cl/Br** (B97D/def2-TZVPP, contour value 0.05, Pd: black, P: violet, Br: red, Cl: green, B: yellow).

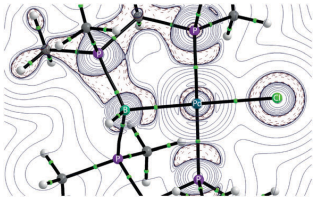

Fig. 4 Molecular graph for complex $\mathbf{3^{Me}}$**-Cl** derived from QTAIM analysis with contour plot of the Laplacian in the B–Pd–P-plane (bcps: green dots; charge depletion ($\nabla^2\rho > 0$): solid blue lines; charge accumulation ($\nabla^2\rho < 0$): dotted red lines).

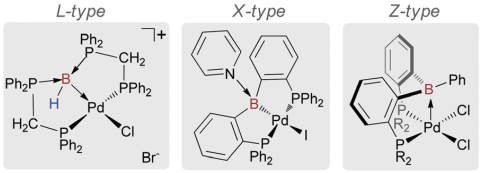

Scheme 3 Representative examples for different boron ligand types in palladium(II) complexes (R = ^{i}Pr).

A look on previously reported palladium PBP-pincer complexes reveals that the three basic ligand types according to the covalent bond classification can formally be realized in palladium(II) complexes (Scheme 3). Using an ambiphilic pincer ligand with a central BR_3-group, Bourissou and co-workers reported the square pyramidal palladium(II) complex **A**, in which the central tricoordinate boron atom (BR_3) acts as a σ-accepting Z-type ligand in the apical position.[49] Very recently, Tauchert and co-workers described the palladium(II) pincer-type complex **B** with a pyridine-stabilized boryl-group,[50] in which the central LR_2B-group can formally be regarded as a X-type ligand. The cationic palladium(II) complex **3** contains a phosphine-stabilized borylene acting as a L-type donor group. In the following, we aimed to identify differences in structural, spectroscopic and quantum chemical data (Table 1).

The long Pd–B-bond and the low pyramidalization of the boron atom in **A** indicate a rather weak interaction, while the interaction in **3** and **B** are found to be significantly stronger. The Pd–P-bond distances, however, are found to be very similar in all three complexes. A clear trend within this series of complexes is observed for the chemical shift in the $^{11}B\{^1H\}$ NMR spectra: the Z-type ligand exhibits a resonance at 59 ppm, the X-type at 17 ppm and the chemical shift for complex **3** is observed at −24.5 ppm.

We performed quantum chemical calculations of the methyl-substituted complexes $\mathbf{3^{Me}}$**-Cl**, $\mathbf{B^{Me}}$ and $\mathbf{A^{Me}}$ to obtain further information within this series: the natural population analysis reveals a positive charge of +0.90*e* at the boron atom of the Z-type ligand in $\mathbf{A^{Me}}$, which is considerably decreased for $\mathbf{B^{Me}}$ (+0.43*e*) and finally results in a negative charge of −0.85*e* for the boron atom in $\mathbf{3^{Me}}$**-Cl**. Using QTAIM analysis, we identified bcps for the Pd–B-bond in all three complexes. The electron and energy

Table 1 Selected quantum chemical and spectroscopic data, bond distances and angles

	3-X (L-type)	**B** (X-type)[a]	**A** (Z-type)[b]
d_{Pd-B}/Å	2.129	2.196	2.650
d_{Pd-P}/Å	2.203–2.204	2.275–2.284	2.288–2.315
$\sum_{B\alpha}$/°	319–343[c]	330.7	354.9
δ_B/ppm	−24.5	17	59
	$\mathbf{3^{Me}}$**-Cl**	$\mathbf{B^{Me}}$	$\mathbf{A^{Me}}$
q_B (NBO)[d]	−0.848	+0.434	+0.902
ρ_{bcp} (Pd–B)[e]	0.091	0.086	0.020
H_{bcp} (Pd–B)[e]	−0.037	−0.029	−0.009

[a] Data taken from ref. 32. [b] Data taken from ref. 31. [c] The BH-group in **3** was disordered and therefor two values are reported; the big discrepancy might be a result of inaccurate location of the hydrogen atoms. [d] Charges from natural bond orbital (NBO) analysis. [e] Electron and energy density at bond critical point (bcp) from QTAIM analysis.

densities at the bcps support this observation as well, although the qualitative interpretation of the orbital shapes and the contour plot of the Laplacians of the electron density appear quite similar for $\mathbf{3^{Me}}$**-Cl** and $\mathbf{B^{Me}}$.[40]

In conclusion, we described a synthetic method for the simple preparation of pincer-type complexes containing a phosphine-stabilized borylene as donor group (L-type). Our study shows that P–B-bond cleavage of **1** can be competitive with nucleophilic metal centres. Based on bonding analysis and the comparison of structural and spectroscopic properties, the boron-based ligand in **3** is best described as an electron donating L-type ligand. With this example, it was possible for the first time to compare structurally related palladium(II) complexes with the three different types of boron-based ligands according to the covalent bond classification.

We gratefully acknowledge financial support from the Deutsche Forschungsgemeinschaft (LA 2830/3-2), the Erich-Becker-Stiftung (R. L.) and the Studienstiftung des deutschen Volkes (L. V.). We also thank Dr Paul Jerabek and Prof. Dr Peter Schwerdtfeger for helpful discussions.

Notes and references

§ Further indication for **3-Cl** being the major isomer is provided by ESI-MS.

1 A. F. Hill, G. R. Owen, A. J. P. White and D. J. Williams, *Angew. Chem., Int. Ed.*, 1999, **38**, 2759–2761.
2 H. Braunschweig and R. D. Dewhurst, *Dalton Trans.*, 2011, **40**, 549–558.
3 G. R. Owen, P. H. Gould, A. Hamilton and N. Tsoureas, *Dalton Trans.*, 2010, **39**, 49–52.
4 G. R. Owen, P. Hugh Gould, J. P. H. Charmant, A. Hamilton and S. Saithong, *Dalton Trans.*, 2010, **39**, 392–400.
5 N. Tsoureas, Y.-Y. Kuo, M. F. Haddow and G. R. Owen, *Chem. Commun.*, 2011, **47**, 484–486.
6 J. S. Figueroa, J. G. Melnick and G. Parkin, *Inorg. Chem.*, 2006, **45**, 7056–7058.
7 V. K. Landry, J. G. Melnick, D. Buccella, K. Pang, J. C. Ulichny and G. Parkin, *Inorg. Chem.*, 2006, **45**, 2588–2597.
8 K. Pang, S. M. Quan and G. Parkin, *Chem. Commun.*, 2006, 5015–5017.
9 K. Pang, J. M. Tanski and G. Parkin, *Chem. Commun.*, 2008, 1008–1010.
10 M. E. Moret and J. C. Peters, *Angew. Chem., Int. Ed.*, 2011, **50**, 2063–2067.
11 M. E. Moret and J. C. Peters, *J. Am. Chem. Soc.*, 2011, **133**, 18118–18121.
12 H. Fong, M. E. Moret, Y. Lee and J. C. Peters, *Organometallics*, 2013, **32**, 3053–3062.
13 I. R. Crossley, A. F. Hill and A. C. Willis, *Organometallics*, 2005, **24**, 1062–1064.
14 I. R. Crossley, A. F. Hill and A. C. Willis, *Organometallics*, 2006, **25**, 289–299.
15 I. R. Crossley, M. R. S. J. Foreman, A. F. Hill, G. R. Owen, A. J. P. White, D. J. Williams and A. C. Willis, *Organometallics*, 2008, **27**, 381–386.
16 I. R. Crossley and A. F. Hill, *Dalton Trans.*, 2008, 201–203.
17 I. R. Crossley, A. F. Hill and A. C. Willis, *Organometallics*, 2008, **27**, 312–315.
18 I. R. Crossley, A. F. Hill and A. C. Willis, *Organometallics*, 2010, **29**, 326–336.
19 M. L. H. Green, *J. Organomet. Chem.*, 1995, **500**, 127–148.
20 J. Cid, H. Gulyas, J. J. Carbo and E. Fernandez, *Chem. Soc. Rev.*, 2012, **41**, 3558–3570.
21 H. Gulyás, A. Bonet, C. Pubill-Ulldemolins, C. Solé, J. Cid and E. Fernández, *Pure Appl. Chem.*, 2012, **84**, 2219.
22 E. Bernhardt, V. Bernhardt-Pitchougina, H. Willner and N. Ignatiev, *Angew. Chem., Int. Ed.*, 2011, **50**, 12085–12088.
23 J. Landmann, F. Keppner, D. B. Hofmann, J. A. P. Sprenger, M. Häring, S. H. Zottnick, K. Müller-Buschbaum, N. V. Ignat'ev and M. Finze, *Angew. Chem., Int. Ed.*, 2017, **56**, 2795–2799.
24 J. Landmann, J. A. P. Sprenger, R. Bertermann, N. Ignat'ev, V. Bernhardt-Pitchougina, E. Bernhardt, H. Willner and M. Finze, *Chem. Commun.*, 2015, **51**, 4989–4992.
25 D. A. Ruiz, G. Ung, M. Melaimi and G. Bertrand, *Angew. Chem., Int. Ed.*, 2013, **52**, 7590–7592.
26 H. Braunschweig, R. D. Dewhurst, F. Hupp, M. Nutz, K. Radacki, C. W. Tate, A. Vargas and Q. Ye, *Nature*, 2015, **522**, 327–330.
27 F. Dahcheh, D. Martin, D. W. Stephan and G. Bertrand, *Angew. Chem., Int. Ed.*, 2014, **53**, 13159–13163.
28 R. Kinjo, B. Donnadieu, M. A. Celik, G. Frenking and G. Bertrand, *Science*, 2011, **333**, 610–613.
29 D. A. Ruiz, M. Melaimi and G. Bertrand, *Chem. Commun.*, 2014, **50**, 7837–7839.
30 M. Soleilhavoup and G. Bertrand, *Acc. Chem. Res.*, 2015, **48**, 256–266.
31 M. A. Celik, R. Sure, S. Klein, R. Kinjo, G. Bertrand and G. Frenking, *Chem. – Eur. J.*, 2012, **18**, 5676–5692.
32 L. Kong, R. Ganguly, Y. Li and R. Kinjo, *Chem. Sci.*, 2015, **6**, 2893–2902.
33 N. Frank, K. Hanau, K. Flosdorf and R. Langer, *Dalton Trans.*, 2013, **42**, 11252–11261.
34 L. Vondung, N. Frank, M. Fritz, L. Alig and R. Langer, *Angew. Chem., Int. Ed.*, 2016, **55**, 14450–14454.
35 S. A. Westcott, H. P. Blom, T. B. Marder, R. T. Baker and J. C. Calabrese, *Inorg. Chem.*, 1993, **32**, 2175–2182.
36 M. Sigl, A. Sehier and H. Schmidbaur, *Chem. Ber.*, 1997, **130**, 1411–1416.
37 T. A. Shuttleworth, M. A. Huertos, I. Pernik, R. D. Young and A. S. Weller, *Dalton Trans.*, 2013, **42**, 12917–12925.
38 K. Owsianik, R. Chauvin, A. Balińska, M. Wieczorek, M. Cypryk and M. Mikołajczyk, *Organometallics*, 2009, **28**, 4929–4937.
39 T. Costa and H. Schmidbaur, *Chem. Ber.*, 1982, **115**, 1374–1378.
40 For further details please see ESI‡.
41 S. Wu, X. Li, Z. Xiong, W. Xu, Y. Lu and H. Sun, *Organometallics*, 2013, **32**, 3227–3237.
42 C. F. Czauderna, A. G. Jarvis, F. J. L. Heutz, D. B. Cordes, A. M. Z. Slawin, J. I. van der Vlugt and P. C. J. Kamer, *Organometallics*, 2015, **34**, 1608–1618.
43 R. G. Holloway, B. R. Penfold, R. Colton and M. J. McCormick, *J. Chem. Soc., Chem. Commun.*, 1976, 485–486.
44 L. Kong, Y. Li, R. Ganguly, D. Vidovic and R. Kinjo, *Angew. Chem., Int. Ed.*, 2014, **53**, 9280–9283.
45 A. Naghipour, A. Ghorbani-Choghamarani, H. Babaee and B. Notash, *Appl. Organomet. Chem.*, 2016, **30**, 998–1003.
46 S. Ganguly, J. T. Mague and D. M. Roundhill, *Inorg. Chem.*, 1992, **31**, 3500–3501.
47 H. Braunschweig, K. Radacki, D. Rais and K. Uttinger, *Angew. Chem., Int. Ed.*, 2006, **45**, 162–165.
48 H. Braunschweig, K. Gruss, K. Radacki and K. Uttinger, *Eur. J. Inorg. Chem.*, 2008, 1462–1466.
49 S. Bontemps, M. Sircoglou, G. Bouhadir, H. Puschmann, J. K. Howard, P. W. Dyer, K. Miqueu and D. Bourissou, *Chem. – Eur. J.*, 2008, **14**, 731–740.
50 D. Schuhknecht, F. Ritter and M. E. Tauchert, *Chem. Commun.*, 2016, **52**, 11823–11826.

Electronic Supplementary Material (ESI) for ChemComm.

Supporting Information

Donor ligands based on tricoordinate boron formed by B-H-activation of bis(phosphine)boronium salts

Maik Grätz,[a] Andreas Bäcker,[a] Lisa Vondung,[a] Leon Maser,[a] Arian Reincke,[a] Robert Langer*[,a,b]

1. **Experimental Details**
2. **NMR spectra**
3. **X-Ray Crystallography**
4. **DFT Calculations**

[a]*Department of Chemistry, Philipps-Universität Marburg, Hans-Meerwein-Str., 35043 Marburg, Germany, Fax: (+)49-6421-2825617, E-mail: robert.langer@chemie.uni-marburg.de*

[b]Lehn Institute of Functional Materials (LIFM), Sun Yat-Sen University (SYSU), Xingang Road West, Guangzhou 510275, PR China.

1. Experimental Details

Material and Methods

All experiments were carried out under an atmosphere of purified argon in a MBraun Labmaster glove box or using standard Schlenk techniques. THF and C_6D_6 were dried and distilled from Na/K alloy and stored over molecular sieves. *n*-Hexane was dried and distilled from $LiAlH_4$ and stored over molecular sieves. Toluene was dried and distilled from sodium and stored over molecular sieves. Bis(diphenylphosphino)methane (dppm) was prepared according to a previously reported procedure.[1]

^{1}H, ^{13}C, ^{31}P and ^{11}B NMR spectra were recorded using Bruker DRX 400, DRX 500 and Avance 500 NMR spectrometers. ^{1}H and $^{13}C\{^{1}H\}$, ^{13}C-APT (attached proton test) NMR chemical shifts are reported in ppm downfield from tetramethylsilane. The resonance of the residual protons in the deuterated solvent was used as internal standard for ^{1}H NMR. The solvent peak of the deuterated solvent was used as internal standard for ^{13}C NMR. ^{31}P NMR chemical shifts are reported in ppm downfield from H_3PO_4 and referenced to an external 85% solution of phosphoric acid in D_2O. ^{11}B NMR chemical shifts are reported in ppm downfield from $BF_3{\cdot}Et_2O$ and referenced to an external solution of $BF_3{\cdot}Et_2O$ in $CDCl_3$. The following abbreviations are used for the description of NMR data: br (broad), s (singlet), d (doublet), t (triplet), q (quartet), quin (quintet), m (multiplet), v (virtual).

FT-IR spectra were recorded by attenuated total reflection of the solid samples on a Bruker Tensor IF37 spectrometer. The intensity of the absorption band is indicated as vw (very weak), w (weak), m (medium), s (strong), vs (very strong) and br (broad).

HR-ESI mass spectra were acquired with a LTQ-FT mass spectrometer (Thermo Fisher Scientific). The resolution was set to 100.000.

Synthesis of $[H_2B(dppm)_2]Br$ (1)

dppm (880 mg, 2.2 mmol) was dissolved in CH_2Cl_2 (6 mL) and a solution of $BH_2Br{\cdot}SMe_2$ in CH_2Cl_2 (1 M, 1.1 mL, 1.1 mmoL) was added. After stirring for 10 d, reaction control via $^{31}P\{^{1}H\}$ NMR indicated no further conversion of *dppm*. The solvent was removed under reduced pressure and the residue was washed with Et_2O/THF (2:1, 5x 10 mL). The solvent was removed under high vacuum to obtain *$[H_2B(dppm)_2]Br$* (560 mg, 0.65 mmol, 59 %) as

colorless crystalline solid (M = 861.51 g·mol^{-1}). ^{1}H-NMR (300 MHz, THF-d_8, 27 °C) δ = 4.05 (d, 4H, $^{3}J_{HH}$ = 12.3 Hz, CH_2) 7.03-7.16 (m, 16H, phenyl-*H*), 7.19-7.27 (m, 8H, phenyl-*H*), 7.51-7.59 (m, 8H, phenyl-*H*), 7.61-7.72 (m, 8H, phenyl-*H*) ppm. Boron-bound protons were not observed. ^{11}B{^{1}H} NMR (96 MHz, CD_2Cl_2, 27 °C) δ = -34.0 (br) ppm. Only resonances that are changing upon ^{11}B-decoupling are listed in the ^{1}H{^{11}B} NMR spectrum. ^{1}H{^{11}B}NMR (300 MHz, THF-d_8, 27 °C) δ = 2.65 (t, 2H, $^{2}J_{HP}$ = 20.4 Hz, BH_2) ppm. ^{31}P{^{1}H} NMR (122 MHz, CD_2Cl_2, 27 °C) δ = -25.2 (d, $^{2}J_{PP}$ = 67.1 Hz, P-CH_2-*P*), 7.5 (br, *P*-BH_2-*P*) ppm. ^{13}C{^{1}H} NMR (76 MHz, CD_2Cl_2, 27 °C) δ = 22,7 (dd, $^{1}J_{PC}$ = 39.2 Hz, $^{1}J_{PC}$ = 34.2 Hz, P-*C*H_2-P), 124.3 (dd, J_{PC} = 61.6 Hz, J_{PC} = 2.8 Hz, phenyl-*C*), 124.3 (d, J_{PC} = 70.6 Hz, phenyl-*C*), 128.9 (s, phenyl-*C*), 129.1 (s, phenyl-*C*), 129.6 (s, phenyl-*C*), 129.8 (d, J_{PC} = 1.5 Hz, phenyl-*C*), 132.8 (s, phenyl-*C*), 132.9 (s, phenyl-*C*), 133.0 (s, phenyl-*C*), 133.2 (s, phenyl-*C*), 133.3 (d, J_{PC} = 2.8 Hz, phenyl-*C*), 136.3 (d, J_{PC} = 7.3 Hz, phenyl-*C*), 136.5 (d, J_{PC} = 7.3 Hz, phenyl-*C*) ppm. FT-IR (ATR) $\tilde{\nu}$/cm^{-1}: 3050 (w), 3008 (w), 2983 (w), 2846 (w), 2440 (w), 2394 (w), 1586 (w), 1482 (w), 1435 (m), 1365 (w), 1314 (w), 1189 (w), 1160 (w), 1106 (m), 1070 (w), 1026 (w) 997 (w), 915 (w), 776 (m), 740 (s), 721 (m), 690 (s), 633 (m). HRMS (ESI^{+}) m/z: 781.2643 (calculated for $C_{50}H_{46}BP_4$), 781.2646 (found, Δ = 0.4 ppm).

Synthesis of [(H_2B{dppm}$_2$)Ni(CO)$_2$]Br (2)

[Ni(CO)$_4$] (24 mg, 0.14 mmol) was added to a solution of **1** (120 mg, 0.14 mmol) in 5 mL THF and the resulting solution was stirred for five hours at ambient temperature. After this period the extent of conversion was checked by ^{31}P{^{1}H} NMR spectroscopy. Addition of 10 mL *n*-hexane resulted in precipitation of **2**. The supernatant solution was decanted off and the precipitate was dried *in vacuo*. Yield: 12 mg (0.012 mmol, 8.5 %). The yield can be increased significantly by removal of all volatiles from the reaction mixture and continuous washing of the residue, but the obtained product contains inseparable byproducts according to the ^{31}P{^{1}H} NMR spectrum. ^{1}H NMR (300 MHz, CD_3CN, 27 °C) δ = 3.82 (br, 4H, CH_2), 7.05-7.14 (m, 10H, phenyl-*H*), 7.19 (dd, 4H, J_{HH} = 7.3 Hz, J_{HH} = 1.1 Hz, phenyl-*H*), 7.24-7.35 (m, 10H, phenyl-*H*), 7.40 (t br, 10H, *J* = 9.0 Hz, phenyl-*H*), 7.62-7.82 (m, 6H, phenyl-*H*) ppm. ^{11}B{^{1}H} NMR (96 MHz, C_6D_6, 27 °C) δ = -35.8 (br) ppm. Only resonances that are changing upon decoupling are listed for the ^{1}H{^{11}B} NMR spectrum. ^{1}H{^{11}B} NMR (300 MHz, C_6D_6, 27 °C) δ = 4.25 (br, 2H, BH_2) ppm. ^{31}P{^{1}H}NMR (122 MHz, $CDCl_3$, 27 °C) δ = 4.9 (br, *P*-B-*P*), 18.1 (ddd, J_{PP} = 38.4 Hz, J_{PP} = 12.0 Hz, J_{PP} = 4.0 Hz, *P*-Ni-*P*) ppm. ^{13}C-APT NMR (76 MHz, CD_3CN, 27 °C) δ = 23.8 (d, $^{1}J_{PC}$ = 36.7 Hz, P-*C*H_2-P), 129.1 (vt, J_{PC} = 4.8 Hz, phenyl-*C*), 129.8 (d, J_{PC} = 11.8 Hz, phenyl-*C*), 130.3 (s, phenyl-*C*), 130.5 (s, phenyl-*C*), 130.6 (s, phenyl-*C*), 133.0 (d, J_{PC} = 9.6 Hz, phenyl-*C*), 133.2 (d, J_{PC} = 2.8 Hz, phenyl-*C*) ppm. The

resonances for carbonyl ligands and for the quaternary carbon atoms of the phenyl rings were not observed. FT-IR (ATR) $\tilde{\upsilon}$/cm^{-1}: 2963 (w) 2905 (w) 2376 (w) 2360 (w) 2349 (w) 2343 (w) 2323 (w) 2298 (w) 2002 (w, ν_{CO}) 1939 (w, ν_{CO}) 1484 (w) 1435 (w) 1413 (w) 1258 (m) 1009 (s) 864 (m) 787 (s) 687 (m) 671 (m) 664 (m) 470 (m) 417 (m). HRMS (ESI$^+$) m/z: 867.1949 (calculated for [(H$_2$B{dppm}$_2$)Ni(CO)]$^+$), 867.1945 (found, Δ = 0.5 ppm); 839.1993 (calculated for [(H$_2$B{dppm}$_2$)Ni]$^+$), 839.1999 ((found, Δ = 0.7 ppm).

Synthesis of [(HB{dppm}$_2$)PdX]X (3, X = Cl, Br)

[H$_2$B(dppm)$_2$]Br (**1**, 40 mg, 0.046 mmol) and [PdCl$_2$(MeCN)$_2$] (12 mg, 0.046 mmol) were dissolved in 5 mL THF and stirred at ambient temperature for 5 hours. During this period, the solution brightened up and precipitate was formed. The supernatant solution was decanted off, the residue was washed with 5 mL THF and dried *in vacuo*. Complex **3** was formed and isolated as a mixture of the two constitutional isomers, with the two cations [[(HB{dppm}$_2$)PdCl]$^+$ (**3-Cl**, ~90 %) and [[(HB{dppm}$_2$)PdBr]$^+$ (**3-Br**, ~10 %). Both isomers are very similar in their spectroscopic properties. In several attempts to grow single crystals with different solvents and under various conditions only single crystals from [**3-Br**]Br could be obtained. Yield: 34.8 mg (0.035 mmol, 76 %). ^{1}H NMR (300 MHz, DMSO-d_6, 27 °C) δ = 2.52 (partly superimposed, 4H, $^2J_{PH}$ = 4.0 Hz, CH_2), 7.10-7.20 (m, 8H, phenyl-*H*), 7.36-7.61 (m, 20H, phenyl-*H*), 7.61-7.79 (m, 10H, phenyl-*H*), 8.50 (br t, 2H, J_{HH} = 2.7 Hz, phenyl-*H*) ppm. ^{11}B{^{1}H} NMR (96 MHz, DMSO-d_6, 27 °C) δ = -24.5 (br) ppm. Only resonances that are changing upon decoupling are listed for the ^{1}H{^{11}B} NMR spectrum. ^{1}H{^{11}B} NMR(300 MHz, DMSO-d_6, 27 °C) δ = 3.57 (br t, 1H, $^2J_{HP}$ = 17.9 Hz, B*H*) ppm. ^{31}P{^{1}H} NMR (122 MHz, DMSO-d_6, 27 °C) δ = 59.3 (br, *P*-B-*P*), 81.8 (dd, $^2J_{PP}$ = 76.4 Hz, $^2J_{PP}$ = 68.1 Hz, Ph$_2$*P*-Pd-Cl), 84.4 (t, $^2J_{PP}$ = 71.9 Hz, Ph$_2$*P*-Pd-Br) ppm. ^{13}C{^{1}H} NMR (76 MHz, DMSO-d_6, 27 °C) δ = 38.5-40.5 (P-*C*H$_2$-P, superimposed by DMSO-d_6), 128.2-128.6 (superimposed resonances, phenyl-*C*), 128.7 (vt, J_{PC} = 5.7 Hz, phenyl-*C*), 129.3 (vt, J_{PC} = 5.7 Hz, phenyl-*C*), 130.8 (s, phenyl-*C*), 131.0 (s, phenyl-*C*), 131.3-131.8 (superimposed resonances, phenyl-*C*), 132.4 (vt, J_{PC} = 6.2 Hz, phenyl-*C*), 132.7 (s, phenyl-*C*), 132.9 (s, phenyl-*C*), 134.0 (dd, $^1J_{PC}$ = 23.7 Hz, J_{PC} = 2.9 Hz, phenyl-*C*) ppm. FT-IR (ATR) $\tilde{\upsilon}$ / cm^{-1}: 3053 (w), 3015 (w), 2963 (w), 2905 (w), 2586 (w), 2370 (w), 2361 (w), 2349 (w) 2343 (w), 2323 (w), 2298 (w), 1587 (w), 1572 (w), 1483 (w), 1435 (m), 1411 (w), 1307 (m), 1259 (s), 1188 (w), 1086 (s), 1013 (s), 935 (m) 865 (w), 792 (s), 737 (m), 689 (s), 665 (m), 619 (w), 604 (w), 559 (m), 533 (m), 504 (m), 485 (m), 451 (w), 406 (w). HRMS (ESI$^+$) m/z: 921.1303 (calculated for [(HB{dppm}$_2$)PdCl]$^+$), 921.1305 (found, Δ = 0.2 ppm).

2. NMR Spectra

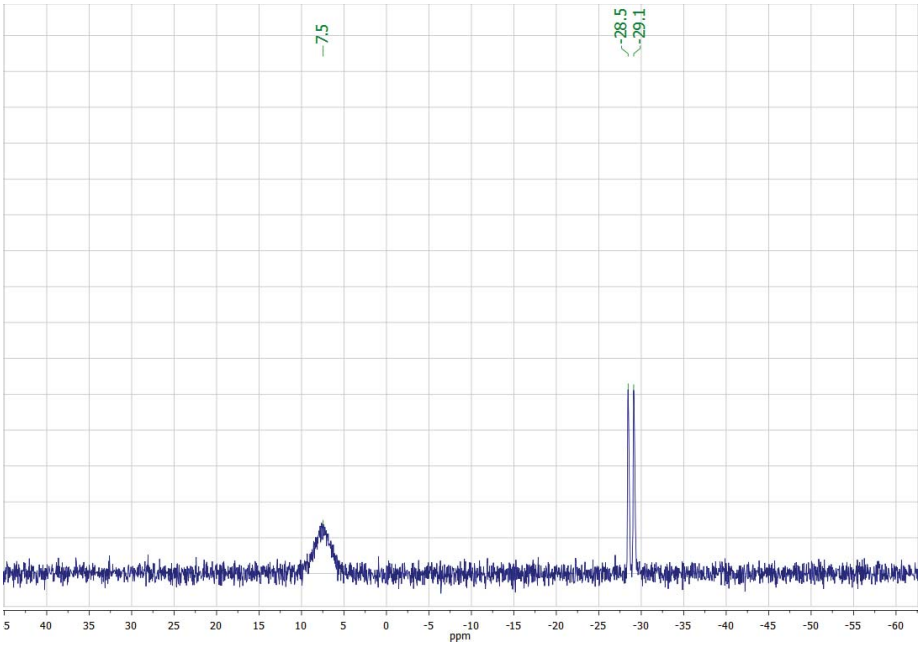

Figure 1 $^{31}P\{^{1}H\}$ NMR spectrum of compound **1** in CD_2Cl_2.

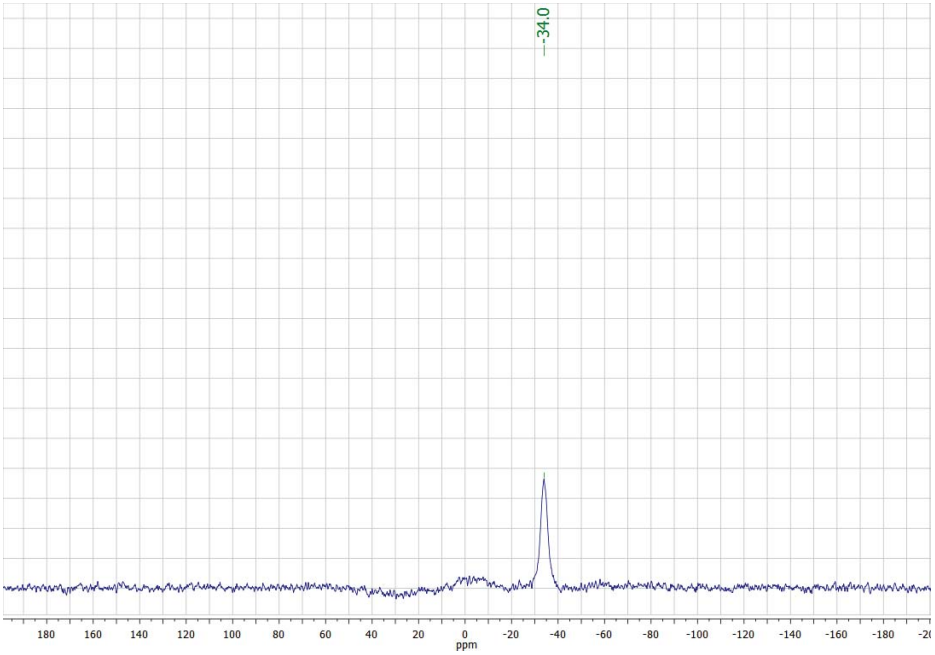

Figure 2 $^{11}B\{^{1}H\}$ NMR spectrum of compound **1** in CD_2Cl_2.

S5

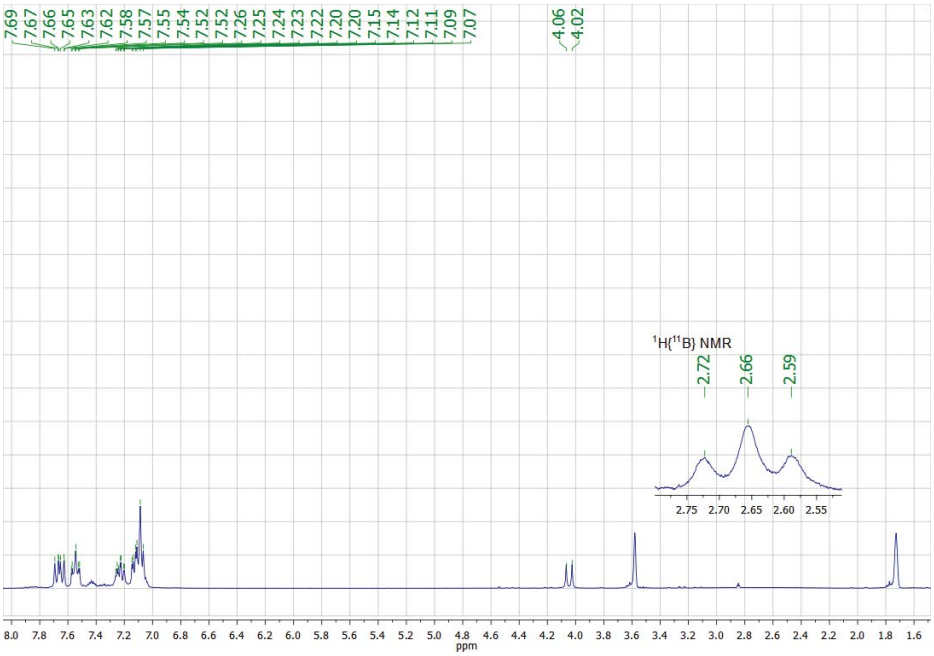

Figure 3 ^{1}H NMR spectrum of compound **1** in THF-d_8, with an inset showing the resonance of the boron-bound H-atoms in the $^{1}H\{^{11}B\}$NMR spectrum .

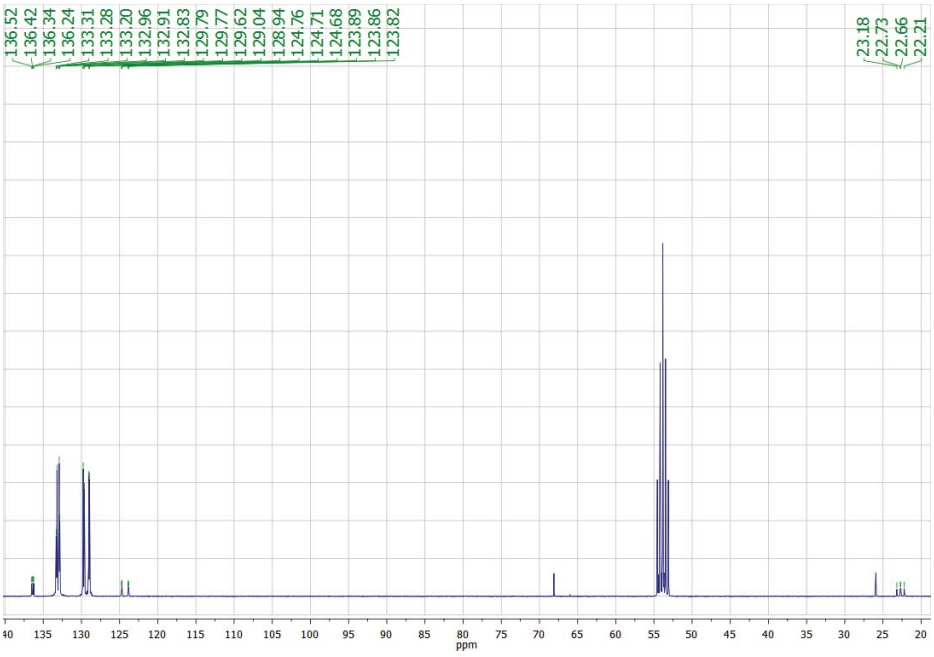

Figure 4 $^{13}C\{^{1}H\}$ NMR spectrum of compound **1** in CD_2Cl_2.

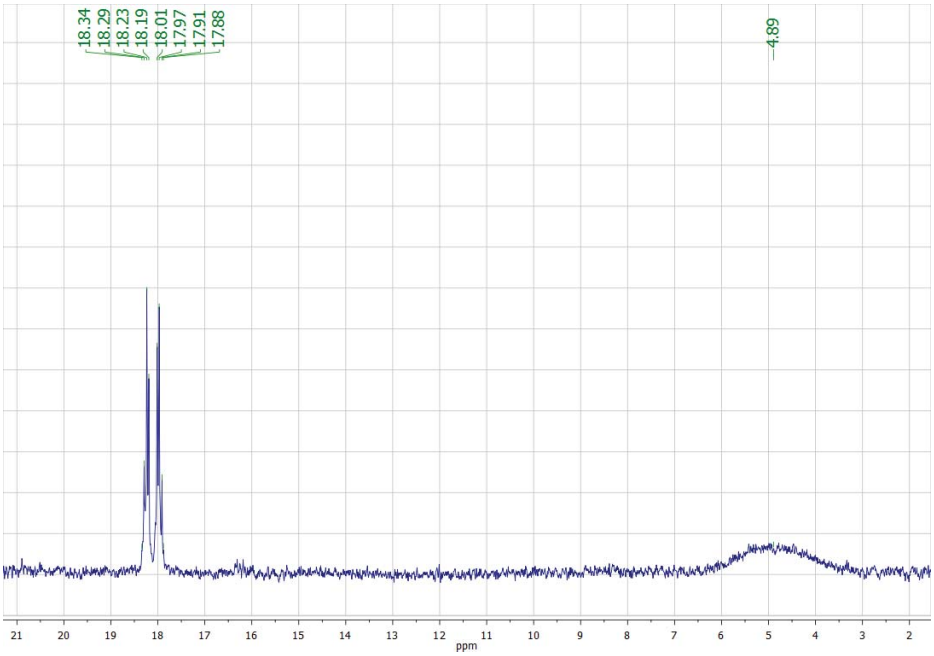

Figure 5 $^{31}P\{^{1}H\}$ NMR spectrum of complex **2** in CD_3CN.

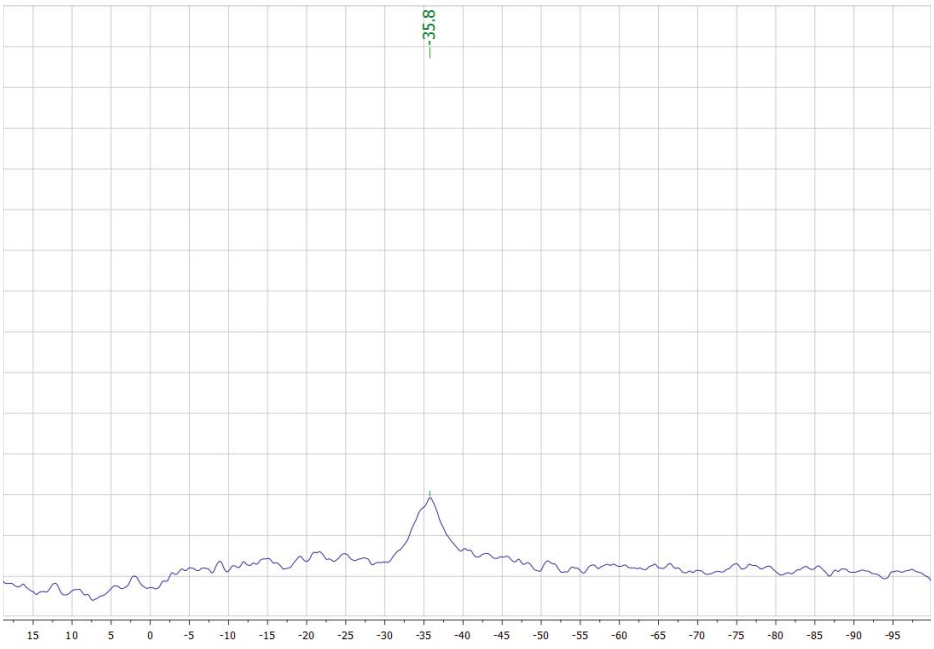

Figure 6 $^{11}B\{^{1}H\}$ NMR spectrum of complex **2** in CD_3CN.

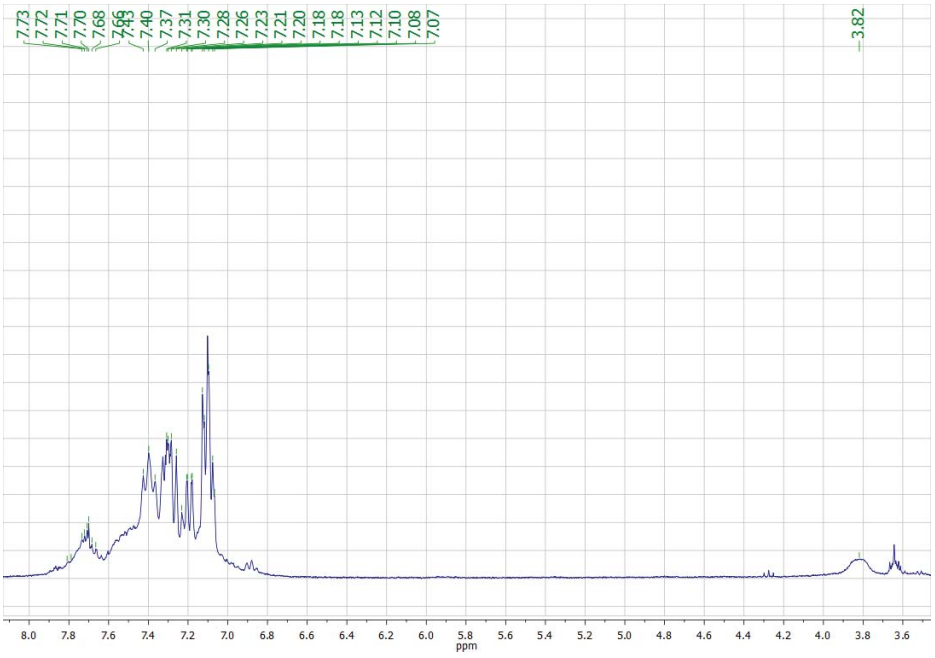

Figure 7 ^{1}H NMR spectrum of complex **2** in CD_3CN.

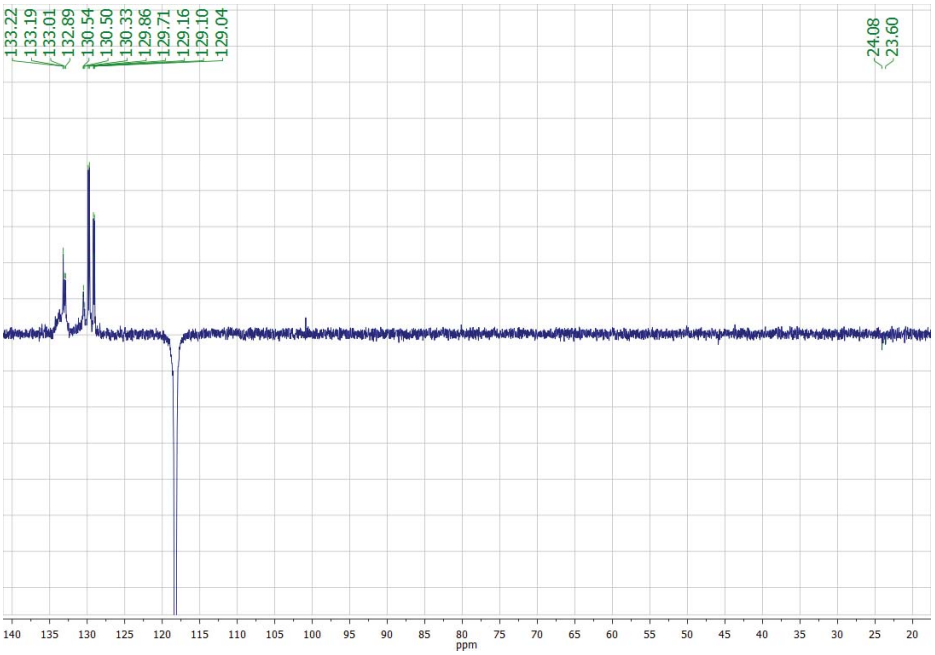

Figure 8 ^{13}C-APT NMR spectrum of complex **2** in CD_3CN.

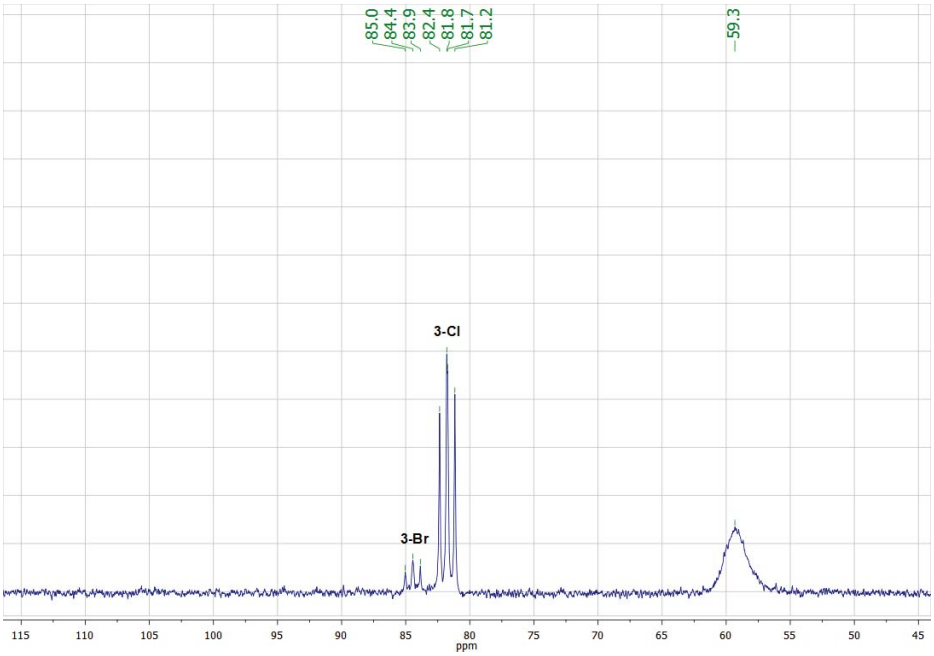

Figure 9 $^{31}P\{^{1}H\}$ NMR spectrum of complex **3** in DMSO-d_6.

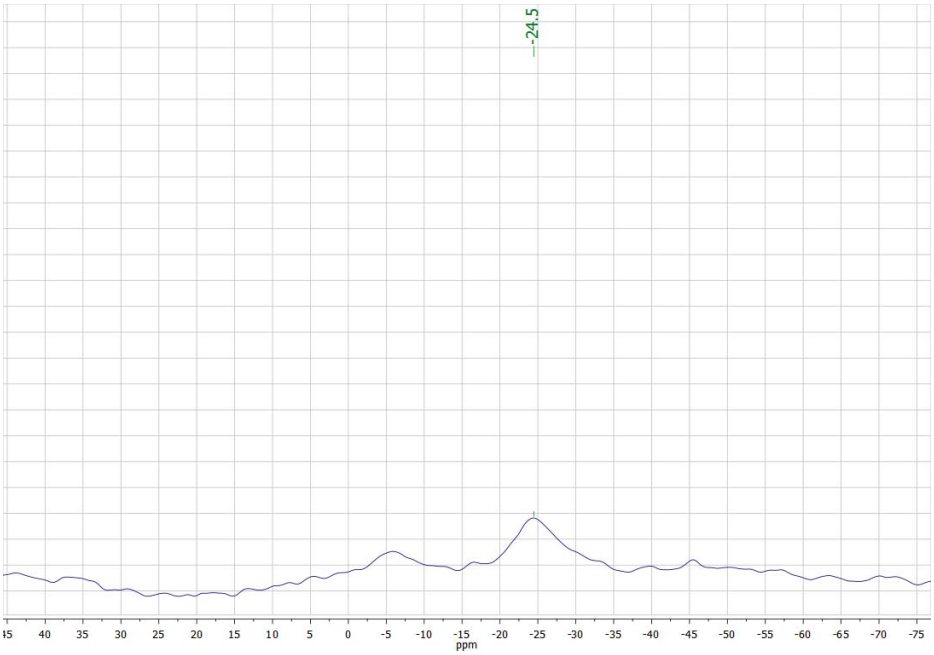

Figure 10 $^{11}B\{^{1}H\}$ NMR spectrum of complex **3** in DMSO-d_6.

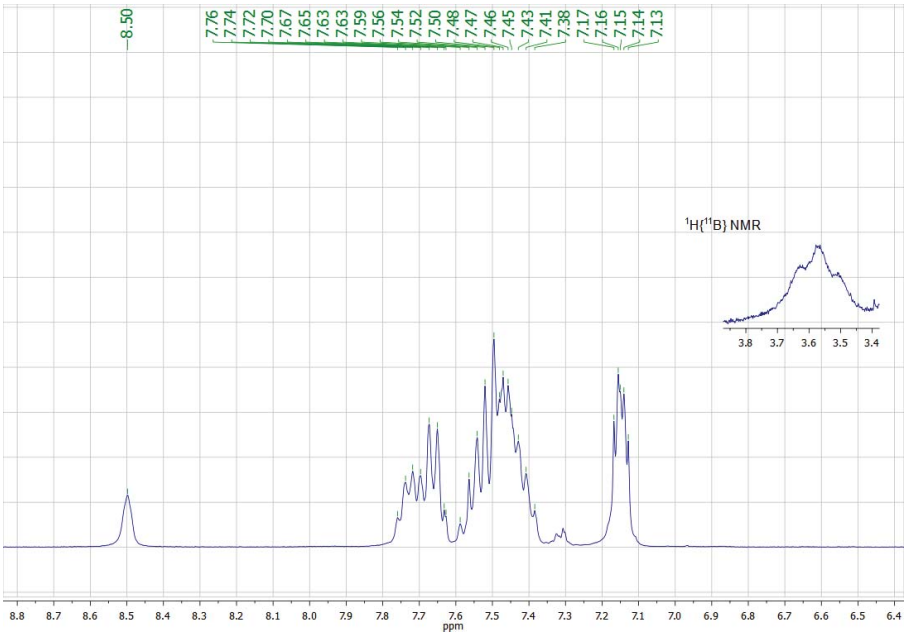

Figure 11 ^{1}H NMR spectrum of complex **3** in DMSO-d_6, with an inset showing the resonance of the boron-bound H-atom in the $^{1}H\{^{11}B\}$NMR spectrum.

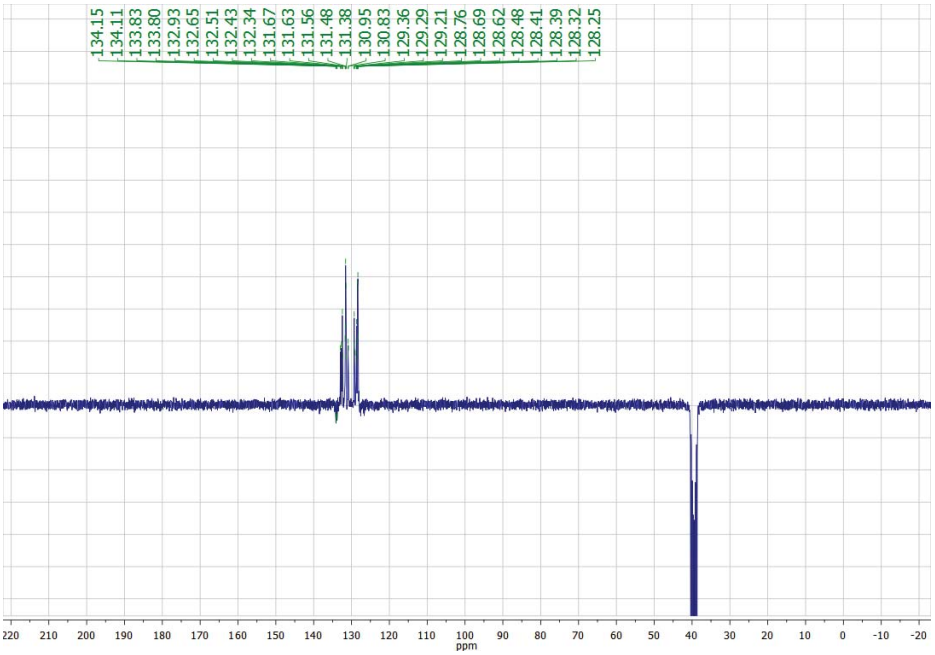

Figure 12 ^{13}C-APT NMR spectrum of complex **3** in DMSO-d_6.

X-Ray Crystallography

The single crystal X-ray diffraction data for the structural analysis of **1** has been collected using graphite-monochromated Mo-K_α-radiation ($\lambda_{MoK\alpha}$ = 0.71073) on the image plate system IPDSII, **2·1$^1/_2$THF** and **[3-Br]Br·1$^1/_4$THF** have been collected using graphite-monochromated Mo-K_α-radiation ($\lambda_{MoK\alpha}$ = 0.71073) on the pixel detector system BRUKER D8-QUEST. The structures were solved by direct methods with SHELXS-97 and refined against F^2 by full-matrix-least-square techniques using SHELXL-97.[2] Based on the crystal descriptions, numerical absorption corrections were applied.[3, 4] Crystallographic data for **1**, **2·1$^1/_2$THF** and **[3-Br]Br·1$^1/_4$THF** have been deposited at Cambridge Crystallographic Data Centre (CCDC 1540277-1540279) and can be obtained free of charge via www.ccdc.cam.ac.uk/. Details of the data collection and the refinement can be found in Table 1. Figure 13 shows the molecular structure of **1** in the solid state.

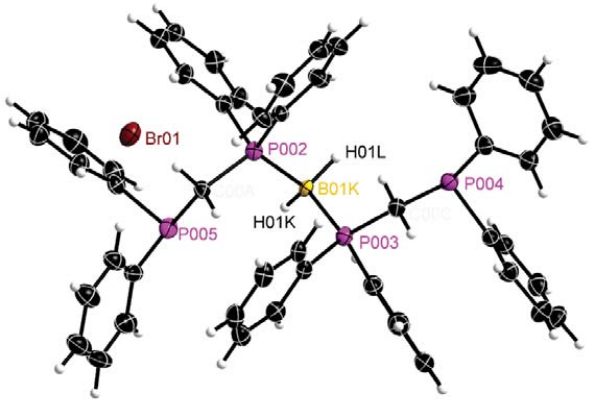

Figure 13 Molecular structure of **1** in the solid state (ellipsoids are drawn at 30 % probability, carbon-bound hydrogen atoms are omitted).

Table 1 Crystallographic data for **1**-**3**.

Compound	**1**	**2**·1^1/$_2$**THF**	**[3-Br]Br**·1^1/$_4$**THF**
Empirical formula	$C_{50}H_{46}BBrP_4$	$C_{52}H_{46}BBrNiO_2P_4 \cdot 1^1/_2C_4H_8O$	$C_{50}H_{45}BBr_2P_4Pd \cdot 1^1/_2C_4H_8O$
Fw/g·mol^{-1}	861.47	1084.35	1136.90
T/K	100(2)	100(2)	110(2)
Crystal system	Orthorhombic	Monoclinic	Monoclinic
Space group	$P2_12_12_1$	$P2_1/c$	$P2_1/n$
a/Å	10.306(2)	16.5199(6)	9.6936(3)
b/Å	13.535(3)	13.4032(6)	24.8956(9)
c/Å	30.934(6)	25.3996(11)	23.1874(10)
α/°	90	90	90
β/°	90	96.7900(10)	91.2630(10)
γ/°	90	90	90
V/Å^3	4315.0(15)	5584.5(4)	5594.4(4)
Z	4	4	4
ρ_{calc}/g·cm^{-3}	1.326	1.290	1.350
$\mu(MoK_\alpha)$/mm^{-1}	1.136	1.220	1.910
F(000)	1784	2248	2304
2θ range/°	2.63-53.44	4.43-53.46	4.51-54.20
Reflections measured	25668	70947	48722
Independent reflections	9087 (R_{Int} = 0.0483)	11812 (R_{Int} = 0.0549)	12151 (R_{Int} = 0.0419)
Ind. reflections (I>2σ(I))	8270	9409	8920
Parameters/Restraints	513/0	624/0	568/39
R_1 *(I>2σ(I))*	0.0350	0.0479	0.0733
wR_2 *(all data)*	0.0840	0.1487	0.2245
GooF (all data)	0.999	0.978	1.047
Max. peak/hole/e·Å^{-3}	0.753/-0.535	2.314/-0.604	1.601/-2.354
CCDC	1540277	1540278	1540279

3. DFT Calculations

DFT calculations were performed with Gaussian 09, Revision C.01.[5] Natural Bond Orbital Analysis was done with NBO 5.9.[6] Grimmes general-gradient approximated and dispersion including B97D functional was used.[7] All geometries were first optimized with the def2-SVP basis set and then reoptimized using the def2-TZVPP basis set.[8, 9] Minima were confirmed with frequency calculations (0 imaginary frequencies). Visualization of molecular orbitals was done with ChemCraft.[10] QTAIM Analysis was performed with AIMAll[11] and pictures were created with Multiwfn.[12] The simplified methyl-substituted complexes **3^{Me}-Br, B^{Me}** and **A^{Me}** were derived by replacing phenyl with methyl groups and subsequent geometry optimization. Bond lengths and selected angles, as well as NBO charges are given in tables 2 and 3.

Table 2 Comparison of experimentally derived bond length and angles of **3-Br** with the results of DFT calculations.

	3-Br (X-Ray)	**3^{Me}-Br** (DFT)	**3^{Me}-Cl** (DFT)
Pd-B	2.129(11)	2.17566	2.17221
Pd-P	2.3031(15)	2.28473	2.28753
Pd-P	2.3041(15)	2.30044	2.29873
P-B	2.005(12)	1.93269	1.92982
P-B	1.929(12)	1.91929	1.91930
P-M-P	170.98(5)	170.37	170.31

Table 3 Charges from Natural Population Analysis for the complexes $\mathbf{3^{Me}}$**-Br**, $\mathbf{B^{Me}}$ and $\mathbf{A^{Me}}$

	$\mathbf{3^{Me}}$**-Cl**	$\mathbf{B^{Me}}$	$\mathbf{A^{Me}}$
Pd	0.116	0.056	0.296
B	-0.848	0.434	0.902
P(Pd)	1.044	1.022	1.15
P(Pd)	1.049	1.01	1.136
P(B)	1.328		
P(B)	1.330		
C(B)		-0.302	-0.368
C(B)		-0.279	-0.367
H(B)	0.051		
N(B)		-0.428	
C(B)			-0.469

Molecular Orbitals (Molecular Orbitals are shown with isocontour values at 0.03; Pd: pale green, P: violet, Cl: green, Br: dark red, C: grey, B: orange)

Complex **3^{Me}-Cl**

LUMO

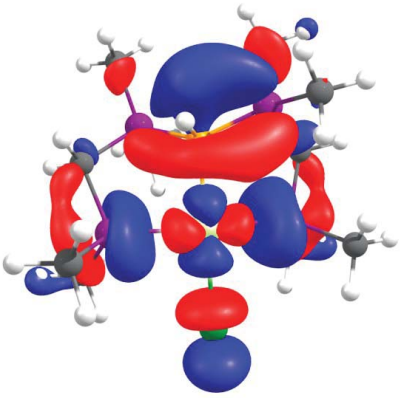

HOMO

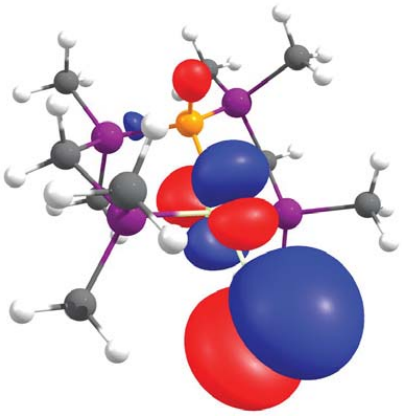

HOMO-1

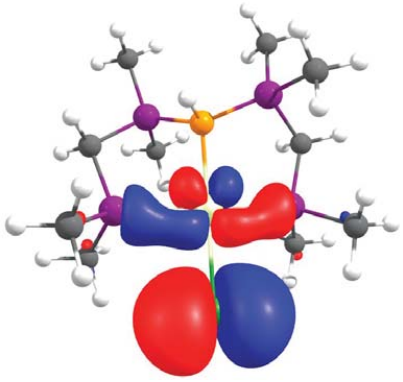

HOMO-2

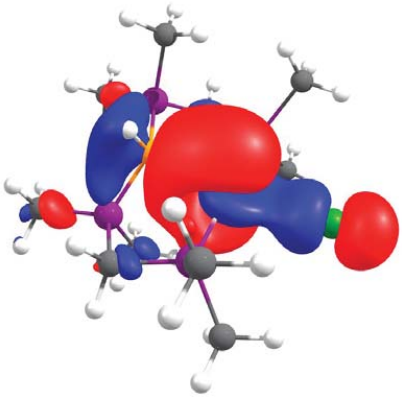

HOMO-3

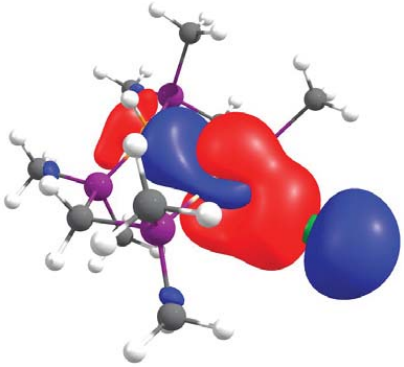

HOMO-4

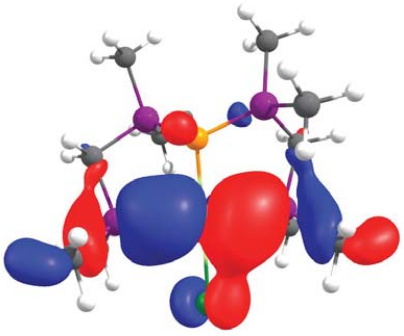

HOMO-5

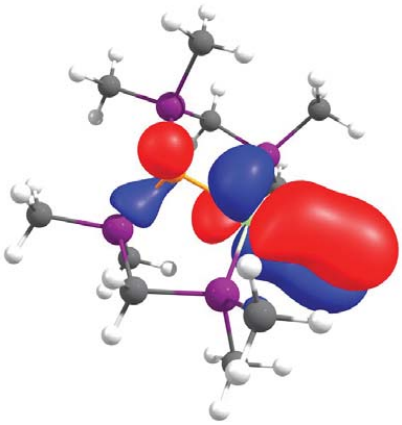

HOMO-8

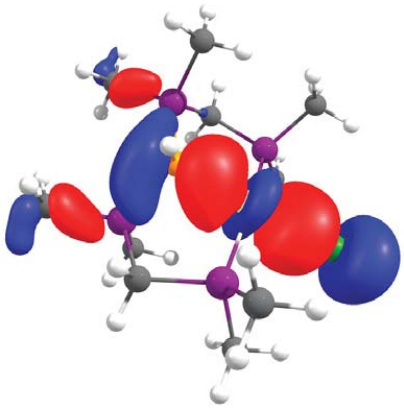

HOMO-9

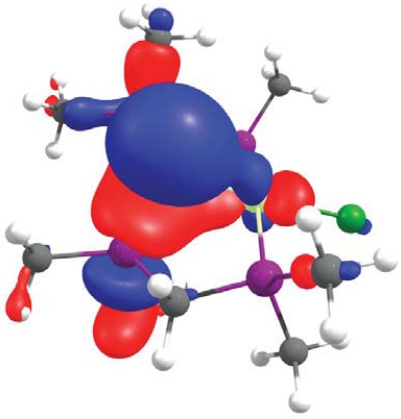

HOMO-10

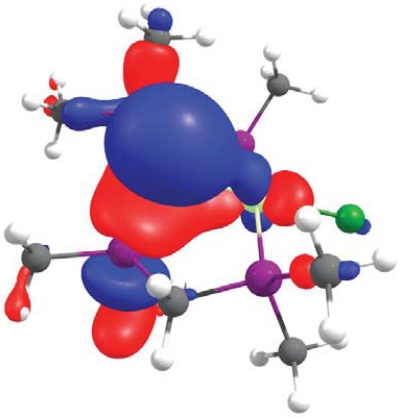

S17

Complex **4^{Me}-Cl/Br**

LUMO

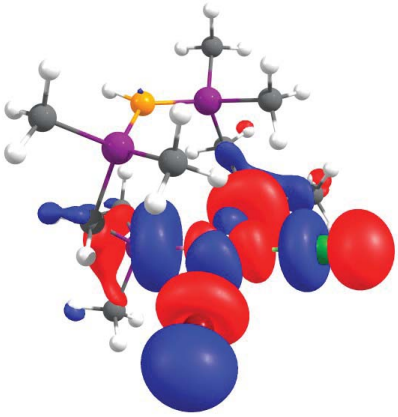

HOMO

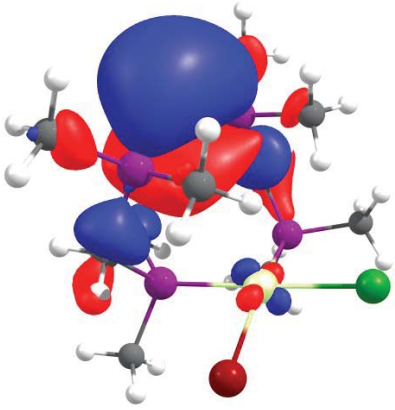

HOMO-1

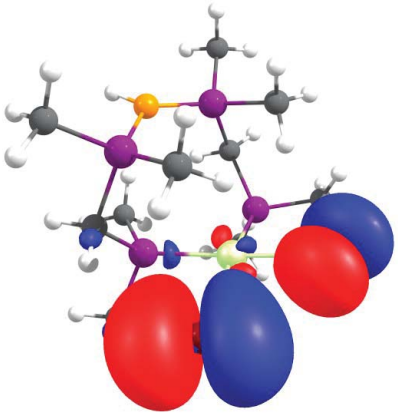

HOMO-2

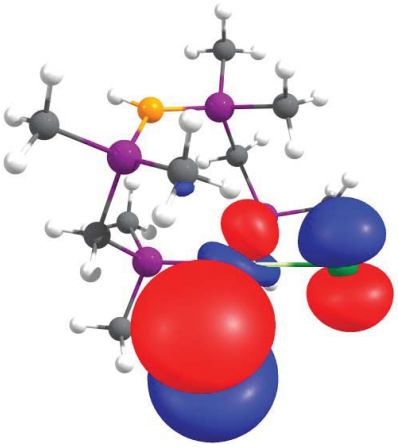

HOMO-3

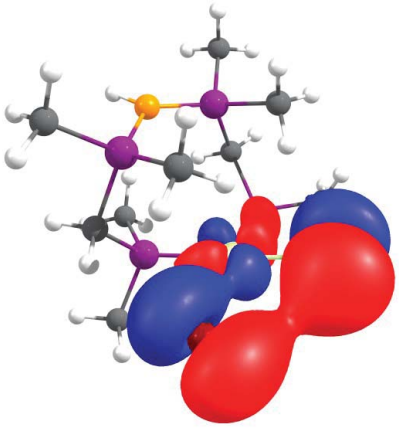

HOMO-4

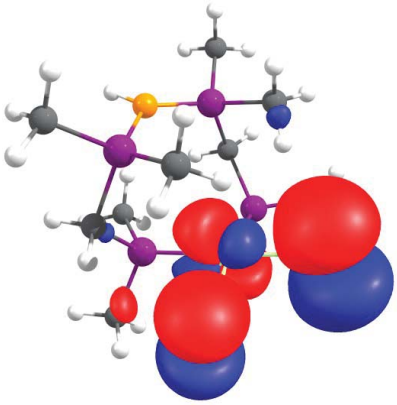

HOMO-10

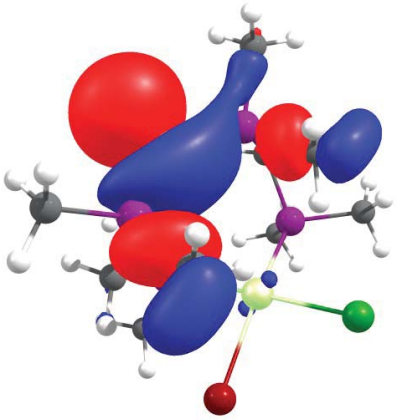

HOMO-11

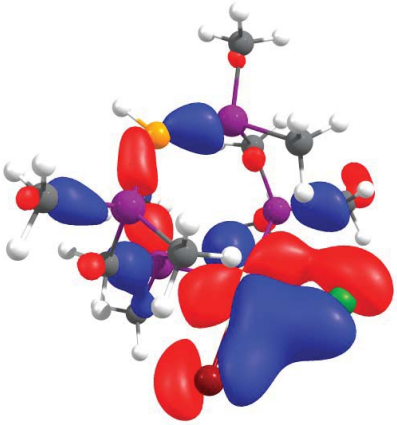

HOMO-12

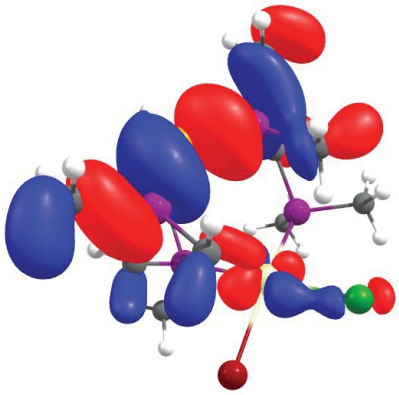

S19

Complex $\mathbf{A}^{\mathbf{Me}}$

LUMO

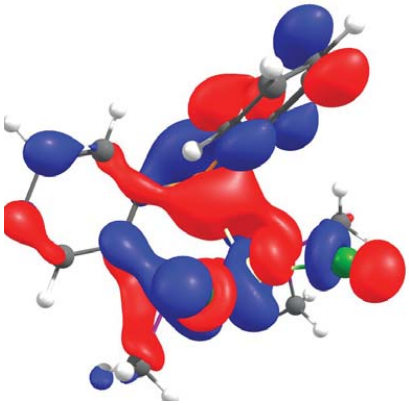

HOMO

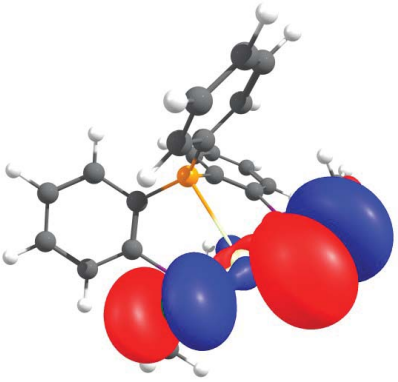

HOMO-1

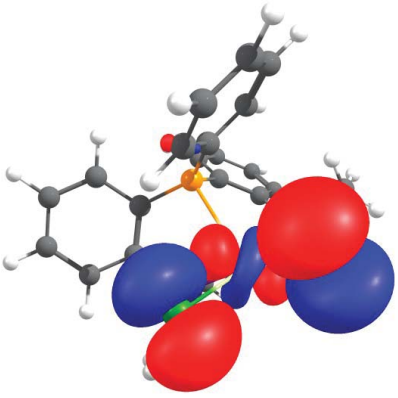

HOMO-2

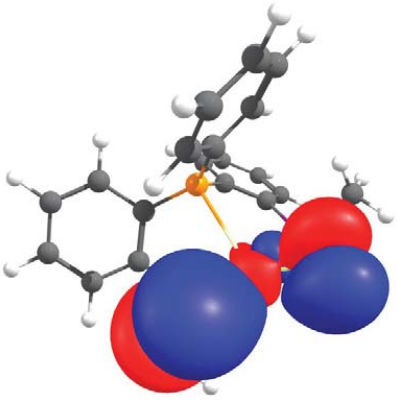

HOMO-3

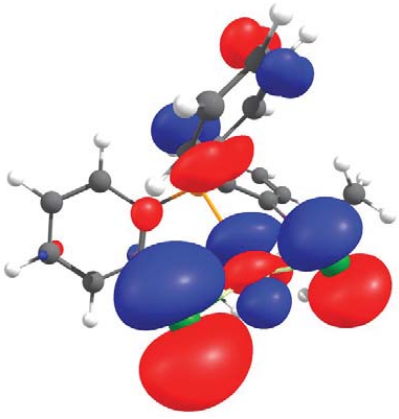

HOMO-4

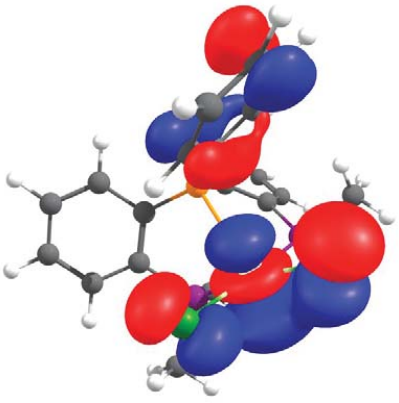

S20

HOMO-5

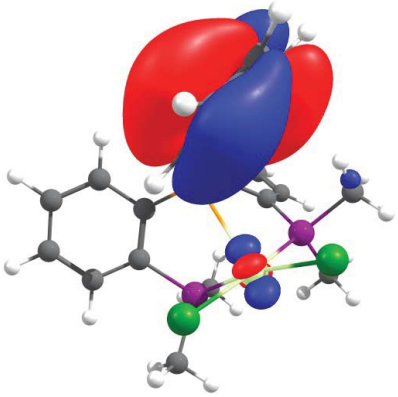

HOMO-6

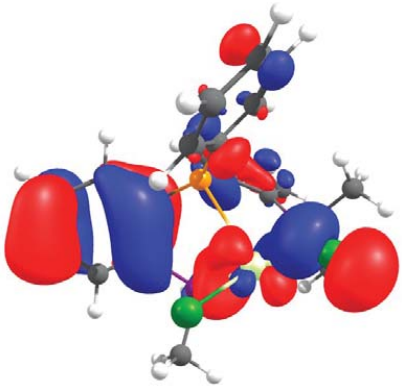

HOMO-12

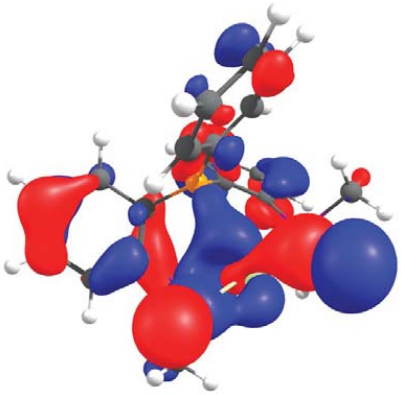

S21

Complex $\mathbf{B}^{\mathbf{Me}}$

LUMO

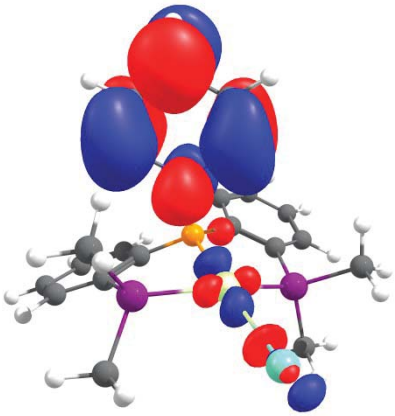

HOMO

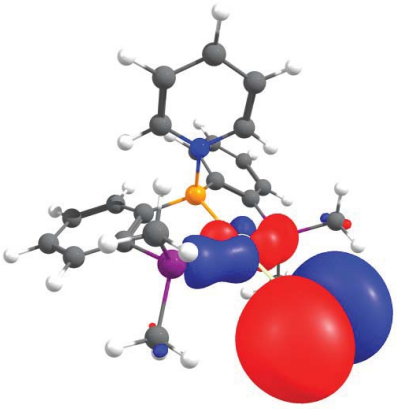

HOMO-1

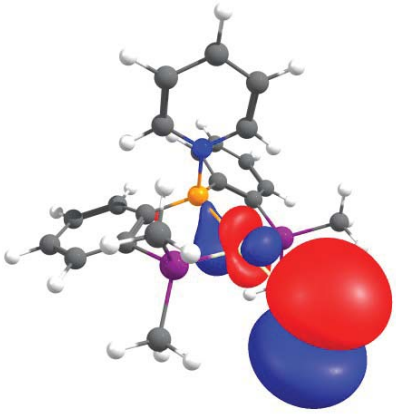

HOMO-2

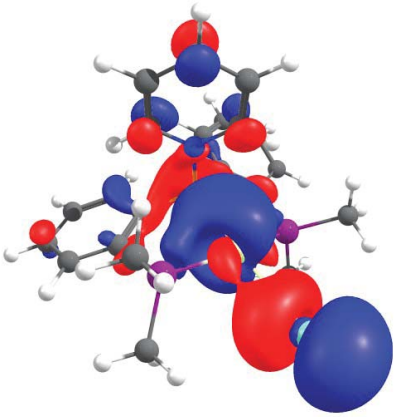

HOMO-3

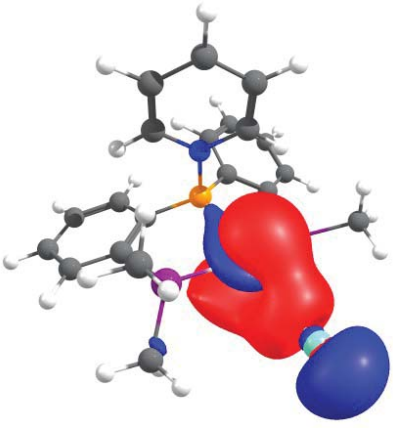

HOMO-4

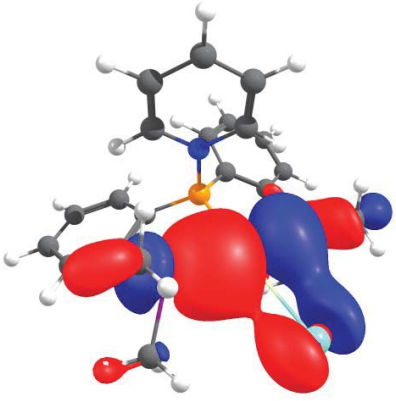

HOMO-5

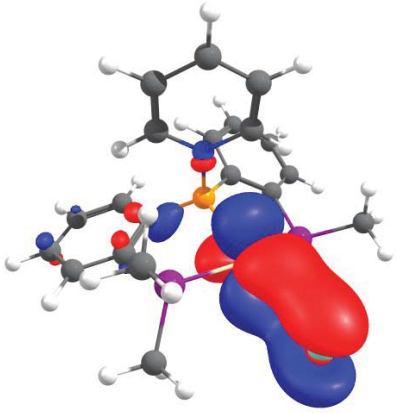

HOMO-12

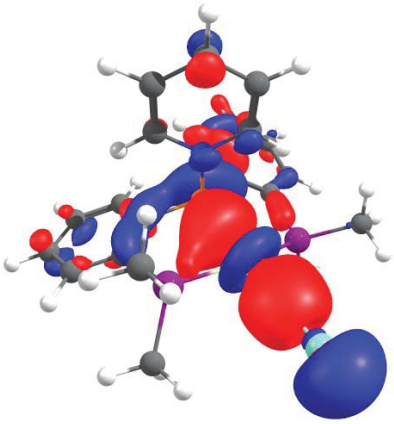

HOMO-15

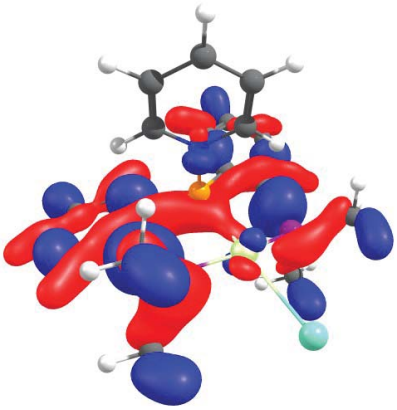

HOMO-17

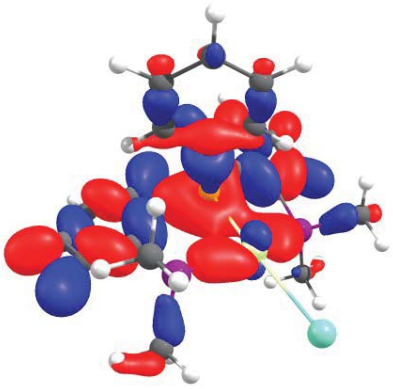

S23

Quantum Theory of Atoms and Molecules (QTAIM)

Table 4 Comparison of bond critical point data in atomic units of the Pd-B-bond in **3^{Me}-Br**, **3^{Me}-Cl**, **A^{Me}** and **B^{Me}**.

	ρ	$\nabla^2\rho$	$\in$	K_{bcp}	V_{bcp}	H_{bcp}
3^{Me}-Br	0.090626	-0.007863	0.063472	0.038974	-0.075977	-0.037003
3^{Me}-Cl	0.091572	-0.008755	0.069699	0.039596	-0.076998	-0.037402
A^{Me}	0.020004	0.029088	0.606243	0.001389	-0.01005	-0.008661
B^{Me}	0.085673	-0.037487	0.026577	0.038215	-0.067059	-0.028844

Table 5 Bond critical point data in atomic units for **3^{Me}-Cl**.

Bond	ρ	$\nabla^2\rho$	∈	K_{bcp}	V_{bcp}	H_{bcp}
Pd1 - Cl2	0.066421	0.187503	0.04863	0.01266	-0.07217	-0.05951
Pd1 - P3	0.103726	0.138338	0.015354	0.040441	-0.115394	-0.074953
Pd1 - B5	0.091572	-0.008755	0.069699	0.039596	-0.076998	-0.037402
Pd1 - P4	0.101723	0.136356	0.025098	0.038802	-0.111626	-0.072824
B5 - P8	0.129748	-0.214093	0.173496	0.120813	-0.188103	-0.06729
B5 - P9	0.128225	-0.217616	0.119375	0.118576	-0.182748	-0.064172
B5 - H14	0.165223	-0.186382	0.012748	0.176202	-0.305809	-0.129607

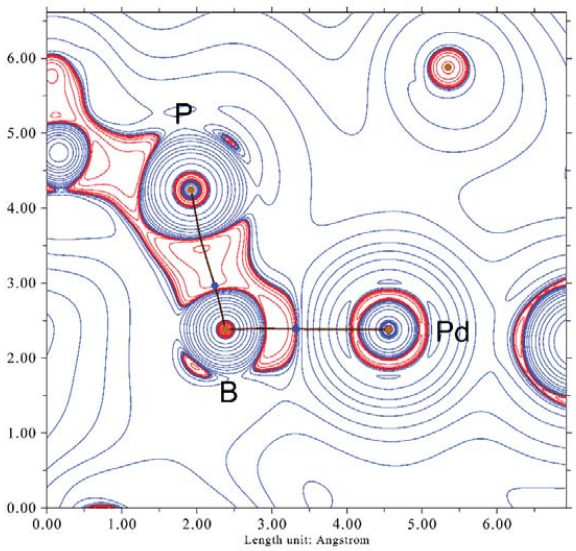

Figure 14 Molecular graph for complex **3^{Me}-Cl** derived from QTAIM analysis with a contour plot of the Laplacian in the P-B-Pd plane. Bond critical points are indicated as blue dots. Positive values of the Laplacian (charge depletion) are depicted as solid blue lines, and negative values (charge accumulation) as red lines.

Table 6 Bond critical point data in atomic units for **3^{Me}-Br**.

Bond	ρ	$\nabla^2\rho$	$\in$	K_{bcp}	V_{bcp}	H_{bcp}
Pd1 - Br2	0.058248	0.137973	0.057183	0.009988	-0.054462	-0.044474
Pd1 - P3	0.103841	0.138583	0.021378	0.04055	-0.115674	-0.075124
Pd1 - P4	0.10133	0.136374	0.027284	0.038493	-0.111015	-0.072522
Pd1 - B5	0.090626	-0.007863	0.063472	0.038974	-0.075977	-0.037003
B5 - P8	0.129942	-0.21554	0.167124	0.121051	-0.188216	-0.067165
B5 - P9	0.127743	-0.217593	0.111006	0.117738	-0.181078	-0.06334
B5 - H14	0.165415	-0.189149	0.016006	0.176547	-0.305807	-0.12926

Table 7 Bond critical point data in atomic units for $\mathbf{A^{Me}}$.

Bond	ρ	$\nabla^2\rho$	∈	K_{bcp}	V_{bcp}	H_{bcp}
Pd1 - Cl2	0.076242	0.19468	0.042741	0.017069	-0.082808	-0.065739
Pd1 - B6	0.020004	0.029088	0.606243	0.001389	-0.01005	-0.008661
Pd1 - Cl3	0.072847	0.190121	0.046568	0.015519	-0.078568	-0.063049
Pd1 - P4	0.111596	0.097202	0.022069	0.048259	-0.120818	-0.072559
Pd1 - P5	0.107013	0.097435	0.029939	0.044407	-0.113174	-0.068767
B6 - C14	0.190579	-0.22681	0.126211	0.211937	-0.367172	-0.155235
B6 - C15	0.180126	-0.225792	0.239159	0.196062	-0.335677	-0.139615

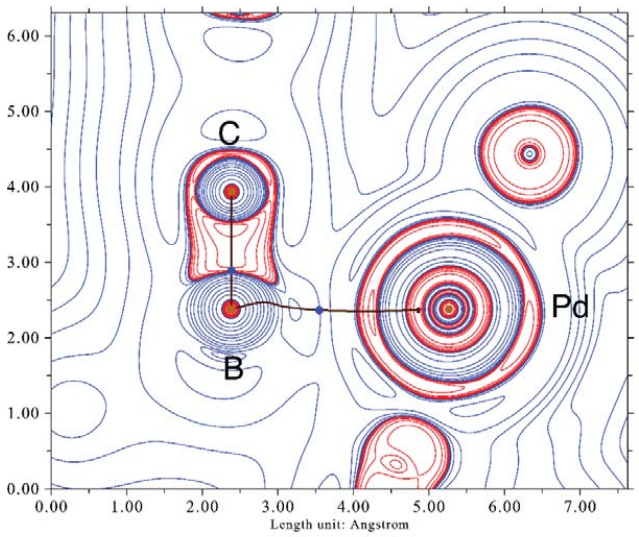

Figure 15 Molecular graph for complex $\mathbf{A^{Me}}$ derived from QTAIM analysis with a contour plot of the Laplacian in the C-B-Pd plane. Bond critical points are indicated as blue dots. Positive values of the Laplacian (charge depletion) are depicted as solid blue lines, and negative values (charge accumulation) as red lines.

Table 8 Bond critical point data in atomic units for $\mathbf{B^{Me}}$.

Bond	ρ	$\nabla^2\rho$	∈	K_{bcp}	V_{bcp}	H_{bcp}
Pd1 - B5	0.085673	-0.037487	0.026577	0.038215	-0.067059	-0.028844
Pd1 - P2	0.108143	0.139611	0.020959	0.044832	-0.124568	-0.079736
Pd1 - P3	0.10403	0.144808	0.025885	0.041348	-0.118898	-0.07755
Pd1 - I4	0.045642	0.087695	0.061059	0.007382	-0.036688	-0.029306
B5 - C12	0.164056	-0.188483	0.08083	0.172342	-0.297562	-0.12522
B5 - C14	0.165549	-0.19283	0.073636	0.174529	-0.300851	-0.126322
B5 - N13	0.116784	0.290182	0.059865	0.089818	-0.252181	-0.162363

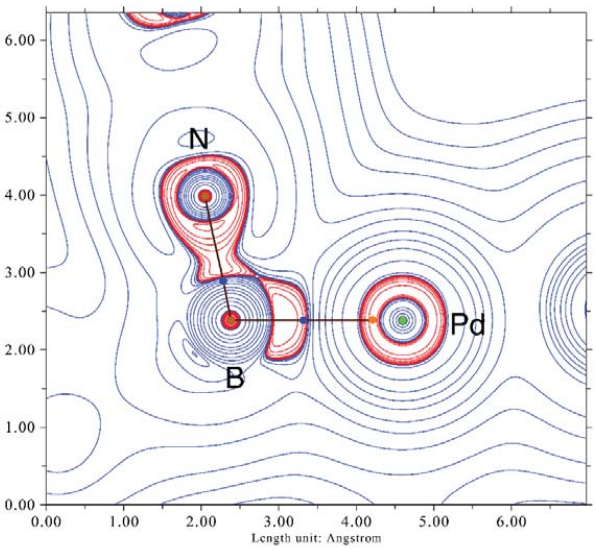

Figure 16 Molecular graph for complex $\mathbf{B^{Me}}$ derived from QTAIM analysis with a contour plot of the Laplacian in the C-B-Pd plane. Bond critical points are indicated as blue dots. Positive values of the Laplacian (charge depletion) are depicted as solid blue lines, and negative values (charge accumulation) as red lines.

Cartesian coordinates of all DFT-optimized geometries

3^{Me}-Br

Pd	0.606577000	-0.127272000	-0.175605000
Br	3.086058000	-0.798753000	0.047385000
P	-0.046345000	-2.240651000	0.396519000
P	1.168859000	2.093162000	-0.388985000
B	-1.441454000	0.455605000	-0.622043000
C	-1.895456000	-2.280717000	0.697725000
C	-0.371783000	3.155193000	-0.255182000
P	-1.693477000	2.061824000	0.397873000
P	-2.648573000	-1.039921000	-0.418159000
H	-2.348010000	-3.274654000	0.589772000
H	-2.056626000	-1.939091000	1.728753000
H	-0.226026000	4.046534000	0.366053000
H	-0.682543000	3.474237000	-1.257445000
H	-1.517254000	0.806530000	-1.784258000
C	-2.835489000	-1.852045000	-2.040536000
H	-3.410594000	-1.194402000	-2.700899000
H	-1.844185000	-2.000275000	-2.478984000
H	-3.348363000	-2.814644000	-1.940037000
C	0.659322000	-2.861447000	1.966244000
H	0.278394000	-3.861494000	2.207505000
H	1.747645000	-2.884845000	1.845028000
H	0.417081000	-2.163789000	2.774716000
C	-1.388791000	1.871740000	2.187529000
H	-2.185112000	1.264108000	2.633189000
H	-0.434076000	1.351181000	2.316409000
H	-1.365072000	2.845164000	2.690415000
C	1.992139000	2.626791000	-1.931771000
H	2.216088000	3.700391000	-1.919975000
H	2.922395000	2.053491000	-2.015065000
H	1.354220000	2.386132000	-2.788550000
C	-4.349663000	-0.734839000	0.191345000
H	-4.924529000	-1.666681000	0.236525000
H	-4.305034000	-0.294282000	1.193499000
H	-4.854163000	-0.035342000	-0.484447000
C	0.286984000	-3.581026000	-0.806275000
H	-0.170847000	-3.352531000	-1.773290000
H	1.373714000	-3.620934000	-0.942315000
H	-0.077481000	-4.549153000	-0.441473000
C	2.244721000	2.706554000	0.959011000
H	1.749991000	2.559551000	1.924791000
H	3.160984000	2.106870000	0.947388000
H	2.479864000	3.769346000	0.822526000
C	-3.271399000	2.984456000	0.251873000
H	-3.216932000	3.947292000	0.772884000
H	-3.486720000	3.157529000	-0.808211000
H	-4.084576000	2.392429000	0.686548000

3^{Me}-Cl

Pd	0.388539000	-0.788850000	-0.184373000
Cl	1.341268000	-3.013909000	0.119741000
P	-1.662582000	-1.591416000	0.426654000
P	2.468770000	0.157512000	-0.431724000
B	-0.419138000	1.180722000	-0.616717000
C	-2.856289000	-0.168537000	0.680799000
C	2.346000000	2.014940000	-0.190745000
P	0.662226000	2.334616000	0.470893000
P	-2.343327000	1.159796000	-0.470844000
H	-3.913975000	-0.438283000	0.566890000
H	-2.702869000	0.199617000	1.703872000
H	3.130697000	2.411167000	0.463826000
H	2.415643000	2.517337000	-1.162943000
H	-0.167323000	1.505325000	-1.761797000
C	-3.015636000	0.704114000	-2.103328000
H	-2.848094000	1.531959000	-2.800278000
H	-2.474166000	-0.172763000	-2.470833000
H	-4.086966000	0.485150000	-2.039562000
C	-1.669615000	-2.469112000	2.031439000
H	-2.674844000	-2.824876000	2.288882000
H	-0.976486000	-3.312126000	1.937582000
H	-1.297396000	-1.801214000	2.815402000
C	0.699097000	1.886029000	2.240219000
H	-0.286439000	2.067778000	2.684606000
H	0.927153000	0.817641000	2.316025000
H	1.446344000	2.477433000	2.781464000
C	3.333725000	-0.066751000	-2.027493000
H	4.311050000	0.430999000	-2.032751000
H	3.467067000	-1.144200000	-2.176869000
H	2.710169000	0.324526000	-2.838020000
C	-3.226730000	2.684731000	0.033028000
H	-4.312382000	2.536247000	0.014354000
H	-2.924344000	2.967649000	1.047510000
H	-2.963470000	3.494218000	-0.657003000
C	-2.498877000	-2.747896000	-0.719840000
H	-2.659418000	-2.276157000	-1.693557000
H	-1.823890000	-3.600422000	-0.856086000
H	-3.456847000	-3.093730000	-0.312796000
C	3.660762000	-0.387768000	0.843109000
H	3.273232000	-0.139017000	1.836598000
H	3.737192000	-1.477964000	0.771742000
H	4.642470000	0.079954000	0.699377000
C	0.400031000	4.149053000	0.421928000
H	1.185306000	4.676085000	0.976058000
H	0.403971000	4.485919000	-0.620405000
H	-0.571137000	4.391253000	0.8684860000

4^{Me}-Cl/Br

Pd	0.675871000	-0.921726000	-0.036269000
Cl	0.604954000	-2.262611000	-2.012409000
P	0.853076000	0.632122000	1.612686000
P	-1.280841000	-1.841928000	0.656085000
B	-1.962320000	2.320745000	-0.034006000
C	1.102115000	2.298809000	0.872801000
C	-2.726349000	-0.729565000	0.818654000
P	-2.809064000	0.768882000	-0.414525000
P	-0.220171000	2.696047000	-0.421839000
H	1.026577000	3.049381000	1.672974000
H	2.103547000	2.329823000	0.429112000
H	-3.631784000	-1.345397000	0.728790000
H	-2.719783000	-0.271779000	1.812800000
H	-2.473430000	2.976457000	0.842929000
C	0.065467000	4.511010000	-0.548927000
H	-0.477167000	4.892707000	-1.419465000
H	-0.332884000	4.991696000	0.351603000
H	1.134903000	4.736337000	-0.642423000
C	2.291809000	0.361591000	2.721759000
H	2.374500000	1.192284000	3.434188000
H	2.139403000	-0.573688000	3.273415000
H	3.198038000	0.276392000	2.117591000
C	-2.483812000	-0.054966000	-2.017938000
H	-2.613934000	0.678061000	-2.819240000
H	-1.468921000	-0.464959000	-2.058131000
H	-3.195357000	-0.877985000	-2.156423000
C	-1.062895000	-2.663564000	2.291194000
H	-2.017263000	-3.055829000	2.664046000
H	-0.359067000	-3.492645000	2.154025000
H	-0.639571000	-1.971727000	3.022768000
C	0.437144000	2.004467000	-1.979208000
H	1.516254000	2.173057000	-2.047114000
H	0.269268000	0.926540000	-2.028904000
H	-0.084463000	2.496899000	-2.806640000
C	-0.485835000	0.963360000	2.833651000
H	-1.343518000	1.382934000	2.298472000
H	-0.776261000	0.057721000	3.373443000
H	-0.111794000	1.697598000	3.559430000
C	-1.945039000	-3.220470000	-0.353308000
H	-2.201773000	-2.857991000	-1.350579000
H	-1.172036000	-3.984160000	-0.469517000
H	-2.829662000	-3.633429000	0.148787000
C	-4.635064000	1.010474000	-0.356348000
H	-5.168140000	0.057755000	-0.462741000
H	-4.898313000	1.472113000	0.601895000
H	-4.921680000	1.693396000	-1.161867000
Br	3.046325000	-0.171578000	-0.691255000

A^{Me}

Pd	4.182481000	8.338374000	0.845033000
Cl	2.385814000	8.531725000	-0.701789000
Cl	5.738825000	8.059590000	-0.958232000
P	2.709098000	8.753549000	2.501525000
P	5.978686000	7.785185000	2.131550000
B	5.165659000	10.792192000	1.996207000
C	2.136971000	7.229050000	3.350611000
C	1.144803000	9.595265000	2.061638000
C	3.431865000	9.831544000	3.791681000
C	7.209870000	9.120893000	1.999776000
C	6.778407000	6.220611000	1.611457000
C	5.798030000	7.476812000	3.942346000
C	4.534096000	10.646038000	3.453267000
C	4.413259000	11.598482000	0.900334000
C	6.703529000	10.431547000	1.854789000
H	1.691445000	6.581540000	2.587770000
H	2.985548000	6.713139000	3.807386000
H	1.386117000	7.452406000	4.117566000
H	1.381935000	10.487788000	1.477909000
H	0.537176000	8.928868000	1.444716000
H	0.621091000	9.869540000	2.986459000
C	2.923696000	9.816494000	5.099550000
C	8.583604000	8.865165000	1.953631000
H	6.030422000	5.422232000	1.668889000
H	7.117965000	6.317060000	0.578828000
H	7.610907000	5.982272000	2.284486000
H	5.350093000	8.331860000	4.449756000
H	5.175181000	6.588802000	4.099928000
H	6.794045000	7.287511000	4.360343000
C	5.109834000	11.419748000	4.479503000
C	4.853003000	11.572189000	-0.442445000
C	3.252902000	12.346325000	1.202191000
C	7.630074000	11.469176000	1.656952000
H	2.082214000	9.175654000	5.352356000
C	3.502686000	10.606244000	6.094147000
C	9.485967000	9.918639000	1.776919000
H	8.956381000	7.846717000	2.027756000
C	4.602175000	11.410193000	5.780253000
H	5.978093000	12.035601000	4.252221000
H	5.719698000	10.971128000	-0.701142000
C	4.149436000	12.240053000	-1.441079000
C	2.556670000	13.032374000	0.208692000
H	2.902308000	12.386116000	2.231468000
H	7.264828000	12.483845000	1.511721000
C	9.006780000	11.220883000	1.625963000
H	3.106827000	10.584041000	7.106554000
H	10.553570000	9.717196000	1.734154000
H	5.070391000	12.019151000	6.550316000
H	4.481407000	12.176291000	-2.474265000
C	3.000525000	12.970814000	-1.117620000

H	1.666413000	13.605508000	0.458867000
H	9.701972000	12.041505000	1.463440000
H	2.446633000	13.486474000	-1.899131000

B^{Me}

Pd	6.662778000	5.352965000	-0.045676000
P	5.513447000	3.426855000	0.224020000
P	7.163134000	7.432768000	-0.825825000
I	6.977295000	5.859125000	2.700391000
B	6.520176000	4.887162000	-2.209419000
C	3.851203000	3.686796000	0.968211000
C	6.197977000	2.061929000	1.254347000
C	5.228709000	2.706600000	-1.431268000
C	6.364567000	7.484413000	-2.479143000
C	6.407047000	8.814289000	0.119704000
C	8.898721000	8.015358000	-1.056569000
C	5.772160000	3.466350000	-2.487268000
N	8.092024000	4.640614000	-2.598706000
C	5.986470000	6.213729000	-2.982267000
H	3.995220000	4.097811000	1.973730000
H	3.303341000	4.415098000	0.362049000
H	3.285616000	2.747512000	1.019802000
H	7.153088000	1.728188000	0.834327000
H	6.379921000	2.467131000	2.256565000
H	5.509660000	1.209322000	1.312103000
C	4.587252000	1.479666000	-1.659537000
C	6.043030000	8.667895000	-3.152436000
H	5.329133000	8.640235000	0.193920000
H	6.827924000	8.793998000	1.131241000
H	6.595725000	9.786173000	-0.353807000
H	9.365403000	8.087544000	-0.067193000
H	9.454955000	7.285603000	-1.653733000
H	8.932864000	8.994449000	-1.551802000
C	5.684302000	2.914462000	-3.781662000
C	8.760852000	3.635508000	-1.972806000
C	8.767500000	5.395432000	-3.498235000
C	5.223730000	6.200128000	-4.163768000
C	4.490384000	0.973404000	-2.955951000
H	4.173752000	0.913905000	-0.826229000
H	6.343776000	9.630694000	-2.742777000
C	5.294754000	8.620119000	-4.333308000
H	6.131331000	3.446109000	-4.620162000
C	5.052293000	1.691555000	-4.018721000
H	8.172604000	3.069916000	-1.260637000
C	10.098820000	3.378339000	-2.205298000
C	10.118140000	5.195703000	-3.768714000
H	8.192022000	6.171735000	-3.986684000
C	4.871766000	7.382629000	-4.825931000
H	4.882714000	5.250926000	-4.568386000
H	3.995050000	0.022195000	-3.137648000
H	5.023079000	9.539473000	-4.847257000

H	5.000206000	1.292440000	-5.029903000
H	10.581570000	2.567591000	-1.668892000
C	10.806672000	4.176744000	-3.114771000
H	10.610031000	5.839038000	-4.492053000
H	4.263866000	7.337637000	-5.727563000
H	11.862349000	4.004241000	-3.303802000

Literature

1. K. Sommer, *Z. Anorg. Allg. Chem.*, 1970, **376**, 37-43.
2. G. M. Sheldrick, *Acta Crystallogr., Sect. A*, 2008, **64**, 112-122.
3. X.-R. 1.01, *Data Reduction Program, Stoe & Cie GmbH, Darmstadt, Germany, 2001*.
4. X.-S. 1.06, *Crystal Optimization for Numerical Absorption Correction Program, Stoe & Cie GmbH, Darmstadt, 1999*.
5. M. J. Frisch, G. W. Trucks, H. B. Schlegel, G. E. Scuseria, M. A. Robb, J. R. Cheeseman, G. Scalmani, V. Barone, B. Mennucci, G. A. Petersson, H. Nakatsuji, M. Caricato, X. Li, H. P. Hratchian, A. F. Izmaylov, J. Bloino, G. Zheng, J. L. Sonnenberg, M. Hada, M. Ehara, K. Toyota, R. Fukuda, J. Hasegawa, M. Ishida, T. Nakajima, Y. Honda, O. Kitao, H. Nakai, T. Vreven, J. A. Montgomery, J. E. P. Jr., F. Ogliaro, M. Bearpark, J. J. Heyd, E. Brothers, K. N. Kudin, V. N. Staroverov, R. Kobayashi, J. Normand, K. Raghavachari, A. Rendell, J. C. Burant, S. S. Iyengar, J. Tomasi, M. Cossi, N. Rega, J. M. Millam, M. Klene, J. E. Knox, J. B. Cross, V. Bakken, C. Adamo, J. Jaramillo, R. Gomperts, R. E. Stratmann, O. Yazyev, A. J. Austin, R. Cammi, C. Pomelli, J. W. Ochterski, R. L. Martin, K. Morokuma, V. G. Zakrzewski, G. A. Voth, P. Salvador, J. J. Dannenberg, S. Dapprich, A. D. Daniels, Farkas, J. B. Foresman, J. V. Ortiz, J. Cioslowski and D. J. Fox, *Gaussian 09 Revision C.01, Gaussian Inc. Wallingford CT 2009*.
6. E. D. Glendening, J.K. Badenhoop, A. E. Reed, J. E. Carpenter, J. A. Bohmann, C. M. Morales and F. Weinhold, *(Theoretical Chemistry Institute, University of Wisconsin, Madison, WI, 2012)*, NBO 5.9, **www.chem.wisc.edu/~nbo5**.
7. S. Grimme, *J. Comput. Chem.*, 2006, **27**, 1787-1799.
8. A. Schäfer, H. Horn and R. Ahlrichs, *J. Chem. Phys.*, 1992, **97**, 2571.
9. F. Weigend and R. Ahlrichs, *Phys. Chem. Chem. Phys.*, 2005, **7**, 3297-3305.
10. *Chemcraft version 1.8*, **www.chemcraftprog.com**.
11. Todd A. Keith and O. P. K. TK Gristmill Software, USA, *AIMAll (Version 17.01.25)*, 2017, **www.aim.tkgristmill.com**.
12. Tian Lu and F. Chen, *J. Comp. Chem.*, 2012, **33**, 580-592.

Dalton Transactions

PAPER

View Article Online
View Journal | View Issue

Cite this: *Dalton Trans.*, 2018, **47**, 10544

Carbodiphosphorane-based nickel pincer complexes and their (de)protonated analogues: dimerisation, ligand tautomers and proton affinities†

Leon Maser, Jan Herritsch and Robert Langer *

Received 29th December 2017,
Accepted 14th February 2018

DOI: 10.1039/c7dt04930g

rsc.li/dalton

The reactivity patterns of carbodiphosphoranes (CDPs) as ligands are much less explored than those of isoelectronic analogues. In the current manuscript, we investigate the reactivity of the carbodiphosphorane-based PCP nickel(II) pincer complex [({dppm}$_2$C)NiCl]Cl (**1**) towards acids and bases, calculate proton affinities, analyse the bonding situation and tautomeric forms with the aim to evaluate whether CDPs can potentially act as cooperative ligands in catalysis (dppm = 1,1-bis(diphenylphosphino)methane). Our investigations show that different tautomeric forms are stable for the coordinated and the uncoordinated ligand. The protonated CDP-based complex **2** represents a rare example of a cationic donor group binding to a cationic metal centre. The continuous arm-deprotonation of **1** leads to the formation of remarkably stable dimers with Ni–C–P–C-metallacycles. In comparison to corresponding boron and amine-based ligands, the coordinated CDP-group exhibits the lowest proton affinity according to DFT calculations, indicating that coordinated CDP ligands can potentially serve as proton relay in cooperative catalysis.

1. Introduction

Carbodiphosphoranes (CDPs) display a carbon in the formal oxidation state 0 with two coordinated, stabilising phosphine moieties. These compounds of the general formulae $(R_3P)_2C$ are observed in linear and bent geometries.[1–4] The bonding situation in the bent form is often described by donor interaction from the two tertiary phosphines to the central carbon atom, which retains two lone pairs (one with σ-, one with π-type symmetry) and formally exhibits the oxidation state 0.[5] Linear forms are often considered as bisylides, but the actual bonding situation is still conversely discussed. Due to the two lone pairs at the carbon center and an unusually high proton affinity that exceeds those of carbenes,[6,7] unusual coordination properties of CDPs were expected and an increased catalytic activity was predicted based on density functional theory calculations. Carbodicarbenes, a related class of carbon(0) compounds, were successfully utilised as ligands in homogeneous catalysts.[8–11]

Several examples of Lewis-acid–base adducts and CDP-coordinated metal complexes were reported so far.[12] The protonation of a coordinated CDP-group formally results in a cationic ligand bound to a cationic metal centre, which in case of monodentate CDP-ligands often results in dissociation and formation of protonated CDP (Fig. 1b). So far, there are only two examples of structurally characterised complexes with protonated, monodentate CDP-ligands. Laguna and co-workers reported the formation of the cationic gold(I) complex $[(Ph_2MeP–C(H)–PPh_2Me)Au(C_6F_5)]^+$ by the reaction of $(Ph_2MeP–C(H)–PPh_2Me)OTf$ with $[Au(C_6F_5)(tht)]$.[13] Neumüller, Petz, Frenking and co-workers reported the cationic silver(I) complex $[Ag(Ph_3P–C(H)–PPh_3)_2]^+$, containing even two cationic ligands coordinated to the cationic metal centre.[5,14] Although examples of polydentate ligands with CDP-groups are limited, the protonated analogues as ligands are more common than protonated, monodentate CDPs as ligands.

We recently reported pincer-type complexes based on phosphine-stabilised borylenes that showed an unusual reactivity: a B–H-reductive elimination is observed in iron(II) complexes, leading to the reversible formation of bisphosphinoboronium- or borate-groups (Fig. 1a).[15] These two groups can facilitate different reversible reactions in solution, which have been used for the catalytic H/D-exchange of C–H-bonds.[16] Amines as donor groups are considered to be isoelectronic to L_2BH-groups (Fig. 1a), but the reductive elimination to ammonium salts is usually not observed and they instead provide a proton,

Department of Chemistry, Philipps-Universität Marburg, Hans-Meerwein-Strasse 4, 35032 Marburg, Germany. E-mail: robert.langer@chemie.uni-marburg.de; Fax: +49-6421-2825653; Tel: +49-6421-2825516

†Electronic supplementary information (ESI) available: Experimental details, spectra, crystallographic data and information about the quantum chemical investigation. CCDC 1814006–1814010. For ESI and crystallographic data in CIF or other electronic format see DOI: 10.1039/c7dt04930g

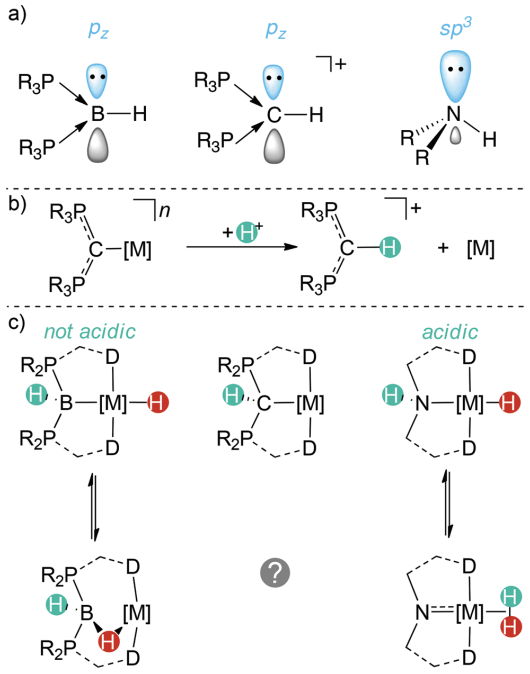

Fig. 1 (a) Schematic drawing of amines, phosphine-stabilized borylenes and CDPs; (b) dissociation of CDP-based ligands upon protonation; (c) examples of reactivity and acidity of the above donor groups within pincer-type ligands.

leading to amido-complexes (Fig. 1c).[17] In combination with metal hydride complexes such amine groups allow for concerted proton-hydride-transfer or reversible protonation of the hydrido ligand, both being import key steps of catalytic (de)hydrogenation reactions.[18]

As a kind of "missing link", we were wondering what kind of reactivity patterns we can expect from CDP-based pincer ligands. Following up the initial reports by Peringer, Schuh and co-workers, we choose the nickel(II) complex **1** as a starting point for our investigations.[19] Herein, we report the reactivity of complex **1** towards different acids and bases. Using quantum chemical methods, we analyse the bonding situation, calculate relative stabilities of tautomeric forms of the pincer ligand as well as proton affinities. These results indicate that protonated CDPs can potentially act as cooperative ligands.

In coordination chemistry, it is uncommon to draw donor arrows or formal charges for transition metal complexes. However, there are different bonding descriptions of coordinated CDP-ligands. For CDP-based pincer-type ligands with two neutral, terminal donor groups D, the bonding descriptions are represented by different resonance structures (**I–IV** Fig. 2). While for transition metal complexes in high oxidation states, such as $[(CDP)ReO_3]^+$, a considerable degree of π-donation of the CDP-ligand is observed,[21] we will show that

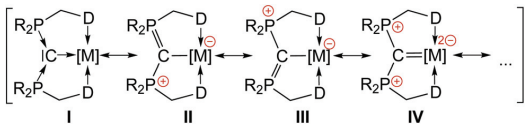

Fig. 2 Possible resonance structures in CDP-based pincer complexes (D = neutral donor group).[20]

this is not the case for the nickel(II) complexes reported herein.

2. Results and discussion

In their original contribution, Peringer and co-workers reported the formation of CDP-based palladium pincer complexes by the reaction of $PdCl_2$ with 1,1-bis(diphenylphosphine)methane (dppm) and CS_2,[22] which was later on demonstrated to work for $NiCl_2{\cdot}H_2O$ and $PtCl_2$ as well.[19] As the template-free synthesis of suitable pre-ligands remained surprisingly challenging, we started to investigate the reactivity of the CDP-based nickel(II) pincer complex **1**, which was previously reported to release $[H_2C(dppm)_2]^{2+}$ upon reaction with HCl.[19] Moreover, the $(R_3P)_2CH^+$-moiety remained uncoordinated in gold(I) complexes containing $[HC(dppm)_2]^+$ as free ligand.[23]

2.1. Reactivity towards acids and bases

Using an acid with a more weakly coordinating anion than chloride, such as $HBF_4{\cdot}Et_2O$, we succeeded to protonate the CDP-moiety in **1** without decoordination of the entire pincer ligand (Fig. 3). The $^{31}P\{^1H\}$ NMR spectrum of complex **2** gives rise to two new triplet resonances at 6.1 and 43.6 ppm ($^2J_{PP}$ = 42.5 Hz). A triplet resonance at 4.37 ppm ($^2J_{PH}$ = 18.7 Hz) is observed in the ^1H NMR spectrum for the CDP-bound proton. The identity of complex **2** was further confirmed by assignment of ^1H and ^{13}C NMR data using 2D NMR spectroscopy as well as single crystal X-ray diffraction. The protonation of the CDP-carbon atom in **1** results in a slight elongation of the Ni–C-bond to 1.990 Å and in significantly longer P–C-bonds (Table 1). The protonated CDP-carbon atom is slightly pyramidalised, as judged by the sum of angles of 349.8° at the central carbon atom $\left(\sum \angle_{C_\alpha^{CDP+H}} = \angle_{P-C-P'} + \angle_{Ni-C-P'} + \angle_{P-C-Ni}\right)$. CDP as a ligand or a donor group is usually considered a σ- and π-donor. However, late transition metal ions, such as nickel(II), are lacking vacant and energetically accessible orbitals for an efficient interaction with π-donors. In consequence, the occupied orbital of π-symmetry at the central carbon atom in complexes like **1** is mainly delocalised over the P-C^{CDP}-P backbone. This interpretation is reflected in significantly longer P–C^{CDP}-bonds in the protonated complex **2**, in which the central tetra-coordinate carbon atom is only σ-bonded. In contrast, the elongation of the Ni–C^{CDP}-bond might be a result of Coulomb repulsion between the cationic $(R_3P)_2CH^+$-donor group and the cationic metal centre.

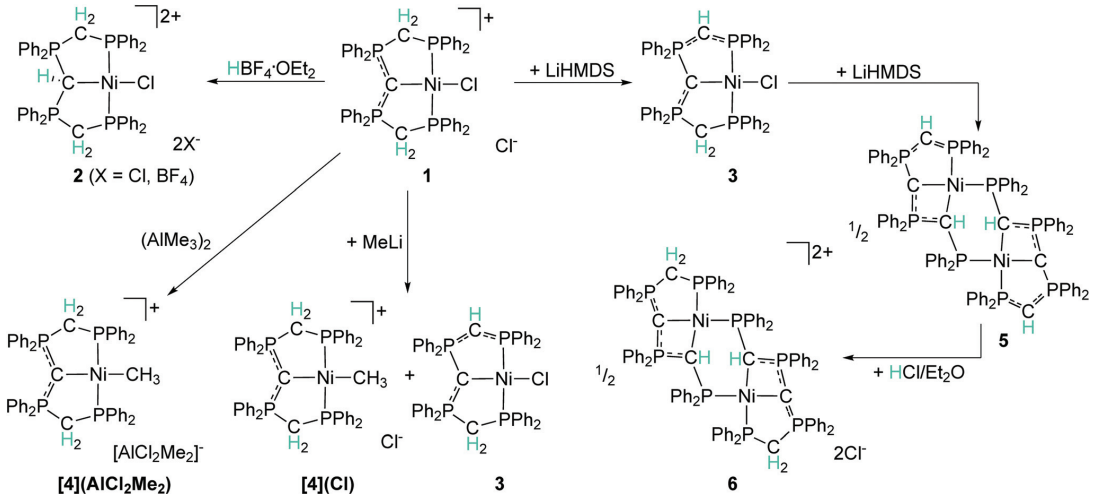

Fig. 3 Reactivity of complex 1 towards acids and bases.

Table 1 Selected bond lengths and angles of CDP-based nickel pincer complexes derived by single crystal XRD

Complex	**1**[19]	**2**	**3**	**4**	*trans*-**5**	*cis*-**5**	*cis*-**6**
d_{Ni-C}^{CDP}/Å	1.930–1.942	1.990	1.933–1.934	1.959	1.983	1.942–1.950	1.951–1.961
d_{Ni-P}/Å	2.177–2.205	2.189–2.195	2.186–2.211	2.105	2.165	2.201–2.222	2.186–2.242
d_{Ni-Cl}/Å	2.192–2.208	2.176	2.198–2.204	—	—	—	—
d_{P-C}^{CDP}/Å	1.690–1.704	1.801–1.834	1.682–1.742	1.697	1.702	1.651–1.714	1.685–1.698
$\angle_{P-C-P}$/°	125.1–126.3	121.1	124.1–124.9	120.9	122.07	137.1–139.8	130.3–142.2
$\sum\angle_{C\alpha}^{CDP}$/°	359.4–360.0	—	355.7–358.7	360.0	360.0	353.7–358.0	347.5–358.8
$\sum\angle_{C\alpha}^{CDP+H}$/°	—	349.8	—	—	330.2	332.2–335.0	323.9–329.4

The arm-deprotonation of P–CH_2–P-group(s) in **1** should lead to π-bonding of the resulting CH-group to the bound phosphorus-atoms and therewith effect the degree of delocalisation of the electron pair at the CDP-carbon atom. We therefor investigated the reactivity of complex **1** towards different bases. The reaction of complex **1** with methyl lithium (MeLi) leads to a mixture of two complexes, which were identified as the neutral deprotonated complex **3** and the methyl complex **4**. However, selective arm-deprotonation can be achieved with lithium hexamethyldisilazanide (LiHMDS) as base, yielding exclusively complex **3**. The reduced symmetry of complex **3** is reflected in the appearance of four doublet of doublets of doublets resonances at 10.4, 17.0, 25.0 and 45.0 ppm in the $^{31}P\{^1H\}$ NMR spectrum. The deprotonation of one P–CH_2–P-group is further indicated by a one proton resonance at 1.34 ppm (ddt) in the ^1H NMR spectrum. The remaining P–CH_2–P-group gives rise to a triplet at 3.46 ppm ($^2J_{PH}$ = 8.6 Hz). The molecular structure of **3** was obtained by single crystal XRD. The Ni–C-bond length of 1.933–1.934 Å in **3** is very similar to those in complex **1** (1.930–1.942 Å), indicating that arm-deprotonation has a minor effect on the Ni–C-bond. However, the two P–C^{CDP}-bond distances are quite different in length, leading to a longer P–C^{CDP}-bond (1.682 Å) relative to those found in **1** at the deprotonated site and a shorter P–C^{CDP}-bond (1.742 Å) at the remaining protonated arm. These observations are in line with a reduced ability for π-bonding to the CDP-bound phosphorus atom at the deprotonated arm. Based on the short P–C^{CDP}-distance, this seems to be compensated by increased π-bonding to the phosphorus atom of the protonated arm.

Selective formation of the methyl complex **4** is achieved by the reaction of trimethylaluminum with **1**, yielding the cationic complex **4** with a dichloridodimethylaluminate counter ion. In agreement with the more symmetric complexes **1** and **2**, two triplet resonances are observed at 27.5 and 31.8 ppm in the $^{31}P\{^1H\}$ NMR spectrum. The new methyl-ligand in *trans*-position to the CDP-group gives rise to triplet at 0.74 ppm in the ^1H NMR spectrum. The methyl ligand, as a strong σ-donor with a strong *trans*-influence, leads to an electron rich nickel centre and a longer Ni–C^{CDP}-bond length (1.959 Å), which can be interpreted in terms of reduced π-donation of the CDP-group. This view is further supported by rather short P–C^{CDP}-bond lengths (1.697 Å). The comparably short Ni–P-distances (2.105 Å) suggest a stronger π-backdonation to the terminal phosphines in **4**.

Treatment of complex **1** with an excess of base leads to the abstraction of the remaining chlorido ligand in **3** and formation of a new complex. The $^{31}P\{^{1}H\}$ NMR spectrum of the reaction mixture shows four regions of resonances that in part appeared to be overlapped. The X-ray diffraction analysis of suitable single crystals revealed the formation of the neutral dimeric nickel complex **5** (Fig. 4). The deprotonation of the second arm results in a change of the binding mode and a overall tetradentate ligand: the square-planar nickel(II) centre in **5** is coordinated by a PPh_2-group, the CDP-group and a $(R_2P)_2CH$-group of the arm, leading to a rare four-membered Ni–C–P–C-metallacycle.[24,25] The fourth coordination site at each nickel atom is occupied by a PPh_2-group of the second PCP-ligand in the dimer. Interestingly, two different stereoisomers are observed in the crystal lattice of **5**, differing in the orientation of the protons in the two $(R_2P)_2CH$-groups. The Ni–C^{CDP}-bond in *trans*-**5** (1.983 Å) is longer than in *cis*-**6** (1.942–1.950 Å). The P–C^{CDP}-bond lengths are comparable to the other reported complexes, but for the *cis*-isomer one short (1.651 Å) and one longer (1.714 Å) distance is observed, while both P–C^{CDP}-bonds are equal in the *trans*-isomer. The sum of angles around the CDP-carbon atom is close to 360° (353.7–360.0°), while the carbon atoms of the $(R_2P)_2CH$-groups are strongly pyramidalised (330.2–335.0°).

Next, we investigated the reversibility of the deprotonation reactions and treated complex **3** and **5** with different proton sources. Protonation of complex **3** yields complex **1** in a clean reaction. To our surprise, the protonation of **5** results in the formation of a new complex and did not lead to **3**. A X-ray diffraction analysis of suitable single crystals grown from methylene chloride confirmed the formation of a new dimeric nickel complex (**6**) that is protonated at the non-coordinated carbon atoms (Fig. 4). In contrast to complex **5**, only the *cis*-isomer is observed in the crystal lattice of **6**. Apart from that, the bond lengths and angles in the dicationic complex **6** are quite similar to *cis*-**5** (Table 1). Complex **6** crystallises with two chloride counter ions and is there with a constitutional isomer of complex **3**. Both isomers exhibit different reactivities: complex **3** is rapidly converted to complex **1** upon exposure to air, while complex **6** initially remains stable.

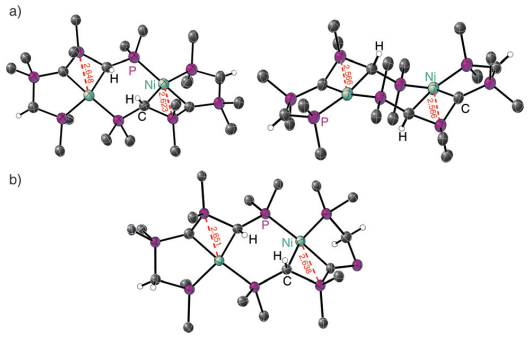

Fig. 4 Molecular structures of *cis*- and *trans*-**5** (a) and *cis*-**6** (b) in the solid state (phenyl-rings and counter ions are omitted for clarity). The labeled H-atoms are either on the same site of the complex, exhibiting a *cis*-configuration, or pointing in opposite directions with a *trans*-arrangement.

2.2. Bonding analysis

To gain further insight into the bonding situation, we performed quantum chemical investigations on the methyl substituted complexes using density functional theory (DFT). The analysis of molecular orbitals reveals that the degree of π-donation from the CDP-group is insignificant for the description of the bonding situation in the reported nickel complexes. The combination of nickel(II), a late transition metal with a d^8 valence electron configuration, with two potentially π-donating ligands in a *trans*-orientation results in a situation where π-anti-bonding states are occupied. The highest occupied molecular orbital (HOMO) of complex $\mathbf{1}^{Me}$ can be described as the doubly anti-bonding interaction of the π-type orbital of the CDP and a p-orbital of the chlorido ligand with a d-orbital of the central metal atom (Fig. 5). The protonated CDP-group in $\mathbf{2}^{Me}$ acts as a pure σ-donor and the HOMO describing the corresponding π-interaction is reduced to an anti-bonding combination of the chlorido p-orbital with a nickel d-orbital.

Based on the different P–C^{CDP}-bond lengths in **3**, we concluded that the arm deprotonation limits the ability for π-back bonding of the involved CDP-bound phosphorus atom. This view is supported by the analysis of the corresponding molecular orbitals. The HOMO of $\mathbf{3}^{Me}$ is very similar to the HOMO in $\mathbf{1}^{Me}$, but a deformation of the π-type orbital at the CDP-moiety towards one phosphorus atom is observed.

Partial charges were calculated using natural population analysis (NPA, Table 2). The high negative partial charge at the central carbon atom of CDP-adducts can be explained by charge donation from the phosphines to the CDP-carbon,[26] which has an even stronger effect than the lone pair of

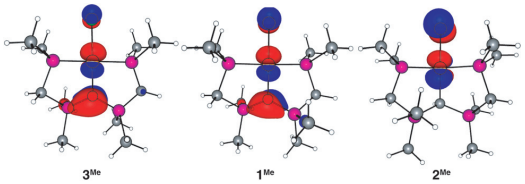

Fig. 5 HOMOs of complex $\mathbf{1}^{Me}$–$\mathbf{3}^{Me}$ (isocontour value 0.05).

Table 2 Partial charges derived by natural population analysis

	q (C^{CDP})	q (Ni)	q (P^{CDP})	q ($\underline{C}H_n$)
$\mathbf{1}^{Me}$	−1.46	+0.38	+1.60	−1.05
$\mathbf{2}^{Me}$	−1.24	+0.37	+1.59	−1.05/−1.06
$\mathbf{3}^{Me}$	−1.41	+0.38	+1.58/+1.61	−1.06/−1.34
cis-$\mathbf{6}^{Me}$	−1.44	+0.36	+1.59/+1.62	−1.05
trans-$\mathbf{6}^{Me}$	−1.44	+0.36	+1.57/+1.62	−1.05/−1.06
cis-$\mathbf{7}^{Me}$	−1.46/−1.48	+0.39/0.43	+1.60/+1.62	−1.06/−1.34

π-symmetry. The negative partial charge of −1.46*e* at the CDP-carbon atom in $\mathbf{1}^{Me}$ is reduced to −1.24*e* upon protonation (complex $\mathbf{2}^{Me}$), while the partial charge of the CDP-bound phosphorus atoms and the central nickel center remains almost unchanged. These findings differ from the protonation of methyl and halogene adducts of hexaphenylcarbodiphosphorane, where the protonation results in a less negative partial charge at the CDP-carbon atom and an increased positive charge at the connected phosphorus atoms.[26]

Deprotonation of the CH_2-group has only a minor effect on the partial charge at the CDP-carbon atom, the coordinated nickel, and the attached phosphorus atoms. The partial charges at the phosphorus atoms in $\mathbf{3}^{Me}$ differ only by 0.03*e*. Similar observations are made for the dimers *cis*-$\mathbf{6}^{Me}$, *trans*-$\mathbf{6}^{Me}$ and *cis*-$\mathbf{7}^{Me}$, which are very similar in their partial charges.

To support the findings above, we examined the electronic structure of the CDP-moiety by QTAIM (quantum theory of atoms in molecules) calculations. The partial charges derived by the AIM analysis are similar to the values in Table 2 and show the same trend. The Laplacian distribution of the electron density $\nabla^2\rho$ in the Ni–C^{CDP}–P-plane of $\mathbf{1}^{Me}$ indicates a high polarity of the P–C^{CDP}-bond towards the CDP-carbon atom, which is increasing upon protonation of the CDP-carbon atom ($\mathbf{2}^{Me}$). The P–C-bonds within the planar five-membered ring of the deprotonated arm in $\mathbf{3}^{Me}$ give rise to a similar laplacian distribution (Fig. 6), clearly illustrating that all P–C-bonds within the cycle show similar bonding characteristics. Overall, the topological analysis reveals a very similar situation in the three complexes (**1**–**3**). As arm-deprotonation has a minor-impact on the donor properties of the CDP-carbon atom, the analysis of the dimeric complexes allows for the direct comparison of protonated and non-protonated CDP-like carbon atoms. Using the example of *cis*-$\mathbf{6}^{Me}$, it becomes evident that the two carbon-based donor groups within the four-membered metallacycle are very similar.

2.3. Relative stability of tautomeric ligands

The bridging, phosphorus-bound carbon atoms in the pincer ligands of the nickel complexes reported herein exhibit very similar environments and just differ in the number of bound hydrogen atoms. For each number of bound hydrogen atoms and the corresponding overall charge, different tautomers can be realised in the (pre)ligands and in complexes. For this reason, we started to investigate the relative stability of all possible isomers for the corresponding methyl-substituted compounds by means of DFT. This includes the pre-ligands with different degrees of protonation, ranging from the doubly protonated CDP to the dianionic ligand observed in **5**.

The relative energies are summarised in Fig. 7. The isomers are unambiguously identified by the number triple *n*-*m*-*o*, representing the number of bound hydrogen atoms at each of the bridging carbon atoms. The resulting charge is given by *q*. For the diprotonated CDP (*q* = +2) only one isomer (2-2-2) with three CH_2-groups is possible. In agreement with the experimental results,[19] the 2-1-2 isomer was calculated to be the most stable one for the protonated CDP (*q* = +1). The non-symmetric 2-2-1 isomer is calculated to be 62 kJ mol^{-1} higher in Gibbs enthalpy. In case of the neutral ligand (*q* = 0) with four hydrogen atoms distributed over three bridging carbon atoms, the 2-1-1 isomer was calculated to be the most stable one. In contrast to complex **1**, where the coordinated 2-0-2 isomer seems to be the most stable one, this isomer is 34 kJ mol^{-1} higher in Gibbs enthalpy than the 2-1-1 isomer. Interestingly,

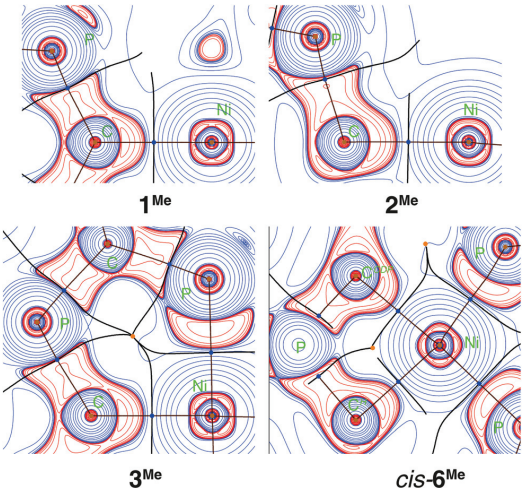

Fig. 6 Contour line diagrams of the Laplacian distribution $\nabla^2\rho$ of $\mathbf{1}^{Me}$–$\mathbf{3}^{Me}$ in the Ni–C–P-plane, as well as $\nabla^2\rho$ of *cis*-$\mathbf{6}^{Me}$ in the C–Ni–C-plane (bond critical points are blue, charge accumulation is depicted as red lines, charge depletion is depicted as blue lines).

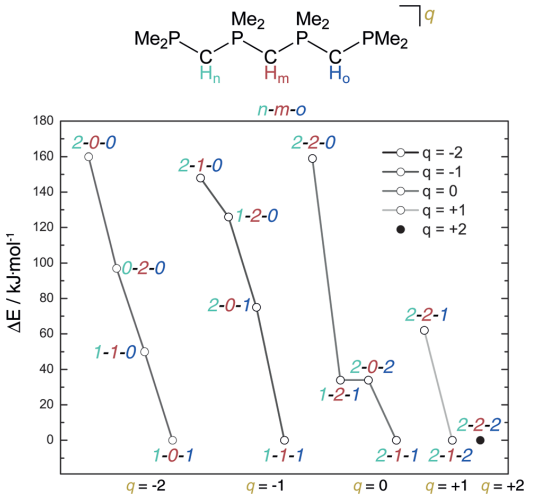

Fig. 7 Relative stability of tautomers for different pre-ligands (B97D, def2-TZVPP, tautomers are connected by a solid line).

the corresponding 1-2-1 isomer is equally stable as the 2-0-2 isomer. For the least stable isomer (2-2-0) with the CDP group located at the arm, the geometry optimisation leads to P–C-bond cleavage. For the anionic compound (q = −1), the 1-1-1 isomer is the most stable, followed by the 2-0-1 isomer (+75 kJ mol^{-1}), the 1-2-0 (+126 kJ mol^{-1}) and the 2-1-0 isomer (+148 kJ mol^{-1}). Again, the isomer observed as ligand in complex **3** (2-0-1) is not the most stable one in the uncoordinated form. As observed in complex **5**, the 1-0-1 isomer of the di-anionic ligand (q = −2) is also the most stable in the non-coordinated form. The non-symmetric 1-1-0 isomer is +50 kJ mol^{-1} in Gibbs enthalpy, while di-CDP isomers 0-2-0 (+97 kJ mol^{-1}) and 2-0-0 (+160 kJ mol^{-1}) are even higher in Gibbs enthalpy. Overall, the calculation of relative stabilities support our experimental observations that the reaction of the protonated or diprotonated CDP-ligand with different bases does not lead to the free CDP.

2.4. Monomer *vs.* dimer stability

The irreversible dimer formation by deprotonation of complex **3** made us to evaluate the relative stability of monomers and dimers for different degrees of ligand protonation (Fig. 8). The monomeric nickel(II) complex **3**^{Me} is 15 kJ mol^{-1} higher in Gibbs enthalpy than one half of the corresponding methyl-substituted dimers *cis*- and *trans*-**6**^{Me}, which were found to be equal in Gibbs enthalpy. These findings indicate that complex **3** is the kinetic reaction product of the deprotonation of **1**. Furthermore, the generation of the Ni–C–P–C-metallacycle seems to result in a particular stable situation.

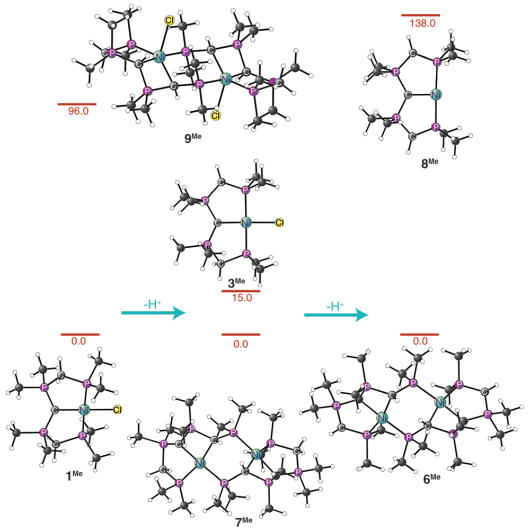

Fig. 8 Optimised geometries of monomers and their corresponding dimers for different degrees of ligand (de)protonation. Relative energies are given in red (B97D/def2-TZVPP; counter ions are included, but are omitted for clarity).

Deprotonation of complex **3** results in the formation of the dimers *cis*- and *trans*-**5**. In this case, the *cis*-isomer of complex **5**^{Me} is 6 kJ mol^{-1} more stable the *trans*-**5**^{Me}. However, the corresponding monomeric, tri-coordinate complex **7**^{Me} is significantly higher in Gibbs enthalpy (+138 kJ mol^{-1}) and most likely not observable.

Protonation of complex **3** yields quantitatively the monomeric complex **1**, which, according to our experimental observations is thermodynamically the most stable isomer. Nonetheless, we investigated the corresponding dimer **8**^{Me} using DFT, by attaching a proton to the two CDP groups in **6**^{Me}. Furthermore, the chloride counter ions in **6** and **8**^{Me} were found to be in proximity (approx. 4.4 Å) to the nickel atoms by both theory and experiment. However, the converged energetic minimum structure of the doubly protonated dimer **8**^{Me} exhibits a Ni-Cl-bond and a nickel(II) centre in a distorted trigonal bipyramidal environment. This species is 96 kJ mol^{-1} higher than the monomer **1**^{Me}.

2.5. Comparison with related donor groups

The first proton affinity of hexaphenylcarbodiphosphorane (1172 kJ mol^{-1})[6] was calculated to be slightly higher than those of N-hetrocyclic carbenes (~1144 kJ mol^{-1})[6] and secondary amines (~950 kJ mol^{-1}), but still lower than the proton affinities of anionic bases (>1300 kJ mol^{-1}),[27,28] that render an important class of bases. However, the second proton affinity of hexaphenylcarbodiphosphorane(777 kJ mol^{-1}) is significantly reduced and lower than the one of secondary amines.[6] The proton affinities of the cationic halogen adducts [Ph_3P-C(X)-PPh_3]$^+$ (X = halogene) were recently reported to be in the same range as the second proton affinity of hexaphenylcarbodiphosphorane.[26]

Interestingly, the proton affinities of metal-bound CDP's have not yet been investigated. As pointed out in the introduction, the CDP-based pincer-ligands represent a link between amine- and L_2BH-based pincer complexes investigated in our group. More importantly, groups with the general formulae R_2NH, R_2CH^-, L_2BH and L_2CH^+ can be formally regarded as isoelectronic (R = anionic substituent such as alkyl, L = neutral substituent such as phosphines). For this reason, we calculated the proton affinities for the corresponding nickel complexes, shown in Fig. 9. The synthesis of complexes of the type

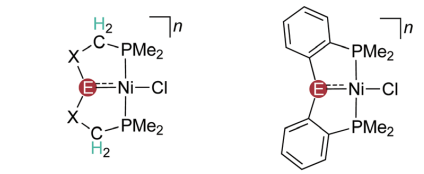

1^{Me}: E = C, X = PMe_2, n = +1
9^{Me}: E = B, X = PMe_2, n = 0
10^{Me}: E = N, X = CH_2, n = 0
11^{Me}: E = C, n = -1
12^{Me}: E = N, n = 0

Fig. 9 Nickel pincer complexes with different central donor groups, considered for the calculation of proton affinities.

Table 3 Calculated proton affinities (PAs) and NPA partial charges at B97D/def2-TZVPP level of theory

Complex	PA (kJ mol^{-1})	q (E)	q (H)	q (Ni)	q (X)
$\mathbf{1}^{Me}$	777.8	−1.44	—	+0.38	+1.59
$\mathbf{2}^{Me}$	—	−1.23	+0.27	+0.37	+1.59
$\mathbf{9}^{Me}$	1225.4	−1.12	—	+0.28	+1.25
$\mathbf{9}^{Me}$ + H^+	—	−0.89	+0.06	+0.27	+1.33
$\mathbf{10}^{Me}$	1066.9	−0.64	—	+0.40	−0.23
$\mathbf{10}^{Me}$ + H^+	—	−0.49	+0.39	+0.41	−0.23
$\mathbf{11}^{Me}$	1461.6	−0.32	—	+0.31	−0.07
$\mathbf{11}^{Me}$ + H^+	—	−0.45	+0.22	+0.35	−0.01
$\mathbf{12}^{Me}$	988.2	−0.56	—	+0.42	+0.16
$\mathbf{12}^{Me}$ + H^+	—	−0.60	+0.40	+0.42	+0.13

10,[29–32] **11** [33] and **12** [34,35] was previously reported with different substituents at the phosphine groups. Transition metal complexes with pincer-type ligands like in **9** + H^+ were recently reported with other metals, but with nickel as central atom it was not possible to stabilise such a complex.[15,36] However, the corresponding deprotonated complexes like **9** are unknown so far.

A qualitative analysis of molecular orbitals revealed that orbitals representing the Ni–E- and the Ni–Cl-interactions are very similar. The HOMO in all complexes is best described as doubly anti-bonding π-interaction between the central donor group E, a nickel-centred d-orbital and the chlorido ligand.[37]

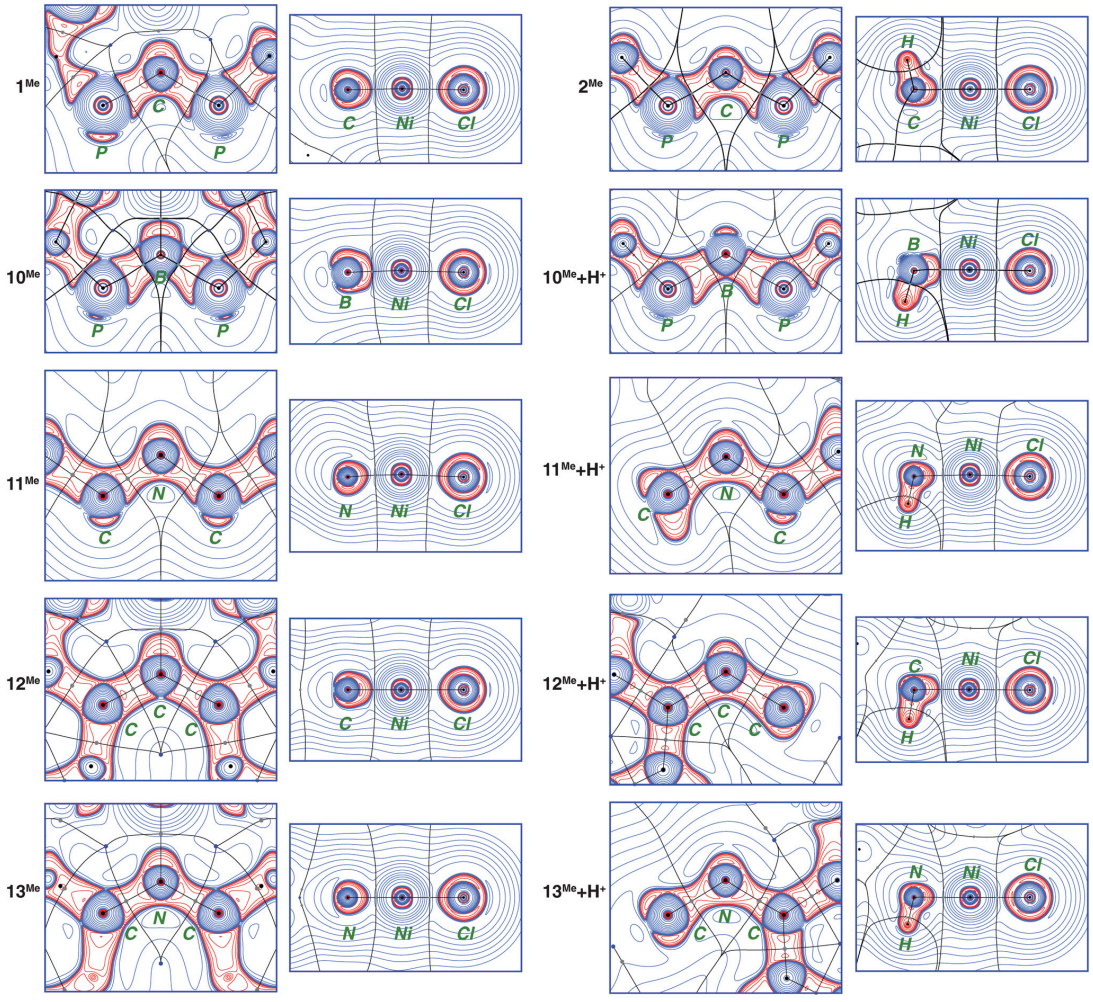

Fig. 10 Contour line diagrams of the Laplacian distribution $\nabla^2\rho$ of different nickel pincer complexes in their deprotonated and protonated form; the left diagram of each complex represents the P–C–P-plane, the right diagram the E–Ni–Cl-plane (E = B, C, N; bond critical points are grey, charge accumulation is depicted as red lines, charge depletion is depicted as blue lines).

View Article Online
Dalton Transactions Paper

Upon protonation of the coordinated donor group E, the HOMO changes to an anti-bonding π-interaction of the nickel-centred d-orbital and the chlorido ligand.

A closer look on partial charges derived by natural population analysis (NPA) reveals that the absolute value of the negative partial charge q(E) decreases in the order L_2CH^+ > L_2BH > R_2NH > R_2CH^- (Table 3). Moreover, the partial charge at the phosphorus atoms in $\mathbf{2}^{Me}$ is more positive than in $\mathbf{9}^{Me}$ + H, leading to the biggest partial charge difference for the C–P-bond. These findings reflect the difference in electronegativity between boron and carbon. Despite the significant charge differences between the P–B- and the P–C-bond, both are often described as a donor interaction from the phosphine to the EH-group.

The calculated proton affinities (PAs) for the nickel complexes in Table 3 do not correlate with the partial charge q(E) at the atom E of the central donor group. The PA of the CDP-based nickel pincer complex $\mathbf{1}^{Me}$ is with 807.5 kJ mol^{-1} only slightly higher than the second PA of hexaphenylcarbodiphosphorane.[38] The amido-based pincer complexes $\mathbf{10}^{Me}$ and $\mathbf{12}^{Me}$ exhibit higher PAs of 1108.1 and 1024.2 kJ mol^{-1}, respectively. The highest proton affinity (1499.3 kJ mol^{-1}) among this series is observed for the alkylidene complex $\mathbf{12}^{Me}$. In summary, complex $\mathbf{1}^{Me}$ exhibits the most negative partial charge (−1.44e) at the atom E of the central donor groups among this series and has the lowest proton affinity.

Taking the PA as measure for the ability of the donor group to act as internal base, the comparison of well established, cooperative amido-based pincer complexes ($\mathbf{10}^{Me}$) with the CDP-based complex $\mathbf{1}^{Me}$ suggests that the CDP-group is a significantly weaker base. In turn, the higher tendency to transfer the proton could be advantageous in reactions involving dihydrogen, in which the concerted proton-hydride-transfer is often rate-determining. Such a situation might be achieved under more acidic conditions.

The unexpected trend in proton affinities that reflects the stabilisation of the corresponding base tempted us to compare the bonding situation in these boron-, carbon- and nitrogen-based pincer-type complexes using QTAIM. Fig. 10 shows the Laplacian distribution $\nabla^2\rho$ for different nickel pincer complexes in their deprotonated and protonated forms. Inspection of the E–P- and E–C-bonds (E = B, C, N) reveals different bonding situations in the back-bone of the four types of complexes. In particular, protonated complexes give meaningful insights, as no π-bonding is expected in these complexes and the Laplacian distribution along the bond path is only related to a σ-bond interaction (Fig. 10 right). The C–C-bond in $\mathbf{11}^{Me}$ + H^+ is best described as a rather non-polar covalent bond. The C–N-bonds in $\mathbf{10}^{Me}$ + H^+ and $\mathbf{12}^{Me}$ + H^+ are similar, but show accumulation of electron density at the nitrogen atom with the bond critical point (bcp) shifted towards the corresponding carbon atom. Interestingly, the bcp of the P–C-bond in $\mathbf{2}^{Me}$ is located near the phosphorus atom, while electron accumulation is observed at the carbon atom of the protonated CDP-moiety. In contrast, the situation is reversed for the P–B-bond in $\mathbf{9}^{Me}$ + H^+ with the bcp located next to the boron atom and electron accumulation at the phosphorus atom. These findings are in line with the electronegativity of boron(2.04), carbon (2.55) and phosphorus (2.19).[39] However, the significant differences in polarity of the E–P-bond (E = B, C) in combination with the contrary Laplacian distribution of both bonds might be taken as indications that the P–C-bond rather has characteristics of a covalent electron sharing interaction, while the P–B-bond is well described by a donor bond from the phosphine to the borylene-moiety.

A qualitative interpretation of the laplacian distribution $\nabla^2\rho$ and the bond path of E–H-bond reveals differences that are in line with the difference in electronegativity of the E–H-bond. The bcp of the N–H-bond in $\mathbf{10}^{Me}$ + H^+ is located near the hydrogen atom, while charge accumulation is observed at the nitrogen atom. The C–H-bond in $\mathbf{2}^{Me}$ appears rather non-polar, while electron accumulation is found near the hydrogen atom of the B–H-bond in $\mathbf{9}^{Me}$ + H^+. Overall, these findings show that the polarity of the E–H-bond does not correlate with the calculated proton affinities and underlines again that PAs rather reflect the stabilisation of the deprotonated form.

3. Conclusions

We reported a comprehensive study on the (de)protonation chemistry of CDP-based nickel pincer complexes. Our investigation shows that protonation of the coordinated CDP-group does not lead to cleavage of the nickel carbon bond. The binding of CDP-groups in late transition metal complexes is characterised by an occupied π-anti-bonding state, which is maintained upon deprotonation of the arm. Continuous deprotonation results in the formation of a dimeric complex, whose protonation leads to a dimer of the initial monomeric complex. A quantum chemical investigation showed that in some cases, monomeric and dimeric complexes are very similar in energy. However, for the uncoordinated tridentate ligand, isomers without a CDP-moiety turn out to be more stable. A comparative quantum chemical study finally revealed differences in proton affinity and the nature of the E–P- and the E–H-bond for different nickel complexes. These results indicate that carbodiphosphoranes as donor groups in pincer-type ligands can potentially act as proton relay in cooperative catalysis.

Conflicts of interest

There are no conflicts to declare.

Acknowledgements

We gratefully acknowledge financial support from the Deutsche Forschungsgemeinschaft (LA 2830/3-2), the Erich-Becker-Stiftung (R. L.).

References

1 P. J. Quinlivan and G. Parkin, *Inorg. Chem.*, 2017, **56**, 5493–5497.
2 G. E. Hardy, J. I. Zink, W. C. Kaska and J. C. Baldwin, *J. Am. Chem. Soc.*, 1978, **100**, 8001–8002.
3 G. E. Hardy, W. C. Kaska, B. P. Chandra and J. I. Zink, *J. Am. Chem. Soc.*, 1981, **103**, 1074–1079.
4 A. T. Vincent and P. J. Wheatley, *J. Chem. Soc., Dalton Trans.*, 1972, 617.
5 R. Tonner, F. Öxler, B. Neumüller, W. Petz and G. Frenking, *Angew. Chem., Int. Ed.*, 2006, **45**, 8038–8042.
6 R. Tonner, G. Heydenrych and G. Frenking, *ChemPhysChem*, 2008, **9**, 1474–1481.
7 R. Tonner and G. Frenking, *Chem. – Eur. J.*, 2008, **14**, 3273–3289.
8 C. Pranckevicius, L. Fan and D. W. Stephan, *J. Am. Chem. Soc.*, 2015, **137**, 5582–5589.
9 Y. C. Hsu, J. S. Shen, B. C. Lin, W. C. Chen, Y. T. Chan, W. M. Ching, G. P. Yap, C. P. Hsu and T. G. Ong, *Angew. Chem., Int. Ed.*, 2015, **54**, 2420–2424.
10 C. C. Roberts, D. M. Matías, M. J. Goldfogel and S. J. Meek, *J. Am. Chem. Soc.*, 2015, **137**, 6488–6491.
11 M. J. Goldfogel, C. C. Roberts and S. J. Meek, *J. Am. Chem. Soc.*, 2014, **136**, 6227–6230.
12 W. Petz, *Coord. Chem. Rev.*, 2015, **291**, 1–27.
13 I. Romeo, M. Bardaji, M. Concepción Gimeno and M. Laguna, *Polyhedron*, 2000, **19**, 1837–1841.
14 W. Petz, F. Öxler and B. Neumüller, *J. Organomet. Chem.*, 2009, **694**, 4094–4099.
15 L. Vondung, N. Frank, M. Fritz, L. Alig and R. Langer, *Angew. Chem., Int. Ed.*, 2016, **55**, 14450–14454.
16 L. Vondung, L. E. Sattler and R. Langer, *Chem. – Eur. J.*, 2018, **24**, 1358.
17 S. Schneider, J. Meiners and B. Askevold, *Eur. J. Inorg. Chem.*, 2012, 412–429.
18 L. Maser, L. Vondung and R. Langer, *Polyhedron*, 2017, DOI: 10.1016/j.poly.2017.09.009.
19 C. Reitsamer, S. Stallinger, W. Schuh, H. Kopacka, K. Wurst, D. Obendorf and P. Peringer, *Dalton Trans.*, 2012, **41**, 3503.
20 Based on a reviewer comment, we felt the need to clarify that the orbitals at the backbone P-atoms that are used for π-bonding in the resonance structures **II** and **III** are best described as a set of σ*-orbitals of two P–C-bonds of the PPh_2R-group (2e representation with approx. C_{3V} local symmetry).
21 J. Sundermeyer, K. Weber and K. Peters, *Organometallics*, 1994, **13**, 2560–2562.
22 S. Stallinger, C. Reitsamer, W. Schuh, H. Kopacka, K. Wurst and P. Peringer, *Chem. Commun.*, 2007, **012**, 510–512.
23 C. Reitsamer, I. Hackl, W. Schuh, H. Kopacka, K. Wurst and P. Peringer, *J. Organomet. Chem.*, 2017, **830**, 150–154.
24 H. Schmidbaur, A. Mörtl and B. Zimmer-Gasser, *Chem. Ber.*, 1981, **114**, 3161–3163.
25 D. J. Brauer, C. Kruger, P. J. Roberts and Y.-h. Tsay, *Chem. Ber.*, 1974, **107**, 3706–3715.
26 W. Petz, I. Kuzu, G. Frenking, D. M. Andrada, B. Neumüller, M. Fritz and J. E. Münzer, *Chem. – Eur. J.*, 2016, **22**, 8536–8546.
27 W. L. Jolly, *Modern Inorganic Chemistry*, McGraw-Hill, New York, 2nd edn, 1991.
28 NIST - Computational Chemistry Comparison and Benchmark DataBase, http://cccbdb.nist.gov/pa1.asp.
29 D. Walther, T. Dohler, K. Heubach, O. Klobes, B. Schweder and H. Gorls, *Z. Anorg. Allg. Chem.*, 1999, **625**, 923–932.
30 P. L. Orioli and C. A. Ghilardi, *J. Chem. Soc. A*, 1970, 1511–1516.
31 S. S. Rozenel, J. B. Kerr and J. Arnold, *Dalton Trans.*, 2011, **40**, 10397.
32 M. Tamizmani and C. Sivasankar, *J. Organomet. Chem.*, 2017, **845**, 82–89.
33 D. V. Gutsulyak, W. E. Piers, J. Borau-Garcia and M. Parvez, *J. Am. Chem. Soc.*, 2013, **135**, 11776–11779.
34 L.-C. Liang, P.-S. Chien, J.-M. Lin, M.-H. Huang, Y.-L. Huang and J.-H. Liao, *Organometallics*, 2006, **25**, 1399–1411.
35 C. Yoo, S. Oh, J. Kim and Y. Lee, *Chem. Sci.*, 2014, **5**, 3853–3858.
36 M. Grätz, A. Bäcker, L. Vondung, L. Maser, A. Reincke and R. Langer, *Chem. Commun.*, 2017, **53**, 7230–7233.
37 For further details please see ESI. †
38 R. Tonner, G. Heydenrych and G. Frenking, *ChemPhysChem*, 2008, **9**, 1474–1481.
39 *CRC Handbook of Chemistry and Physics*, ed. W. M. Haynes, CRC Press, 97th edn, 2016.

Electronic Supplementary Material (ESI) for Dalton Transactions.

Supporting Information

Carbodiphosphorane-based nickel pincer complexes and their (de)protonated analogues: dimerisation, ligand tautomers and proton affinities

Leon Maser[a], Jan Heritsch[a] and Robert Langer*[a]

1. Syntheses

1.1 Materials and Methods

All experiments were carried out under an atmosphere of purified argon or nitrogen in the MBraun glove boxes LABmaster 130 and UNIlab or using standard Schlenk techniques.

THF and diethyl ether were dried over Na/K alloy, *n*-hexane was dried over $LiAlH_4$, toluene was dried over sodium and dichloromethane was dried over CaH_2. Deuterated solvents were sparged with argon and stored over molecular sieves.

1 was obtained following the reported procedure by REITSAMER *et al.*[1]

^{1}H, ^{13}C, and ^{31}P NMR spectra were recorded using Bruker AVANCE 300 A, DRX 400, DRX 500 and Avance 500 NMR spectrometers at 300 K. ^{1}H and $^{13}C\{^{1}H\}$, ^{13}C-APT (attached proton test) NMR chemical shifts are reported in ppm downfield from tetramethylsilane. The resonance of the residual protons in the deuterated solvent was used as internal standard for ^{1}H NMR. The solvent peak of the deuterated solvent was used as internal standard for ^{13}C NMR. ^{31}P NMR chemical shifts are reported in ppm downfield from H_3PO_4 and referenced to an external 85 % solution of phosphoric acid in D_2O. The following abbreviations are used for the description of NMR data: br (broad), s (singlet), d (doublet), t (triplet), q (quartet), quin (quintet), m (multiplet), v (virtual).

FT-IR spectra were recorded by attenuated total reflection of the solid samples on a Bruker Tensor IF37 spectrometer. The intensity of the absorption band is indicated as w (weak), m (medium), s (strong), vs (very strong) and br (broad).

HR-ESI mass spectra were acquired with a LTQ-FT mass spectrometer (Thermo Fisher Scientific). HR-APCI mass spectra were acquired with a LTQ-FT mass spectrometer (Thermo Fisher Scientific). In both cases the resolution was set to 100.000. Elemental analyses were performed on a Vario Micro Cube Elemental Analyzer.

None of the compounds have been characterised by elemental analysis.

1.2 *Synthesis of Complex* **2**

To a suspension of 100 mg **1** (110 µmol, 1.0 eq.) in 10 ml diethyl ether, 0.15 ml of a solution of $HBF_4 \cdot OEt_2$ in diethyl ether (109 µmol, 1.0 eq.) were added. After stirring for 16 h, the solvent was removed *in vacuo* and the remaining orange solid was dissolved in 10 ml DCM. After filtration, layering of the solution with *n*-hexane yields 72 mg **2** (68.6 µmol, 62 %) as orange crystals.

Due to the low solubility of **2** in CD_2Cl_2 and MeCN-d_3 and its decomposition in DMSO-d_6 and D_3COD, the resonances of the bridging CH and CH_2 carbons could not be observed in 1D spectra and were assigned via 2D crosspeaks.

^{1}H NMR (300 MHz, CD_2Cl_2) δ_H: 4.39 – 4.05 (4H, m, CH_2), 4.37 (1H, t, $^2J_{H,P}$ = 18.7 Hz, P-C*H*-P), 7.75 – 7.11 (m, 32H, Phenyl-*H*), 7.83 (vq, 4H, *J* = 6.4 Hz, Phenyl-*H*), 7.91 (vq, 4H, *J* = 6.6 Hz, Phenyl-*H*) ppm.

^{13}C APT NMR (75 MHz, CD_2Cl_2) δ_C: 8.8 (P-*C*H-P), 31.5 (P-*C*H_2-P), 129.4 (vt, $J_{C,P}$ = 5.6 Hz, Phenyl-*C*), 130.3 (d, $J_{C,P}$ = 4.6 Hz, Phenyl-*C*), 130.4 (d, $J_{C,P}$ = 3.9 Hz, Phenyl-*C*), 133.0 – 132.7 (m, Phenyl-*C*), 133.3 (d, $J_{C,P}$ = 11.5 Hz, Phenyl-*C*), 133.8 (vt, $J_{C,P}$ = 6.4 Hz, Phenyl-*C*), 134.1 (vt, $J_{C,P}$ = 6.1 Hz, Phenyl-*C*), 135.0 (d, $J_{C,P}$ = 1.8 Hz, Phenyl-*C*), 135.8 (s, Phenyl-*C*) ppm.

^{31}P{^{1}H} NMR (121 MHz, CD_2Cl_2) δ_P: 6.1 (t, $^2J_{P,P}$ = 42.5 Hz), 43.6 (t, $^2J_{P,P}$ = 42.5 Hz) ppm.

FT-IR (ATR) $\tilde{}$/cm^{-1}: 3061 (w), 2972 (w), 2914 (w), 2325 (w), 1587 (w), 1485 (w), 1437 (s), 1367 (w), 1339 (w), 1314 (w), 1284 (w), 1191 (w), 1144 (m), 1098 (vs), 1050 (vs), 996 (vs), 884 (m), 838 (w), 783 (m), 732 (vs), 684 (vs), 643 (m), 578 (w), 525 (s), 506 (m), 489 (m), 470 (s).

ESI-MS (+) / : 873 (15%, M - H$^+$), 782 (100, M - NiClHR-ESI-MS (+) / : 873.1430 (calc. for [M] - H$^+$), 873.1436 (found, Δ = 0.7 ppm)

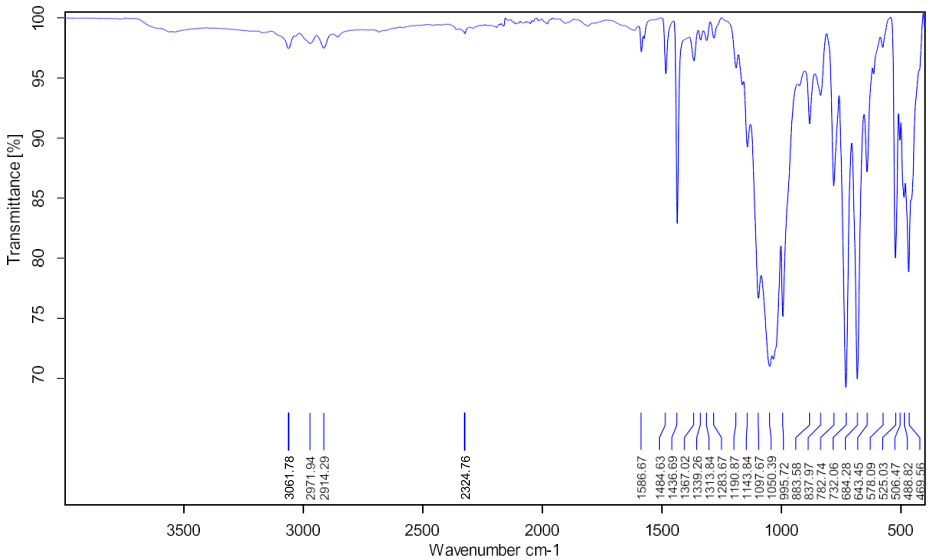

Figure 1- FT-IR spectrum of complex 2.

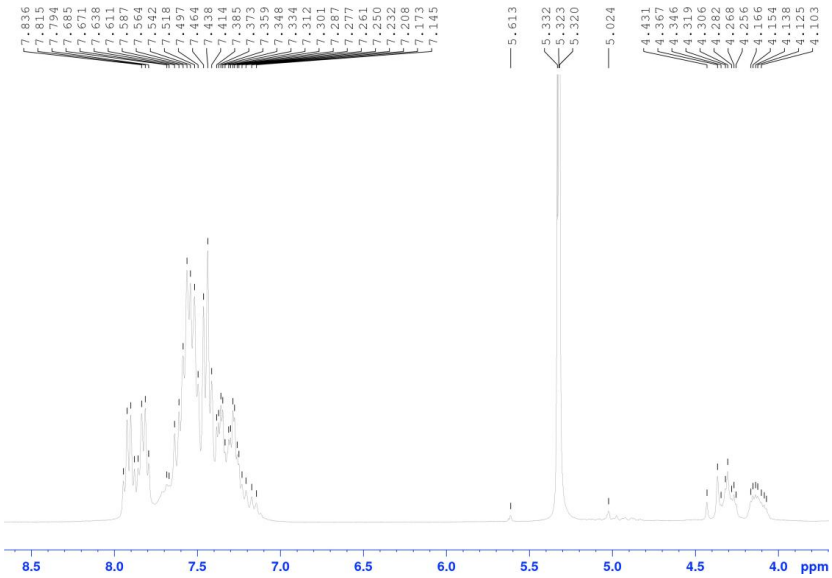

Figure 2 - ^{1}H NMR spectrum of complex 2 in CD_2Cl_2.

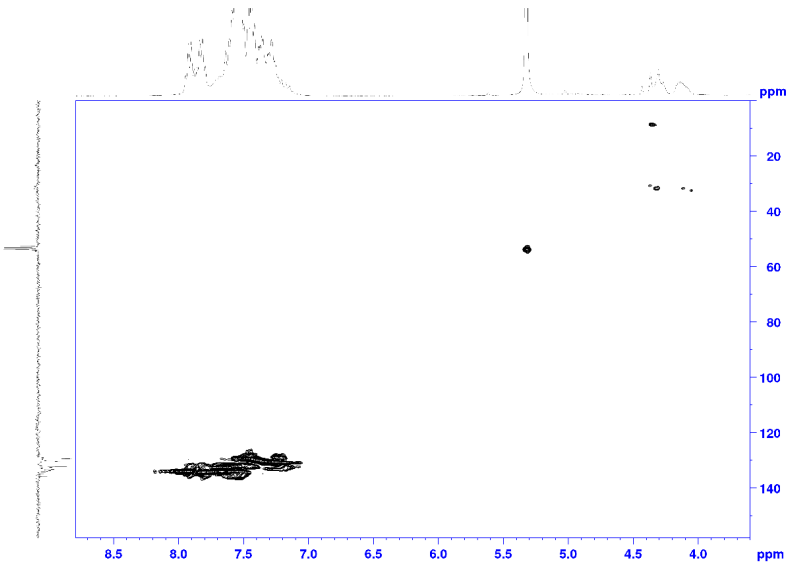

Figure 3 - $^{1}H,^{13}C$ HMQC NMR spectrum of complex 2 in CD_2Cl_2.

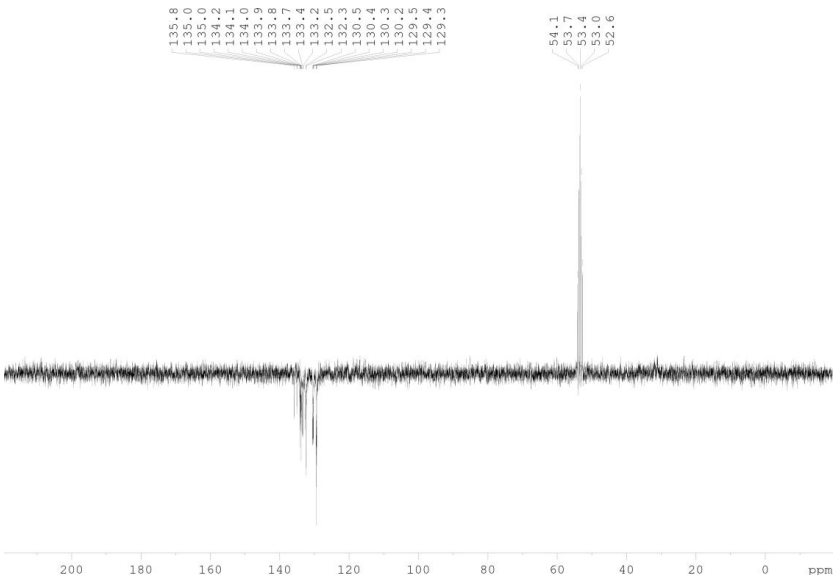

Figure 4 - ^{13}C APT NMR spectrum of complex 2 in CD_2Cl_2.

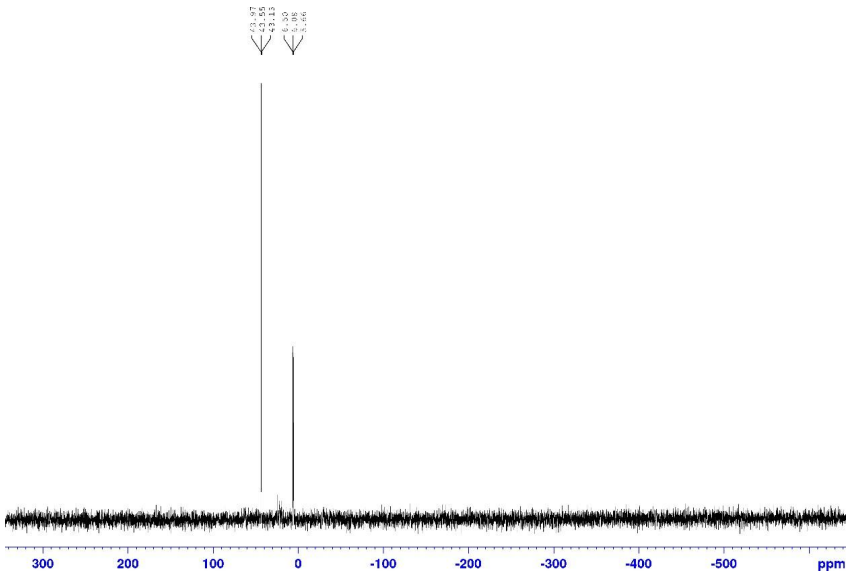

Figure 5 - $^{31}P\{^1H\}$ NMR spectrum of complex 2 in CD_2Cl_2.

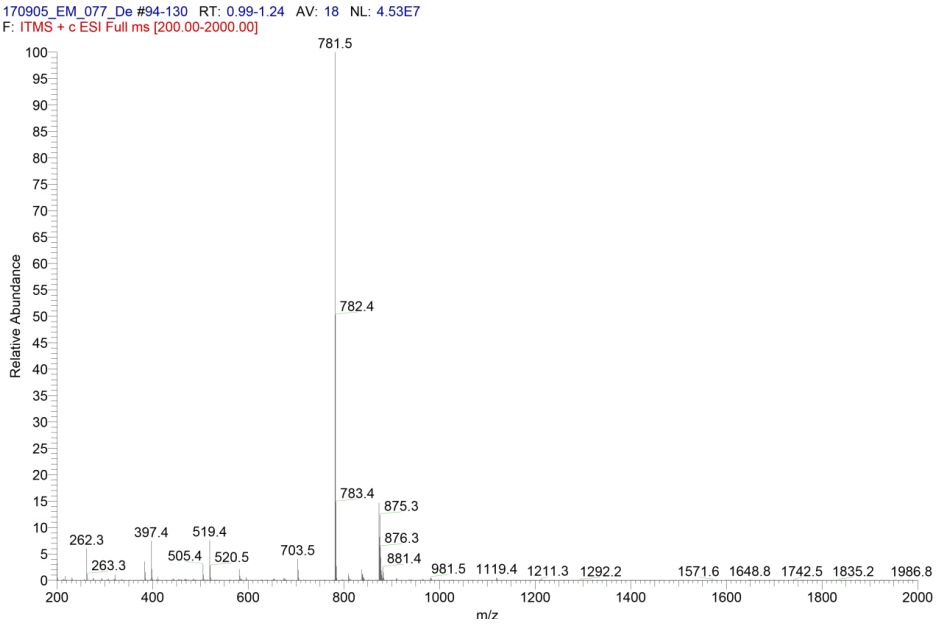

Figure 6 - ESI(+) MS spectrum of complex 2.

1.3 *Synthesis of Complex* **3**

200 mg **1** (220 µmol, 0.9 eq.) and 41 mg LiHMDS (245 µmol, 1.0 eq.) were dissolved in 20 ml THF and stirred for 16 h. After removal of the solvent in vacuo, the remaining dark brown solid was extracted with 20 ml of toluene. Removal of the solvent in vacuo yielded 120 mg (137 µmol, 56 %) **3** as dark red powder.

Crystals suitable for single-crystal X-ray diffraction measurements were obtained by layering a solution of **3** in THF with *n*-hexane and storing it at 4 °C.

Due to low solubility in most deuterated solvents (e.g. C_6D_6, CD_2Cl_2,...), NMR measurements were carried out in DMSO-d_6. **3** is only stable for a limited amount of time in DMSO-d_6 and shows decomposition to **1** and free ligand.

^{1}H NMR (300 MHz, DMSO-d_6) δ_H: 1.34 (1H, ddvt, $J_{H,P}$ = 16.5 Hz, $J_{H,P}$ = 5.2 Hz, $J_{H,P}$ = 2.4 Hz, P-C*H*-P), 3.46 (vt, 2H, $^2J_{H,P}$ = 9.3 Hz, P-CH_2-P), 6.90 - 7.07 (8H, m, Phenyl-*H*), 7.12 - 7.42 (24H, m, Phenyl-*H*), 7.67 - 7.77 (4H, m, Phenyl-*H*), 7.84 - 7.94 (4H, m, Phenyl-*H*) ppm.

^{13}C{^{1}H} NMR (126 MHz, DMSO-d_6) δ_C: 24.2 (s, P-*C*H-P), 36.8 (d, $^1J_{C,P}$ = 148.7 Hz, P-*C*H_2-P), 127.1 (d, $J_{C,P}$ = 6.7 Hz, Phenyl-*C*), 127.7 (d, $J_{C,P}$ = 13.2 Hz, Phenyl-*C*), 127.7 (s, Phenyl-*C*), 128.3 (d, $J_{C,P}$ = 14.8 Hz, Phenyl-*C*), 128.7 (s, Phenyl-*C*), 129.7 (s, Phenyl-*C*), 129.9 (s, Phenyl-*C*), 130.5 – 130.8 (m Phenyl-*C*), 131.1 (s, Phenyl-*C*), 131.2 (s, Phenyl-*C*), 131.9 (s, Phenyl-*C*), 132.0 (s, Phenyl-*C*), 132.3 (d, $J_{C,P}$ = 10.9 Hz, Phenyl-*C*), 132.6 (d, $J_{C,P}$ = 6.2 Hz, Phenyl-*C*), 133.4 (d, $J_{C,P}$ = 23.5 Hz, Phenyl-*C*), 139.0 (s, Phenyl-*C*), 141.7 (s, Phenyl-*C*) ppm.

^{31}P{^{1}H} NMR (101 MHz, C_6D_6) δ_P: 10.4 (ddd, $J_{P,P}$ = 42.6, 82.5, 348.1 Hz), 17.0 (ddd, $J_{P,P}$ = 28.1, 52.7, 81.8 Hz), 25.0 (ddd, $J_{P,P}$ = 27.1, 143.6, 348.3 Hz), 45.0 (ddd, $J_{P,P}$ = 40.7, 52.5, 144.0 Hz) ppm.

^{31}P{^{1}H} NMR (101 MHz, DMSO-d_6) δ_P: 10.3 (ddd, $J_{P,P}$ = 39.5, 84.1, 338.9 Hz), 20.7 (ddd, $J_{P,P}$ = 25.7, 52.0, 83.6 Hz), 23.8 (ddd, $J_{P,P}$ = 25.2, 147.8, 339.1 Hz), 44.8 (ddd, $J_{P,P}$ = 39.4, 52.0, 147.6 Hz) ppm.

FT-IR (ATR) $\tilde{}$/cm^{-1}: 3045 (w), 2321 (w), 1585 (w), 1480 (w), 1433 (m), 1377 (w), 1306 (w), 1184 (w), 1131 (m), 1092 (s), 1025 (w), 998 (w), 911 (m), 856 (m), 798 (m), 739 (vs), 689 (vs), 529 (m), 496 (vs), 475 (s), 441 (m), 416 (w).

ESI-MS (+) /: 873 (100%, $[M]H^+$), 782 (17, $[M]H_2^+$ - $NiCl^+$), 704 (28, $[M]H^+$ - PhNiCl).

HR-ESI-MS (+) /: 873.1430 (calc. for $[M]H^+$), 873.1432 (found, Δ = 0.2 ppm).

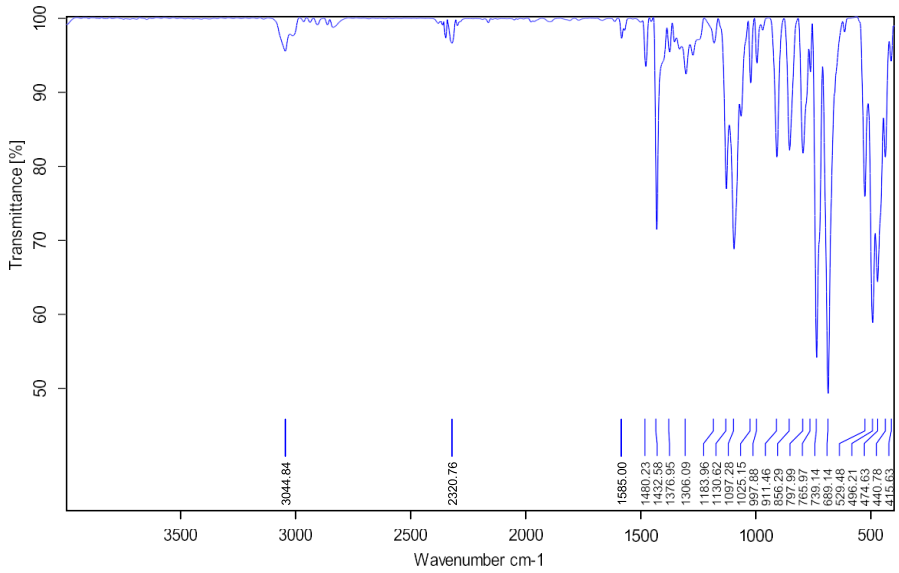

Figure 7 - FT-IR spectrum of complex 3.

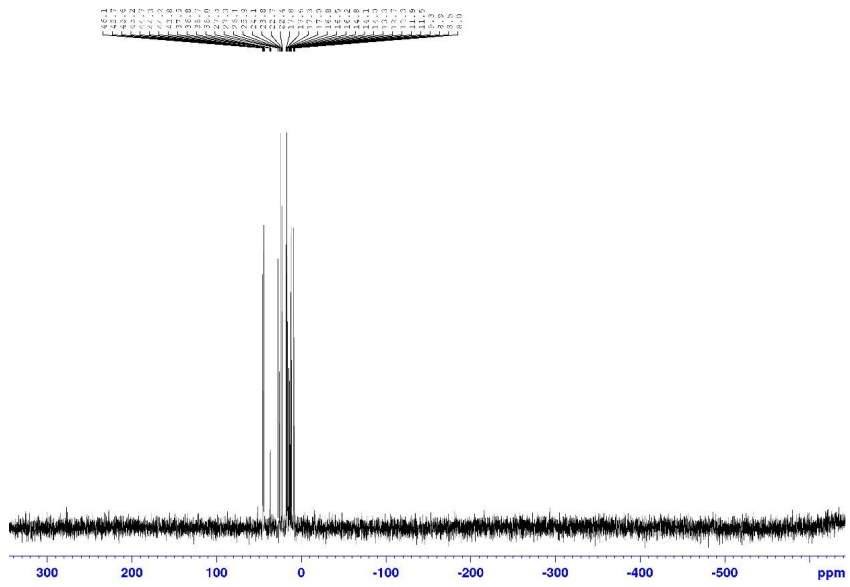

*Figure 8 - $^{31}P\{^{1}H\}$ NMR spectrum of complex **3** in C_6D_6.*

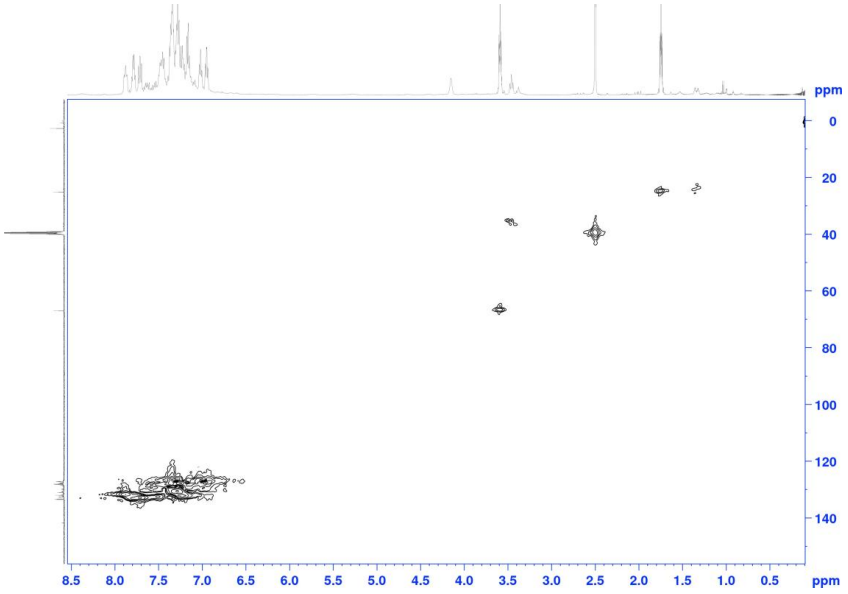

*Figure 9 - $^{1}H,^{13}C$ HMQC NMR spectrum of complex **3** in DMSO-d_6.*

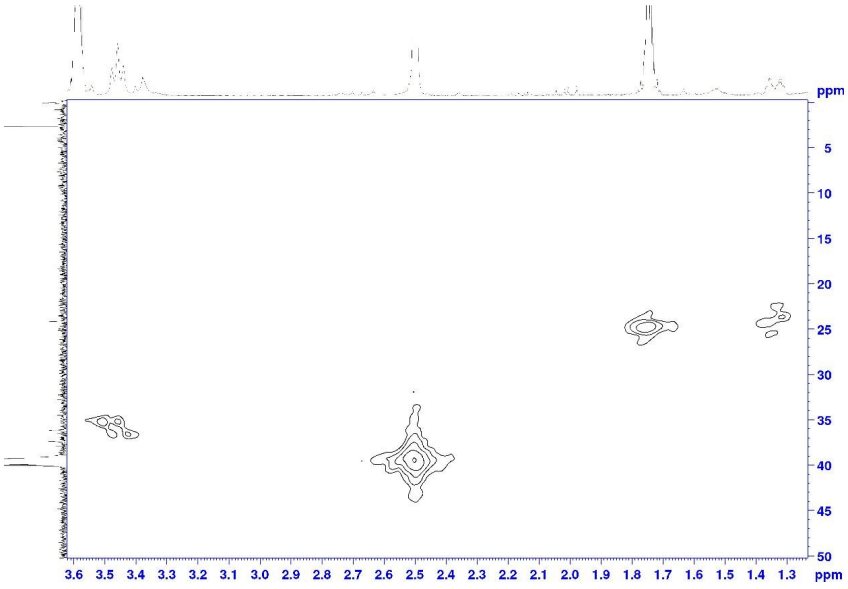

*Figure 10 – Detail of the $^{1}H,^{13}C$ HMQC NMR spectrum of complex **3** in DMSO-d_6, area of PCHP and PCH_2P resonances.*

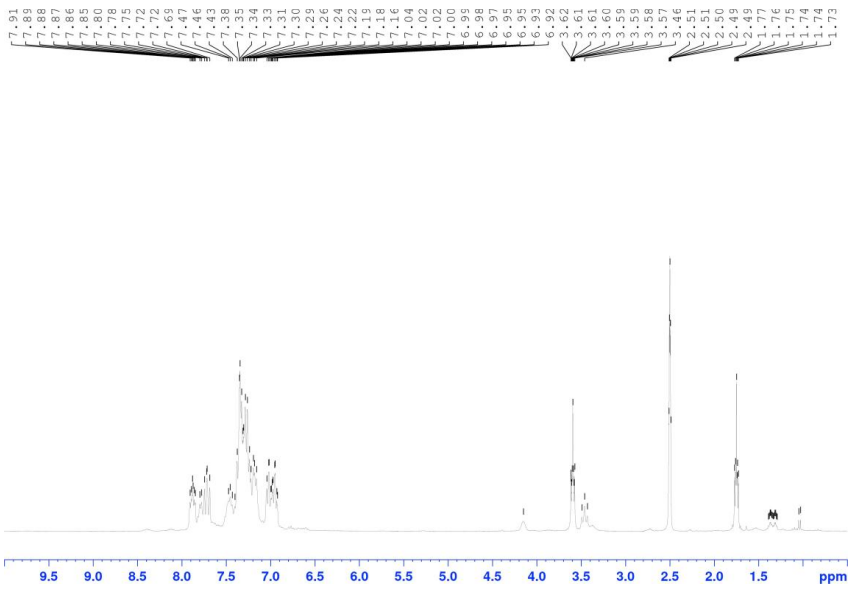

*Figure 11 - ^{1}H NMR spectrum of complex **3** in DMSO-d_6.*

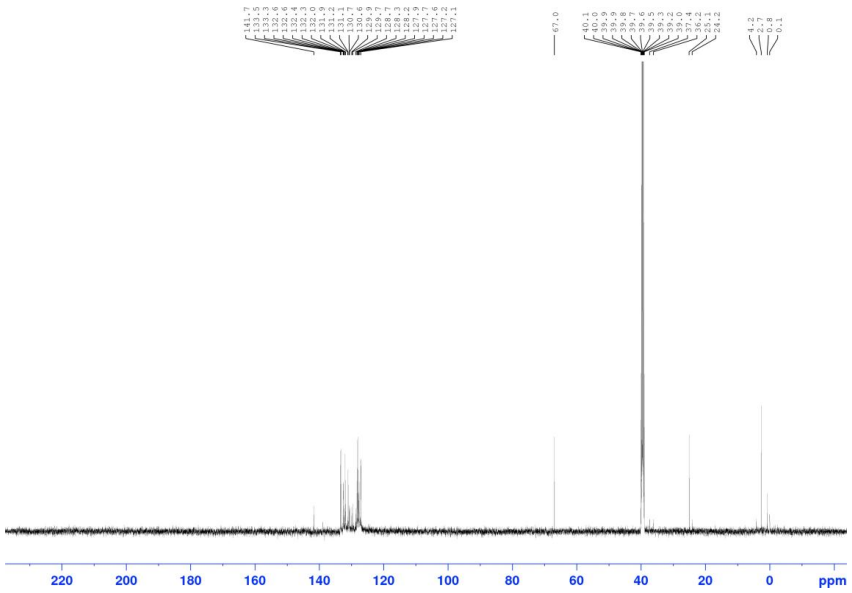

*Figure 12 - $^{13}C\{^{1}H\}$ NMR spectrum of complex **3** in DMSO-d_6.*

1.4 *Synthesis of Complex* **4**

488 mg **1** (536 µmol, 1.0 eq.) was suspended in 50 ml toluene and 10 ml of a solution of $AlMe_3$ in toluene (163 mmol/L, 1.79 mmol, 3.0 eq.) was added dropwise. After stirring for 15 h, the solvent was evaporated, the solids dissolved in 100 ml THF and filtered. Removal of the solvent *in vacuo* yielded 480 mg **4** (490 µmol, 91 %) as a dark orange solid.

The resonances of the bridging CH and CH_2 carbons could not be observed in 1D spectra and were assigned via 2D crosspeaks.

^{1}H NMR (300 MHz, CD_2Cl_2) δ_H: -0.78 (6H, s, $AlCl_2(CH_3)_2$), -0.74 (3H, t, $^{3}J_{H,P}$ = 9.6 Hz, Ni-CH_3), 3.81 (4H, vq, $^{2}J_{C,P}$ = 4.0 Hz, P-CH_2-P), 7.12 - 7.21 (8H, m, Phenyl-*H*), 7.24 - 7.34 (8H, m, Phenyl-*H*), 7.34 - 7.42 (12H, m, Phenyl-*H)*, 7.43 - 7.53 (12H, m, Phenyl-*H*) ppm.

^{13}C APT NMR (75 MHz, CD_2Cl_2) δ_C: -7.3 (Ni-CH_3), 45.7 (P-CH_2-P), 129.1 (t, $J_{C,P}$ = 5.8 Hz, Phenyl-*C*), 129.3 (t, $J_{C,P}$ = 5.0 Hz, Phenyl-*C*), 131.3 (t, $J_{C,P}$ = 1.1 Hz, Phenyl-*C*), 132.3 (t, $J_{C,P}$ = 1.7 Hz, Phenyl-*C*), 132.5 (t, $J_{C,P}$ = 5.0 Hz, Phenyl-*C*), 133.6 (t, $J_{C,P}$ = 6.4 Hz, Phenyl-*C*) ppm.

^{31}P{^{1}H} NMR (121 MHz, CD_2Cl_2) δ_P: 27.5 (t, $^{2}J_{P,P}$ = 53.5 Hz), 31.8 (t, $^{2}J_{P,P}$ = 53.4 Hz) ppm.

FT-IR (ATR) $\tilde{}$/cm^{-1}: 3057 (w), 2926 (w), 1587 (w), 1574 (w), 1484 (w), 1436 (s), 1362 (w), 1307 (w), 1261 (w), 1173 (m), 1099 (vs), 1025 (m), 999 (m), 816 (m), 774 (s), 760 (m), 735 (vs), 718 (s), 688 (vs), 668 (vs), 572 (m), 528 (m), 495 (s), 481 (s), 471 (s), 443 (m), 422 (w). JHV-8

ESI-MS (+) *m/z*: 874 (100%, $[M]ClH^+$ - Me^-), 798 (23, $[M]OH^+$ - $NiMe^+$), 704 (26, $[M]H^+$ - PhNiMe).

HR-ESI-MS (+) *m/z*: 873.1430 (calc. for $[M]ClH^+$ - Me^-), 873.1432 (found, Δ = 0.2 ppm).

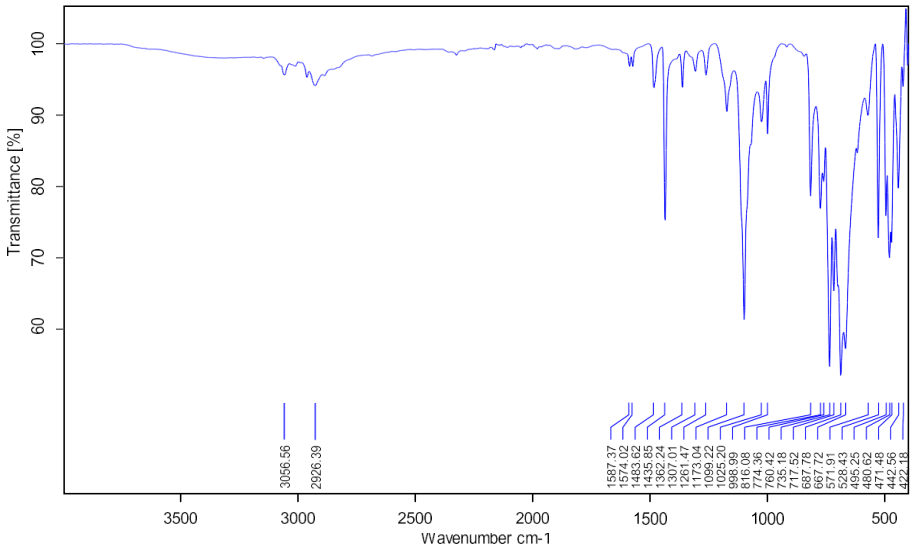

Figure 13 - FT IR spectrum of complex ***4****.*

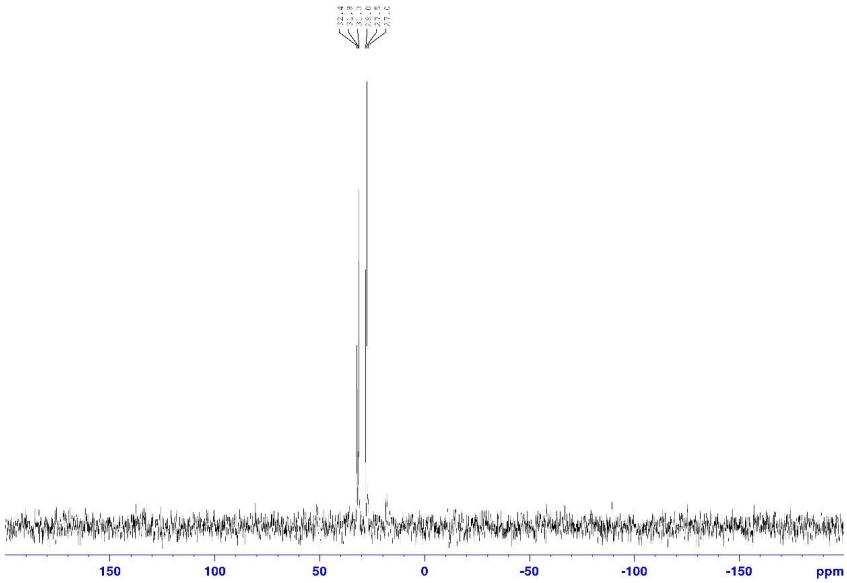

*Figure 14 – $^{31}P\{^{1}H\}$ NMR spectrum of complex **4** in CD_2Cl_2.*

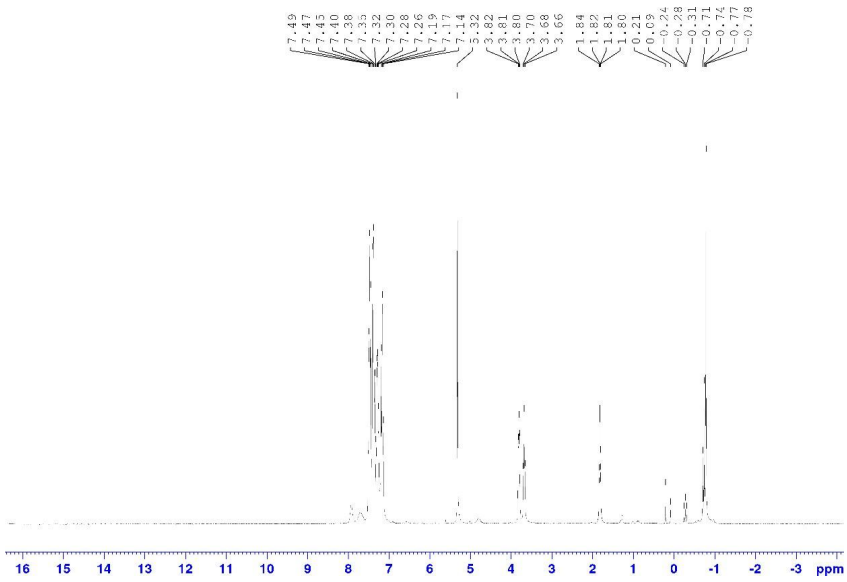

*Figure 15 - ^{1}H NMR spectrum of complex **4** in CD_2Cl_2.*

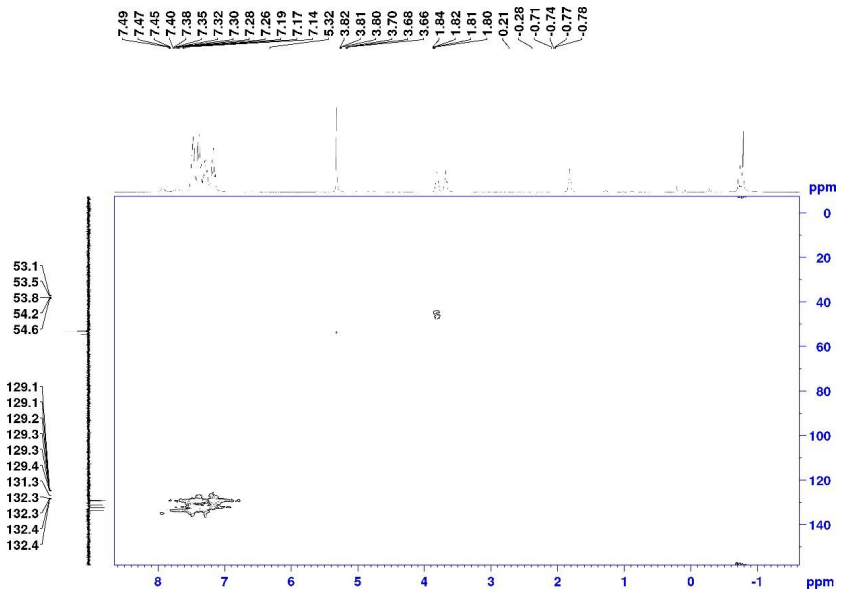

*Figure 16 - $^{1}H,^{13}C$ HMQC NMR spectrum of complex **4** in CD_2Cl_2.*

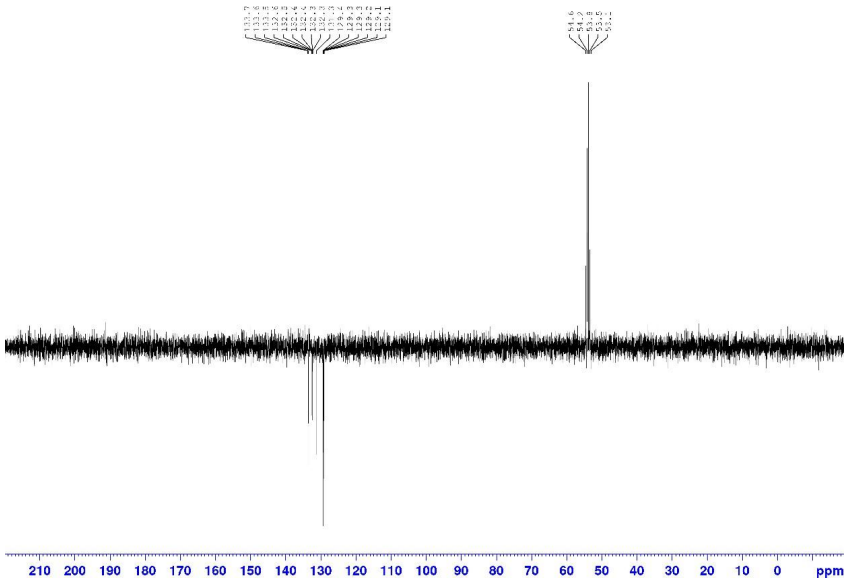

*Figure 17 - $^{13}C\{^{1}H\}$ NMR spectrum of complex **4** in CD_2Cl_2.*

1.5 *Synthesis of Complex* **5**

770 mg **1** (846 µmol, 1.0 eq.) and 460 mg LiHMDS (2.75 mmol, 3.3 eq.) were suspended in 50 ml toluene and stirred for 16 h. The resulting red-brown solution was filtered and layered with 100 ml *n*-hexane. After 7 d at -21 °C, the solvent was decanted from the formed dark brown crystals and they were dried *in vacuo*. 428 mg **5** (60 %, 256 mol) was obtained.

Crystals suitable for single-crystal X-ray diffraction measurements were obtained by layering a solution of **5** in THF with *n*-hexane.

5 decomposes in CD_2Cl_2. For this reason, saturated solution in C_6D_6 (15 mg in 0.6 ml) was used for NMR experiments. Due to the low concentration of the solution, unambiguous assignment of ^{13}C resonances was not possible in all cases. Furthermore, selective ^{31}P decoupling of ^{1}H NMR spectra was used to identify the proton resonances corresponding to the methyl-backbone of the ligand.

^{1}H NMR (300 MHz, C_6D_6) δ_H: 1.01 (2H, ddd, $^{2}J_{H,P}$ = 4.2 Hz, $^{2}J_{H,P}$ = 4.7 Hz, , $^{2}J_{H,P}$ = 10.7 Hz, P-C*H*-P), 1.13-1.23 (2H, br m, P-C*H*-P), 6.60-7.96 (80H, superimposed resonances, Phenyl-*H*) ppm.

$^{13}C\{^{1}H\}$ NMR (126 MHz, C_6D_6) δ_C: 30.2 (m, P-*C*H-P), 125.5-127.8 (m, Phenyl-*C*, *meta*+*para*) 131.0-133.0 (m, Phenyl-*C*, *ortho*) ppm.

$^{31}P\{^{1}H\}$ NMR (122 MHz, C_6D_6) δ_P: 14.8 (dd, $^{2}J_{P,P}$ = 24.7, $^{2}J_{P,P}$ = 48.2 Hz), 23.6 (dd, $^{2}J_{P,P}$ = 21.9, $^{2}J_{P,P}$ = 39.6 Hz), 37.1 (dd, $^{2}J_{P,P}$ = 23.2, $^{2}J_{P,P}$ = 153.4 Hz), 41.5 (dd, $^{2}J_{P,P}$ = 25.8, $^{2}J_{P,P}$ = 153.4 Hz) ppm.

FT-IR (ATR) ˜/cm^{-1}: 3374 (br w), 3052 (m), 2953 (m), 2896 (w), 2326 (w), 1980 (w), 1665 (br w), 1586 (w), 1481 (m), 1434 (s), 1307 (w), 1249 (m), 1178 (m), 1132 (m), 1097 (s), 1026 (w), 999 (w), 929 (s), 884 (w), 836 (s), 737 (vs), 690 (vs), 617 (w), 527 (m), 479 (s).

HR-FD-MS (+) /: 1673.32591 (calc. for M^{+}), 1673.32437 (found, Δ = -0.9 ppm)

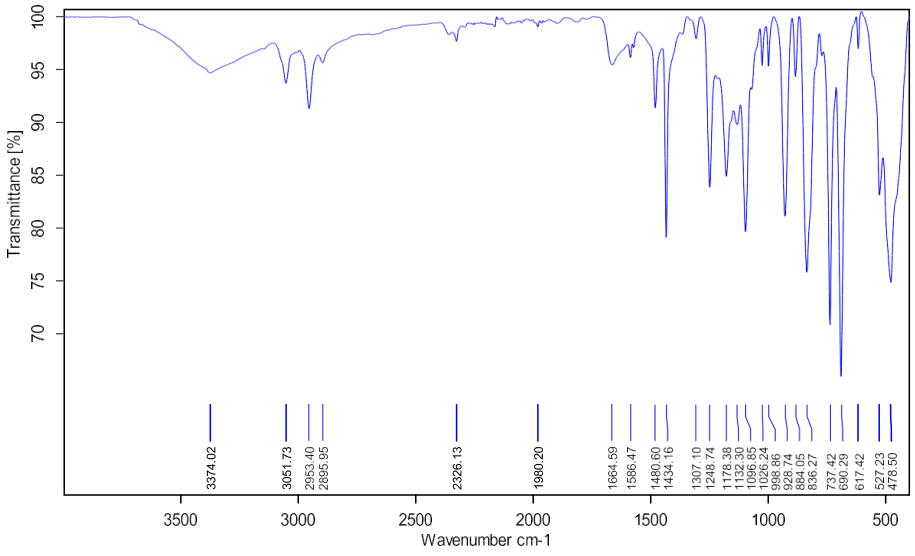

Figure 18 - FT IR spectrum of complex ***5****.*

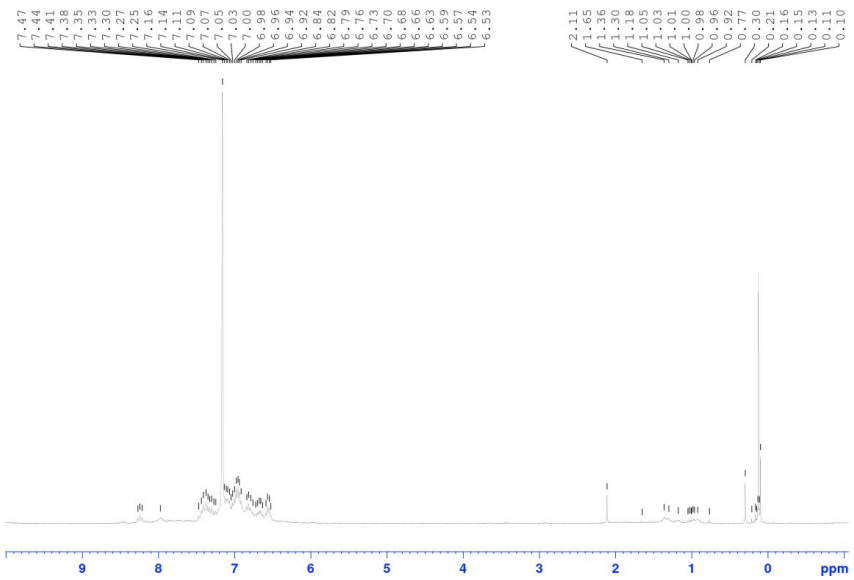

*Figure 19 - ^{1}H NMR spectrum of complex **5** in C_6D_6.*

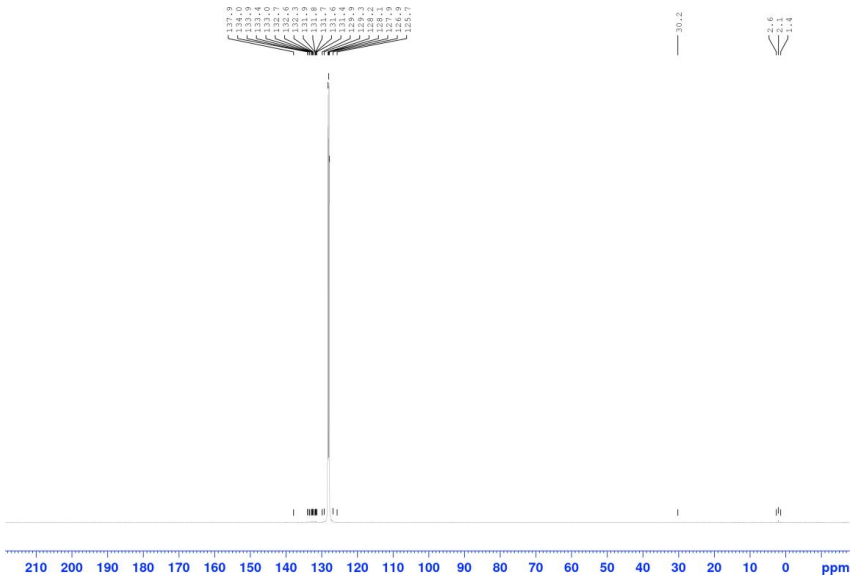

*Figure 20 - $^{13}C\{^{1}H\}$ NMR spectrum of complex **5** in C_6D_6.*

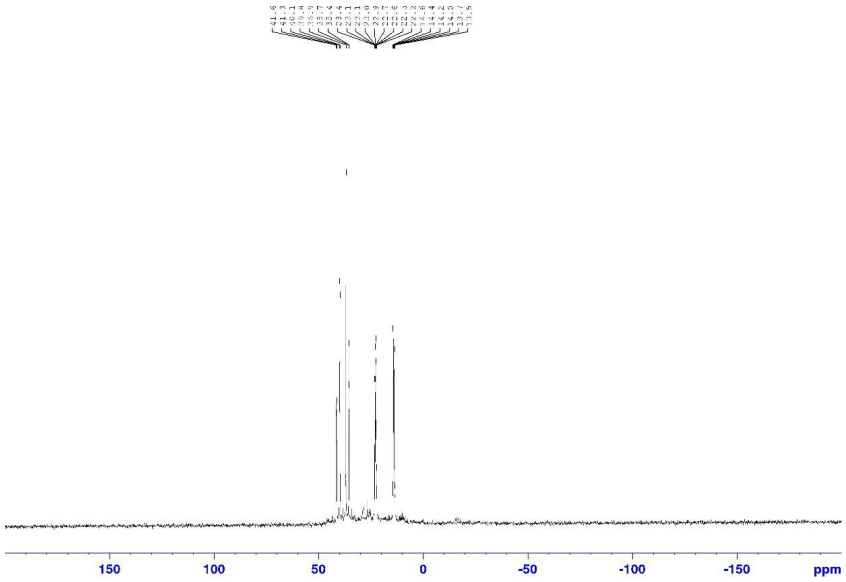

*Figure 21 – $^{31}P\{^{1}H\}$ NMR spectrum of complex **5** in C_6D_6.*

1.6 *Synthesis of Complex* **6**

To 81.0 mg **5** (48.4 µmol, 1.0 eq.), dissolved in 5 ml toluene, 50 µml HCl in DEE (2 M, 100 µmol, 2.1 eq.) were added. After stirring for 2 h, the solvents were removed in vacuo and 5 ml of DCM were added. After filtration through a syringe filter, the solvent was removed in vacuo and 52 mg **6** (29.8 µmol, 62 %) were obtained in form of a dark red solid.

The $^{31}P\{^{1}H\}$ NMR spectrum shows just three instead of the expected four resonances. This is most likely due to the overlapping of two resonances with similar shifts in the area of 22 to 25 ppm. The presence of two isomers in the crystal structure of **5** suggests a similar equilibrium for **6**, even though only one isomer is present in the isolated single crystals. ^{1}H NMR spectroscopy yields evidence for a second isomer in solution. The phosphorous bridging -CH- and -CH_2- groups of the second isomer display two low intensity resonances shifted +0.2 - 0.3 ppm compared to the main isomer (1.84-1.93 vs. 1.52-1.63 ppm and 3.63-3.81 vs. 3.48 ppm). The absent third resonance is superimposed by the main isomer resonance at 3.48 ppm, as suggested by a slightly bigger integral for the corresponding main isomer resonance and observed via 2D $^{1}H,^{1}H$ COSY and $^{1}H,^{13}C$ HSQC NMR coupling. The shifts of the phosphorous atoms are expected to be nearly identical for the two isomers and thus, no new resonances are expected to be present. ^{13}C NMR spectroscopy proves to be difficult because of low resonance intensities in $^{13}C\{^{1}H\}$ NMR spectra even with a saturated solution (~30 mg in 0.6 ml CD_2Cl_2). ^{13}C NMR shifts had to be extracted from a $^{1}H,^{13}C$ HSQC NMR spectrum. Furthermore, **6** is prone to slow decomposition in CD_2Cl_2 and partially forms complex **1**. In THF-d_8, the solubility is worse and decomposition is observed, whereas in C_6D_6, almost no solubility is observed. The following assignment is for the main isomer only.

^{1}H NMR (300 MHz, CD_2Cl_2) δ_H: 1.52-1.63 (2H, m, P-C*H*-P), 3.22 (2H, ddd, $^{2}J_{H,H}$ = 14.4 Hz, $^{2}J_{H,P}$ = 14.9 Hz, $^{2}J_{H,P}$ = 8.5 Hz), 3.48 (2H, ddd, $^{2}J_{H,H}$ = 14.4 Hz, $^{2}J_{H,P}$ =10.2 Hz, $^{2}J_{H,P}$ = 4.5 Hz), 6.34-6.52 (10H, superimposed resonances, Phenyl-*H*), 6.69 (4H, dt, $J_{H,H}$ = 7.6 Hz, $J_{H,H}$ = 2.6 Hz, Phenyl-*H*), 6.76-6.89 (10H, superimposed resonances, Phenyl-*H*), 6.98-7.47 (44H, superimposed resonances, Phenyl-*H*), 7.54-7.67 (8H, superimposed resonances, Phenyl-*H*), 7.79 (4H, dd, $J_{H,H}$ = 7.9 Hz, $J_{H,H}$ = 11.1 Hz, Phenyl-*H*) ppm.

$^{13}C\{^{1}H\}$ NMR (75 MHz, CD_2Cl_2) δ_C: -9.5-8.3 (m, P-*C*H-P), 42.6 (dd, $^{1}J_{C,P}$ = 24.1 Hz, $^{1}J_{C,P}$ = 64.8 Hz, P-*C*H_2-P), 127.8-130.0 (superimposed resonances, Phenyl-*C*), 130.2-133.4 (superimposed resonances, Phenyl-*C*), 134.6-135.06 (superimposed resonances, Phenyl-*C*) ppm.

$^{31}P\{^{1}H\}$ NMR (101 MHz, CD_2Cl_2) δ_P: 22.5-24.8 (m), 28.9 (dd, $^{2}J_{P,P}$ = 81.2 Hz, $^{2}J_{P,P}$ = 28.5 Hz), 38.8 (dd, $^{2}J_{P,P}$ = 81.7 Hz, $^{2}J_{P,P}$ = 16.6 Hz) ppm.

FT-IR (ATR) ~/cm^{-1}: 3049 (w), 2361 (w), 2337 (br w), 1585 (w), 1480 (w), 1434 (m), 1308 (w), 1245 (br w), 1157 (br w), 1096 (m), 1026 (w), 998 (w), 905 (w), 835 (w), 794 (w), 737 (s), 689 (vs), 528 (m), 481 (br s).

HR-ESI-MS (+) /: 1747.2781 (calc. for MH^+), 1747.2812 (found, Δ = 1.8 ppm).

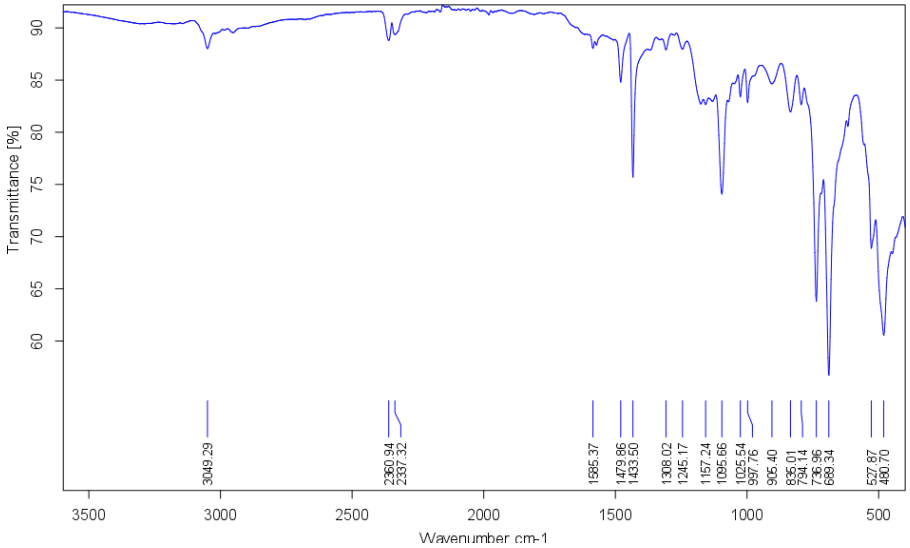

*Figure 22 - FT IR spectrum of complex **6**.*

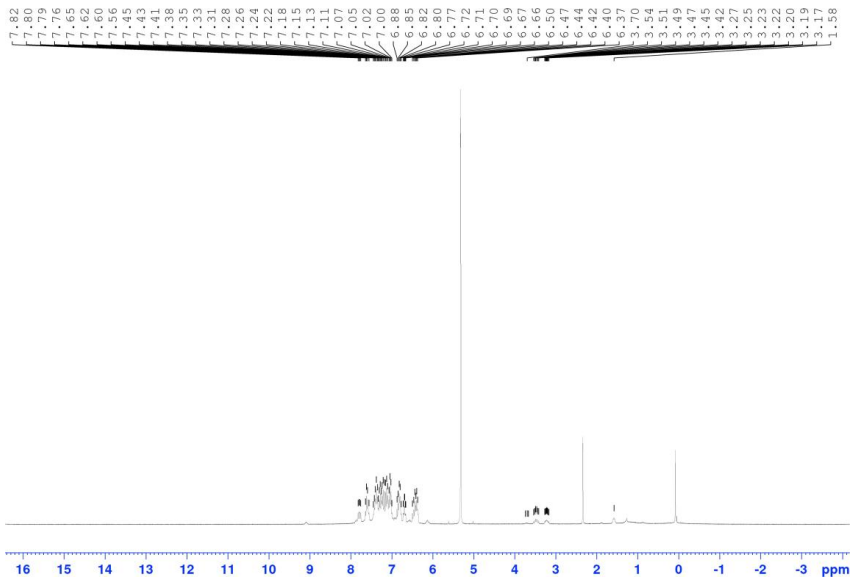

*Figure 23 - ^{1}H NMR spectrum of complex **6** in CD_2Cl_2.*

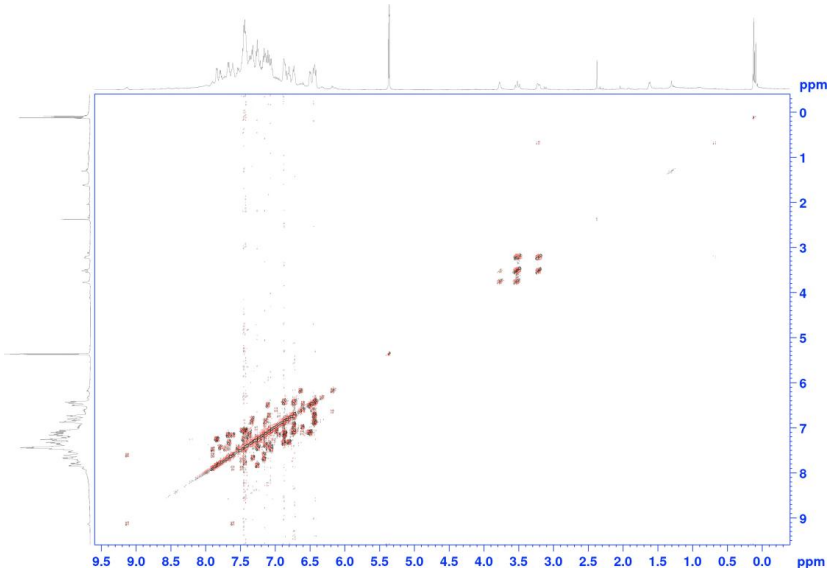

*Figure 24 - $^{1}H,^{1}H$ COSY NMR spectrum of complex **6** in CD_2Cl_2.*

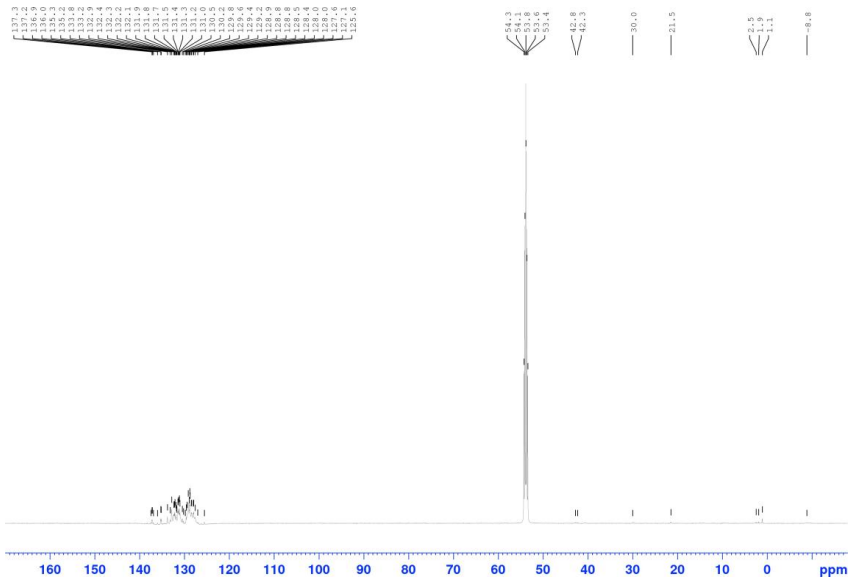

*Figure 25 - $^{13}C\{^{1}H\}$ NMR spectrum of complex **6** in CD_2Cl_2.*

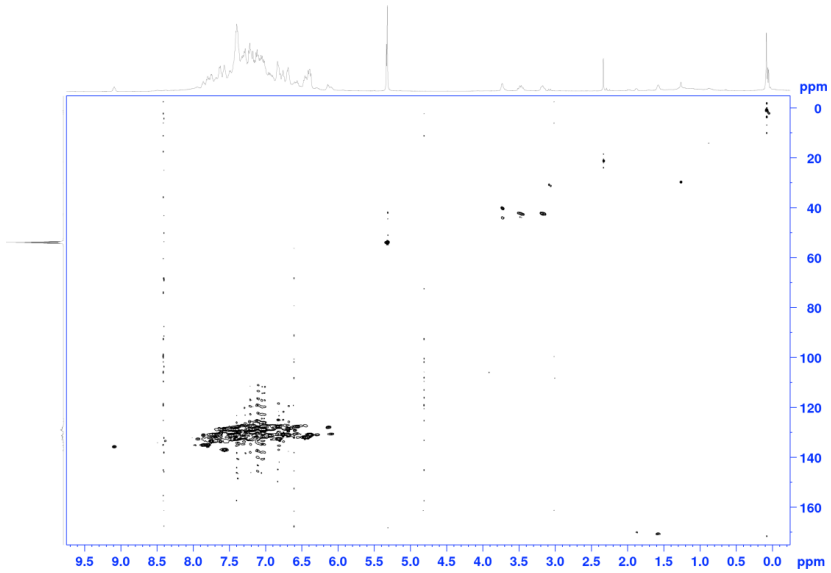

*Figure 26 - $^{1}H,^{1}H$ COSY NMR spectrum of complex **6** in CD_2Cl_2.*

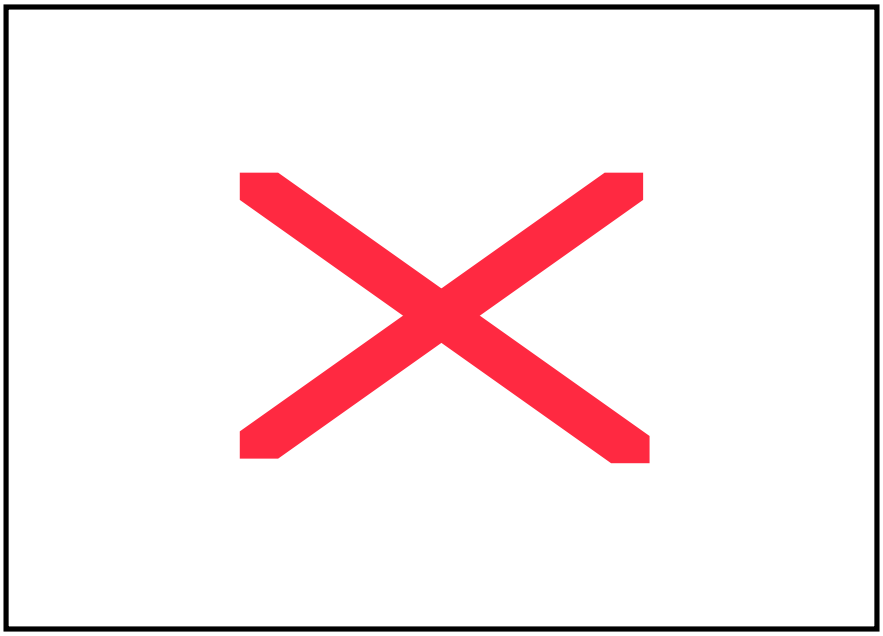

*Figure 27 - $^{13}C\{^{1}H\}$ NMR spectrum of complex **6** in CD_2Cl_2.*

2. X-ray crystallography

The single crystal X-ray diffraction data for the structural analysis were collected using graphite-monochromated Mo-Kα-radiation ($\lambda_{MoK\alpha}$= 0.71073) on the imaging plate detector systems STOE IPDS2 and STOE IPDS2T or on the pixel detector system Bruker Quest D8. The structures were solved with the Olex2 software by direct methods with SHELXT and refined against F^2 by full-matrix-least-square techniques using SHELXL.[2–5]

Complex	**2**	**3 · ½ Toluene**	**[4](AlCl$_2$Me$_2$)**	**5 · ¼ THF · $^3/_8$ *n*-hexane**	**6 · 2½ DCM**
Formula	$C_{51}H_{44}B_2ClF_8NiP_4$	$C_{51}H_{43}ClNiP_4$ · ½ C_7H_8	$C_{54}H_{53}AlCl_4NiP_2$	$C_{102}H_{84}Ni_2P_8$ · ¼ C_4H_8O · $^3/_8$ C_6H_{14}	$C_{102}H_{86}Cl_2Ni_2P_8$ · 2½ CH_2Cl_2
$D_{calc.}$/ g cm^{-3}	1.474	1.293	1.326	1.293	1.398
μ/mm^{-1}	0.671	0.639	0.724	0.613	0.791
Formula Weight	1048.52	919.96	991.39	1741.99	1960.10
Colour	orange	red	orange	red	red
Shape	block	block	block	plate	needle
Size/mm^3	0.50×0.41×0.41	0.52×0.36×0.14	0.31×0.26×0.21	0.19×0.18×0.07	0.60×0.22×0.19
T/K	100.0	100.0	100.0	100.0	100.0
Crystal System	monoclinic	monoclinic	monoclinic	triclinic	triclinic
Space Group	$P2_1/c$	$P2_1/c$	$C2/c$	$P\bar{1}$	$P\bar{1}$
a/Å	12.2896(6)	21.4394(11)	13.3928(6)	14.102(3)	13.590(3)
b/Å	18.9342(10)	19.5780(10)	20.9075(10)	14.186(3)	17.439(4)
c/Å	20.4715(11)	23.3621(12)	18.7057(11)	39.126(8)	22.442(5)
α/°	90	90	90	91.13(3)	88.48(3)
β/°	97.295(2)	105.447(2)	108.4890(10)	97.92(3)	72.40(3)
γ/°	90	90	90	119.53(3)	67.39(3)
V/Å^3	4725.0(4)	9451.8(8)	4967.4(4)	6710(3)	4656(2)
Z	4	8	4	3	2
Z'	1	2	0.5	1.5	1
Wavelength/Å	0.710730	0.710730	0.710730	0.710730	0.71073
Radiation type	MoK$_\alpha$	MoK$_\alpha$	MoK$_\alpha$	MoK$_\alpha$	MoK$_a$
Φ_{min}/°	2.128	2.229	2.261	1.585	1.675
Φ_{max}/°	24.971	21.448	24.392	26.772	26.800
Measured Refl.	48535	54585	26730	80180	41177
Independent Refl.	8254	10705	4055	28059	19516
R_{int}	0.0513	0.0687	0.0519	0.0695	0.1289
Parameters	604	1115	284	1584	1111
Restraints	0	0	0	0	0
Largest Peak	1.036	0.397	0.372	1.045	1.431
Deepest Hole	-0.533	-0.349	-0.370	-0.564	-0.933
GooF	1.027	1.013	1.047	0.841	0.949
wR_2 (all data)	0.1118	0.0884	0.0779	0.1379	0.1638
wR_2	0.1035	0.0799	0.0741	0.1099	0.1507
R_1 (all data)	0.0571	0.0570	0.0466	0.1491	0.0931
R_1	0.0445	0.0376	0.0352	0.0536	0.0641
CCDC	1814009	1814006	1814010	1814007	1814008

3. DFT Calculations

DFT calculations were done with Grimme's B97D functional including dispersion[6] and the def2-TZVPP basis set after a preoptimisation with the def2-SVP basis set.[7,8] Crystals structures were used as starting models, where possible, and the phenyl groups were substituted by methyl groups. After optimization, a frequency calculation was run to ascertain that a ground state was found (no imaginary modes). QTAIM charges and critical point data were calculated by the AIMQB module of the AIMStudio software bundle.[9] Laplacian contour line plots were created with the program multiwfn, molecular orbital visualizations with ChemCraft.[10,11]

Table 1 - QTAIM charges for the monomeric complexes

	1^{Me}	**2**^{Me}	**3**^{Me}	**7**^{Me}
Ni	0.39	0.40	0.38	0.29
C^{CDP}	-2.00	-1.38	-1.91	-1.80
P1	1.62	1.60	1.81	1.74
P2	2.60	2.47	2.68	2.68
P3	2.60	2.46	2.54	2.68
P4	1.62	1.60	1.60	1.74
Cl	-0.57	-0.49	-0.62	
C1	-1.02	-1.04	-1.73	-1.73
C2	-1.02	-1.03	-1.02	-1.73

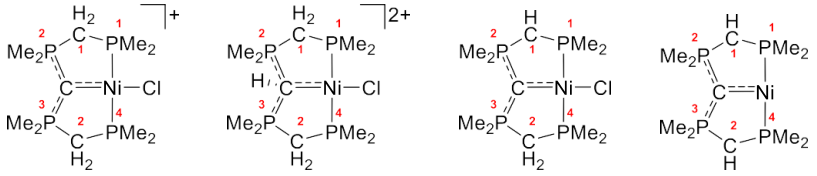

1^{Me} **2**^{Me} **3**^{Me} **7**^{Me}

Figure 28 - Numbering scheme for the monomeric complexes.

Table 2 - QTAIM charges for the dimeric complexes

	***cis*-5**^{Me}	***trans*-5**^{Me}	***cis*-6**^{Me}	**8**^{Me}
Ni	0.30 / 0.30	0.31 / 0.31	0.34 / 0.37	0.38 / 0.38
C^{CDP}	-2.01 / -2.02	-2.02 / -2.02	-2.08 / -2.03	-1.55 / -1.55
P1	1.76 / 1.75	1.76 / 1.76	1.61 / 1.62	1.52 / 1.52
P2	2.73 / 2.73	2.74 / 2.74	2.63 / 2.62	2.56 / 2.56
P3	2.65 / 2.65	2.64 / 2.64	2.68 / 2.66	2.60 / 2.60
P4	1.63 / 1.63	1.62 / 1.62	1.68 / 1.66	1.74 / 1.74
C1	-1.71 / -1.71	-1.71 / -1.71	-1.05 / -1.04	-1.02 / -1.02
C2	-1.41 / -1.41	-1.40 / -1.40	-1.39 / -1.41	-1.43 / -1.43

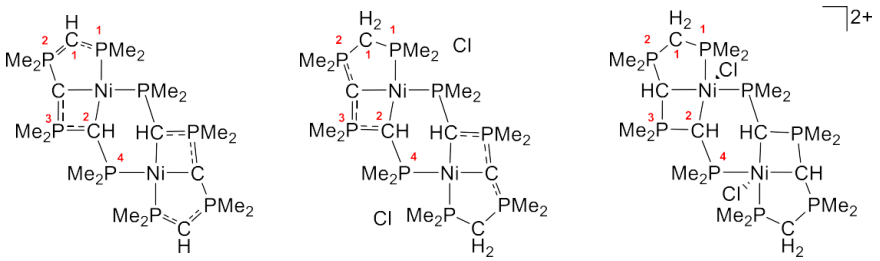

5^{Me} **6^{Me}** **8^{Me}**

Figure 29 - Numbering scheme for the dimeric complexes.

*Table 3 - Bond critical point data in atomic units for **1^{Me}**.*

Bond	ρ	∇ ρ	ε	K	V	H
Ni—Cl	7.7819929557E-02	2.2181081510E-01	8.7875160579E-02	2.2576453210E-02	-1.2885065495E-01	-1.0627420174E-01
Ni—C^{CDP}	1.0312936845E-01	1.9335851481E-01	4.4694435662E-02	4.0255513124E-02	-1.2885065495E-01	-8.8595141826E-02
Ni—P^{1}	1.0000341562E-01	1.2488957623E-01	2.4765883313E-02	4.2316537577E-02	-1.1585546921E-01	-7.3538931633E-02
Ni—P^{4}	9.9879996194E-02	1.2527452645E-01	2.5191501105E-02	4.2211315226E-02	-1.1574126206E-01	-7.3529946834E-02
C^{CDP}—P^{2}	1.9259576604E-01	-3.1807034153E-02	2.0883773828E-01	1.9295253512E-01	-3.7795331169E-01	-1.8500077657E-01
C^{CDP}—P^{3}	1.9256151834E-01	-3.2988339036E-02	2.0752867024E-01	1.9294284997E-01	-3.7763861517E-01	-1.8469576520E-01
C^{1}—P^{1}	1.5336636795E-01	-2.3611257883E-01	9.4722245481E-02	1.4071579481E-01	-2.2240344491E-01	-8.1687650100E-02
C^{2}—P^{4}	1.5347020994E-01	-2.3478459830E-01	9.4566512067E-02	1.4087743051E-01	-2.2305871145E-01	-8.2181280940E-02
C^{1}—P^{2}	1.6749618925E-01	-2.7423720639E-01	3.0325424187E-02	1.6253976852E-01	-2.5652023544E-01	-9.3980466920E-02
C^{2}—P^{3}	1.6752565952E-01	-2.7340462009E-01	3.1204734505E-02	1.6257553389E-01	-2.5679991277E-01	-9.4224378880E-02
C^{1}—H	2.7644941915E-01	-9.6288428438E-01	1.2525170948E-02	2.8841433328E-01	-3.3610759546E-01	-4.7693262180E-02
C^{1}—H'	2.7710488995E-01	-9.6903880263E-01	9.5183203650E-03	2.8908765694E-01	-3.3591561323E-01	-4.6827956290E-02
C^{2}—H	2.7645999359E-01	-9.6288827059E-01	1.3123924426E-02	2.8844223335E-01	-3.3616239905E-01	-4.7720165700E-02
C^{2}—H'	2.7706567731E-01	-9.6902509095E-01	9.6888542281E-03	2.8903192127E-01	-3.3580756981E-01	-4.6775648540E-02

*Table 4 - Bond critical point data in atomic units for **2^{Me}**.*

Bond	ρ	∇ ρ	ε	K	V	H
Ni—Cl	8.7034415332E-02	2.2244556475E-01	7.8279026363E-02	2.8173140155E-02	-1.1195767150E-01	-8.3784531345E-02
Ni—C^{CDP}	8.6566512754E-02	2.0243840378E-01	9.9767303730E-02	2.7349319763E-02	-1.0530824047E-01	-7.7958920707E-02
Ni—P^{1}	9.6311499621E-02	1.1524253304E-01	2.1220749829E-02	3.9045614423E-02	-1.0690186211E-01	-6.7856247687E-02
Ni—P^{4}	9.8530697766E-02	1.1591583586E-01	6.2038183095E-03	4.0992075266E-02	-1.1096310950E-01	-6.9971034234E-02
C^{CDP}—P^{2}	1.7326632469E-01	-2.5374400290E-01	5.0579948604E-02	1.7000059839E-01	-2.7656519606E-01	-1.0656459767E-01
C^{CDP}—P^{3}	1.7138607006E-01	-2.8405612669E-01	3.8944957540E-02	1.6721978949E-01	-2.6342554730E-01	-9.6205757810E-02
C^{CDP}—H	2.7008562022E-01	-9.0740558063E-01	2.2585187362E-02	2.7824977002E-01	-3.2964814489E-01	-5.1398374870E-02
C^{1}—P^{1}	1.4872424108E-01	-2.2039020691E-01	1.0552449368E-01	1.3409791946E-01	-2.1309828720E-01	-7.9000367740E-02
C^{2}—P^{4}	1.4864986771E-01	-2.1668539376E-01	9.5106480354E-02	1.3401975496E-01	-2.1386816148E-01	-7.9848406520E-02
C^{1}—P^{2}	1.7322329479E-01	-3.1504197714E-01	1.5787527233E-02	1.7048212126E-01	-2.6220374824E-01	-9.1721626980E-02
C^{2}—P^{3}	1.7450367485E-01	-2.9777355229E-01	2.4996015707E-02	1.7243005716E-01	-2.7041672626E-01	-9.7986669100E-02
C^{1}—H	2.7775108663E-01	-9.7964363966E-01	5.9774417084E-03	2.8966344047E-01	-3.3441597103E-01	-4.4752530560E-02
C^{1}—H'	2.7630789130E-01	-9.6615658374E-01	3.8870417403E-03	2.8747792031E-01	-3.3341669469E-01	-4.5938774380E-02

C^2—H	2.7713558623E-01	-9.7615652234E-01	7.3436619885E-03	2.8856811604E-01	-3.3309710148E-01	-4.4528985440E-02
C^2—H'	2.7564654360E-01	-9.5963565249E-01	6.1422704426E-03	2.8684058856E-01	-3.3377226399E-01	-8.3784531345E-02

Table 5 - Bond critical point data in atomic units for ***3^{Me}***.

Bond	ρ	∇ ρ	ε	K	V	H
Ni—Cl	7.0724447948E-02	2.1466043483E-01	9.5536525902E-02	1.8541979834E-02	-9.0749068376E-02	-7.2207088542E-02
Ni—C^{CDP}	1.0540748784E-01	1.8908602834E-01	3.5047022575E-02	4.2223070587E-02	-1.3171764826E-01	-8.9494577673E-02
Ni—P^1	9.7925285290E-02	9.2706245507E-02	1.3635439603E-02	4.0555921790E-02	-1.0428840496E-01	-6.3732483170E-02
Ni—P^4	1.0151514258E-01	1.5028055473E-01	1.5875378264E-02	4.3859647289E-02	-1.2528943326E-01	-8.1429785971E-02
C^{CDP}—P^2	1.8170578921E-01	-1.3252718596E-01	1.4260667846E-01	1.8018283374E-01	-3.2723387098E-01	-1.4705103724E-01
C^{CDP}—P^3	1.9639325357E-01	-4.4289122888E-02	2.7487731681E-01	1.9949076703E-01	-3.8790925335E-01	-1.8841848632E-01
C^1—P^1	1.8004703534E-01	-3.9372684078E-02	1.3221125750E-01	1.7403244441E-01	-3.3822171781E-01	-1.6418927340E-01
C^2—P^4	1.5309446555E-01	-2.2165598033E-01	9.5968649468E-02	1.4043062518E-01	-2.2544725527E-01	-8.5016630090E-02
C^1—P^2	1.9490650037E-01	-3.4307894427E-02	2.9560013071E-01	1.9612306314E-01	-3.8366915267E-01	-1.8754608953E-01
C^2—P^3	1.6657314657E-01	-2.5230849427E-01	3.9434657512E-02	1.6108718684E-01	-2.5909725011E-01	-9.8010063270E-02
C^1—H	2.7255738213E-01	-9.2574581707E-01	6.4785031932E-02	2.8764858597E-01	-3.4386071767E-01	-5.6212131700E-02
C^2—H	2.7616437553E-01	-9.5862973123E-01	1.6310172028E-02	2.8844473810E-01	-3.3723204338E-01	-4.8787305280E-02
C^2—H'	2.7571515070E-01	-9.5668541192E-01	1.1704353023E-02	2.8758556447E-01	-3.3599977596E-01	-4.8414211490E-02

Table 6 - Bond critical point data in atomic units for ***7^{Me}***.

Bond	ρ	∇ ρ	ε	K	V	H
Ni—C^{CDP}	1.2364308535E-01	1.1355553875E-01	2.2545212155E-02	5.9718955321E-02	-1.4782679533E-01	-8.8107840009E-02
Ni—P^1	9.6107139736E-02	1.1039272239E-01	9.8909277442E-03	3.9082655774E-02	-1.0576349215E-01	-6.6680836376E-02
Ni—P^4	9.6731827180E-02	1.0962775526E-01	8.7108590924E-03	3.9589183184E-02	-1.0658530518E-01	-6.6996121996E-02
C^{CDP}—P^2	1.8380349677E-01	-1.0373922121E-01	2.1544752992E-01	1.8240540970E-01	-3.3887601409E-01	-1.5647060439E-01
C^{CDP}—P^3	1.8376345353E-01	-1.0501970413E-01	2.1561292998E-01	1.8238246566E-01	-3.3851000529E-01	-1.5612753963E-01
C^1—P^1	1.8372841055E-01	-1.9271540208E-02	1.5392144088E-01	1.7874028279E-01	-3.5266268053E-01	-1.7392239774E-01
C^2—P^4	1.8379554269E-01	-1.9371897802E-02	1.5519609638E-01	1.7883791576E-01	-3.5283285706E-01	-1.7399494130E-01
C^1—P^2	1.9155286698E-01	-5.9287230913E-02	2.6466101829E-01	1.9199765930E-01	-3.6917351088E-01	-1.7717585158E-01
C^2—P^3	1.9154359180E-01	-5.8201321863E-02	2.6402180281E-01	1.9193890150E-01	-3.6932747253E-01	-1.7738857103E-01
C^1—H	2.7265352958E-01	-9.2569876437E-01	6.6977287165E-02	2.8788732036E-01	-3.4434994963E-01	-5.6462629270E-02
C^2—H	2.7272055563E-01	-9.2627350189E-01	6.7063805306E-02	2.8799343080E-01	-3.4441848613E-01	-5.6425055330E-02

Table 7 - Bond critical point data in atomic units for ***trans-5^{Me}***.

Bond	ρ	∇ ρ	ε	K	V	H
Ni—P^*	9.7701999899E-02	1.0885138534E-01	1.2730821185E-02	4.0347555111E-02	-1.0790795656E-01	-6.7560401449E-02
Ni—C^{CDP}	1.0824975677E-01	1.8280046870E-01	4.7105307880E-02	4.5113124736E-02	-1.3592636665E-01	-9.0813241914E-02
Ni—C^2	8.0544861682E-02	1.6892490216E-01	1.6952808795E-01	2.3620649345E-02	-8.9472524231E-02	-6.5851874886E-02

Ni—P^{4}	9.7972124906E-02	1.4618299518E-01	1.9447294673E-02	4.0927927226E-02	-1.1840160325E-01	-7.7473676024E-02
C^{CDP}—P^{2}	1.8874486804E-01	-3.3260300298E-02	1.2722331843E-01	1.8689308703E-01	-3.6547109899E-01	-1.7857801196E-01
C^{CDP}—P^{3}	1.9791384453E-01	6.6666902757E-02	1.8187828883E-01	1.9720419320E-01	-4.1107511208E-01	-2.1387091888E-01
C^{1}—P^{1}	1.8041031068E-01	-6.1624578174E-02	1.6845040122E-01	1.7551874984E-01	-3.3563135514E-01	-1.6011260530E-01
C^{2}—P^{4}	1.6415131755E-01	-1.8754884371E-01	4.5368931650E-02	1.5554209818E-01	-2.6419698543E-01	-1.0865488725E-01
C^{1}—P^{2}	1.9250419262E-01	-4.1546368779E-02	2.7096654376E-01	1.9271660128E-01	-3.7504661036E-01	-1.8233000908E-01
C^{2}—P^{3}	1.7560483183E-01	-1.8107802411E-01	1.1114491716E-01	1.7249643829E-01	-2.9972337055E-01	-1.2722693226E-01
Ni^{1}—P^{1*}	9.7702417071E-02	1.0885067081E-01	1.2731947821E-02	4.0347904507E-02	-1.0790847672E-01	-6.7560572213E-02
Ni^{1}—C^{CDP*}	1.0824960687E-01	1.8280011740E-01	4.7102633011E-02	4.5112997463E-02	-1.3592602428E-01	-9.0813026817E-02
Ni^{1}—C^{2*}	8.0543945818E-02	1.6892363665E-01	1.6952474985E-01	2.3620057435E-02	-8.9471024033E-02	-6.5850966598E-02
Ni^{1}—P^{*}	9.7971465370E-02	1.4618341174E-01	1.9440979810E-02	4.0927328351E-02	-1.1840050964E-01	-7.7473181289E-02
C^{CDP*}—P^{2*}	1.8874479587E-01	-3.3262432293E-02	1.2722460903E-01	1.8689306200E-01	-3.6547051592E-01	-1.7857745392E-01
C^{CDP*}—P^{3*}	1.9791428898E-01	6.6669803206E-02	1.8187918233E-01	1.9720474078E-01	-4.1107693236E-01	-2.1387219158E-01
C^{1*}—P^{1*}	1.8041032249E-01	-6.1625440544E-02	1.6845217772E-01	1.7551880021E-01	-3.3563124028E-01	-1.6011244007E-01
C^{2*}—P^{4*}	1.6415134549E-01	-1.8754858363E-01	4.5365904329E-02	1.5554210769E-01	-2.6419706947E-01	-1.0865496178E-01
C^{1*}—P^{2*}	1.9250416828E-01	-4.1546145335E-02	2.7096682458E-01	1.9271655660E-01	-3.7504657686E-01	-1.8233002026E-01
C^{2*}—P^{3*}	1.7560557846E-01	-1.8107384387E-01	1.1114093174E-01	1.7249742926E-01	-2.9972639754E-01	-1.2722896828E-01
C^{1}—H	2.7247445158E-01	-9.2453624341E-01	6.8204003872E-02	2.8764975195E-01	-3.4416544305E-01	-5.6515691100E-02
C^{1*}—H	2.7247536593E-01	-9.2454196294E-01	6.8204122232E-02	2.8765148684E-01	-3.4416748293E-01	-5.6515996090E-02
C^{2}—H	2.7604156316E-01	-9.4441666922E-01	3.0771980182E-02	2.8987896012E-01	-3.4365375293E-01	-5.3774792810E-02
C^{2*}—H	2.7604192366E-01	-9.4441886419E-01	3.0772245873E-02	2.8987955659E-01	-3.4365439713E-01	-5.3774840540E-02

Table 8 - Bond critical point data in atomic units for ***cis-5^{Me}****.*

Bond	ρ	∇ ρ	ε	K	V	H
Ni—P^{*}	9.8282487699E-02	1.1005573198E-01	2.5580517277E-02	4.0954968359E-02	-1.0942386971E-01	-6.8468901351E-02
Ni—C^{CDP}	1.0471137949E-01	1.8261612561E-01	5.5469007052E-02	4.2026397249E-02	-1.2970682590E-01	-8.7680428651E-02
Ni—C^{2}	8.6691769438E-02	1.7488788976E-01	1.3102872043E-01	2.7788957653E-02	-9.9299887747E-02	-7.1510930094E-02
Ni—P^{4*}	9.8403314142E-02	1.4636023743E-01	1.4590951488E-02	4.1169092445E-02	-1.1892824425E-01	-7.7759151805E-02
C^{CDP}—P^{2}	1.8823582371E-01	-4.0941951500E-02	1.2465196184E-01	1.8646979774E-01	-3.6270410761E-01	-1.7623430987E-01
C^{CDP}—P^{3}	1.9736196477E-01	4.9892114007E-02	1.6777269636E-01	1.9710013084E-01	-4.0667329017E-01	-2.0957315933E-01
C^{1}—P^{1}	1.8039663792E-01	-6.3457887084E-02	1.7012507842E-01	1.7554549062E-01	-3.3522650948E-01	-1.5968101886E-01
C^{2}—P^{4}	1.6605898418E-01	-1.7380343874E-01	7.9330590060E-02	1.5816798110E-01	-2.7288510252E-01	-1.1471712142E-01
C^{1}—P^{2}	1.9173343518E-01	-5.4449699696E-02	2.6595890408E-01	1.9205873275E-01	-3.7050504057E-01	-1.7844630782E-01
C^{2}—P^{3}	1.7701914237E-01	-1.7066323779E-01	1.0702002400E-01	1.7428579137E-01	-3.0590577329E-01	-1.3161998192E-01
Ni^{1}—P^{1*}	9.8031850885E-02	1.1096068160E-01	2.3658705985E-02	4.0720747090E-02	-1.0918166458E-01	-6.8460917490E-02
Ni^{1}—C^{CDP*}	1.0509501611E-01	1.8309977998E-01	5.3638568497E-02	4.2359628452E-02	-1.3049420190E-01	-8.8134573448E-02
Ni^{1}—C^{2*}	8.6094334957E-02	1.7337297559E-01	1.3253884596E-01	2.7375057619E-02	-9.8093359136E-02	-7.0718301517E-02
Ni^{1}—P^{4}	9.8950364806E-02	1.4581211706E-01	1.2916551367E-02	4.1640615901E-02	-1.1973426107E-01	-7.8093645169E-02
C^{CDP*}—P^{2*}	1.8852644352E-01	-3.4979281441E-02	1.2586011511E-01	1.8666164749E-01	-3.6457847461E-01	-1.7791682712E-01
C^{CDP*}—P^{3*}	1.9764115546E-01	5.5855160569E-02	1.6986673335E-01	1.9727849273E-01	-4.0852077561E-01	-2.1124228288E-01
C^{1*}—P^{1*}	1.8033196311E-01	-6.3413024685E-02	1.6930479336E-01	1.7545252197E-01	-3.3505178777E-01	-1.5959926580E-01
C^{2*}—P^{4*}	1.6594927288E-01	-1.7340700743E-01	7.8243943476E-02	1.5800892806E-01	-2.7266610426E-01	-1.1465717620E-01
C^{1*}—P^{2*}	1.9179321359E-01	-5.3441711020E-02	2.6686942886E-01	1.9210789736E-01	-3.7085536697E-01	-1.7874746961E-01
C^{2*}—P^{3*}	1.7702311367E-01	-1.6985658941E-01	1.0602814983E-01	1.7426870859E-01	-3.0607326982E-01	-1.3180456123E-01

C^{1}—H	2.7219647256E-01	-9.2288417872E-01	6.7495772305E-02	2.8712792142E-01	-3.4353479816E-01	-5.6406876740E-02
$C^{1'}$—H	2.7217430288E-01	-9.2260953450E-01	6.7527093062E-02	2.8709835010E-01	-3.4354431657E-01	-5.6445966470E-02
C^{2}—H	2.7496185438E-01	-9.3650366714E-01	2.9966227323E-02	2.8878750320E-01	-3.4344908962E-01	-5.4661586420E-02
$C^{2'}$—H	2.7508124835E-01	-9.3718863371E-01	2.9825679088E-02	2.8895042918E-01	-3.4360369994E-01	-5.4653270760E-02

Table 9 - Bond critical point data in atomic units for ***cis-6^{Me}***.

Bond	ρ	∇ ρ	ε	K	V	H
Ni—P^{1}	1.0142507744E-01	1.3514828329E-01	3.1925753366E-02	4.4027800501E-02	-1.2184267182E-01	-7.7814871319E-02
Ni—C^{CDP}	9.8811836487E-02	1.9429705357E-01	9.1469508730E-02	3.7287569161E-02	-1.2314940171E-01	-8.5861832549E-02
Ni—C^{2}	8.9926361103E-02	1.6785851968E-01	1.2546803080E-01	3.0077850099E-02	-1.0212033012E-01	-7.2042480021E-02
Ni—P^{4}	1.0138806086E-01	1.2328956102E-01	1.3442869211E-02	4.3684763767E-02	-1.1819191779E-01	-7.4507154023E-02
C^{CDP}—P^{2}	1.9597661606E-01	5.0126402180E-02	1.6067691129E-01	1.9480644466E-01	-4.0214448986E-01	-2.0733804520E-01
C^{CDP}—P^{3}	1.9409230361E-01	4.9934220197E-02	1.1875131556E-01	1.9183419488E-01	-3.9615194481E-01	-2.0431774993E-01
C^{1}—P^{1}	1.5711863437E-01	-2.5654278943E-01	6.2051419698E-02	1.4618410550E-01	-2.2823251364E-01	-8.2048408140E-02
C^{2}—P^{4}	1.6253575939E-01	-1.7073557365E-01	8.2609828103E-02	1.5329226072E-01	-2.6390062802E-01	-1.1060836730E-01
C^{1}—P^{2}	1.6792917106E-01	-2.7910574641E-01	2.8140695052E-02	1.6323157274E-01	-2.5668670887E-01	-9.3455136130E-02
C^{2}—P^{3}	1.7826066051E-01	-1.9112662278E-01	8.8099259835E-02	1.7656151111E-01	-3.0534136652E-01	-1.2877985541E-01
Ni^{i}—P^{1i}	1.0247707601E-01	1.3290748226E-01	4.6944905712E-02	4.4924326825E-02	-1.2307552422E-01	-7.8151197395E-02
Ni^{i}—C^{CDPi}	9.4470637280E-02	1.8502748030E-01	9.4915454857E-02	3.3894477319E-02	-1.1404582471E-01	-8.0151347391E-02
Ni^{i}—C^{2i}	9.0360637427E-02	1.7701477809E-01	1.1934324830E-01	3.0460131684E-02	-1.0517395789E-01	-7.4713826206E-02
Ni^{i}—P^{4}	1.0121686636E-01	1.2933066342E-01	2.8888703379E-02	4.3689902534E-02	-1.1971247092E-01	-7.6022568386E-02
C^{CDPi}—P^{2i}	1.9602432218E-01	-9.1207953626E-03	1.3513266932E-01	1.9722010168E-01	-3.9216000453E-01	-1.9493990285E-01
C^{CDPi}—P^{3i}	1.9299600553E-01	1.5300933361E-02	1.0676603017E-01	1.9173234734E-01	-3.8728992802E-01	-1.9555758068E-01
C^{1i}—P^{1i}	1.5587582094E-01	-2.4540898350E-01	6.1008946040E-02	1.4454324121E-01	-2.2773423654E-01	-8.3190995330E-02
C^{2i}—P^{4i}	1.6710381678E-01	1.7513617421E-01	7.8890945620E-02	1.5962100208E-01	-2.7545796061E-01	-1.1583695853E-01
C^{1i}—P^{2i}	1.6890345503E-01	-2.6748839033E-01	2.1375993559E-02	1.6455998665E-01	-2.6224787571E-01	-9.7687889060E-02
C^{2i}—P^{3i}	1.7674922323E-01	-1.6840905386E-01	1.0885672069E-01	1.7385704357E-01	-3.0561182368E-01	-1.3175478011E-01
C^{1}—H	2.7454904618E-01	-9.4776806501E-01	2.5169490210E-03	2.8600905349E-01	-3.3507609072E-01	-4.9067037230E-02
C^{1}—H'	2.7862904150E-01	-9.9039226886E-01	1.4311750984E-02	2.9034669484E-01	-3.3309532248E-01	-4.2748627640E-02
C^{1i}—H	2.7474020630E-01	-9.4979732420E-01	3.5521464630E-03	2.8615121077E-01	-3.3485309050E-01	-4.8701879730E-02
C^{1i}—H'	2.7888570564E-01	-9.8572601405E-01	1.7157644084E-02	2.9100262945E-01	-3.3557375539E-01	-4.4571125940E-02
C^{2}—H	2.7532326390E-01	-9.4143902082E-01	2.3541475379E-02	2.8862708146E-01	-3.4189440772E-01	-5.3267326260E-02
C^{2i}—H	2.7548411437E-01	-9.4247968575E-01	2.9063286755E-02	2.8909846435E-01	-3.4257700726E-01	-5.3478542910E-02

Table 10 - Bond critical point data in atomic units for ***trans-8^{Me}***.

Bond	ρ	∇ ρ	ε	K	V	H
Ni—P^{1}	9.0803576173E-02	1.4894693266E-01	1.5596554590E-02	3.4544545104E-02	-1.0632582337E-01	-7.1781278266E-02
Ni—C^{CDP}	7.9901080481E-02	1.8187583251E-01	1.2550093290E-01	2.3521234519E-02	-9.2511427164E-02	-6.8990192645E-02
Ni—C^{2}	8.1565337017E-02	1.7964687689E-01	1.2340836724E-01	2.3728019094E-02	-9.2367757409E-02	-6.8639738315E-02
Ni—P^{4}	1.0379056046E-01	1.0379056046E-01	1.8214762908E-02	4.5897664366E-02	-1.1443841475E-01	-6.8540750384E-02
Ni—Cl	4.3249341463E-02	1.2995552405E-01	3.7112708384E-02	5.6557866059E-03	-4.3800454225E-02	-3.8144667619E-02
C^{CDP}—P^{2}	1.8125691977E-01	-1.7892913454E-01	8.6434423569E-02	1.8030517120E-01	-3.1587805878E-01	-1.3557288758E-01
C^{CDP}—P^{3}	1.7785815018E-01	-1.1985066695E-01	1.0415527247E-01	1.7376799276E-01	-3.1757331878E-01	-1.4380532602E-01

C^{1}—P^{1}	1.4820687686E-01	-2.1980167739E-01	8.7263969666E-02	1.3327541403E-01	-2.1160040872E-01	-7.8324994690E-02
C^{2}—P^{4}	1.6479647940E-01	-1.9377827763E-01	6.6309155831E-02	1.5680381012E-01	-2.6516305083E-01	-1.0835924071E-01
C^{1}—P^{2}	1.7240226980E-01	-2.7954704518E-01	2.3291608931E-02	1.6944902219E-01	-2.6901128309E-01	-9.9562260900E-02
C^{2}—P^{3}	1.8192743366E-01	-1.9960374846E-01	9.2980759458E-02	1.8191591983E-01	-3.1393090255E-01	-1.3201498272E-01
Ni'—$P^{1'}$	9.0804035933E-02	1.4894721348E-01	1.5595730899E-02	3.4544919084E-02	-1.0632664154E-01	-7.1781722456E-02
Ni'—$C^{CDP,}$	7.9900676279E-02	1.8187428190E-01	1.2549953128E-01	2.3520984932E-02	-9.2510540340E-02	-6.8989555408E-02
Ni'—$C^{2'}$	8.1564155626E-02	1.7964479073E-01	1.2340760098E-01	2.3727239546E-02	-9.2365676775E-02	-6.8638437229E-02
Ni'—P^{4}	1.0379094407E-01	9.0572915975E-02	1.8214765905E-02	4.5898016058E-02	-1.1443926111E-01	-6.8541245052E-02
Ni'—Cl'	4.3250136333E-02	1.2995838154E-01	3.7110808067E-02	5.6560249956E-03	-4.3801645376E-02	-3.8145620380E-02
$C^{CDP,}$—$P^{2'}$	1.8125700014E-01	-1.7892830272E-01	8.6435221315E-02	1.8030526503E-01	-3.1587845438E-01	-1.3557318935E-01
$C^{CDP,}$—$P^{3'}$	1.7785807316E-01	-1.1985169699E-01	1.0415470652E-01	1.7376790820E-01	-3.1757289216E-01	-1.4380498396E-01
$C^{1'}$—$P^{1'}$	1.4820704301E-01	-2.1980131289E-01	8.7262830856E-02	1.3327565744E-01	-2.1160098665E-01	-7.8325329210E-02
$C^{2'}$—$P^{4'}$	1.6479658510E-01	-1.9377758572E-01	6.6308662967E-02	1.5680393883E-01	-2.6516348123E-01	-1.0835954240E-01
$C^{1'}$—$P^{2'}$	1.7240218103E-01	-2.7954644954E-01	2.3291597430E-02	1.6944888496E-01	-2.6901115754E-01	-9.9562272580E-02
$C^{2'}$—$P^{3'}$	1.8192790654E-01	-1.9959931852E-01	9.2980415266E-02	1.8191652481E-01	-3.1393321999E-01	-1.3201669518E-01
C^{1}—H	2.7699641488E-01	-9.7104170635E-01	7.6514856820E-03	2.8864425514E-01	-3.3452808370E-01	-4.5883828560E-02
C^{1}—H'	2.7622511210E-01	-9.5933876869E-01	8.3977826276E-03	2.8807007367E-01	-3.3630545516E-01	-4.8235381490E-02
$C^{1'}$—H	2.7699595231E-01	-9.7103877534E-01	7.6516503992E-03	2.8864338878E-01	-3.3452708373E-01	-4.5883694950E-02
$C^{1'}$—H'	2.7622477350E-01	-9.5933692318E-01	8.3980225158E-03	2.8806943179E-01	-3.3630463279E-01	-4.8235201000E-02
C^{2}—H	2.7790846899E-01	-9.6687295250E-01	1.8608761733E-02	2.9053128175E-01	-3.3934432539E-01	-4.8813043640E-02
$C^{2'}$—H	2.7790834766E-01	-9.6687201294E-01	1.8609129218E-02	2.9053107318E-01	-3.3934414312E-01	-4.8813069940E-02
C^{CDP}—H	2.7540372870E-01	-9.4868918562E-01	2.3611531652E-02	2.8742294267E-01	-3.3767358893E-01	-5.0250646260E-02
$C^{CDP,}$—H	2.7540360991E-01	-9.4868875709E-01	2.3611131645E-02	2.8742270824E-01	-3.3767322721E-01	-5.0250518970E-02

3.1 Molecular orbitals

All Molecular Orbitals are shown with a contour value of 0.03 and the atoms are color-coded as follows: Ni: orange; P: violet; Cl: green; C: grey.

1^{Me}

LUMO

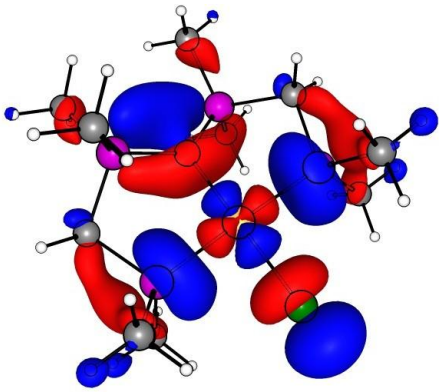

HOMO

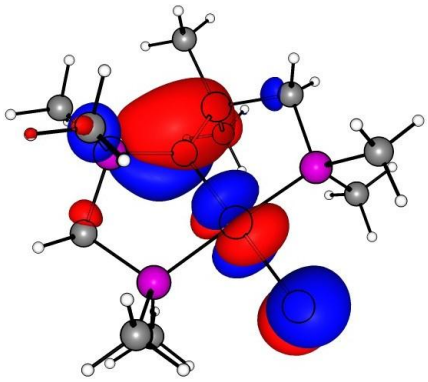

HOMO-1

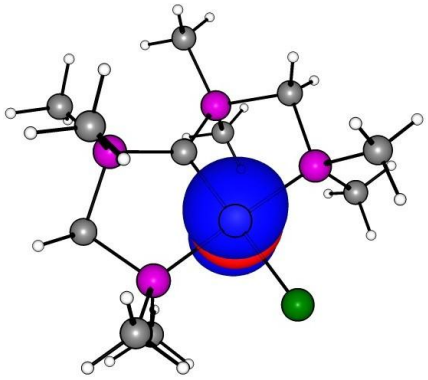

HOMO-2

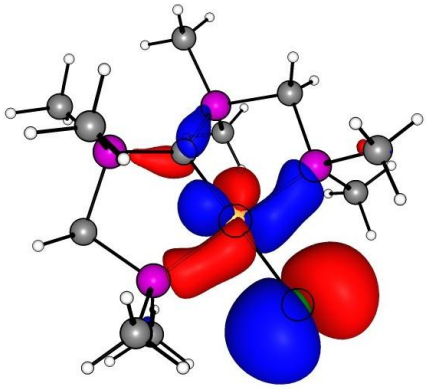

HOMO-3

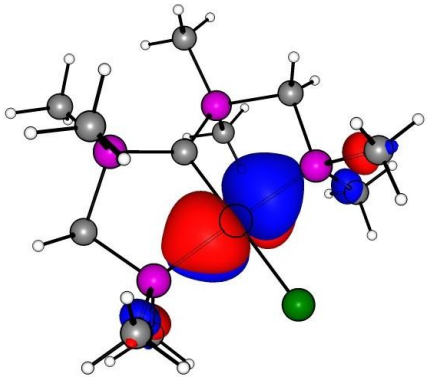

HOMO-4

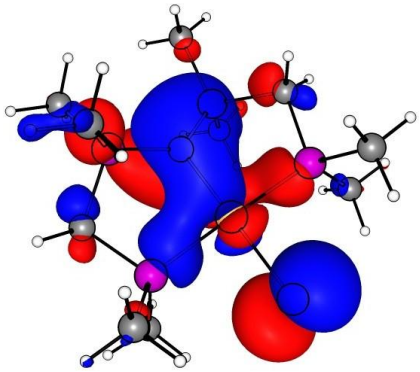

28

HOMO-5

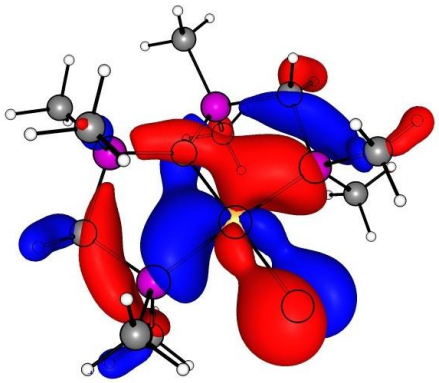

HOMO-6

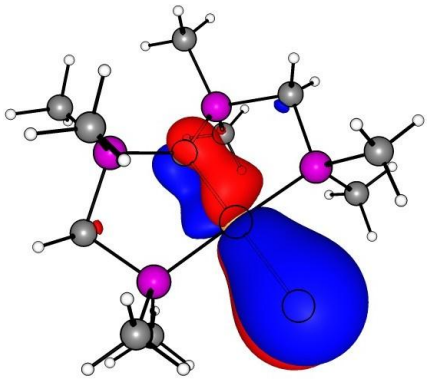

HOMO-7

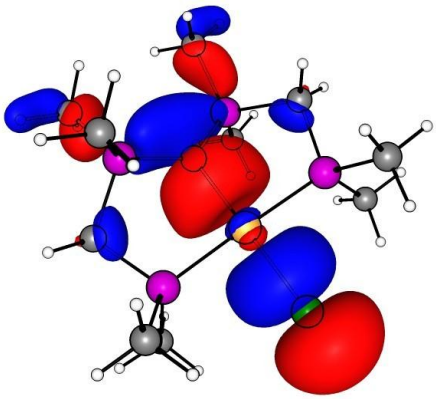

HOMO-8

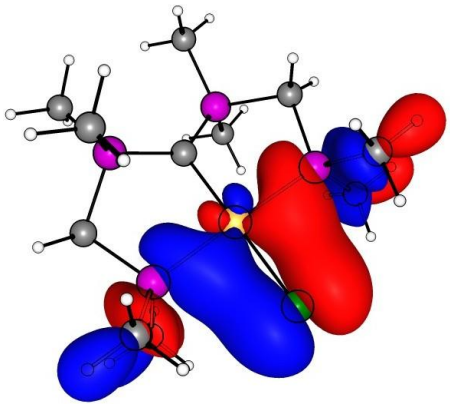

HOMO-9

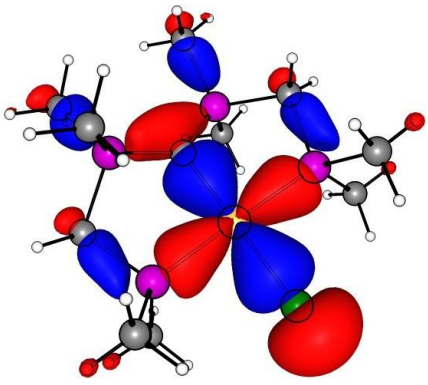

HOMO-10

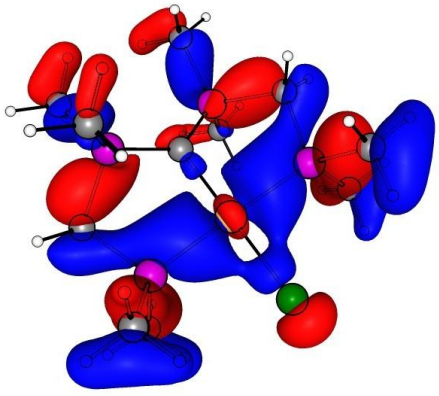

2^{Me}

LUMO

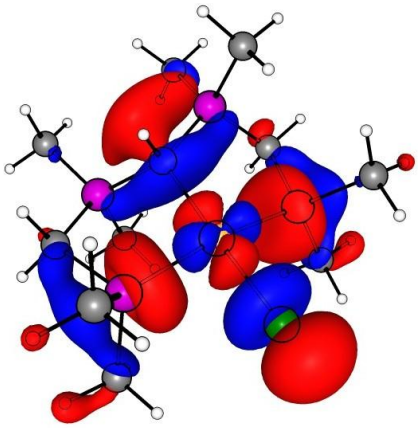

HOMO

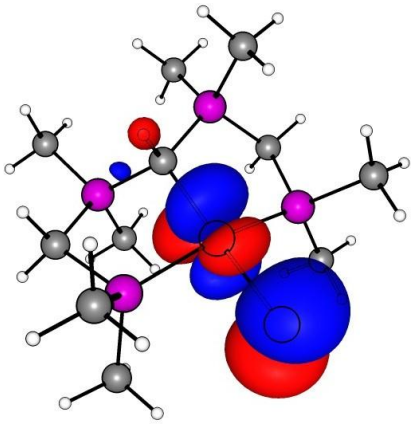

HOMO-1

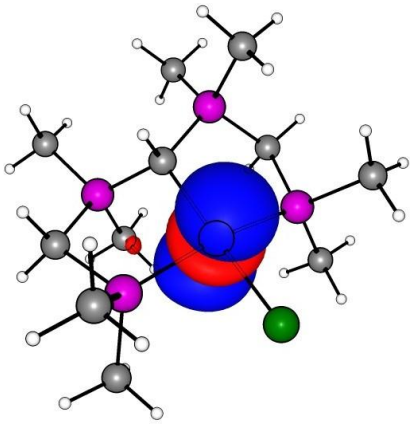

HOMO-2

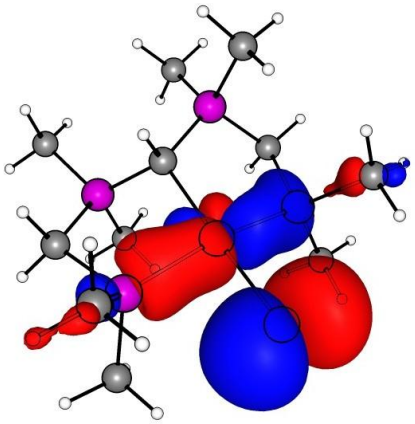

HOMO-3

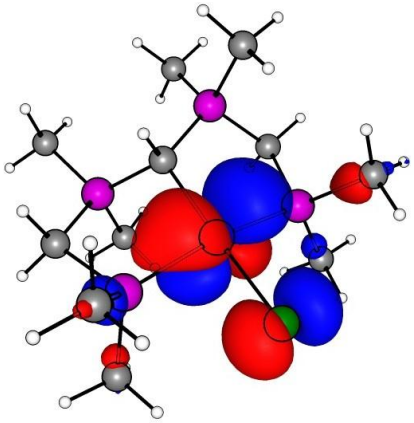

HOMO-4

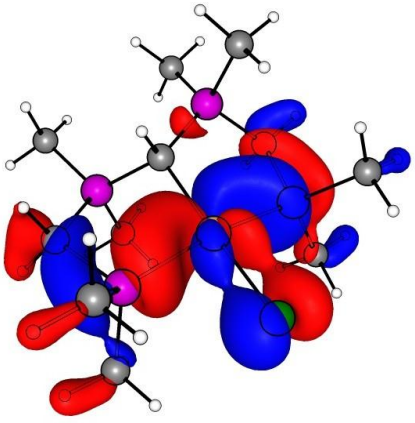

30

HOMO-5

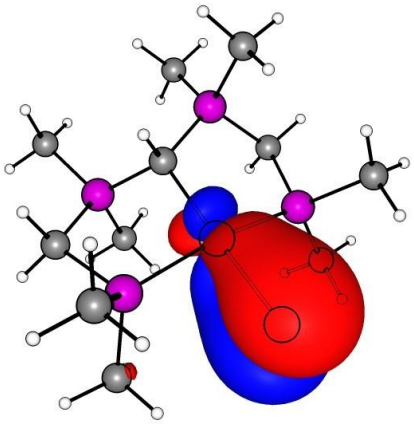

HOMO-6

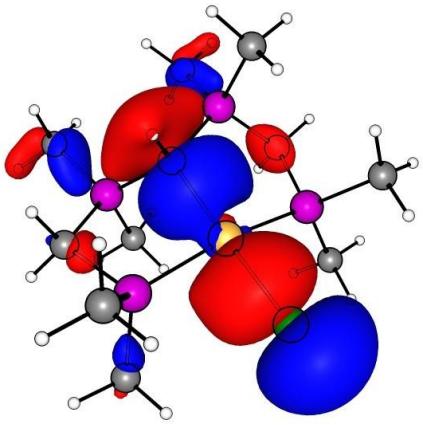

HOMO-7

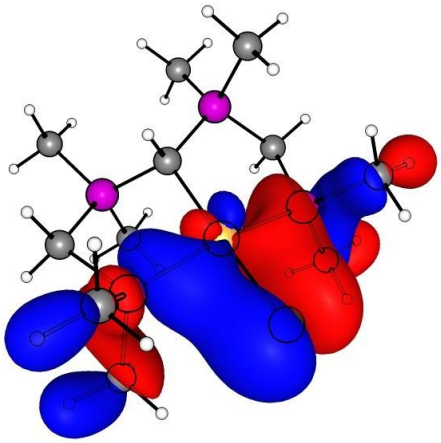

HOMO-8

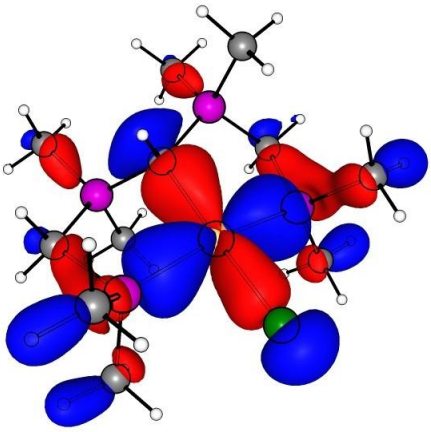

HOMO-9

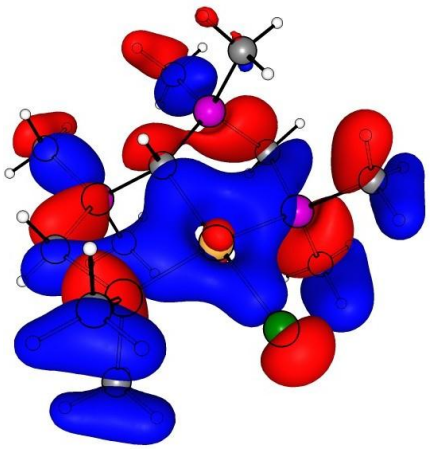

HOMO-10

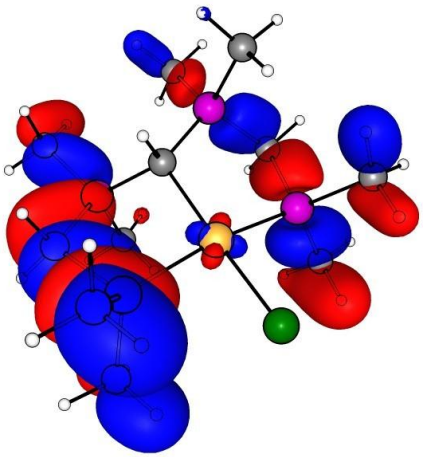

31

3^{Me}

LUMO

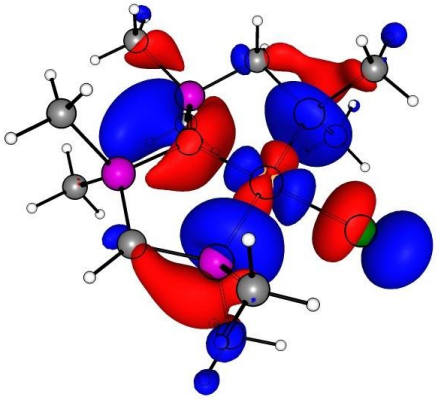

HOMO

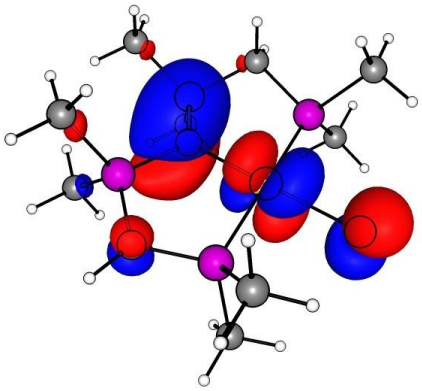

HOMO-1

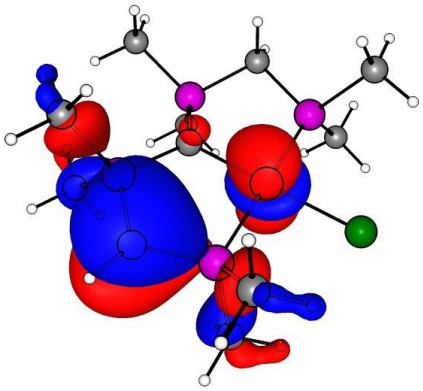

HOMO-2

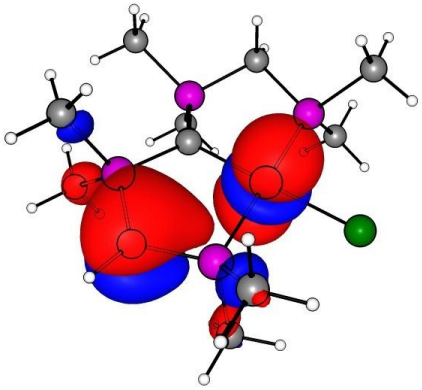

HOMO-3

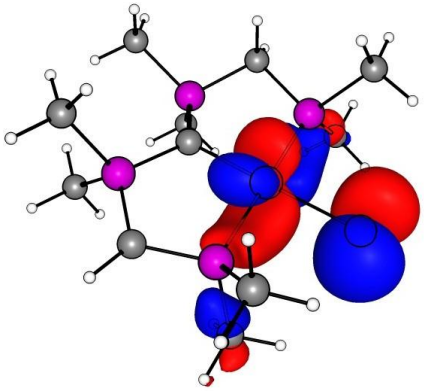

HOMO-4

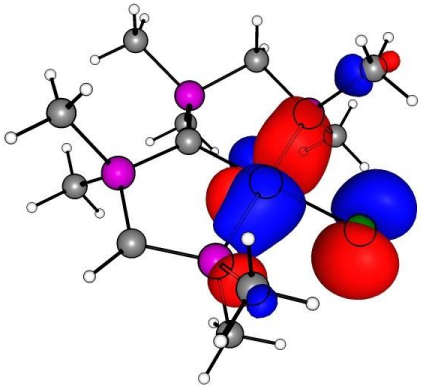

32

HOMO-5

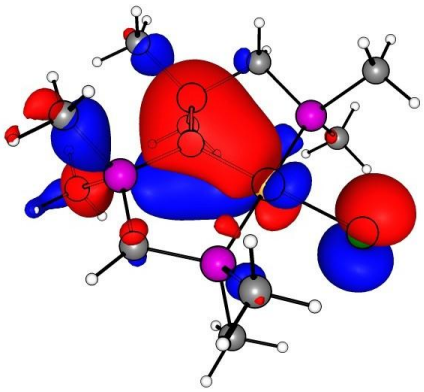

HOMO-6

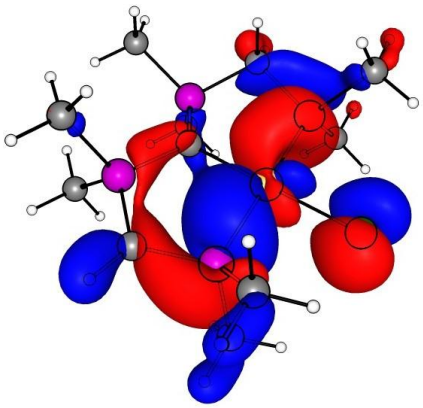

HOMO-7

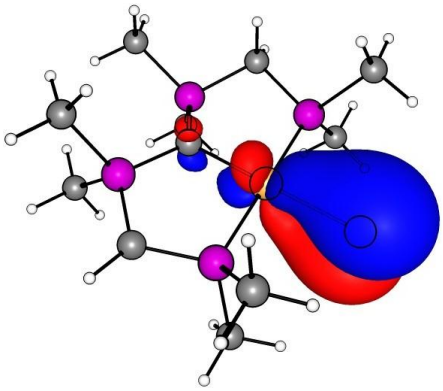

HOMO-8

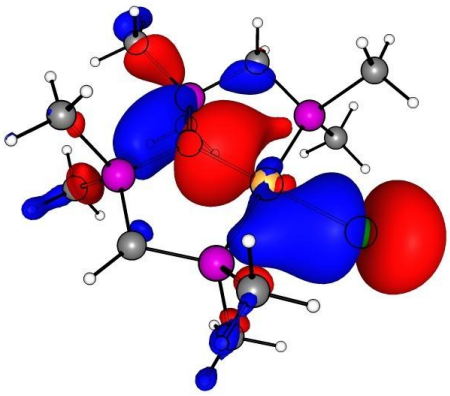

HOMO-9

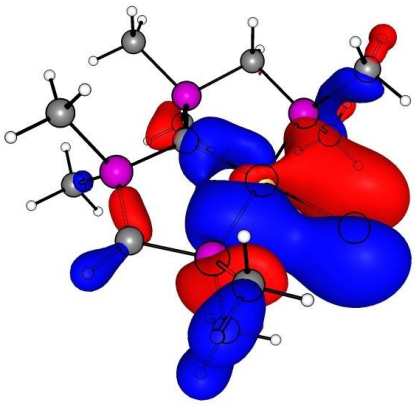

HOMO-10

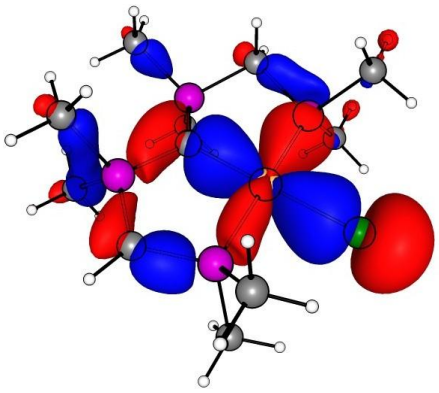

7^{Me}

LUMO

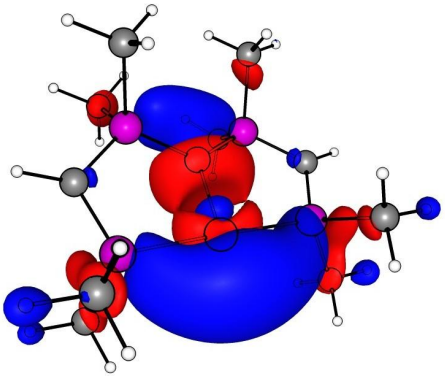

HOMO

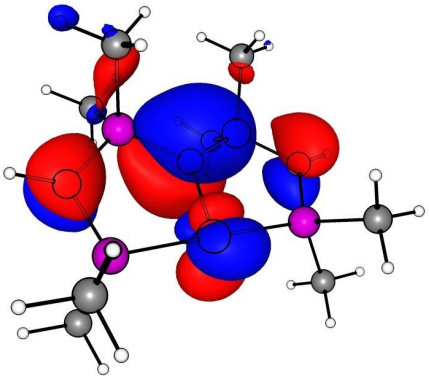

HOMO-1

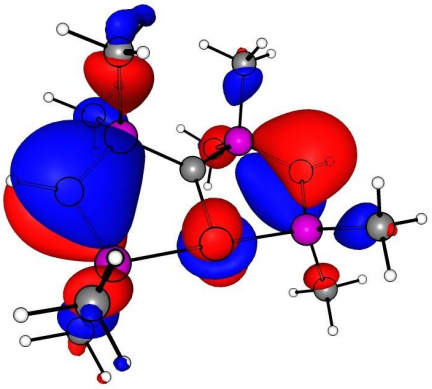

HOMO-2

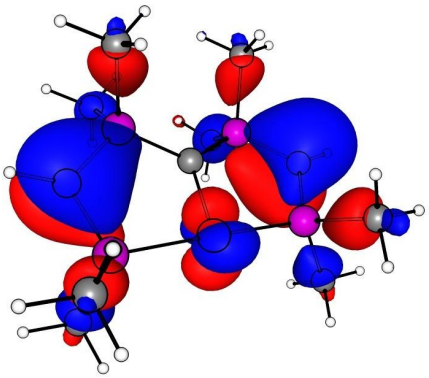

HOMO-3

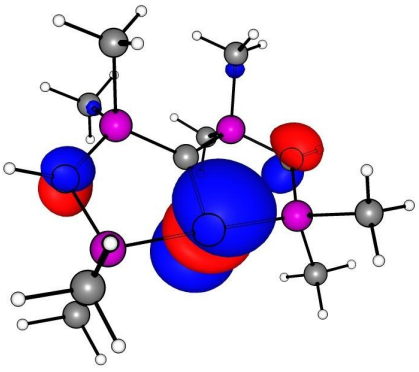

HOMO-4

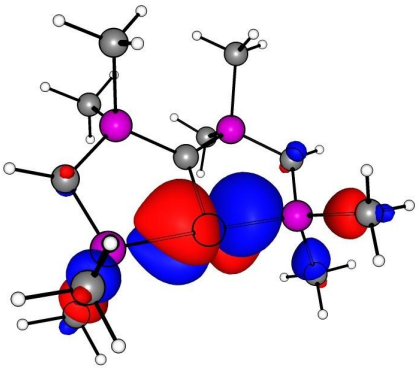

HOMO-5

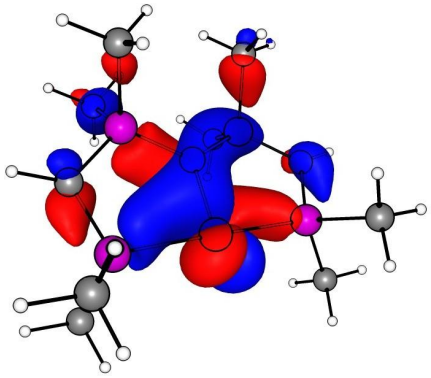

HOMO-6

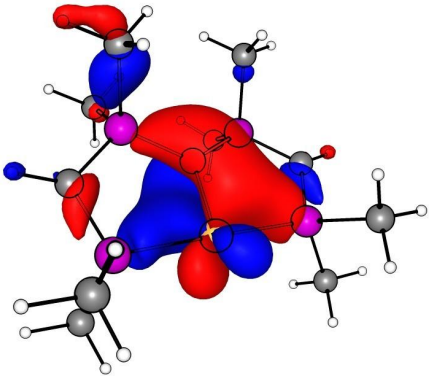

HOMO-7

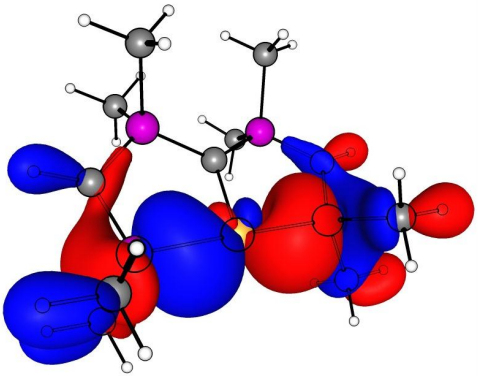

HOMO-8

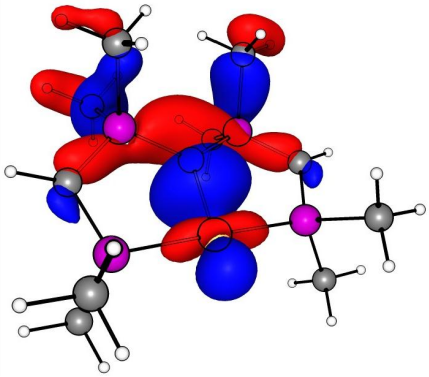

HOMO-9

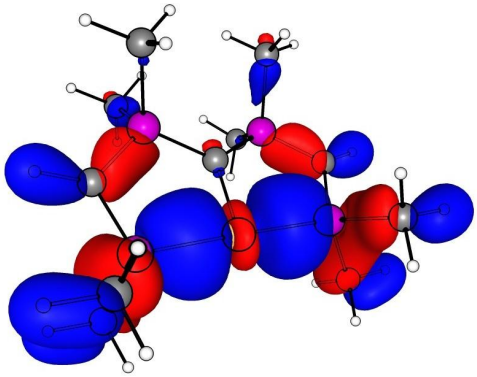

HOMO-10

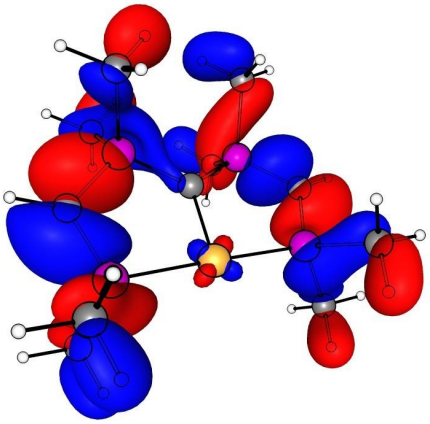

***cis*-5^{Me}**

LUMO

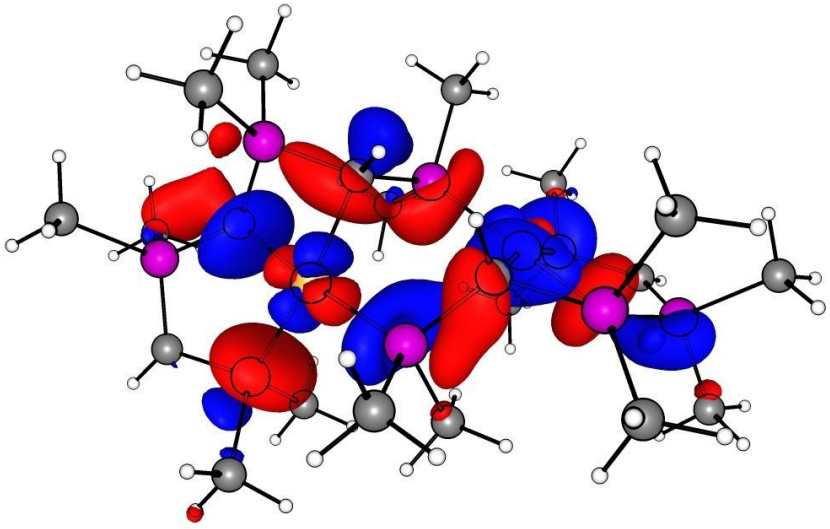

HOMO

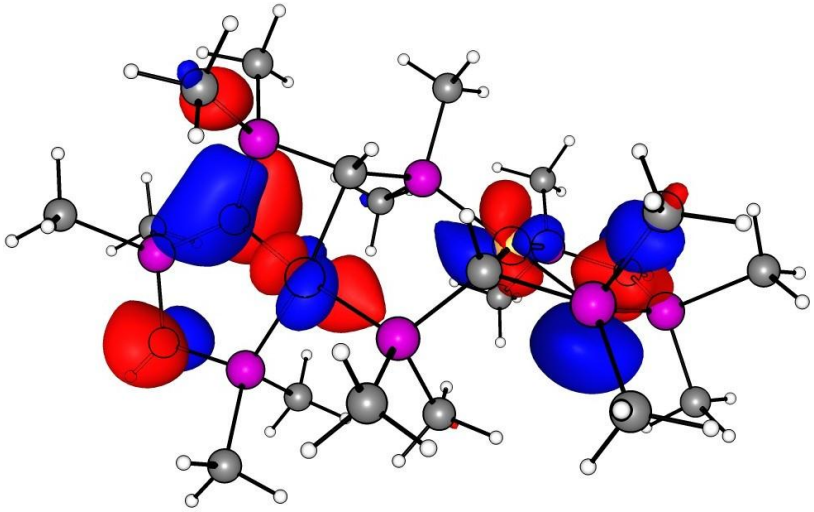

36

HOMO-1

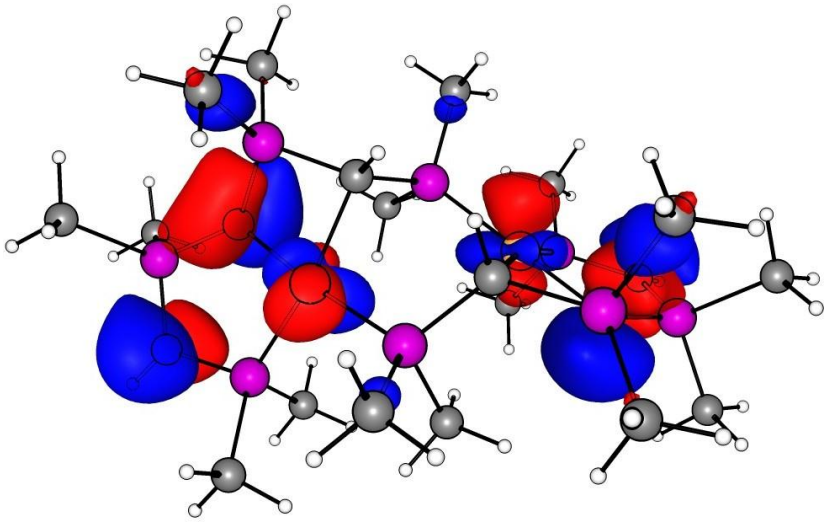

HOMO-2

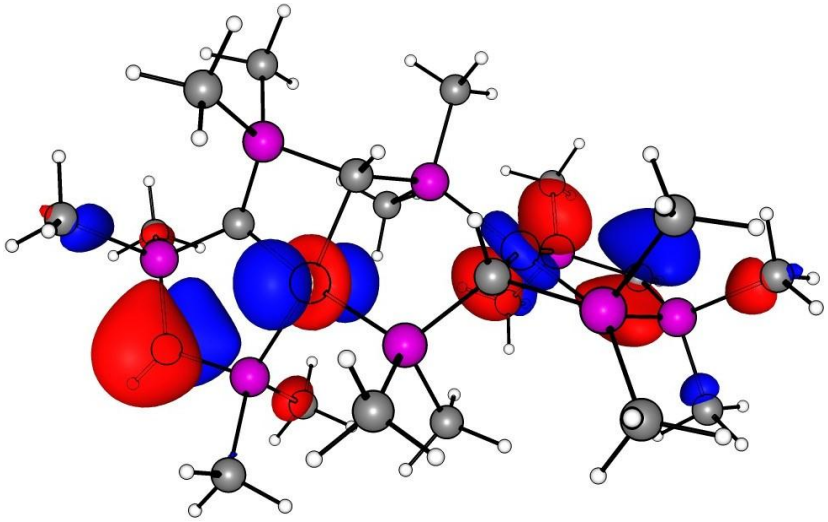

HOMO-3

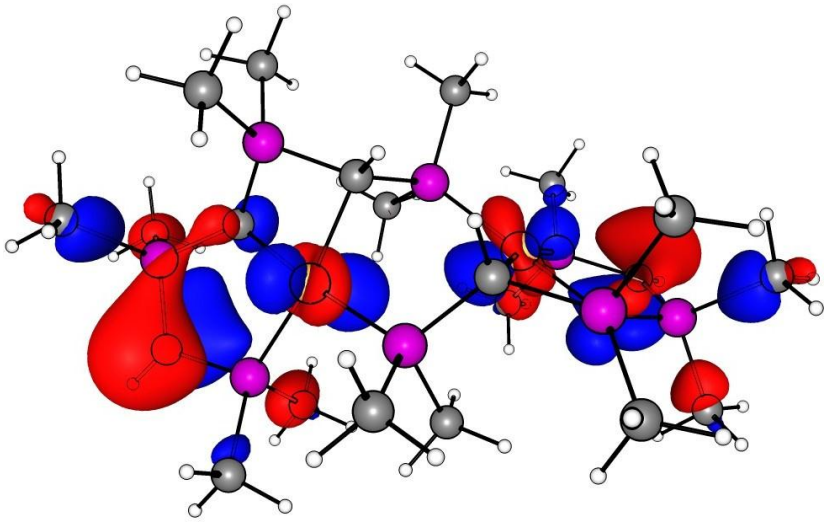

HOMO-4

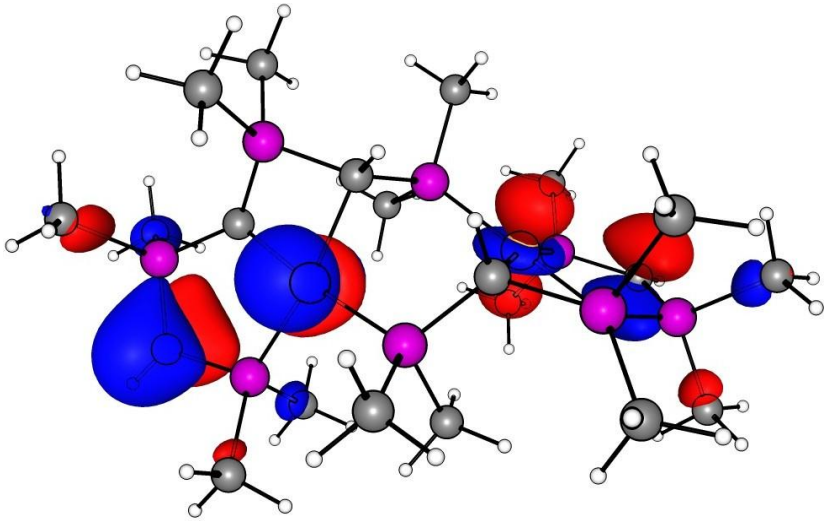

38

HOMO-5

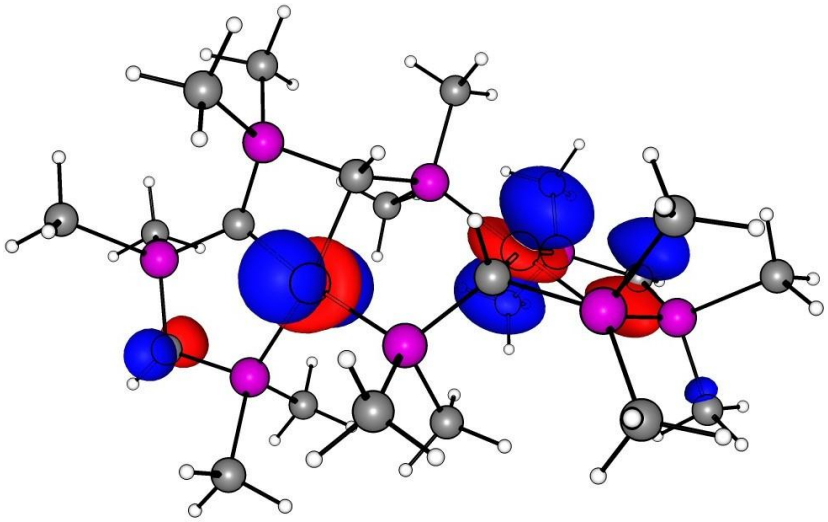

HOMO-6

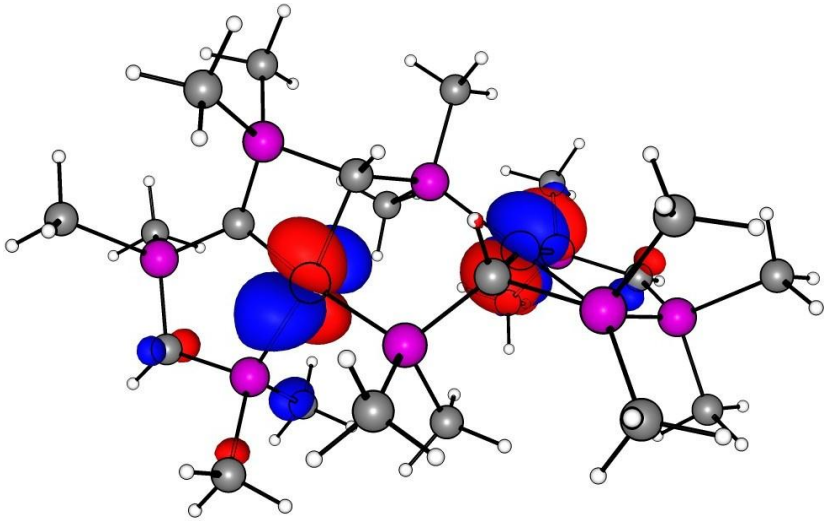

HOMO-7

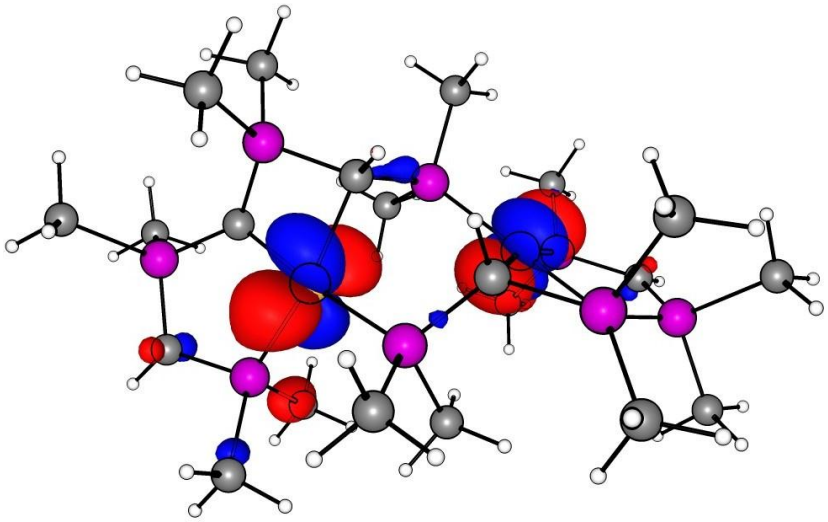

HOMO-8

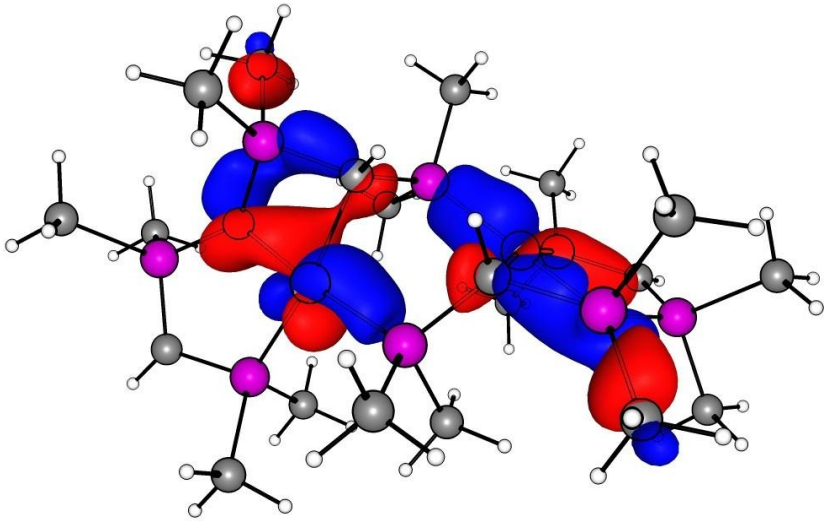

40

HOMO-9

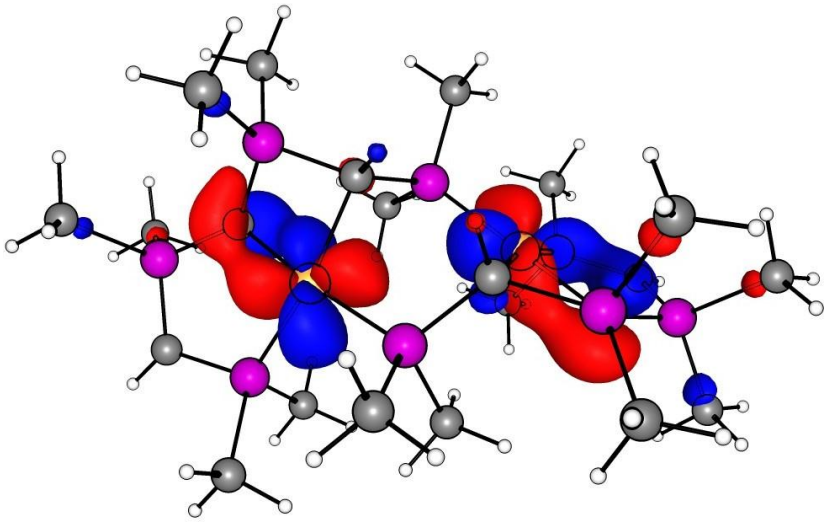

HOMO-10

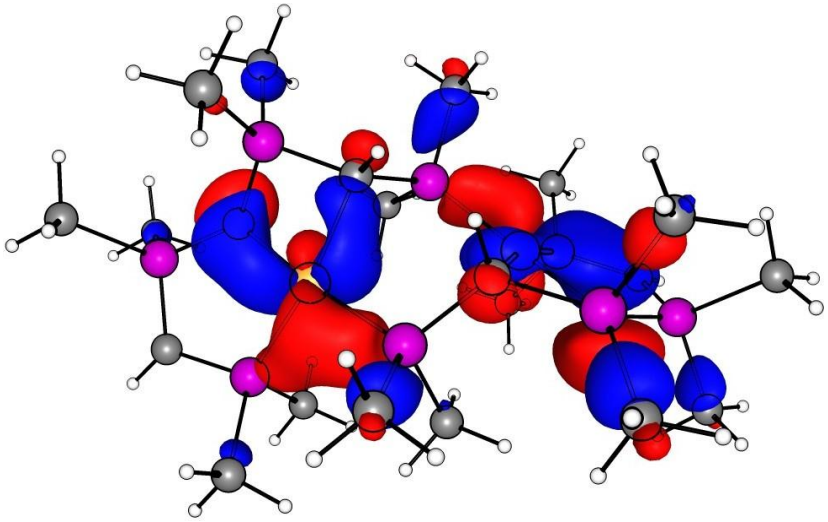

***trans*-5^{Me}**

LUMO

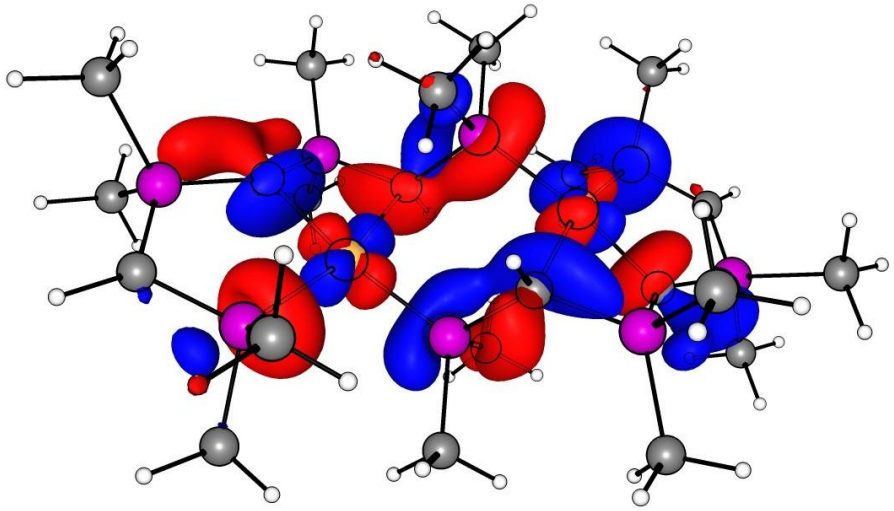

HOMO

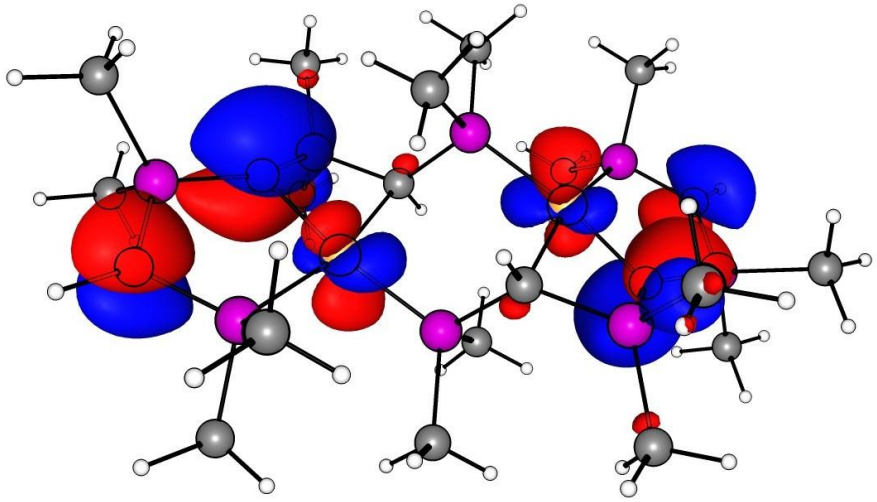

HOMO-1

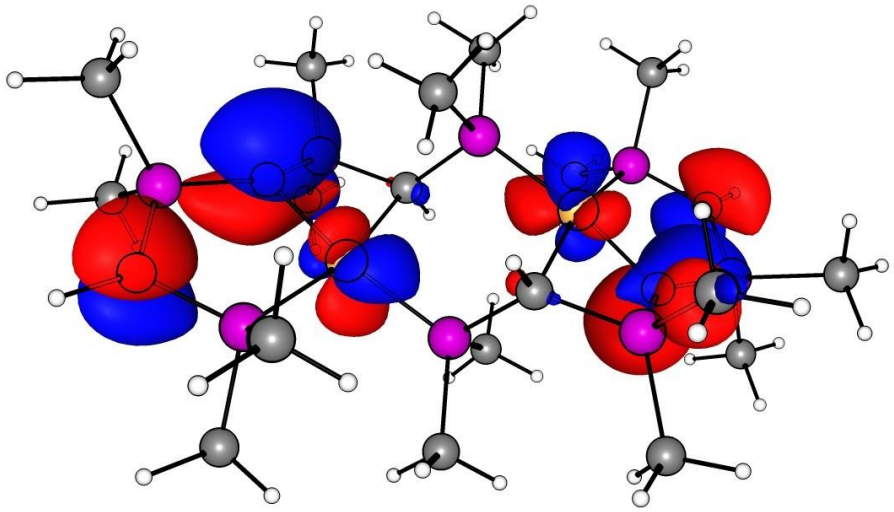

HOMO-2

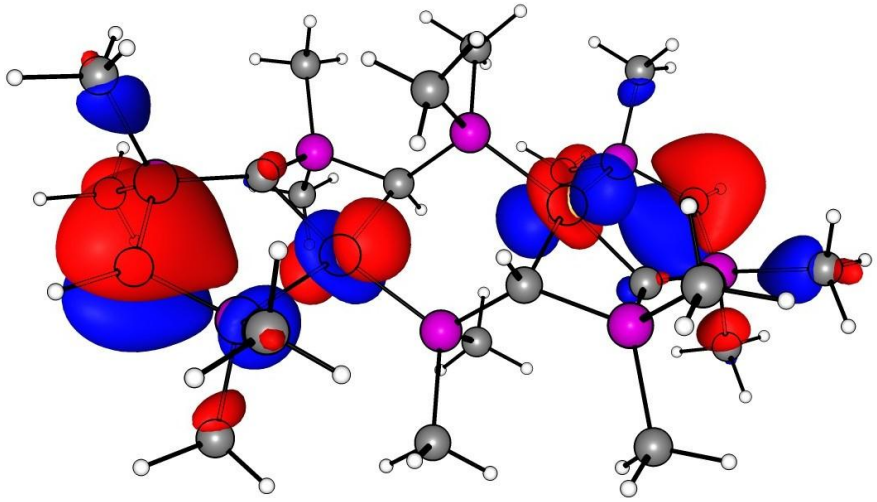

HOMO-3

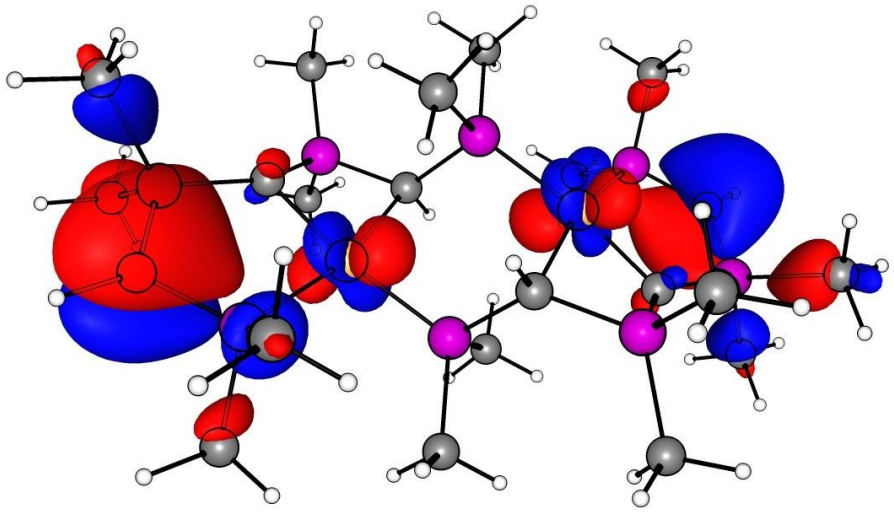

HOMO-4

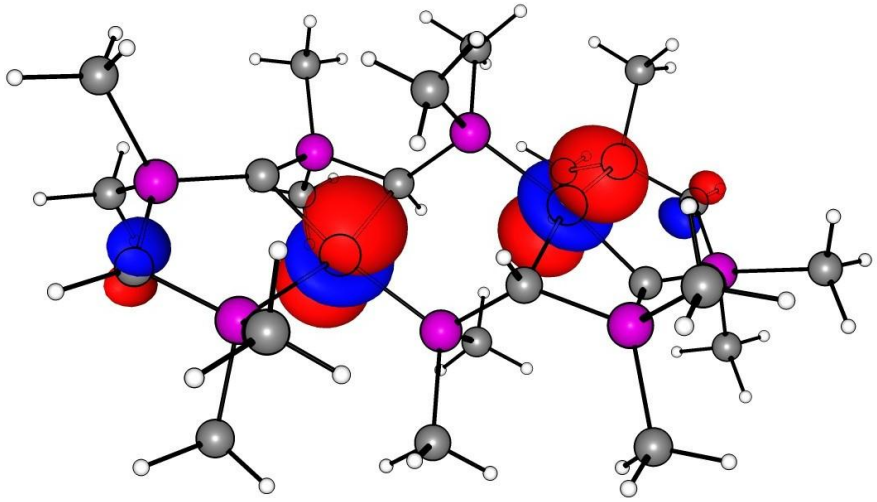

HOMO-5

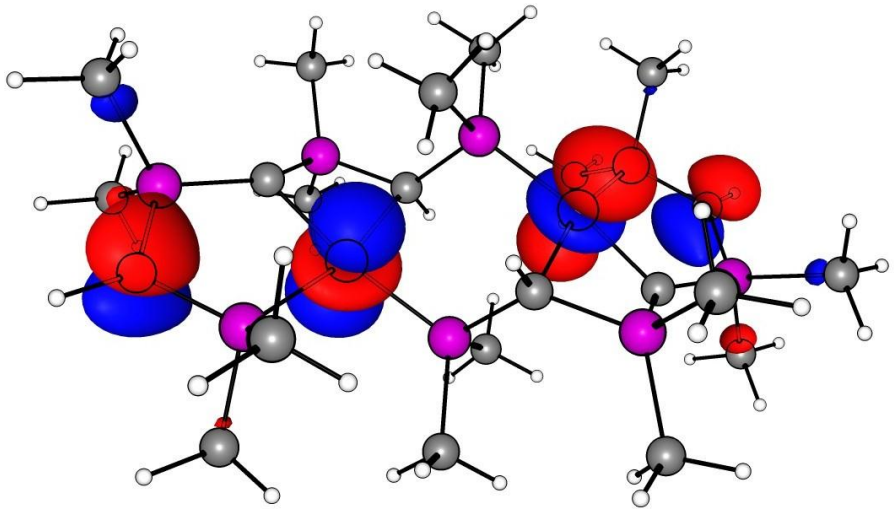

HOMO-6

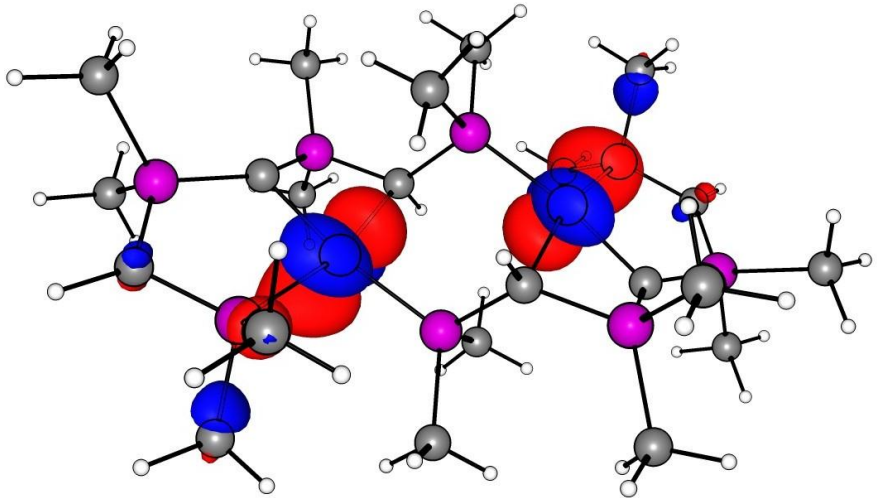

HOMO-7

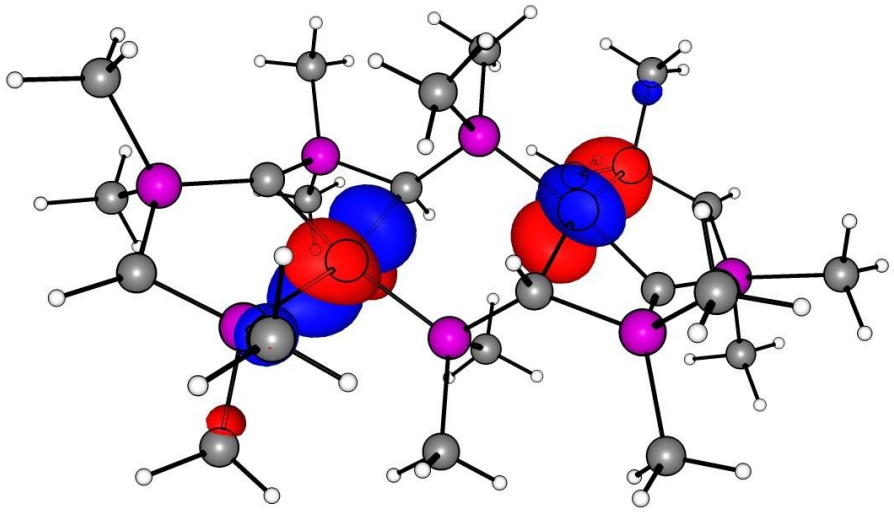

HOMO-8

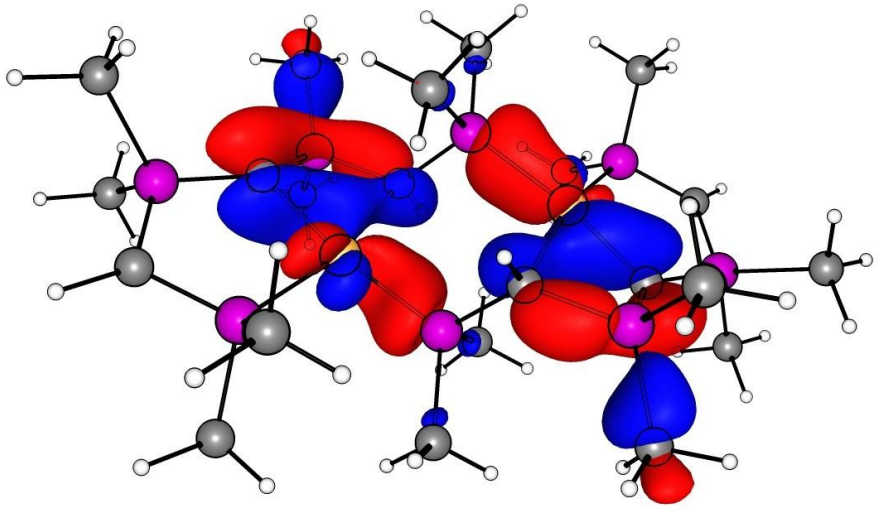

HOMO-9

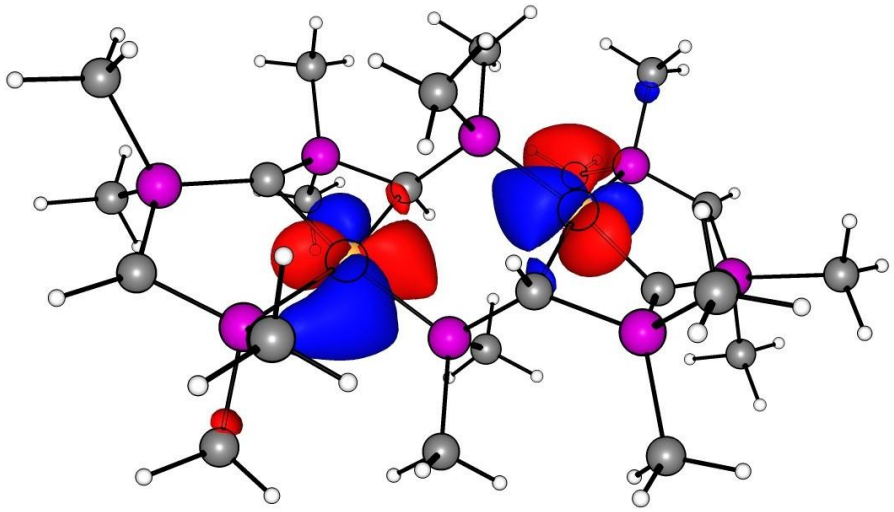

HOMO-10

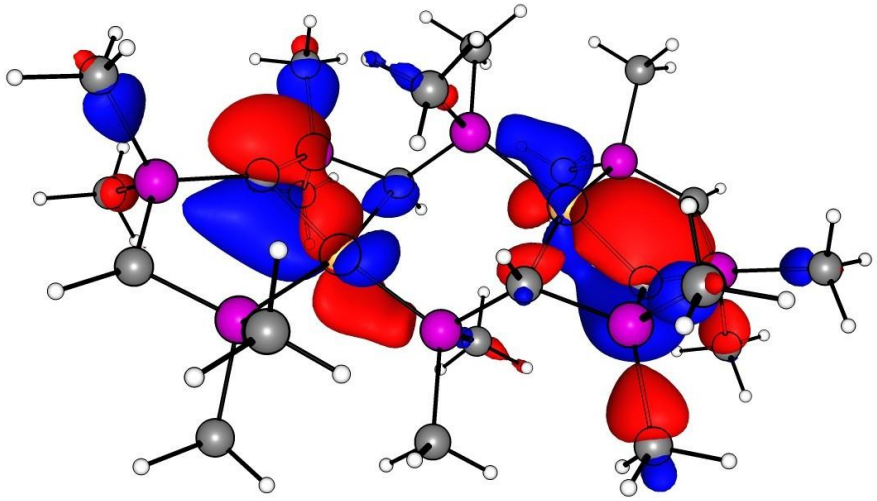

***cis*-6^{Me}**

LUMO

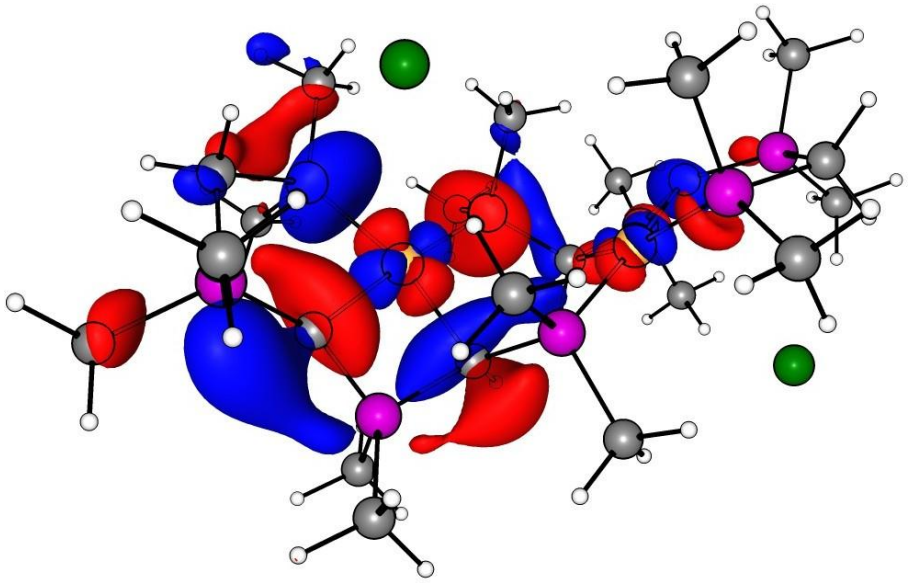

HOMO

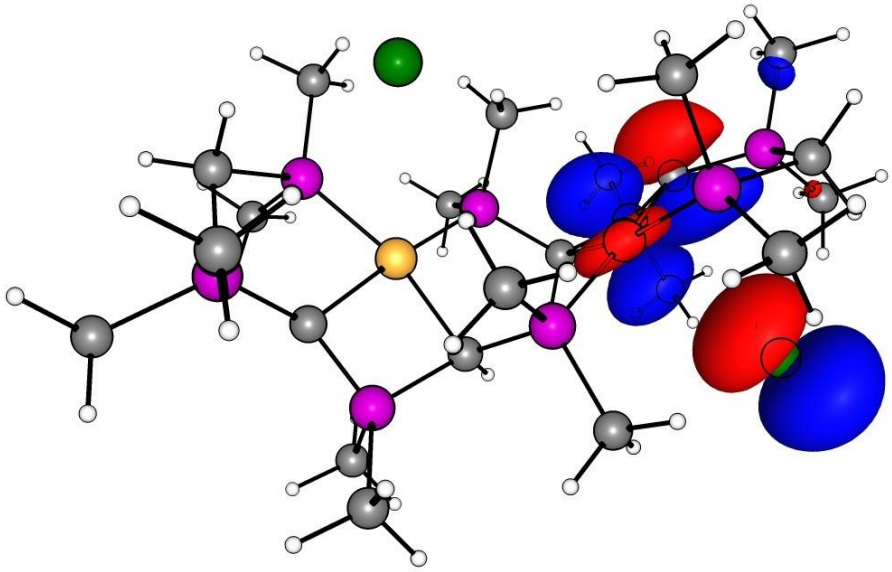

48

HOMO-1

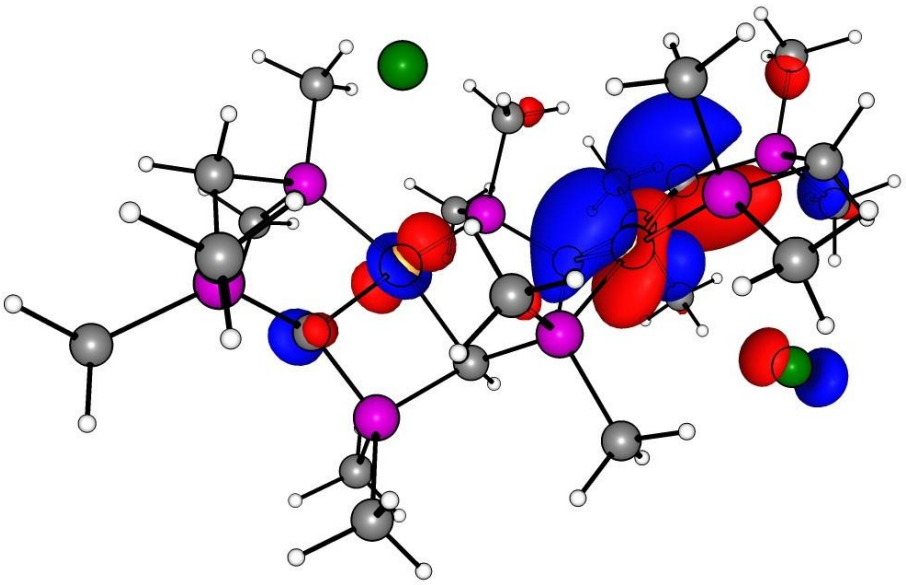

HOMO-2

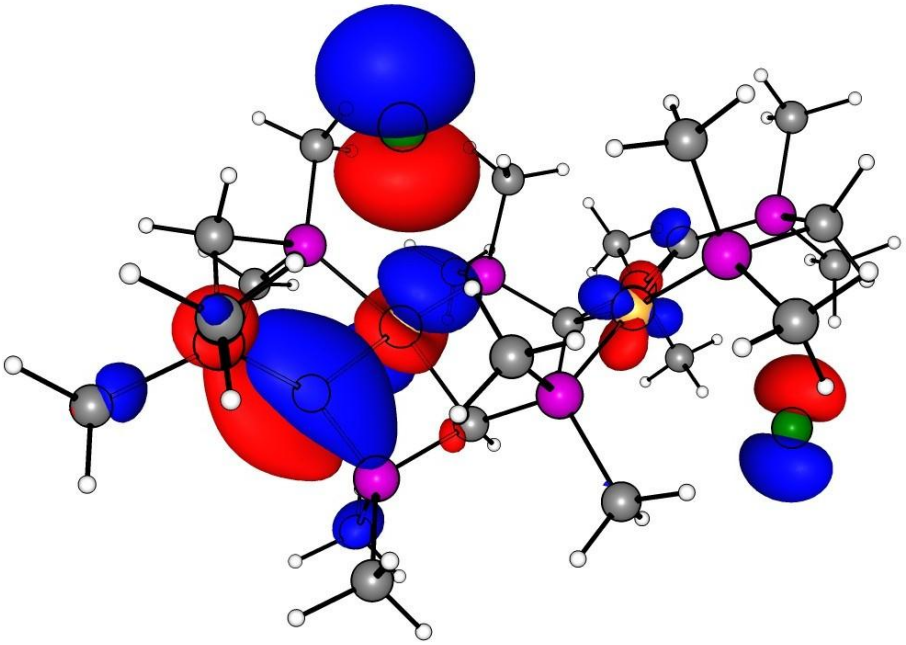

HOMO-3

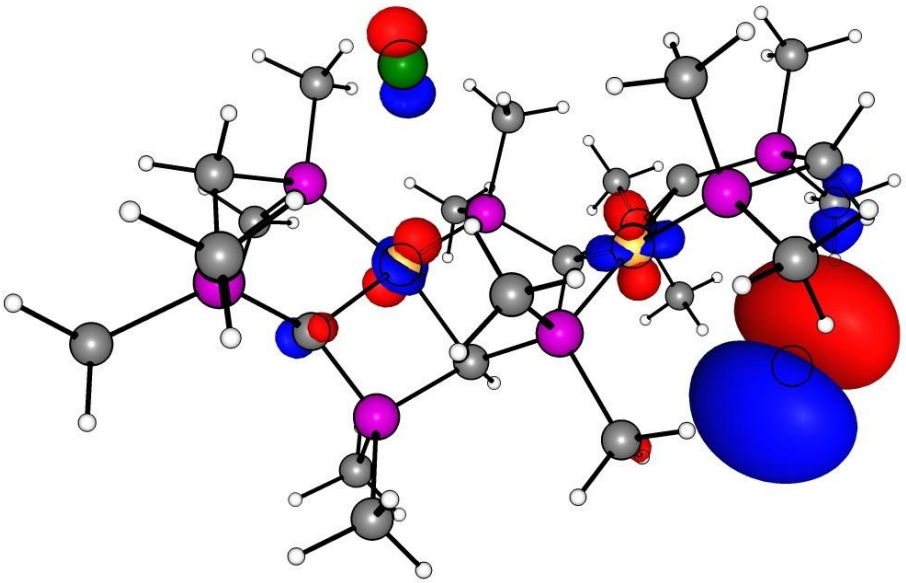

HOMO-4

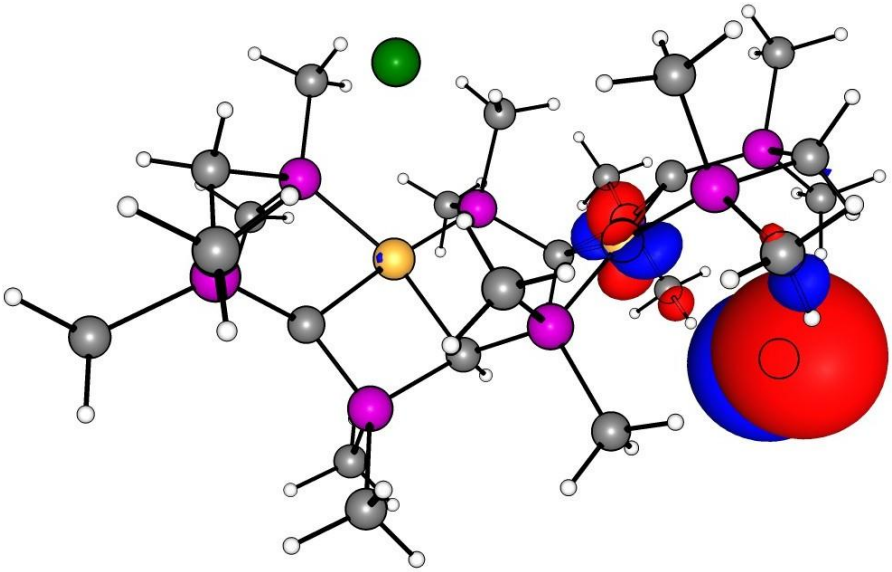

50

HOMO-5

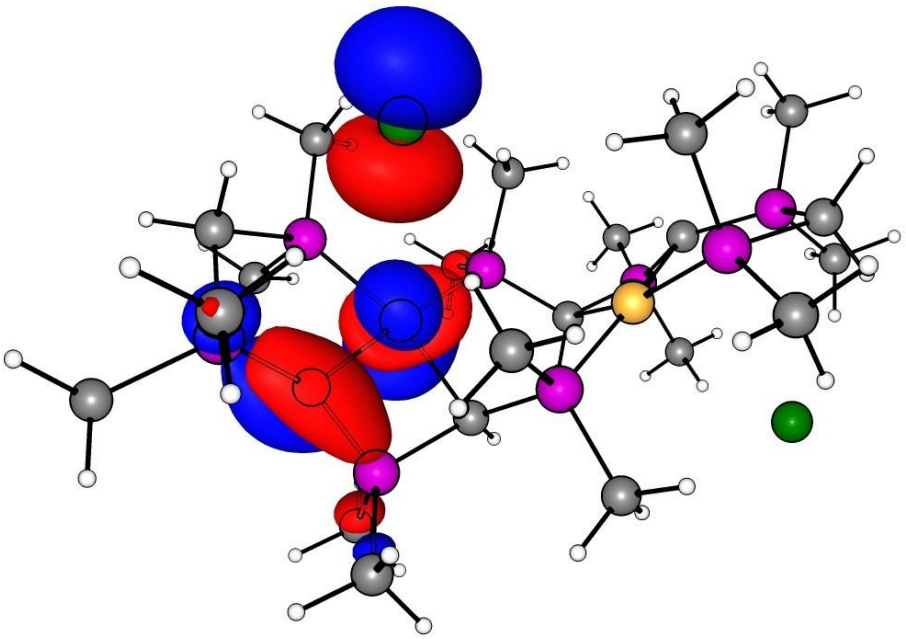

HOMO-6

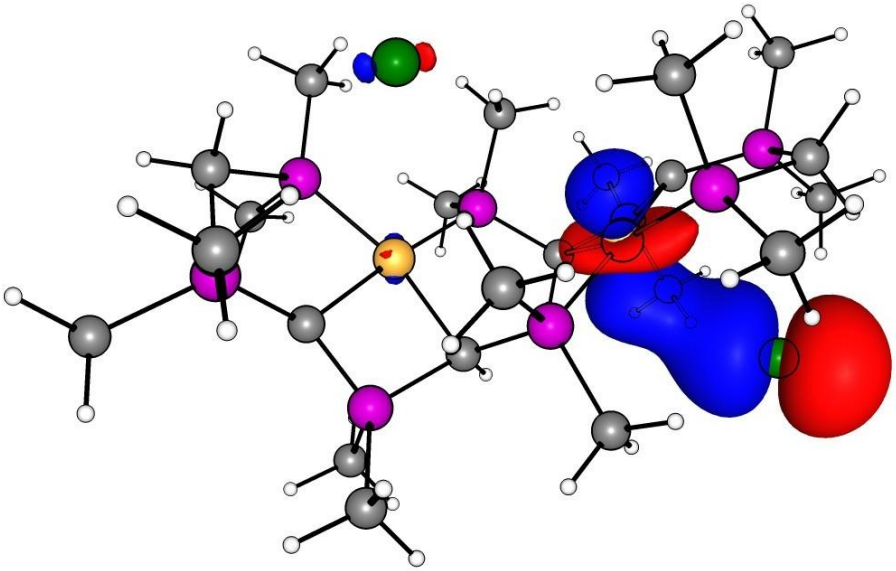

HOMO-7

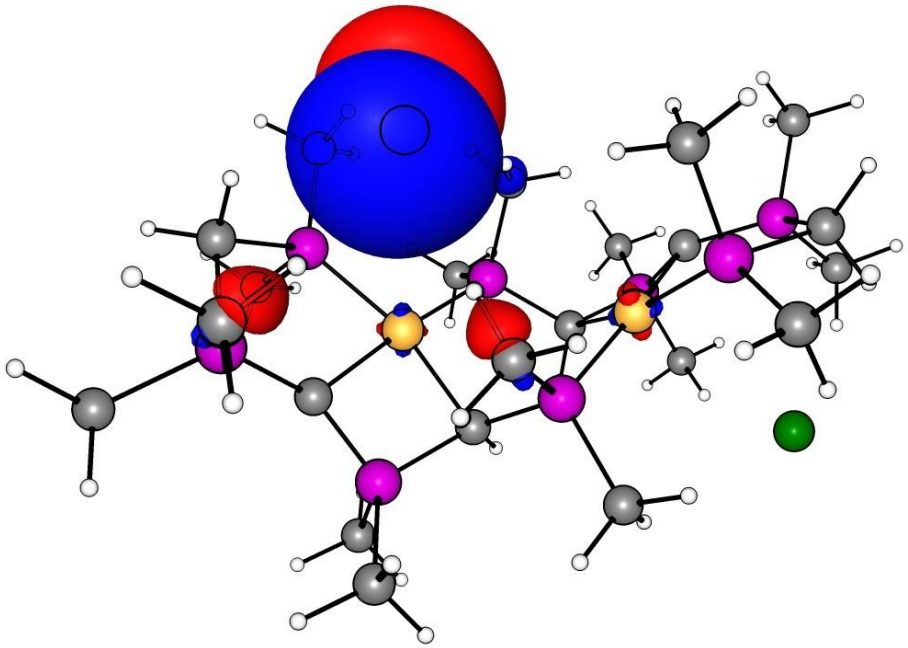

HOMO-8

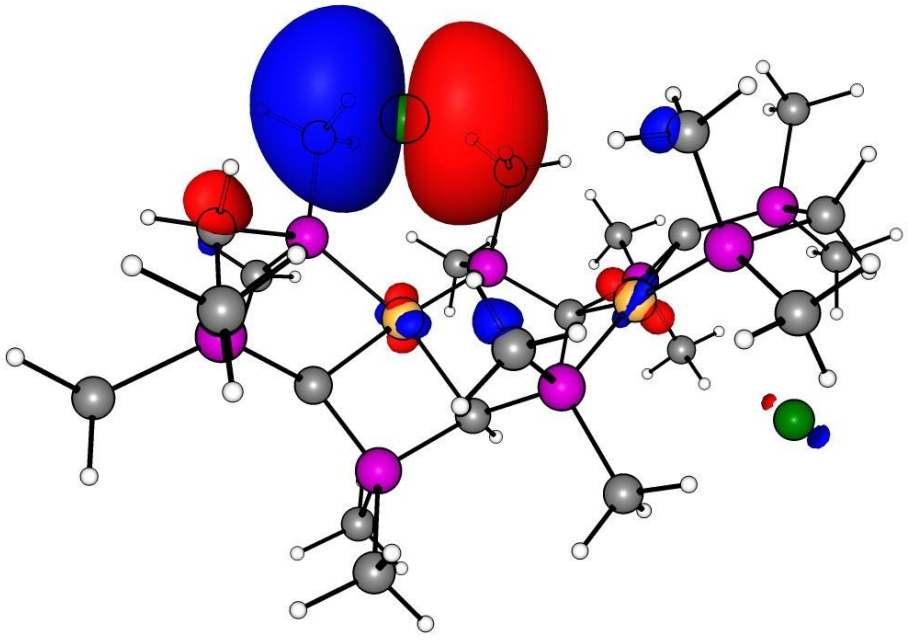

52

HOMO-9

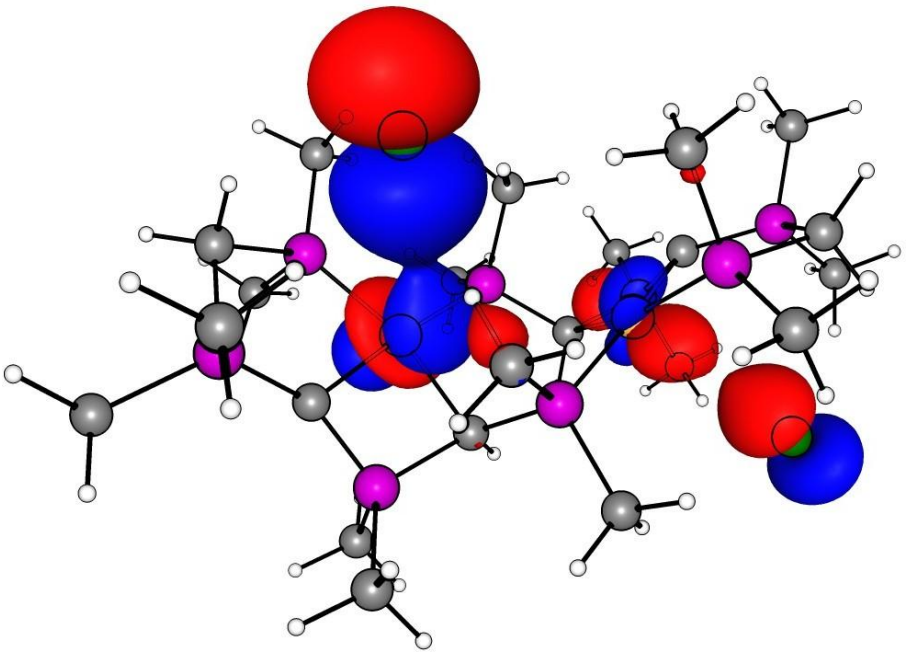

HOMO-10

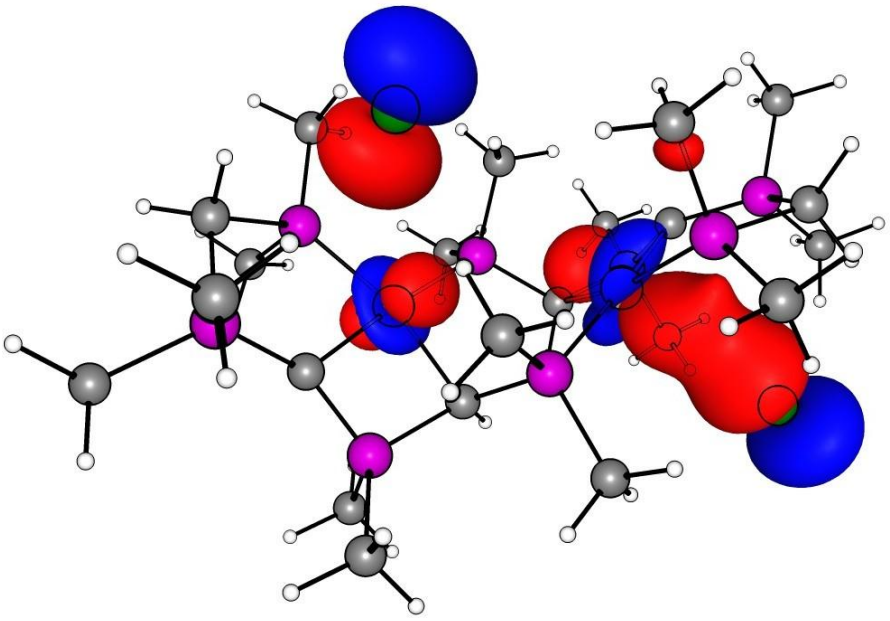

***trans*-8^{Me}**

LUMO

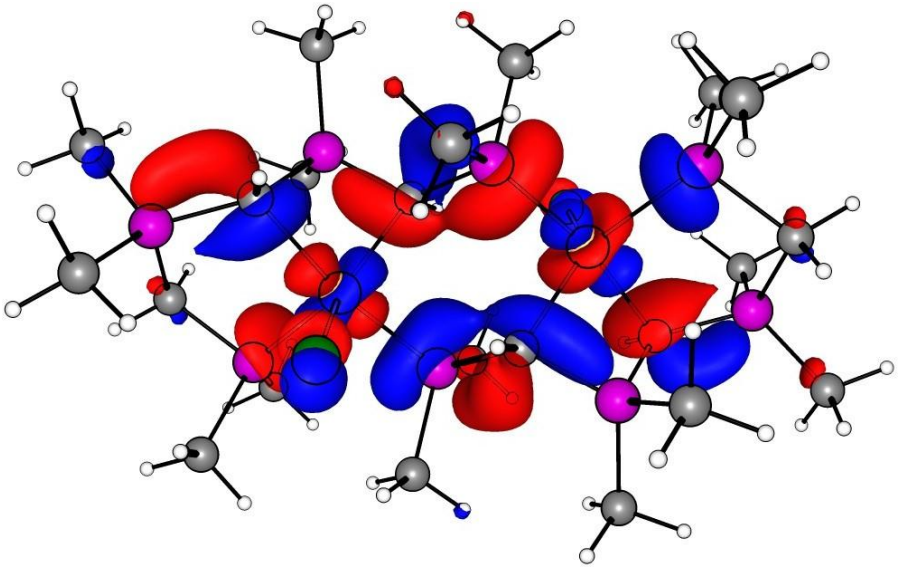

HOMO

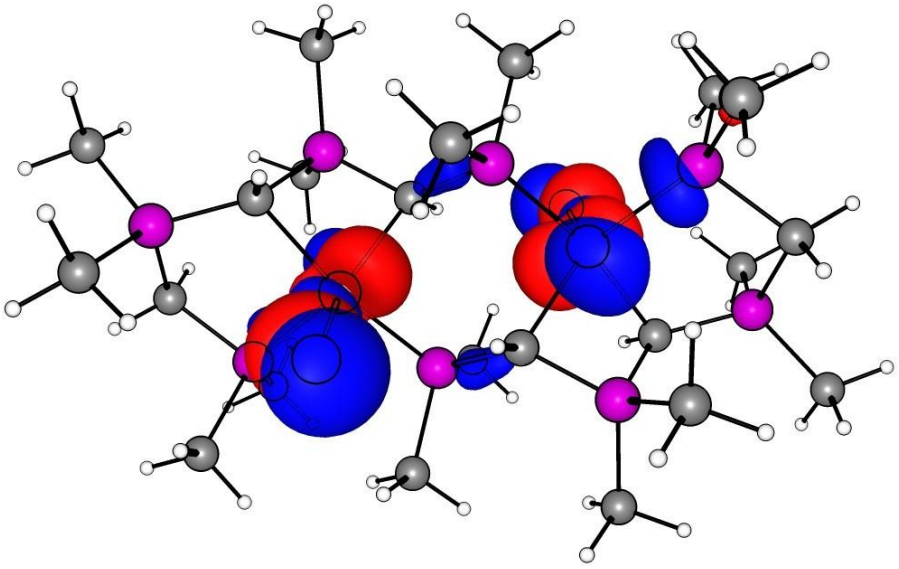

54

HOMO-1

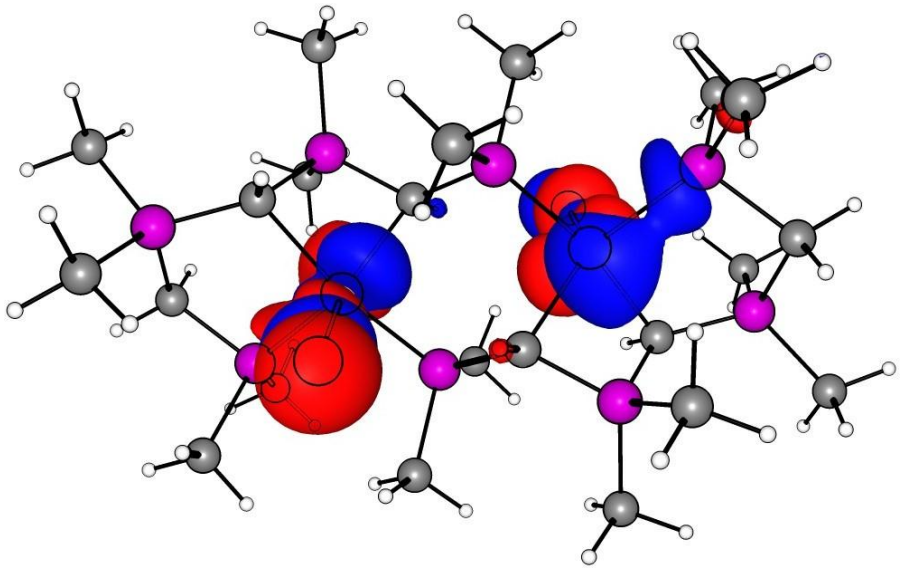

HOMO-2

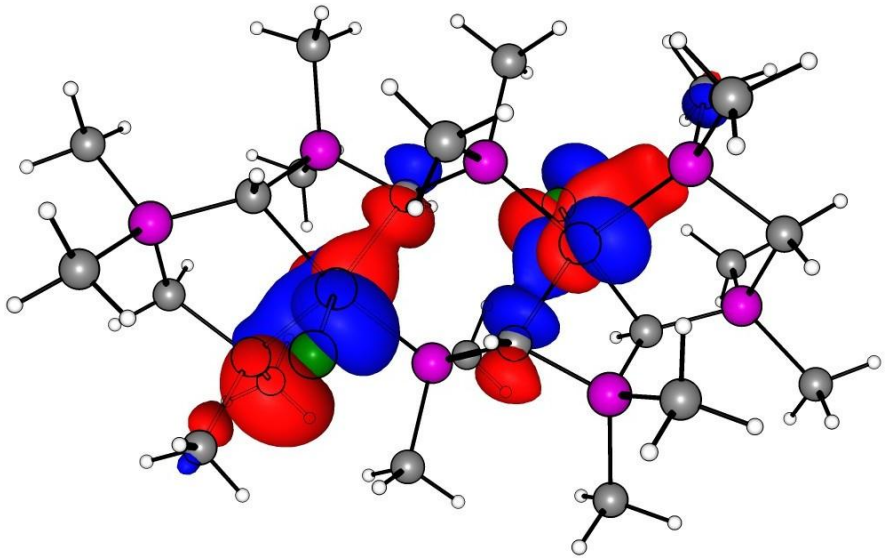

HOMO-3

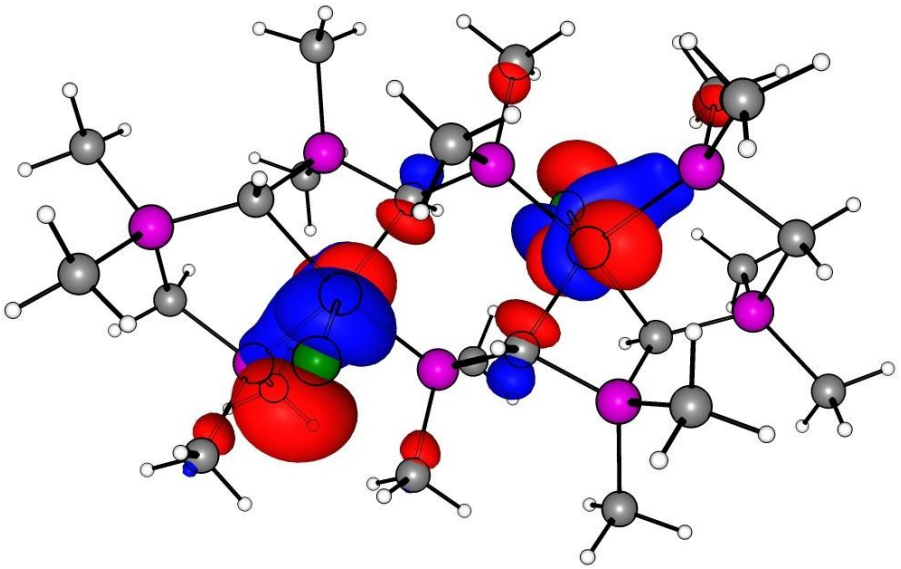

HOMO-4

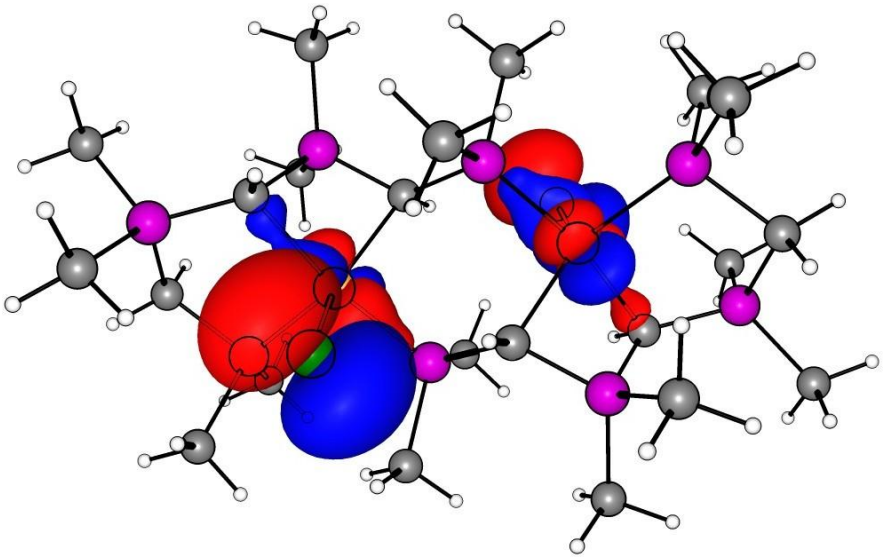

56

HOMO-5

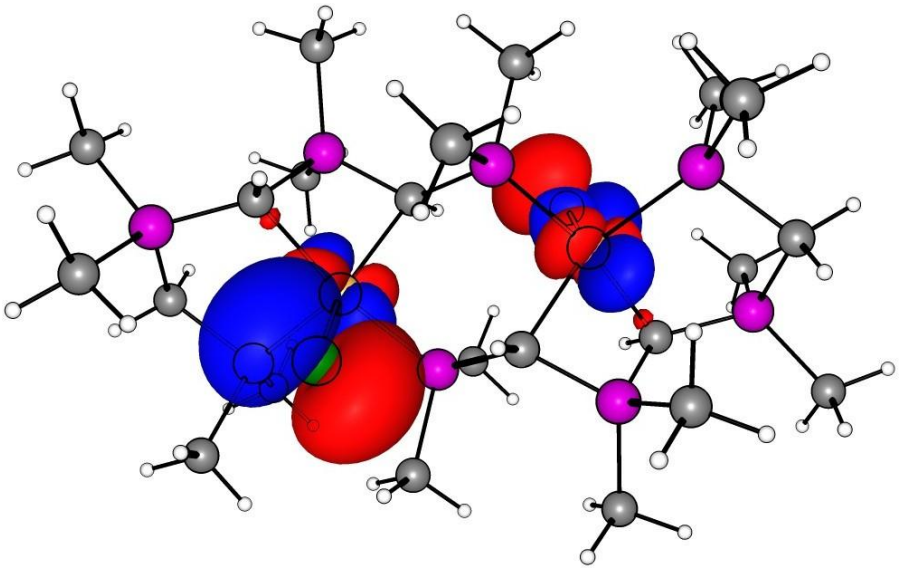

HOMO-6

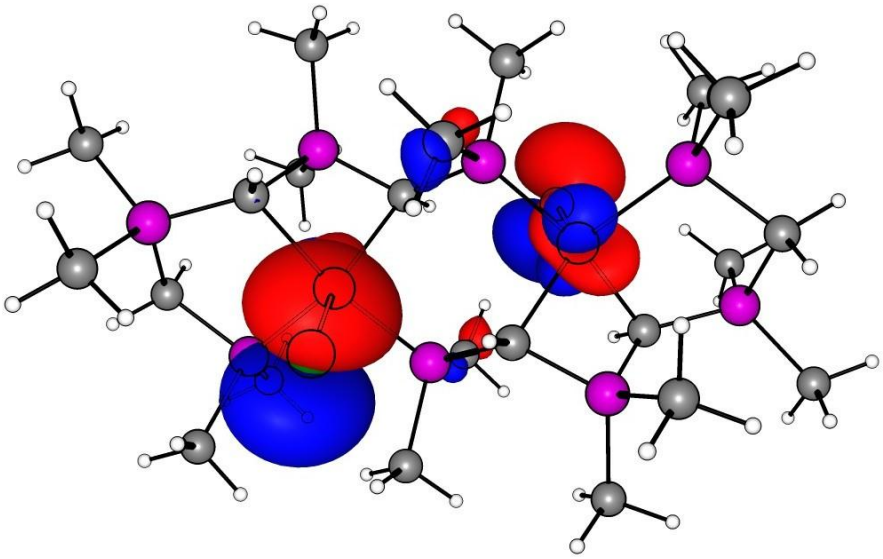

HOMO-7

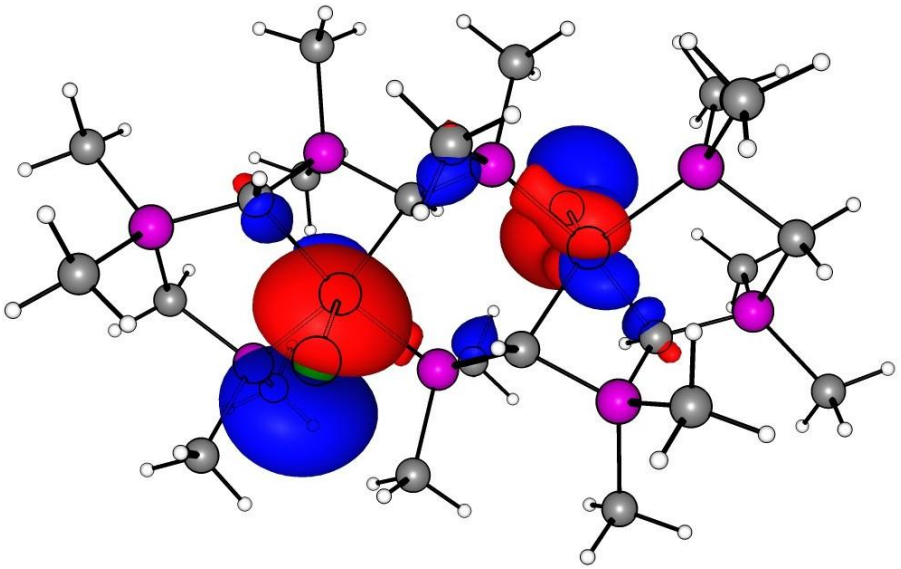

HOMO-8

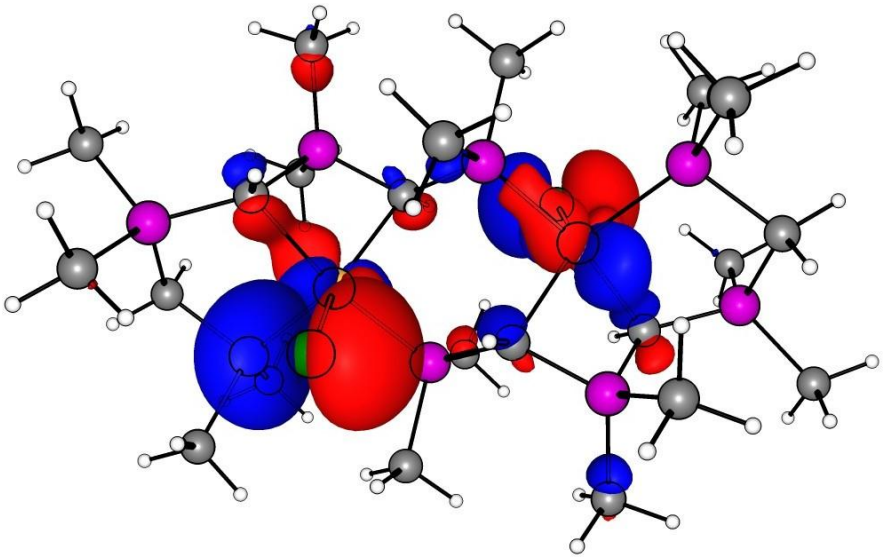

58

HOMO-9

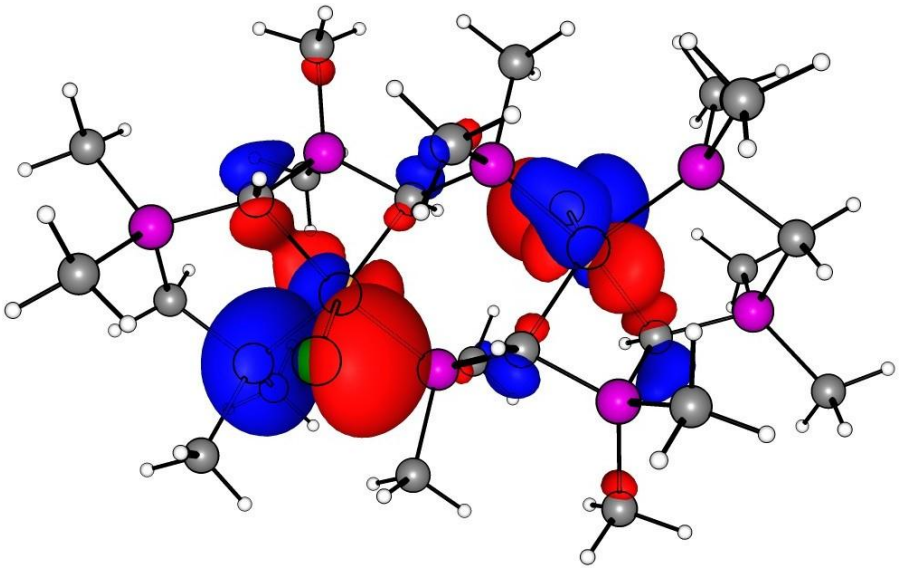

HOMO-10

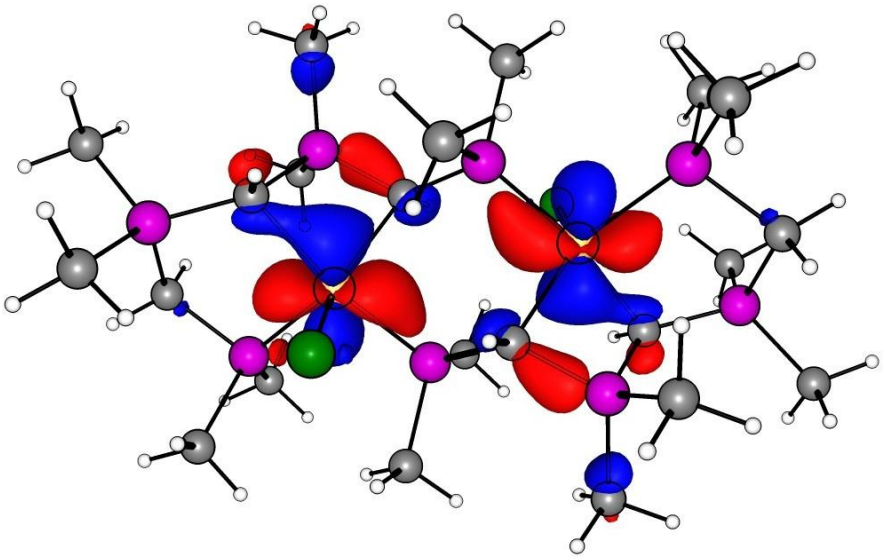

3.2 Cartesian coordinates of all DFT-optimized geometries

1^{Me}

Ni	-1.161450	0.218978	0.009839
Cl	-3.368419	0.447311	-0.139963
P	-0.927795	1.902346	-1.358476
P	-1.460213	-1.463147	1.368012
C	0.791344	0.018530	0.137406
C	-1.679424	3.486358	-0.828778
C	-1.563147	1.625409	-3.052378
C	0.889558	2.282060	-1.569984
C	-2.412618	-2.877811	0.699380
C	-2.273189	-1.059058	2.956768
C	0.201586	-2.178283	1.833043
P	1.337231	-1.540774	0.541761
P	1.693322	1.429511	-0.158738
H	-2.747445	3.308093	-0.668195
H	-1.234014	3.812090	0.116844
H	-1.536684	4.263153	-1.589624
H	-1.072597	0.747933	-3.486417
H	-2.637556	1.428056	-2.976039
H	-1.386735	2.502280	-3.687309
H	1.248709	1.816209	-2.495218
H	1.102816	3.356633	-1.604104
H	-3.391554	-2.499041	0.388634
H	-1.903249	-3.290101	-0.177772
H	-2.535141	-3.662493	1.455604
H	-1.696868	-0.283745	3.472410
H	-3.269950	-0.666459	2.729990
H	-2.355891	-1.947154	3.595243
H	0.514339	-1.753005	2.793967
H	0.197732	-3.271821	1.907855
C	1.216191	-2.767733	-0.813756
C	3.048073	-1.714730	1.166063
C	1.658715	2.664856	1.194830
C	3.468486	1.237918	-0.559015
H	0.197817	-2.734642	-1.215230
H	1.912095	-2.489238	-1.613117
H	1.446499	-3.781030	-0.462842
H	3.763078	-1.448911	0.381554
H	3.196988	-1.064937	2.034583
H	3.224491	-2.755590	1.459848
H	0.613343	2.857696	1.458739
H	2.165947	2.249878	2.072974
H	2.145937	3.601732	0.898407
H	4.010872	0.854769	0.310762
H	3.588241	0.547479	-1.400191
H	3.889630	2.212623	-0.829870

2^{Me}

Ni	7.730152	15.712988	7.418858
P	8.263177	15.744453	9.563689
P	7.623069	15.894786	5.232888
Cl	7.453928	17.874381	7.510381
C	7.746740	13.660602	7.412980
C	6.941562	16.067345	10.779413
C	9.641140	16.860401	9.998217
C	8.914794	14.024354	9.960423
C	6.047522	16.433266	4.483761
C	7.975777	14.182121	4.542100
C	8.909966	16.947905	4.478853
P	9.200317	13.194329	8.365589
P	7.377510	12.989326	5.771931
H	6.884783	13.384706	8.041987
H	6.561312	17.077524	10.589566
H	6.121918	15.352857	10.649113
H	7.329247	16.007872	11.803420
H	10.520248	16.640920	9.383402
H	9.321714	17.886845	9.792869
H	9.895752	16.752538	11.059439
H	9.832084	14.040151	10.560392
H	8.158783	13.447475	10.508639
H	5.224036	15.775571	4.777776
H	5.837247	17.440121	4.861144
H	6.127943	16.459762	3.390458
H	7.529497	13.990991	3.558192
H	9.064101	14.069583	4.450330
H	8.739536	17.974580	4.818716
H	9.903008	16.627924	4.811554
H	8.851871	16.902186	3.384614
C	10.698284	13.849234	7.586694
C	9.442128	11.417640	8.666260
C	8.058010	11.345834	5.402007
C	5.572647	12.892364	5.665274
H	10.873073	13.346295	6.628339
H	10.566502	14.922675	7.414751
H	11.565160	13.673119	8.233828
H	8.532255	10.986553	9.098842
H	9.686692	10.898666	7.734410
H	10.270466	11.280189	9.371972
H	9.152931	11.372427	5.415200
H	7.695247	10.617109	6.134942
H	7.728904	11.037868	4.402286
H	5.209474	12.103284	6.333329
H	5.139273	13.849929	5.970777
H	5.272019	12.660854	4.637498

3^{Me}

Ni	-1.327645	-0.006321	0.150559
Cl	-3.580851	0.164109	0.071349
P	-1.474409	-1.576014	-1.327066
P	-1.176650	1.547311	1.711724
C	0.622844	-0.165690	0.183647
C	-2.141314	-1.111913	-2.978095
C	-2.464099	-3.059103	-0.879970
C	0.223835	-2.254116	-1.698663
C	-2.199805	1.135665	3.193335
C	-1.953357	3.137518	1.177755
C	0.480729	1.779507	2.179781
P	1.562687	0.838926	1.263016
P	1.350348	-0.919231	-1.144491
H	-3.136333	-0.684337	-2.815292
H	-1.503435	-0.344599	-3.429774
H	-2.207444	-1.978011	-3.649263
H	-2.053707	-3.498234	0.035768
H	-3.486102	-2.721421	-0.678597
H	-2.461293	-3.805658	-1.684922
H	0.402327	-3.127349	-1.060706
H	0.370752	-2.536352	-2.748155
H	-3.248826	1.034704	2.894603
H	-1.847784	0.188152	3.614311
H	-2.100294	1.924844	3.951578
H	-1.425976	3.509296	0.292826
H	-3.005082	2.960526	0.926930
H	-1.879193	3.884070	1.980561
H	0.813240	2.431938	2.983821
C	2.692718	-0.162874	2.334767
C	2.816739	1.875719	0.360887
C	1.648830	0.065250	-2.687814
C	2.997830	-1.695820	-0.868706
H	2.087855	-0.912567	2.855008
H	3.472089	-0.662527	1.747150
H	3.172792	0.490951	3.074627
H	3.556456	1.266101	-0.175997
H	2.284059	2.516913	-0.349243
H	3.351157	2.511168	1.079088
H	0.700836	0.526560	-2.985199
H	2.364356	0.863521	-2.462111
H	2.037374	-0.551541	-3.509318
H	3.730692	-0.927005	-0.602160
H	2.923019	-2.416552	-0.048633
H	3.336236	-2.202816	-1.780116

***cis*-5^{Me}**

Ni	-2.291904	7.482863	8.092790
P	-3.167491	5.501956	7.748392
P	-3.160616	9.201477	9.868334
P	-0.486900	7.335714	6.879568
C	-2.025655	9.485707	8.534786
C	-3.825155	7.780348	9.286657
C	-2.088145	4.006961	7.549244
C	-3.991374	5.529643	6.076498
C	-4.326768	5.108541	8.986746
C	-4.314277	10.583656	10.307965
C	-2.123677	9.145193	11.402155
C	0.348102	8.925512	6.672429
C	0.781523	6.170126	7.580586
C	-0.688438	6.688007	5.162369
P	-2.393606	10.366631	7.000161
H	-1.021457	9.738148	8.883675
P	-4.764216	6.485220	9.907815
H	-1.429006	4.101939	6.678901
H	-1.482196	3.877121	8.452008
H	-2.719287	3.117821	7.417851
H	-4.742262	6.326861	6.093000
H	-3.271885	5.734207	5.275763
H	-4.493615	4.571748	5.881912
H	-4.883416	4.173956	9.009161
H	-4.950225	10.827334	9.452017
H	-4.955245	10.261228	11.139802
H	-3.754629	11.476026	10.615696
H	-2.742548	8.830904	12.250853
H	-1.331002	8.405878	11.246838
H	-1.682810	10.126380	11.622903
Ni	-0.897992	10.042683	5.451291
P	1.613496	9.295308	5.485485
H	0.541329	9.378310	7.647799
H	1.090083	6.543882	8.563700
H	0.345395	5.174396	7.709516
H	1.661964	6.102970	6.929929
H	-1.003446	5.639660	5.202087
H	-1.450969	7.285997	4.656023
H	0.238046	6.776055	4.586087
C	-2.588926	12.157157	7.462632
C	-4.126898	9.891863	6.581141
C	-4.559102	6.228447	11.732520
C	-6.575316	6.859015	9.831721
P	-1.923281	10.907502	3.714979
C	0.607564	9.740283	4.226757
C	2.880549	7.981879	5.158668
C	2.678184	10.586243	6.280235
H	-3.377383	12.289186	8.213544
H	-1.637609	12.514245	7.873338
H	-2.826475	12.749813	6.573731
H	-4.130117	8.850350	6.248676
H	-4.792995	9.966974	7.446351
H	-4.488268	10.539121	5.775038
H	-3.499099	6.041737	11.933034

H	-4.891227	7.112570	12.293642
H	-5.145596	5.361154	12.063064
H	-6.818392	7.718531	10.469986
H	-6.833392	7.092125	8.793634
H	-7.160046	5.991942	10.165911
C	-2.990625	12.414419	3.906939
C	-3.201497	9.691792	3.107062
C	-0.792515	11.262012	2.438883
P	0.735552	10.539134	2.715322
H	3.425423	7.725062	6.076042
H	2.396981	7.086641	4.756455
H	3.596106	8.356778	4.414186
H	2.026649	11.403983	6.605732
H	3.227299	10.180042	7.140051
H	3.395027	10.973026	5.545968
H	-3.840734	12.226405	4.573467
H	-2.386027	13.233100	4.310937
H	-3.376057	12.714343	2.923218
H	-2.689062	8.747607	2.892768
H	-3.986247	9.511206	3.850882
H	-3.659139	10.063546	2.179651
H	-1.086969	11.685787	1.480984
C	1.237254	9.374379	1.367159
C	2.132855	11.754810	2.637458
H	2.237915	8.966312	1.561161
H	0.510027	8.556500	1.336779
H	1.245390	9.889870	0.397837
H	1.975339	12.503003	3.420995
H	3.098303	11.254097	2.792064
H	2.148150	12.255646	1.660506

***trans*-5^{Me}**

Ni	-3.447788	-3.755352	19.981523
P	-2.936084	-3.140970	22.463704
P	-4.931933	-5.250896	19.356697
P	-2.458550	-3.287394	18.097600
C	-2.363137	-2.281997	21.014890
C	-4.249152	-3.900434	21.759621
C	-1.487770	-4.157486	23.014859
C	-3.264304	-2.183704	24.018690
C	-6.121582	-4.470288	18.152122
C	-5.810575	-5.879523	20.722571
C	-4.402278	-6.735058	18.370312
C	-3.028040	-1.658712	17.537023
C	-2.593871	-4.451734	16.656016
C	-0.619144	-3.166480	18.184164
P	-2.932623	-0.653314	20.454312
H	-1.280095	-2.350491	20.885777
P	-5.359082	-5.135410	22.192942
H	-1.810641	-4.857224	23.794955
H	-1.129733	-4.727418	22.151142
H	-0.677969	-3.528286	23.408041
H	-2.397464	-1.577196	24.308584
H	-4.137085	-1.538683	23.880131
H	-3.482387	-2.899467	24.823307
H	-6.596977	-3.618850	18.650823
H	-5.601473	-4.113415	17.254089
H	-6.898919	-5.189313	17.858673
H	-6.580105	-6.643475	20.639531
H	-4.144501	-6.483048	17.337718
H	-3.540699	-7.203640	18.858337
H	-5.231799	-7.454627	18.363609
Ni	-1.943386	-0.185357	18.570389
P	-2.455098	-0.799738	16.088208
H	-4.111081	-1.590219	17.666139
H	-2.243675	-5.442674	16.964125
H	-3.634981	-4.534948	16.329625
H	-1.982122	-4.103215	15.818522
H	-0.336902	-2.483782	18.988990
H	-0.203597	-4.164171	18.374742
H	-0.222380	-2.755540	17.249079
C	-2.797298	0.511027	21.895895
C	-4.772029	-0.774224	20.367750
C	-4.679599	-6.325811	23.443369
C	-6.799550	-4.456041	23.132326
P	-0.459231	1.310175	19.195217
C	-1.142031	-0.040269	16.792288
C	-3.903417	0.216772	15.537055
C	-2.126877	-1.757003	14.533221
H	-3.409045	0.162511	22.733391
H	-1.756187	0.594241	22.222284
H	-3.147493	1.501967	21.587784
H	-5.054273	-1.456923	19.562925
H	-5.168794	-1.185161	21.302835
H	-5.187573	0.223468	20.177169
H	-3.779945	-6.784612	23.020190

H	-4.424530	-5.808215	24.378257
H	-5.413143	-7.112025	23.665882
H	-6.468249	-4.015881	24.081866
H	-7.271718	-3.683908	22.516468
H	-7.528504	-5.249589	23.342575
C	0.730411	0.529558	20.399791
C	0.419419	1.938795	17.829343
C	-0.988876	2.794341	20.181601
P	-0.032097	1.194704	16.358968
H	-4.713216	-0.412433	15.143877
H	-4.261454	0.786704	16.400772
H	-3.580552	0.916510	14.756957
H	-1.254093	-2.402022	14.671779
H	-2.993715	-2.363514	14.243328
H	-1.908797	-1.041239	13.728604
H	0.210299	0.172686	21.297823
H	1.205800	-0.321884	19.901088
H	1.507754	1.248576	20.693241
H	1.188939	2.702757	17.912381
H	-1.850450	3.262929	19.693575
H	-1.246657	2.542332	21.214195
H	-0.159350	3.513904	20.188307
C	-0.711587	2.385126	15.108564
C	1.408355	0.515335	15.419560
H	-0.966668	1.867543	14.173672
H	-1.611234	2.843925	15.531760
H	0.021959	3.171339	14.886055
H	1.880524	-0.256809	16.035402
H	1.077038	0.075189	14.470018
H	2.137312	1.308880	15.209311

***cis*-6^{Me}**

Ni	-2.025679	0.597417	-0.549669
P	-0.263571	1.865515	-0.681784
P	-2.800632	-1.615865	-1.699488
P	-3.394035	1.949829	0.434266
C	-3.580286	-0.641854	-0.572033
C	-1.150138	-0.989772	-1.517856
C	1.154263	1.041668	-1.434796
C	-0.583680	3.400430	-1.683882
C	0.300901	2.524099	0.940198
C	-3.063082	-3.444198	-1.625500
C	-3.277748	-1.259842	-3.440041
C	-2.951913	3.346384	1.544565
C	-4.487337	2.761291	-0.816086
C	-4.599101	0.973936	1.459236
P	-4.656268	-0.699339	0.714996
P	0.110873	-1.704725	-0.420074
H	-0.692770	-0.716429	-2.472711
Ni	1.785511	-0.363510	-0.084820
P	2.817154	1.661294	-1.367362
H	0.893522	0.621344	-2.408987
H	-0.826659	3.112484	-2.713192
H	-1.439578	3.941520	-1.263141
H	0.289150	4.063677	-1.693108
H	-0.117585	3.525110	1.093195
H	-0.070925	1.861212	1.731195
H	1.394807	2.553461	0.978360
H	-2.508796	-3.940432	-2.431098
H	-2.735050	-3.846173	-0.663701
H	-4.134897	-3.647800	-1.752242
H	-4.341252	-1.485269	-3.582241
H	-3.109940	-0.193414	-3.621901
H	-2.679029	-1.856314	-4.139918
H	-2.385307	2.933683	2.386486
H	-2.337173	4.068275	0.995842
H	-3.858823	3.849479	1.904329
H	-3.886931	3.419459	-1.454528
H	-4.930861	1.980201	-1.441757
H	-5.276363	3.351462	-0.331616
H	-4.154368	0.895739	2.460959
H	-5.589743	1.443702	1.506388
C	-6.409110	-1.042505	0.264295
C	-4.320580	-1.872715	2.079865
C	-0.811008	-2.211446	1.081060
C	0.620999	-3.294608	-1.202260
P	2.676237	-1.386337	1.593643
C	3.243815	1.002695	0.129248
C	3.674713	1.029943	-2.858859
C	2.998212	3.493215	-1.527834
H	-6.745046	-0.300693	-0.467989
H	-6.471960	-2.039663	-0.188049
H	-7.056506	-1.013299	1.149067
H	-4.240142	-2.890307	1.679420
H	-3.376044	-1.564936	2.547144
H	-5.124961	-1.837087	2.825743

H	-1.148769	-1.316020	1.620364
H	-1.673918	-2.839719	0.839622
H	-0.144866	-2.776005	1.739208
H	-0.249591	-3.934723	-1.393443
H	1.160014	-3.077126	-2.129509
H	1.331035	-3.806962	-0.546856
C	2.030840	-0.742795	3.192157
C	4.498532	-1.012025	1.648739
C	2.725256	-3.214497	1.801373
P	4.741095	0.580460	0.786663
H	3.700572	-0.066721	-2.790065
H	3.153067	1.358194	-3.767191
H	4.702107	1.412143	-2.880456
H	2.620985	3.843981	-2.496913
H	2.449708	3.982942	-0.717254
H	4.061811	3.754294	-1.442919
H	2.241443	0.331293	3.234770
H	0.940091	-0.853721	3.236563
H	2.497659	-1.247174	4.048807
H	4.910313	-1.024485	2.665937
H	4.970521	-1.782659	1.026713
H	1.718990	-3.631450	1.894320
H	3.213200	-3.615986	0.905417
H	3.300974	-3.475699	2.698678
C	6.158700	0.350359	-0.349914
C	5.367827	1.767270	2.047127
H	5.877975	-0.455247	-1.041388
H	6.344766	1.281685	-0.898201
H	7.062920	0.075688	0.207920
H	5.516537	2.744546	1.572747
H	4.615801	1.873608	2.836130
H	6.317257	1.427982	2.480014
Cl	-1.716622	0.446448	3.215420
Cl	4.021395	-2.358434	-1.480874

7^{Me}

Ni	0.875232	0.007883	-0.007592
P	0.931393	-2.203042	-0.169116
P	0.889370	2.214983	0.169822
C	-1.014957	-0.007056	-0.020575
C	2.057662	-2.976497	1.092209
C	1.738834	-2.807191	-1.730431
C	-0.677117	-2.800128	-0.009028
C	2.016155	3.013951	-1.074620
C	1.676380	2.813635	1.743773
C	-0.725962	2.790469	0.001427
P	-1.845013	1.509230	-0.207501
P	-1.815101	-1.534883	0.196511
H	3.094422	-2.642855	0.950005
H	1.719814	-2.690816	2.093807
H	2.028062	-4.071650	1.003559
H	1.178293	-2.415240	-2.585433
H	2.781057	-2.466010	-1.792982
H	1.723212	-3.905654	-1.763958
H	-0.948216	-3.846474	0.105510
H	3.055605	2.691291	-0.926501
H	1.689995	2.733532	-2.081541
H	1.972760	4.107776	-0.976149
H	1.115223	2.404572	2.590301
H	2.722751	2.486411	1.810635
H	1.645057	3.911363	1.788880
H	-1.013489	3.834126	-0.095411
C	-2.718873	1.659465	-1.835482
C	-3.288471	1.656596	0.943346
C	-2.675004	-1.690549	1.832189
C	-3.263352	-1.714821	-0.943832
H	-1.973638	1.522579	-2.625712
H	-3.506478	0.905038	-1.942418
H	-3.164862	2.659054	-1.927060
H	-4.040522	0.884995	0.738867
H	-2.929488	1.558879	1.972197
H	-3.754680	2.641319	0.811082
H	-1.926951	-1.533946	2.616169
H	-3.477332	-0.952106	1.941207
H	-3.099382	-2.698577	1.933774
H	-4.030956	-0.958736	-0.738340
H	-2.912282	-1.614302	-1.975150
H	-3.707384	-2.708671	-0.804051

***trans*-8^{Me}**

Ni	-3.911916	-3.650354	19.862321
P	-2.936658	-3.466810	22.251409
P	-4.592434	-5.720449	19.440938
P	-3.040010	-3.194207	17.931412
C	-2.391248	-2.579294	20.829339
C	-4.632232	-3.693595	21.827328
C	-2.030470	-5.043960	22.318738
C	-2.693463	-2.741312	23.917352
C	-6.123507	-5.978444	18.456083
C	-5.060667	-6.444115	21.114641
C	-3.462728	-7.031613	18.800677
C	-3.012428	-1.388666	17.764005
C	-4.038247	-3.866304	16.537241
C	-1.352467	-3.797975	17.567685
P	-2.363663	-0.773752	20.661938
H	-1.400968	-2.925939	20.517916
P	-5.660711	-5.085664	22.165219
H	-2.090519	-5.531053	21.342708
H	-0.982050	-4.827652	22.552290
H	-2.434588	-5.695205	23.101562
H	-3.257430	-1.807346	24.007881
H	-3.059522	-3.447552	24.673396
H	-1.630108	-2.543192	24.095467
H	-6.854193	-5.209110	18.721444
H	-5.884892	-5.851689	17.395836
H	-6.532714	-6.983594	18.612145
H	-5.799257	-7.252267	21.046213
H	-4.152584	-6.848649	21.578679
H	-3.187376	-6.790706	17.768107
H	-2.547195	-7.066664	19.401670
H	-3.943059	-8.017556	18.812280
Ni	-1.491769	-0.317587	18.731031
P	-2.467024	-0.501147	16.341936
H	-4.002709	-1.042022	18.075432
H	-3.984480	-4.960254	16.548111
H	-5.075833	-3.548479	16.672837
H	-3.654113	-3.519097	15.574073
H	-0.634349	-3.344180	18.259295
H	-1.324937	-4.888850	17.661217
H	-1.071181	-3.537642	16.538673
C	-1.365417	-0.101666	22.056107
C	-4.051204	-0.169982	21.025675
C	-5.681915	-5.666936	23.891629
C	-7.346748	-4.643603	21.690084
P	-0.811306	1.752521	19.152424
C	-0.771456	-0.274316	16.766021
C	-3.373249	1.075980	16.274592
C	-2.710187	-1.226672	14.676001
H	-1.749535	-0.448893	23.019273
H	-0.327829	-0.419480	21.920494
H	-1.419193	0.992283	22.045256
H	-4.769329	-0.623798	20.334087
H	-4.332471	-0.430286	22.054700
H	-4.078740	0.920890	20.932111

H	-4.673944	-5.965888	24.199000
H	-6.033184	-4.857163	24.540866
H	-6.355656	-6.525669	23.994275
H	-7.757663	-3.955233	22.437046
H	-7.309766	-4.131170	20.720541
H	-7.971514	-5.542068	21.643217
C	0.719776	2.010536	20.137263
C	-0.343102	2.476212	17.478725
C	-1.941030	3.063653	19.792716
P	0.256984	1.117783	16.428142
H	-4.421673	0.859639	16.041084
H	-3.313181	1.563102	17.250607
H	-2.969175	1.727213	15.491736
H	-2.146210	-2.160634	14.585498
H	-3.773537	-1.424805	14.497872
H	-2.344122	-0.520442	13.919952
H	0.481173	1.883792	21.197514
H	1.450460	1.241200	19.871902
H	1.128979	3.015685	19.981187
H	0.395463	3.284387	17.547156
H	-1.251197	2.880719	17.014687
H	-2.856579	3.098683	19.191746
H	-2.216350	2.822735	20.825292
H	-1.460724	4.049608	19.781105
C	0.278185	1.699069	14.701736
C	1.943029	0.675760	16.903284
H	0.629440	0.889297	14.052491
H	-0.729783	1.998038	14.394373
H	0.951938	2.557794	14.599095
H	1.906046	0.163271	17.872798
H	2.353986	-0.012550	16.156290
H	2.567761	1.574246	16.950216
H	-0.197952	-1.203200	16.701456
H	-5.205706	-2.764693	21.891892
Cl	0.609381	-1.513691	19.475935
Cl	-6.013060	-2.454236	19.117391

2-2-2

C	5.264874000	-0.471342000	-0.183858000
P	4.024924000	0.809909000	-0.696983000
H	6.250318000	-0.135832000	-0.529313000
H	5.299821000	-0.602567000	0.904831000
H	5.059303000	-1.433389000	-0.666778000
C	4.450611000	2.192963000	0.461204000
C	2.482877000	0.132339000	0.259447000
H	4.535880000	1.856714000	1.501579000
H	5.416984000	2.602111000	0.142261000
H	3.707163000	2.994547000	0.384134000
P	1.370808000	-0.697494000	-0.888981000
H	2.766875000	-0.556490000	1.066784000
H	1.954473000	0.988533000	0.694957000
C	0.694747000	0.495776000	-2.066310000
C	2.249355000	-1.994860000	-1.792078000
C	-0.000829000	-1.577305000	-0.015975000
H	0.197063000	1.315458000	-1.538252000
H	1.533403000	0.905539000	-2.641679000
H	-0.010863000	0.003845000	-2.744617000
H	3.069810000	-1.528603000	-2.349710000
H	2.654978000	-2.731443000	-1.089779000
H	1.570105000	-2.490427000	-2.494694000
P	-1.368475000	-0.700854000	0.866561000
H	0.477615000	-2.239625000	0.719554000
H	-0.482412000	-2.229218000	-0.758743000
C	-0.687861000	0.479838000	2.053921000
C	-2.249867000	-2.003542000	1.759260000
C	-2.479122000	0.142795000	-0.273245000
H	0.015849000	-0.020276000	2.728224000
H	-0.187291000	1.302246000	1.532909000
H	-1.525153000	0.887696000	2.632646000
H	-2.658000000	-2.733214000	1.051218000
H	-1.570972000	-2.506543000	2.456926000
H	-3.068506000	-1.540001000	2.321792000
P	-4.016788000	0.817895000	0.691900000
H	-2.766949000	-0.538300000	-1.085735000
H	-1.948148000	1.000538000	-0.702557000
C	-5.263370000	-0.451936000	0.166720000
C	-4.437594000	2.215171000	-0.450899000
H	-5.302105000	-0.569282000	-0.923439000
H	-5.059810000	-1.420715000	0.636881000
H	-6.246466000	-0.117132000	0.519455000
H	-3.690354000	3.012486000	-0.366586000
H	-4.525990000	1.890140000	-1.494563000
H	-5.401608000	2.625353000	-0.126191000

2-1-2

C	-5.309071000	-0.717672000	-0.457123000
P	-4.221834000	0.044836000	0.847498000
H	-6.319412000	-0.827064000	-0.045594000
H	-5.360441000	-0.096951000	-1.361261000
H	-4.948586000	-1.717058000	-0.724522000
C	-4.941503000	1.760172000	0.888342000
C	-2.687081000	0.419600000	-0.206019000
H	-5.027938000	2.197099000	-0.114771000
H	-5.939259000	1.708333000	1.339994000
H	-4.319250000	2.408494000	1.516212000
P	-1.333947000	-0.816438000	-0.107394000
H	-2.942989000	0.553279000	-1.266288000
H	-2.258313000	1.367576000	0.146465000
C	-0.840160000	-0.819373000	1.646347000
C	-2.081233000	-2.431806000	-0.474380000
C	-0.005171000	-0.556111000	-1.160333000
H	-0.360457000	0.132699000	1.899229000
H	-1.733135000	-0.937847000	2.270155000
H	-0.137612000	-1.638198000	1.828167000
H	-2.933868000	-2.601504000	0.191606000
H	-2.425363000	-2.443765000	-1.514382000
H	-1.333696000	-3.218031000	-0.331992000
P	1.334629000	0.489698000	-0.916901000
H	-0.061847000	-1.033331000	-2.134931000
C	0.887413000	2.181293000	-0.394224000
C	2.221144000	0.633464000	-2.495776000
C	2.539165000	-0.068600000	0.346930000
H	0.278672000	2.651509000	-1.173140000
H	0.306729000	2.136661000	0.534413000
H	1.795708000	2.767965000	-0.214861000
H	2.569010000	-0.356032000	-2.809849000
H	1.543324000	1.038593000	-3.253601000
H	3.079321000	1.302135000	-2.373746000
P	4.134711000	0.955824000	0.448108000
H	2.749135000	-1.131885000	0.169113000
H	2.028904000	0.009244000	1.316006000
C	5.235053000	-0.103400000	-0.616389000
C	4.699230000	0.394366000	2.130144000
H	5.195237000	-1.159735000	-0.319741000
H	4.954461000	-0.013372000	-1.671355000
H	6.266241000	0.254600000	-0.513521000
H	4.047751000	0.820910000	2.901770000
H	4.705064000	-0.699650000	2.220041000
H	5.715269000	0.769873000	2.300055000

2-2-1

C	1.513654000	-0.909141000	-2.343901000
P	2.582139000	-0.772162000	-0.813482000
H	2.137887000	-0.751287000	-3.232046000
H	1.036390000	-1.895869000	-2.422853000
H	0.738649000	-0.133074000	-2.340691000
C	3.767768000	-2.159387000	-1.188217000
C	1.543311000	-1.467525000	0.480375000
H	3.235577000	-3.101526000	-1.375367000
H	4.364804000	-1.904234000	-2.072637000
H	4.444573000	-2.295983000	-0.337547000
P	1.346126000	-0.725800000	1.969787000
H	1.047865000	-2.435592000	0.370806000
C	1.149142000	-1.890448000	3.359225000
C	2.665817000	0.454889000	2.395320000
C	-0.234402000	0.350469000	2.255999000
H	0.364973000	-2.614573000	3.110653000
H	2.093446000	-2.426523000	3.498634000
H	0.878646000	-1.364919000	4.282336000
H	3.593989000	-0.105008000	2.547584000
H	2.820299000	1.147800000	1.563364000
H	2.411288000	1.003932000	3.308321000
P	-0.846175000	1.199552000	0.775347000
H	-0.061893000	1.088551000	3.050540000
H	-1.038860000	-0.319457000	2.587011000
C	0.471729000	2.153681000	-0.008072000
C	-2.154909000	2.356791000	1.264329000
C	-1.505615000	-0.023847000	-0.374631000
H	0.829217000	2.920977000	0.687653000
H	1.302237000	1.490640000	-0.289615000
H	0.065990000	2.630411000	-0.907198000
H	-2.984510000	1.812777000	1.727965000
H	-1.755811000	3.087550000	1.976019000
H	-2.515925000	2.880410000	0.372170000
P	-2.221185000	0.719491000	-1.971088000
H	-2.245041000	-0.637792000	0.159324000
H	-0.646835000	-0.663566000	-0.622058000
C	-4.013145000	0.829495000	-1.477772000
C	-2.262367000	-0.846769000	-2.968862000
H	-4.379858000	-0.111722000	-1.047460000
H	-4.171314000	1.642484000	-0.760602000
H	-4.601431000	1.059584000	-2.373993000
H	-1.240304000	-1.147625000	-3.221136000
H	-2.764243000	-1.662978000	-2.434120000
H	-2.803392000	-0.645776000	-3.900917000

2-1-1

C	-4.344678000	0.689660000	-0.249316000
P	-2.818053000	1.469850000	0.489940000
H	-5.182447000	1.393513000	-0.172438000
H	-4.192825000	0.430626000	-1.306261000
H	-4.612064000	-0.217100000	0.304668000
C	-2.503574000	2.775433000	-0.803989000
C	-1.532384000	0.221582000	-0.075601000
H	-2.493837000	2.352173000	-1.817423000
H	-3.286978000	3.540902000	-0.743108000
H	-1.537492000	3.254787000	-0.608126000
P	-1.085470000	-1.121904000	1.094887000
H	-1.825488000	-0.248456000	-1.023926000
H	-0.575690000	0.736653000	-0.241903000
C	-0.575538000	-0.218013000	2.606999000
C	-2.631160000	-1.973534000	1.570359000
C	0.000319000	-2.267223000	0.465345000
H	0.335879000	0.337763000	2.367463000
H	-1.359504000	0.477006000	2.930758000
H	-0.358462000	-0.946526000	3.395918000
H	-3.318028000	-1.263288000	2.042330000
H	-3.099800000	-2.407632000	0.681554000
H	-2.394259000	-2.773456000	2.280113000
P	1.426789000	-1.750347000	-0.401030000
H	-0.269212000	-3.317031000	0.554985000
C	1.147674000	-1.708738000	-2.220332000
C	2.594808000	-3.182846000	-0.251788000
C	1.963391000	-0.217073000	0.122476000
H	0.756440000	-2.684294000	-2.532382000
H	0.419740000	-0.927528000	-2.458724000
H	2.080127000	-1.489545000	-2.751817000
H	2.912984000	-3.267837000	0.793055000
H	2.114205000	-4.121718000	-0.558735000
H	3.472501000	-2.999081000	-0.882690000
P	2.633286000	1.029132000	-0.958848000
H	2.145669000	-0.155380000	1.199731000
C	4.392068000	1.274958000	-0.341110000
C	1.924792000	2.604057000	-0.213536000
H	4.416634000	1.401599000	0.751564000
H	4.991272000	0.394655000	-0.604572000
H	4.845983000	2.159075000	-0.810460000
H	0.847830000	2.653820000	-0.417514000
H	2.078003000	2.638146000	0.875616000
H	2.400950000	3.485761000	-0.664034000

1-2-1

C	-3.966200000	-1.957632000	0.620799000
P	-2.211728000	-1.564901000	0.090334000
H	-4.132064000	-3.043104000	0.589918000
H	-4.168647000	-1.599609000	1.640960000
H	-4.670926000	-1.475778000	-0.067431000
C	-1.336973000	-2.401983000	1.520433000
C	-2.076092000	0.173783000	0.482007000
H	-1.677396000	-2.006055000	2.488955000
H	-1.537559000	-3.481832000	1.494294000
H	-0.254193000	-2.251335000	1.427768000
P	-1.478271000	1.316441000	-0.597805000
H	-2.413737000	0.566858000	1.445955000
C	-0.939754000	0.604113000	-2.179910000
C	-2.645347000	2.678823000	-1.040965000
C	-0.036044000	2.332835000	0.005226000
H	-0.053680000	-0.008987000	-1.997457000
H	-1.744255000	-0.013411000	-2.589615000
H	-0.694518000	1.418448000	-2.871466000
H	-3.497934000	2.242351000	-1.573542000
H	-3.012489000	3.144634000	-0.118620000
H	-2.165968000	3.443312000	-1.665931000
P	1.438622000	1.361491000	0.604997000
H	-0.398042000	2.976807000	0.819421000
H	0.305032000	2.992332000	-0.805678000
C	0.923188000	0.626633000	2.184495000
C	2.559649000	2.760367000	1.053665000
C	2.072000000	0.242707000	-0.479381000
H	0.648170000	1.430029000	2.877681000
H	0.059706000	-0.017147000	1.999258000
H	1.748421000	0.037107000	2.594197000
H	2.914189000	3.238723000	0.132808000
H	2.053407000	3.508321000	1.677563000
H	3.424328000	2.351502000	1.588688000
P	2.274417000	-1.489652000	-0.089962000
H	2.393563000	0.649430000	-1.443138000
C	4.043407000	-1.815575000	-0.618860000
C	1.432665000	-2.355267000	-1.522521000
H	4.234192000	-1.448467000	-1.638081000
H	4.728837000	-1.309111000	0.071255000
H	4.249807000	-2.894150000	-0.589608000
H	0.345124000	-2.245645000	-1.429579000
H	1.757595000	-1.943402000	-2.489677000
H	1.673770000	-3.426825000	-1.499759000

2-0-2

C	5.143258000	0.019338000	0.618367000
P	4.096022000	-0.445716000	-0.854340000
H	6.197800000	-0.172273000	0.384787000
H	5.022230000	1.080261000	0.877621000
H	4.867201000	-0.591868000	1.483468000
C	4.638151000	0.915952000	-2.014584000
C	2.451183000	0.285467000	-0.315444000
H	4.553900000	1.906098000	-1.545793000
H	5.681594000	0.749856000	-2.311005000
H	4.019125000	0.895264000	-2.919618000
P	1.255770000	-0.779835000	0.649859000
H	2.604903000	1.201951000	0.271358000
H	1.906667000	0.571142000	-1.226094000
C	0.913575000	-2.132719000	-0.572638000
C	2.303835000	-1.636704000	1.890901000
C	-0.002339000	-0.000492000	1.370788000
H	0.363468000	-1.713184000	-1.423468000
H	1.843222000	-2.590401000	-0.934330000
H	0.287059000	-2.891010000	-0.089944000
H	3.137233000	-2.167154000	1.415219000
H	2.685132000	-0.899395000	2.604998000
H	1.670543000	-2.349257000	2.430290000
P	-1.258018000	0.779423000	0.646268000
C	-0.911805000	2.133049000	-0.574274000
C	-2.310160000	1.635747000	1.884248000
C	-2.450268000	-0.285275000	-0.323532000
H	-0.286604000	2.890859000	-0.089134000
H	-0.359218000	1.713967000	-1.423707000
H	-1.840238000	2.591199000	-0.938491000
H	-2.693876000	0.898187000	2.596790000
H	-1.678706000	2.348134000	2.426006000
H	-3.141922000	2.166382000	1.405919000
P	-4.092876000	0.446352000	-0.868562000
H	-2.606380000	-1.201842000	0.262492000
H	-1.902396000	-0.570911000	-1.232176000
C	-5.146023000	-0.019865000	0.599568000
C	-4.630226000	-0.914401000	-2.032129000
H	-5.026357000	-1.081093000	0.858180000
H	-4.873019000	0.590343000	1.466347000
H	-6.199584000	0.172402000	0.362146000
H	-4.007527000	-0.892866000	-2.934623000
H	-4.547761000	-1.904954000	-1.563878000
H	-5.672469000	-0.748157000	-2.332659000

2-2-0

C	-3.246686000	1.290204000	-1.712471000
P	-2.620103000	1.899720000	-0.043714000
H	-3.642535000	2.137586000	-2.288835000
H	-2.462171000	0.799945000	-2.304595000
H	-4.063243000	0.577495000	-1.546464000
C	-1.222826000	2.999058000	-0.633467000
C	-1.853458000	0.633593000	0.845696000
H	-0.492046000	2.454725000	-1.246034000
H	-1.634133000	3.827901000	-1.224247000
H	-0.710852000	3.413152000	0.242177000
P	-1.881244000	-0.987294000	0.895277000
C	-1.410416000	-1.747620000	2.497528000
C	-3.240081000	-2.063919000	0.239222000
C	0.177796000	-2.642884000	-0.267417000
H	-0.512375000	-1.244975000	2.869131000
H	-2.215781000	-1.623927000	3.232518000
H	-1.201593000	-2.813116000	2.350678000
H	-4.123807000	-2.007366000	0.887984000
H	-3.509643000	-1.719054000	-0.763850000
H	-2.892081000	-3.102368000	0.183756000
P	1.194765000	-1.393909000	-0.828688000
H	-0.341839000	-3.211492000	-1.038086000
H	0.542732000	-3.224714000	0.577858000
C	0.307481000	-0.408720000	-2.072933000
C	2.811623000	-1.796119000	-1.635163000
C	1.612742000	-0.260723000	0.539904000
H	-0.021129000	-1.063582000	-2.887478000
H	-0.563666000	0.031997000	-1.578766000
H	0.955323000	0.380697000	-2.466556000
H	3.437369000	-2.353145000	-0.928284000
H	2.620963000	-2.430165000	-2.508787000
H	3.336705000	-0.885257000	-1.952095000
P	2.693546000	1.214614000	0.108049000
H	2.044534000	-0.849483000	1.361695000
H	0.645980000	0.145328000	0.877871000
C	4.358760000	0.571192000	0.654167000
C	2.266402000	2.258246000	1.590048000
H	4.311528000	0.138373000	1.663099000
H	4.716972000	-0.191519000	-0.046472000
H	5.080745000	1.397024000	0.655840000
H	1.208542000	2.537675000	1.529567000
H	2.437954000	1.716895000	2.530208000
H	2.875072000	3.170574000	1.583629000

78

2-1-0

C	3.712258000	6.636720000	6.949356000
P	5.494234000	6.161590000	7.282244000
H	3.042468000	6.032878000	7.576717000
H	3.536836000	7.701363000	7.161777000
H	3.467503000	6.443072000	5.898692000
C	5.635628000	6.830182000	9.022637000
C	6.381389000	7.547025000	6.403994000
H	5.297048000	7.874178000	9.079604000
H	5.036739000	6.218323000	9.710815000
H	6.686589000	6.790710000	9.331827000
P	6.915757000	7.320638000	4.648979000
H	5.797487000	8.477912000	6.442338000
H	7.348200000	7.746958000	6.894220000
C	7.940300000	5.793926000	4.694486000
C	5.394150000	6.777259000	3.757754000
C	7.507375000	8.694903000	3.867009000
H	8.898212000	6.111326000	5.126355000
H	7.466790000	5.012681000	5.305384000
H	8.078783000	5.439513000	3.664369000
H	5.024702000	5.837492000	4.184275000
H	4.620755000	7.548441000	3.841603000
H	5.635930000	6.623775000	2.699811000
P	8.936991000	9.447246000	4.605627000
H	7.052401000	8.987372000	2.919941000
C	8.503800000	11.266730000	4.833221000
C	10.138858000	9.653191000	3.164902000
C	9.432012000	8.546206000	5.906604000
H	8.209078000	11.745772000	3.887156000
H	7.674838000	11.329475000	5.547906000
H	9.374351000	11.786051000	5.255587000
H	10.512457000	8.655292000	2.905177000
H	9.670249000	10.112642000	2.279305000
H	10.983377000	10.275050000	3.493969000
P	10.230639000	9.258330000	7.285242000
C	11.802861000	8.208492000	7.521024000
C	9.341622000	8.454292000	8.769198000
H	11.553128000	7.135827000	7.452402000
H	12.513593000	8.448335000	6.718158000
H	12.282780000	8.413365000	8.493139000
H	8.337261000	8.889189000	8.868618000
H	9.239826000	7.366921000	8.602270000
H	9.890946000	8.624360000	9.709404000

2-0-1

C	4.598700000	1.091031000	1.071685000
P	3.179231000	1.260005000	-0.179418000
H	5.352217000	1.884192000	0.938927000
H	4.215521000	1.136150000	2.104188000
H	5.084411000	0.117255000	0.925950000
C	2.572013000	2.921540000	0.490726000
C	1.935719000	0.134197000	0.365780000
H	2.296860000	2.835631000	1.554335000
H	3.345522000	3.698661000	0.386369000
H	1.682037000	3.228784000	-0.073311000
P	1.422020000	-1.276528000	-0.525436000
H	1.726002000	0.066414000	1.438725000
C	1.330079000	-0.740811000	-2.307946000
C	2.787165000	-2.541765000	-0.683934000
C	0.037904000	-2.118480000	-0.014570000
H	0.502670000	-0.029669000	-2.409896000
H	2.263028000	-0.248671000	-2.613926000
H	1.135229000	-1.620251000	-2.935298000
H	3.685114000	-2.069826000	-1.106023000
H	3.014202000	-2.920353000	0.319951000
H	2.467369000	-3.380220000	-1.318185000
P	-1.212915000	-1.257521000	0.608276000
C	-1.118667000	-0.585931000	2.348637000
C	-2.759536000	-2.265810000	0.707019000
C	-1.747007000	0.307795000	-0.303339000
H	-0.898918000	-1.420130000	3.026025000
H	-0.284184000	0.123656000	2.377477000
H	-2.044588000	-0.079848000	2.657420000
H	-3.084628000	-2.519266000	-0.308290000
H	-2.517146000	-3.194020000	1.237422000
H	-3.560900000	-1.733002000	1.235984000
P	-3.264811000	1.272574000	0.183860000
H	-1.797220000	0.042564000	-1.369739000
H	-0.866265000	0.956163000	-0.171986000
C	-4.561807000	0.359779000	-0.811830000
C	-3.060428000	2.741274000	-0.964574000
H	-4.236548000	0.221147000	-1.853526000
H	-4.745784000	-0.624586000	-0.368753000
H	-5.501710000	0.927694000	-0.802686000
H	-2.207320000	3.343160000	-0.628547000
H	-2.874275000	2.413403000	-1.997469000
H	-3.960619000	3.371288000	-0.943862000

1-1-1

C	4.847801000	-0.861875000	0.037237000
P	3.115279000	-1.046748000	0.776571000
H	5.503120000	-1.688911000	0.352371000
H	4.804439000	-0.845225000	-1.063416000
H	5.284642000	0.084410000	0.381982000
C	2.694209000	-2.641272000	-0.139272000
C	2.152626000	0.165312000	-0.075170000
H	2.793463000	-2.505948000	-1.227847000
H	3.352768000	-3.464426000	0.177572000
H	1.654550000	-2.910211000	0.083402000
P	1.248042000	1.417969000	0.670000000
H	2.219686000	0.258513000	-1.162112000
C	0.666786000	0.801565000	2.311908000
C	2.235937000	2.914157000	1.195196000
C	-0.006593000	2.100619000	-0.303764000
H	-0.128118000	0.073921000	2.119116000
H	1.490560000	0.313056000	2.847775000
H	0.266829000	1.638238000	2.898445000
H	3.036208000	2.583652000	1.869101000
H	2.686200000	3.363197000	0.301910000
H	1.607212000	3.658661000	1.703786000
P	-1.242269000	1.164141000	-1.066906000
H	-0.005603000	3.175924000	-0.460700000
C	-0.639373000	0.144000000	-2.485317000
C	-2.245600000	2.451040000	-1.976979000
C	-2.137018000	0.141178000	-0.020682000
H	-0.233301000	0.803602000	-3.262577000
H	0.154419000	-0.504247000	-2.100694000
H	-1.453481000	-0.471595000	-2.888487000
H	-2.704538000	3.119559000	-1.238885000
H	-1.623436000	3.037466000	-2.667751000
H	-3.038986000	1.940388000	-2.536864000
P	-3.024940000	-1.305108000	-0.510480000
H	-2.216600000	0.517425000	1.002317000
C	-4.766418000	-1.025196000	0.173952000
C	-2.519392000	-2.579818000	0.786650000
H	-4.729135000	-0.704371000	1.227257000
H	-5.259445000	-0.237848000	-0.411035000
H	-5.368923000	-1.944433000	0.106360000
H	-1.464212000	-2.836838000	0.633586000
H	-2.633962000	-2.172982000	1.803698000
H	-3.126330000	-3.494141000	0.699147000

1-2-0

C	2.564250000	7.740101000	5.717880000
P	4.077011000	6.973685000	6.534337000
H	1.661440000	7.536511000	6.312312000
H	2.682367000	8.829678000	5.614363000
H	2.436683000	7.306095000	4.718637000
C	4.012519000	8.021020000	8.102733000
C	5.411891000	7.660314000	5.592456000
H	4.022659000	9.094443000	7.859278000
H	3.107603000	7.797993000	8.688037000
H	4.892887000	7.797107000	8.717728000
P	6.826647000	6.757560000	5.293950000
H	5.528229000	8.740792000	5.493502000
C	7.913092000	6.339532000	6.718786000
C	6.394914000	5.085051000	4.658339000
C	7.897979000	7.561656000	4.072659000
H	8.284658000	7.258642000	7.186492000
H	7.314259000	5.767998000	7.440425000
H	8.783348000	5.755086000	6.398325000
H	5.677269000	4.628688000	5.351179000
H	5.923220000	5.189556000	3.675584000
H	7.293009000	4.459828000	4.582802000
P	9.154950000	8.938356000	4.685312000
H	7.244950000	7.934527000	3.272807000
H	8.573071000	6.799805000	3.661309000
C	7.941070000	10.162068000	5.441528000
C	9.393221000	9.698471000	3.003908000
C	10.543107000	8.466504000	5.383529000
H	7.035583000	10.289570000	4.831833000
H	7.657409000	9.809198000	6.439235000
H	8.455348000	11.125554000	5.544606000
H	9.955496000	8.992458000	2.381869000
H	8.436978000	9.946531000	2.520232000
H	9.995714000	10.605971000	3.129658000
P	10.841507000	8.466817000	7.110636000
C	12.461479000	9.440509000	7.268757000
C	11.661319000	6.782511000	7.417883000
H	13.191089000	9.082105000	6.524566000
H	12.258547000	10.501909000	7.073265000
H	12.884938000	9.339427000	8.281245000
H	10.903847000	5.989815000	7.356298000
H	12.428117000	6.593252000	6.649252000
H	12.123227000	6.747006000	8.417569000

2-0-0

C	-4.499469000	0.542371000	-0.774433000
P	-3.143021000	1.219878000	0.340950000
H	-5.418018000	1.141048000	-0.670643000
H	-4.179552000	0.557109000	-1.828297000
H	-4.721183000	-0.494290000	-0.494315000
C	-2.907440000	2.852902000	-0.572584000
C	-1.681706000	0.283512000	-0.292454000
H	-2.752184000	2.680947000	-1.648510000
H	-3.777707000	3.514509000	-0.434575000
H	-2.014575000	3.350109000	-0.172967000
P	-1.147423000	-1.418779000	0.369250000
H	-1.748406000	0.177183000	-1.386906000
H	-0.740986000	0.840607000	-0.079974000
C	-1.047742000	-0.993344000	2.192306000
C	-2.725266000	-2.403417000	0.324906000
C	0.078207000	-2.178618000	-0.409273000
H	-0.164786000	-0.341732000	2.267646000
H	-1.946579000	-0.480328000	2.572614000
H	-0.872380000	-1.921723000	2.753777000
H	-3.526896000	-1.893890000	0.881011000
H	-3.027347000	-2.547681000	-0.720123000
H	-2.526777000	-3.386133000	0.772446000
P	1.574945000	-1.284133000	-0.458195000
C	2.188322000	-1.439297000	-2.249839000
C	2.872795000	-2.453383000	0.299485000
C	1.644435000	0.287151000	0.170082000
H	2.231705000	-2.491878000	-2.574214000
H	1.474139000	-0.896311000	-2.882745000
H	3.178941000	-0.967012000	-2.334165000
H	2.679294000	-2.490870000	1.379923000
H	2.801875000	-3.471418000	-0.119419000
H	3.879133000	-2.038866000	0.129219000
P	3.027727000	1.291996000	-0.102750000
C	3.588098000	1.878682000	1.647636000
C	2.285718000	3.017634000	-0.512891000
H	2.699905000	2.195285000	2.226218000
H	4.052433000	1.028703000	2.169488000
H	4.317090000	2.711361000	1.600346000
H	1.834287000	2.973952000	-1.514799000
H	1.487148000	3.250868000	0.216764000
H	3.049298000	3.818857000	-0.495919000

1-1-0

C	4.504270000	-1.364213000	-0.503872000
C	3.149398000	-0.766291000	-0.808083000
H	4.562768000	-2.417507000	-0.841699000
H	5.394287000	-0.858856000	-0.964000000
H	4.707700000	-1.384594000	0.579557000
P	2.456340000	0.560939000	0.011682000
H	2.752257000	-0.915231000	-1.812598000
C	3.026207000	0.368911000	1.807687000
C	3.239572000	2.278501000	-0.254297000
C	0.793173000	0.858721000	-0.238566000
H	2.569404000	-0.539980000	2.215877000
H	4.122529000	0.300595000	1.901395000
H	2.668179000	1.237579000	2.375542000
H	4.325787000	2.214700000	-0.090377000
H	3.045637000	2.583800000	-1.290185000
H	2.814432000	3.030363000	0.429089000
P	-0.597591000	-0.243919000	-0.095142000
H	0.497888000	1.906053000	-0.192999000
C	-0.078309000	-1.497281000	1.231550000
C	-0.453413000	-1.429639000	-1.563551000
C	-2.045621000	0.539259000	0.166676000
H	0.944473000	-1.869135000	1.055942000
H	-0.139149000	-0.990177000	2.203144000
H	-0.791228000	-2.335680000	1.220205000
H	-0.574010000	-0.838396000	-2.480001000
H	0.533882000	-1.912919000	-1.562471000
H	-1.258346000	-2.177417000	-1.509914000
P	-3.548131000	-0.177080000	-0.305332000
C	-4.625656000	1.337652000	-0.793051000
C	-4.543175000	-0.429086000	1.335035000
H	-4.515781000	2.126733000	-0.025849000
H	-4.257325000	1.735125000	-1.750425000
H	-5.693492000	1.068335000	-0.901576000
H	-4.104007000	-1.275046000	1.885251000
H	-4.449860000	0.476904000	1.963187000
H	-5.613970000	-0.643567000	1.147625000

1-0-1

C	5.343584000	0.237824000	-0.020485000
P	3.765269000	-0.557304000	-0.774029000
H	6.244879000	0.028784000	-0.625762000
H	5.223147000	1.331437000	0.067846000
H	5.491305000	-0.174130000	0.987472000
C	3.859921000	0.491317000	-2.363163000
C	2.408348000	0.103231000	0.101850000
H	3.804808000	1.565924000	-2.119560000
H	4.792289000	0.303200000	-2.924433000
H	3.001013000	0.239721000	-2.998914000
P	1.237361000	-0.817471000	1.057233000
H	2.338207000	1.182343000	0.268786000
C	0.746405000	-2.267518000	-0.036150000
C	2.198868000	-1.787726000	2.345315000
C	-0.000217000	-0.024071000	1.852397000
H	0.062831000	-1.881340000	-0.801377000
H	1.629811000	-2.715673000	-0.516556000
H	0.219130000	-3.019377000	0.569153000
H	3.032003000	-2.322175000	1.864840000
H	2.596050000	-1.066816000	3.071187000
H	1.537452000	-2.497016000	2.865234000
P	-1.231289000	0.787373000	1.065372000
C	-0.731160000	2.259585000	0.006789000
C	-2.200301000	1.731299000	2.367302000
C	-2.396518000	-0.110977000	0.082100000
H	-0.206569000	2.997062000	0.631759000
H	-0.043251000	1.888617000	-0.762056000
H	-1.610959000	2.719436000	-0.469156000
H	-2.606181000	0.995529000	3.073195000
H	-1.540631000	2.425973000	2.908657000
H	-3.027268000	2.279726000	1.891897000
P	-3.746173000	0.570180000	-0.789523000
H	-2.332835000	-1.193106000	0.231644000
C	-5.334319000	-0.221790000	-0.052028000
C	-3.841478000	-0.459233000	-2.390487000
H	-5.223496000	-1.317453000	0.022386000
H	-5.482411000	0.178122000	0.960724000
H	-6.231596000	0.003024000	-0.657683000
H	-2.978508000	-0.206372000	-3.020173000
H	-3.794629000	-1.536776000	-2.158531000
H	-4.770494000	-0.258385000	-2.952774000

0-2-0

C	5.298710000	0.138840000	-0.914505000
P	4.021057000	-0.333316000	0.440363000
H	6.327211000	-0.148670000	-0.627846000
H	5.026910000	-0.353493000	-1.864895000
H	5.267473000	1.227319000	-1.068495000
C	4.402791000	-2.192922000	0.293654000
C	2.464285000	-0.202077000	-0.331560000
H	4.198932000	-2.533665000	-0.736200000
H	5.453203000	-2.409052000	0.556024000
H	3.742924000	-2.745444000	0.976655000
P	1.440136000	1.031074000	0.035456000
C	1.209232000	1.603156000	1.825442000
C	1.812121000	2.739571000	-0.710721000
C	-0.322730000	0.843447000	-0.534532000
H	0.729674000	0.799620000	2.393400000
H	2.209634000	1.782083000	2.240552000
H	0.601935000	2.517712000	1.903143000
H	2.753771000	3.104610000	-0.274940000
H	1.955692000	2.604918000	-1.790353000
H	1.012059000	3.476702000	-0.531787000
P	-1.395352000	-0.713694000	-0.274607000
H	-0.335199000	1.000421000	-1.622331000
H	-0.899923000	1.667929000	-0.091096000
C	-0.834430000	-1.241785000	1.438118000
C	-0.454631000	-1.905618000	-1.319284000
C	-2.992929000	-0.606509000	-0.673260000
H	0.262939000	-1.273327000	1.495240000
H	-1.240919000	-0.537764000	2.174582000
H	-1.257129000	-2.235613000	1.635471000
H	-0.723432000	-1.716938000	-2.366153000
H	0.626186000	-1.757358000	-1.163288000
H	-0.763000000	-2.926587000	-1.055385000
P	-4.166625000	0.050393000	0.435361000
C	-5.706133000	-1.035528000	0.110665000
C	-4.921156000	1.553704000	-0.488588000
H	-5.859175000	-1.142957000	-0.978187000
H	-5.529049000	-2.034628000	0.534043000
H	-6.612126000	-0.604962000	0.573937000
H	-4.186573000	2.371808000	-0.492741000
H	-5.132383000	1.273405000	-1.536112000
H	-5.848667000	1.911418000	-0.004381000

10^{Me}

Ni	-0.007599000	-1.016766000	-0.042566000
P	2.129808000	-0.998869000	-0.131474000
P	-2.145123000	-0.966221000	-0.133941000
P	1.609021000	1.864765000	-0.053630000
P	-1.580361000	1.889378000	-0.049159000
B	0.007076000	0.975142000	-0.228820000
C	2.897556000	0.651761000	-0.543773000
C	-2.888159000	0.697340000	-0.539871000
H	3.864121000	0.814355000	-0.049952000
H	3.035427000	0.714542000	-1.629193000
H	-3.027561000	0.765777000	-1.624770000
H	-3.851096000	0.873155000	-0.043491000
C	-1.851175000	3.428849000	-1.045828000
H	-1.125794000	4.191661000	-0.738892000
H	-1.692115000	3.199757000	-2.104226000
H	-2.862123000	3.828316000	-0.895194000
C	-2.155973000	2.484822000	1.624487000
H	-3.166541000	2.916621000	1.596899000
H	-2.131275000	1.635109000	2.314706000
H	-1.451142000	3.241853000	1.989893000
C	-2.903207000	-2.091561000	-1.381184000
H	-2.542607000	-1.811633000	-2.377009000
H	-2.559724000	-3.106882000	-1.156486000
H	-4.000104000	-2.043679000	-1.354351000
C	-3.023310000	-1.458231000	1.413251000
H	-4.109820000	-1.515893000	1.265625000
H	-2.631740000	-2.438272000	1.706391000
H	-2.796422000	-0.740047000	2.208328000
C	2.874500000	-2.140642000	-1.371960000
H	3.971895000	-2.107361000	-1.343295000
H	2.516986000	-3.150153000	-1.143131000
H	2.519620000	-1.860793000	-2.369862000
C	2.998690000	-1.495976000	1.419422000
H	2.782143000	-0.770122000	2.210385000
H	2.592115000	-2.468410000	1.717462000
H	4.084330000	-1.570952000	1.273114000
C	1.902266000	3.397853000	-1.053801000
H	2.918538000	3.783735000	-0.903486000
H	1.740626000	3.168672000	-2.111811000
H	1.187114000	4.171102000	-0.749154000
C	2.196219000	2.454520000	1.617977000
H	1.504767000	3.224473000	1.981947000
H	2.157349000	1.607075000	2.310306000
H	3.214040000	2.868756000	1.588454000
Cl	-0.026365000	-3.307955000	0.321029000

10^{Me}+H^+

Ni	0.001072000	-0.936694000	-0.079415000
P	2.169019000	-0.989887000	-0.171802000
P	-2.166722000	-0.994454000	-0.171279000
P	1.639146000	1.880673000	-0.082644000
P	-1.643354000	1.877383000	-0.083464000
B	-0.001159000	1.065707000	-0.666411000
C	2.912257000	0.676970000	-0.600670000
C	-2.913593000	0.670523000	-0.601190000
H	3.892856000	0.864805000	-0.148351000
H	3.005606000	0.745867000	-1.691794000
H	-3.006602000	0.738614000	-1.692397000
H	-3.894822000	0.856321000	-0.149416000
C	-2.112368000	3.515084000	-0.758958000
H	-1.394923000	4.270777000	-0.418467000
H	-2.084614000	3.471152000	-1.853090000
H	-3.117180000	3.805057000	-0.430901000
C	-1.795781000	2.032369000	1.731042000
H	-2.830611000	2.255192000	2.013225000
H	-1.478624000	1.093842000	2.195253000
H	-1.151385000	2.841615000	2.089404000
C	-2.840030000	-2.126248000	-1.445480000
H	-2.456232000	-1.838419000	-2.429892000
H	-2.482460000	-3.133609000	-1.208608000
H	-3.936724000	-2.105745000	-1.452255000
C	-3.031696000	-1.487447000	1.370177000
H	-4.115087000	-1.546498000	1.210212000
H	-2.640442000	-2.467489000	1.661499000
H	-2.818831000	-0.774318000	2.172871000
C	2.844100000	-2.119373000	-1.447104000
H	3.940751000	-2.096767000	-1.454244000
H	2.488561000	-3.127608000	-1.210865000
H	2.459403000	-1.831536000	-2.431161000
C	3.035484000	-1.482383000	1.368966000
H	2.821155000	-0.770544000	2.172416000
H	2.646514000	-2.463586000	1.659427000
H	4.118970000	-1.538820000	1.208714000
C	2.104873000	3.519819000	-0.756929000
H	3.109470000	3.811121000	-0.429394000
H	2.076330000	3.476866000	-1.851080000
H	1.386513000	4.274052000	-0.415138000
C	1.790930000	2.034686000	1.731999000
H	1.144418000	2.841932000	2.091041000
H	1.476191000	1.094937000	2.195386000
H	2.825163000	2.259956000	2.014433000
H	-0.000871000	1.084908000	-1.884531000
Cl	0.003346000	-3.129584000	0.477064000

88

11^{Me}

Ni	0.000000000	-0.257344000	-0.126652000
P	2.153353000	-0.093888000	0.008646000
P	-2.153352000	-0.093881000	0.008648000
C	1.193223000	2.394215000	0.022139000
C	-1.193211000	2.394218000	0.022140000
N	0.000005000	1.654734000	-0.387793000
C	2.451648000	1.663457000	-0.463187000
C	-2.451640000	1.663465000	-0.463185000
Cl	-0.000012000	-2.492138000	-0.018429000
H	3.374484000	2.080365000	-0.040849000
H	2.505838000	1.703927000	-1.557944000
H	-2.505830000	1.703935000	-1.557942000
H	-3.374472000	2.080379000	-0.040847000
C	-3.238932000	-1.158025000	-1.014603000
H	-3.011503000	-0.985710000	-2.072222000
H	-3.007701000	-2.202266000	-0.777301000
H	-4.301017000	-0.954696000	-0.827053000
C	-2.820859000	-0.273752000	1.712404000
H	-3.905490000	-0.106360000	1.740671000
H	-2.592408000	-1.283787000	2.069880000
H	-2.322713000	0.450235000	2.366879000
C	3.238934000	-1.158037000	-1.014598000
H	4.301018000	-0.954709000	-0.827045000
H	3.007702000	-2.202277000	-0.777292000
H	3.011508000	-0.985727000	-2.072219000
C	2.820857000	-0.273757000	1.712405000
H	2.322716000	0.450235000	2.366877000
H	2.592399000	-1.283790000	2.069884000
H	3.905490000	-0.106373000	1.740672000
H	-1.256903000	2.534055000	1.124275000
H	1.256917000	2.534053000	1.124274000
H	-1.157657000	3.411585000	-0.409555000
H	1.157671000	3.411582000	-0.409557000

11^{Me}+H^+

Ni	0.011756000	-0.260668000	-0.241719000
P	-2.156394000	-0.191158000	0.092109000
P	2.185605000	-0.077497000	0.007119000
C	-1.391973000	2.391079000	-0.307162000
C	1.018356000	2.362843000	0.468951000
N	-0.026291000	1.747719000	-0.423618000
C	-2.309410000	1.584816000	0.612947000
C	2.386125000	1.772179000	0.105951000
Cl	0.103907000	-2.421992000	-0.164823000
H	-3.338424000	1.961120000	0.564063000
H	-1.973589000	1.650786000	1.655149000
H	3.149289000	2.071012000	0.832825000
H	2.702403000	2.138042000	-0.879840000
C	2.744803000	-0.742701000	1.614967000
H	2.170648000	-0.281773000	2.425888000
H	2.553600000	-1.820662000	1.622357000
H	3.813758000	-0.547635000	1.764473000
C	3.367736000	-0.710913000	-1.231070000
H	4.401907000	-0.501499000	-0.931996000
H	3.221401000	-1.793869000	-1.311070000
H	3.166886000	-0.257022000	-2.207284000
C	-2.842715000	-1.219423000	1.431076000
H	-3.904187000	-0.995277000	1.591801000
H	-2.721801000	-2.270931000	1.150436000
H	-2.281106000	-1.041775000	2.353922000
C	-3.271804000	-0.427028000	-1.339809000
H	-3.002801000	0.262648000	-2.146913000
H	-3.147540000	-1.452245000	-1.705897000
H	-4.318365000	-0.266290000	-1.053396000
H	1.009029000	3.453469000	0.342840000
H	-1.813245000	2.420998000	-1.317419000
H	0.744654000	2.129501000	1.502409000
H	-1.278012000	3.425245000	0.039647000
H	0.289046000	1.919423000	-1.380070000

12^{Me}

Ni	0.000000000	1.134729000	-0.000002000
C	-0.000001000	-0.849949000	-0.000004000
Cl	0.000005000	3.447600000	-0.000021000
C	2.728467000	-3.454298000	0.646654000
C	1.462123000	-2.897055000	0.539908000
C	3.901187000	-2.712087000	0.392003000
H	0.606784000	-3.505907000	0.812025000
H	4.885720000	-3.166916000	0.475514000
C	1.259051000	-1.523842000	0.151550000
C	3.751009000	-1.354923000	0.080585000
H	4.633678000	-0.731217000	-0.070977000
C	2.485244000	-0.781469000	-0.015010000
H	2.813522000	-4.496322000	0.959115000
P	2.120950000	0.955289000	-0.272556000
C	-1.259056000	-1.523838000	-0.151555000
C	-1.462132000	-2.897049000	-0.539921000
C	-2.485247000	-0.781464000	0.015017000
C	-2.728478000	-3.454289000	-0.646665000
C	-3.751014000	-1.354916000	-0.080576000
C	-3.901195000	-2.712078000	-0.392003000
H	-0.606795000	-3.505899000	-0.812049000
H	-2.813536000	-4.496310000	-0.959133000
H	-4.633681000	-0.731210000	0.070995000
H	-4.885729000	-3.166904000	-0.475511000
P	-2.120947000	0.955291000	0.272567000
C	-3.194001000	1.919850000	-0.877015000
H	-2.970330000	1.611088000	-1.903612000
H	-4.259752000	1.750957000	-0.669939000
H	-2.946137000	2.981541000	-0.762806000
C	-2.788954000	1.456189000	1.921383000
H	-2.289911000	0.861441000	2.693755000
H	-2.559129000	2.516737000	2.080078000
H	-3.874236000	1.294024000	1.978905000
C	2.788974000	1.456185000	-1.921366000
H	2.559155000	2.516734000	-2.080064000
H	3.874256000	1.294015000	-1.978877000
H	2.289936000	0.861438000	-2.693741000
C	3.193996000	1.919841000	0.877038000
H	2.946142000	2.981534000	0.762826000
H	2.970311000	1.611081000	1.903633000
H	4.259748000	1.750940000	0.669975000

12^{Me}+H^+

Ni	0.240931000	-1.157810000	-0.210325000
C	-0.129748000	0.788074000	-0.664157000
Cl	0.614392000	-3.327750000	0.232085000
H	0.109186000	0.790010000	-1.742476000
C	1.721631000	3.642061000	1.178189000
C	0.668421000	2.895302000	0.635167000
C	3.037505000	3.179441000	1.113099000
H	-0.343337000	3.282744000	0.699771000
H	3.849738000	3.764558000	1.537247000
C	0.908510000	1.657776000	0.019605000
C	3.292978000	1.931025000	0.533019000
H	4.306055000	1.533220000	0.525156000
C	2.240127000	1.173109000	0.019375000
H	1.506620000	4.594720000	1.657863000
P	2.325475000	-0.571178000	-0.507055000
C	-1.577169000	1.233289000	-0.540493000
C	-2.023889000	2.481986000	-1.008905000
C	-2.529343000	0.352102000	-0.002679000
C	-3.368456000	2.844248000	-0.908468000
C	-3.880511000	0.711806000	0.102933000
C	-4.301057000	1.964627000	-0.343268000
H	-1.310818000	3.168229000	-1.459362000
H	-3.694873000	3.813279000	-1.279848000
H	-4.602330000	0.011531000	0.519122000
H	-5.347563000	2.250318000	-0.268346000
P	-1.806336000	-1.265413000	0.405778000
C	-2.032828000	-1.522462000	2.212419000
H	-1.490137000	-0.741840000	2.755176000
H	-3.094832000	-1.491422000	2.487186000
H	-1.606260000	-2.498489000	2.469033000
C	-2.903778000	-2.535406000	-0.341081000
H	-2.952142000	-2.377674000	-1.423404000
H	-2.454984000	-3.515050000	-0.143853000
H	-3.915220000	-2.491565000	0.082145000
C	3.584872000	-1.375589000	0.556395000
H	3.603401000	-2.442001000	0.307608000
H	4.579336000	-0.935399000	0.412626000
H	3.279677000	-1.272704000	1.602344000
C	3.101711000	-0.599808000	-2.180420000
H	3.187408000	-1.640630000	-2.514032000
H	2.462536000	-0.054730000	-2.883164000
H	4.096884000	-0.137268000	-2.162334000

13^{Me}

Ni	-0.000007000	-1.131536000	-0.000088000
N	0.000029000	0.819822000	-0.000034000
Cl	-0.000040000	-3.335223000	-0.000251000
C	-2.599293000	3.386635000	0.861286000
C	-1.343816000	2.809959000	0.692053000
C	-3.777276000	2.685715000	0.566355000
H	-0.461764000	3.374253000	0.971368000
H	-4.750233000	3.150030000	0.700268000
C	-1.207811000	1.485955000	0.199499000
C	-3.670208000	1.361588000	0.140981000
H	-4.569069000	0.775538000	-0.043791000
C	-2.416605000	0.765882000	-0.023930000
H	-2.658928000	4.401778000	1.248893000
P	-2.133921000	-0.980894000	-0.374101000
C	1.207901000	1.485909000	-0.199547000
C	1.343966000	2.809893000	-0.692133000
C	2.416659000	0.765788000	0.023915000
C	2.599472000	3.386500000	-0.861394000
C	3.670291000	1.361422000	-0.141028000
C	3.777421000	2.685529000	-0.566454000
H	0.461942000	3.374220000	-0.971466000
H	2.659156000	4.401626000	-1.249037000
H	4.569123000	0.775335000	0.043762000
H	4.750401000	3.149788000	-0.700394000
P	2.133867000	-0.980949000	0.374198000
C	3.250510000	-1.948805000	-0.709797000
H	3.038960000	-1.695607000	-1.753340000
H	4.303517000	-1.736431000	-0.486984000
H	3.038859000	-3.011962000	-0.552572000
C	2.726093000	-1.362160000	2.070949000
H	2.167078000	-0.755520000	2.790533000
H	2.537703000	-2.422853000	2.272973000
H	3.798426000	-1.150388000	2.169229000
C	-2.726673000	-1.362311000	-2.070617000
H	-2.538385000	-2.423036000	-2.272562000
H	-3.799032000	-1.150519000	-2.168573000
H	-2.167875000	-0.755783000	-2.790464000
C	-3.250281000	-1.948588000	0.710342000
H	-3.038655000	-3.011770000	0.553245000
H	-3.038478000	-1.695206000	1.753789000
H	-4.303345000	-1.736261000	0.487750000

13^{Me}+H^+

Ni	0.261952000	-1.133383000	-0.218972000
N	-0.147524000	0.807686000	-0.662397000
Cl	0.660249000	-3.202617000	0.258000000
H	0.086260000	0.875788000	-1.655749000
C	1.566438000	3.590023000	1.288090000
C	0.540279000	2.846190000	0.689230000
C	2.889782000	3.152880000	1.236132000
H	-0.481369000	3.203446000	0.740068000
H	3.678658000	3.738104000	1.699684000
C	0.854283000	1.652348000	0.048459000
C	3.192653000	1.937377000	0.614385000
H	4.215059000	1.568729000	0.616220000
C	2.178279000	1.170085000	0.033226000
H	1.318508000	4.517631000	1.796345000
P	2.374414000	-0.550753000	-0.558215000
C	-1.569137000	1.200599000	-0.558995000
C	-2.006803000	2.412992000	-1.096248000
C	-2.471806000	0.304478000	0.023361000
C	-3.357952000	2.754950000	-1.003419000
C	-3.824452000	0.663648000	0.121532000
C	-4.263820000	1.888985000	-0.381086000
H	-1.300248000	3.085353000	-1.575328000
H	-3.702852000	3.696405000	-1.421482000
H	-4.537262000	-0.024130000	0.569318000
H	-5.313410000	2.159662000	-0.309077000
P	-1.791561000	-1.334867000	0.451018000
C	-2.006466000	-1.589887000	2.247889000
H	-1.458728000	-0.816946000	2.796070000
H	-3.067875000	-1.553767000	2.521130000
H	-1.591367000	-2.571520000	2.501163000
C	-2.859349000	-2.578466000	-0.354366000
H	-2.878368000	-2.401483000	-1.434209000
H	-2.423587000	-3.564595000	-0.161070000
H	-3.879515000	-2.537932000	0.045242000
C	3.645621000	-1.333705000	0.488897000
H	3.708337000	-2.390470000	0.208144000
H	4.622606000	-0.855804000	0.353817000
H	3.336225000	-1.271384000	1.536384000
C	3.102672000	-0.498639000	-2.243177000
H	3.223781000	-1.526801000	-2.603394000
H	2.435469000	0.036104000	-2.927859000
H	4.079353000	0.000172000	-2.228898000

4. References

1 S. Stallinger, C. Reitsamer, W. Schuh, H. Kopacka, K. Wurst and P. Peringer, *Chem. Commun.*, 2007, **12**, 510–512.

2 O. V. Dolomanov, L. J. Bourhis, R. J. Gildea, J. A. K. Howard and H. Puschmann, *J. Appl. Crystallogr.*, 2009, **42**, 339–341.

3 L. J. Bourhis, O. V. Dolomanov, R. J. Gildea, J. a. K. Howard and H. Puschmann, *Acta Crystallogr. Sect. A Found. Adv.*, 2015, **71**, 59–75.

4 G. M. Sheldrick, *Acta Crystallogr. Sect. A Found. Crystallogr.*, 2007, **64**, 112–122.

5 G. M. Sheldrick, *Acta Crystallogr. Sect. C Struct. Chem.*, 2015, **71**, 3–8.

6 S. Grimme, *J. Comput. Chem.*, 2006, **27**, 1787–1799.

7 F. Weigend, R. Ahlrichs, K. A. Peterson, T. H. Dunning, R. M. Pitzer and A. Bergner, *Phys. Chem. Chem. Phys.*, 2005, **7**, 3297.

8 F. Weigend, C. Hättig, H. Patzelt, R. Ahlrichs, S. Spencer and A. Willets, *Phys. Chem. Chem. Phys.*, 2006, **8**, 1057.

9 *AIMAll* Version 16.05.18, Todd A. Keith, TK Gristmill Software, Overland Park KS, USA, **2017** aim.tkgristmill.com.

10 T. Lu and F. Chen, *J. Comput. Chem.*, 2012, **33**, 580–592.

11 *Chemcraft* Version 1.8, www.chemcraftprog.com.

ARTICLE IN PRESS

Polyhedron xxx (2017) xxx–xxx

Contents lists available at ScienceDirect

Polyhedron

journal homepage: www.elsevier.com/locate/poly

The ABC in pincer chemistry – From amine- to borylene- and carbon-based pincer-ligands

Leon Maser [1], Lisa Vondung [1], Robert Langer *

Department of Chemistry, Philipps-Universität Marburg, Hans-Meerwein-Str., 35032 Marburg, Germany

ARTICLE INFO

Article history:
Received 30 June 2017
Accepted 13 September 2017
Available online xxxx

Keywords:
Pincer ligand
Amines
Borylenes
Carbodiphosphoranes
Coordination chemistry

ABSTRACT

The platform of pincer ligands offers the opportunity to stabilize elusive groups in the coordination sphere of a metal. These groups often exhibit unusual bonding properties and can show unprecedented reactivity patterns, which are potentially useful for (cooperative) catalysis. In the current review, we compare pincer ligands whose central donor group exhibits a sp^3-hybridized atom. The primary focus lies on the comparison of reactivity patterns of these formally isoelectronic donor groups. In particular, secondary amine groups, well known to act cooperatively as a proton relay, are compared with recently reported ligands that are based on boron and carbon. In the **ABC** in pincer chemistry, we will demonstrate that in contrast to **A**mine donor-groups, ligand-stabilized **B**orylenes are not acting as a proton source and rather undergo a reversible redox-reaction with the coordinated metal centre. The different types of **C**arbon-based ligands rather show characteristics of amine reactivity, but there is evidence for some complexes that a reversible redox reaction might be a possible exchange mechanism. Moreover, this review tries to analyze the bonding situation of the aforementioned species and to distinguish them from other related ligand types and their reactivity patterns.

1. Introduction

Tridentate ligands adopting a meridional coordination mode in (octahedral) transition metal complexes are commonly called pincer-ligands. Over the past decades, publications on different types of pincer-ligands and various applications of pincer-type complexes have seen a steady growth (Fig. 1), illustrating the continuously increasing interest in pincer chemistry [1]. The more or less constrained coordination geometry of pincer ligands is ideal for octahedral and square planar transition metal complexes and usually prevents the adoption of tetrahedral geometries. It is well known that coordination compounds with polydentate ligands exhibit an increased thermodynamic stability due to the chelate effect. In pincer-type ligands, the terminal donor groups adopt a *trans*-arrangement (Fig. 2, D^1 and D^3). The modification of those is often used to tune steric and electronic properties of the metal complex and to induce hemilability, which reversibly generates a vacant coordination site. The central donor group in pincer-type complexes is usually in *trans*-position to an ancillary ligand and thus directly affects the reactivity of the complex by its *trans*-effect and -influence. In some cases the increased stability of the pincer ligands is used to prepare unusual or very reactive groups in the coordination sphere of a transition metal, such as cationic donor groups or ligand stabilized borylenes [2–4]. The increasing number of publications and the huge variety of donor groups realized in pincer-type complexes make it difficult to provide a comprehensive overview on this emerging topic. The present review details properties and the typical reactivity patterns of pincer ligands with formally isoelectronic central donor groups, such as amines, ligand-stabilized borylenes, alkyls and protonated carbodiphosphoranes.

A similar comparison of isoelectronic donor groups can be made using boryls, carbenes and nitrenium ions as ligands [2,5–7]. After the initial publication on stabilized boryllithium in 2006, a number of transition metal complexes containing a cyclic diamido boryl ligand were reported [8]. Shortly afterwards, the first transition metal pincer complex with a cyclic diamido boryl ligand as the central donor group was reported, followed by studies on cooperative bond activation with such complexes. The PBP-type cobalt(I) pincer complex **1** for example, activates two equivalents dihydrogen, leading to the cobalt(III) dihydride complex **2** (Scheme 1) [9]. Interestingly, complex **1** is an active pre-catalyst for the hydrogenation of olefins. Quantum chemical investigations on the Lewis-acid cooperative H_2-activation reveal a synergistic heterolytic cleavage of the coordinated H_2-ligand as the most favorable mechanistic pathway [10].

* Corresponding author.
E-mail address: robert.langer@chemie.uni-marburg.de (R. Langer).
[1] Authors contributed equally.

https://doi.org/10.1016/j.poly.2017.09.009
0277-5387/

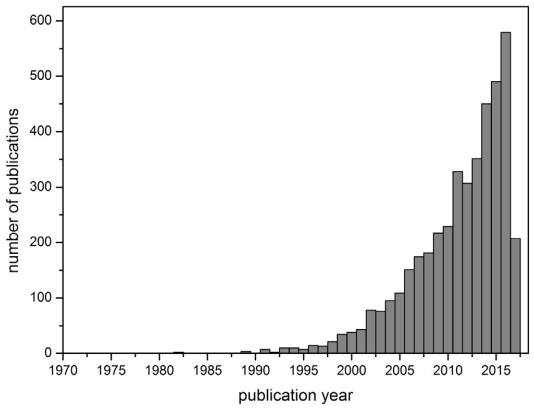

Fig. 1. Number of publications about pincer ligands [1].

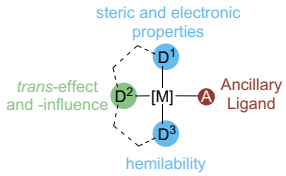

Fig. 2. Basic arrangement of D^2-based pincer-type complexes.

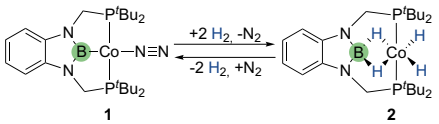

Scheme 1. Cooperative activation of H_2 with the boryl-based cobalt pincer complex **1**.

Structurally characterized pincer-type complexes with a central carbene-donor group have been reported with rhodium [11–13], iridium [12], palladium [13] and molybdenum [14]. The latter is an active catalyst for the reduction of nitrogen to ammonia.

In 2011 *Gandelman* and co-workers managed to employ a nitrenium cation as central donor group in a pincer-type complex (**3**), which is formally isoelectronic to boryl-anions and carbenes ligands (Scheme 2) [2,3,15]. In this case, the pincer-platform was necessary to sufficiently stabilize the metal complex. The Coulomb repulsion arising from the interaction of the nitrenium cation and the cationic metal center has to be compensated by the bonding of additional donor groups. Without the two terminal phosphine groups 1,3-dialkyl triazolium species would remain non-coordinative [3].

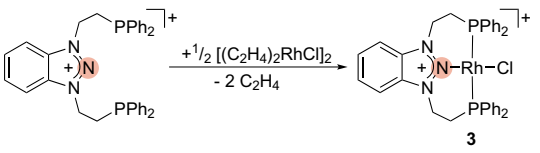

Scheme 2. Synthesis of the first metal complex with a nitrenium cation as ligand.

In parallel, different structural parameters and C–O-stretching vibrations on transition metal complexes were used to compare the donor properties of boryl anions and nitrenium cations with carbenes, respectively. These investigations showed that the nitrenium ligand is the weakest σ-donor among this series (Fig. 3). The strength of σ-donation subsequently increases when going to N–heterocyclic carbenes and boryl ligands [2,8]. Below, we will compare in detail the properties and, most importantly, the reactivity patterns of isoelectronic ligands with the general formula R_2EH (E = N, R = alkyl, aryl; E = C, R = alkyl, L-type donor; E = B, R = L-type donor, aryl). This includes amines, ligand-stabilized borylenes, protonated carbodiphosphoranes and alkyl-groups. While amines are very common ligands in coordination chemistry, their potential as cooperative donor group is often only highlighted in two-, three- or four-dentate ligands. Although mono-dentate borylenes and protonated carbones have been reported as ligands in metal complexes, some elusive donor groups are only stabilized by additional donor groups within a pincer ligand. This review will show that the pincer ligand platform can be used to stabilize very reactive donor groups and that it allows to examine unusual reactivity patterns in those complexes, which in many cases would not be possible with mono-dentate systems.

2. Amine-based pincer-type complexes

Increasing attention has recently been paid to pincer-type complexes with a central amine-group, due to their excellent activity in cooperative catalysis [16–21]. In pioneering work by the groups of *Noyori*, *Okhuma* and *Ikariya*, the term *bifunctional catalysis* was introduced for ruthenium hydrogenation catalysts, which contain bidentate ligands with an amine donor group and posses the ability to transfer a proton together with a metal-bound hydride to the substrate [22,23]. A related term frequently used in this context is *cooperative ligand* or *cooperative catalysis*, meaning essentially the same as *bifunctional catalysis*. Nowadays, the mechanistic view for *Noyori*-type catalysts is somehow revised in such a way that the amine only serves for a strong pre-coordination of the substrate via hydrogen bonds and therewith stabilizes the transition state. The amine-bound proton is most likely not transferred to the carbonyl substrate [22,24–26]. However, the NH-function of amine ligands in organometallic catalysis was recently reviewed [27]. In this section, we will focus on the identification of typical reactivity patterns of transition metal complexes with amine-based pincer-type ligands.

Fig. 4 summarizes common types of amine-based pincer ligands. In principle, the amine can be bound to carbon atoms in alkyl-, alkenyl- or aryl-groups as well as heteroatom-containing groups such as $Si(CH_3)_2$-groups. The terminal donor groups vary from tertiary phosphines to carbenes, silylenes, heterocycles and thioethers. Amine-based pincer ligands with dibenzotropyl-substituents, for example, coordinate via two terminal olefine groups and the amine-group to the central metal atom (Fig. 4 right) [20]. Following these reports about bidentate ligands with cooperative

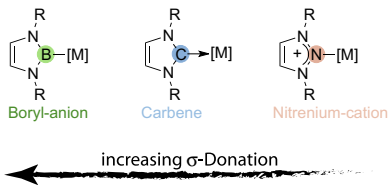

Fig. 3. Comparison of isoelectronic donor groups. Some of those can only be stabilized using a pincer ligand as platform.

Please cite this article in press as: L. Maser et al., Polyhedron (2017), https://doi.org/10.1016/j.poly.2017.09.009

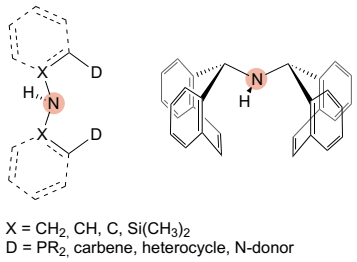

Fig. 4. Common ligand frameworks in amine-based pincer-type ligands.

amine groups, a lot of tri- and tetra-dentate ligands containing amine-groups or groups that are being transferred into amine groups during catalysis were reported [20,21,27]. In particular, pincer-type complexes turned out to be robust catalysts for various hydrogenation and dehydrogenation reactions (Fig. 5), ranging from hydrogenation of challenging substrates like amides, carbamates and ureas to the acceptorless dehydrogenation of alcohols as well as several dehydrocoupling reactions. In 2011, *Kuriyama* and co-workers reported high catalytic activity for the hydrogenation of esters to alcohol, utilizing complex **4** as a pre-catalyst [28]. This pre-catalyst is currently used for the hydrogenation of enantiomerically pure methyl lactate (**9**) to 1,2-propanediol (**10**), while the configuration of the stereocenter is retained. The corresponding manganese(I)-(**6**) and iron(II)-complexes (**5**) are active catalysts for the hydrogenation of carbonyl compounds as well, including challenging substrates such as esters and amides [29–44]. Moreover, ruthenium(II)-complexes with terminal donor groups different than phosphines (complexes **7** and **8**) were demonstrated to be active catalysts too [45,46].

In agreement with the *Valence Shell Electron Pair Repulsion* (VSEPR) theory, amines with the general formula NR_3 typically exhibit a trigonal pyramidal or pseudo-tetrahedral geometry. As ligands in metal complexes, they are regarded as pure σ-donors, leading to moderate ligand field splitting.

Common reactivity patterns of metal complexes with secondary amine-based pincer-type ligands involve the transfer of the amine proton. In combination with coordinated hydrido ligands (e. g. ruthenium complex **11**), secondary amine ligands are able to provide a proton for a concerted proton–hydride transfer to an unsaturated substrate [27]. Typically, the transition state (TS) is assumed to be a six membered ring (Scheme 3, $\mathbf{TS_1}$), leading to an amido-coordinated complex (**12**) [47]. Coordination of H_2 (**13**) followed by heterolytic cleavage of H_2 across the ruthenium nitrogen bond regenerates the hydride complex **11**. However, recent studies show that the amine does not get deprotonated during this reaction and only serves as donor for hydrogen bonds to the substrate ($\mathbf{TS_2}$) [22,24–26]. The resulting complex **14** contains the substrate bound via a hydrogen bond to the amine ligand. Dihydrogen coordination and subsequent heterolytic cleavage by the NH-bound alkoxide product in complex **15** regenerates the ruthenium hydride complex **11**.

Although different mechanistic pathways for the catalytic hydrogenation by ruthenium complexes have been discussed, there is strong experimental evidence that the secondary amine group in pincer-type complexes serves indeed as a proton relay. The groups of *Schneider* and *Schmedt auf der Günne* demonstrated that the proton hydride exchange in **16** is stereoselective and significantly faster when a protic molecule such as water is involved (Fig. 6) [48]. Based on quantitative ^{1}H EXSY (exchange spectroscopy) NMR spectra, the rate constant for the exchange between the nitrogen-proton and the ruthenium-bound hydrido ligand atom is with 0.02 s^{-1} several orders of magnitude smaller than the rate constants for the exchange with a water molecule. A six membered ring as transition state ($\mathbf{TS_3}$) was suggested on the basis of density functional theory (DFT) calculations for this proton hydride exchange, leading to the dihydrogen intermediate **17**. These complexes often liberate dihydrogen under formation of amide complexes (**18**). Depending on the substituents of the central R_2NH-group in such pincer-type complexes, different reaction pathways are possible in addition to the proton-transfer. For substituents with CH_2-groups like in $HN(CH_2CH_2PR_2)_2$, the coordinated pincer ligand can get further dehydrogenated under certain reaction conditions. The liberation of hydrogen from hydrido complexes with the amine-based pincer ligand to the amido-based ligand **19** was discussed above. This species can react reversibly via β-hydride elimination to give a new hydrido complex with an imine-based pincer ligand (Scheme 4, **20**). However, this species can usually not be detected and was calculated to be higher in energy than the isomeric complex **19**, as well as the corresponding enamide tautomer that can subsequently eliminate dihydrogen (complex **21**). Depending on the central metal atom, this reaction

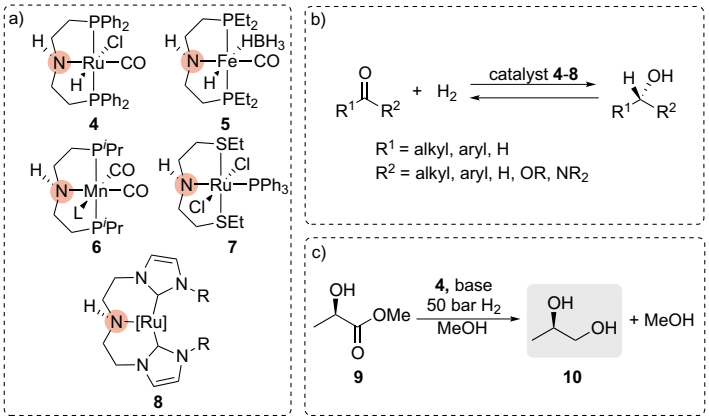

Fig. 5. a) Examples of highly active pre-catalysts with amine-based pincer-type ligands. b) Hydrogenation of various carbonyl compounds as well as for the acceptorless dehydrogenation of alcohols. c) Hydrogenation of methyl lactate.

Please cite this article in press as: L. Maser et al., Polyhedron (2017), https://doi.org/10.1016/j.poly.2017.09.009

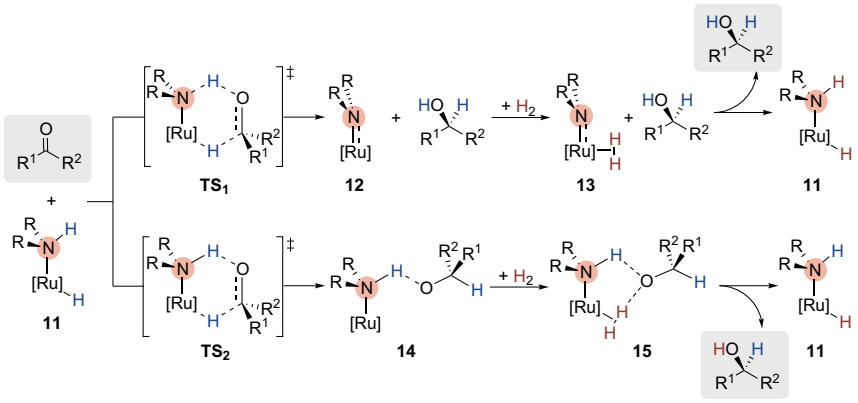

Scheme 3. Mechanistic pathways for the hydrogenation of carbonyl compounds, using *bifunctional catalysts* ([Ru] = [(diphosphine) Ru(H)], [(η^6-$C_6R'_6$) Ru] (R′ = H, Me), R_2NH = 1,2-diamine, 1,2-aminoalcohol).

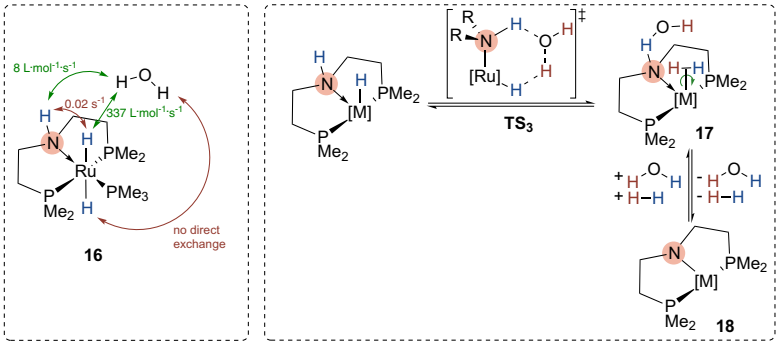

Fig. 6. Chemical exchange in the amine-based pincer-type ruthenium(II) dihydride complex **16**, detected by quantitative ^{1}H EXSY NMR spectroscopy (left); calculated reaction pathway for the solvent-assisted proton hydride exchange (right).

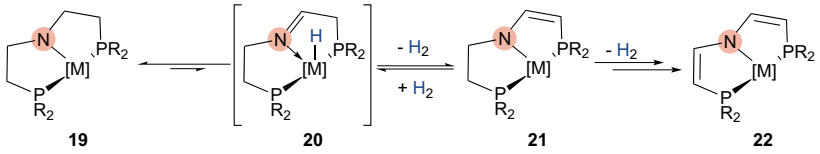

Scheme 4. Ligand backbone dehydrogenation of amido-based complexes (**19**) to enamido-based pincer type complexes **21** and **22** (M = Ru, Ir).

pathway can only be observed in the presence of a hydrogen acceptor like quinone (e.g. M = Ir) or it is induced by ancillary ligands. Overall, up to three equivalents of dihydrogen can be eliminated starting from a hydride complex with a coordinated secondary amine.

3. Carbon-based pincer-type ligands

sp^3-hybridized carbon-based ligands with different substituents are formally isoelectronic to amines. In the following chapter we discuss pincer-type ligands with different central carbon-based donor groups.

3.1. Alkyl-based pincer-type ligands

The coordination versatility in *sp*^{3}-hybridized alkyl-based pincer-type complexes was recently reviewed by *Gelman* and co-workers [49]. It is not our intention to give a comprehensive overview of the recent achievements in this field of research and in the following, we will rather identify typical reactivity patterns of this ligand type using selected examples.

Shaw and co-workers demonstrated that rhodium(III) hydride complexes (**23**, M = Rh) undergo a rapid reversible C–H-bond fission of the coordinated PC^{sp3}P-type pincer ligand. Upon heating in isopropanol, the coordinated pincer ligand gets dehydrogenated,

Please cite this article in press as: L. Maser et al., Polyhedron (2017), https://doi.org/10.1016/j.poly.2017.09.009

yielding the olefine-coordinated complex **24** (Scheme 5) [50,51]. A similar observation was made for amide-based pincer-type complexes, where a β-hydride elimination leads to a coordinated imine-group. However, the β-hydride elimination of a coordinated alkyl-ligand results in the formation and subsequent coordination of an olefine. Upon heating, the corresponding iridium(III) complex (**23**, M = Ir) liberates dihydrogen as well, but in contrast to the rhodium(III) complex the alkylidene complex **25** is formed [52,53]. Interestingly, this reaction is similar to the dihydrogen elimination from hydride complexes with coordinated amine-groups. It should be noted that other iridium pincer-type complexes preferably react via β-hydride elimination to the coordinated olefin complexes [54].

Gusev and co-workers reported ruthenium complexes with the same alkyl-based pincer ligand [55]. The reaction of 1,5-*Bis*(di-*tert*-butylphosphino)pentane ($^tBu_2P$-$(CH_2)_5$-P^tBu_2) with $[RuCl_2(cymene)]_2$ leads to a mixture of **27** and **28** (Scheme 6). Under hydrogen atmosphere, the mixture of the two complexes reversibly reacts to complex **26**. Based on the H···H-distance (estimated by NMR measurements), **26** is best described as a compressed dihydride complex. In the absence of dihydrogen, a mixture of **27** and **28** is formed again.

A series of rhodium and iridium complexes (**29**–**31**) with an alkyl-based pincer ligand were reported to catalyze the H/D-exchange of vinyl-groups, using C_6D_6 as deuterium source (Scheme 7, top) [54]. The reaction proceeds with high selectivity, high functional group tolerance and no detectable isomerisation of the olefin is observed. Although β-hydride elimination from the coordinated alkyl ligand is an observable reaction pathway in the current case, it is too slow to account for the operative mechanism of the catalytic H/D-exchange. A possible mechanism involves the formation of the tricoordinated iridium(I) complex **32**, which subsequently reacts with C_6D_6 in an oxidative addition step to complex **33** (Scheme 7, bottom). Two different pathways are conceivable for the actual H/D-exchange. The first one involves α-hydrogen elimination and formation of the iridium(III) carbene complex **34a**. Alternatively, a reductive C-D-elimination from **33**, leading to complex **34b** as an intermediate, was considered. In both cases the complex **33'** is formed, followed by reductive C–H-elimination of C_6D_5H.

In summary, alkyl-based donor groups in pincer-type ligands are less acidic than amines, but show a wide range of related reactivity patterns. α- and β-hydride elimination were identified as common reaction pathways, which can both be completely reversible. Furthermore, reductive C–H-elimination was proposed as an alternative pathway and cannot be excluded so far.

3.2. Carbodiphosphorane-based pincer complexes and their protonated analogues

Carbodiphosphoranes (CDP), their first representative, hexaphenylcarbodiphosphorane, being synthesized by *Ramirez* and co-workers in 1961 [56], contain a central carbon atom, which is only bound to two PR_3-groups. Different structures for hexaphenylcarbodiphosphorane have been observed: An angled form, in which two free electron pairs are located at the central carbon atom, has been described as a coordinated carbon(0) [57–67]. Still, some controversity remains about this description [68–71]. More recently, *Parkin* and co-workers reported a linear form of hexa-phenyl-carbo-di-phosphorane, which is intuitively in agreement with bonding of an ylid [72]. The two free electron pairs render it a σ- and π-donating ligand and soon after its initial discovery, transition metal complexes were reported by *Kaska et al.* [73,74]. Since then, other adducts were reported, some of which led to unusual binding modes prompting further investigations [75–78].

Several reviews about carbodiphosphorane and heavier homologues [79], transition metal complexes [80] and main-group Lewis acids [81] have already discussed the coordination chemistry of CDPs. In principle, there are three types of adducts derived from carbodiphosphoranes. Due to their two electron pairs, carbodiphosphoranes can act as donors for two or one acceptors, as shown in Fig. 7. If they only coordinate to one acceptor, they can either donate both electron pairs or retain one as a free electron pair, depending on the electron deficiency of the acceptor [81].

Even though numerous examples of complexes and adducts containing monodentate or μ-bridging carbodiphosphorane complexes have been structurally characterized, pincer-type ligands based on a carbodiphosphorane-backbone (**35**) are rare [76,82–88]. The structural motif of ligands with a central carbon atom that is only bound to two phosphorous atoms is nevertheless well represented in coordination chemistry, but these ligands are rather described as bis(phosphorous-stabilized) carbenes **36** (Fig. 8).

Even though iminophosphorano- and sulfidophosphorano-based pincer ligands share obvious similarities with carbodiphosphorane-based pincer ligands, investigations on their bonding properties and reactivities have placed them closer to carbene-based ligands [89]. However, this review will focus on the lesser explored complexes of carbodiphosphorane-based pincer ligands containing only carbon-bound phosphorous atoms in the ligand backbone.

"True" carbodiphosphorane-based pincer-type ligands are limited to two structural examples. Rhodium and platinum complexes were reported with the dianionic CCC-type ligand in **37** (Fig. 9). The second type of pincer ligand with a central carbodiphosphorane exhibits two terminal phosphine groups (**38**).

37a is derived from hexaphenylcarbonyldiphosphorane by *ortho*-C–H activation of a phenyl-group of each phosphorous atom (Scheme 8). It was first described by *Cavell* and co-workers in 2005 as the reaction product of hexaphenylcarbodiphosphorane and rhodium or platinum precursors [76].

In the case of platinum, the double *ortho*-metalation directly takes place, whereas starting with $[RhCl(cod)]_2$ (cod = cyclooctadiene) first yields a κ^2-P,C coordination, which is expanded to a κ^3-P,C,P' coordination upon addition of PMe_3. In the following years, only two additional complexes were published [83,82]. The publication by *Petz* and *Neumüller* describes an interesting reactivity of a platinum complex. They were able to isolate platinum(II) complex **39**, in which a protonated CDP-carbon coordinates to the metal centre (Scheme 9). They proposed that this complex is formed due the high proton affinity of carbodiphosphorane adducts of type **40** and stabilized by the chelating effect of the pincer ligand.

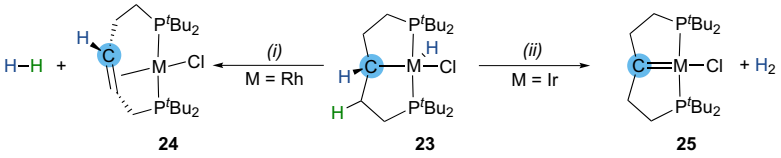

Scheme 5. Reaction pathways of $PC^{sp^3}P$-type pincer complexes. Reaction conditions: *(i)* refluxing isopropanol, *(ii)* refluxing decalin or heating *in vacuo*.

Please cite this article in press as: L. Maser et al., Polyhedron (2017), https://doi.org/10.1016/j.poly.2017.09.009

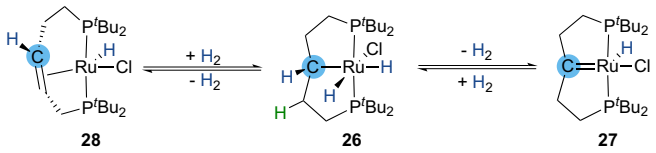

Scheme 6. Different reaction pathways for hydrogen release from complex **26**.

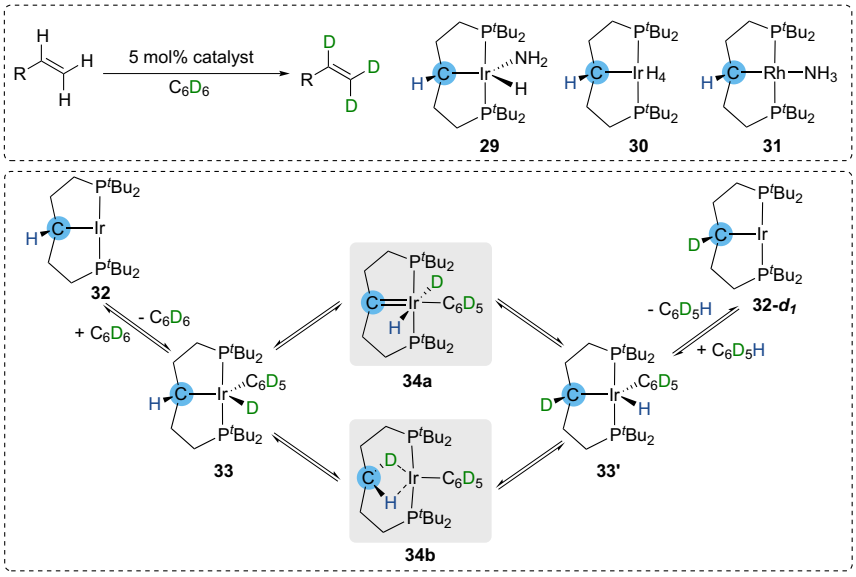

Scheme 7. Catalytic H/D-exchange of olefines catalyzed by **29**–**31** (top). Possible mechanistic pathways for the exchange (bottom).

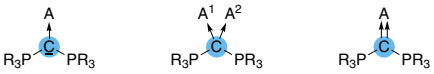

Fig. 7. Modes for carbodiphosphorane-adducts.

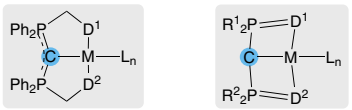

Fig. 8. Structurally most represented complexes with **35** and **36** as ligands.

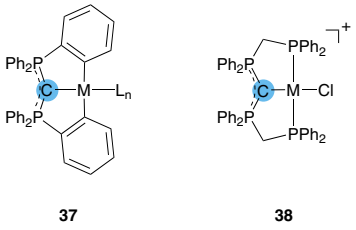

Fig. 9. General structures of complexes with the two known carbodiphosphorane-based pincer ligands **37a,b** (M = Pt, Rh) [76,82,83] and **38a–c** (M = Pd, Pt, Ni) [84–88].

In the second publication, *Kubo* et al. describe the formation of the dimeric species **41** upon ligand exchange from **37a** with L = SMe_2 to L = PEt_3 and addition of silver trifluoromethanesulfonate. They were furthermore able to cleave **41** by addition of two equivalents of a phosphine and obtained the corresponding monomeric complexes **42** (Scheme 10) [83].

The formation of a second metal carbon bond to a different metal in these dimers indicate that the Pt-C bond interaction is mostly σ-based and that the second electron pair at the central carbon is available for donation to a second lewis acid, be it a proton or a second metal.

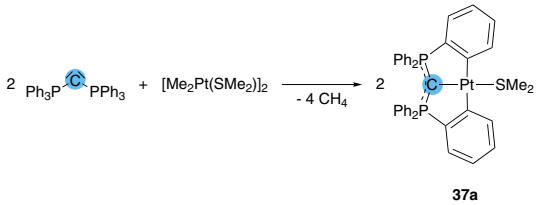

Scheme 8. Synthesis of the first hexaphenylcarbodiphoshorane-based platinum-pincer complex **37a** (L = SMe_2) by *Cavell* and co-workers [76].

Please cite this article in press as: L. Maser et al., Polyhedron (2017), https://doi.org/10.1016/j.poly.2017.09.009

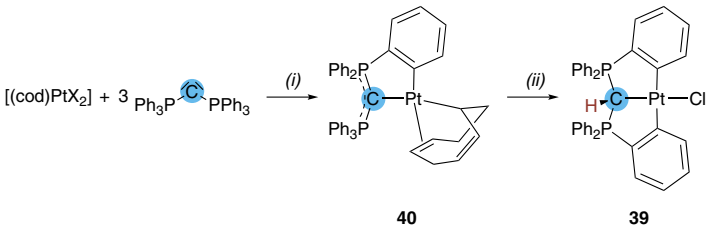

40 39

Scheme 9. Formation of the protonated carbodiphosphorane-based platinum pincer complex **39** as reported by *Petz* and *Neumüller*. X = Cl, I; *(i)* = −2 (HC{PPh_3}$_2$) X; *(ii)* = CH_2Cl_2 or $CHCl_3$ [82].

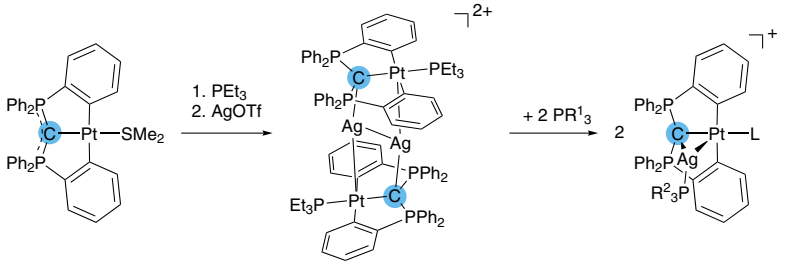

37a 41 42

Scheme 10. Formation of the Ag-bridged dimeric complex **41** and its cleavage leading to monomeric complexes **42** (R^1 = Ph, R^2 = Ph, L = PEt_3 or R^1 = OPh, R^2 = Et, L = $P(OPh)_3$) [83].

Complex **38c** was first obtained by *Peringer* and co-workers via template synthesis with nickel(II) (Scheme 11) using carbon disulfide as carbon source. Based on NMR-spectra, it was also postulated that the protonated complex **43a** (M = Ni) can be formed [84]. In later works, the reversibility of the reaction was assured and **43b** (M = Pd) was also synthesized. Notably, **43b** is already deprotonated by water, indicating the acidic nature of protonated CDP ligands [87].

Already in 2009, reaction of **38a** with [AuCl(tht)] (tht = tetrahydrothiophene) yielded the first binucleating carbodiphosphorane pincer complex **44** with two different complexated metals (Scheme 12) [85]. **44** shows striking structural similarities to **42**, indicating that the ability for a μ^2-coordination mode is similar in both carbodiphosphorane-based pincer ligand systems.

Based on **43a**, in 2011 they were able to synthesize the homodimetallic complex **45** in a two-step reaction (Scheme 13) [86].

In contrast to **44** and **42**, **45** does not show a κ^3-P,C,P'-coordination but rather a κ^3-P,C,C'-coordination by involving the aliphatic ligand backbone. Nevertheless, **45** further exemplifies the general tendency of carbodiphosphorane-based ligands to form bimetallic complexes.

In their works, *Schuh* and co-workers also observed the formation of the free diprotonated carbodiphosphorane ligand **46** by treatment of **38c** hydrochlorid acid (Scheme 14) [87]. **46** can be further transformed to its monoprotonated form **47** by aqueous ammonia. **46** enabled access to a variety of gold(I)-(**48**,**49**) and gold(III)-complexes (**50**,**51** in Scheme 15).

The square-planar coordination of the gold(III)-complexes **50** and **51** is to be expected, whereas the trigonal-planar coordination of **48** and linear coordination of **49** is without significant interaction between carbon atom and the metal centre.

Based on the observed reactivities, it seems likely that in the unprotonated complexes as well as their protonated counterparts, the carbodiphosphorane mainly acts as a σ-donor. Thus, the free electron pair can form a bond to the proton or be delocated over the phosphine groups. This is indicated by the planar geometry of the carbon, which changes to a tetragonal geometry as soon as it is protonated or acts as a binucleating ligand. It can be assumed that the σ-donor-abilities outweigh its π-donor-abilities, depending on the electron accumulation at the central metal atom. This is seen in the marginal changes in C-M atom distances of deprotonated versus protonated complexes of late transition metal complexes (Pd-C: 2.062(2)Å, Pd-CH: 2.102(3)Å; Pt-C: 2.054(4)-2.060(4)Å, Pt-CH: 2.106(4)Å [84,87]). It is also important to note that the protonation, though easily carried out with hydrochloric acid, does not take place with water in the reaction mixture, as demonstrated by the use of $NiCl_2{\cdot}6\,H_2O$ as a starting material for the template synthesis. Instead, the protonated complexes show a higher acidity than water and revert to their unprotonated counterparts when water is added (Scheme 11).

The ability for deprotonation at the donor atom is shared by the already discussed amine-based pincer ligands, where it is an integral part in the versatility of the ligand system. In comparison to amine-based pincer ligands, the carbodiphosphorane-based pincer ligands are capable of delocalizing the free electron pair on the phosphine groups as well as by π-donation to the metal (Scheme 16). In contrast to amido- and alkyl-based pincer complexes, β-hydride elimination can not take place, as the β-position is occupied by tertiary phosphine donor moieties.

The first and second proton affinity (PA) of carbodiphosphoranes and their adducts have already attracted some attention, as they can be used to distinguish between carbodiphosphoranes and carbenes [63,90]. For carbodiphosphoranes, the calculated values for the first proton affinity are in the order of 1100 kJ mol^{-1}

Please cite this article in press as: L. Maser et al., Polyhedron (2017), https://doi.org/10.1016/j.poly.2017.09.009

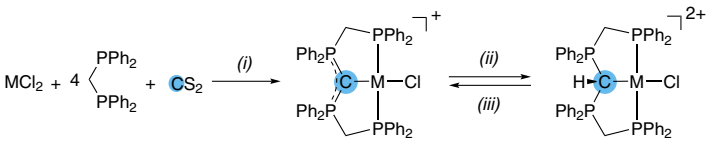

Scheme 11. *Peringer* and co-workers' template synthesis for complexes **38a–c** (M = Pd, Pt, Ni) of their CDP-based ligand and its protonated forms **43b,c** (M = Pd, Pt). (i) = −2 dppmS; *(ii)* = HCl; (iii) = H_2O. dppm = 1,1-*Bis*(diphenylphosphino)methane [84,87].

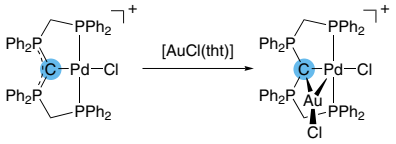

Scheme 12. Synthesis of the first heterodimetallic carbodiphosphorane-based pincer complex **44** by *Schuh* and co-workers [85].

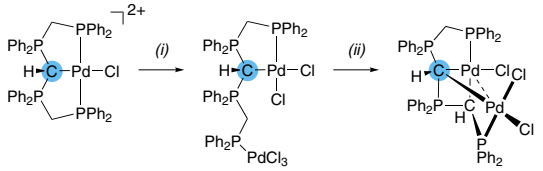

Scheme 13. Synthesis of the homodimetallic pincer complex **45**. (i) = + $[PdCl_2(MeCN)_2]$, −2 MeCN; (ii) = + H_2O, −2 HCl [86].

(1^{st} PA hexaphenylcarbodiphosphorane: 1172 kJ mol^{-1}) and the second is about 450 kJ mol^{-1} lower (2^{nd} PA hexaphenylcarbodiphosphorane: 654 kJ mol^{-1}) [63], which is equal to the first proton affinity of carbodiphosphorane Lewis acid adducts [90]. Such as it is, the calculated values for the first proton affinities of secondary amines (e.g. Me_2NH = 930 kJ mol^{-1}, Et_2NH = 955 kJ mol^{-1}, $^{i}Pr_2NH$ = 964 kJ mol^{-1}) [91] are significantly higher than those of protonated carbodiphosphoranes, but still lower than those of carbodiphosphoranes [91–93]. This observation might be due to the anionic form of the deprotonated amine versus the neutral character of the carbodiphosphorane and the positive charge on a protonated carbodiphosphorane. The easy protonation and lower proton affinity nevertheless suggests that carbodiphosphoranes could be better proton donors in cooperative ligands.

4. Boron-based pincer ligands

Boron containing pincer ligands represent a rather novel field in organometallic chemistry. So far, only a few ligand types are known, but the research on boron-based pincer ligands is rapidly evolving. For the comparison of properties and reactivities it is useful to make distinctions by the number of substituents at the boron atom as well as by the bonding modes between the transition metal and boron atom. In the following chapter, we will give an overview on complexes with ligands based on bi- and tricoordinate boron, their bonding situations and reactivity.

4.1. Boryl-based pincer complexes

Boryl groups with the general formula BR_2^- were used for the first time as donor groups in a pincer-type ligand in 2009 in seminal works of the groups of *Nozaki* and *Yamashita* on a pincer ligand with an amidostabilized boryl group (**I**, Fig. 10) [94]. Following up on the boryl-pincer-ligand design **I**, the groups of *Yamashita*, *Nozaki*, *Murakami*, *Hill*, *Peters*, *López-Serrano* and *Rodriguez* reported complexes with different transition metals and numerous ancillary ligands [5–7,9,95–104]. Until mid 2017, only two more motifs for boryl pincer ligands were reported: The group of *Ozerov* employed *Bourissou*'s borane-based pincer ligand in the reaction with iridium precursors, which results in oxidative C-B-addition and formation of complex **II** (Fig. 10) [105]. The utilization of a rhodium precursor leads to a mixture of boryl-complexes and the corresponding boratrane complex, which can be converted to boryl complexes under H_2-atmosphere.

Boryl-based pincer complexes can react with two equivalents of H_2, as reported by the group of *Peters*. As pointed out in Scheme 1, pincer ligands based on N-heterocyclic boryl groups can act as cooperative ligands in small molecule activation. In this case, the cobalt(I) boryl complex is able to cleave two equivalents of dihydrogen to give the cobalt(III) dihydride complex with a dihydrido borate group. The remaining Lewis acidity at the boron atom in a coordinated boryl ligand is believed to be responsible for this reactivity [9].

Encouraged by these results, several boryl pincer complexes were tested and optimized for catalytic reactions (Fig. 10). The group of *Peters* reported the ability of cobalt boryl pincer complex **52** to catalyze olefin hydrogenation, amine-borane

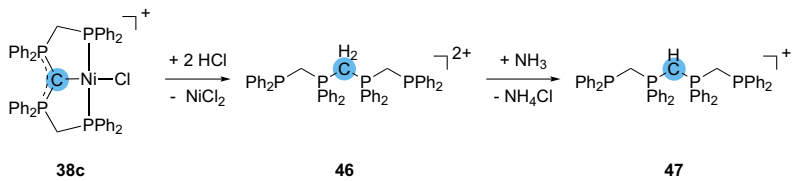

Scheme 14. Synthesis of the free mono-(**47**) or diprotonated (**46**) carbodiphosphorane-based ligand [87].

Please cite this article in press as: L. Maser et al., Polyhedron (2017), https://doi.org/10.1016/j.poly.2017.09.009

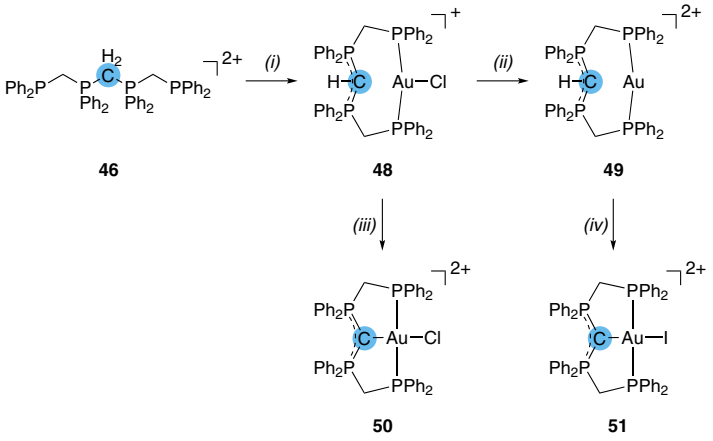

Scheme 15. Synthesis of the Au-complexes **48**–**51** starting with the diprotonated carbodiphosphorane-based ligand **46**. *(i)* = +[AuCl(tht)], −THT; *(ii)* = +2 TlOTf, −2 TlCl; *(iii)* = +*xs.* HNO_3, −n NO_x, −m HCl, −k H_2O; *(iv)* = +I_2, +TlOTf, −TlI, −TfOH [88].

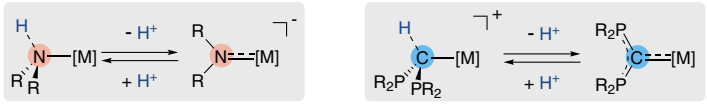

Scheme 16. Possible π-bonding upon deprotonation of amine- or carbodiphosphorane-based ligands.

dehydrogenation and transfer hydrogenation between amine-borane and styrene [9].

Yamashita and co-workers reported on the application of platinum complex **53** with a PBP-boryl pincer ligand in the hydrosilylation of 1-decene [96]. Although the performance was lower than that of established homogeneous catalysts, it showed the potential of boryl pincer complexes. Further catalytic applications of the diamido-boryl pincer complexes were demonstrated by *Yamashita*'s group with rhodium and iridium complexes. The most active rhodium complex **54** from this study is obtained from the PBP-ligand and a ruthenium-hydrido-acetato precursor by subsequent ligand exchange of $[BH_4]^-$ [101]. The iridium complexes were able to catalyze the dehydrogenation of cyclooctane after exchange of the bulky *tert*-butyl phosphines for sterically less demanding *iso*-propyl phosphines (complex **55**) or expansion of the alkyl bridge in the backbone (complex **56**) [102,103]. Very low catalyst loadings can be achieved, but the turn over numbers are still moderate.

4.2. Carborane-based pincer complexes

In the same year as the first boryl-pincer ligands were reported, the group of *Mirkin* introduced functionalized *m*-carboranes as boron-containing pincer ligands (**III**, Fig. 11) [106]. *Planas* and co-workers showed in 2014 that *o*-carboranes are also suitable for use in pincer ligands (**IV**, Fig. 11) [107]. Further variants of *m*-carborane based pincer complexes were reported by the groups of *Nakamura* and *Peryshkov*, varying the backbone between carborane and donor atom [108,109].

From the group of *Nakamura*, the application of carborane based pincer complexes **57** as chiral catalysts in asymmetric conjugated reduction and reductive aldol reactions was reported in 2011. The carborane structure provides good means to invoke chirality and for electronic fine-tuning [108].

Planas and co-workers found the *o*-carborane **58** to be highly active in Suzuki coupling reactions in water with very low catalyst loadings [107].

4.3. Bonding and classification for ligands based on tricoordinate boron

Pincer complexes based on tricoordinate boron can be assigned to all three coordination types according to the *covalent bond classification* by *Green* (Fig. 12) [110]. Borane or boratrane complexes with a central BR_3-moiety in a pincer ligand act as Z-type ligand, with a dative metal-boron bond which donates electron density to the electron-deficient boron atom. In these complexes, the boron atom can occupy an additional coordination site of the metal complex. The palladium(II) complex **59** with a Z-type ligand group adopts a square-planar coordination geometry for the X- and L-type PR_3- and Cl^--ligands, whereas the borane adopts the additional apical position. This class of compounds was the first to incorporate boron as central atom in tridentate ligands and is described very well in a review by *Braunschweig* and co-workers [111].

Boryl complexes with a tricoordinate boron atom contain a R_2LB-group (**60**), which consists of the already described BR_2^- moiety and an additional donor group, stabilizing the boron atom. They thus possess an electron which participates in a covalent bond with the metal. These complexes are classified as X-type complexes and are strong σ-donors.

If π-accepting and σ-donating substituents are utilized on the boron atom, an *Umpolung* of the boron atom to a Lewis-base is possible. Such a Lewis-base stabilized L_2RB-group acts as a donor ligand in transition metal complexes and is classified as L-type ligand (**61**). So far, in boron chemistry, the Z-type ligands were dominating, with X-type boryl ligands emerging in the last years,

Please cite this article in press as: L. Maser et al., Polyhedron (2017), https://doi.org/10.1016/j.poly.2017.09.009

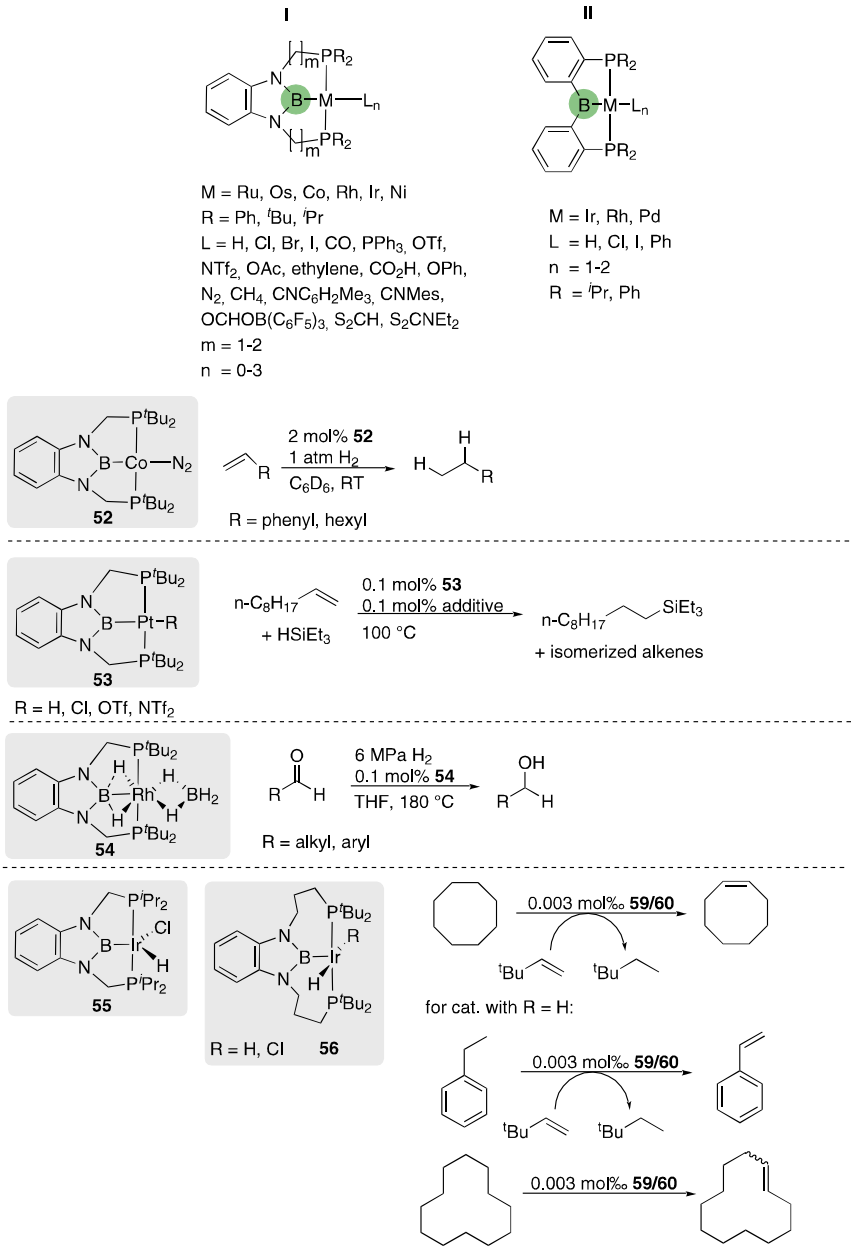

Fig. 10. Known types of boryl-based pincer ligands and their application in homogeneous catalysis.

while for L-type borylene-based pincer complexes only very few examples are known [4,112].

The assignment of complexes with boron-containing pincer ligands as L-, X- or Z-type can often be ambiguous. Nonetheless, different experimental and theoretical parameters show trends for the different ligand types. Table 1 summarizes different parameters for palladium complexes of all three types, as shown in Fig. 12. From experimental data, Pd-B and Pd-P bond lengths show an increase when going from donating (L-type) via covalent (X-type) to accepting (Z-type) boron ligands. The bond angle sum at the boron atom ($\Sigma_{B\alpha}$) also becomes larger the more accepting the ligand type. Another experimentally easy accessible value is the ^{11}B NMR chemical shift. For the L-type borylene ligand, the signal is shifted highfield, while the Z-type borane ligand gives a signal

Please cite this article in press as: L. Maser et al., Polyhedron (2017), https://doi.org/10.1016/j.poly.2017.09.009

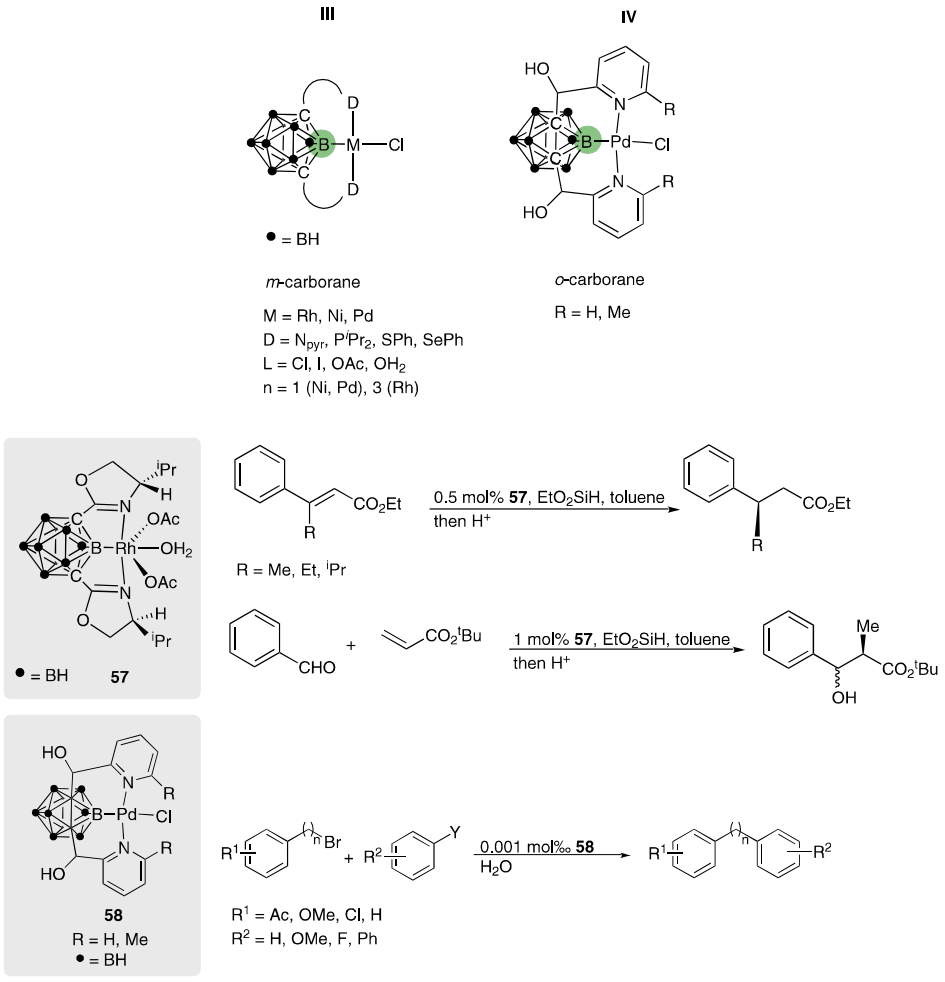

Fig. 11. Complexes with carborane-based pincer ligands and their application in catalytic reactions.

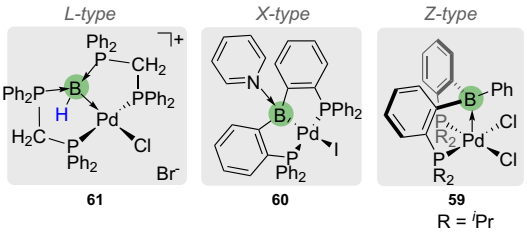

Fig. 12. Examples for L-, X- and Z-type boron-based pincer complexes based on tricoordinate boron ligands [112–114].

lowfield compared to the X-type boryl ligand. Further insight can be gained from quantum chemical calculations. One tool for bonding analysis is the *Quantum Theory of Atoms in Molecules* (QTAIM) method, which provides information on where bonds are located and different values for the so called bond critical points (bcp). From Table 1, it can be concluded that the electron and energy densities (ρ and H*bcp*) at the bcps both decrease when going from L- to X- and Z-type ligands. Also, the charge at the boron atom (q_B), as derived from *Natural Bond Orbital* (NBO) analysis, is a good hint for the ligand type.

Table 1
Comparison of different parameters derived from X-ray crystal structures and QTAIM analysis for L-, X- and Z-type boron-containing palladium pincer complexes.

	61 (L-type)	**60** (X-type)	**59** (Z-type)
Ligand formula	L_2BX	LBX_2	BX_3
d_{Pd-B}/Å	2.129	2.196	2.650
d_{Pd-P}/Å	2.203–2.204	2.275–2.284	2.288–2.315
Σ_{Bz}/°	319–343	331	355
δ_B/ ppm	−24.5	17	59
q_B (NBO)/e	−0.848	+0.434	+0.902
ρ_B/ e·Å^{-3}	0.091	0.086	0.020
H*bcp* (Pd-B)/ Ha·Å^{-3}	−0.037	−0.029	−0.009

Please cite this article in press as: L. Maser et al., Polyhedron (2017), https://doi.org/10.1016/j.poly.2017.09.009

4.4. Pincer ligands based on tricoordinate boron (Z-type)

The first examples for tridentate ligands with tricoordinate boron in the central position were borane or boratrane complexes. *Hill* and co-workers reported the formation of the ruthenium boratrane complex **62** from a poly(azolyl)borate via B-H activation with a ruthenium complex (Fig. 13) [115]. In the following years, metallaboratranes were explored further using similar ligand scaffolds (for a more detailed review see [111]). In 2007 *Bourissou*, *Maron* and co-workers found the first borane-based pincer-type ligand, whose central BR_3-group acts as a Z-type ligand for AuCl (complex **63**) [116]. Interestingly, the formed complex exhibits a square-planar coordination geometry and at the same time the formal oxidation state of the gold atom was demonstrated to be +I. This shows the unusual bonding modes which are possible with borane-ligands.

In these complexes, the metal-atom donates electron density towards the boron atom, which has a pyramidalized coordination sphere. Since a borane does not have any electrons left for bonding with a metal, the metal-boron bond is solely a donor bond from the metal to the borane atom, which is in line with the description of a σ-acceptor [111].

Complexes with Z-type ligands based on boron react with dihydrogen to hydrido hydridoborate complexes [117–119]. Mechanistic investigations revealed a synergistic heterolytic cleavage as the most likely pathway, in which a hydride is transfered to the borane and oxidative protonation of the metal center occurs (Fig. 15) [105].

4.5. Pincer ligands based on tricoordinate boron (L-type)

For the third complex type, the L-type borylenes, only few examples are known so far. This is mostly owed to the high reactivity of borylenes.

So far, free borylenes RB: have not been isolated at ambient conditions. A few examples were observed in the gas-phase or with matrix isolation techniques at low temperatures [120–123]. Only when σ-donating and π-accepting substituents are installed at the boron atom, borylenes can be isolated in synthetic amounts. The first example was reported by *Bertrand* and co-workers with cyclic (alkyl)(amino) carbenes [124]. Because of their filled p_z-orbital, borylenes act as strong σ-donors in transition metal complexes. In 2014, the group of *Kinjo* was able to isolate the first borylene (chromium) complex, using an oxazol-2-ylidenes to stabilize a PhB: fragment [125].

For the incorporation of borylenes as strong σ-donors in pincer ligands, so far only one ligand type is known. Recently, our group showed that phosphine-stabilized borylenes can be employed as PBP-pincer complexes of type **64** for iron and palladium (Fig. 14) [4,112]. Metal complexes containing a non-stabilized borylene can react with H_2 by a symmetric insertion into the boron-metal bond to σ-coordinated borane-ligands (Fig. 15) [126]. Recent studies on pincer-type complexes with a ligand-stabilized borylene as central donor group showed that they are able to undergo reversible intramolecular redox-processes by B-H reductive elimination between the ligand and the metal [4]. Since boryls and borylenes are more reactive and even stronger donors than their N- and C-based analogues, using them in pincer ligands seems very attractive in order to control the reactivity.

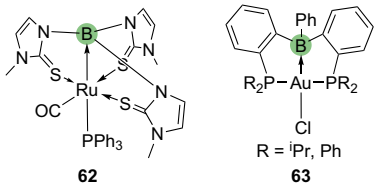

Fig. 13. First example of a metallaboratrane by *Hill* (left) and first pincer borane complex by *Bourissou* (right) [115,116].

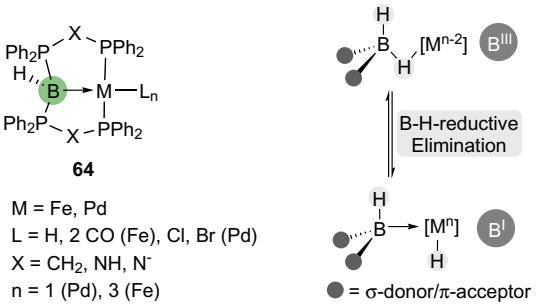

Fig. 14. Borylene-based pincer ligands in transition metal complexes.

5. Comparison

Although amines (**A**), ligand-stabilized borylenes (**B**) and protonated carbodiphosphoranes (**C**) as well as carbanions are formally isoelectronic, there are significant differences in the geometry and the bonding (Fig. 16). In agreement with the VSEPR theory, amines exhibit a trigonal pyramidal or pseudo-tetrahedral geometry, which is best explained by hybridization of *s*- and *p*-orbitals to sp^3-orbitals. Ligand-stabilized borylenes and protonated carbodiphosphoranes in contrast, are trigonal planar and require π-accepting substituents L to stabilize the occupied p_z-orbital. A closer look on the bonding situation of **B** and **C** reveals that the highest occupied molecular orbital (HOMO) in these two compound classes is of π-type symmetry [127], illustrating a significant degree of π-back-bonding from the central boron or carbon atom to the π-accepting substituent. The deprotonation of secondary amines (**C**) is easily achieved with a number of bases, leading to metal amides, an important class of compounds and bases. In a similar manner, species like **B** can be deprotonated. The deprotonation of ligand-stabilized borylenes **B** to species like **D** has not been reported so far (Fig. 17). The proton affinity of secondary amines **A** (930–980 kJ mol^{-1}) is significantly lower than for neutral borylene species **B** (1221 kJ mol^{-1}, L = PPh_3). With 779 kJ mol^{-1} the cationic species **C** exhibits the lowest proton affinity among this series.

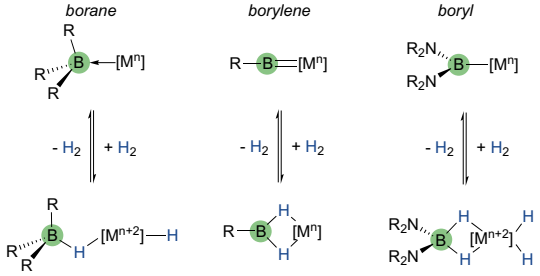

Fig. 15. Known reactivity patterns of borane, borylene and boryl complexes towards dihydrogen.

Please cite this article in press as: L. Maser et al., Polyhedron (2017), https://doi.org/10.1016/j.poly.2017.09.009

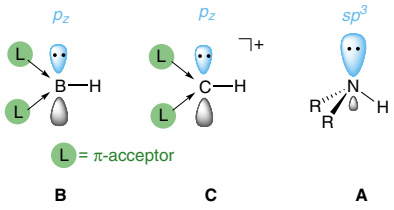

Fig. 16. Structural differences between ligand-stabilized borylens, protonated carbodiphosphoranes and amines.

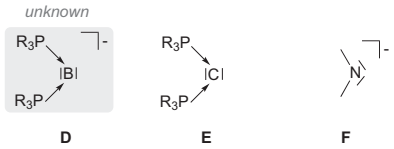

Fig. 17. Deprotonation products of **A**–**C**.

However, the neutral carbodiphosphoranes (**E**) exhibit higher proton affinities than secondary amines, but lower affinities than the corresponding anionic amides **F** (1600–1700 kJ mol^{-1}). When employed as ligands in a transition metal complex, the metal-bound atom E in the discussed ligands adopts a tetrahedral environment (E = B, C, N). Representative examples of transition metal complexes show fundamentally different reaction pathways for boron- and nitrogen-based ligands: secondary amines are well known to act as a proton source, which is capable of protonating metal hydrides as well as binding substrates by hydrogen bonds (Fig. 18). Boron based ligands act either as cooperative Lewis-acid, like boranes, or they exhibit a distinct redox reactivity, which leads to a reversible reduction of the coordinated metal center [4]. As gap-bridging element, different carbon-based ligands show facets of both types of reactivity: while protonated carbodiphosphoranes are not known to be redox active, they can easily be deprotonated. Like with amines, β-hydride elimination can occur with alkyl-based pincer-type complexes. However, the formation of carbene complexes is known as well, and a reductive elimination could not be ruled out as an exchange pathway for iridium complexes.

6. Conclusion

The widespread applications of pincer-type complexes were subjected in several reviews and the interest in this class of compounds is continuously increasing. The key-feature of this ligand class is the meridonal coordination mode with all donor groups in one plane, leading to a *trans*-arrangement of the terminal donor groups. Generally, this provides an enhanced stability of the corresponding transition metal complexes and has led to major breakthroughs in organometallic chemistry and catalysis in the last decades. The enhanced stability in combination with unusual donor properties or cooperative behavior of the central donor group developed into a fruitful concept in homogenous catalysis. The ability of donor groups to participate in important reaction steps lowers reaction barriers and can open entirely new directions in catalysis. In this context, it is worth noting that novel reactivity patterns between a coordinated ligand and the central metal atom can be potentially applied in cooperative bond activation.

One of the most successfully applied, cooperative pincer-type ligands are based on amines. In the current review, we compared five different classes of pincer-type ligands based on the elements nitrogen, carbon and boron. The isoelectronic donor groups in these ligands show different reactivity patterns, ranging from proton transfer and β-hydride elimination for amines to redox activity and Lewis-acid cooperativity of ligand-stabilized borylenes and boranes. Numerous applications of pincer-type complexes with different central groups as catalysts have been discussed in this review, highlighting the enormous potential of cooperative pincer-type ligands. Although detailed mechanistic information about the catalytic reactions discussed herein is limited, the reviewed

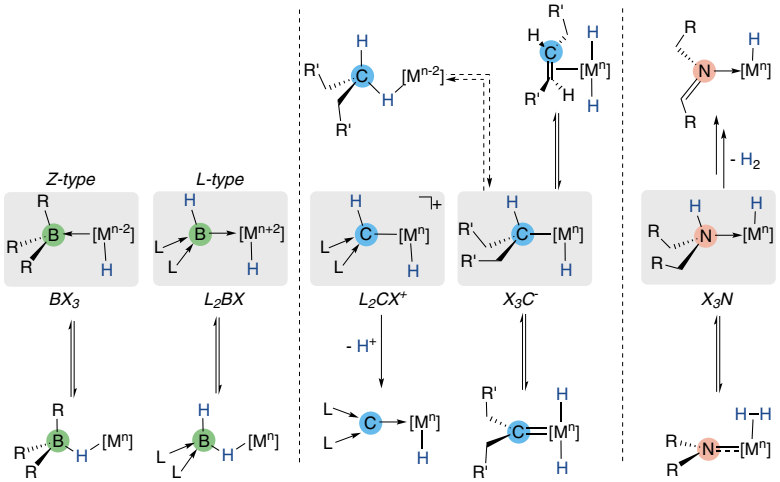

Fig. 18. Comparison of reactivity patterns in metal complexes containing tricoordinated boron (left), carbodiphosphoranes or alkyls (middle) and secondary amines (right) as ligands.

Please cite this article in press as: L. Maser et al., Polyhedron (2017), https://doi.org/10.1016/j.poly.2017.09.009

examples show that the investigation of novel reactivity patterns has the potential to open new directions in cooperative catalysis.

Acknowledgement

We gratefully acknowledge financial support from the Deutsche Forschungsgemeinschaft (LA 2830/3-2), the Erich-Becker-Stiftung (R. L.) and the Studienstiftung des deutschen Volkes (L. V.).

References

[1] Based on a web of science search for the keyword pincer 18.06.2017.
[2] Y. Tulchinsky, M.A. Iron, M. Botoshansky, M. Gandelman, Nat. Chem. 3 (7) (2011) 525.
[3] Y. Tulchinsky, S. Kozuch, P. Saha, M. Botoshansky, L.J.W. Shimon, M. Gandelman, Chem. Sci. 5 (4) (2014) 1305.
[4] L. Vondung, N. Frank, M. Fritz, L. Alig, R. Langer, Angew. Chem. Int. Ed. 55 (46) (2016) 14450.
[5] Y. Masuda, M. Hasegawa, M. Yamashita, K. Nozaki, N. Ishida, M. Murakami, J. Am. Chem. Soc. 135 (19) (2013) 7142.
[6] M. Hasegawa, Y. Segawa, M. Yamashita, K. Nozaki, Angew. Chem. Int. Ed. 51 (2012) 6956.
[7] Y. Segawa, M. Yamashita, K. Nozaki, Organometallics 28 (21) (2009) 6234.
[8] Y. Segawa, M. Yamashita, K. Nozaki, Science (80-) 314 (2006) 113.
[9] T.P. Lin, J.C. Peters, J. Am. Chem. Soc. 135 (41) (2013) 15310.
[10] Y. Li, C. Hou, J. Jiang, Z. Zhang, C. Zhao, A.J. Page, Z. Ke, ACS Catal. 6 (3) (2016) 1655.
[11] D.A. Valyaev, O.A. Filippov, N. Lugan, G. Lavigne, N.A. Ustynyuk, Angew. Chem. Int. Ed. 54 (21) (2015) 6315.
[12] A.F. Hill, C.M.A. Mcqueen, Organometallics 31 (23) (2012) 8051.
[13] A. Plikhta, A. Pöthig, E. Herdtweck, B. Rieger, Inorg. Chem. 54 (19) (2015) 9517.
[14] A. Eizawa, K. Arashiba, H. Tanaka, S. Kuriyama, Y. Matsuo, K. Nakajima, K. Yoshizawa, Y. Nishibayashi, Nat. Commun. 8 (2017) 14874.
[15] Y. Tulchinsky, S. Kozuch, P. Saha, A. Mauda, G. Nisnevich, Chem. Eur. J. 21 (2015) 7099.
[16] H. Grützmacher, Angew. Chem. Int. Ed. 47 (10) (2008) 1814.
[17] C. Gunanathan, D. Milstein, Science (80-) 341 (2013), 1229712–1229712.
[18] J.R. Khusnutdinova, D. Milstein, Angew. Chem. Int. Ed. 54 (42) (2015) 12236.
[19] D.G.H. Hetterscheid, S.H. Chikkali, B. DeBruin, J.N.H. Reek, ChemCatChem 5 (10) (2013) 2785.
[20] S. Schneider, J. Meiners, B. Askevold, Eur. J. Inorg. Chem. 3 (2012) 412.
[21] J.I. Van Der Vlugt, Eur. J. Inorg. Chem. 3 (2012) 363.
[22] P.A. Dub, T. Ikariya, ACS Catal. 2 (8) (2012) 1718.
[23] R. Noyori, T. Ohkuma, Angew. Chem. Int. Ed. 40 (1) (2001) 40.
[24] P.A. Dub, J.C. Gordon, Dalton Trans. 45 (16) (2016) 6756.
[25] P.A. Dub, T. Ikariya, J. Am. Chem. Soc. 135 (7) (2013) 2604.
[26] P.A. Dub, N.J. Henson, R.L. Martin, J.C. Gordon, J. Am. Chem. Soc. 136 (9) (2014) 3505.
[27] B. Zhao, Z. Han, K. Ding, Angew. Chem. Int. Ed. 52 (18) (2013) 4744.
[28] W. Kuriyama, T. Matsumoto, O. Ogata, Y. Ino, K. Aoki, S. Tanaka, K. Ishida, T. Kobayashi, N. Sayo, T. Saito, Org. Process Res. Dev. 16 (1) (2012) 166.
[29] S. Werkmeister, K. Junge, B. Wendt, E. Alberico, H. Jiao, W. Baumann, H. Junge, F. Gallou, M. Beller, Angew. Chem. Int. Ed. 53 (33) (2014) 8722.
[30] M. Perez, S. Elangovan, A. Spannenberg, K. Junge, M. Beller, ChemSusChem 10 (1) (2017) 83.
[31] M. Peña-López, H. Neumann, M. Beller, ChemCatChem 7 (5) (2015) 865.
[32] N.T. Fairweather, M.S. Gibson, H. Guan, Organometallics 34 (1) (2015) 335.
[33] J.F. Sonnenberg, A.J. Lough, R.H. Morris, Organometallics 33 (22) (2014) 6452.
[34] F. Kallmeier, T. Irrgang, T. Dietel, R. Kempe, Angew. Chem. Int. Ed. 55 (39) (2016) 11806.
[35] S. Elangovan, C. Topf, S. Fischer, H. Jiao, A. Spannenberg, W. Baumann, R. Ludwig, K. Junge, M. Beller, J. Am. Chem. Soc. 138 (28) (2016) 8809.
[36] P.O. Lagaditis, P.E. Sues, J.F. Sonnenberg, K.Y. Wan, A.J. Lough, R.H. Morris, J. Am. Chem. Soc. 136 (4) (2014) 1367.
[37] E.A. Bielinski, P.O. Lagaditis, Y. Zhang, B.Q. Mercado, C. Würtele, W.H. Bernskoetter, N. Hazari, S. Schneider, J. Am. Chem. Soc. 136 (29) (2014) 10234.
[38] S. Chakraborty, W.W. Brennessel, W.D. Jones, J. Am. Chem. Soc. 136 (24) (2014) 8564.
[39] S. Chakraborty, H. Dai, P. Bhattacharya, N.T. Fairweather, M.S. Gibson, J.A. Krause, H. Guan, J. Am. Chem. Soc. 136 (22) (2014) 7869.
[40] M.B. Widegren, G.J. Harkness, A.M. Slawin, D.B. Cordes, M.L. Clarke, A Highly Active Manganese Catalyst for Enantioselective Ketone and Ester Hydrogenation, 2017.
[41] S. Elangovan, M. Garbe, H. Jiao, A. Spannenberg, K. Junge, M. Beller, Angew. Chem. Int. Ed. 55 (49) (2016) 15364.
[42] E. Alberico, P. Sponholz, C. Cordes, M. Nielsen, H.-J. Drexler, W. Baumann, H. Junge, M. Beller, Angew. Chem. Int. Ed. 52 (52) (2013) 14162.
[43] E.A. Bielinski, M. Förster, Y. Zhang, W.H. Bernskoetter, N. Hazari, M.C. Holthausen, ACS Catal. 5 (4) (2015) 2404.
[44] F. Schneck, M. Assmann, M. Balmer, K. Harms, R. Langer, Organometallics 35 (11) (2016) 1931.
[45] G.A. Filonenko, M.J.B. Aguila, E.N. Schulpen, R. van Putten, J. Wiecko, C. Müller, L. Lefort, E.J.M. Hensen, E.A. Pidko, J. Am. Chem. Soc. 137 (24) (2015) 7620.
[46] D. Spasyuk, S. Smith, D.G. Gusev, Angew. Chem. Int. Ed. 52 (9) (2013) 2538.
[47] M. Yamakawa, H. Ito, R. Noyori, J. Am. Chem. Soc. 122 (7) (2000) 1466.
[48] A. Friedrich, M. Drees, J.S. Auf Der Günne, S. Schneider, J. Am. Chem. Soc. 131 (48) (2009) 17552.
[49] D. Gelman, S. Musa, ACS Catal. 2 (12) (2012) 2456.
[50] B.L. Shaw, J. Organomet. Chem. 200 (1980) 307.
[51] C. Crocker, R.J. Errington, W.S. McDonald, K.J. Odell, B.L. Shaw, R.J. Goodfellow, J. Chem. Soc., Chem. Commun. (498) (1979) 498.
[52] R.J. Errington, W.S. McDonald, B.L. Shaw, J. Chem. Soc., Dalton Trans. 2 (9) (1982) 1829.
[53] H.D. Empsall, E.M. Hyde, R. Markham, W.S. McDonald, M.C. Norton, B.L. Shaw, B. Weeks, J. Chem. Soc. Chem. Commun. 006 (17) (1977) 589.
[54] J. Zhou, J.F. Hartwig, Angew. Chem. Int. Ed. 47 (31) (2008) 5783.
[55] D.G. Gusev, A.J. Lough, Organometallics 21 (13) (2002) 2601.
[56] F. Ramirez, N.B. Desai, B. Hansen, N. McKelvie, J. Am. Chem. Soc. 83 (16) (1961) 3539.
[57] H. Schmidbaur, Nachrichten aus Chemie, Tech. und Lab. 27 (10) (1979) 620.
[58] H. Schmidbaur, Angew. Chem. Int. Ed. 22 (12) (1983) 907.
[59] H. Schmidbaur, Angew. Chem. 95 (12) (1983) 980.
[60] O.I. Kolodiazhnyi, Tetrahedron 52 (6) (1996) 1855.
[61] R. Tonner, F. Öxler, B. Neumüller, W. Petz, G. Frenking, Angew. Chem. 118 (47) (2006) 8206.
[62] R. Tonner, F. Öxler, B. Neumüller, W. Petz, G. Frenking, Angew. Chem. Int. Ed. 45 (47) (2006) 8038.
[63] R. Tonner, G. Frenking, Chem. – A Eur. J. 14 (11) (2008) 3260.
[64] G. Frenking, R. Tonner, Pure Appl. Chem. 81 (2009) 4.
[65] C.A. Dyker, V. Lavallo, B. Donnadieu, G. Bertrand, Angew. Chem. Int. Ed. 47 (17) (2008) 3206.
[66] C.A. Dyker, G. Bertrand, Nat. Chem. 1 (4) (2009) 265.
[67] M. Melaimi, P. Parameswaran, B. Donnadieu, G. Frenking, G. Bertrand, Angew. Chem. Int. Ed. 48 (26) (2009) 4792.
[68] D. Himmel, I. Krossing, A. Schnepf, Angew. Chem. Int. Ed. 53 (2) (2014) 370.
[69] D. Himmel, I. Krossing, A. Schnepf, Angew. Chem. 126 (2) (2014) 378.
[70] D. Himmel, I. Krossing, A. Schnepf, Angew. Chem. Int. Ed. 53 (24) (2014) 6047.
[71] D. Himmel, I. Krossing, A. Schnepf, Angew. Chem. 126 (24) (2014) 6159.
[72] P.J. Quinlivan, G. Parkin, Inorg. Chem. 56 (10) (2017) 5493.
[73] W.C. Kaska, D.K. Mitchell, R. Reichelderfer, J. Organomet. Chem. 47 (2) (1973) 391.
[74] W.C. Kaska, D.K. Mitchell, R.F. Reichelderfer, W.D. Korte, J. Am. Chem. Soc. 96 (9) (1974) 2847.
[75] W. Petz, F. Weller, J. Uddin, G. Frenking, Organometallics 18 (4) (1999) 619.
[76] K. Kubo, N.D. Jones, M.J. Ferguson, R. McDonald, R.G. Cavell, J. Am. Chem. Soc. 127 (15) (2005) 5314.
[77] W. Petz, C. Kutschera, M. Heitbaum, G. Frenking, R. Tonner, B. Neumüller, Inorg. Chem. 44 (5) (2005) 1263.
[78] R. Tonner, G. Frenking, Chem. – A Eur. J. 14 (11) (2008) 3273.
[79] G. Frenking, R. Tonner, S. Klein, N. Takagi, T. Shimizu, A. Krapp, K.K. Pandey, P. Parameswaran, Chem. Soc. Rev. 43 (14) (2014) 5106.
[80] W. Petz, G. Frenking, Carbodiphosphoranes and Related Ligands (2010) 49.
[81] W. Petz, Coord. Chem. Rev. 291 (2015) 1.
[82] W. Petz, B. Neumüller, Polyhedron 30 (11) (2011) 1779.
[83] K. Kubo, H. Okitsu, H. Miwa, S. Kume, R.G. Cavell, T. Mizuta, Organometallics 36 (2) (2017) 266.
[84] S. Stallinger, C. Reitsamer, W. Schuh, H. Kopacka, K. Wurst, P. Peringer, Chem. Commun. 012 (5) (2007) 510.
[85] C. Reitsamer, W. Schuhe, H. Kopacka, K. Wurst, P. Peringer, Organometallics 28 (22) (2009) 6617.
[86] C. Reitsamer, W. Schuh, H. Kopacka, K. Wurst, E.P. Ellmerer, P. Peringer, Organometallics 30 (15) (2011) 4220.
[87] C. Reitsamer, S. Stallinger, W. Schuh, H. Kopacka, K. Wurst, D. Obendorf, P. Peringer, Dalton Trans. 41 (12) (2012) 3503.
[88] C. Reitsamer, I. Hackl, W. Schuh, H. Kopacka, K. Wurst, P. Peringer, J. Organomet. Chem. 830 (2017) 150.
[89] S.T. Liddle, D.P. Mills, A.J. Wooles, Chem. Soc. Rev. 40 (5) (2011) 2164.
[90] W. Petz, I. Kuzu, G. Frenking, D.M. Andrada, B. Neumüller, M. Fritz, J.E. Münzer, Chem. – A Eur. J. 22 (25) (2016) 8536.
[91] V.S. Bryantsev, M.S. Diallo, W.A. Goddard, J. Phys. Chem. A 111 (20) (2007) 4422.
[92] E.P.L. Hunter, S.G. Lias, J. Phys. Chem. Ref. Data 27 (3) (1998) 413.
[93] G. Raabe, Y. Wang, J. Fleischhauer, Zeitschrift für Naturforsch. A 55 (2000) 8.
[94] Y. Segawa, M. Yamashita, K. Nozaki, J. Am. Chem. Soc. 131 (2009) 9201.
[95] A.F. Hill, S.B. Lee, J. Park, R. Shang, A.C. Willis, Organometallics 29 (21) (2010) 5661.
[96] H. Ogawa, M. Yamashita, Dalton Trans. 42 (3) (2013) 625.
[97] T. Miyada, M. Yamashita, Organometallics 32 (19) (2013) 5281.
[98] T.P. Lin, J.C. Peters, J. Am. Chem. Soc. 136 (39) (2014) 13672.
[99] N. Curado, C. Maya, J. López-Serrano, A. Rodríguez, Chem. Commun. 50 (99) (2014) 15718.
[100] A.F. Hill, C.M.A. McQueen, Organometallics 33 (8) (2014) 1977.
[101] T. Miyada, E. Huang Kwan, M. Yamashita, Organometallics 33 (23) (2014) 6760.
[102] K. Tanoue, M. Yamashita, Organometallics 34 (16) (2015) 4011.
[103] E.H. Kwan, Y.J. Kawai, S. Kamakura, M. Yamashita, Dalton Trans. 13 (c) (2016) 15931.

Please cite this article in press as: L. Maser et al., Polyhedron (2017), https://doi.org/10.1016/j.poly.2017.09.009

[104] C.M.A. McQueen, A.F. Hill, M. Sharma, S.K. Singh, J.S. Ward, A.C. Willis, R.D. Young, Polyhedron 120 (2016) 185.
[105] W.-C. Shih, W. Gu, M.C. MacInnis, S.D. Timpa, N. Bhuvanesh, J. Zhou, O.V. Ozerov, J. Am. Chem. Soc. 138 (7) (2016) 2086.
[106] A.M. Spokoyny, M.G. Reuter, C.L. Stern, M.A. Ratner, T. Seideman, C.A. Mirkin, J. Am. Chem. Soc. 131 (27) (2009) 9482.
[107] M.Y. Tsang, C. Viñas, F. Teixidor, J.G. Planas, N. Conde, R. SanMartin, M.T. Herrero, E. Domínguez, A. Lledós, P. Vidossich, D. Choquesillo-Lazarte, Inorg. Chem. (2014).
[108] M.E. El-Zaria, H. Arii, H. Nakamura, Inorg. Chem. 50 (9) (2011) 4149.
[109] B.J. Eleazer, M.D. Smith, D.V. Peryshkov, J. Organomet. Chem. 829 (2017) 42.
[110] M. Green, J. Organomet. Chem. 500 (1–2) (1995) 127.
[111] H. Braunschweig, R.D. Dewhurst, A. Schneider, Chem. Rev. 110 (2010) 3924.
[112] M. Grätz, A. Bäcker, L. Vondung, L. Maser, A. Reincke, R. Langer, Chem. Commun. (2017) 1.
[113] D. Schuhknecht, F. Ritter, M.E. Tauchert, Chem. Commun. 52 (79) (2016) 11823.
[114] S. Bontemps, M. Sircoglou, G. Bouhadir, H. Puschmann, J.A.K. Howard, P.W. Dyer, K. Miqueu, D. Bourissou, Chem. – A Eur. J. 14 (2) (2008) 731.
[115] A. Hill, G. Owen, A. White, D. Williams, Angew. Chem. Int. Ed. 38 (18) (1999) 2759.
[116] M. Sircoglou, S. Bontemps, M. Mercy, N. Saffon, M. Takahashi, G. Bouhadir, L. Maron, D. Bourissou, Angew. Chem. Int. Ed. 46 (45) (2007) 8583.
[117] N. Tsoureas, Y.-Y. Kuo, M.F. Haddow, G.R. Owen, Chem. Commun. 47 (1) (2011) 484.
[118] W.H. Harman, J.C. Peters, J. Am. Chem. Soc. 134 (11) (2012) 5080.
[119] H. Fong, M.E. Moret, Y. Lee, J.C. Peters, Organometallics 32 (2013) 3053.
[120] P.L. Timms, J. Am. Chem. Soc. 89 (6) (1967) 1629.
[121] M. Nomoto, T. Okabayashi, T. Klaus, M. Tanimoto, J. Mol. Struct. 413–414 (1997) 471.
[122] L. Andrews, P. Hassanzadeh, J.M.L. Martin, P.R. Taylor, J. Phys. Chem. 97 (22) (1993) 5839.
[123] H.F. Bettinger, J. Am. Chem. Soc. 128 (8) (2006) 2534.
[124] R. Kinjo, B. Donnadieu, M.A. Celik, G. Frenking, G. Bertrand, Science 333 (2011) 610.
[125] L. Kong, Y. Li, R. Ganguly, D. Vidovic, R. Kinjo, Angew. Chem. Int. Ed. 53 (35) (2014) 9280.
[126] G. Alcaraz, U. Helmstedt, E. Clot, L. Vendier, S. Sabo-Etienne, J. Am. Chem. Soc. 130 (39) (2008) 12878.
[127] M.A. Celik, R. Sure, S. Klein, R. Kinjo, G. Bertrand, G. Frenking, 2012, 0403, 5676–5692.

Please cite this article in press as: L. Maser et al., Polyhedron (2017), https://doi.org/10.1016/j.poly.2017.09.009

JACS
JOURNAL OF THE AMERICAN CHEMICAL SOCIETY
Article
Cite This: J. Am. Chem. Soc. 2019, 141, 7596−7604
pubs.acs.org/JACS

Quantifying the Donor Strength of Ligand-Stabilized Main Group Fragments

Leon Maser, Christian Schneider, Lisa Vondung, Lukas Alig, and Robert Langer*

Department of Chemistry, Philipps-Universität Marburg, Hans-Meerwein-Str. 4, 35032 Marburg, Germany

Supporting Information

ABSTRACT: Unusual binding properties, enabling the stabilization of elusive species, and beneficial properties for homogeneous catalysts have been predicted and demonstrated for ligand-stabilized main group fragments, such as carbodiphosphoranes and -carbenes. However, the quantification and comparison of their binding properties by experimental means still represent major challenges. In this article, we describe a series of iridium(III) pincer complexes of the type $[(PEP)IrCl(CO)(H)]^q$ enabling the quantification of the donor strength of the central donor group E (q = 0, +1, +2). Our investigations show that phosphine-stabilized boron(I) and carbon(0) compounds are exceptionally strong neutral donor groups in comparison to common spectator ligands in homogeneous catalysis such as carbenes and phosphines. Our experimental and computational results for the first time allow and justify the comparison of the donor strength of cationic, neutral, and anionic ligands. On the basis of quantum chemical investigations, we further demonstrate that the heavier homologues of phosphine-stabilized borylenes and carbon(0) compounds exhibit slightly diminished donor properties.

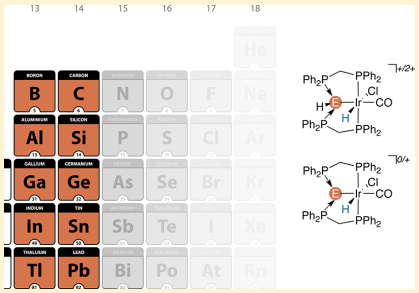

INTRODUCTION

The nucleophilicity of electron-rich main group compounds and fragments, often stabilized by supporting ligands or substituents, can be illustrated by coordination to suitable metal centers.[1−8] All too often, their application as ligands in transition-metal complexes is limited only to exemplify their nucleophilic nature, whereas their coordination chemistry has not yet been systematically explored. In homogeneous catalysis, neutral ligands with tunable steric and electronic properties can serve as versatile spectator ligands.[9−11] Thus, the investigation of the coordination properties of nucleophilic main group compounds generally offers the potential to replace common spectator ligands, such as phosphines and carbenes. Substituting these by more powerful alternatives may facilitate new catalytic reactions. In particular, increased donor abilities of ancillary ligands can enable unusual bond activations and speed up precatalyst activation.[12−16]

In this context, we became interested in the coordination chemistry of nucleophilic boron compounds, specifically phosphine-stabilized borylenes[17−21] and their heavier homologues. In recent years, it has been a matter of particular interest as to whether neutral, tricoordinate boron compounds can serve as electron-donating ligands rather than pure acceptor ligands, as they are commonly viewed. Notably, a majority of tricoordinate boron compounds of the type BR_3 are known to act as Lewis acids and σ-accepting or Z-type ligands in transition-metal complexes.[22−25] By manipulation of the R substituents in BR_3, it is possible to cause a dramatic change in these properties: formally anionic substituents, such as hydrides, alkyls, aryls, halogenides, and most anionic N-heterocycles lead to classical Lewis acids or Z-type ligands.[22,26−58] In these cases, the vacant p_z-orbital of the trigonal planar boron compound is stabilized either by π-donation of the substituents or by dimerization and the formation of two-electron, three-center bonds. Replacing one of the substituents R on boron by a neutral σ-donating and π-accepting substituent L formally results in a partially filled p_z-orbital at the boron atom in BR_2L. This ligand-stabilized boryl ligand acts as an X-type ligand and contributes one electron to a covalent bond. In the absence of a neutral, stabilizing substituent, X-type boryl ligands BR_2 result.[59−61] If a second anionic substituent at boron is replaced by a neutral σ-donating and π-accepting substituent, then the p_z-orbital is filled and stabilized by π-accepting substituents. The resulting boron compounds BRL_2 now act as Lewis bases or L-type ligands.[1,2,5,62−68]

The direct coordination to transition metals was documented for only a few isolable nucleophilic boron compounds.[2,65] Based on chemical intuition, we expect these ligand-stabilized main group fragments to be very strong donor ligands, but quantification often represents a major challenge. As the strong donor ability is accompanied by increased reducing properties,[69] the reaction with the metal complexes may result in metal reduction rather than coordination of the main group fragment. Drawing from our experience with iron

Received: March 14, 2019
Published: April 17, 2019

DOI: 10.1021/jacs.9b02598
J. Am. Chem. Soc. 2019, 141, 7596−7604

and palladium complexes,[70,71] we herein developed a simple synthesis protocol that allows the stabilization of a number of main group fragments as donor groups in iridium pincer complexes by the oxidative addition of suitable preligands. The analysis of these complexes by experimental and quantum chemical methods reveals that ligands of the type BRL_2 are exceptionally strong and neutral donor ligands in comparison to common spectator ligands in organometallic chemistry and homogeneous catalysis (Chart 1). It is further demonstrated

Chart 1. (Top) Common Spectator Ligands in Coordination Chemistry and Homogeneous Catalysis, Ordered by Their Donor Strength According to the Tolman Electronic Parameter (TEP) and (Bottom) Reported Phosphine-Stabilized Group 13 and 14 Fragments with Their Approximate TEP Range

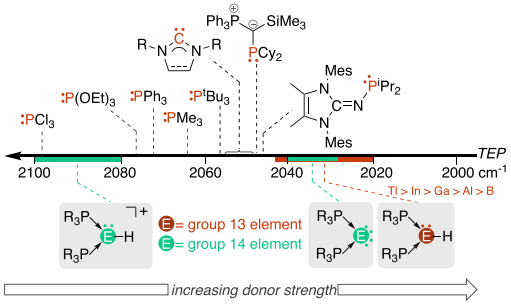

that heavier homologues also act as strong donor ligands, but because of the stabilization of s-orbitals with increasing atomic number, the geometry of the donor fragment is less favorable for efficient orbital overlap with the central metal atom. Overall, our results suggest that neutral donor ligands based on tricoordinate boron should be superb spectator ligands in homogeneous catalysis.

RESULTS AND DISCUSSION

Preligands **a**–**h** exhibit two terminal PPh_2 groups and a central group with at least one E–H bond (Chart 2), which ranges from simple ammonium (**c**), pyridinium (**b**), and imidazolium ions (**d**) to mono- (**e**) and diprotonated carbodiphosphoranes (**a**), a bisphosphino-boronium ion (**f**), and aryl (**g**) and alkyl moieties (**h**). A series of isotypical iridium pincer complexes with different central donor groups were synthesized by E–H oxidative addition of preligands **a**–**h** to $[IrCl(CO)(PPh_3)_2]$ or $[IrCl(CO)_2(p\text{-}NH_2\text{–}C_6H_4\text{–}CH_3)]$. In most cases, the reaction with both complexes results in the formation of the desired complexes (**1a**–**h**) as major products, but only the best method is reported for each complex, respectively. The resulting iridium(III) complexes of the type $[(\kappa^3P,E,P\text{-PEP})IrCl(CO)(H)]^q$ (**1a**–**h**, q = 0, +1, +2) were characterized by means of single-crystal XRD (Figure 1), mass spectrometry, and multinuclear NMR and IR spectroscopy, clearly indicating the presence of an iridium(III) complex for each investigated ligand.

Resonances between −7.5 and 32.1 ppm are observed in the $^{31}P\{^1H\}$ NMR spectra for the two terminal, magnetically equivalent PPh_2 groups, which adopt a *trans*-orientation in iridium complexes **1a**–**h**. The E–H oxidative addition leads to the formation of a hydrido ligand, which gives rise to specific

Chart 2. Synthesis of Iridium(III) Pincer-Type Complexes 1a–h ($L^1 = L^2 = PPh_3$; L^1 = CO, L^2 = p-$H_2N\text{–}C_6H_4\text{–}CH_3$, X = Cl, Br)

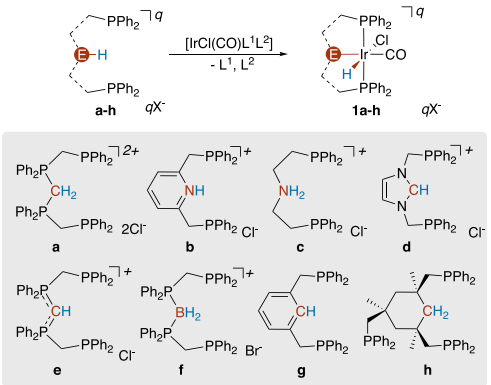

triplet resonances between −14.38 and −17.74 ppm in the ^1H NMR spectra of **1a**–**h**.

Among this series of iridium complexes (**1a**–**h**), we characterized the unusual iridium complex **1f** with a neutral central donor group based on tricoordinate boron. The ^{11}B chemical shift of −31.1 ppm and all other spectroscopic data are in line with previously reported complexes of tricoordinate, nucleophilic boron compounds.[2,65,72] The molecular structures of **1a**–**h** in the solid state display an octahedral coordination environment with a meridionally coordinated pincer ligand. The carbonyl ligand is situated in the position *trans* to the central donor group of the pincer ligand, while the hydrido and the chlorido ligands occupy two opposing vertices. Further evidence for the presence of iridium(III) and electron donors in **1a**–**h** is provided by the τ_5 parameter of the pentacoordinated iridium fragment $[(R_3P)_2IrCl(CO)(H)]$ (= ML_5) without the central donor group (Table 1).[73] If a Z-type ligand is present, then no significant change to the coordination geometry of the metal upon coordination of the ML_5 fragment is expected.[22] Thus, a Z-type ligand would bridge an edge of a trigonal bipyramid ($\tau_5 \approx 1$) in an ML_5Z complex. With the observed τ_5 values of 0.01–0.22, clearly a square-pyramidal fragment ML_5 is present, with the L-type donor groups in **1a**–**h** occupying a vertex of the octahedral coordination polyhedron.

The Ir–P bond lengths to the terminal PPh_2 groups in **1a**–**h** are found to be very similar (2.293–2.347 Å), along with the Ir–Cl bond lengths (2.457–2.536 Å). The ^{31}P NMR chemical shifts assignable to the iridium-bound PPh_2 groups for ligands of the type (dppm)$_2$E (E = CH^+ (**1a**), C (**1e**) and BH (**1f**)) range between 0.8 and 10.2 ppm, and the corresponding values of the remaining complexes are detected between 25.1 and 32.1 ppm. For complexes with a tetrahedral environment at the central donor group E (**1a**, **1c**, **1f**, and **1h**), two isomers can be observed, differing in the relative orientation of the hydrido ligand and the hydrogen atom bound to the central donor atom E. As depicted in Chart 3, *cis*- and *trans*-isomers can be defined, which are usually observed in solution and in the solid state. In case of **1a**, two independent molecules for *cis*- and *trans*-**1a** were refined in the crystal structure, while NMR spectra indicate the presence of an approximately 1:1 mixture

DOI: 10.1021/jacs.9b02598
J. Am. Chem. Soc. 2019, 141, 7596–7604

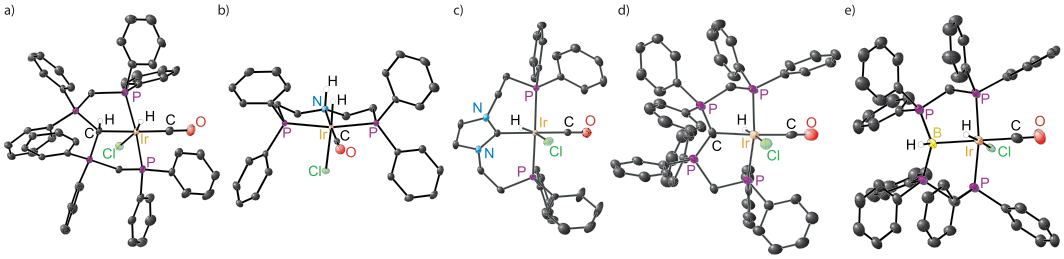

Figure 1. Selected molecular structures of cationic iridium pincer complexes in the solid state: **1a** (a), **1c** (b), **1d** (c), **1e** (d), and **1f** (e). (Ellipsoids are drawn at the 50% probability level, and hydrogen atoms of the CH_2 and phenyl groups are omitted for clarity.)

Table 1. Structural and Spectroscopic Data for 1a–h[a]

complex	donor group	τ_5[b]	d_{Ir-P}/Å	d_{Ir-Cl}/ Å	δ_P(Ir–P)/ppm	δ_H(Ir–H)/ppm	$\tilde{\nu}_{CO}$/cm^{-1}
cis-**1a**[c]	$(R_3P)_2CH^+$	0.05	2.335(3)–2.347(3)	2.500(3)	0.8	−15.88	2049
trans-**1a**[c]	$(R_3P)_2CH^+$	0.07	2.344(4)	2.479(5)	2.0	−14.38	2049
1b	pyridine	0.02	2.305(5)–2.333(6)	2.466(6)–2.553(6)	21.6	−14.90	2040
cis-**1c**	R_2NH	0.09	2.335(1)–2.336(1)	2.457(1)	29.4	−16.12	2030
trans-**1c**	R_2NH				30.8	−15.48	2030
1d	carbene	0.08–0.12	2.341(1)–2.355(1)	2.467(1)–2.477(1)	−7.8	−16.69	2040
1e	$(R_3P)_2C$	0.03	2.313(2)–2.337(2)	2.499(2)	7.8	−16.51	2015
cis-**1f**	$(R_3P)_2BH$	0.01	2.293(2)–2.305(2)	2.536(1)	11.6	−17.73	2015
trans-**1f**	$(R_3P)_2BH$				10.2	−16.66	2015
1g	$C_6R_2H_3^-$	0.22	2.307(1)–2.315(1)[d]	2.507(1)[d]	25.1[d]	−17.74[d]	2012
1h[e]	R_2CH^-		2.303(2)–2.306(2)	2.495(2)	32.1	−17.70	1992

[a]The structural data is derived from single-crystal diffraction experiments. NMR spectroscopic data was acquired in CD_2Cl_2 or CH_2Cl_2. [b]τ_5 parameter for the IrL_5 fragment (ref 73). [c]The crystal structure of **1a** contains two independent molecules of *cis*-**1a** and *trans*-**1a**. The latter is disordered with respect to the chloride and the hydrido ligands. [d]Reference 78. [e]Reference 79.

Chart 3. *cis*- and *trans*-Isomers in Iridium(III) Pincer-Type Complexes 1

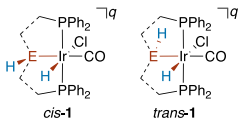

of both isomers in solution. In the crystal lattice of **1c** and **1f**, only the *cis*-isomer was detected. However, the NMR spectroscopic analysis of different crystalline samples always indicates the presence of minor quantities of the corresponding *trans*-isomer.

As isotypical complexes **1a–h** are sufficiently similar in their structural properties and mainly influenced by the properties of the central donor group, we used the C–O stretching vibration of the carbonyl ligand *trans* to the central donor group of interest as a qualitative measure of the net donor properties of the corresponding donor. With the ligand environment in **1a–h**, potential falsification by the coupling of vibrational modes or symmetry breaking of various donor groups is avoided. Although *cis*- and *trans*-isomers are detectable by NMR spectroscopy for donor atoms with tetrahedral environments, usually only one band is observed in the IR spectrum. This indicates that the difference between the isomers is lower than the resolution limit. Most importantly, the current setup allows us to obtain experimental values for rare cationic, neutral, and anionic ligands. For common electronic ligand parameters such as the Tolman electronic ligand parameter (TEP),[74] $[LRhCl(CO)_2]$[75] and $[LIrCl(CO)_2]$[76,77] are limited to neutral ligands and are strongly affected by the coupling of vibrational modes and the symmetry breaking of the different ligands.

A detailed comparison of IR spectra reveals that the formal charge of the central donor group has the strongest influence on the wavenumber corresponding to the C–O stretching vibration. Iridium complex **1a** with the cationic donor group $[(dppm)_2CH]^+$ exhibits the highest value (2049 cm^{-1}) and represents the weakest net donor. The iridium pincer complexes with neutral central donor groups (**1b–e**) give rise to lower values for $\tilde{\nu}_{CO}$ (2040 to 2015 cm^{-1}), while the complexes with anionic donor groups (**1g–h**) have the lowest values (2012 and 1996 cm^{-1}). Among the neutral pincer ligands, the net donor ability is found to increase in the order pyridine < R_2NH < $(R_3P)_2C$ ≈ $(R_3P)_2BH$. As the CDP-based group $(R_3P)_2C$ exhibits two lone pairs, enabling σ- and π-donation, the assumption that $(R_3P)_2BH$ with only one lone pair is the stronger σ-donor is justified.

The chemical shift of the triplet resonance for the hydrido ligand in the ^{1}H NMR spectra of **1a–h** can serve as an additional measure for the donor properties of the investigated central donor groups. These values range from −14.38 ppm for the cationic pincer ligand in *trans*-**1a** to −17.74 ppm for the anionic donor groups in **1g**.

On the basis of the framework of eight experimentally characterized iridium complexes (**1a–h**) and their measured values for the C–O stretching vibration, we started to use quantum chemical methods to (i) investigate the agreement between theory and experiment, (ii) shed light on the meaning of the obtained ligand parameter, and (iii) extend the number of examples, which provides the possibility to predict unknown molecules and to identify trends within the periodic table.

DOI: 10.1021/jacs.9b02598
J. Am. Chem. Soc. 2019, 141, 7596–7604

Chart 4. Iridium(III) Pincer-Type Complexes 1i−1q, 1a−1a[4], 1e−1e[2], 1f−1f[4], and 1q−1q[2] That Were Considered for Quantum Chemical Investigations in Addition to 1a−1h

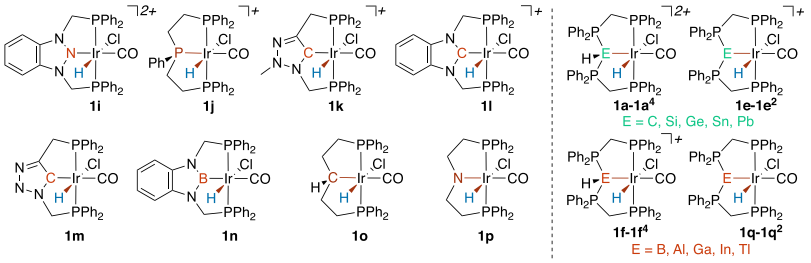

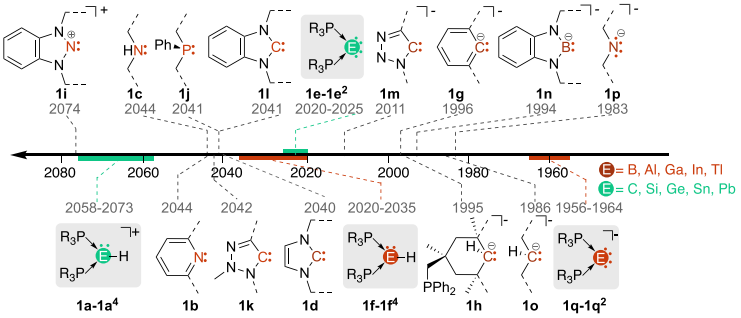

Figure 2. Calculated wavenumbers for the C−O stretching vibration of iridium(III) pincer-type complexes **1a−1q[2]** (G16 B97D/def2-TZVPP). Only the central donor group and its connectivity for each complex is shown.

Quantum chemical investigations using density functional theory (DFT) were performed to expand the scope of this study and obtain meaningful insights into the vibration-based ligand parameter. C−O stretching frequencies of the calculated ground state structures are in good agreement with the experimental values. Wavenumbers for C−O stretching vibrations of additional iridium complexes (**1i−q**) were calculated for well-known pincer-type ligands (Chart 4 and Figure 2).[80−86] In addition, we analyzed the ligand-stabilized main group fragments of the heavier homologues (**1a^n**, **1e^n**, **1f^n**, and **1q^n**; ***n*** = 1−4). The experimentally observed trend that $\tilde{\nu}_{CO}$ decreases in the order cationic > neutral > anionic ligand is confirmed by the calculations for a series of 29 complexes. In line with the weakest net donor ability, the complexes with cationic ligands (**1a^n** and **1i**) give rise to the highest values.

Within the series of neutral ligands, the boron-based ligand in **1f** is found to be a significantly stronger donor than carbenes (**1d**, **1k**, and **1l**) and phosphines (**1j**), two of the most common classes of spectator ligands in homogeneous catalysis. The π-acceptance or π-donation ability of the donor group seems to account for the value of $\tilde{\nu}_{CO}$, resulting in higher values for π-accepting phosphines and carbenes. These findings are repeated for the anionic donor groups in **1g**, **1h**, and **1m−1q**, where the σ-donating and π-accepting boryl ligand gives rise to a higher value (1994 cm^{-1}) than the σ- and π-donating amide-based ligand (1983 cm^{-1}). Interestingly, an isomer of a related boryl-based hydrido chloride iridium(III) pincer complex was obtained by a different route.[86,87] Although the boryl-based ligand is known to be the stronger σ-donor, these findings might be rationalized by the comparably high oxidation state of the central iridium atom (+III) and the positive charge of the diagnostic metal fragment in comparison to previously reported vibration-based electronic ligand parameters.

The strongest net donor within this series was found to be the deprotonated analogue of **1f**, complex **1q** ($\tilde{\nu}_{CO}$ = 1956 cm^{-1}), whose central donor group can be described as a ligand-stabilized boride ion. An analysis using CM5 charges shows that the value of $\tilde{\nu}_{CO}$ is correlated with the charge transfer from the central donor group to the carbonyl ligand, while the charge at the central iridium atom is affected only to a minor extent.[88]

While ligand-stabilized borylenes and other boron(I) compounds as well as corresponding carbon(0) compounds are sufficiently stabilized only by π-accepting substituents, their heavier homologues are expected to be more stable as a result of the subsequent stabilization of the valence s-orbital and therewith oxidation state +I (group 13), 0 (group 14), or +II (group 14). To investigate the influence of these changes within a group on the donor properties, we performed DFT calculations on complexes of the type *cis*-[{(dppm)$_2$EH}IrCl(CO)(H)]^q (E = B−Tl, q = +1; E = C−Pb, q = +2). Apart from two complexes, the geometry optimizations resulted in energetic minima, as confirmed by the absence of imaginary frequencies. Only for E = Sn and E = Pb does the geometry optimization lead to the cleavage of one E−P bond. In all cases, the Ir−E distances are close to the sum of covalent radii, and the determined τ_5 parameters of the pentacoordinated iridium fragments within these structures again indicated the presence of a donor group (τ_5 = 0.06−0.16).

As with the other complexes, we used the calculated value of $\tilde{\nu}_{CO}$ to estimate their donor strength (Table 2). In the case of the group 13 fragments, the following trend was found for $\tilde{\nu}_{CO}$:

DOI: 10.1021/jacs.9b02598
J. Am. Chem. Soc. 2019, 141, 7596−7604

Table 2. Calculated $\tilde{\nu}_{CO}$ Values for 1a−1a[4], 1e−1e[2], 1f−1f[4], and 1q−1q[2] (G16, B97D/def2-TZVPP)

	group 13			group 14	
E =	EH	E	E =	EH	E
B	2020 (**1f**)	1956 (**1q**)	C	2058 (**1a**)	2021 (**1e**)
Al	2025 (**1f**[1])	1960 (**1q**[1])	Si	2073 (**1a**[1])	2024 (**1e**[1])
Ga	2027 (**1f**[2])	1964 (**1q**[2])	Ge	2069 (**1a**[2])	2025 (**1e**[2])
In	2026 (**1f**[3])		Sn	2066 (**1a**[3])	
Tl	2035 (**1f**[4])		Pb	2068 (**1a**[4])	

B < Al < Ga ≈ In < Tl. It should be noted that there is a direct correlation between $\tilde{\nu}_{CO}$ and the Ir−E−H angle (R^2 = 0.84), which increased from an almost ideal tetrahedral angle of 110.9° for E = B to close to linearity with 158.6° for E = Tl. These findings suggest a decreasing contribution of the valence s-orbital to the actual donor orbital, which in turn results in less favorable overlap with metal-located orbitals (Figure 3). The main contribution to the Ir−E bond is given by the HOMO in all complexes, which contains an antibonding component of the Ir−Cl bond. As a consequence, the decreasing donor strength with increasing atomic number for the group 13 fragments is reflected in shorter Ir−Cl bond distances for the heavier homologues.

In addition to the C−O stretching vibration, we analyzed the Ir−H stretching vibration for the hydrido ligand *cis* to the central donor group. In line with recent reports on the empiric influence of ligands on the wavenumber of terminal hydride stretching vibrations in octahedral complexes,[89] we observed no systematic influence of the central donor in the *cis*-position.

Noticeably, the C−O stretching vibrations for reported iridium complexes **1** (experimental values and those obtained by DFT calculations) show an excellent correlation to the A_1-symmetric stretching vibrations $\tilde{\nu}_{CO}(A_1)$ for the corresponding monodentate ligands in $[LNi(CO)_3]$, the TEP.[74,90] The linear dependence of the values (e.g., $\tilde{\nu}_{CO}$ in **1d** and the TEP of the corresponding carbene[90]) allowed us to extrapolate the TEP of $(Ph_2MeP)_2BH$ to be 2021 cm^{-1}, which is an unprecedented low value for a neutral ligand. Equally interesting is the TEP range for the cationic ligands in this study (2080−2100 cm^{-1}), which is in the range of neutral ligands with significant π-acceptor properties.

Next, we were interested in the relation between $\tilde{\nu}_{CO}$ and the metal ligand bond in complexes of type **1**. Previous attempts to rationalize the TEP showed that corrected values for $\tilde{\nu}_{CO}(A_1)$ are correlated with the intrinsic bond strength of the Ni−L bond.[91−93] We therefore used energy decomposition analysis (EDA) to analyze the metal−ligand interaction. During EDA, the interaction between two fragments is analyzed. Because of multiple bonding interactions, chelating ligands provide a challenge. To mitigate this problem and to examine the central donor−iridium bond on its own, we used C_s-symmetric monodentate model complexes of type **2** (Chart 5). This additionally allows for the separation of the orbital interactions into σ- and π-type contributions. Donor groups E in these complexes are bound to a $[IrCl(CO)(H)(PPh_2Me)_2]^+$ fragment. To justify this simplification, we compared the optimized structures for type **1** and **2** complexes, showing only minor differences in the Ir−L bond length. Furthermore, the C−O stretching vibrations in **2** display a strong correlation to the values found for **1**.

Chart 5. Pincer-Type Complexes 1 and Their Monodentate Model Complexes 2 Used for the EDA Study

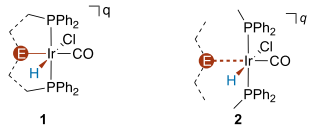

The EDA results confirm the trends seen in the CO stretching frequencies. Complex **2a** with a cationic ligand (E = CH^+) turned out to be unstable toward ligand dissociation (dissociation energy D_e = −31.7 kcal·mol^{-1}), showing the importance of the pincer ligand for the stabilization of the synthesized pincer analogue **1a**. Neutral lutidine-coordinated complex **2b** also gave rise to just a marginally positive value for the dissociation energy of 0.2 kcal·mol^{-1}. Among the series of neutral ligands, the dissociation energies rise in the order E = Me_2NH (**2c**, 21.1 kcal·mol^{-1}) < ^{Benz}NHC (**2l**, 35.7 kcal·mol^{-1}) < $PhMe_2P$ (**2j**, 48.7 kcal·mol^{-1}) < $(Ph_2MeP)_2C$ (**2e**, 68.7 kcal·mol^{-1}) < $(Ph_2MeP)_2BH$ (**2f**, 73.8 kcal·mol^{-1}). Interestingly, the calculated interaction energies (ΔE_{Int}) for the lutidine- (**2b**) and the amine-containing complex (**2c**) are similar, but their dissociation energies differ significantly. This is due to a much smaller preparation energy (E_{prep}) for the amine-containing complexes, meaning fewer changes from the free ligand to its state in the complex. Overall, the anionic phenyl- (**2g**) and the *iso*-propyl-ligand (**2o**) have the highest D_e values (133.1 and 169.3 73.8 kcal·mol^{-1} respectively).

A similar trend with an almost identical succession of the investigated ligands is found for the interaction energy (ΔE_{Int}) of the ligand and metal fragment ($-D_e = E_{prep} + \Delta E_{Int}$). Again, the ligand based on tricoordinated boron in **2f** exhibits the strongest interaction (ΔE_{Int}) among the neutral ligands, complementing the observations on the CO stretching frequency.

An analysis of the different energy terms contributing to ΔE_{Int} reveals that a large interaction energy is usually caused by high values for electrostatic (ΔE_{elstat}) and orbital interactions (ΔE_{orb}), which are only partially compensated for by an increased Pauli repulsion (ΔE_{Pauli}). Apart from the cationic ligand in **2a**, the electrostatic interaction ΔE_{elstat} represents the

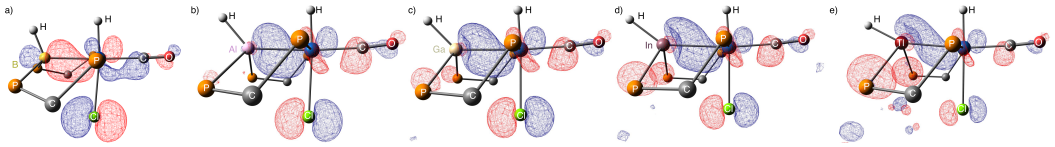

Figure 3. Highest occupied molecular orbitals for complexes of the type *cis*-[{$(dppm)_2$EH}IrCl(CO)(H)]$^+$ (**1e−1e**[4]) with E = B, Al, Ga, In, Tl. (Phenyl rings and nonrelevant hydrogen atoms were omitted for clarity.)

DOI: 10.1021/jacs.9b02598
J. Am. Chem. Soc. 2019, 141, 7596−7604

dominating attractive energy term for the metal ligand interaction in **2** (55.7−68.5%). Although the EDA might overestimate electrostatic interactions between a ligand and the cationic iridium fragment, given that a majority of metal complexes contain a central metal atom with a positive formal oxidation state and the interaction of ligands with cationic metal fragments is generally far more common in coordination chemistry than for neutral fragments, the relative values are still meaningful. Keeping this in mind, the EDA gives useful insights into metal−ligand bonding.

As expected, the anionic ligands in **2g** (phenyl) and **2o** (*iso*-propyl) give rise to the strongest electrostatic (ΔE_{elstat}) and orbital interactions (ΔE_{orb}), which are partially compensated for by the strongest Pauli repulsion. For the neutral ligands, the absolute values of the attractive (ΔE_{elstat} and ΔE_{orb}) and the repulsive terms (ΔE_{Pauli}) are significantly reduced. The largest interaction energy within the neutral ligands is obtained for the borylene-containing ligand, further confirming the experimental observations that this is the strongest neutral σ-donor ligand in the series investigated.

The extent of the dispersion energy (ΔE_{disp}) is closely related to the number of atoms in the ligand L and therefore higher for bulky ligands (up to −53.0 kcal·mol^{-1} in **2e**). Even though potential π-acceptors are among the studied ligands, π-backbonding ($\Delta E_{orb}(\pi)$) seems to be an insignificant contribution to ΔE_{orb}, ranging from −6.0 to −16.5 kcal·mol^{-1}.

Plotting the different energy terms versus the C−O stretching vibration in pincer-type complexes **1** reveals a linear dependence of the total interaction energy (Figure 4), ΔE_{int},

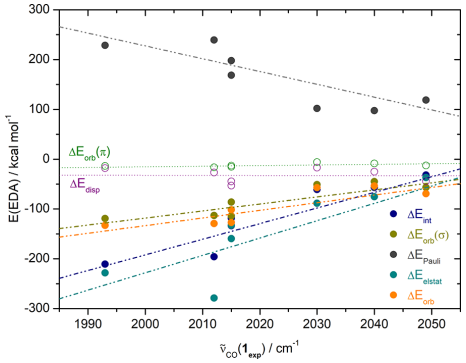

Figure 4. Relationship between the C−O stretching vibration in **1a**−**1h** and the different energy contributions to the metal−ligand interaction in monodentate analogues **2a**−**2h**.

on $\tilde{\nu}_{CO}(\mathbf{1}_{exp})$ and $\tilde{\nu}_{CO}(\mathbf{1}_{DFT})$ (R^2 = 0.95...0.99). Comparably good correlations are observed for the major contributions to the total interaction energy (ΔE_{elstat}, ΔE_{orb}, $\Delta E_{orb}(\sigma)$, and ΔE_{Pauli}). These findings have two important consequences: all of the investigated metal-ligand-bonds show characteristic contributions of energy terms, which are comparable to a fingerprint. Furthermore, the intrinsic strength of the metal ligand bond and the net charge donation are well reflected by the newly developed ligand parameter based on the C−O stretching vibration in type **1** complexes.

Finally, the quantum chemical investigations underline that the experimentally obtained values are meaningful parameters for comparing the net donor strength and suggest that both mono- and tridentate ligands might be used for the comparison of ligand properties in iridium(III) complexes. Considering the simplicity of the reactions leading to **1a**−**h** and the favored oxidative addition of the utilized precursors, we believe that the reported method represents a powerful synthesis tool for evaluating the donor strength of ligands.

CONCLUSIONS

Using a newly developed ligand parameter based on the C−O stretching vibration in iridium pincer complexes, we demonstrated that neutral tricoordinated boron compounds with π-accepting substituents are exceptionally strong donor ligands. This allows, for the first time, to obtain and compare experimental values for cationic, neutral, and anionic ligands. The comparison with spectator ligands common in homogeneous catalysis revealed that the boron-based ligands reported herein are stronger donors and exhibit stronger metal−ligand bonds. This indicates that this new class of boron-based ligands is expected to serve as superb spectator ligands. In continuation of these results, we currently develop monodentate versions of the reported ligands for applications in homogeneous catalysis and bond activation reactions.

ASSOCIATED CONTENT

Supporting Information

The Supporting Information is available free of charge on the ACS Publications website at DOI: 10.1021/jacs.9b02598.

Experimental details, spectra of the synthesized compounds, X-ray crystallographic data, details of the DFT calculation and the EDA results, and Cartesian coordinates for all complexes and ligands (PDF)

cif file compound **1a** (CIF)

cif file compound **1b** (CIF)

cif file compound **1c** (CIF)

cif file compound **1d** (CIF)

cif file compound **1e** (CIF)

cif file compound **1f** (CIF)

cif file compound **1g** (CIF)

AUTHOR INFORMATION

Corresponding Author

*robert.langer@chemie.uni-marburg.de

ORCID

Robert Langer: 0000-0001-5746-9940

Funding

We gratefully acknowledge financial support from the Deutsche Forschungsgemeinschaft (LA 2830/3-2, 2830/5-1, and 2830/6-1), the Erich-Becker-Stiftung, and the Studienstiftung des Deutschen Volkes.

Notes

The authors declare no competing financial interest.

ACKNOWLEDGMENTS

R.L. is grateful to Prof. S. Dehnen for her continuous support.

REFERENCES

(1) Kinjo, R.; Donnadieu, B.; Celik, M. A.; Frenking, G.; Bertrand, G. Synthesis and Characterization of a Neutral Tricoordinate Organoboron Isoelectronic with Amines. *Science (Washington, DC, U. S.)* **2011**, *333* (6042), 610−613.

DOI: 10.1021/jacs.9b02598
J. Am. Chem. Soc. 2019, 141, 7596−7604

(2) Ruiz, D. A.; Ung, G.; Melaimi, M.; Bertrand, G. Deprotonation of a Borohydride: Synthesis of a Carbene-Stabilized Boryl Anion. *Angew. Chem., Int. Ed.* **2013**, *52* (29), 7590−7592.
(3) Kong, L.; Li, Y.; Ganguly, R.; Vidovic, D.; Kinjo, R. Isolation of a Bis(Oxazol-2-Ylidene)-Phenylborylene Adduct and Its Reactivity as a Boron-Centered Nucleophile. *Angew. Chem., Int. Ed.* **2014**, *53* (35), 9280−9283.
(4) Kong, L.; Ganguly, R.; Li, Y.; Kinjo, R. Diverse Reactivity of a Tricoordinate Organoboron L_2PhB: (L = Oxazol-2-Ylidene) towards Alkali Metal, Group 9 Metal, and Coinage Metal Precursors. *Chem. Sci.* **2015**, *6* (5), 2893−2902.
(5) Braunschweig, H.; Dewhurst, R. D.; Hupp, F.; Nutz, M.; Radacki, K.; Tate, C. W.; Vargas, A.; Ye, Q. Multiple Complexation of CO and Related Ligands to a Main-Group Element. *Nature* **2015**, *522* (7556), 327−330.
(6) Hicks, J.; Mansikkamäki, A.; Vasko, P.; Goicoechea, J. M.; Aldridge, S. A Nucleophilic Gold Complex. *Nat. Chem.* **2019**, *11* (March), 237−241.
(7) Hicks, J.; Vasko, P.; Goicoechea, J. M.; Aldridge, S. Synthesis, Structure and Reaction Chemistry of a Nucleophilic Aluminyl Anion. *Nature* **2018**, *557* (7703), 92−95.
(8) Serrano, O.; Hoppe, E.; Power, P. P. Synthesis of the Sterically Related Nickel Gallanediyl Complexes $[Ni(CO)_3(GaAr')]$ (Ar′ = C_6H_3-2,6-(C_6H_3-2,6-IPr_2)$_2$) and $[Ni(CO)_3(GaL)]$ (L = HC[C-(CH_3)N(C_6H_3-2,6-IPr_2)]$_2$): Thermal Decomposition of $[Ni(CO)_3(GaAr')]$. *J. Cluster Sci.* **2010**, *21* (3), 449−460.
(9) Hartwig, J. F. *Organotransition Metal Chemistry: From Bonding to Catalysis*; University Science Books: Sausalito, CA, 2010.
(10) Steinborn, D. *Grundlagen der Metallorganischen Komplexkatalyse*; Springer Vieweg: Wiesbaden, Germany, 2010.
(11) Crabtree, R. H. NHC Ligands versus Cyclopentadienyls and Phosphines as Spectator Ligands in Organometallic Catalysis. *J. Organomet. Chem.* **2005**, *690* (24−25), 5451−5457.
(12) Littke, A. F.; Fu, G. C. Palladium-Catalyzed Coupling Reactions of Aryl Chlorides. *Angew. Chem., Int. Ed.* **2002**, *41* (22), 4176−4211.
(13) Martin, R.; Buchwald, S. L. Palladium-Catalyzed Suzuki−Miyaura Cross-Coupling Reactions Employing Dialkylbiaryl Phosphine Ligands. *Acc. Chem. Res.* **2008**, *41* (11), 1461−1473.
(14) Li, H.; Johansson Seechurn, C. C. C.; Colacot, T. J. Development of Preformed Pd Catalysts for Cross-Coupling Reactions, beyond the 2010 Nobel Prize. *ACS Catal.* **2012**, *2* (6), 1147−1164.
(15) Zapf, A.; Beller, M. The Development of Efficient Catalysts for Palladium-Catalyzed Coupling Reactions of Aryl Halides. *Chem. Commun.* **2005**, No. 4, 431−440.
(16) Grubbs, R. H. Olefin-Metathesis Catalysts for the Preparation of Molecules and Materials (Nobel Lecture). *Angew. Chem., Int. Ed.* **2006**, *45* (23), 3760−3765.
(17) Légaré, M.-A.; Pranckevicius, C.; Braunschweig, H. Metallomimetic Chemistry of Boron. *Chem. Rev.* **2019**, DOI: 10.1021/acs.chemrev.8b00561.
(18) Soleilhavoup, M.; Bertrand, G. Borylene: Eine Aufstrebende Verbindungsklasse. *Angew. Chem.* **2017**, *129* (35), 10416−10426.
(19) Soleilhavoup, M.; Bertrand, G. Borylenes: An Emerging Class of Compounds. *Angew. Chem., Int. Ed.* **2017**, *56* (35), 10282−10292.
(20) Goettel, J. T.; Braunschweig, H. Recent Advances in Boron-Centered Ligands and Their Transition Metal Complexes. *Coord. Chem. Rev.* **2019**, *380*, 184−200.
(21) Braunschweig, H.; Dewhurst, R. D.; Gessner, V. H. Transition Metal Borylene Complexes. *Chem. Soc. Rev.* **2013**, *42* (8), 3197−3208.
(22) Amgoune, A.; Bourissou, D. σ-Acceptor, Z-Type Ligands for Transition Metals. *Chem. Commun.* **2011**, *47* (3), 859−871.
(23) Li, Y.; Hou, C.; Jiang, J.; Zhang, Z.; Zhao, C.; Page, A. J.; Ke, Z. General H2 Activation Modes for Lewis Acid-Transition Metal Bifunctional Catalysts. *ACS Catal.* **2016**, *6* (3), 1655−1662.
(24) Li, Y.; Zhang, J.; Shu, S.; Shao, Y.; Liu, Y.; Ke, Z. Boron-Based Lewis Acid Transition Metal Complexes as Potential Bifunctional Catalysts. *Youji Huaxue* **2017**, *37* (9), 2187.
(25) Zhang, J.; Lin, J.; Li, Y.; Shao, Y.; Huang, X.; Zhao, C.; Ke, Z. The Effect of Auxiliary Ligand on the Mechanism and Reactivity: DFT Study on H_2 activation by Lewis Acid-Transition Metal Complex (Tris(Phosphino)Borane)Fe(L). *Catal. Sci. Technol.* **2017**, *7* (20), 4866−4878.
(26) Owen, G. R. Hydrogen Atom Storage upon Z-Class Borane Ligand Functions: An Alternative Approach to Ligand Cooperation. *Chem. Soc. Rev.* **2012**, *41* (9), 3535.
(27) Tsoureas, N.; Hamilton, A.; Haddow, M. F.; Harvey, J. N.; Orpen, A. G.; Owen, G. R. Insight into the Hydrogen Migration Processes Involved in the Formation of Metal−Borane Complexes: Importance of the Third Arm of the Scorpionate Ligand. *Organometallics* **2013**, *32* (9), 2840−2856.
(28) Tsoureas, N.; Nunn, J.; Bevis, T.; Haddow, M. F.; Hamilton, A.; Owen, G. R. Strong Agostic-Type Interactions in Ruthenium Benzylidene Complexes Containing 7-Azaindole Based Scorpionate Ligands. *Dalt. Trans.* **2011**, *40* (4), 951−958.
(29) Zech, A.; Haddow, M. F.; Othman, H.; Owen, G. R. Utilizing the 8-Methoxycyclooct-4-En-1-Ide Unit As a Hydrogen Atom Acceptor En Route to "Metal−Borane Pincers". *Organometallics* **2012**, *31* (19), 6753−6760.
(30) Tsoureas, N.; Bevis, T.; Butts, C. P.; Hamilton, A.; Owen, G. R. Further Exploring the "Sting of the Scorpion": Hydride Migration and Subsequent Rearrangement of Norbornadiene to Nortricyclyl on Rhodium(I). *Organometallics* **2009**, *28* (17), 5222−5232.
(31) Owen, G. R.; Gould, P. H.; Hamilton, A.; Tsoureas, N. Unexpected Pincer-Type Coordination (κ^3-SBS) within a Zerovalent Platinum Metallaboratrane Complex. *Dalt. Trans.* **2010**, *39* (1), 49−52.
(32) Tsoureas, N.; Kuo, Y.-Y.; Haddow, M. F.; Owen, G. R. Double Addition of H_2 to Transition Metal−Borane Complexes: A 'Hydride Shuttle' Process between Boron and Transition Metal Centres. *Chem. Commun.* **2011**, *47* (1), 484−486.
(33) Owen, G. R.; Hugh Gould, P.; Charmant, J. P. H.; Hamilton, A.; Saithong, S. A New Hybrid Scorpionate Ligand: A Study of the Metal−Boron Bond within Metallaboratrane Complexes. *Dalt. Trans.* **2010**, *39* (2), 392−400.
(34) Landry, V. K.; Melnick, J. G.; Buccella, D.; Pang, K.; Ulichny, J. C.; Parkin, G. Synthesis and Structural Characterization of $[\kappa^3$-B,S,S-$B(Mim^R)_3]Ir(CO)(PPh_3)H$ (R = *t*Bu, Ph) and $[\kappa^4$-$B(Mim^{But})_3]M(PPh_3)Cl$ (M = Rh, Ir): Analysis of the Bonding in Metal Borane Compounds. *Inorg. Chem.* **2006**, *45* (6), 2588−2597.
(35) Figueroa, J. S.; Melnick, J. G.; Parkin, G. Reactivity of the Metal→BX_3 Dative σ-Bond: 1,2-Addition Reactions of the Fe→BX_3 Moiety of the Ferraboratrane Complex $[\kappa^4$-B(MimBut) $_3]Fe(CO)_2$. *Inorg. Chem.* **2006**, *45* (18), 7056−7058.
(36) Pang, K.; Tanski, J. M.; Parkin, G. Reactivity of the Ni→B Dative σ-Bond in the Nickel Boratrane Compounds $[\kappa^4$-$B(Mim^{But})_3]$-NiX (X = Cl, OAc, NCS, N_3): Synthesis of a Series of B-Functionalized Tris(2-Mercapto-1-*tert*-Butylimidazolyl)-Borato Complexes, $[YTm^{But}]NiZ$. *Chem. Commun.* **2008**, No. 8, 1008.
(37) Crossley, I. R.; Hill, A. F.; Willis, A. C. Metallaboratranes: Bis- and Tris(Methimazolyl)Borane Complexes of Group 9 Metal Carbonyls and Thiocarbonyls. *Organometallics* **2010**, *29* (2), 326−336.
(38) López-Gómez, M. J.; Connelly, N. G.; Haddow, M. F.; Hamilton, A.; Orpen, A. G. Fluxional Rhodium Scorpionate Complexes of the Hydrotris(Methimazolyl)Borate (Tm) Ligand and Their Static Boratrane Derivatives. *Dalt. Trans.* **2010**, *39* (22), 5221.
(39) Blagg, R. J.; Connelly, N. G.; Haddow, M. F.; Hamilton, A.; Lusi, M.; Orpen, A. G.; Ridgway, B. M. Isomerism in Rhodium(i) N,S-Donor Heteroscorpionates: Ring Substituent and Ancillary Ligand Effects. *Dalt. Trans.* **2010**, *39* (48), 11616.
(40) López-Gómez, M. J.; Connelly, N. G.; Haddow, M. F.; Hamilton, A.; Lusi, M.; Baisch, U.; Orpen, A. G. Potassium S_2N-

DOI: 10.1021/jacs.9b02598
J. Am. Chem. Soc. 2019, 141, 7596−7604

Heteroscorpionates: Structure and Iridaboratrane Formation. *Dalt. Trans.* **2011**, *40* (17), 4647.
(41) Blagg, R. J.; Charmant, J. P. H.; Connelly, N. G.; Haddow, M. F.; Orpen, A. G. Redox Activation of a B−H Bond: A New Route to Metallaboratrane Complexes. *Chem. Commun.* **2006**, No. 22, 2350−2352.
(42) Blagg, R. J.; Adams, C. J.; Charmant, J. P. H.; Connelly, N. G.; Haddow, M. F.; Hamilton, A.; Knight, J.; Orpen, A. G.; Ridgway, B. M. A Novel Route to Rhodaboratranes $[Rh(CO)(PR_3)\{B(Taz)_3\}]^+$ via the Redox Activation of Scorpionate Complexes [RhLL′Tt]. *Dalt. Trans.* **2009**, No. 40, 8724.
(43) Holler, S.; Tüchler, M.; Roschger, M. C.; Belaj, F.; Veiros, L. F.; Kirchner, K.; Mösch-Zanetti, N. C. Three-Fold-Symmetric Selenium-Donor Metallaboratranes of Cobalt and Nickel. *Inorg. Chem.* **2017**, *56* (21), 12670−12673.
(44) Nuss, G.; Saischek, G.; Harum, B. N.; Volpe, M.; Belaj, F.; Mösch-Zanetti, N. C. Pyridazine Based Scorpionate Ligand in a Copper Boratrane Compound. *Inorg. Chem.* **2011**, *50* (24), 12632−12640.
(45) Nuss, G.; Saischek, G.; Harum, B. N.; Volpe, M.; Gatterer, K.; Belaj, F.; Mösch-Zanetti, N. C. Novel Pyridazine Based Scorpionate Ligands in Cobalt and Nickel Boratrane Compounds. *Inorg. Chem.* **2011**, *50* (5), 1991−2001.
(46) Holler, S.; Tüchler, M.; Steller, B. G.; Belaj, F.; Veiros, L. F.; Kirchner, K.; Mösch-Zanetti, N. C. Thiopyridazine-Based Palladium and Platinum Boratrane Complexes. *Inorg. Chem.* **2018**, *57* (12), 6921−6931.
(47) Holler, S.; Tüchler, M.; Knaus, A. M.; Belaj, F.; Mösch-Zanetti, N. C. Di-Tert-Butyl Thiopyridazine Boratrane Complexes of Co, Ni and Cu. *Polyhedron* **2017**, *125*, 122−129.
(48) Foreman, M. R. S.-J.; Hill, A. F.; Ma, C.; Tshabang, N.; White, A. J. P. Synthesis and Ligand Substitution Reactions of κ^4 - B, S, S′,S″-Ruthenaboratranes. *Dalt. Trans.* **2019**, *48* (1), 209−219.
(49) Holler, S.; Tüchler, M.; Belaj, F.; Veiros, L. F.; Kirchner, K.; Mösch-Zanetti, N. C. Thiopyridazine-Based Copper Boratrane Complexes Demonstrating the Z-Type Nature of the Ligand. *Inorg. Chem.* **2016**, *55* (10), 4980−4991.
(50) Qin, Y.; Ma, Q.; Jia, A.-Q.; Chen, Q.; Zhang, Q.-F. Synthesis and Structural Characterization of Ruthenium Complexes with 1-Aryl-Imidazole-2-Thione. *J. Coord. Chem.* **2013**, *66* (8), 1405−1415.
(51) Mihalcik, D. J.; White, J. L.; Tanski, J. M.; Zakharov, L. N.; Yap, G. P. A.; Incarvito, C. D.; Rheingold, A. L.; Rabinovich, D. Cobalt Tris(Mercaptoimidazolyl)Borate Complexes: Synthetic Studies and the Structure of the First Cobaltaboratrane. *Dalt. Trans.* **2004**, No. 10, 1626.
(52) Senda, S.; Ohki, Y.; Hirayama, T.; Toda, D.; Chen, J.-L.; Matsumoto, T.; Kawaguchi, H.; Tatsumi, K. Mono{hydrotris-(Mercaptoimidazolyl)Borato} Complexes of Manganese(II), Iron(II), Cobalt(II), and Nickel(II) Halides. *Inorg. Chem.* **2006**, *45* (24), 9914−9925.
(53) Hill, A. F.; Owen, G. R.; White, A. J. P.; Williams, D. J. The Sting of the Scorpion: A Metallaboratrane. *Angew. Chem., Int. Ed.* **1999**, *38* (18), 2759−2761.
(54) Crossley, I. R.; Foreman, M. R. S.-J.; Hill, A. F.; White, A. J. P.; Williams, D. J. The First Rhodaboratrane: $[RhCl(PPh_3)\{B(Mt)_3\}]$-(Rh→B) (Mt = Methimazolyl). *Chem. Commun.* **2005**, No. 2, 221−223.
(55) Crossley, I. R.; Hill, A. F.; Humphrey, E. R.; Willis, A. C. The First Bimetallic Metallaboratrane: $[Rh_2\{B(Mt)_3\}_2\{\kappa^2$-S,S′-$HB(Mt)_3\}]$ Cl and Its Synthesis from the Fluxional Rhodaboratrane Salt $[Rh\{B(Mt)_3\}(\eta^4$-$C_8H_{12})]Cl$, (Rh → B, Mt = Methimazolyl). *Organometallics* **2005**, *24* (16), 4083−4086.
(56) Hill, A. F.; Schwich, T.; Xiong, Y. 5-Mercaptotetrazolyl-Derived Metallaboratranes. *Dalt. Trans.* **2019**, *48* (7), 2367−2376.
(57) Crossley, I. R.; Hill, A. F.; Willis, A. C. Retention of Pt→B Bonding in Oxidative Addition Reactions of the Platinaboratrane $[Pt(PPh_3)\{B(Mt)_3\}]$ *(Pt→B)*[10] (Mt = Methimazolyl). *Organometallics* **2008**, *27* (3), 312−315.
(58) Tsoureas, N.; Haddow, M. F.; Hamilton, A.; Owen, G. R. A New Family of Metallaboratrane Complexes Based on 7-Azaindole: B−H Activation Mediated by Carbon Monoxide. *Chem. Commun.* **2009**, No. 18, 2538.
(59) Irvine, G. J.; Lesley, M. J. G.; Marder, T. B.; Norman, N. C.; Rice, C. R.; Robins, E. G.; Roper, W. R.; Whittell, G. R.; Wright, L. J. Transition Metal-Boryl Compounds: Synthesis, Reactivity, and Structure. *Chem. Rev.* **1998**, *98* (8), 2685−2722.
(60) Yamashita, M. The Organometallic Chemistry of Boron-Containing Pincer Ligands Based on Diazaboroles and Carboranes. *Bull. Chem. Soc. Jpn.* **2016**, *89* (3), 269−281.
(61) Braunschweig, H. Transition Metal Complexes of Boron. *Angew. Chem., Int. Ed.* **1998**, *37* (13−14), 1786−1801.
(62) Landmann, J.; Keppner, F.; Hofmann, D. B.; Sprenger, J. A. P.; Häring, M.; Zottnick, S. H.; Müller-Buschbaum, K.; Ignatiev, N. V.; Finze, M. Deprotonation of a Hydridoborate Anion. *Angew. Chem., Int. Ed.* **2017**, *56* (10), 2795−2799.
(63) Landmann, J.; Sprenger, J. A. P.; Bertermann, R.; Ignatiev, N.; Bernhardt-Pitchougina, V.; Bernhardt, E.; Willner, H.; Finze, M. Convenient Access to the Tricyanoborate Dianion $B(CN)_3^{2-}$ and Selected Reactions as a Boron-Centred Nucleophile. *Chem. Commun.* **2015**, *51* (24), 4989−4992.
(64) Celik, M. A.; Sure, R.; Klein, S.; Kinjo, R.; Bertrand, G.; Frenking, G. Borylene Complexes $(BH)L_2$ and Nitrogen Cation Complexes $(N^+)L_2$: Isoelectronic Homologues of Carbones CL_2. *Chem. - Eur. J.* **2012**, *18* (18), 5676−5692.
(65) Kong, L.; Ganguly, R.; Li, Y.; Kinjo, R. Diverse Reactivity of a Tricoordinate Organoboron L_2PhB: (L = Oxazol-2-Ylidene) towards Alkali Metal, Group 9 Metal, and Coinage Metal Precursors. *Chem. Sci.* **2015**, *6* (5), 2893−2902.
(66) Bernhardt, E.; Bernhardt-Pitchougina, V.; Willner, H.; Ignatiev, N. "Umpolung" at Boron by Reduction of $[B(CN)_4]^-$ and Formation of the Dianion $[B(CN)_3]^{2-}$. *Angew. Chem., Int. Ed.* **2011**, *50* (50), 12085−12088.
(67) Cid, J.; Gulyás, H.; Carbó, J. J.; Fernández, E. Trivalent Boron Nucleophile as a New Tool in Organic Synthesis: Reactivity and Asymmetric Induction. *Chem. Soc. Rev.* **2012**, *41* (9), 3558.
(68) Ruiz, D. A.; Melaimi, M.; Bertrand, G. An Efficient Synthetic Route to Stable Bis(Carbene)Borylenes $[(L_1)(L_2)BH]$. *Chem. Commun.* **2014**, *50* (58), 7837−7839.
(69) Frank, R.; Howell, J.; Tirfoin, R.; Dange, D.; Jones, C.; Mingos, D. M. P.; Aldridge, S. Circumventing Redox Chemistry: Synthesis of Transition Metal Boryl Complexes from a Boryl Nucleophile by Decarbonylation. *J. Am. Chem. Soc.* **2014**, *136* (44), 15730−15741.
(70) Vondung, L.; Frank, N.; Fritz, M.; Alig, L.; Langer, R. Phosphine-Stabilized Borylenes and Boryl Anions as Ligands? Redox Reactivity in Boron-Based Pincer Complexes. *Angew. Chem., Int. Ed.* **2016**, *55* (46), 14450−14454.
(71) Grätz, M.; Bäcker, A.; Vondung, L.; Maser, L.; Reincke, A.; Langer, R. Donor Ligands Based on Tricoordinate Boron Formed by B−H-Activation of Bis(Phosphine)Boronium Salts. *Chem. Commun.* **2017**, *53* (53), 7230−7233.
(72) Kong, L.; Li, Y.; Ganguly, R.; Vidovic, D.; Kinjo, R. Isolation of a Bis(Oxazol-2-Ylidene)-Phenylborylene Adduct and Its Reactivity as a Boron-Centered Nucleophile. *Angew. Chem., Int. Ed.* **2014**, *53* (35), 9280−9283.
(73) Addison, A. W.; Rao, T. N.; Reedijk, J.; van Rijn, J.; Verschoor, G. C.; Trans, D.; Addison, A. W.; Rao, T. N. Synthesis, Structure, and Spectroscopic Properties of Copper(II) Compounds Containing Nitrogen−Sulphur Donor Ligands; the Crystal and Molecular Structure of Aqua[1,7-Bis(N-Methylbenzimidazol-2′-Yl)-2,6-Dithiaheptane]Copper(II) Perchlorate. *J. Chem. Soc., Dalton Trans.* **1984**, No. 7, 1349−1356.
(74) Tolman, C. A. Steric Effects of Phosphorus Ligands in Organometallic Chemistry and Homogeneous Catalysis. *Chem. Rev.* **1977**, *77* (3), 313−348.
(75) Wolf, S.; Plenio, H. Synthesis of (NHC)Rh(Cod)Cl and $(NHC)RhCl(CO)_2$ complexes - Translation of the Rh- into the Ir-

DOI: 10.1021/jacs.9b02598
J. Am. Chem. Soc. 2019, 141, 7596−7604

Scale for the Electronic Properties of NHC Ligands. *J. Organomet. Chem.* **2009**, *694* (9−10), 1487−1492.
(76) Chianese, A. R.; Li, X.; Janzen, M. C.; Faller, J. W.; Crabtree, R. H. Rhodium and Iridium Complexes of N-Heterocyclic Carbenes via Transmetalation: Structure and Dynamics. *Organometallics* **2003**, *22* (8), 1663−1667.
(77) Kelly, R. A., III; Clavier, H.; Giudice, S.; Scott, N. M.; Stevens, E. D.; Bordner, J.; Samardjiev, I.; Hoff, C. D.; Cavallo, L.; Nolan, S. P. Determination of N-Heterocyclic Carbene (NHC) Steric and Electronic Parameters Using the [(NHC)Ir(CO)$_2$Cl] System. *Organometallics* **2008**, *27*, 202−210.
(78) Li, R.-X.; Li, X.-J.; Wong, N.-B.; Tin, K.-C.; Zhou, Z.-Y.; Mak, T. C. Syntheses and Characterizations of Iridium Complexes Containing Bidentate Phosphine Ligands and Their Catalytic Hydrogenation Reactions to α,β-Unsaturated Aldehydes. *J. Mol. Catal. A: Chem.* **2002**, *178* (1−2), 181−190.
(79) Mayer, H. A.; Fawzi, R.; Steimann, M. Synthesis, X-Ray Structure and Complexation Behavior of the New Tripodal Phosphane Ligand *cis*,cis-1,3,5-Tris[(Diphenylphosphanyl)-Methyl]-1−1,3,5-Trimethylcyclohexane (Tdppmtmcy). Crystal Structure of Ir(Tdppmtmcy)(CO)Cl. *Chem. Ber.* **1993**, *126* (6), 1341−1346.
(80) Tulchinsky, Y.; Iron, M. A.; Botoshansky, M.; Gandelman, M. Nitrenium Ions as Ligands for Transition Metals. *Nat. Chem.* **2011**, *3* (7), 525−531.
(81) Plikhta, A.; Pöthig, A.; Herdtweck, E.; Rieger, B. Toward New Organometallic Architectures: Synthesis of Carbene-Centered Rhodium and Palladium Bisphosphine Complexes. Stability and Reactivity of [PC^{BIm}PRh(L)][PF$_6$] Pincers. *Inorg. Chem.* **2015**, *54* (19), 9517−9528.
(82) Schuster, E. M.; Botoshansky, M.; Gandelman, M. 1,2,3-Triazolylidene Based Complexes via Post-Modification of Pincer Click Ligands. *Dalt. Trans.* **2011**, *40* (35), 8764.
(83) Schuster, E. M.; Botoshansky, M.; Gandelman, M. Pincer Click Ligands. *Angew. Chem., Int. Ed.* **2008**, *47* (24), 4555−4558.
(84) Chatt, J.; Watson, H. R. 980. The Reactions of Di- and Tri-Tertiary Phosphines with the Hexacarbonyls of Metals of Group VI. *J. Chem. Soc.* **1961**, No. 0, 4980.
(85) Neo, K. E.; Neo, Y. C.; Chien, S. W.; Tan, G. K.; Wilkins, A. L.; Henderson, W.; Hor, T. S. A. PdCl[PPh$_2$CH$_2$CH $_2$CHCH$_2$CH$_2$PPh$_2$] as a Precursor to Homo- and Hetero-Metallic Species Directed by ESMS (Electrospray Ionisation Mass Spectrometry). *Dalt. Trans.* **2004**, No. 15, 2281−2287.
(86) Segawa, Y.; Yamashita, M.; Nozaki, K. Diphenylphosphino- or Dicyclohexylphosphino-Tethered Boryl Pincer Ligands: Syntheses of PBP Iridium(III) Complexes and Their Conversion to Iridium−Ethylene Complexes. *Organometallics* **2009**, *28* (21), 6234−6242.
(87) Segawa, Y.; Yamashita, M.; Nozaki, K. Syntheses of PBP Pincer Iridium Complexes: A Supporting Boryl Ligand. *J. Am. Chem. Soc.* **2009**, *131* (26), 9201−9203.
(88) Marenich, A. V.; Jerome, S. V.; Cramer, C. J.; Truhlar, D. G. Charge Model 5: An Extension of Hirshfeld Population Analysis for the Accurate Description of Molecular Interactions in Gaseous and Condensed Phases. *J. Chem. Theory Comput.* **2012**, *8* (2), 527−541.
(89) Morris, R. H. Estimating the Wavenumber of Terminal Metal-Hydride Stretching Vibrations of Octahedral d^6 Transition Metal Complexes. *Inorg. Chem.* **2018**, *57* (21), 13809−13821.
(90) Perrin, L.; Clot, E.; Eisenstein, O.; Loch, J.; Crabtree, R. H. Computed Ligand Electronic Parameters from Quantum Chemistry and Their Relation to Tolman Parameters, Lever Parameters, and Hammett Constants. *Inorg. Chem.* **2001**, *40* (23), 5806−5811.
(91) Setiawan, D.; Kalescky, R.; Kraka, E.; Cremer, D. Direct Measure of Metal-Ligand Bonding Replacing the Tolman Electronic Parameter. *Inorg. Chem.* **2016**, *55* (5), 2332−2344.
(92) Cremer, D.; Kraka, E. Generalization of the Tolman Electronic Parameter: The Metal-Ligand Electronic Parameter and the Intrinsic Strength of the Metal-Ligand Bond. *Dalt. Trans.* **2017**, *46* (26), 8323−8338.
(93) Kalescky, R.; Kraka, E.; Cremer, D. New Approach to Tolman's Electronic Parameter Based on Local Vibrational Modes. *Inorg. Chem.* **2014**, *53*, 478−495.

DOI: 10.1021/jacs.9b02598
J. Am. Chem. Soc. 2019, 141, 7596−7604

Quantifying the donor strength of ligand-stabilized main group fragments

Leon Maser, Christian Schneider, Lisa Vondung, Lukas Alig and Robert Langer*

Table of Contents

Experimental Procedures and Spectra

Materials and Methods

All experiments were carried out under an atmosphere of purified argon or nitrogen in the MBraun glove boxes LABmaster 130 and UNIlab or using standard Schlenk techniques.
THF and diethyl ether were dried over Na/K alloy, *n*-hexane was dried over $LiAlH_4$, toluene was dried over sodium, dichloromethane was dried over CaH_2, methanol was dried over magnesium and ethyl acetate was dried over potassium carbonate. After drying, solvents were stored over appropriate molecular sieves. Deuterated solvents were degassed with freeze-pump-thaw cycles and stored over appropriate molecular sieves under argon atmosphere.
^1H, ^{13}C, ^{11}B and ^{31}P NMR spectra were recorded using Bruker Avance HD 250, 300 A, DRX 400, DRX 500 and Avance 500 NMR spectrometers at 300 K. ^1H and ^{13}C {^1H}, ^{13}C-APT (attached proton test) NMR chemical shifts are reported in ppm downfield from tetramethylsilane. The resonance of the residual protons in the deuterated solvent was used as internal standard for ^1H NMR spectra. The solvent peak of the deuterated solvent was used as internal standard for ^{13}C NMR spectra. The assignment of resonances in ^1H and ^{13}C NMR spectra was further supported by ^1H COSY, ^1H NOESY, ^1H,^{13}C HMQC and ^1H,^{13}C HMBC NMR spectra. ^{11}B NMR chemical shifts are reported in ppm downfield from $BF_3{\cdot}Et_2O$ and referenced to an external solution of $BF_3{\cdot}Et_2O$ in $CDCl_3$. ^{31}P NMR chemical shifts are reported in ppm downfield from H_3PO_4 and referenced to an external 85 % solution of phosphoric acid in D_2O. The following abbreviations are used for the description of NMR data: br (broad), s (singlet), d (doublet), t (triplet), q (quartet), quin (quintet), m (multiplet).
FT-IR spectra were recorded by attenuated total reflection of the solid samples on a Bruker Tensor IF37 spectrometer. The intensity of the absorption band is indicated as w (weak), m (medium), s (strong), vs (very strong) and br (broad).
HR-ESI mass spectra were acquired with a LTQ-FT mass spectrometer (Thermo Fisher Scientific). The resolution was set to 100.000.
Elemental analyses were done by combustion analysis in a vario Micro cube (Elementar). In a glovebox, samples were weighed in Sn-crucibles of known mass and kept under exclusion of ambient air by cold pressure welding. Measurements were performed as double determinations, the values presented herein are the arithmetic mean.

Bis(diphenylphosphino)methane (dppm) was synthesized following the procedure published by K. Sommer.[1] Vaska's complex ([*trans*-$Ir(PPh_3)_2(CO)Cl$]) and [*cis*-$Ir(CO)_2Cl$(*para*-toluidine)] were prepared according to literature procedures.[2] $[H_2C(dppm)_2]Cl_2$ and $[HC(dppm)_2]Cl$ were synthesized according to the literature by Peringer and coworkers.[3] $[H_2B(dppm)_2]Br$ was synthesized according to our previously published method.[4] Bis(diphenylphosphinoethyl)amine (dpea) and its hydrochloride salt $[H_2N([CH_2]_2PPh_2)_2]Cl$ (dpea·HCl) were synthesized according to a procedure published by Kahn and Rao.[5] 1,3-Bis(diphenylphosphinomethyl)benzene (dpmb) and 2,6-bis(diphenylphosphinomethyl)pyridine (dpmp) were synthesized according to the literature by Wu and coworkers.[6]
1,3-Bis(2-diphenylphosphanylethyl)-3*H*-imidazol-1-ium chloride was prepared according to the literature.[7]

*Synthesis of [{κ^3P,C,P-HC(dppm)$_2$}IrCl(CO)H]Cl$_2$ (**1a**)*

1a can easily be synthesized by oxidative addition of $[H_2C(dppm)_2]Cl_2$ to $[IrCl(CO)(PPh_3)]$, but the following procedure yields a purer product.
To a yellow solution of 96.6 mg [{κ^3*P,C,P*-C(dppm)$_2$}IrCl(CO)H]Cl (**1e**, 90.0 µmol, 1.0 eq.) in 5 ml CH_2Cl_2, a solution of HCl in DEE (2 M, 0.13 ml, 26.0 µmol, 2.9 eq.) was added dropwise until complete discoloration. The volume of the solution was reduced to ~1 ml in vacuo and addition of 8 ml DEE lead to a colorless precipitate. Filtration and drying in vacuo yielded 87 mg (78.4 µmol, 87 %) of a mixture of the *cis*- and *trans*-isomers **1a** in approx. 1:1 ratio. Single crystals suitable for X-ray diffraction experiments were obtained by layering a solution of [{κ^3*P,C,P*-HC(dppm)$_2$}IrCl(CO)H]Cl_2 in CH_2Cl_2 with *n*-hexane. Both isomers are observed in the crystal structure.

^1H NMR (300 MHz, CD_2Cl_2) δ_H: -15.88 (t, 1H, $^2J_{H,P}$ = 11.8 Hz, Ir*H cis*-**1a)**, -14.38 (t, 1H, $^2J_{H,P}$ = 11.7 Hz, Ir*H trans*-**1a**), 5.13 (m, 4H, C*H*$_2$ *cis*- + *trans* **1a**), 6.58 (t, superimposed, 1H, $J_{H,P}$ = 21.2 Hz, C*H*$_2$ *cis*- + *trans*-**1a**), 6.62 (m, superimposed, 1H, C*H*$_2$ *cis*- + *trans*-**1a**), 6.85 (br s, 2H, C*H*$_2$ *cis*- + *trans*-**1a**), 7.15 (td, 4H, $J_{H,P}$ = 7.6 Hz, $J_{H,P}$ = 2.7 Hz, *H*$_{arom.}$), 7.20–7.54 (m, 44H, *H*$_{arom.}$), 7.63 (dd, 4H, $J_{H,P}$ = 13.2 Hz, $J_{H,P}$ = 7.9 Hz, *H*$_{arom.}$), 7.67–7.77 (m, 8H, *H*$_{arom.}$), 7.77–7.85 (m, 8H, *H*$_{arom.}$), 7.96 (dd, 4H, $J_{H,P}$ = 12.9 Hz, $J_{H,P}$ = 7.3 Hz, *H*$_{arom.}$), 8.09 (dd, 4H, $J_{H,P}$ = 12.9 Hz, $J_{H,P}$ = 7.8 Hz, *H*$_{arom.}$), 8.12–8.19 (m, 4H, *H*$_{arom.}$) ppm.
$^1H\{^{31}P\}$ NMR (300 MHz, CD_2Cl_2) δ_H: (only additionally appearing resonances are listed) 3.69 (br s, 2H, C*H*) ppm. ^{13}C APT NMR (126 MHz, CD_2Cl_2) δ_C: 1.4 (t, $J_{C,P}$ = 33.6 Hz, P-*C*H-P), 9.5 (t, $J_{C,P}$ = 37.8 Hz, P-*C*H-P), 33.3–34.2 (m, *C*H$_2$), 35.7 (dt, $J_{C,P}$ = 61.3 Hz, $J_{C,P}$ = 14.0 Hz, *C*H$_2$), 115.6 (dd, $J_{C,P}$ = 237.2 Hz, $J_{C,P}$ = 83.5 Hz, *C*$_{arom}$), 119.6 (dd, $J_{C,P}$ = 81.4 Hz, $J_{C,P}$ = 12.2 Hz, *C*$_{arom}$), 126.1 (td, $J_{C,P}$ = 30.3 Hz, $J_{C,P}$ = 9.6 Hz, *C*$_{arom}$), 127.3 (t, $J_{C,P}$ = 31.7 Hz, *C*$_{arom}$), 128.1 (d, $J_{C,P}$ = 32.0 Hz, *C*$_{arom}$), 128.4–129.0 (m, *C*H$_{arom}$), 129.0–129.4 (m, *C*H$_{arom}$), 129.9 (d, $J_{C,P}$ = 13.2 Hz, *C*H$_{arom}$), 132.2 (dd, $J_{C,P}$ = 44.7 Hz, $J_{C,P}$ = 19.0 Hz, *C*H$_{arom}$), 132.8–133.1 (m, *C*H$_{arom}$), 133.2–133.5 (m, *C*H$_{arom}$), 133.9 (dt, $J_{C,P}$ = 43.8 Hz, $J_{C,P}$ = 6.9 Hz, *C*H$_{arom}$), 134.5–134.9 (m, *C*H$_{arom}$), 134.9–135.2 (m, *C*H$_{arom}$), 164.7 (d, $J_{C,P}$ = 25.7 Hz, *C*$_{arom}$) ppm. The resonance corresponding to the carbonyl ligand was not observed. $^{31}P\{^1H\}$ NMR (121 MHz, CD_2Cl_2) δ_P: 0.8 (t, 2P, $^2J_{P,P}$ = 31.3 Hz, *P*-Ir-P, *cis*-**1a**), 2.0 (t, 2P, $^2J_{P,P}$ = 30.2 Hz, *P*-Ir-P, *trans*-**1a**), 44.0 (t, 2P, $^2J_{P,P}$ = 29.1 Hz, *P*-CH-*P, trans*-**1a**), 45.0 (t, 2P, $^2J_{P,P}$ = 32.0 Hz, *P*-CH-*P*, *cis*-**1a**) ppm. FT-IR $\tilde{\nu}$/cm^{-1}: 3054 (w), 2961 (w), 2792 (w), 2194 (w, IrH), 2049 (s, CO), 1586 (w), 1485 (w), 1435 (s), 1361 (w), 1262 (m), 1099 (s), 1027 (w), 998 (m), 879 (w), 788 (m), 736 (vs), 687 (vs), 615 (w), 553 (s), 524 (s), 500 (s), 480 (s). HRMS:

(ESI+, MeOH) m/z: 1001.1969 [(HC{dppm}$_2$)Ir(CO)]$^+$ measured, 1001.1972 calculated, Δ = -0.30 ppm. Elemental analysis (measured [calculated] for $C_{52}H_{46}Cl_3IrOP_4$ / %): 57.33 [56.30] C, 4.34 [4.18] H, 0.17 [0.00] N.

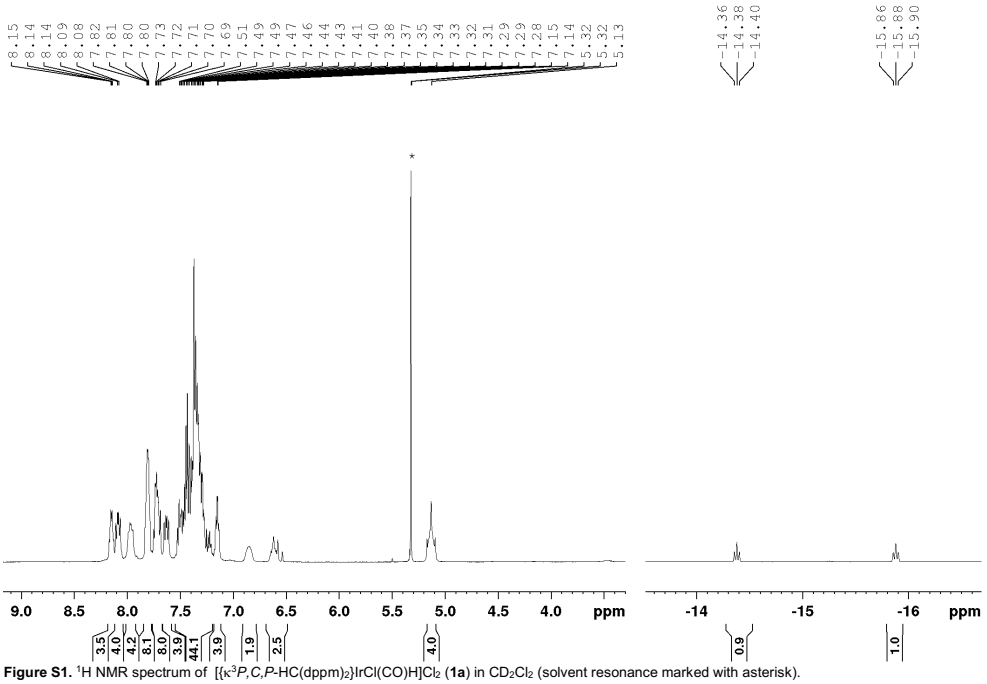

Figure S1. ^{1}H NMR spectrum of [{κ^3*P,C,P*-HC(dppm)$_2$}IrCl(CO)H]Cl$_2$ (**1a**) in CD_2Cl_2 (solvent resonance marked with asterisk).

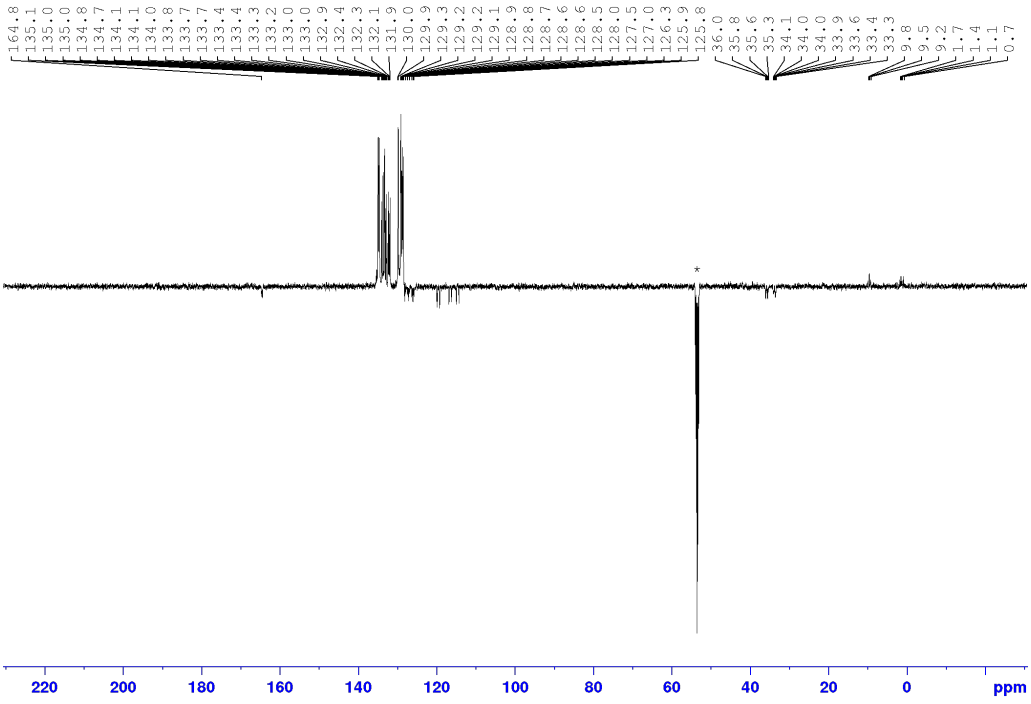

Figure S2. ^{13}C APT NMR spectrum of [{κ^3*P,C,P*-HC(dppm)$_2$}IrCl(CO)H]Cl$_2$ (**1a**) in CD_2Cl_2 (solvent resonance marked with asterisk).

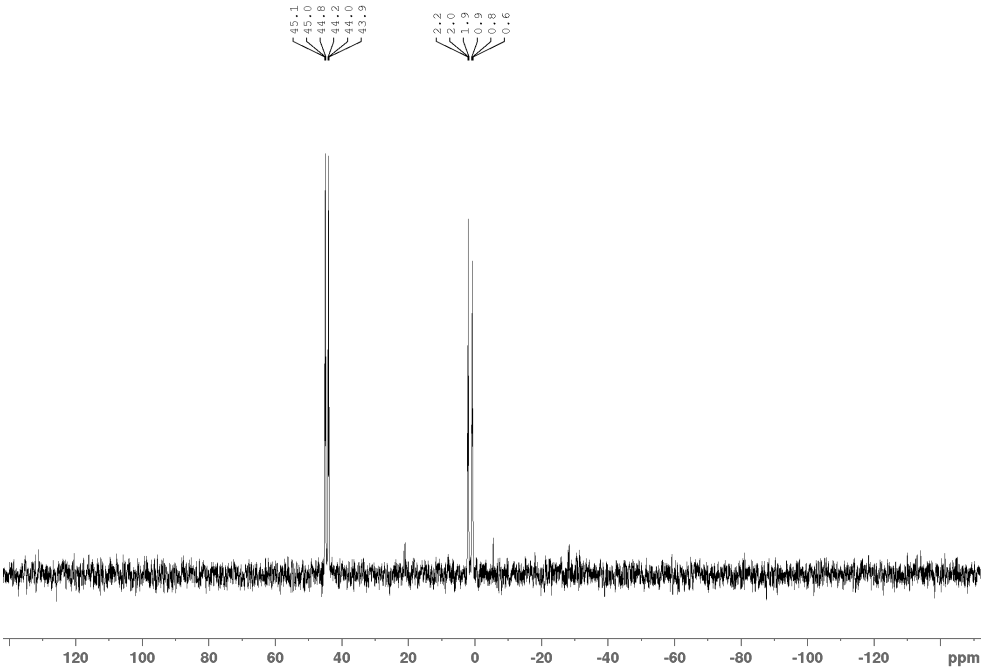

Figure S3. $^{31}P\{^1H\}$ NMR spectrum of [{κ^3*P,C,P*-HC(dppm)$_2$}IrCl(CO)H]Cl$_2$ (**1a**) in CD_2Cl_2.

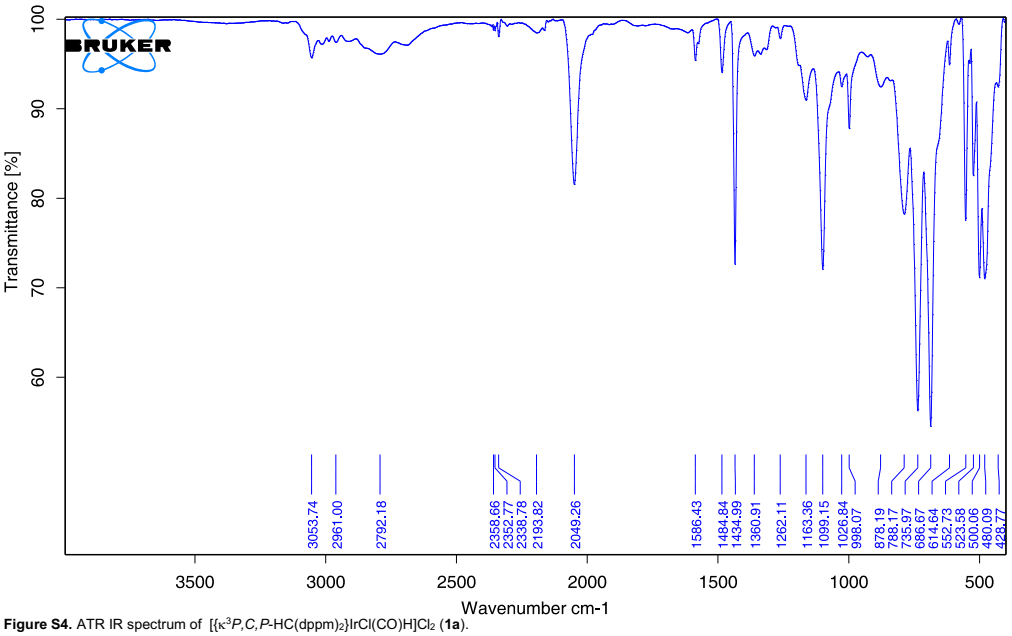

Figure S4. ATR IR spectrum of [{κ^3*P,C,P*-HC(dppm)$_2$}IrCl(CO)H]Cl$_2$ (**1a**).

*Synthesis of [(κ³P,N,P-^{Ph}PN^{Py}P)IrCl(CO)H]Cl (**1b**)*

50 mg dpmp (105 µmol, 1.0 eq.) were dissolved in 5 ml toluene. On addition of 0.05 ml of a solution of HCl in DEE (2 M, 100 µmol, 1.0 eq.), a colorless precipitate formed. After drying in vacuo, the remaining colorless solid was suspended in 5 ml toluene. To the suspension, a solution of 42 mg [IrCl(CO)$_2$(*p*-toluidine)] (108 µmol, 1.0 eq.) in 5 ml toluene were added. The orange suspension was heated to reflux. After cooling to room temperature, the solution was decanted and the remaining colorless solid was washed 2x with 2 ml toluene. After drying in vacuo, 5 ml CH_2Cl_2 were added and the resulting solution was layered with 10 ml *n*-hexane. After 7 d, crystals suitable for X-ray diffraction could be obtained. 37 mg of [(κ³*P,N,P*-^{Ph}PN^{Py}P)IrCl(CO)H]Cl (48.2 µmol, 46 %) were isolated in the form of colorless needles.

^{1}H NMR (300 MHz, CD_2Cl_2) δ_H: -14.90 (t, 1H, $^2J_{H,P}$ = 11.5 Hz, Ir-H), 4.85 (dt, 2H, $^2J_{H,H}$ = 17.4 Hz, $^2J_{H,P}$ = 5.3 Hz, C*H*$_2$), 5.35 (dt, superimposed on solvent resonance, 2H, $^2J_{H,H}$ = 17.6 Hz, $^2J_{H,P}$ = 5.3 Hz, C*H*$_2$), 7.49–7.65 (m, 12H, phenyl *ortho*,*para* *H*$_{arom.}$), 7.71–7.89 (m, 8H, phenyl *meta* *H*$_{arom.}$), 7.99 (t, 1H, $^3J_{H,H}$ = 7.8 Hz, pyridine *para* C*H*), 8.12 (d, 2H, $^3J_{H,H}$ = 7.8 Hz, pyridine *meta* C*H*) ppm. ^{13}C{^{1}H} NMR (75 MHz, CD_2Cl_2) δ_C: 44.8 (t, $^1J_{C,P}$ = 17.8 Hz, *C*H$_2$), 124.4 (t, $^3J_{C,P}$ = 6.0 Hz, pyridine *meta* *C*H), 125.3 (t, $^1J_{C,P}$ = 31.0 Hz, P*C*), 129.3 (t, $^1J_{C,P}$ = 31.7 Hz, P*C*), 129.5 (t, $J_{C,P}$ = 5.9 Hz, phenyl *C*$_{arom.}$), 130.0 (t, $J_{C,P}$ = 5.8 Hz, phenyl *C*$_{arom.}$), 132.9 (br s, phenyl *C*$_{arom.}$), 133.1 (br s, phenyl *C*$_{arom.}$), 133.2 (t, $J_{C,P}$ = 6.7 Hz, phenyl *C*$_{arom.}$), 133.7 (t, $J_{C,P}$ = 6.2 Hz, phenyl *C*$_{arom.}$), 142.2 (s, pyridine *para* *C*H), 162.1 (t, $J_{C,P}$ = 3.2 Hz, pyridine *ortho* *C*), 165.3 (t, $J_{C,P}$ = 7.7 Hz, *C*$_{arom.}$) ppm. The resonance corresponding to the carbonyl ligand was not observed. ^{31}P{^{1}H} NMR (121 MHz, CD_2Cl_2) δ_P: 21.6 (s, 2P, *P*Ph$_2$) ppm. FT-IR $\tilde{\nu}$/cm^{-1}: 3055 (w), 3020 (w), 2914 (w), 2872 (w), 2179 (w, IrH), 2041 (vs, CO), 1967 (w), 1605 (w), 1589 (w), 1564 (w), 1485 (w), 1466 (m), 1435 (s), 1393 (w), 1337 (w), 1312 (w), 1261 (w), 1190 (w), 1161 (w), 1144 (w), 1099 (s), 1074 (w), 1028 (w), 999 (m), 962 (w), 845 (m), 800 (m), 756 (m), 744 (m), 723 (m), 708 (s), 690 (vs), 608 (m), 567 (w), 540 (m), 511, (vs), 478 (vs), 461 (s), 413 (w). HRMS: (ESI+, MeCN) m/z: 732.0966 [(^{Ph}PN^{Py}P)IrCl(CO)H]$^+$ measured; 732.0952 calculated, Δ = 1.91 ppm. Elemental analysis (measured [calculated] for $C_{32}H_{28}ClIrNOP_2 \cdot$ ½ CH_2Cl_2 / %): 48.82 [48.19] C, 3.89 [3.61] H, 1.87 [1.73] N.

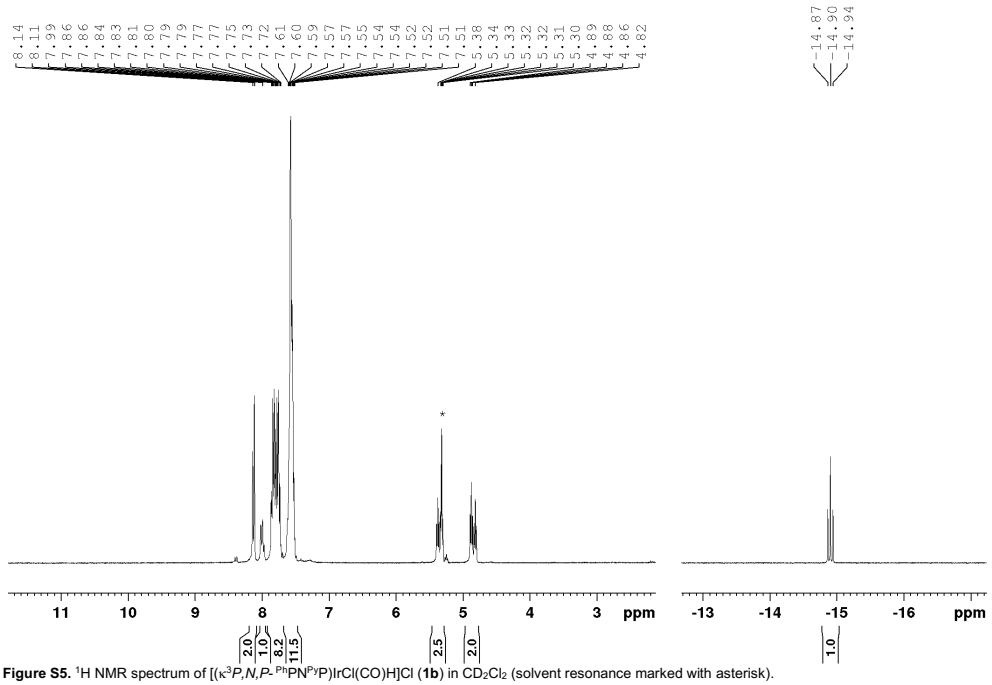

Figure S5. ^{1}H NMR spectrum of [(κ³*P,N,P*-^{Ph}PN^{Py}P)IrCl(CO)H]Cl (**1b**) in CD_2Cl_2 (solvent resonance marked with asterisk).

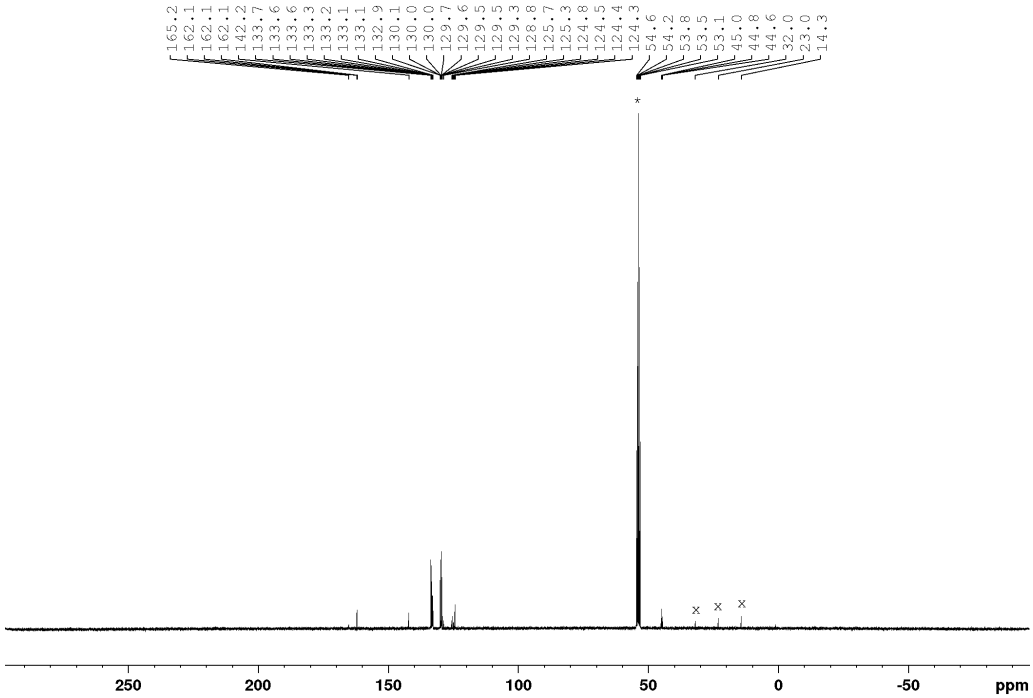

Figure S6. $^{13}C\{^{1}H\}$ NMR spectrum of [(κ^3*P,N,P*-$^{Ph}PN^{Py}P$)IrCl(CO)H]Cl (**1b**) in CD_2Cl_2 (solvent resonance marked with asterisk). Resonances corresponding to residual *n*-hexane are marked with x.

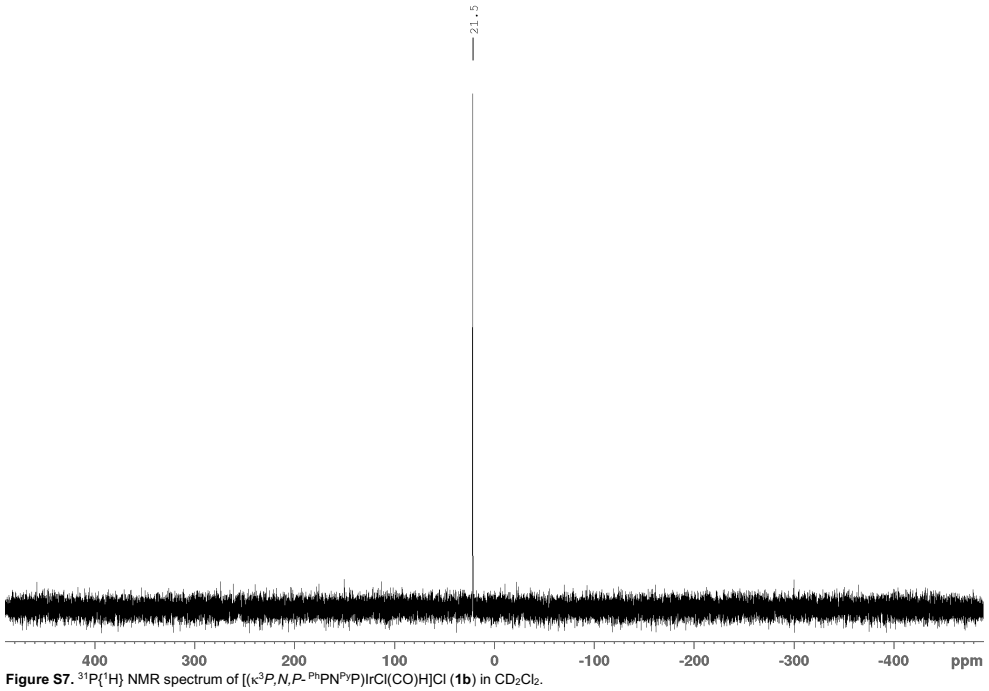

Figure S7. $^{31}P\{^{1}H\}$ NMR spectrum of [(κ^3*P,N,P*-$^{Ph}PN^{Py}P$)IrCl(CO)H]Cl (**1b**) in CD_2Cl_2.

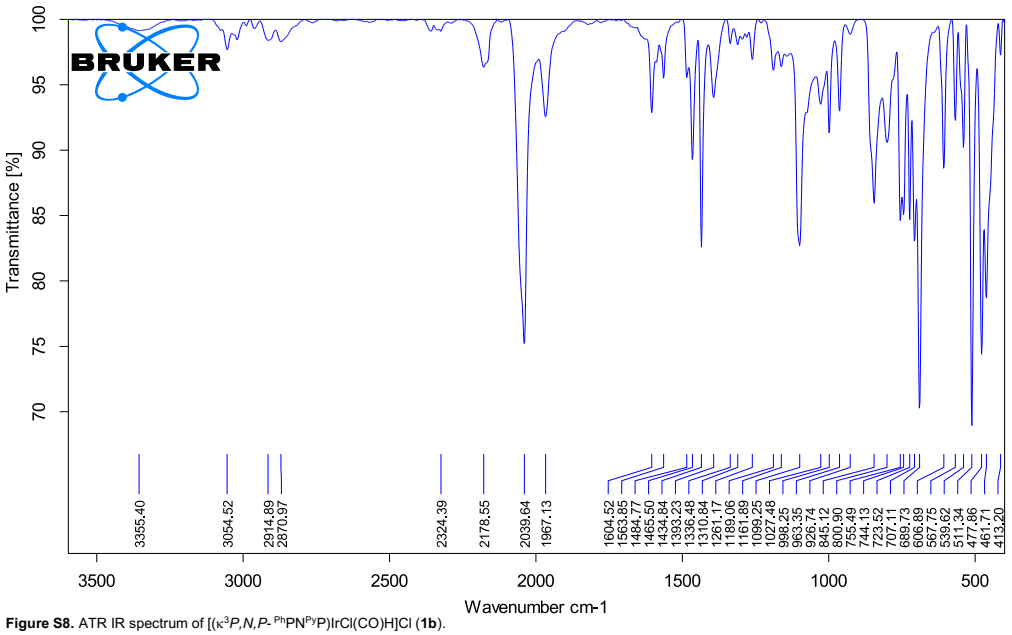

Figure S8. ATR IR spectrum of [(κ^3*P,N,P*-^{Ph}PN^{Py}P)IrCl(CO)H]Cl (**1b**).

*Synthesis of [(κ³P,N,P-^{Ph}PN^{H}P)IrCl(CO)H]Cl (**1c**)*

1c was synthesized based on the procedure by *Khan* and *Rao*.[5] 110 mg [IrCl(CO)(PPh_3)$_2$] (141 µmol, 1.0 eq.) and 100 mg [($Ph_2PCH_2CH_2$)NH_2]Cl (209 µmol, 1.5 eq.) were suspended in 5 ml hot toluene and heated to reflux. After 6 h, the formed precipitate was collected by filtration, washed 3x with 5 ml toluene and dried in vacuo. 98.0 mg [(κ³*P,N,P*-^{Ph}PN^{H}P)IrCl(CO)H]Cl (128 µmol, 95 %) were isolated as a yellow solid, containing the *trans*-isomer as major product. Both the *cis*- and the *trans*-isomer were detected by NMR spectroscopy, and are assigned on the base of NOE-correlations in phase-sensitive ^{1}H NOESY NMR spectra. Layering of a saturated solution of [(κ³*P,N,P*-^{Ph}PN^{H}P)IrCl(CO)H]Cl (**1c**) in CH_2Cl_2 with *n*-hexane resulted in the formation single crystals of *cis*-**1c** suitable for X-ray diffraction experiments.

Major isomer (*cis*-**1c**) resonances listed below, observable resonances of the minor isomer (t*rans*-**1c**) further down.
^{1}H NMR (300 MHz, CD_2Cl_2) δ_H: -15.48 (t, 1H, $^2J_{H,P}$ = 12.0 Hz, Ir*H*), 3.12–3.34 (m, superimposed on resonance of minor isomer, 8H, N(CH_2CH_2P)$_2$), 7.44–7.52 (m, 5H, $H_{arom.}$), 7.54–7.62 (m, 5H, $H_{arom.}$), 7.68–7.78 (m, 10H, $H_{arom.}$), 10.26 (br s, 1H, N*H*) ppm. ^{13}C{^{1}H} NMR (75 MHz, CD_2Cl_2) δ_C: 32.7 (t, $^1J_{C,P}$ = 16.4 Hz, PCH_2), 51.7 (t, $^2J_{C,P}$ = 2.2 Hz, NCH_2), 125.5 (t, $J_{C,P}$ = 29.9 Hz, $C_{arom.}$), 129.4 (t, $J_{C,P}$ = 5.6 Hz, $C_{arom.}$), 129.7 (t, $J_{C,P}$ = 5.7 Hz, $C_{arom.}$), 132.3 (s, $C_{arom.}$), 132.5 (s, $C_{arom.}$), 133.2 (t, $J_{C,P}$ = 6.5 Hz, $C_{arom.}$), 134.1 (t, $J_{C,P}$ = 5.8 Hz, $C_{arom.}$) ppm. The resonance corresponding to the carbonyl ligand was not observed. ^{31}P{^{1}H} NMR (121 MHz, CD_2Cl_2) δ_P: 30.8 (s, 2P, *P*Ph_2) ppm.
Observed minor isomer (t*rans*-**1c**) resonances (marked with x in the spectra; due to low signal strength, complete assignment is not possible): ^{1}H NMR (300 MHz, CD_2Cl_2) δ_H: -16.12 (t, $^2J_{H,P}$ = 10.4 Hz, Ir*H*), 3.34–3.49 (m, superimposed on resonace of major isomer, N(CH_2CH_2P)$_2$), 7.10–7.27 (m, $H_{arom.}$), 7.29–7.37 (m, $H_{arom.}$) ppm. (75 MHz, CD_2Cl_2) δ_C: 125.8 ($C_{arom.}$), 128.7 ($C_{arom.}$), 129.0 ($C_{arom.}$), 129.3 ($C_{arom.}$), 131.8 ($C_{arom.}$), 132.7 ($C_{arom.}$), 133.8 (t, $J_{C,P}$ = 6.0 Hz, $C_{arom.}$), 134.4 ($C_{arom.}$) ppm. ^{31}P{^{1}H} NMR (121 MHz, CD_2Cl_2) δ_P: 29.4 (s, 2P, *P*Ph_2) ppm.
FT-IR $\tilde{\nu}$/cm^{-1}: 3371 (w, br, NH), 3050 (w), 2936 (w), 2764 (w), 2707 (w), 2663 (w), 2605 (w), 2472 (w), 2350 (w), 2198 (w, IrH), 2030 (s, CO), 1666 (w), 1620 (w), 1586 (w), 1573 (w), 1482 (w), 1455 (w), 1434 (s), 1397 (w), 1340 (w), 1311 (w), 1270 (w), 1220 (w), 1179 (w), 1150 (m), 1102 (s), 1066 (m), 1028 (w), 997 (m), 850 (m), 794 (m), 744 (s), 723 (s), 691 (vs), 617 (w), 577 (s), 557 (s), 546 (m), 534 (s), 504 (vs), 489 (vs), 468 (s), 455 (s), 436 (m). HRMS: (ESI+, MeOH) m/z: 662.1342 [(^{Ph}PN^{H}P)Ir(CO)Cl]$^+$ measured; 662.1349 calculated, Δ = 1.06 ppm. Elemental analysis (measured [calculated] for $C_{29}H_{30}Cl_2IrNOP_2 \cdot C_7H_8$ / %): 51.69 [52.36] C, 4.76 [4.64] H, 2.35 [1.70] N.

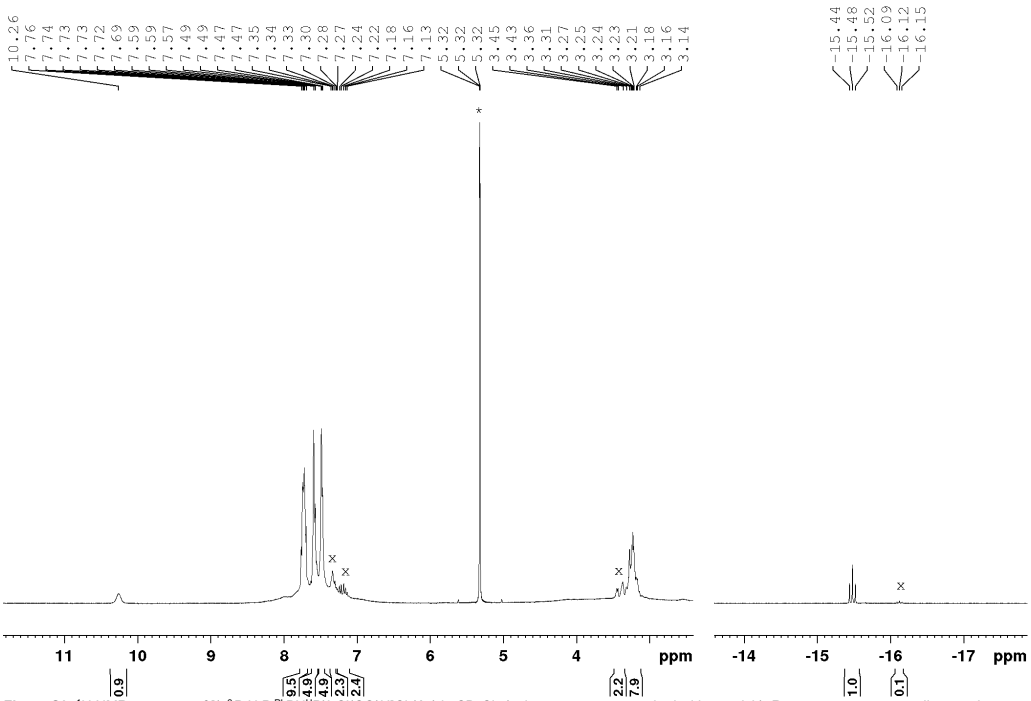

Figure S9. ^{1}H NMR spectrum of [(κ³*P,N,P*-^{Ph}PN^{H}P)IrCl(CO)H]Cl (**1c**) in CD_2Cl_2 (solvent resonance marked with asterisk). Resonances corresponding to minor isomer are marked with x.

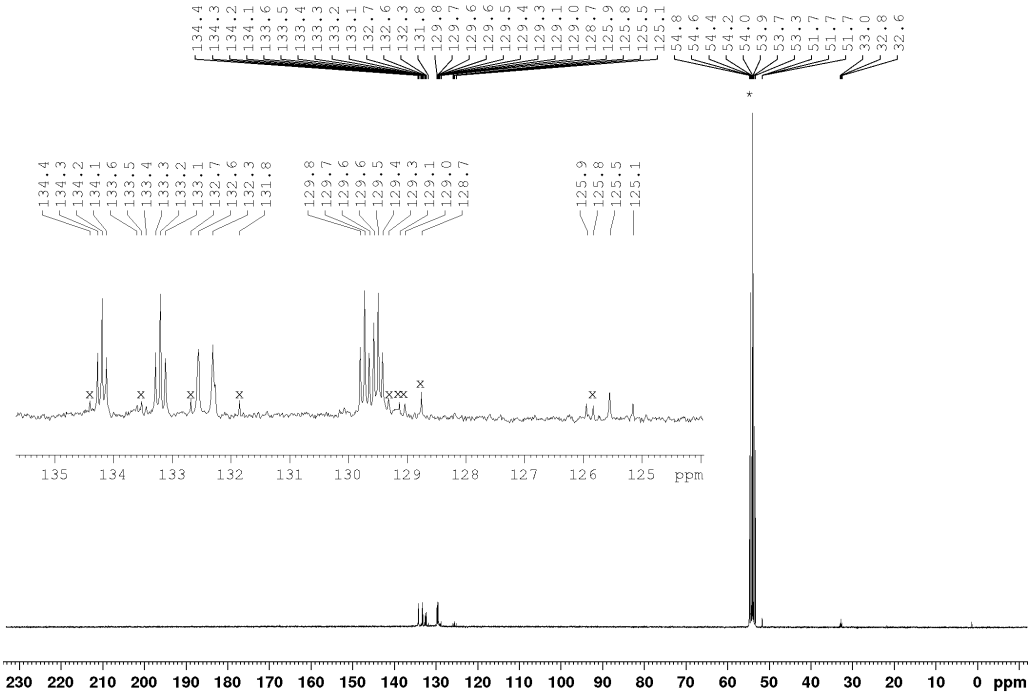

Figure S10. $^{13}C\{^{1}H\}$ NMR spectrum of [(κ^3*P,N,P*-^{Ph}PN^{H}P)IrCl(CO)H]Cl (**1c**) in CD_2Cl_2 (solvent resonance marked with asterisk). Resonances corresponding to minor isomer are marked with x.

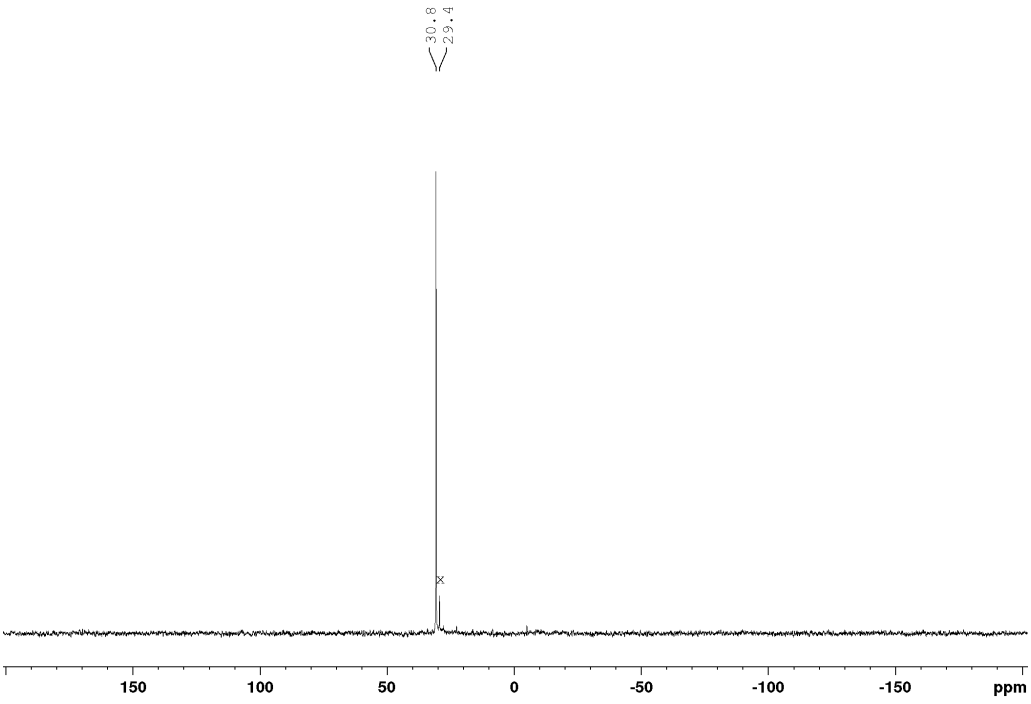

Figure S11. $^{31}P\{^{1}H\}$ NMR spectrum of [(κ^3*P,N,P*-^{Ph}PN^{H}P)IrCl(CO)H]Cl (**1c**) in CD_2Cl_2. Resonance corresponding to minor isomer is marked with x.

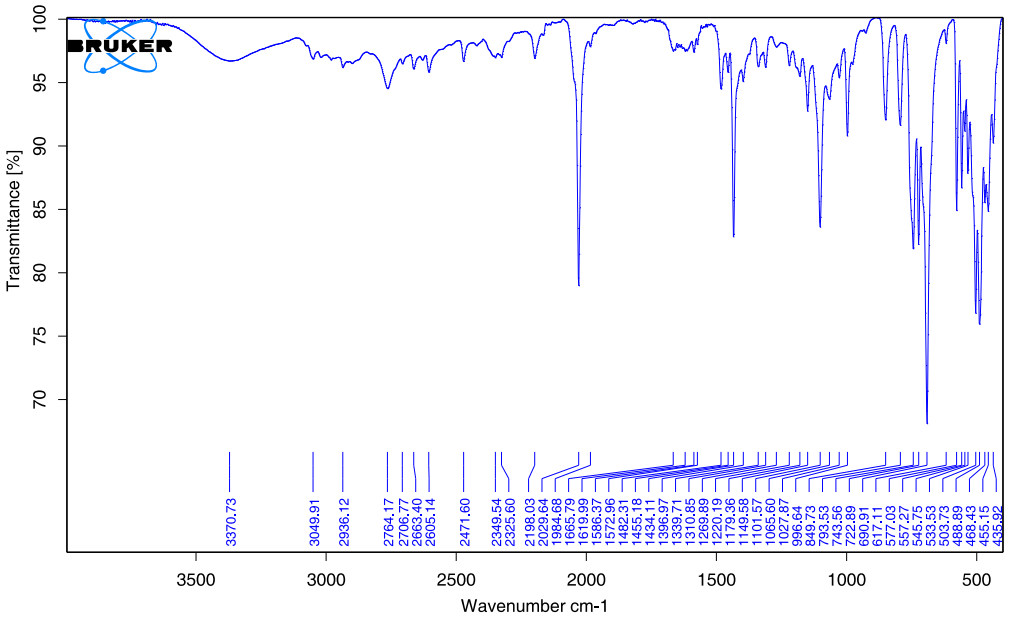

Figure S12. ATR IR spectrum of [(κ^3*P,N,P*-^{Ph}PN^{H}P)IrCl(CO)H]Cl (**1c**).

*Synthesis of [(κ³P,C,P-^{Ph}PC^{im}P)Ir(H)(CO)(Cl)]Cl (**1d**)*

59 mg 1,3-Bis(2-diphenylphosphanylethyl)-3*H*-imidazol-1-ium chloride (112 µmol, 1.0 eq.) and 50 mg [*cis*-Ir(CO)$_2$Cl(*para*-toluidine)] (128 µmol, 1.1 eq.) were dissolved in 5 ml of toluene. After stirring over night, the solvent was removed in vacuo and to the resulting brown solids, 5 ml of dichloromethane were added. Filtration of the suspension yielded a yellow solution, which was layered with 10 ml *n*-hexane. After several weeks, 33.6 mg [(κ³*P,N,P*-^{Ph}PC^{bim}P)Ir(H)(CO)(Cl)]Cl (42.8 µmol, 38 %) were isolated as colorless needles.

^{1}H NMR (300 MHz, CD_2Cl_2) δ_H: -16.69 (t, 1H, $^2J_{H,P}$ = 10.8 Hz, Ir-*H*), 2.57–3.01 (m, 4H, C*H*$_2$P), 4.24 (m, 2H, NC*H*$_2$), 5.19 (m, superimposed on solvent, 2H, NC*H*$_2$), 7.36–7.43 (m, 6H, *H*$_{arom.}$), 7.43–7.52 (m, 10H, *H*$_{arom.}$), 7.58–7.71 (m, 6H, NC*H*, *H*$_{arom.}$) ppm. ^{13}C{^{1}H} NMR (75 MHz, CD_2Cl_2) δ_C: 26.5 (s, PCH$_2$), 47.4 (s, NCH$_2$), 124.0 (s, NCH), 129.0 (t, $J_{C,P}$ = 5.4 Hz, *C*$_{arom.}$), 129.9 (t, $J_{C,P}$ = 11.0 Hz, *C*$_{arom.}$), 131.3 (s, *C*$_{arom.}$), 132.0 (s, *C*$_{arom.}$), 133.1 (t, $J_{C,P}$ = 5.3 Hz, *C*$_{arom.}$), 134.2 (t, $J_{C,P}$ = 6.1 Hz, *C*$_{arom.}$) ppm. ^{31}P{^{1}H} NMR (121 MHz, CD_2Cl_2) δ_P: -7.8 (s, *P*-Ir-*P*) ppm. FT-IR $\tilde{\nu}$/cm^{-1}: 3082 (w), 3053 (w), 3026 (w), 2365 (w), 2203 (w, IrH), 2096 (w), 2041 (vs, CO), 2000 (w), 1967 (w), 1572 (w), 1481 (m), 1433 (s), 1402 (m), 1381 (w), 1352 (w), 1335 (m), 1310 (w), 1281(w), 1252 (w), 1238 (w), 1192 (w), 1151 (w), 1096 (s), 1072 (w), 1057 (w), 1028 (w), 997 (m), 970 (w), 868 (m), 841 (w), 808 (m), 783 (m), 746 (s), 721 (vs), 706 (vs), 689 (vs), 638 (w), 617 (w), 546 (vs), 530 (m), 515 (vs), 503 (s), 488 (s), 476 (s), 459 (s), 415 (m). HRMS (ESI+, MeCN) m/z: 749.1245 [(^{Ph}PC^{bim}P)Ir(H)(CO)(Cl)]$^+$ measured, 749.1229 calculated, Δ = 2.14 ppm. Elemental analysis (measured [calculated] for $C_{32}H_{31}Cl_2IrN_2OP_2 \cdot CH_2Cl_2$ / %): 45.73 [45.58] C, 3.93 [3.83] H, 3.38 [3.22] N.

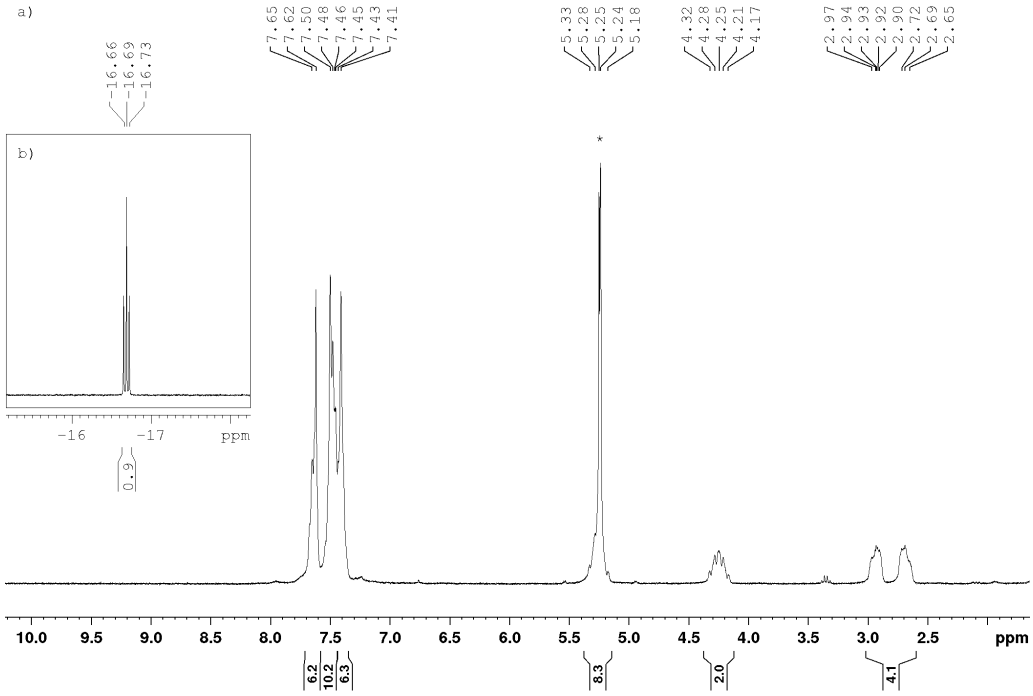

Figure S13. a) ^{1}H NMR spectrum of [(κ³*P,N,P*-^{Ph}PC^{im}P)Ir(H)(CO)(Cl)]Cl (**1d**) in CD_2Cl_2 (solvent resonance marked with asterisk). b) Cutout of the hydride resonance of [(κ³*P,N,P*-^{Ph}PC^{im}P)Ir(H)(CO)(Cl)]Cl (**1d**) in CD_2Cl_2.

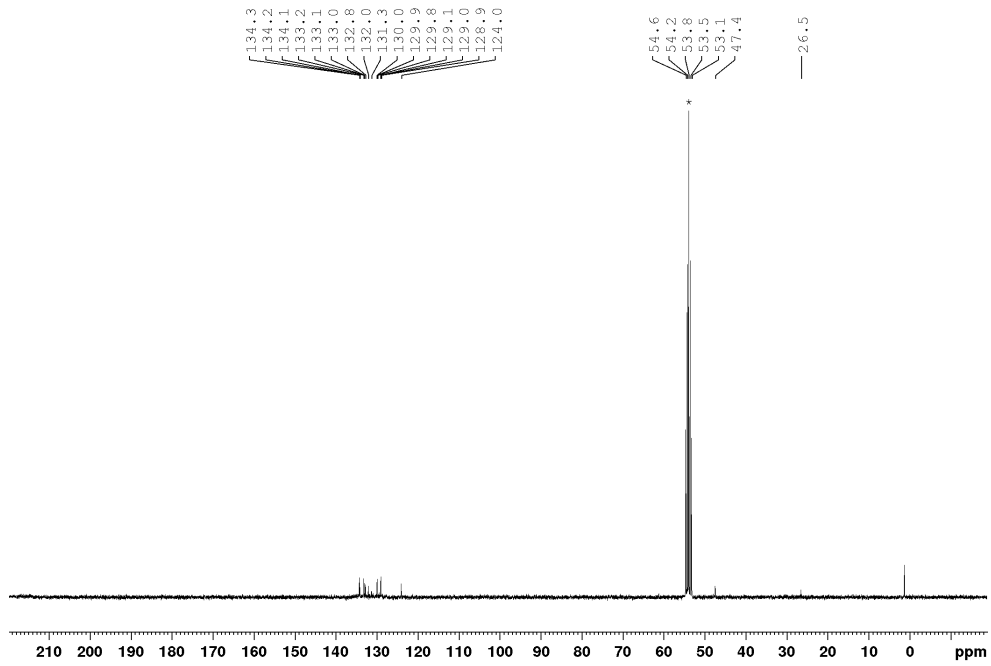

Figure S14. $^{13}C\{^{1}H\}$ NMR spectrum of [(κ^{3}*P,N,P*-^{Ph}PC^{Im}P)Ir(H)(CO)(Cl)]Cl (**1d**) in CD_2Cl_2 (solvent resonance marked with asterisk).

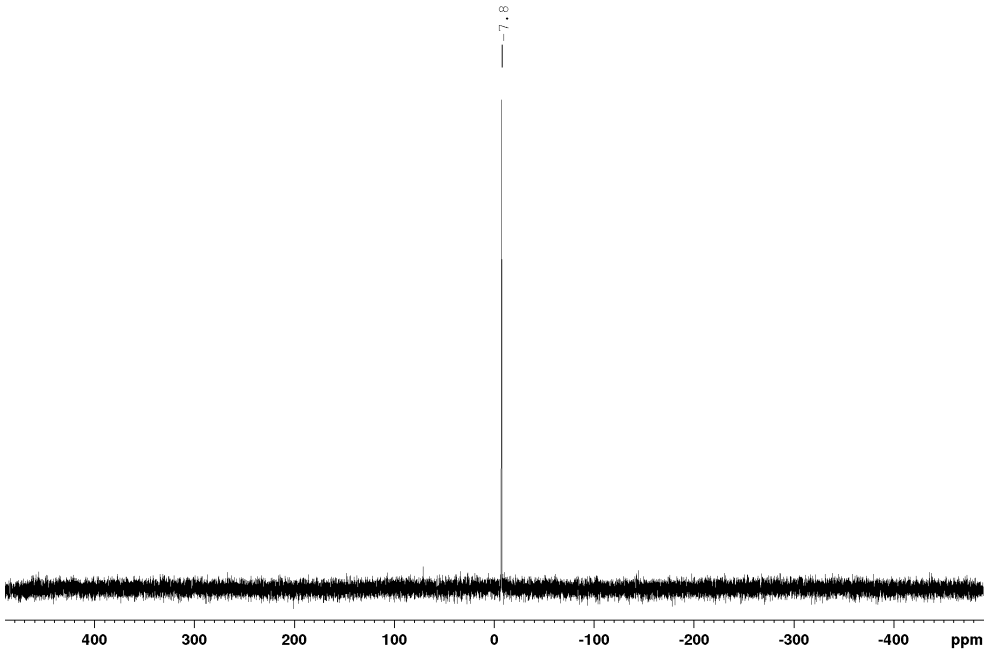

Figure S15. $^{31}P\{^{1}H\}$ NMR spectrum of [(κ^{3}*P,N,P*-^{Ph}PC^{Im}P)Ir(H)(CO)(Cl)]Cl (**1d**) in CD_2Cl_2.

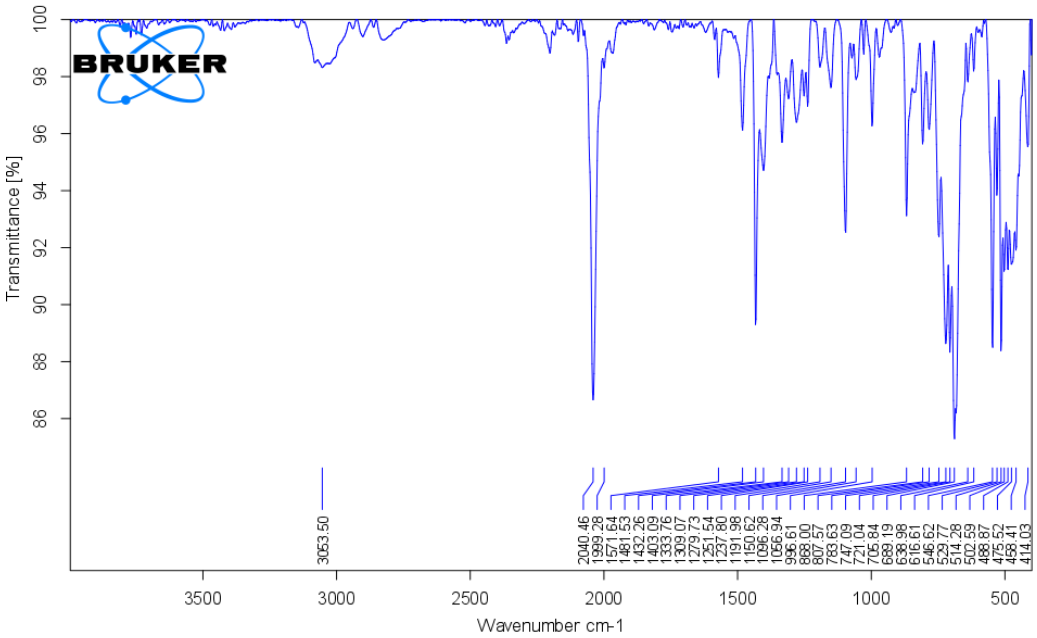

Figure S16. ATR IR spectrum of [(κ^3*P,N,P*-^{Ph}PC^{im}P)Ir(H)(CO)(Cl)]Cl (**1d**).

*Synthesis of [{κ³P,C,P-C(dppm)₂}IrCl(CO)H]Cl (**1e**)*

68.7 mg [IrCl(CO)(PPh₃)] (88.0 µmol, 1.0 eq.) and 72.0 mg [HC(dppm)₂]Cl (88.6 µmol, 1.0 eq.) were dissolved in 5 ml $CHCl_3$. After stirring for 1 h, the solvent was removed in vacuo. The remaining yellow solid was dissolved in 5 ml CH_2Cl_2 and precipitated by adding 10 ml ethyl acetate. After decanting the supernatant solution, the precipitate was washed 3x with 3 ml ethyl acetate. Drying in vacuo yielded 87.0 mg [{κ³*P,C,P*-C(dppm)₂}IrCl(CO)H]Cl (81.1 µmol, 89 %) as a yellow solid. Single crystals suitable for X-ray diffraction experiments were obtained by layering a solution of [{κ³*P,C,P*-C(dppm)₂}IrCl(CO)H]Cl in CH_2Cl_2 with *n*-hexane.

^{1}H NMR (300 MHz, CD_2Cl_2) δ_H: -16.51 (t, 1H, $^2J_{H,P}$ = 10.4 Hz, Ir*H*), 4.33 (m, 2H, CH_2), 4.55 (m, 2H, CH_2), 7.02 (t, 4H, $J_{H,P}$ = 7.3 Hz, $H_{arom.}$), 7.13 (q, $J_{H,P}$ = 7.5 Hz, 4H, $H_{arom.}$), 7.20–7.43 (m, 20H, $H_{arom.}$), 7.43–7.49 (m, 4H, $H_{arom.}$), 7.65 (q, 4H, $J_{H,P}$ = 6.8 Hz, $H_{arom.}$), 7.68–7.73 (m, 4H, $H_{arom.}$) ppm. ^{13}C{^{1}H} NMR (126 MHz, CD_2Cl_2) δ_C: 37.2–38.1 (m, CH_2), 127.8 (t, $J_{C,P}$ = 30.8 Hz, $C_{arom.}$), 128.8 (t, $J_{C,P}$ = 5.9 Hz, $C_{arom.}$), 129.0–129.4 (m, $C_{arom.}$), 131.4 (s, $C_{arom.}$), 131.9 (s, $C_{arom.}$), 132.2–132.5 (m, $C_{arom.}$), 132.6–132.8 (m, $C_{arom.}$), 132.9 (t, $J_{C,P}$ = 4.9 Hz, $C_{arom.}$), 133.3 (t, $J_{C,P}$ = 5.1 Hz, $C_{arom.}$), 133.5 (t, $J_{C,P}$ = 7.1 Hz, $C_{arom.}$), 134.3 (t, $J_{C,P}$ = 5.9 Hz, $C_{arom.}$) ppm. Neither the carbonyl nor the carbodiphosphorane carbon resonances were observed. ^{31}P{^{1}H} NMR (121 MHz, CD_2Cl_2) δ_P: 7.8 (t, 2P, $^2J_{P,P}$ = 34.8 Hz, *P*-Ir-*P*) , 31.8 (t, 2P, $^2J_{P,P}$ = 35.2 Hz, *P*-CH_2-*P*), ppm. FT-IR $\tilde{\nu}$/cm^{-1}: 3053 (w), 3014 (w), 2929 (w), 2844 (w), 2271 (w, IrH), 2015 (s, CO), 1930 (w), 1728 (s), 1587 (w), 1484 (m), 1433 (s), 1370 (m), 1314 (w), 1242 (m), 1190 (w), 1157 (m), 1100 (vs), 1041(m), 998 (m), 939 (w), 833 (m), 784 (s), 739 (s),690 (vs), 610 (vs), 559 (s), 538 (s), 504 (vs), 475 (vs). HRMS: (ESI+, CH_2Cl_2) m/z: 1001.1986 [{C(dppm)₂}IrCl(CO)H]$^+$ measured; 1001.1972 calculated, Δ = 1.40 ppm. Elemental analysis (measured [calculated] for $C_{52}H_{45}Cl_2IrOP_4$ / %): 57.49 [58.21] C, 4.45 [4.23] H, 0.00 [0.00] N.

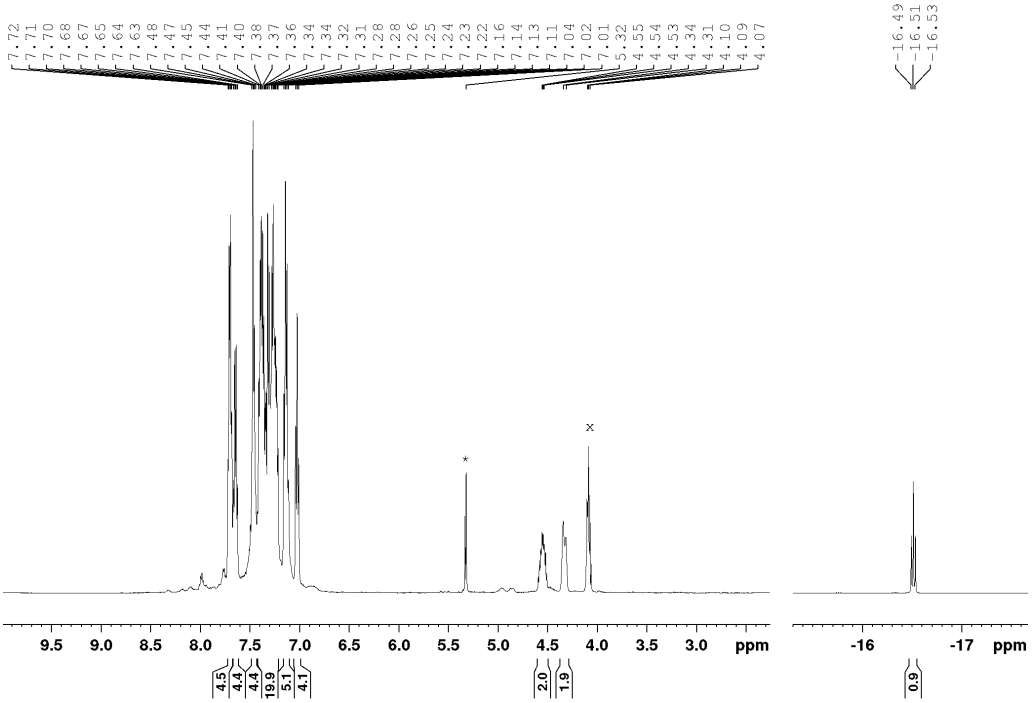

Figure S17. ^{1}H NMR spectrum of [(κ³*P,C,P*- C(dppm)₂}IrCl(CO)H]Cl (**1e**) in CD_2Cl_2 (solvent resonance marked with asterisk). Residual ethyl acetate resonance marked with x.

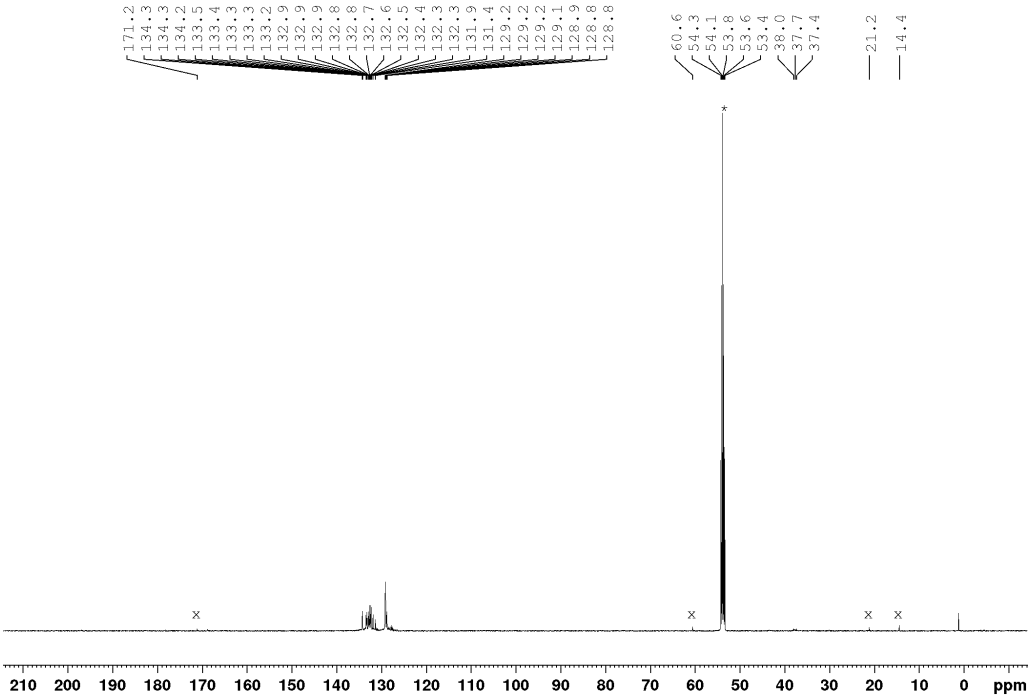

Figure S18. $^{13}C\{^{1}H\}$ NMR spectrum of [(κ^3*P,C,P*- C(dppm)$_2$}IrCl(CO)H]Cl (**1e**) in CD_2Cl_2 (solvent resonance marked with asterisk). Residual ethyl acetate resonance marked with x.

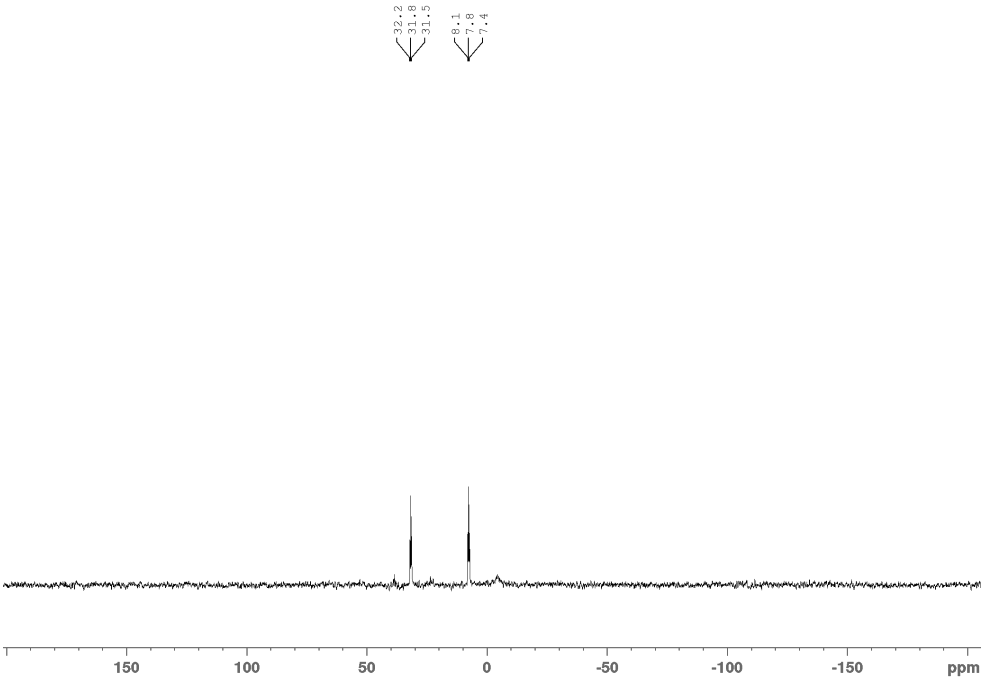

Figure S19. $^{31}P\{^{1}H\}$ NMR spectrum of [(κ^3*P,C,P*- C(dppm)$_2$}IrCl(CO)H]Cl (**1e**) in CD_2Cl_2.

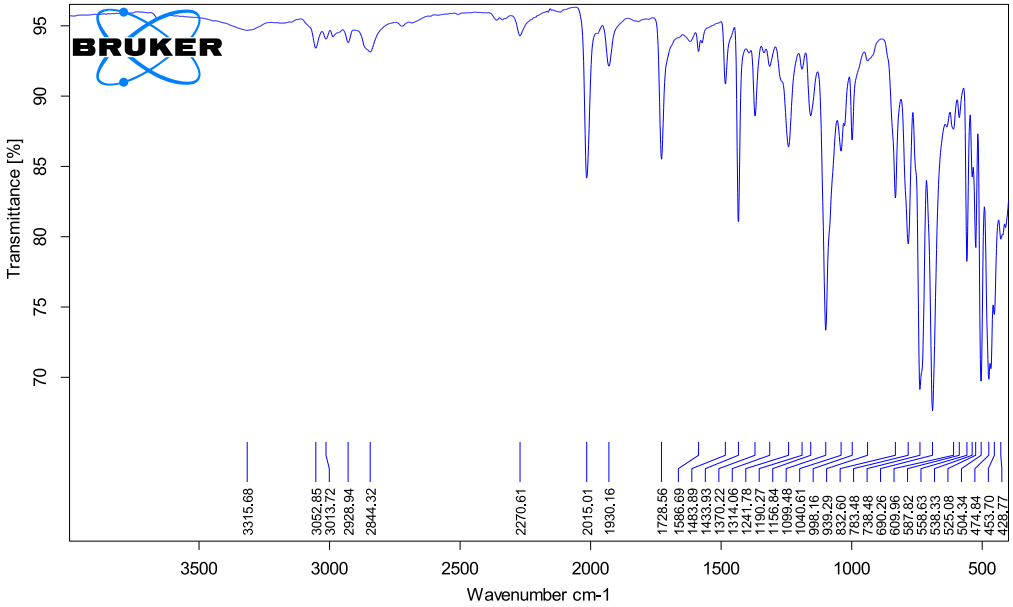

Figure S20. ATR IR spectrum of [(κ^3*P,C,P*- C(dppm)$_2$}IrCl(CO)H]Cl (**1e**).

S17

*Synthesis of [{κ³P,B,P-HB(dppm)₂}IrCl(CO)H]Br (**1f**)*

1f was synthesized by adaptation of the procedure for [{κ³*P,C,P*-C(dppm)₂}IrCl(CO)H]Cl (**1e**). 45.0 mg [Ir(Cl)(CO)(PPh₃)₂] (57.7 µmol, 1.0 eq.) were dissolved in 5 ml CH_2Cl_2 and cooled to -74 °C. Dropwise addition of a solution of 50.0 mg [H₂B(dppm)₂]Br (58.0 µmol, 1.0 eq.) in 5 ml CH_2Cl_2 led to a colorless precipitate. After stirring at -74 °C for 1 h, the precipitate was filtered and dried in vacuo. The resulting colorless solid was washed 3x with 5 ml *n*-hexane and dried in vacuo. 43.8 mg of [{κ³*P,B,P*-HB(dppm)₂}IrCl(CO)H]Br (39.2 µmol, 68 %) were obtained as a colorless solid, consisting of a mixture of the *cis*- and *trans*-isomer (approx. 9:1 ratio). Both the *cis*- and the *trans*-isomer were detected by NMR spectroscopy, and are assigned on the base of NOE-correlations in phase-sensitive ^{1}H NOESY NMR spectra. Single crystals of *cis*-**1f** suitable for X-ray diffraction experiments were obtained by layering a solution of **1f** in CH_2Cl_2 with *n*-hexane.

Main isomer (*cis*-**1f**) resonances listed below, observable resonances of the minor isomer (*trans*-**1f)** are listed separately.
^{1}H NMR (300 MHz, CD_2Cl_2) δ_H: -17.73 (t, 1H, $^2J_{H,P}$ = 12.4 Hz, Ir*H*,) 4.43 (m, 2H, CH_2), 4.91 (m, 2H, CH_2), 7.04 (td, 5H, $J_{H,P}$ = 11.7 Hz, $J_{H,P}$ = 2.8 Hz, $H_{arom.}$), 7.11–7.49 (m, 26H, $H_{arom.}$), 7.59–7.86 (m, 9H, $H_{arom.}$) ppm. ^{1}H{^{11}B} NMR (300 MHz, CD_2Cl_2) δ_H: (only additionally observed resonances are listed) 3.84 (t, 1H, $^2J_{H,P}$ = 25.3 Hz, B*H*) ppm. ^{11}B{^{1}H} NMR (96 MHz, CD_2Cl_2, with reduced glass peak) δ_B: -30.1 (br s, *B*H) ppm. ^{13}C{^{1}H} NMR (75 MHz, CD_2Cl_2) δ_C: 36.6–38.0 (m, *C*H₂), 124.4–125.4 (m, $C_{arom.}$), 127.1 (dd, $^1J_{C,P}$ = 61.9 Hz, $^3J_{C,P}$ = 3.4 Hz, $C_{arom.}$), 128.7 (br s, $C_{arom.}$), 128.8–129.2 (m, *C*H$_{arom.}$), 129.2–129.6 (m, *C*H$_{arom.}$), 131.4 (s, superimposed on minor isomer resonances, *C*H$_{arom.}$), 131.9–132.3 (m, *C*H$_{arom.}$), 132.5–133.0 (m, superimposed on minor isomer resonances, *C*H$_{arom.}$), 133.3–133.5 (m, superimposed on minor isomer resonances, *C*H$_{arom.}$), 134.3 (t, superimposed on minor isomer resonances, $J_{C,P}$ = 6.9 Hz, *C*H$_{arom.}$) ppm. ^{31}P{^{1}H} NMR (100 MHz, CD_2Cl_2) δ_P: 22.7 (br s, 2P, *P*-BH-*P*), 11.6 (t, 2P, $^2J_{P,P}$ = 51.5 Hz, *P*-Ir-*P*) ppm.
Observed minor isomer (*trans*-**1f)** resonances (marked with x in the spectra; due to low signal strength, complete assignment is not possible): ^{1}H NMR (300 MHz, CD_2Cl_2) δ_H: -16.66 (t, 1H, $^2J_{H,P}$ = 12.3 Hz, Ir*H*,) 4.19–4.33 (m, 2H, CH_2), 4.60–4.83 (m, 2H, CH_2), 7.48–7.60 (m, superimposed on major isomer resonances, $H_{arom.}$), 7.95–8.05 (m, $H_{arom.}$) ppm. ^{13}C{^{1}H} NMR (75 MHz, CD_2Cl_2) δ_C: 128.4 (s, $C_{arom.}$), 129.7 (t, $J_{C,P}$ = 5.2 Hz, $C_{arom.}$), 131.3–131.7 (m, superimposed on major isomer resonances, *C*H$_{arom.}$), 132.8–133.3 (m, superimposed on major isomer resonances, *C*H$_{arom.}$), 133.8–134.2 (m, superimposed on major isomer resonances, *C*H$_{arom.}$), 134.3–134.7 (m, superimposed on major isomer resonances, *C*H$_{arom.}$), 134.8–135.2 (m, *C*H$_{arom.}$) ppm. ^{31}P{^{1}H} NMR (100 MHz, CD_2Cl_2) δ_P: 10.2 (t, $^2J_{P,P}$ = 51.1 Hz, *P*-Ir-*P*) ppm.
FT-IR $\tilde{\nu}$/cm^{-1}: 3051 (w), 3016 (w), 2917 (w), 2852 (w), 2234 (w, IrH), 2015 (s, CO), 1587 (w), 1574 (w), 1484 (m), 1434 (s), 1365 (w), 1332 (w), 1310 (w), 1277 (w), 1190 (w), 1158 (m), 1097 (s), 1071 (m), 1027 (w), 999 (m), 793 (m), 739 (s), 728 (s), 687 (vs), 525 (s), 482 (vs), 427 (m). HRMS: (ESI+, CH_2Cl_2) m/z: 1037.1908 [{HB(dppm)₂}IrCl(CO)H]$^+$ measured, 1037.1908 calculated, Δ = 0.00 ppm. Elemental analysis (measured [calculated] for $C_{51}H_{46}BBrClIrOP_4$ / %): 54.43 [54.07] C, 4.34 [4.15] H, 0.00 [0.00] N.

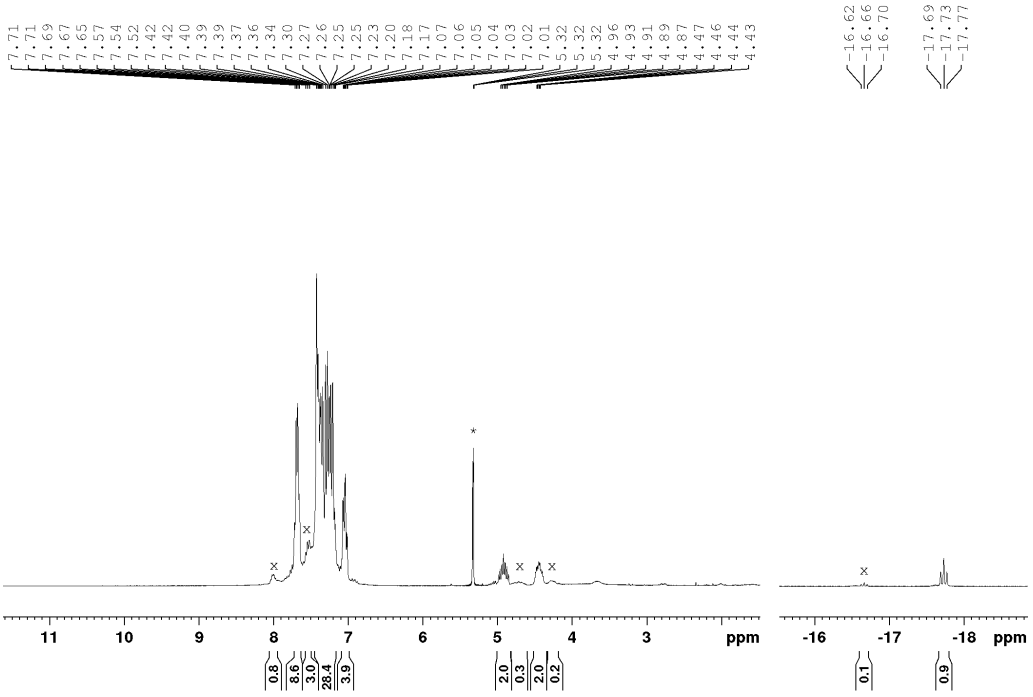

Figure S21. ^{1}H NMR spectrum of [(κ³*P,B,P*- HB(dppm)₂}IrCl(CO)H]Br (**1f**) in CD_2Cl_2 (solvent resonance marked with asterisk). Resonances corresponding to minor isomer are marked with x.

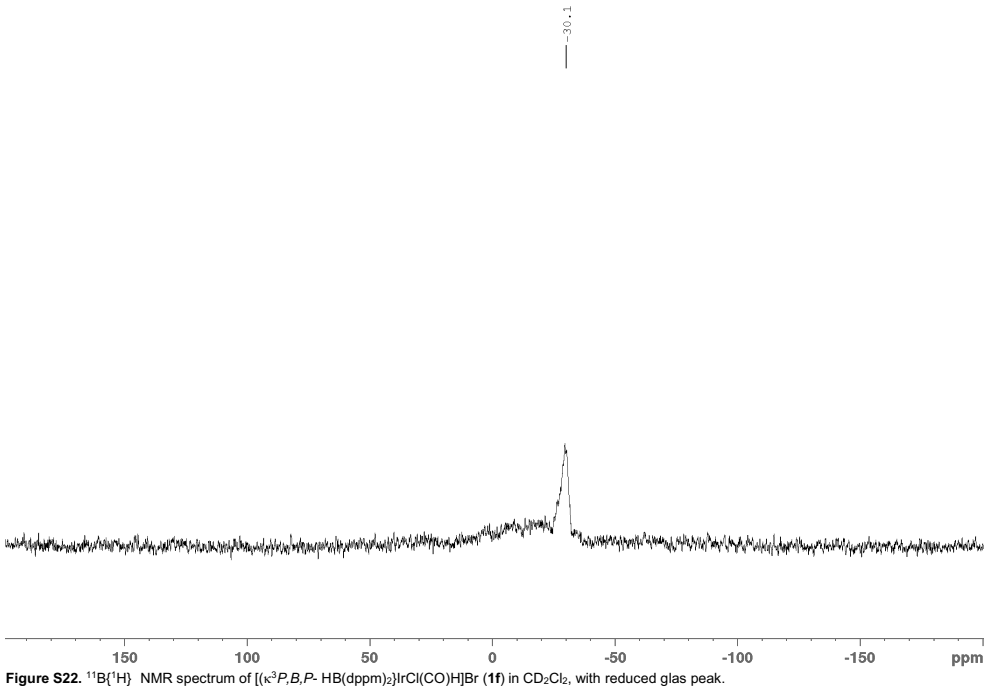

Figure S22. $^{11}B\{^1H\}$ NMR spectrum of [(κ^3*P,B,P*- HB(dppm)$_2$}IrCl(CO)H]Br (**1f**) in CD_2Cl_2, with reduced glas peak.

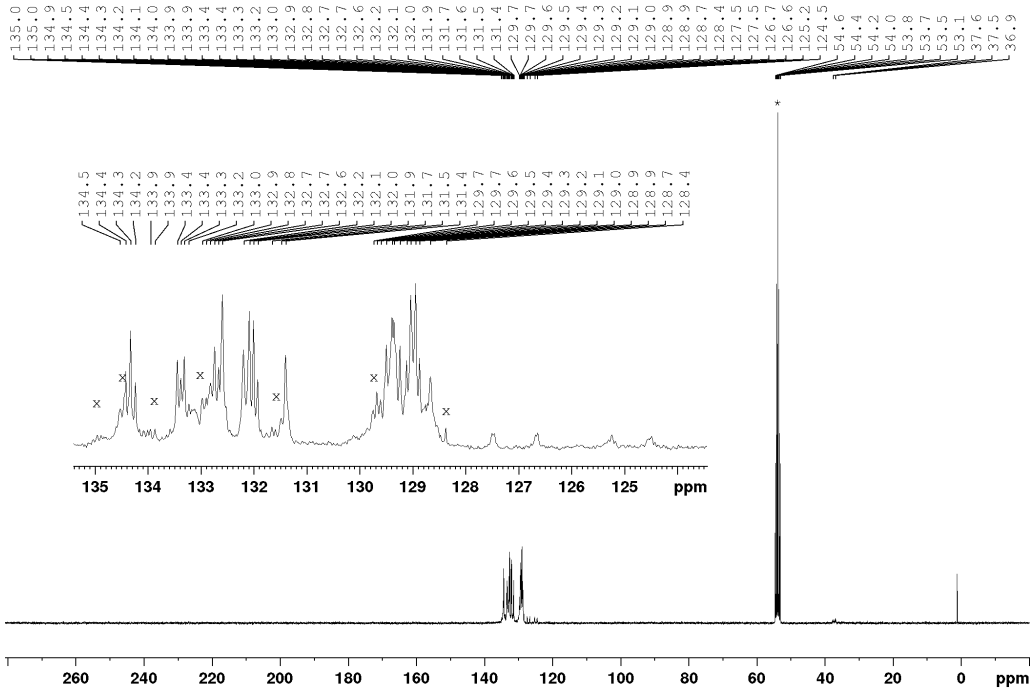

Figure S23. $^{13}C\{^1H\}$ NMR spectrum of [(κ^3*P,B,P*- HB(dppm)$_2$}IrCl(CO)H]Br (**1f**) in CD_2Cl_2 (solvent resonance marked with asterisk). Resonances corresponding to minor isomer are marked with x.

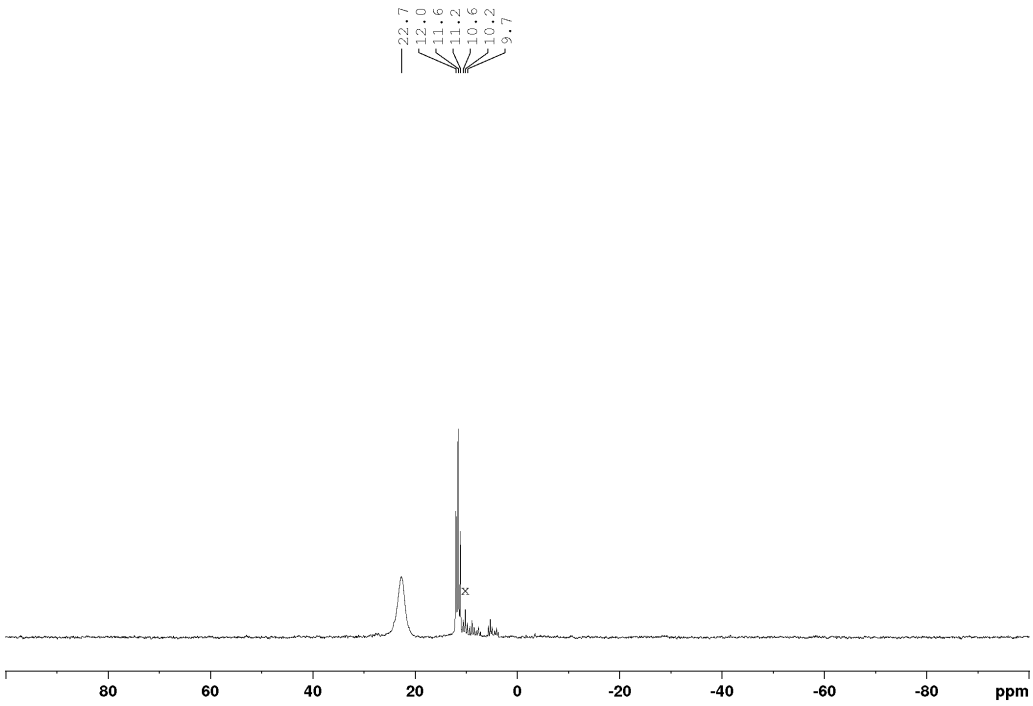

Figure S24. $^{31}P\{^{1}H\}$ NMR spectrum of [(κ^3*P,B,P*- HB(dppm)$_2$}IrCl(CO)H]Br (**1f**) in CD_2Cl_2. Resonances corresponding to minor isomer are marked with x.

Figure S25. ATR IR spectrum of [(κ^3*P,B,P*- HB(dppm)$_2$}IrCl(CO)H]Br (**1f**) in CD_2Cl_2.

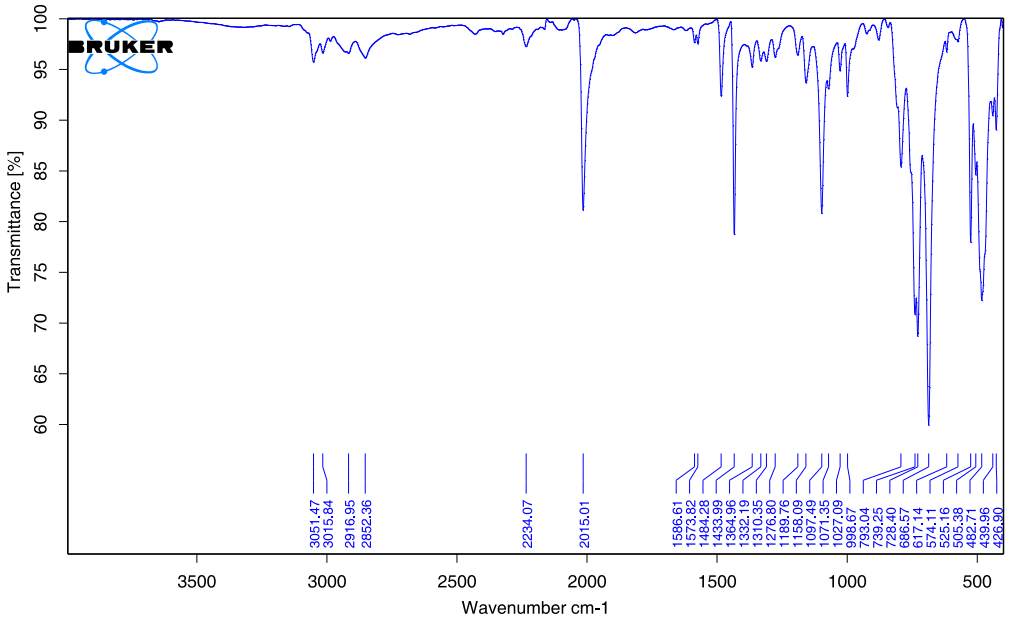

*Synthesis of [(κ³P,C,P-^{Ph}PC^{Ph}P)IrCl(CO)H] (**1g**)*

1g was synthesized following the general procedure by Li and coworkers.[8] 55.0 mg [Ir(Cl)(CO)(PPh_3)$_2$] (70.5 µmol, 1.0 eq.) and 30.0 mg dpmb (63.2 µmol, 0.9 eq.) were suspended in 5 ml toluene. After refluxing for 30 min, crystals formed upon cooling to RT. The supernatant solution was decanted, the crystalline precipitate washed with 2x 3 ml toluene and dried in vacuo. Single crystals suitable for X-ray diffraction were taken from the reaction mixture. 19.6 mg [(κ³*P,C,P*-^{Ph}PC^{Ph}P)IrCl(CO)H] (26.8 µmol, 42.4 %) were isolated as crystalline solid.

^{1}H NMR (300 MHz, $CDCl_3$) δ_H: -17.64 (t, 1H, $^1J_{H,P}$ = 13.3 Hz, Ir-*H*), 3.95 (td, 2H, $^2J_{H,H}$ = 16.2, $^2J_{P,H}$ = 4.9 Hz, C*H*$_2$ (a)), 4.49 (td, 2H, $^2J_{H,H}$ = 16.2, $^2J_{P,H}$ = 4.7 Hz, C*H*$_2$ (b)), 7.02 (t, 1H, $^3J_{H,H}$ = 7.4 Hz, aryl *para* C*H*), 7.19 (d, 2H, $^3J_{H,H}$ = 7.4 Hz, aryl *meta* C*H*), 7.35–7.48 (m, 12H, phenyl *ortho, para* C*H*), 7.56–7.65 (m, 4H, phenyl *meta* C*H* (a)), 7.67–7.77 (m, 4H, phenyl *meta* C*H* (b)) ppm. ^{13}C{^{1}H} NMR (122 MHz, $CDCl_3$) δ_C: 46.0 (t, $J_{C,P}$ = 19.8 Hz, *C*H$_2$), 122.2 (t, $^3J_{C,P}$ = 9.1 Hz, aryl *meta* H*C*), 125.5 (s, aryl *para* H*C*), 128.5 (t, $J_{C,P}$ = 5.3 Hz, phenyl *ortho*, *meta* H*C* (a)), 128.8 (t, $J_{C,P}$ = 5.2 Hz, phenyl *ortho*, *meta* H*C* (b)), 130.1 (t, $^1J_{C,P}$ = 26.9 Hz, phenyl P*C* (a)), 130.9 (br s, phenyl *para* H*C*), 132.6 (t, $J_{C,P}$ = 6.2 Hz, phenyl *ortho*, *meta* H*C* (a)), 133.2 (t, $J_{C,P}$ = 5.7 Hz, phenyl *ortho*, *meta* H*C* (b)), 134.9 (t, $^1J_{C,P}$ = 28.2 Hz, phenyl P*C* (b)), 147.1 (t, $^2J_{C,P}$ = 8.5 Hz, *C*CH$_2$) ppm. ^{31}P{^{1}H} NMR (121 MHz, $CDCl_3$) δ_P: 25.9 (s, *P*Ph$_2$) ppm. The resonance corresponding to the carbonyl ligand was not observed. A minor second set of resonances can be observed in the NMR spectra, indicating a second complex (resonances marked with x in the spectra). ^{1}H NMR (300 MHz, $CDCl_3$) δ_H: -16.70 (t, $J_{H,P}$ = 13.0 Hz), 4.03 (t, superimposed, $J_{H,P}$ = 5.0 Hz), 4.55 (m, superimposed) ppm. ^{31}P{^{1}H} NMR (121 MHz, $CDCl_3$) δ_P: 23.6 (s) ppm. Formation of a penta-coordinate compound through either loss of the carbon monoxide ligand or expulsion of the chloride ligand from the coordination sphere seem likely possibilities, though formation of dimeric species can also occur. The high similarity in the chemical shifts of the resonances points to a rather small change. FT-IR $\tilde{\nu}$/cm^{-1}: 3076 (w), 3053 (w), 3020 (w), 2885 (w), 2829 (w), 2181 (w, IrH), 2012 (s, CO), 1967 (w), 1574 (w), 1493 (w), 1485 (w), 1452 (w), 1435 (s), 1418 (m), 1398 (m), 1379 (w), 1356 (w), 1329 (w), 1304 (w), 1279 (w), 1248 (w), 1194 (w), 1184 (w), 1161 (w), 1105 (m), 1082 (w), 1068 (w), 1028 (w), 999 (w), 964 (m), 897 (w), 843 (m), 793 (m), 771 (w), 756 (m), 733 (vs), 717 (s), 708 (s), 689 (vs), 590 (s), 550 (w). Elemental analysis (measured [calculated] for $C_{33}H_{28}ClIrOP_2$ / %): 54.12 [54.28] C, 4.24 [3.87] H, 0.00 [0.00] N.

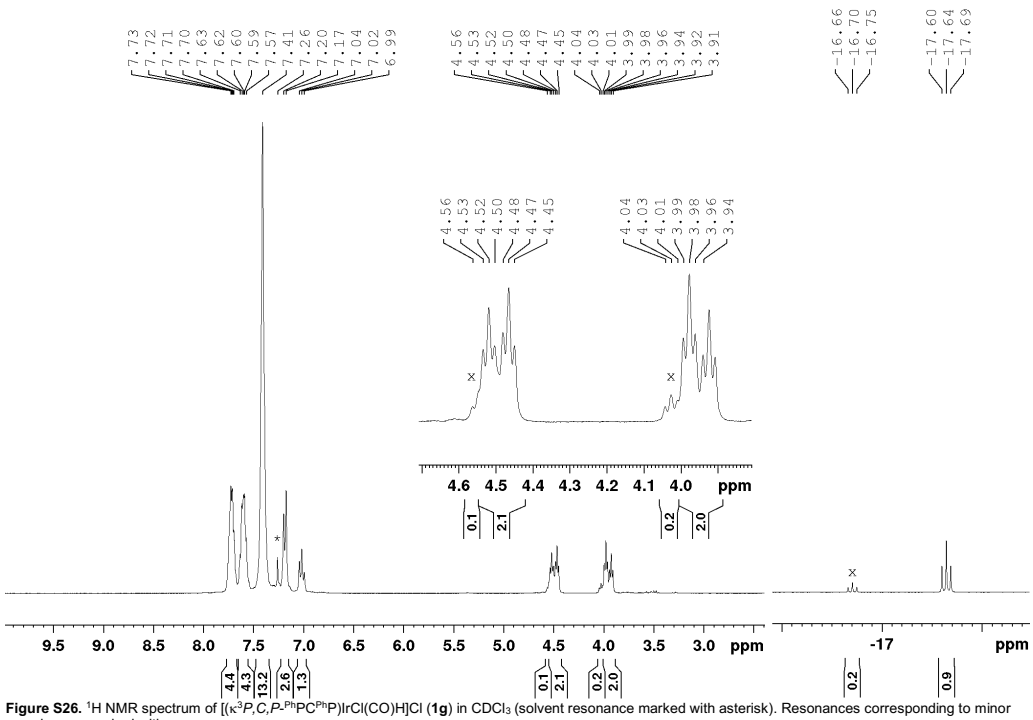

Figure S26. ^{1}H NMR spectrum of [(κ³*P,C,P*-^{Ph}PC^{Ph}P)IrCl(CO)H]Cl (**1g**) in $CDCl_3$ (solvent resonance marked with asterisk). Resonances corresponding to minor complex are marked with x.

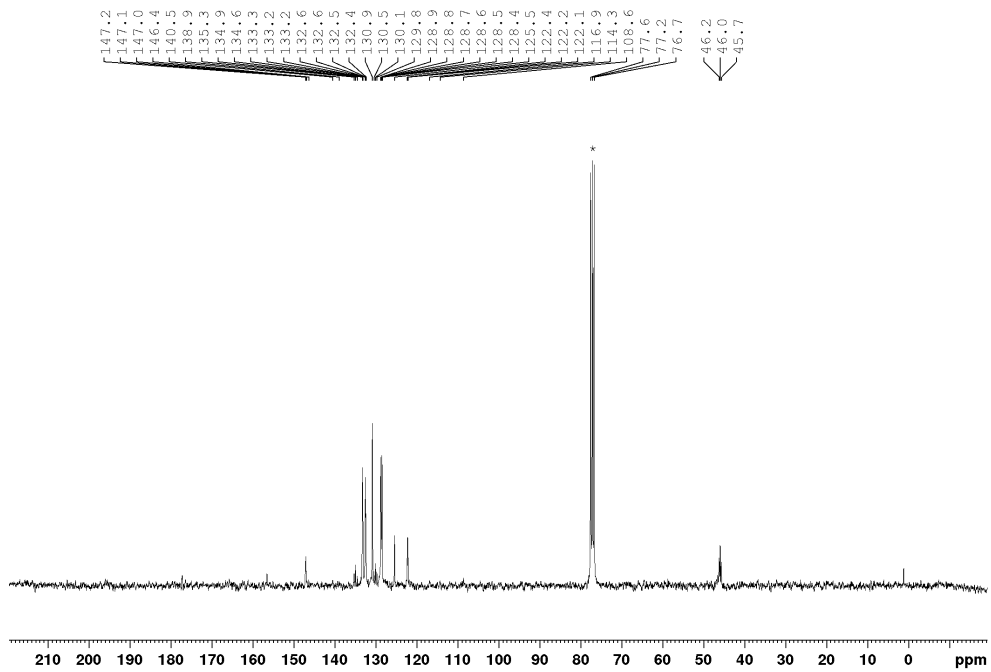

Figure S27. $^{13}C\{^{1}H\}$ NMR spectrum of [(κ^3*P,C,P*-$^{Ph}PC^{Ph}P$)IrCl(CO)H]Cl (**1g**) in $CDCl_3$ (solvent resonance marked with asterisk).

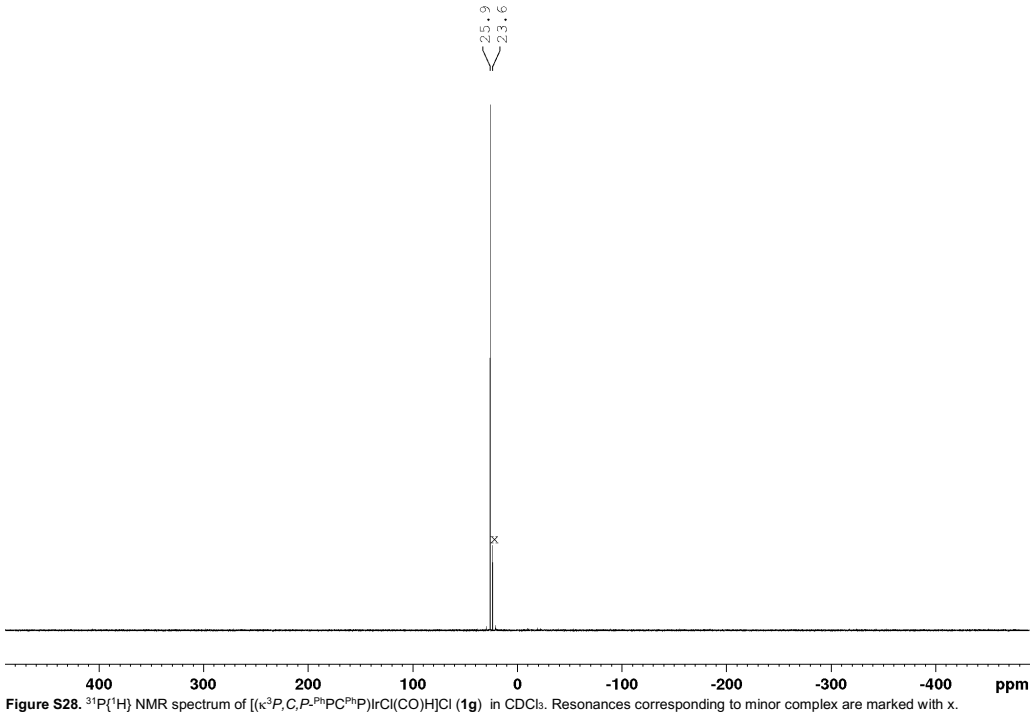

Figure S28. $^{31}P\{^{1}H\}$ NMR spectrum of [(κ^3*P,C,P*-$^{Ph}PC^{Ph}P$)IrCl(CO)H]Cl (**1g**) in $CDCl_3$. Resonances corresponding to minor complex are marked with x.

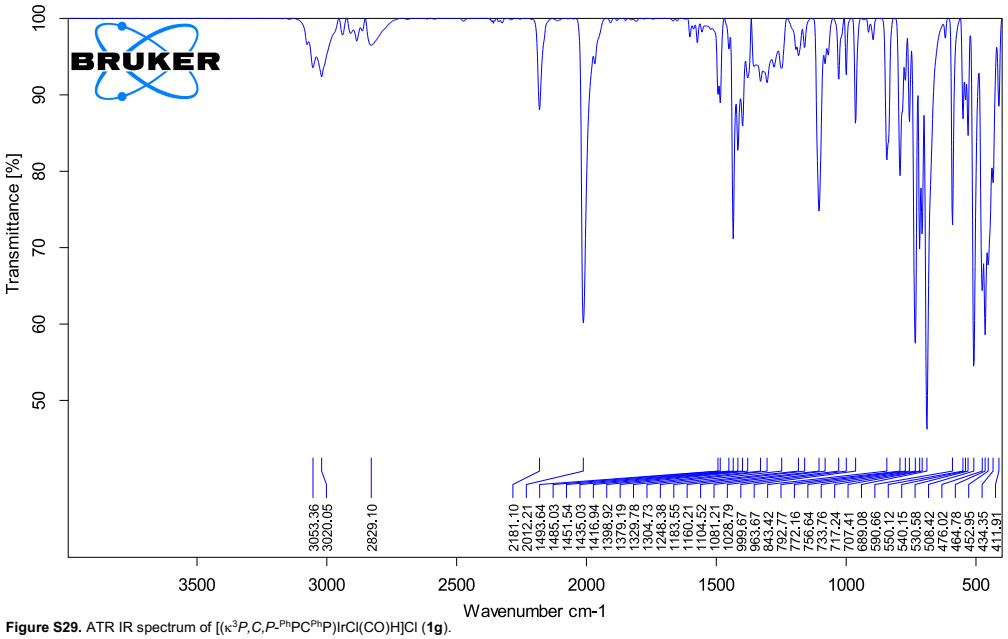

Figure S29. ATR IR spectrum of [(κ^3*P,C,P*-^{Ph}PC^{Ph}P)IrCl(CO)H]Cl (**1g**).

X-Ray Crystallography

The single crystal X-ray diffraction data for the structural analysis were collected using graphite-monochromated Mo-K_α-radiation ($\lambda_{MoK\alpha}$= 0.71073) on the imaging plate detector systems STOE IPDS2 and STOE IPDS2T or on the pixel detector system Bruker Quest D8. The structures were solved with the Olex2 software by direct methods with SHELXT and refined against F^2 by full-matrix-least-square techniques using SHELXL.[9–12] Crystallographic data for **1a-1g** was deposited at Cambridge Crystallographic Data Centre (CCDC 1879155-1879160) and can be obtained free of charge via www.ccdc.cam.ac.uk/.

Table S1. Crystallographic data of complexes **1a-f**.

Complex	**1a**	**1b**	**1c**	**1d**	**1e**	**1f**	**1g**
Formula	$C_{52}H_{46}Cl_3IrOP_4$ · 0.1 CH_2Cl_2	$C_{32}H_{27}ClIrNOP_2$	$C_{29}H_{30}Cl_2IrNOP_2$	$C_{32}H_{31}Cl_2IrN_2OP_2$ · CH_2Cl_2	$C_{55}H_{51}Cl_8IrOP_4$	$C_{52}H_{48}BBrCl_3IrOP_4$	$C_{33}H_{28}ClIrOP_2$ · $^5/_4$ C_7H_8
M / g·mol^{-1}	1117.81	731.13	733.58	869.55	1327.66	1202.05	845.31
T/K	100(2)	100(2)	100(2)	100(2)	100(2)	110(2)	100(2)
Crystal System	monoclinic	triclinic	triclinic	triclinic	monoclinic	orthorhombic	triclinic
Space Group	*C*2/*c*	*P*1	$P\bar{1}$	$P\bar{1}$	$P2_1/c$	*Pbca*	$P\bar{1}$
a / Å	41.384(3)	15.2943(10)	10.603(2)	14.0605(6)	12.265(2)	23.3229(7)	9.6658(4)
b / Å	12.1155(7)	16.0822(10)	11.764(2)	14.4113(6)	24.523(5)	16.5703(5)	14.2713(7)
c / Å	32.393(2)	17.6097(12)	12.732(3)	19.6677(9)	22.176(6)	25.2090(7)	14.7670(7)
α / °	90	108.002(2)	97.860(7)	88.181(2)	90	90	107.989(2)
β / °	109.788(2)	92.021(2)	109.324(7)	79.515(2)	121.94(2)	90	96.128(2)
γ / °	90	109.2707(19)	107.162(5)	63.8870(10)	90	90	104.806(2)
V / Å^3	15282(2)	3842.8(4)	1382.7(4)	3513.5(3)	5660(2)	9742.5(5)	1834.52(15)
Z	12	4	2	4	4	8	2
$\rho_{calc.}$ / g·cm^{-3}	1.457	1.264	1.762	1.644	1.558	1.639	1.530
μ / mm^{-1}	2.950	3.647	5.161	4.224	2.888	3.896	3.830
F(000)	6698	1432	720	1712	2648	4768	841
Θ_{min}/°	2.100	2.178	2.185	2.115	1.661	2.136	2.225
Θ_{max}/°	24.439	25.500	27.480	31.310	26.760	27.404	27.484
Measured Refl.	172870	135821	61214	169650	41514	215064	43359
Independent Refl.	12590 (R_{int} = 0.0556)	27324 (R_{int} = 0.0701)	6342 (R_{int} = 0.0228)	20487 (R_{int} = 0.0380)	11918 (R_{int} = 0.1514)	11063 (R_{int} = 0.0820)	8351 (R_{int} = 0.0337)
Ind. Refl. (I>2σ(I))	11787	22938	6177	18107	8433	8582	7750
Parameters/ Restraints	844/5	1214/1923	329/1	783/0	622/0	575/4	439/122
R_1	0.0648	0.0563	0.0132	0.0248	0.0693	0.0522	0.0273
R_1 (all data)	0.0697	0.0732	0.0140	0.0324	0.1044	0.0750	0.0312
wR_2	0.1532	0.1310	0.0332	0.0497	0.1415	0.1311	0.0662
wR_2 (all data)	0.1555	0.1421	0.0335	0.0519	0.1575	0.1492	0.0680
GooF	1.249	1.046	1.039	1.033	1.017	1.159	1.056
Max. peak + hole / e·Å^{-3}	1.982/-3.720	3.173/-3.218	1.114/-0.916	1.866/-1.392	2.338/-2.727	4.008/-2.222	1.857/-1.365
CCDC	1879160	1879158	1879156	1901950	1879155	1879159	1879157

DFT Calculations

DFT calculations were performed with Grimme's B97D functional including dispersion[13] and the def2TZVPP basis set after a preoptimisation with the def2SVP basis set[14,15] in Gaussian16.[16] For the EDA, the BP86 functional with a triple-zeta STO basis set TZ2P+[17] in conjunction with the zero-order regular approximation (ZORA),[18] and Grimme's D3 dispersion correction together with Becke-Johnson damping as implemented in the ADF2016 program package was employed.[19–23] In order to be able to separate interactions between the fragments in the EDA in σ- and π-bonding interactions, the pincer ligands where simplified into monodentate ligands and the complexes were optimized in C_s symmetry. Crystal structures were used as starting models, where possible. After optimization, a frequency calculation was run to ascertain that a ground state was found (no imaginary modes). From these calculations, C–O stretching frequencies were obtained. Hirshfeld and charge model 5 (CM5) charge analyses were also performed in Gaussian16.[24] Additional Population analysis calculations were done with NBO 6.0.[25] Laplacian contour line plots were created with the program Multiwfn.[26]

Table S2. Results of NPA, Hirshfeld and CM5 charge analyses. Donor and free donor values correspond to the central donor atom of the pincer ligand.

	NPA charge				Hirshfeld charge				CM5 charge			
	Ir	donor	free donor	Δ_{charge} donor	Ir	donor	free donor	Δ_{charge} donor	Ir	donor	free donor	Δ_{charge} donor
cis-**1a**	-0.031	-1.224	-1.350	0.126	-0.040	-0.159	-0.250	-0.090	0.279	-0.171	-0.215	0.045
trans-**1a**	-0.027	-1.232	-1.350	0.118	-0.036	-0.161	-0.250	-0.088	0.286	-0.171	-0.215	0.044
1b	0.039	-0.435	-0.435	0.000	-0.011	-0.031	-0.152	-0.121	0.364	-0.287	-0.336	0.049
cis-**1c**	0.037	-0.558	-0.599	0.041	-0.013	-0.020	-0.127	-0.107	0.347	-0.438	-0.488	0.050
trans-**1c**	0.031	-0.573	-0.599	0.026	-0.014	-0.023	-0.127	-0.104	0.347	-0.442	-0.488	0.046
1d	-0.053	0.223	0.068	0.155	-0.052	0.031	-0.126	-0.157	0.277	0.130	0.009	0.121
1e	-0.025	-1.400	-1.441	0.041	-0.038	-0.267	-0.355	-0.087	0.290	-0.214	-0.256	0.043
cis-**1f**	-0.122	-0.779	-1.010	0.231	-0.094	-0.129	-0.236	-0.107	0.272	-0.376	-0.425	0.049
trans-**1f**	-0.112	-0.832	-1.010	0.178	-0.088	-0.140	-0.236	-0.096	0.282	-0.399	-0.425	0.026
1g	-0.042	-0.173	-0.317	0.144	-0.058	-0.065	-0.202	-0.137	0.276	-0.065	-0.205	0.140
1h	-0.016	-0.427	-0.441	0.014	-0.050	-0.083	-0.173	-0.091	0.280	-0.163	-0.225	0.062
1i	0.019	-0.039	0.011	-0.050	-0.016	0.056	-0.004	-0.060	0.347	-0.064	-0.050	-0.014
cis-**1j**	-0.192	1.167	0.758	0.409	-0.070	0.255	0.103	-0.152	0.295	0.017	-0.027	0.045
trans-**1j**	-0.186	1.159	0.758	0.401	-0.071	0.253	0.103	-0.150	0.294	0.016	-0.027	0.044
1k	-0.051	0.008	-0.168	0.176	-0.051	-0.031	-0.220	-0.189	0.282	0.010	-0.141	0.151
1l	-0.054	0.262	0.119	0.143	-0.052	0.044	-0.104	-0.148	0.277	0.143	0.032	0.111
1m	-0.035	-0.064	-0.211	0.147	-0.060	-0.059	-0.249	-0.190	0.276	-0.015	-0.168	0.153
1n	-0.181	0.661	0.344	0.317	-0.113	0.058	-0.115	-0.173	0.300	-0.105	-0.147	0.041
cis-**1o**	-0.035	-0.395	-0.450	0.055	-0.059	-0.076	-0.163	-0.087	0.266	-0.165	-0.222	0.057
trans-**1o**	-0.031	-0.406	-0.450	0.044	-0.057	-0.077	-0.163	-0.086	0.268	-0.167	-0.222	0.055
1p	0.046	-0.653	-0.691	0.038	-0.026	-0.175	-0.239	-0.065	0.354	-0.441	-0.443	0.002
1q	-0.121	-0.948	-0.978	0.030	-0.088	-0.218	-0.302	-0.084	0.294	-0.407	-0.406	-0.001

Table S3. Comparision of calculated and experimentally determined wavenumbers for the CO stretching vibration $\tilde{\nu}_{CO}$ and for the IrH stretching vibration $\tilde{\nu}_{IrH}$.

	$\tilde{\nu}_{CO}$ (DFT)	$\tilde{\nu}_{CO}$ (exp)	$\tilde{\nu}_{IrH}$ (DFT)	$\tilde{\nu}_{IrH}$ (exp)
cis-**1a**	2058	2049[a]	2291	2194[a]
trans-**1a**	2046	2049[a]	2276	2194[a]
1b	2045	2040	2228	2179
cis-**1c**	2042	2030[b]	2194	2198[b]
trans-**1c**	2045	2030[b]	2245	2198[b]
1d	2040	2040	2235	2203
1e	2021	2015	2313	2271
cis-**1f**	2021	2015	2306	2234
1g	1996	2012	2239	2181
1h	1995	1992[c]	2229	2194[c]

[a] *cis*- and *trans*-**1a** were measured as an approx. 1:1 mixture. [b] *cis*- and *trans*-**1c** were measured as an approx. 9:1 mixture. [c] Ref. [27].

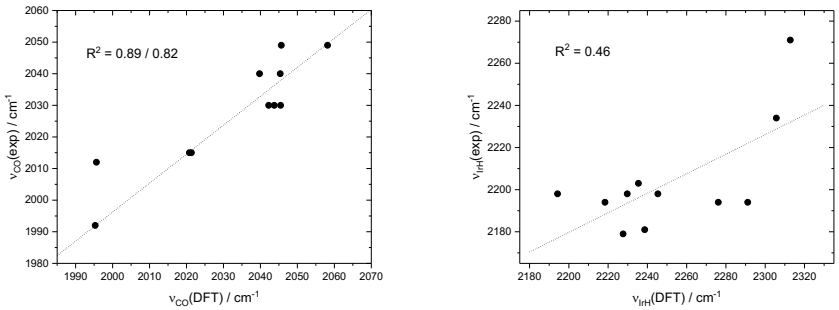

Figure S30. Left: correlation between calculated and experimental values of $\tilde{\nu}_{CO}$. Right: correlation between calculated and experimental values of $\tilde{\nu}_{IrH}$.

Laplacian contour line plots

The plane of the contour line plots is defined parallel to the donor-iridium bond (D-Ir) and normal to the plane defined by the donor atom and the two connected atoms A and B from the pincer ligand backbone.

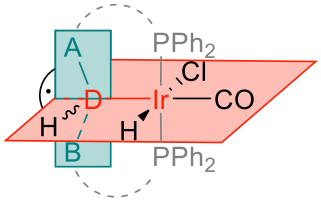

Figure S31. Cutting pattern for contour line plots. The plotted plane is depicted in red, the plane formed by A, B and D is depicted in blue.

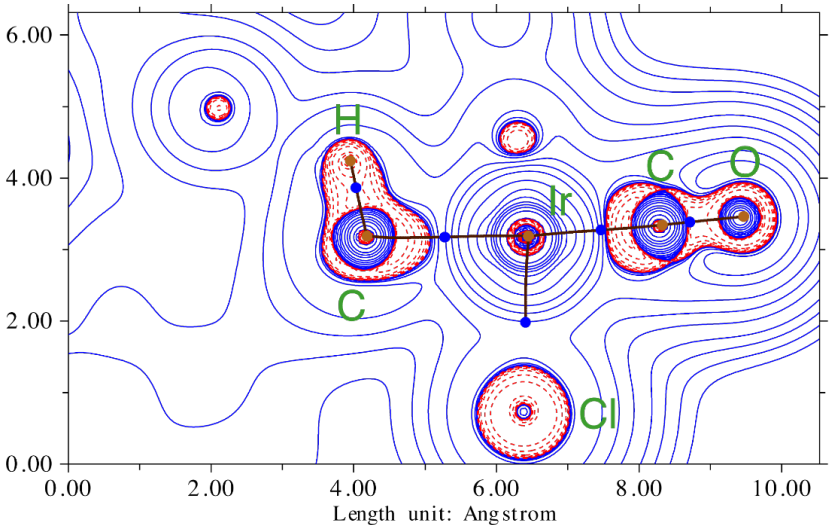

Figure S32. Contour line diagrams of the Laplacian distribution $\nabla^2\rho$ of *cis*-**1a** (bond critical points are blue, charge accumulation is depicted as dashed red lines, charge depletion is depicted as blue lines).

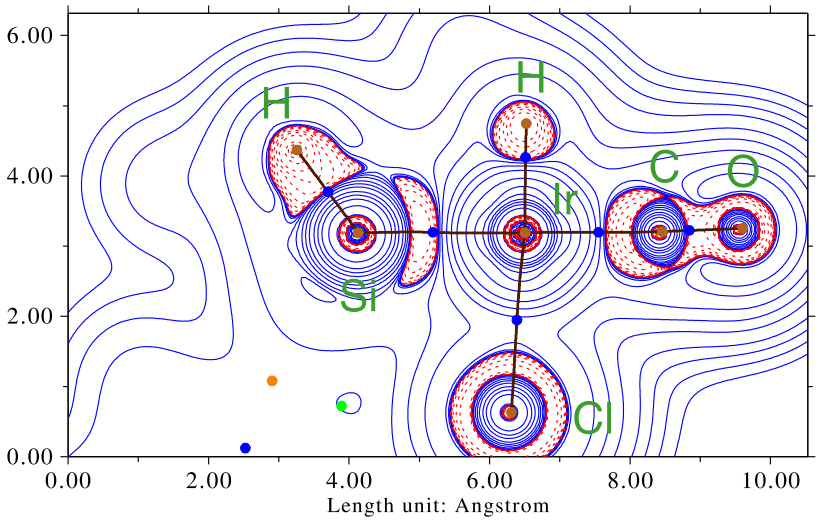

Figure S33. Contour line diagrams of the Laplacian distribution $\nabla^2\rho$ of **1a**[1] (bond critical points are blue, charge accumulation is depicted as dashed red lines, charge depletion is depicted as blue lines).

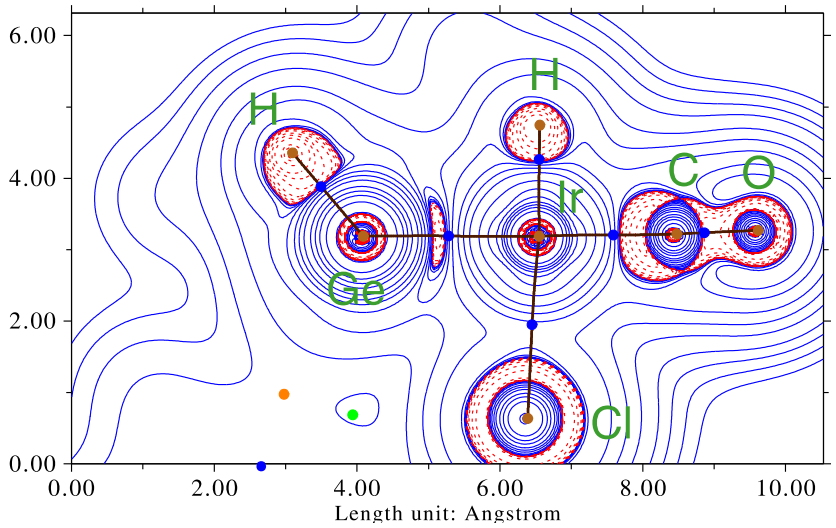

Figure S34. Contour line diagrams of the Laplacian distribution $\nabla^2\rho$ of **1a²** (bond critical points are blue, charge accumulation is depicted as dashed red lines, charge depletion is depicted as blue lines).

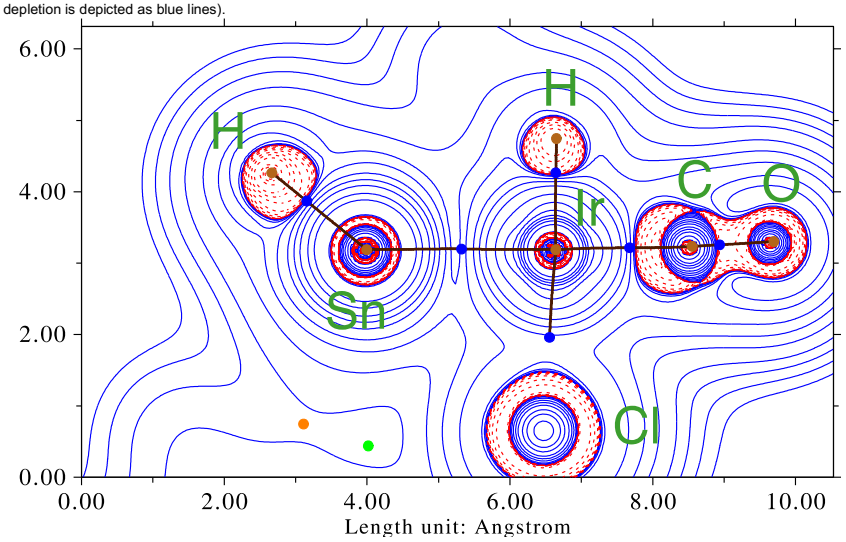

Figure S35. Contour line diagrams of the Laplacian distribution $\nabla^2\rho$ of **1a³** (bond critical points are blue, charge accumulation is depicted as dashed red lines, charge depletion is depicted as blue lines).

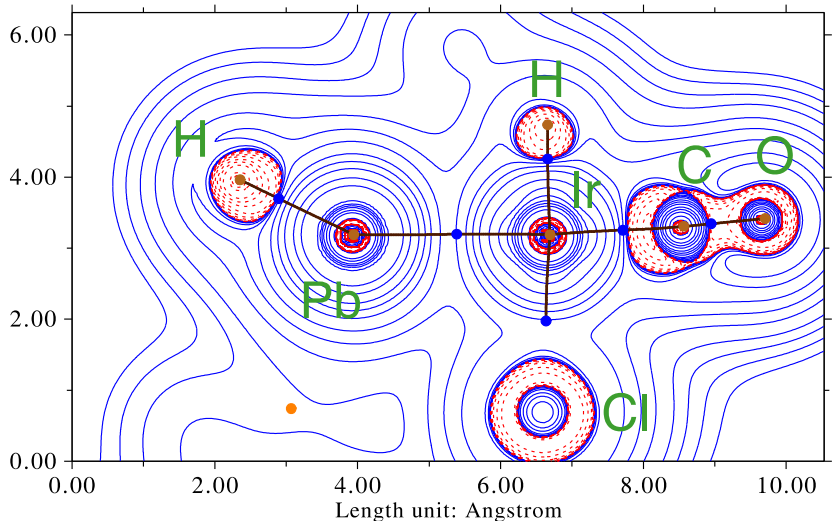

Figure S36. Contour line diagrams of the Laplacian distribution $\nabla^2\rho$ of **1a**[4] (bond critical points are blue, charge accumulation is depicted as dashed red lines, charge depletion is depicted as blue lines).

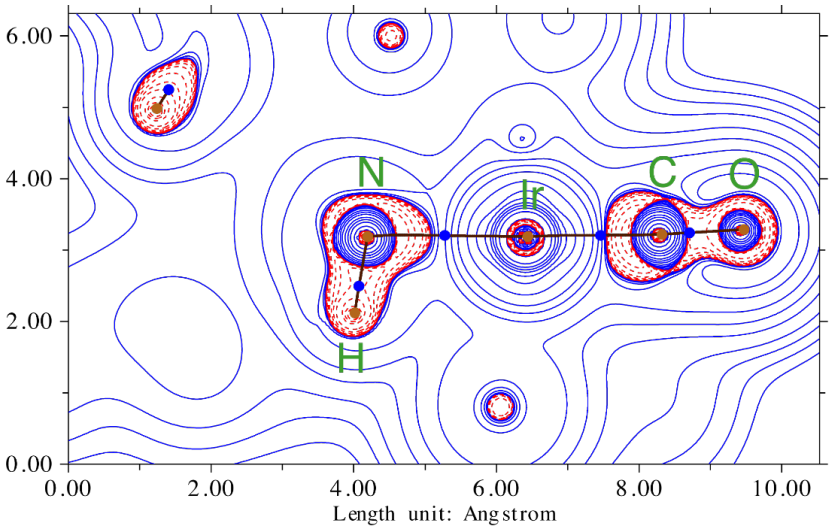

Figure S37. Contour line diagrams of the Laplacian distribution $\nabla^2\rho$ of *trans*-**1a** (bond critical points are blue, charge accumulation is depicted as dashed red lines, charge depletion is depicted as blue lines).

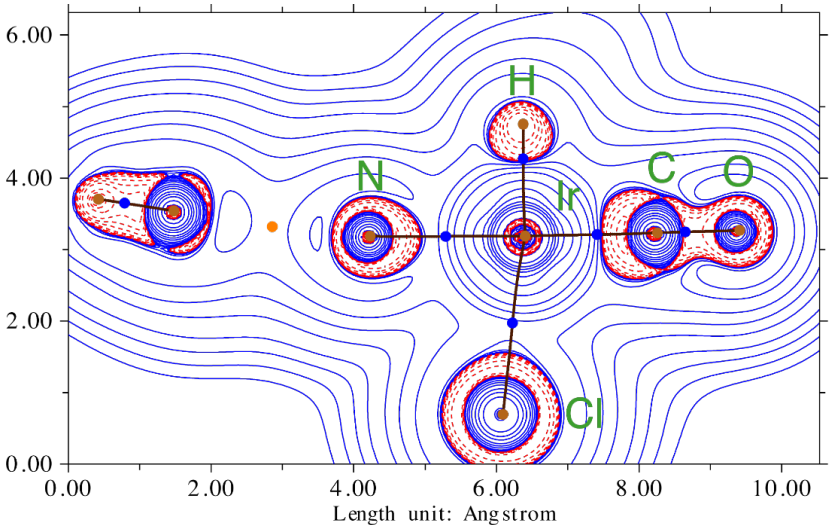

Figure S38. Contour line diagrams of the Laplacian distribution $\nabla^2\rho$ of **1b** (bond critical points are blue, charge accumulation is depicted as dashed red lines, charge depletion is depicted as blue lines).

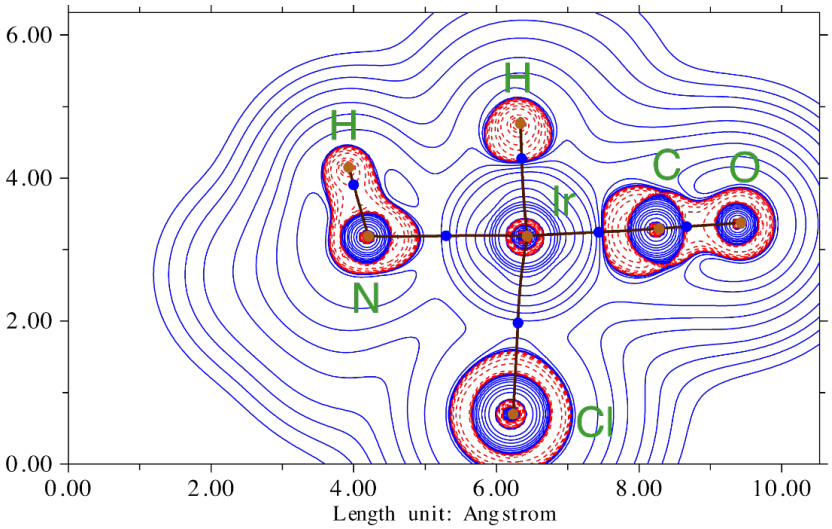

Figure S39. Contour line diagrams of the Laplacian distribution $\nabla^2\rho$ of *cis*-**1c** (bond critical points are blue, charge accumulation is depicted as dashed red lines, charge depletion is depicted as blue lines).

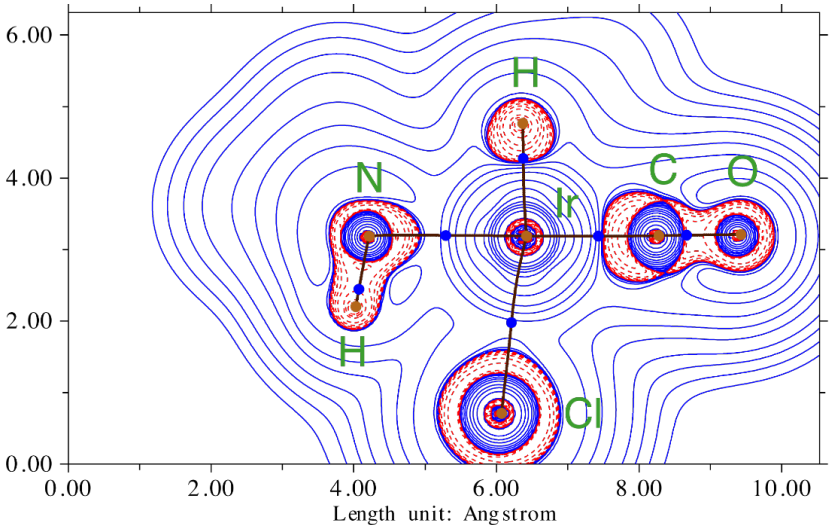

Figure S40. Contour line diagrams of the Laplacian distribution $\nabla^2\rho$ of *trans*-**1c** (bond critical points are blue, charge accumulation is depicted as dashed red lines, charge depletion is depicted as blue lines).

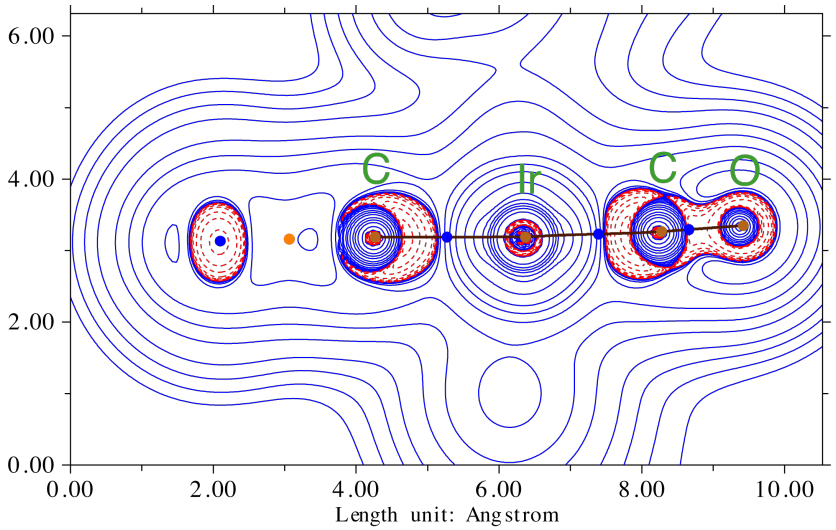

Figure S41. Contour line diagrams of the Laplacian distribution $\nabla^2\rho$ of **1d** (bond critical points are blue, charge accumulation is depicted as dashed red lines, charge depletion is depicted as blue lines).

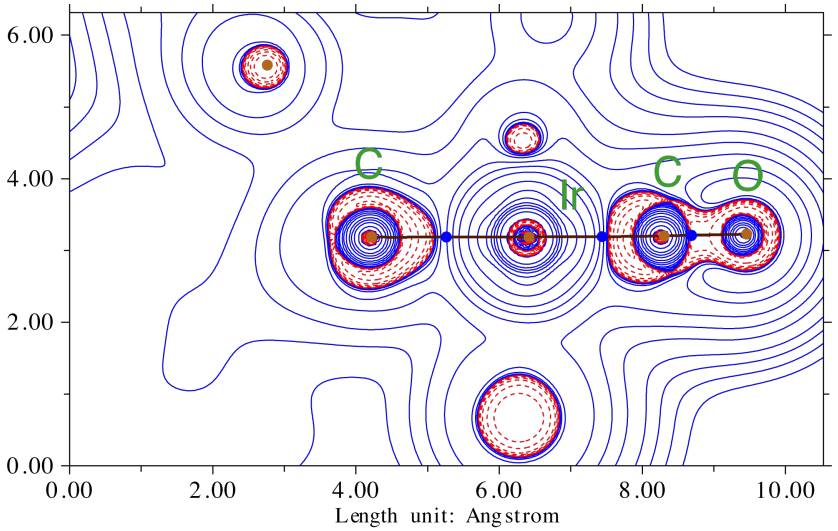

Figure S42. Contour line diagrams of the Laplacian distribution $\nabla^2\rho$ of **1e** (bond critical points are blue, charge accumulation is depicted as dashed red lines, charge depletion is depicted as blue lines).

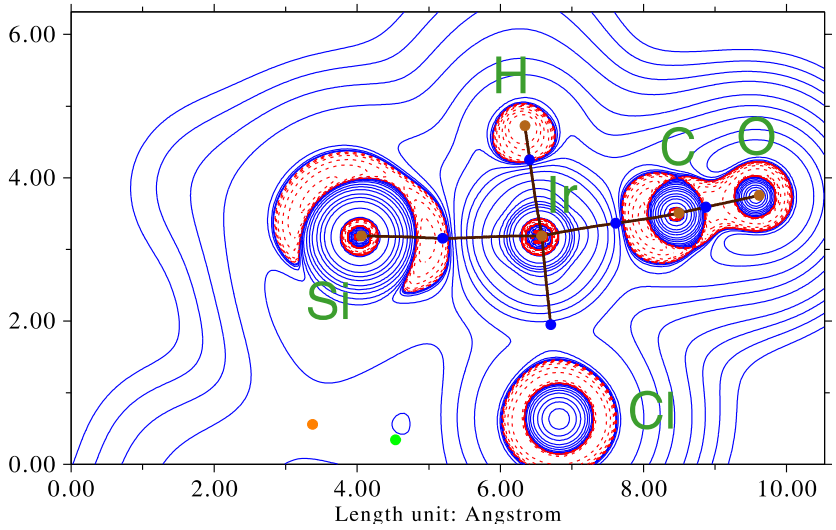

Figure S43. Contour line diagrams of the Laplacian distribution $\nabla^2\rho$ of **1e**[1] (bond critical points are blue, charge accumulation is depicted as dashed red lines, charge depletion is depicted as blue lines).

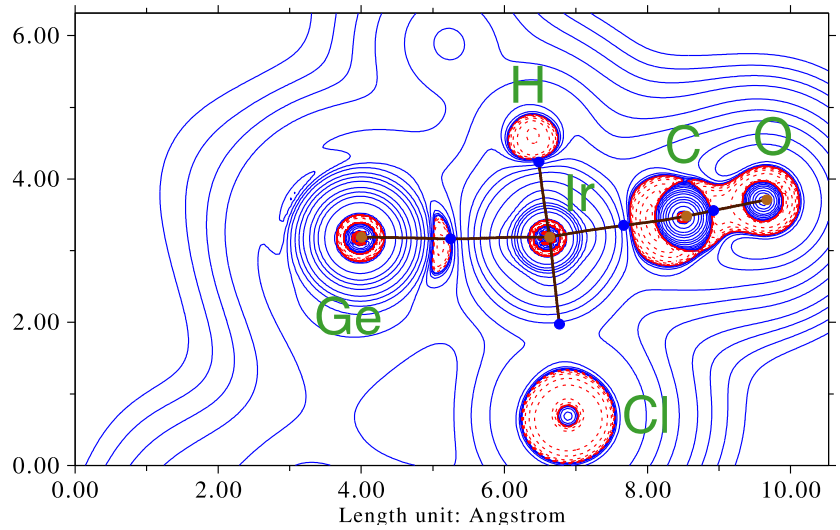

Figure S44. Contour line diagrams of the Laplacian distribution $\nabla^2\rho$ of **1e²** (bond critical points are blue, charge accumulation is depicted as dashed red lines, charge depletion is depicted as blue lines).

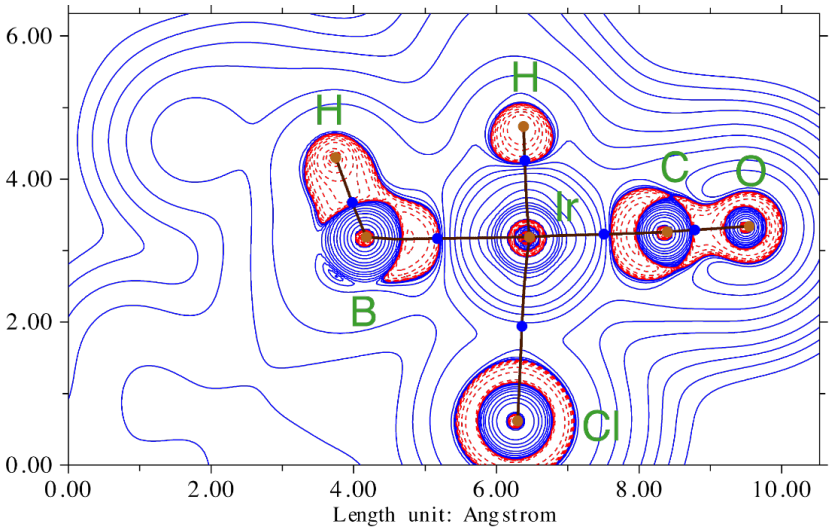

Figure S45. Contour line diagrams of the Laplacian distribution $\nabla^2\rho$ of *cis*-**1f** (bond critical points are blue, charge accumulation is depicted as dashed red lines, charge depletion is depicted as blue lines).

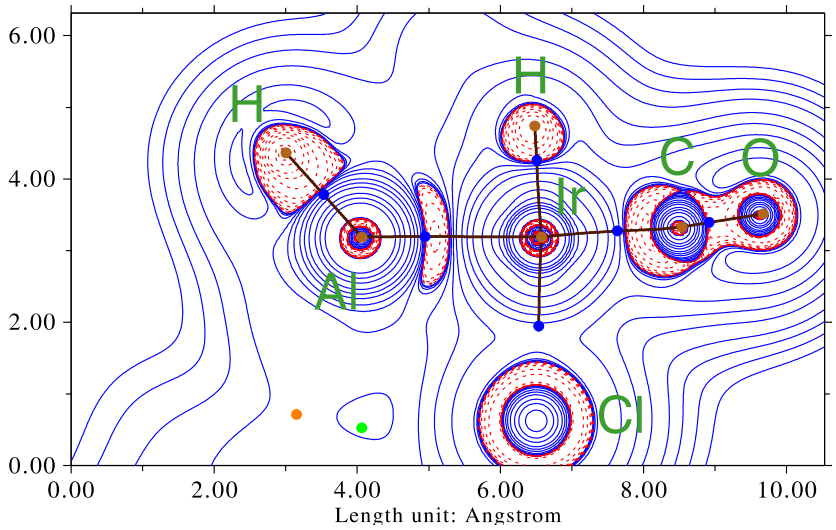

Figure S46. Contour line diagrams of the Laplacian distribution $\nabla^2\rho$ of **1f**[1] (bond critical points are blue, charge accumulation is depicted as dashed red lines, charge depletion is depicted as blue lines).

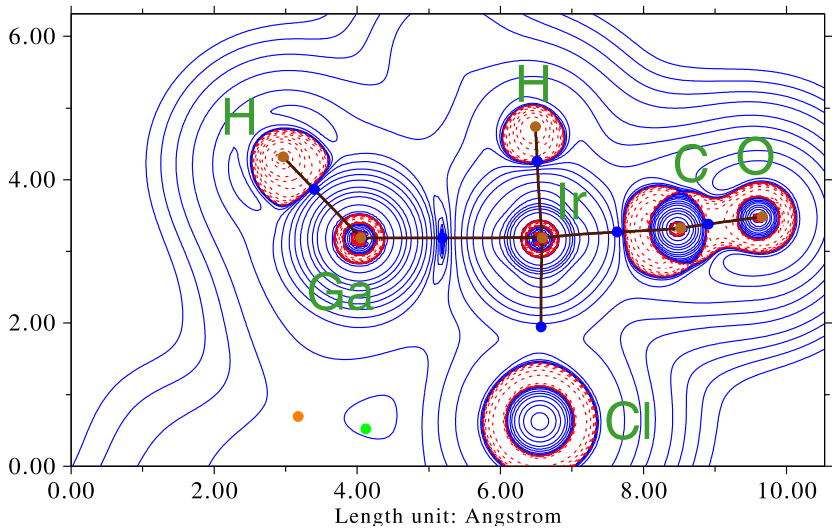

Figure S47. Contour line diagrams of the Laplacian distribution $\nabla^2\rho$ of **1f**[2] (bond critical points are blue, charge accumulation is depicted as dashed red lines, charge depletion is depicted as blue lines).

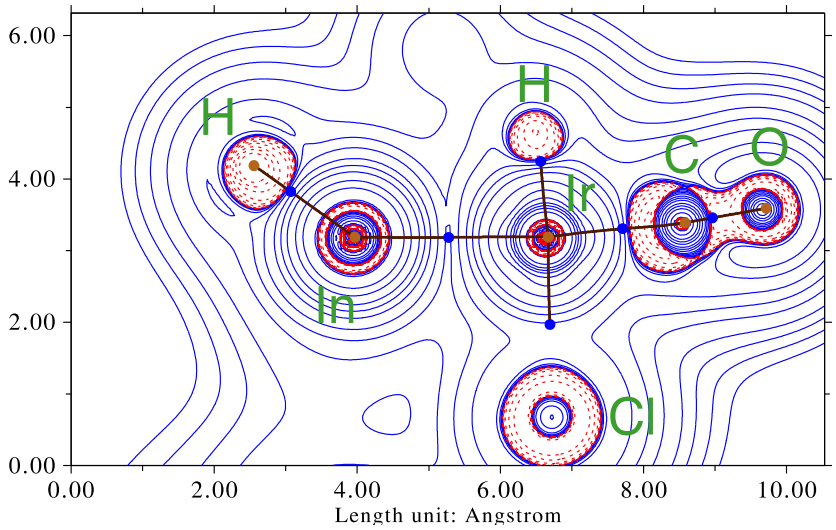

Figure S48. Contour line diagrams of the Laplacian distribution $\nabla^2\rho$ of **1f**[3] (bond critical points are blue, charge accumulation is depicted as dashed red lines, charge depletion is depicted as blue lines).

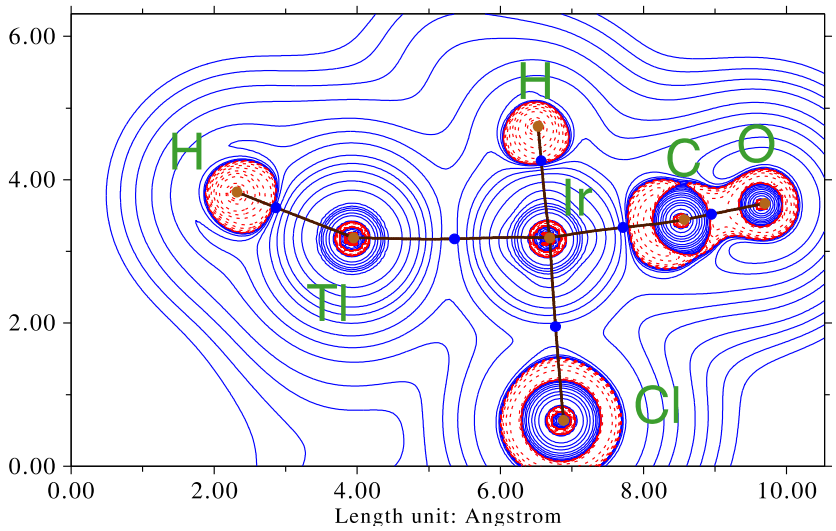

Figure S49. Contour line diagrams of the Laplacian distribution $\nabla^2\rho$ of **1f**[4] (bond critical points are blue, charge accumulation is depicted as dashed red lines, charge depletion is depicted as blue lines).

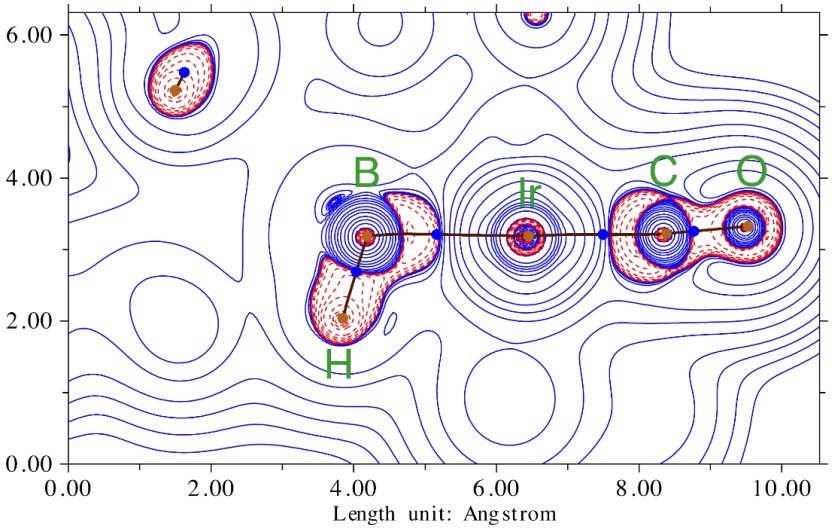

Figure S50. Contour line diagrams of the Laplacian distribution $\nabla^2\rho$ of *trans*-**1f** (bond critical points are blue, charge accumulation is depicted as dashed red lines, charge depletion is depicted as blue lines).

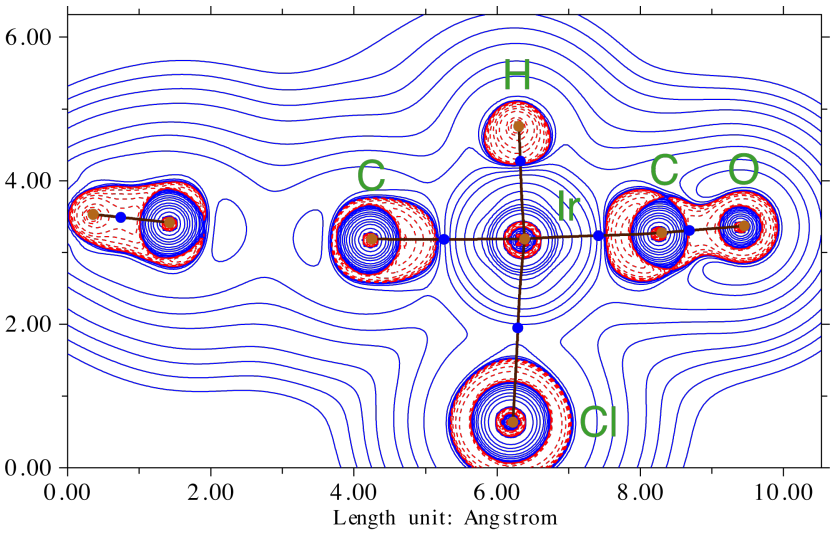

Figure S51. Contour line diagrams of the Laplacian distribution $\nabla^2\rho$ of **1g** (bond critical points are blue, charge accumulation is depicted as dashed red lines, charge depletion is depicted as blue lines).

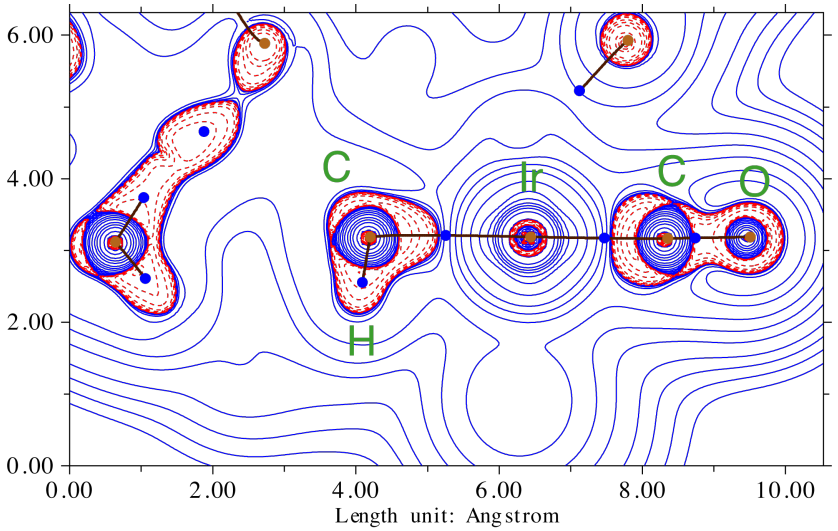

Figure S52. Contour line diagrams of the Laplacian distribution $\nabla^2\rho$ of **1h** (bond critical points are blue, charge accumulation is depicted as dashed red lines, charge depletion is depicted as blue lines).

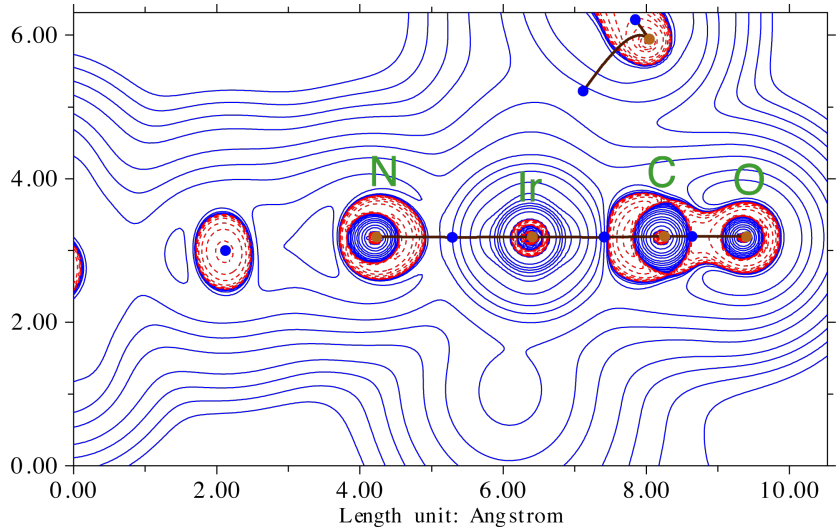

Figure S53. Contour line diagrams of the Laplacian distribution $\nabla^2\rho$ of **1i** (bond critical points are blue, charge accumulation is depicted as dashed red lines, charge depletion is depicted as blue lines).

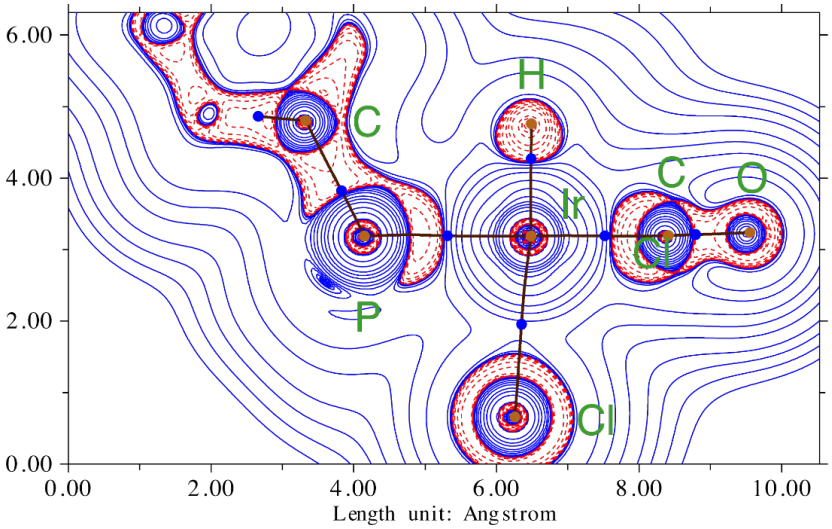

Figure S54. Contour line diagrams of the Laplacian distribution $\nabla^2\rho$ of *cis*-**1j** (bond critical points are blue, charge accumulation is depicted as dashed red lines, charge depletion is depicted as blue lines).

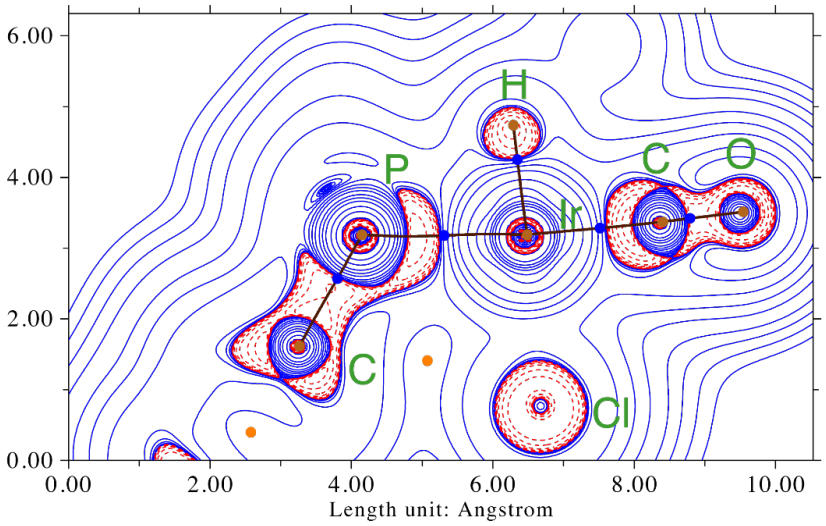

Figure S55. Contour line diagrams of the Laplacian distribution $\nabla^2\rho$ of *trans*-**1j** (bond critical points are blue, charge accumulation is depicted as dashed red lines, charge depletion is depicted as blue lines).

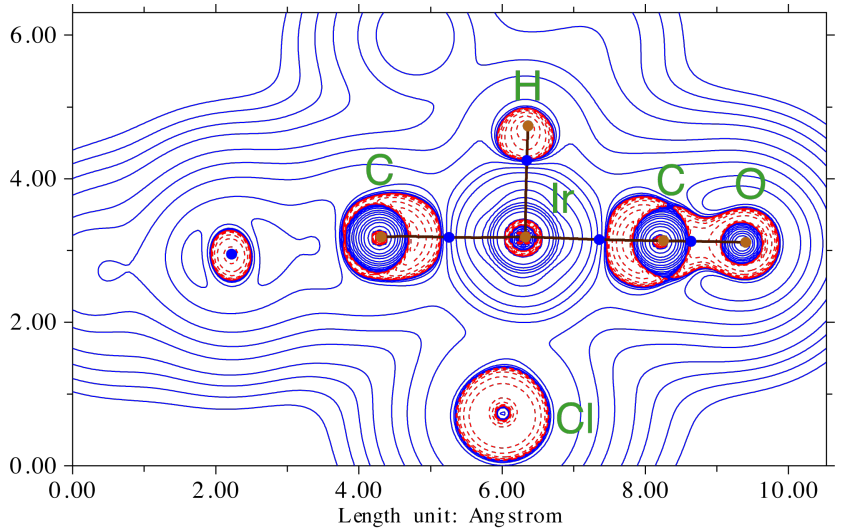

Figure S56. Contour line diagrams of the Laplacian distribution $\nabla^2\rho$ of **1k** (bond critical points are blue, charge accumulation is depicted as dashed red lines, charge depletion is depicted as blue lines).

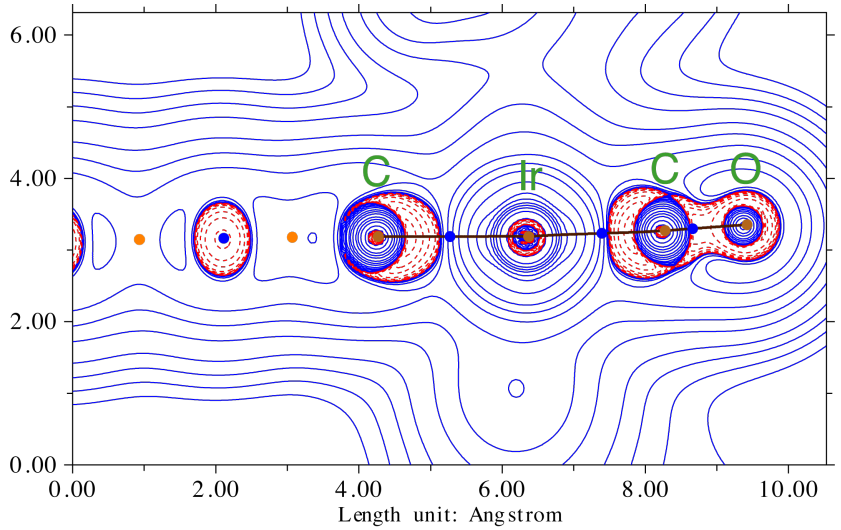

Figure S57. Contour line diagrams of the Laplacian distribution $\nabla^2\rho$ of **1l** (bond critical points are blue, charge accumulation is depicted as dashed red lines, charge depletion is depicted as blue lines).

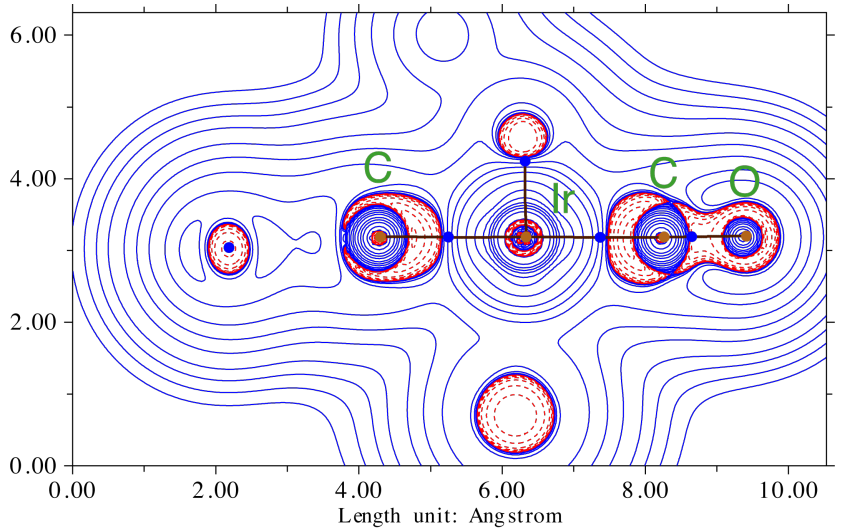

Figure S58. Contour line diagrams of the Laplacian distribution $\nabla^2\rho$ of **1m** (bond critical points are blue, charge accumulation is depicted as dashed red lines, charge depletion is depicted as blue lines).

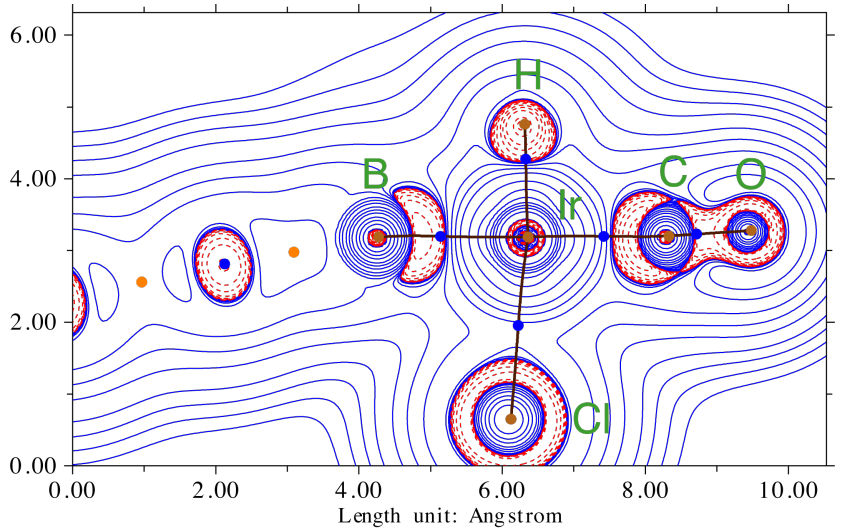

Figure S59. Contour line diagrams of the Laplacian distribution $\nabla^2\rho$ of **1n** (bond critical points are blue, charge accumulation is depicted as dashed red lines, charge depletion is depicted as blue lines).

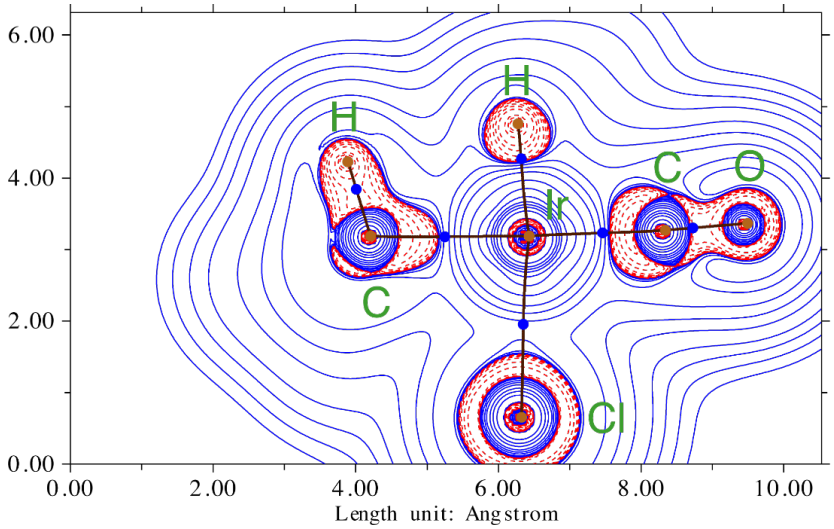

Figure S60. Contour line diagrams of the Laplacian distribution $\nabla^2\rho$ of *cis*-**1o** (bond critical points are blue, charge accumulation is depicted as dashed red lines, charge depletion is depicted as blue lines).

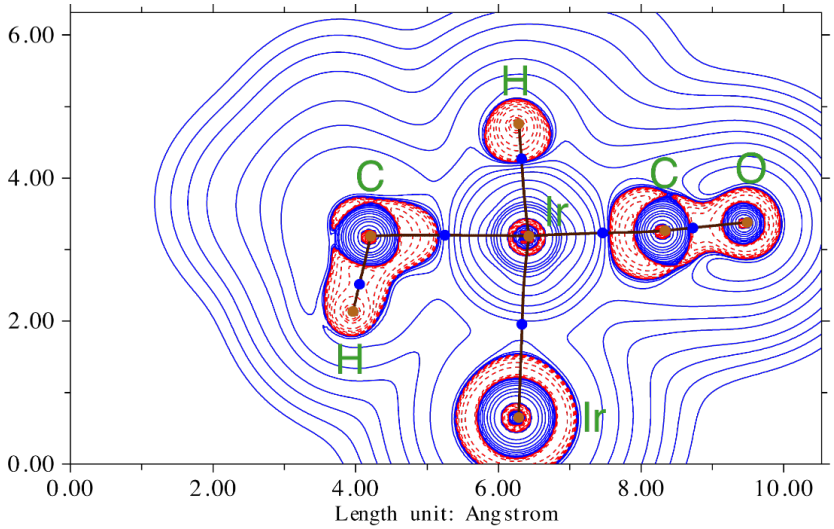

Figure S61. Contour line diagrams of the Laplacian distribution $\nabla^2\rho$ of *trans*-**1o** (bond critical points are blue, charge accumulation is depicted as dashed red lines, charge depletion is depicted as blue lines).

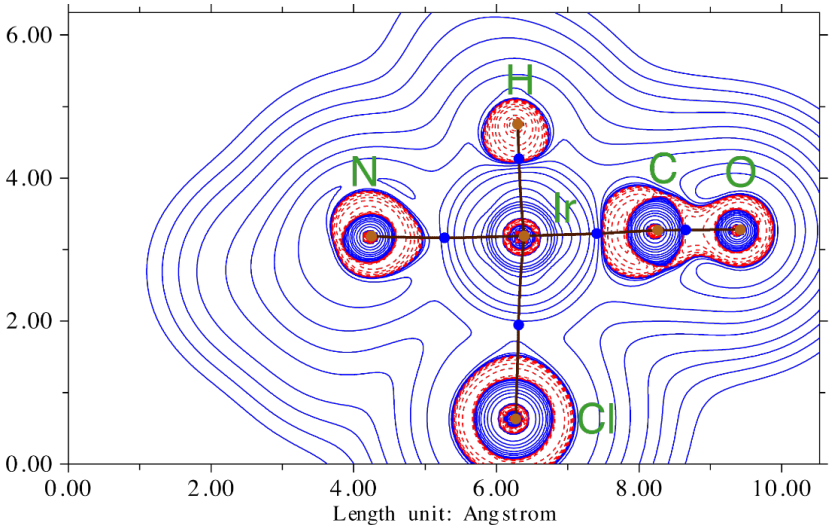

Figure S62. Contour line diagrams of the Laplacian distribution $\nabla^2\rho$ of **1p** (bond critical points are blue, charge accumulation is depicted as dashed red lines, charge depletion is depicted as blue lines).

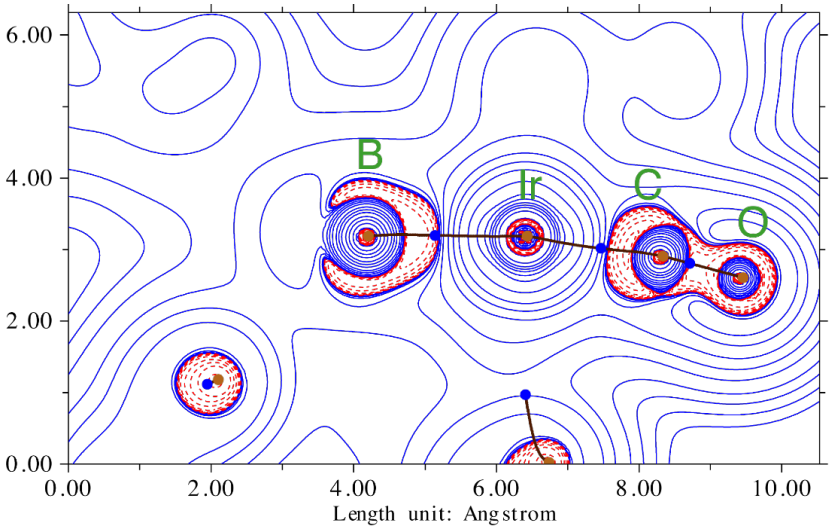

Figure S63. Contour line diagrams of the Laplacian distribution $\nabla^2\rho$ of **1q** (bond critical points are blue, charge accumulation is depicted as dashed red lines, charge depletion is depicted as blue lines).

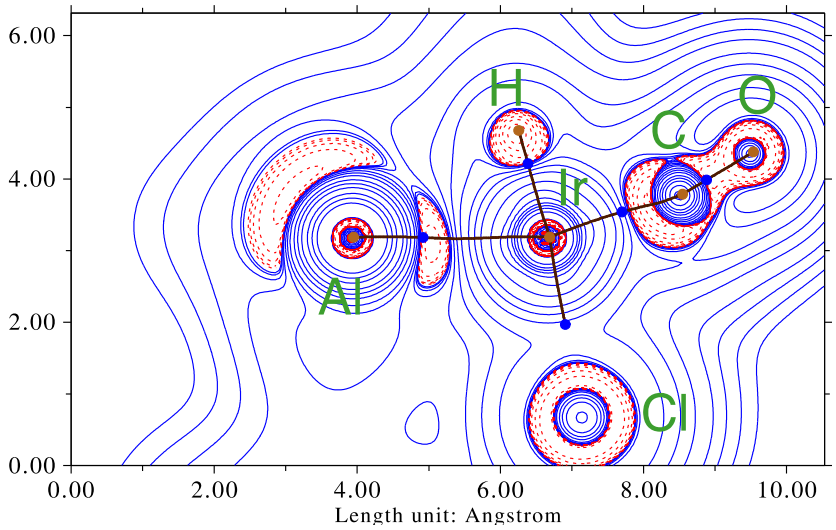

Figure S64. Contour line diagrams of the Laplacian distribution $\nabla^2\rho$ of **1q**[1] (bond critical points are blue, charge accumulation is depicted as dashed red lines, charge depletion is depicted as blue lines).

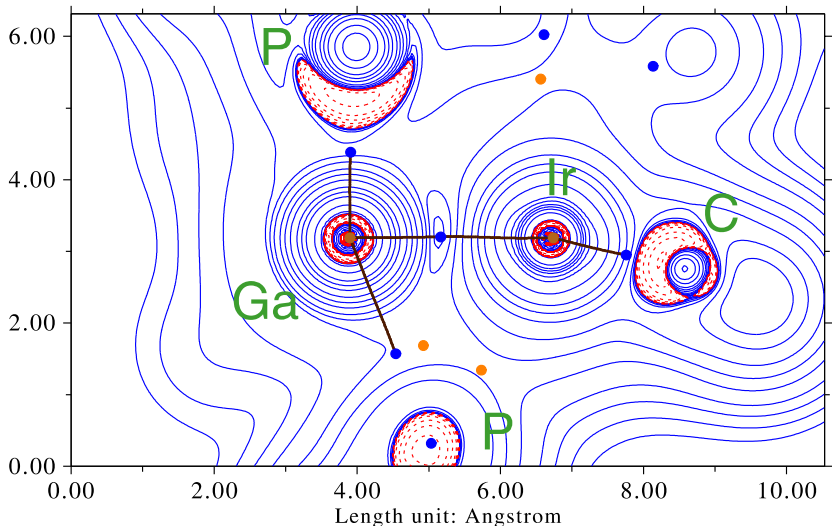

Figure S65. Contour line diagrams of the Laplacian distribution $\nabla^2\rho$ of **1q**[2] (bond critical points are blue, charge accumulation is depicted as dashed red lines, charge depletion is depicted as blue lines).

EDA

EDA (also known as extended transition-state method, ETS) was developed independently by Morokuma[28] and Ziegler and Rauk.[29] It analyses the interaction energy ΔE_{int} of a bond in the molecule A-B with fragments A and B in the frozen geometry of AB and the particular electronic reference state. The interaction energy can be described as the sum of three interactions:

$$\Delta E_{\mathrm{int}} = \Delta E_{\mathrm{elstat}} + \Delta E_{\mathrm{Pauli}} + \Delta E_{\mathrm{orb}} + \Delta E_{\mathrm{disp}}$$

ΔE_{elstat} describes the quasiclassical Coulomb interaction between the unperturbed charge distributions of the fragments A and B. ΔE_{Pauli} is the Pauli repulsion, which is destabilizing and describes the interaction between electrons of the same spin between the two fragments. The third interaction ΔE_{orb} is the orbital interaction, which includes the charge transfer and polarization effects. Further details on the EDA method and examples on bond analysis using EDA can be found in the literature.[30–32]
Table S4 shows the used cutting scheme and summarizes our EDA results for complexes of type **2**. For complexes **1a**, **1c**, **1f** and **1h**, isomers with a *cis*- or *trans*-orientation of the hydrido ligand in respect to the hydrogen atom attached to the central donor group are possible and usually both isomers can be observed by NMR spectroscopy. However, the IR spectra of these mixtures gave rise to only one band for the C-O stretching vibration. Therefor, we analyzed the corresponding isomers of the model complexes **2a**, **2c**, **2f** and **2h** by EDA as well. For **2c**, **2f** and **2h** we found very similar values of the different energy terms for the *cis*- and the *trans*-isomer, but *cis*-**2a** turned out to be an unstable arrangement and could not be analyzed. For this reason, we analyzed trends between the experimentally observed C-O stretching vibration of **1** (mix of *cis* and *trans*) and the energy terms of the corresponding *trans*-isomers in **2** (if applicable).
In case of complex **2f**, we encountered problems with the geometry optimization, which resulted in either unstable or structurally not meaninginful complexes.To avoid potential falsification of the energy terms by the apparent steric overload, we analyzed the interaction with $[(Ph_2PH)_2IrCl(CO)H]^+$ for **2e** and **2f** as well.

Table S4. EDA results for **2a-h** in kcal·mol^{-1} (BP86/TZ2P).

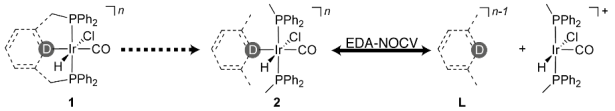

	L =	D_e	E_{Prep}	ΔE_{int}	ΔE_{elstat} [a]	ΔE_{orb} [a]	ΔE_{Pauli}	ΔE_{Disp}	$\Delta E_{orb}(\sigma)$ [b]	$E_{orb}(\pi)$ [b]
trans-**2a**	$(Ph_2MeP)_2CH^+$	-31.7	63.5	-31.8	-36.8 (34.6%)	-69.4 (65.4%)	118.8	-44.4	-56.9 (82.0%)	-12.5 (18.0%)
2b	lutidine	0.2	56.5	-56.7	-75.3 (58.3%)	-53.7 (41.7%)	97.4	-25.2	-45.0 (83.8%)	-8.7 (16.2%)
trans-**2c**	Me_2NH	21.1	39.2	-60.7	-88.5 (60.8%)	-57.1 (39.2%)	102.0	-17.3	-51.1 (89.5%)	-6.0 (10.5%)
cis-**2c**	Me_2NH	23.0	37.5	-60.6	-86.5 (61.4%)	-54.5 (38.6%)	99.0	-18.6	-47.5 (87.3%)	-6.9 (12.7%)
2e	$(Ph_2MeP)_2C$	41.8	67.0	-108.8	-121.4 (56.9%)	-91.8 (43.1%)	147.8	-43.4	-77.5 (84.4%)	-14.3 (15.6 %)
2e[c]	$(Ph_2MeP)_2C$	68.7	49.9	-118.6	-132.8 (56.7%)	-101.4 (43.3%)	168.6	-53.0	-85.9 (84.7%)	-15.5 (15.3%)
trans-**2f**[c]	$(Ph_2MeP)_2BH$	73.8	59.7	-133.5	-159.6 (55.7%)	-127.1 (44.3%)	198.1	-44.8	-114.0 (89.7%)	-13.1 (10.3%)
cis-**2f**[c]	$(Ph_2MeP)_2BH$	56.5	82.6	-139.1	-166.3 (55.8%)	-131.8 (44.2%)	198.5	-39.6	-118.5 (89.9%)	-13.2 (10.1%)
2g	*o*-Me_2-$C_6H_3^-$	133.1	62.6	-195.7	-278.9 (68.3%)	-129.4 (31.7%)	239.3	-26.8	-112.9 (87.2%)	-16.5 (12.8 %)
trans-**2o**	Me_2HC^-	169.3	41.4	-210.7	-228.3 (68.5%)	-132.9 (31.5%)	228.6	-18.2	-119.2 (89.7%)	-13.7 (10.3%)
cis-**2o**	Me_2HC^-	165.0	46.2	-211.2	-286.3 (68.1%)	-134.4 (31.9%)	228.3	-18.8	-119.9 (89.2%)	-14.5 (10.8%)
2j	$PhMe_2P$	48.7	43.1	-91.8	-137.7 (59.7%)	-92.8 (40.3%)	168.9	-30.2	-80.9 (87.2%)	-11.9 (12.8%)
2l	^{Benz}NHC	35.7	61.0	-96.7	-170.4 (60.1%)	-95.6 (39.9%)	194.3	-25.0	-84.2 (88.1%)	-11.4 (11.9%)

[a] The percentage of contribution to $\Delta E_{elstat} + \Delta E_{orb}$ is given in parenthesis. [b] The percentage of contribution to ΔE_{orb} is given in parenthesis. [c] The $[(Ph_2PH)_2IrCl(CO)H]^+$ fragment was used instead to avoid falsification due to steric overload.

A comparison of the experimental and calculated values of $\tilde{\nu}_{CO}$ (Table S3) reveals a rather big difference of 16 cm^{-1} for complex **1g**, which seems not to be based on deviations between the experimentally derived and the optimized structure. In our analysis we observed that the experimental value $\tilde{\nu}_{CO}$(**1g$_{exp}$**) substantially deviates from the observed trend and was therefor treated as an outlier. In the following figures we report two values for the coefficient of correlation R^2 of our linear regression analysis, with and without the discussed outlier $\tilde{\nu}_{CO}$(**1g$_{exp}$**).

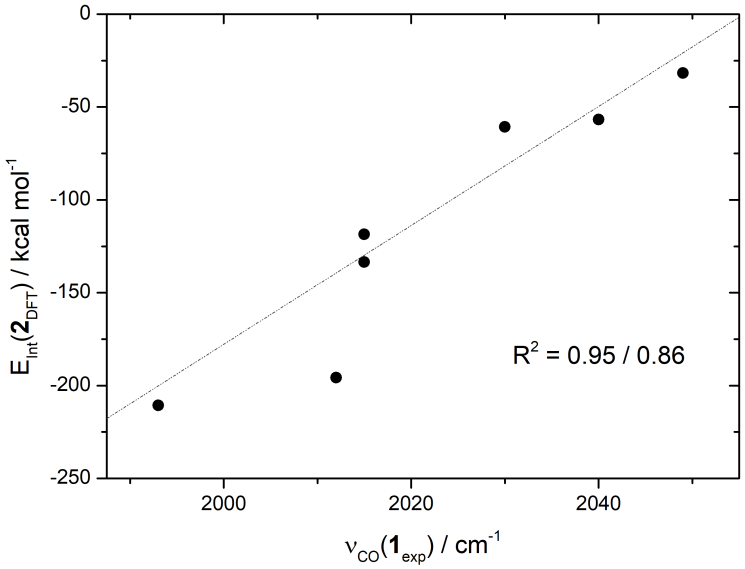

Figure S66. Correlation between the interation energy ΔE_{int} in **2** and the experimental value of $\tilde{\nu}_{CO}$ in **1**.

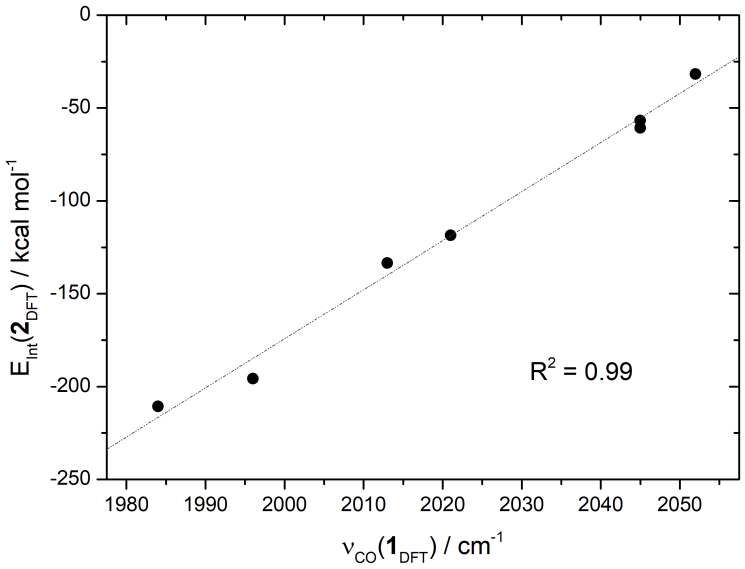

Figure S67. Correlation between the interaction energy ΔE_{int} in **2** and the calculated value of $\tilde{\nu}_{CO}$ in **1**.

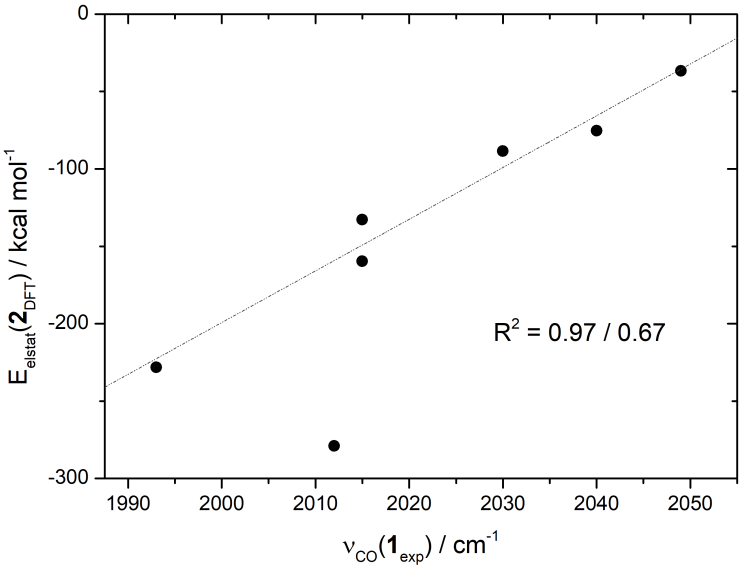

Figure S68. Correlation between the electrostatic interaction energy term ΔE_{elstat} in **2** and the experiment value of $\tilde{\nu}_{CO}$ in **1**.

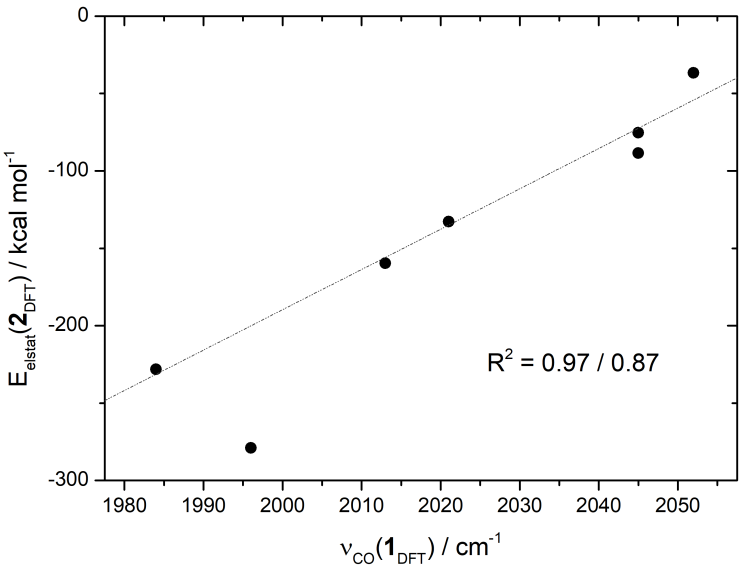

Figure S69. Correlation between the electrostatic interaction energy term ΔE_{elstat} in **2** and the calculated value of $\tilde{\nu}_{CO}$ in **1**.

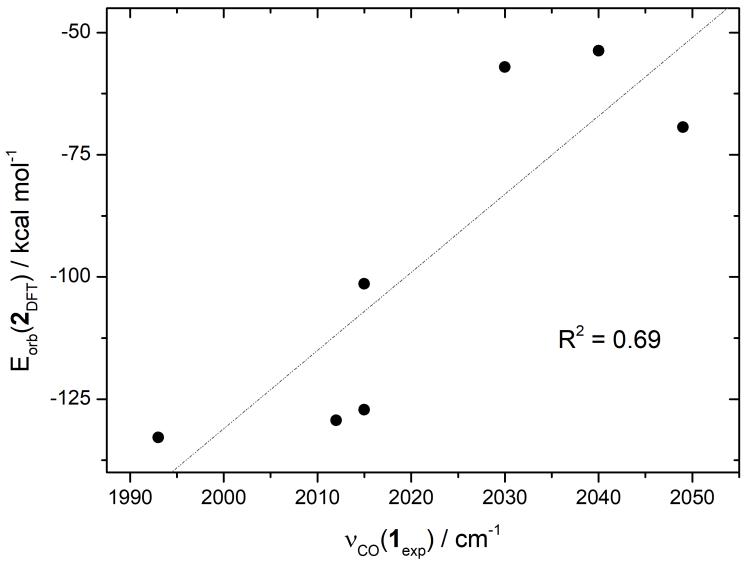

Figure S70. Correlation between the orbital interaction energy term ΔE_{orb} in **2** and the experimental value of $\tilde{\nu}_{CO}$ in **1**.

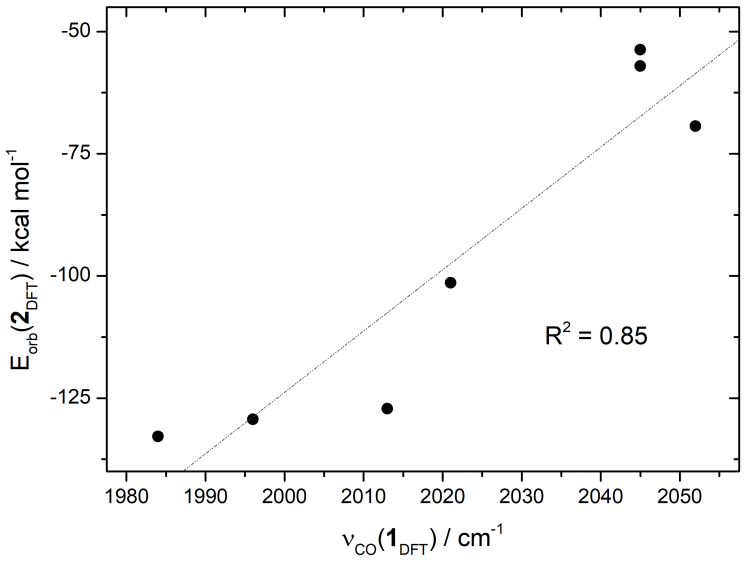

Figure S71. Correlation between the orbital interaction energy term ΔE_{orb} in **2** and the calculated value of $\tilde{\nu}_{CO}$ in **1**.

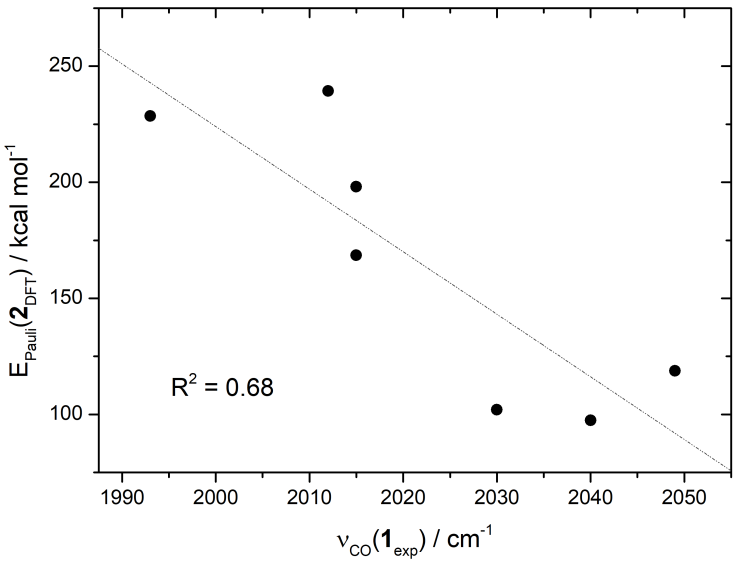

Figure S72. Correlation between the Pauli repulsion energy term ΔE_{Pauli} in **2** and the experimental value of $\tilde{\nu}_{CO}$ in **1**.

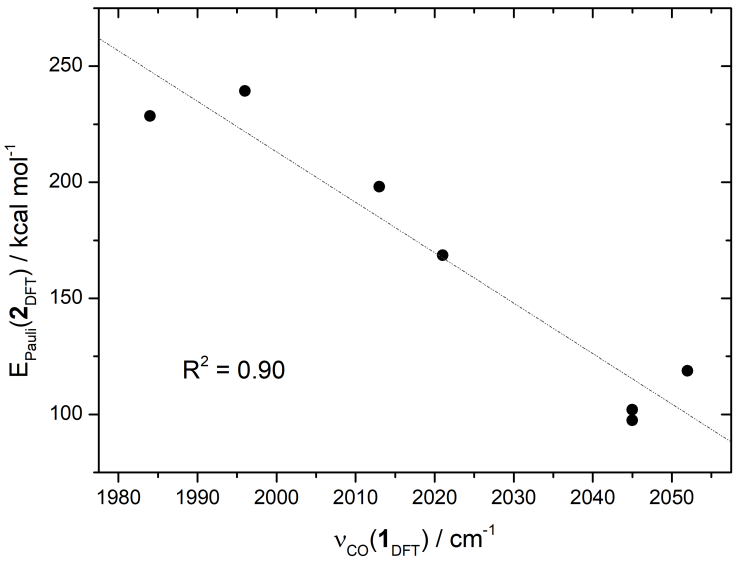

Figure S73. Correlation between the Pauli repulsion energy term ΔE_{Pauli} in **2** and the calculated value of $\tilde{\nu}_{CO}$ in **1**.

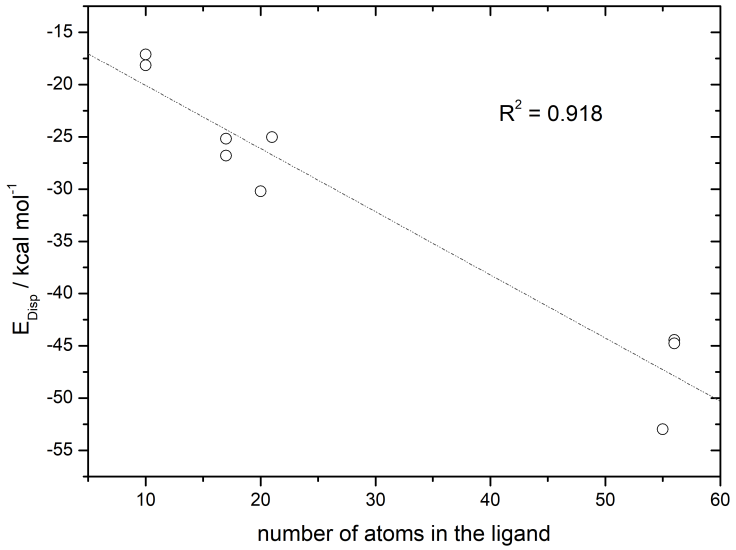

Figure S74. Correlation between the dispersion energy term ΔE_{disp} in **2** and the number of atoms in the ligand fragment.

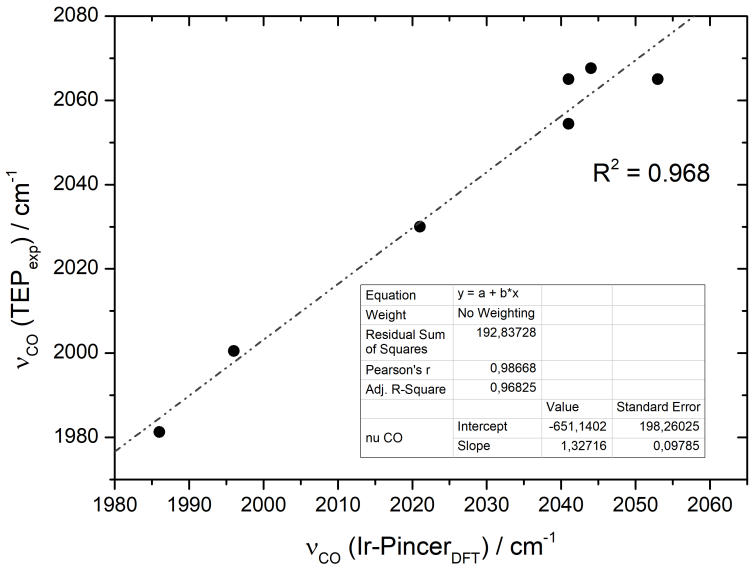

Figure S75. Correlation between the electronic Tolman parameter (TEP) and the ligand parameter reported herein, based on the value of $\tilde{\nu}_{CO}$ in **1**.

The molecular orbitals of the complexes corresponding to σ-donation and π-backdonation were selected by visual inspection of the complexes MOs and are depicted in the following. Additionally, for the ligand and iridium fragments the corresponding occupied and unoccupied MOs were identified which show matching symmetry and MO shape. Occupied MOs are depicted in blue and red, unoccupied MOs are depicted in orange and turquoise.

a) b) c)

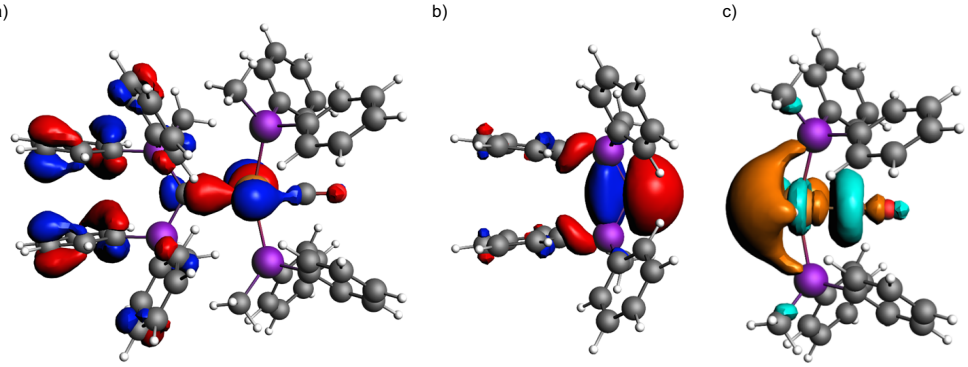

Figure S76. MO corresponding to the σ-donor bond in *trans*-**2a** (a) with the corresponding occupied MO of the ligand fragment (b) and the unoccupied MO of the $[(Ph_2PMe)_2IrCl(CO)H]^+$ fragment (c). Contour values are set to 0.03.

a) b) c)

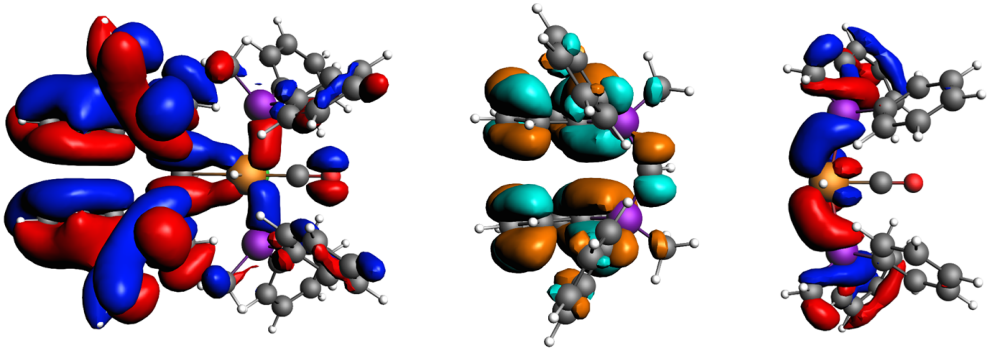

Figure S77. MO corresponding to the π-acceptor bond in *trans*-**2a** (a) with the corresponding unoccupied MO of the ligand fragment (b) and the occupied MO of the $[(Ph_2PMe)_2IrCl(CO)H]^+$ fragment (c). Contour values are set to 0.01.

a) b) c)

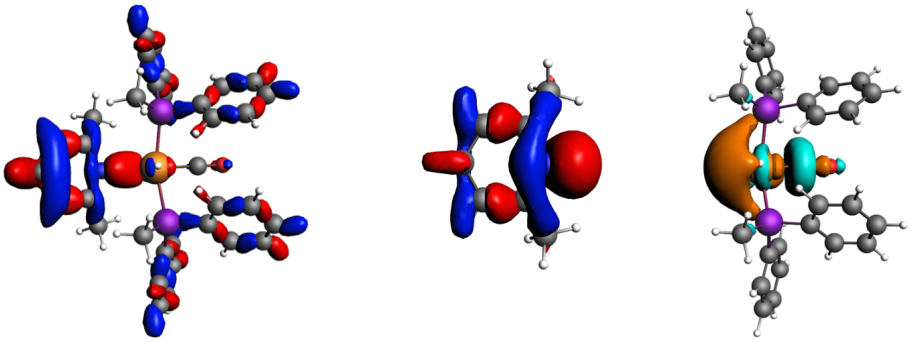

Figure S78. MO corresponding to the σ-donor bond in **2b** (a) with the corresponding occupied MO of the ligand fragment (b) and the unoccupied MO of the $[(Ph_2PMe)_2IrCl(CO)H]^+$ fragment (c). Contour values are set to 0.03.

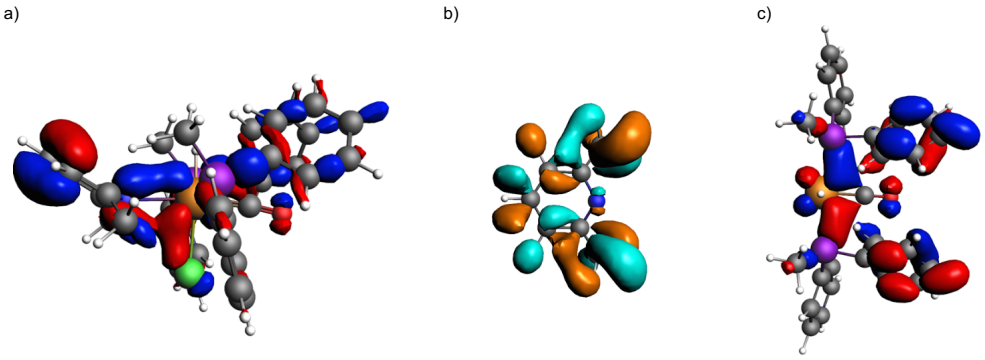

Figure S79. MO corresponding to the π-acceptor bond in **2b** (a) with the corresponding unoccupied MO of the ligand fragment (b) and the occupied MO of the $[(Ph_2PMe)_2IrCl(CO)H]^+$ fragment (c). Contour values are set to 0.01.

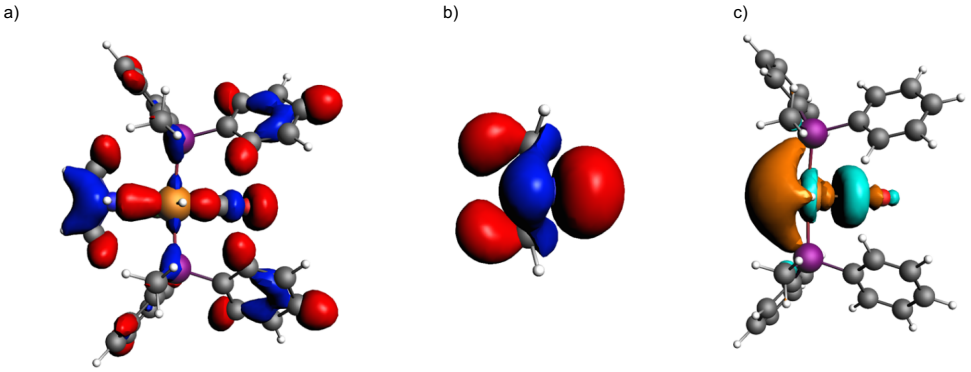

Figure S80. MO corresponding to the σ-donor bond in *cis*-**2c** (a) with the corresponding occupied MO of the ligand fragment (b) and the unoccupied MO of the $[(Ph_2PMe)_2IrCl(CO)H]^+$ fragment (c). Contour values are set to 0.03.

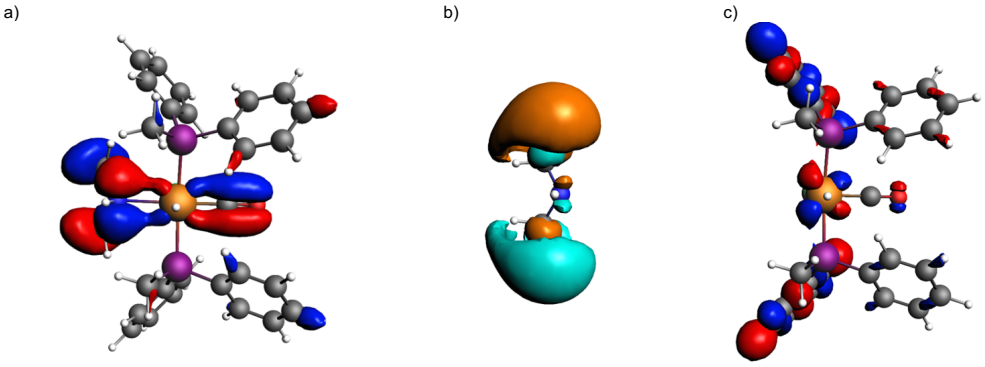

Figure S81. MO corresponding to the π-acceptor bond in *cis*-**2c** (a) with the corresponding unoccupied MO of the ligand fragment (b) and the occupied MO of the $[(Ph_2PMe)_2IrCl(CO)H]^+$ fragment (c). Contour values are set to 0.03.

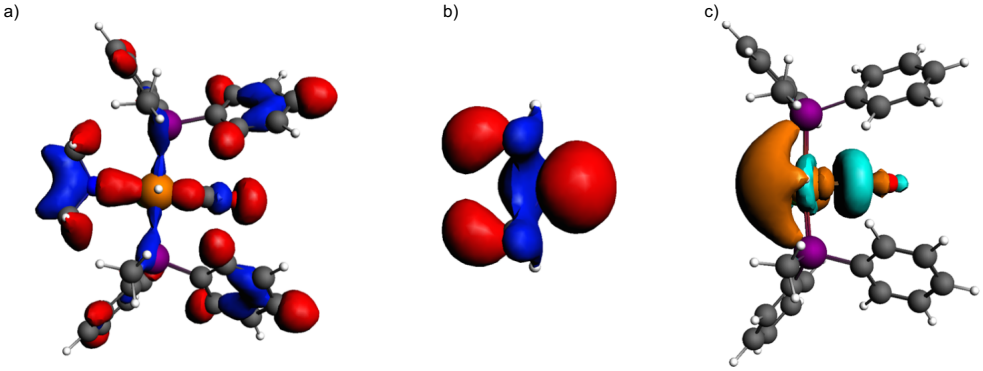

Figure S82. MO corresponding to the σ-donor bond in *trans*-**2c** (a) with the corresponding occupied MO of the ligand fragment (b) and the unoccupied MO of the $[(Ph_2PMe)_2IrCl(CO)H]^+$ fragment (c). Contour values are set to 0.03.

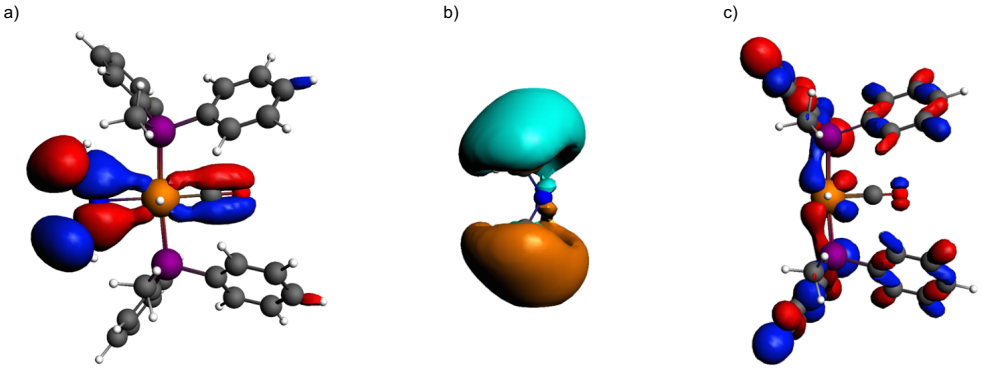

Figure S83. MO corresponding to the π-acceptor bond in *trans*-**2c** (a) with the corresponding unoccupied MO of the ligand fragment (b) and the occupied MO of the $[(Ph_2PMe)_2IrCl(CO)H]^+$ fragment (c). Contour values are set to 0.03.

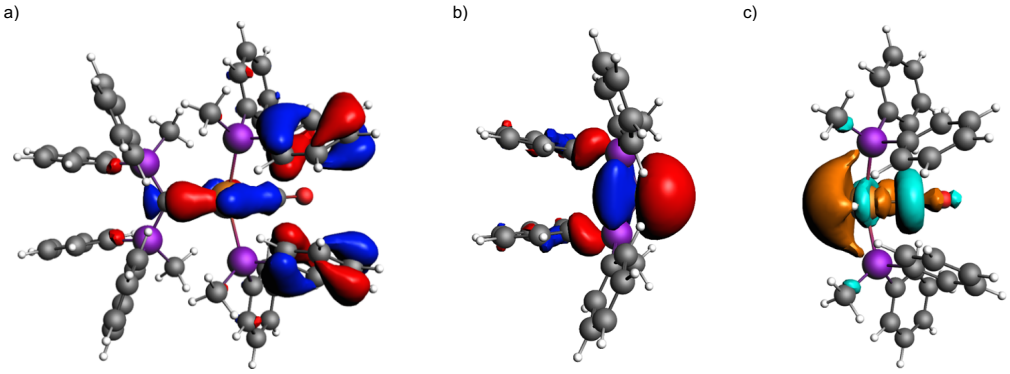

Figure S84. MO corresponding to the σ-donor bond in **2e** (a) with the corresponding occupied MO of the ligand fragment (b) and the unoccupied MO of the $[(Ph_2PMe)_2IrCl(CO)H]^+$ fragment (c). Contour values are set to 0.03.

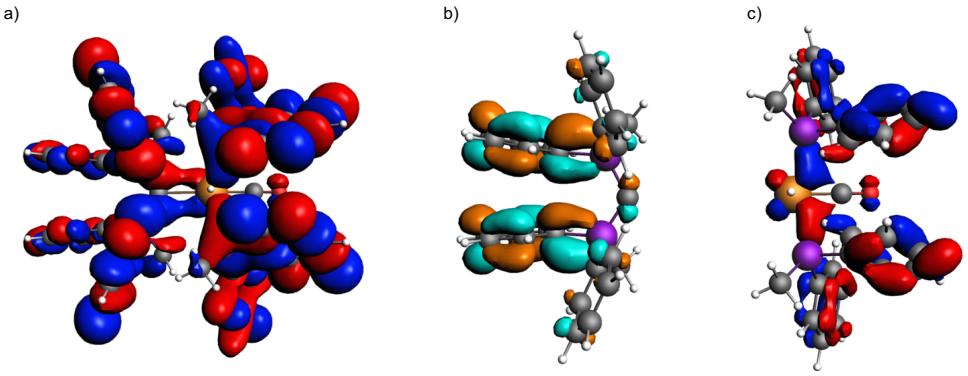

Figure S85. MO corresponding to the π-acceptor bond in **2e** (a) with the corresponding unoccupied MO of the ligand fragment (b) and the occupied MO of the $[(Ph_2PMe)_2IrCl(CO)H]^+$ fragment (c). Contour values are set to 0.01 (a) or 0.03 (b and c).

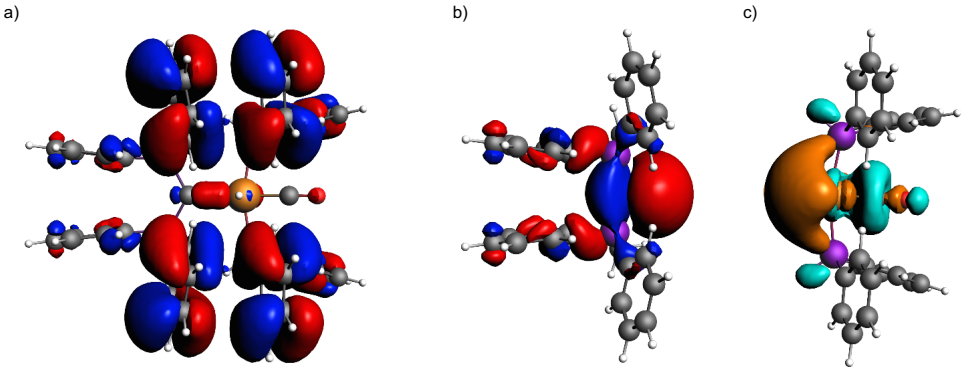

Figure S86. MO corresponding to the σ-donor bond in **2e** (a) with the corresponding occupied MO of the ligand fragment (b) and the unoccupied MO of the $[(Ph_2PH)_2IrCl(CO)H]^+$ fragment (c). Contour values are set to 0.015 (a) or 0.02 (b and c).

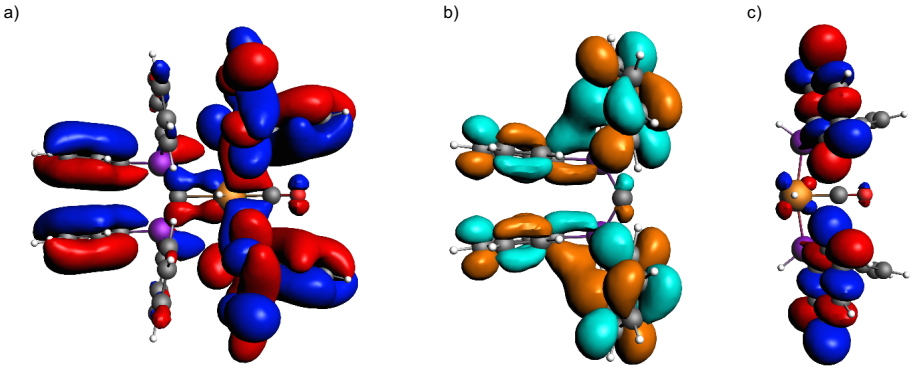

Figure S87. MO corresponding to the π-acceptor bond in **2e** (a) with the corresponding unoccupied MO of the ligand fragment (b) and the occupied MO of the $[(Ph_2PH)_2IrCl(CO)H]^+$ fragment (c). Contour values are set to 0.01 (a and c) or 0.02 (b).

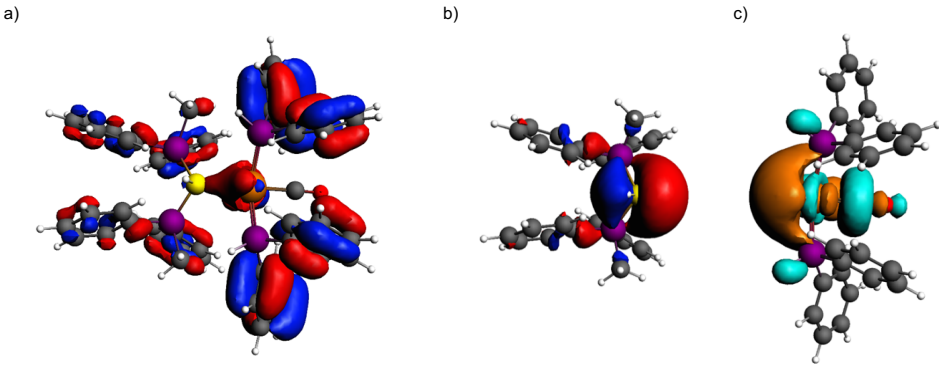

Figure S88. MO corresponding to the σ-donor bond in *cis*-**2f** (a) with the corresponding occupied MO of the ligand fragment (b) and the unoccupied MO of the $[(Ph_2PMe)_2IrCl(CO)H]^+$ fragment (c). Contour values are set to 0.02 (a and c) or 0.03 (b).

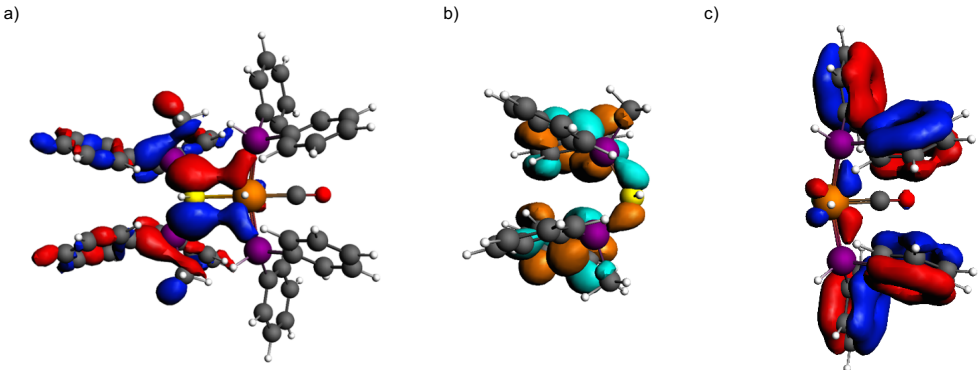

Figure S89. MO corresponding to the π-acceptor bond in *cis*-**2f** (a) with the corresponding unoccupied MO of the ligand fragment (b) and the occupied MO of the $[(Ph_2PMe)_2IrCl(CO)H]^+$ fragment (c). Contour values are set to 0.2 (c), 0.25 (b) or 0.3 (a).

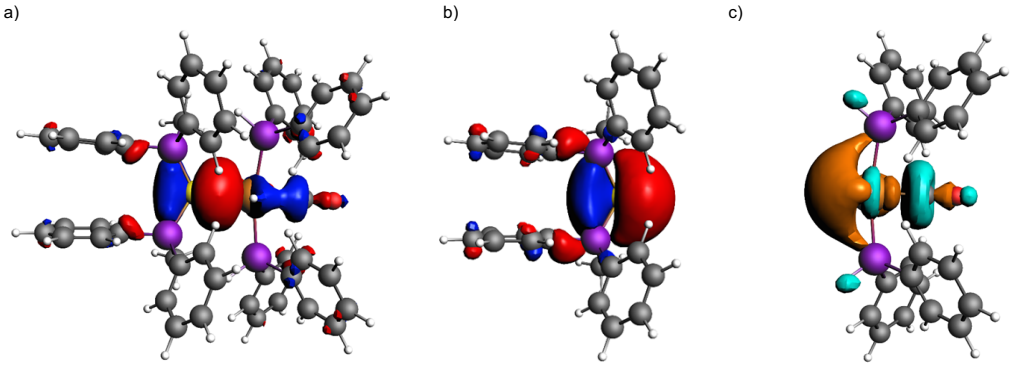

Figure S90. MO corresponding to the σ-donor bond in *trans*-**2f** (a) with the corresponding occupied MO of the ligand fragment (b) and the unoccupied MO of the $[(Ph_2PMe)_2IrCl(CO)H]^+$ fragment (c). Contour values are set to 0.03.

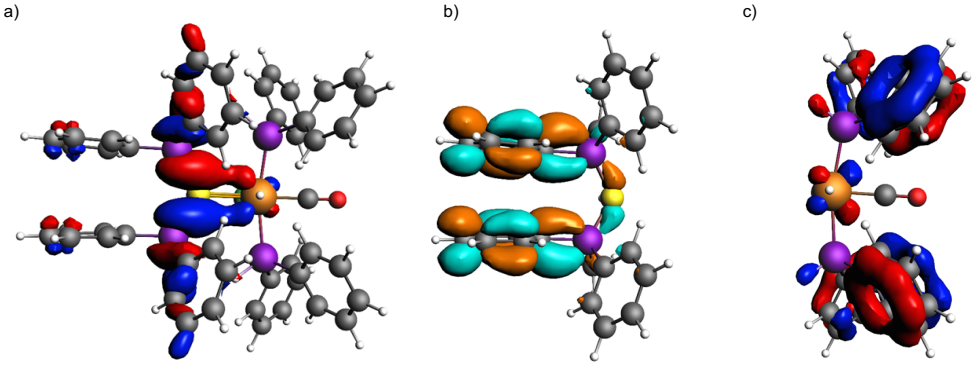

Figure S91. MO corresponding to the π-acceptor bond in *trans*-**2f** (a) with the corresponding unoccupied MO of the ligand fragment (b) and the occupied MO of the $[(Ph_2PMe)_2IrCl(CO)H]^+$ fragment (c). Contour values are set to 0.03.

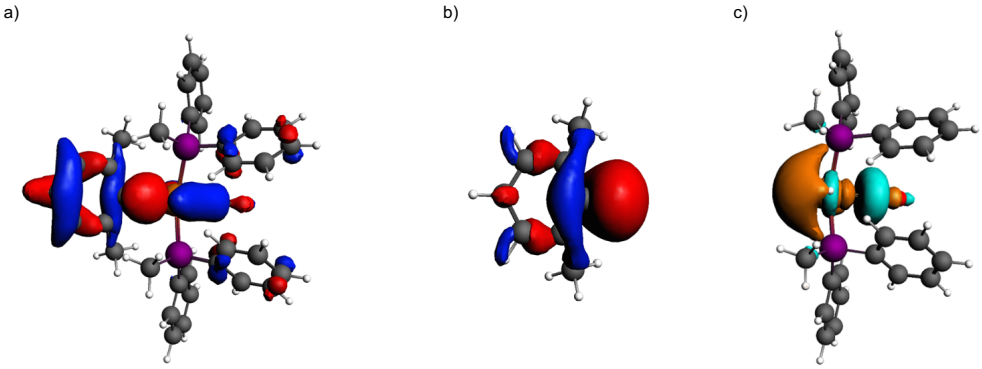

Figure S92. MO corresponding to the σ-donor bond in **2g** (a) with the corresponding occupied MO of the ligand fragment (b) and the unoccupied MO of the $[(Ph_2PMe)_2IrCl(CO)H]^+$ fragment (c). Contour values are set to 0.03.

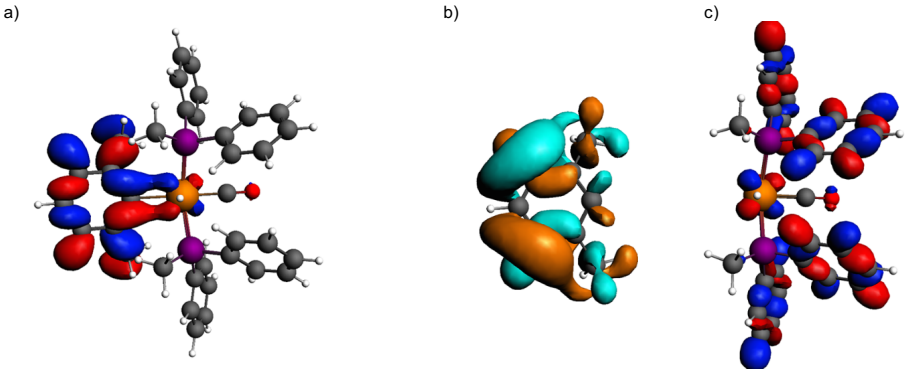

Figure S93. MO corresponding to the π-acceptor bond in **2g** (a) with the corresponding unoccupied MO of the ligand fragment (b) and the occupied MO of the $[(Ph_2PMe)_2IrCl(CO)H]^+$ fragment (c). Contour values are set to 0.25.

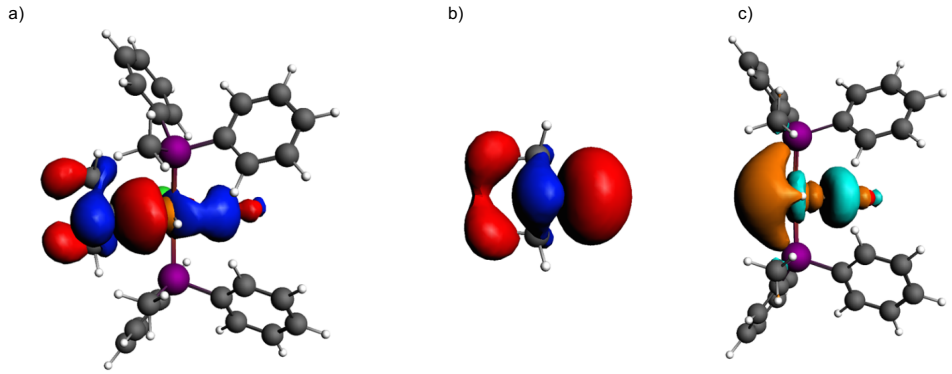

Figure S94. MO corresponding to the σ-donor bond in *cis*-**2o** (a) with the corresponding occupied MO of the ligand fragment (b) and the unoccupied MO of the $[(Ph_2PMe)_2IrCl(CO)H]^+$ fragment (c). Contour values are set to 0.03.

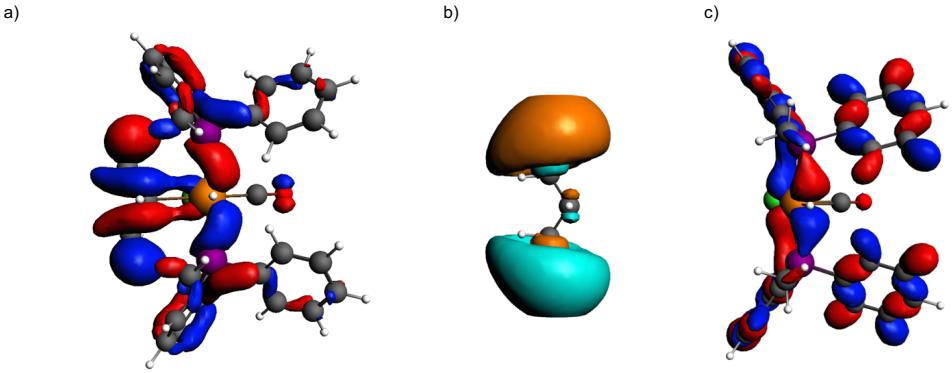

Figure S95. MO corresponding to the π-acceptor bond in *cis*-**2o** (a) with the corresponding unoccupied MO of the ligand fragment (b) and the occupied MO of the $[(Ph_2PMe)_2IrCl(CO)H]^+$ fragment (c). Contour values are set to 0.25.

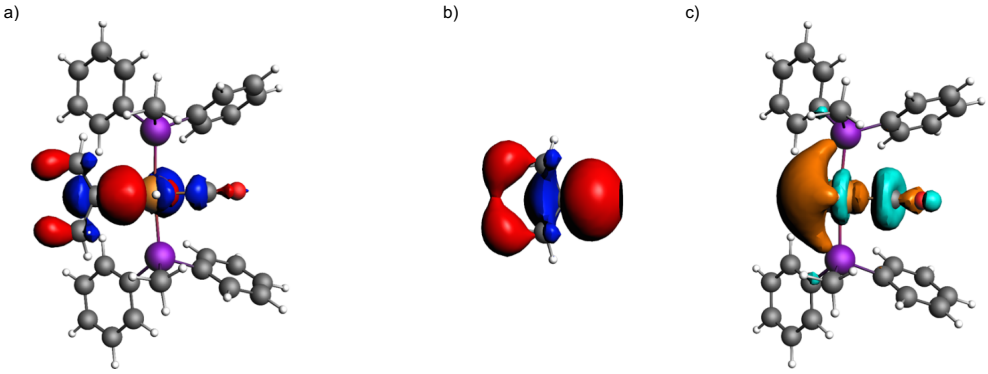

Figure S96. MO corresponding to the σ-donor bond in *trans*-**2o** (a) with the corresponding occupied MO of the ligand fragment (b) and the unoccupied MO of the $[(Ph_2PMe)_2IrCl(CO)H]^+$ fragment (c). Contour values are set to 0.03 (b and c) or 0.035 (a).

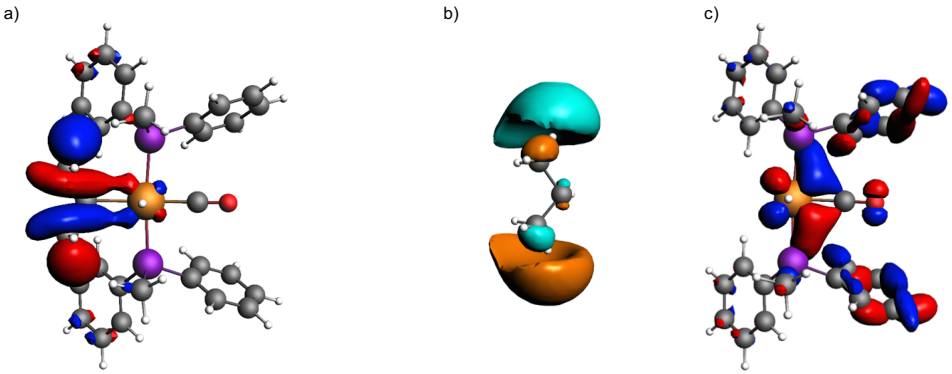

Figure S97. MO corresponding to the π-acceptor bond in *trans*-**2o** (a) with the corresponding unoccupied MO of the ligand fragment (b) and the occupied MO of the $[(Ph_2PMe)_2IrCl(CO)H]^+$ fragment (c). Contour values are set to 0.03.

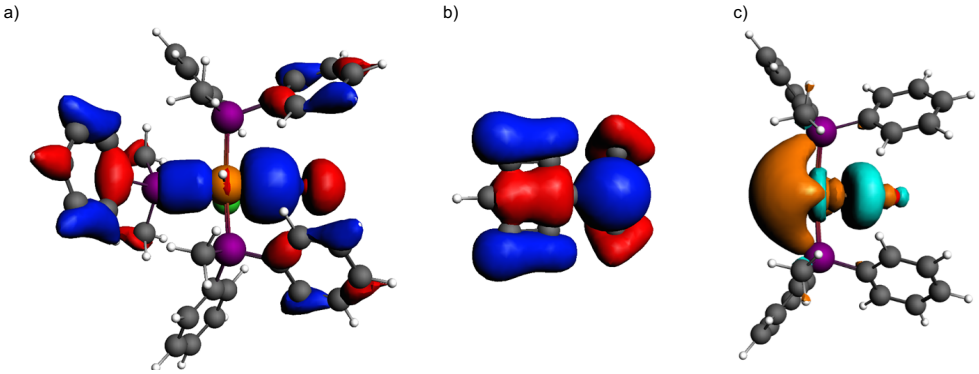

Figure S98. MO corresponding to the σ-donor bond in **2j** (a) with the corresponding occupied MO of the ligand fragment (b) and the unoccupied MO of the $[(Ph_2PMe)_2IrCl(CO)H]^+$ fragment (c). Contour values are set to 0.025.

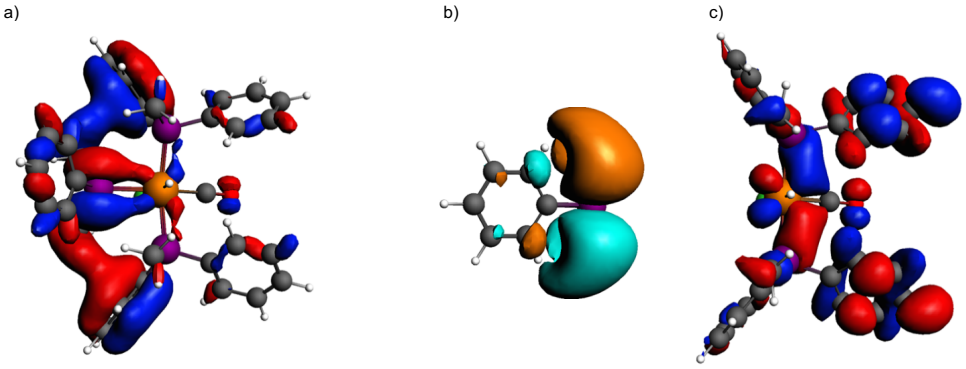

Figure S99. MO corresponding to the π-acceptor bond in **2j** (a) with the corresponding unoccupied MO of the ligand fragment (b) and the occupied MO of the $[(Ph_2PMe)_2IrCl(CO)H]^+$ fragment (c). Contour values are set to 0.02 (a and c) or 0.025 (b).

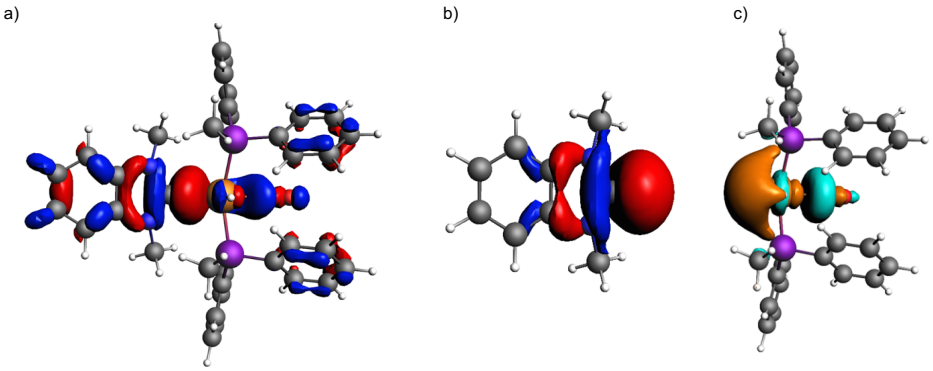

Figure S100. MO corresponding to the σ-donor bond in **2l** (a) with the corresponding occupied MO of the ligand fragment (b) and the unoccupied MO of the $[(Ph_2PMe)_2IrCl(CO)H]^+$ fragment (c). Contour values are set to 0.03.

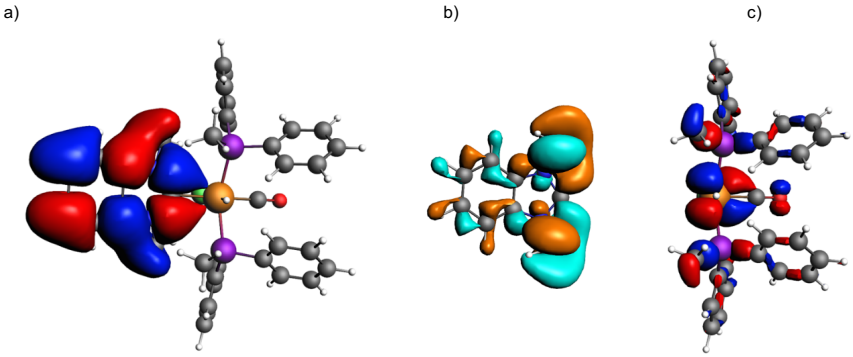

Figure S101. MO corresponding to the π-acceptor bond in **2l** (a) with the corresponding unoccupied MO of the ligand fragment (b) and the occupied MO of the $[(Ph_2PMe)_2IrCl(CO)H]^+$ fragment (c). Contour values are set to 0.03.

Cartesian coordinates of all DFT-optimized geometries

Complexes

Table S5. Cartesian coordinates for the optimized geometry of *cis*-**1a**.

Atomic Number	X	Y	Z
77	5.251429	16.072135	6.823380
1	5.551045	17.591470	7.095322
15	7.564166	15.649142	6.644729
17	4.906966	13.659415	6.146426
15	2.955336	16.558177	6.629087
6	5.214121	16.658667	4.635992
6	5.224563	15.731879	8.674892
6	7.776423	15.258614	4.841157
6	8.267999	14.241399	7.540034
6	8.629397	17.062338	7.035268
6	1.837130	15.900973	7.883787
6	2.546412	18.305394	6.341284
6	2.487061	15.716969	5.034820
15	6.840412	16.470819	3.851474
15	3.692645	16.169670	3.735506
8	5.209063	15.547037	9.807536
1	8.819739	15.212846	4.514178
1	7.297164	14.281987	4.707259
6	8.914531	14.487921	8.764840
6	8.113853	12.921432	7.083395
6	8.203958	17.988972	7.997911
6	9.905007	17.187755	6.464055
6	0.851355	16.701540	8.483490
6	2.003877	14.561157	8.280932
6	1.367868	18.653315	5.657633
6	3.387725	19.322575	6.816028
1	1.474016	15.954817	4.699407
1	2.574837	14.642802	5.222021
6	6.857393	15.935495	2.133770
6	7.688472	18.059428	3.948310
6	3.751360	14.840345	2.515302
6	3.031492	17.628081	2.888994
1	9.045988	15.504000	9.125035
6	9.402527	13.421325	9.520214
1	7.587865	12.709727	6.159624
6	8.615179	11.863122	7.841684
1	7.219167	17.891898	8.444513
6	9.044305	19.036163	8.380830
1	10.260535	16.461973	5.737557
6	10.733322	18.247074	6.833501
6	0.029073	16.156764	9.472545
1	0.729695	17.739883	8.190424
1	2.780805	13.946917	7.832271
6	1.170585	14.027334	9.262788
1	0.686172	17.885960	5.303262

6	1.054195	19.992965	5.431256
6	3.069491	20.663651	6.591545
1	4.284387	19.065731	7.370674
6	6.670282	16.892838	1.120857
6	7.061474	14.586745	1.800285
6	7.318346	19.032130	4.891344
6	8.806364	18.272901	3.121682
6	3.738324	15.175146	1.149081
6	3.723143	13.490816	2.907177
6	3.753595	18.819153	2.733050
6	1.732205	17.527908	2.358211
6	9.256552	12.109670	9.059422
1	9.902479	13.617285	10.464636
1	8.498477	10.844383	7.482594
1	8.715479	19.743910	9.137051
6	10.305355	19.170300	7.794040
1	11.716768	18.345223	6.382235
1	-0.730309	16.776636	9.941101
6	0.184722	14.822743	9.859065
1	1.295984	12.992454	9.569090
6	1.907105	21.000506	5.892812
1	0.141892	20.249494	4.900187
1	3.723614	21.444288	6.970689
1	6.521982	17.938433	1.373689
6	6.707926	16.501439	-0.216451
1	7.193565	13.835703	2.572282
6	7.093716	14.204876	0.459657
6	8.049863	20.215024	4.989030
1	6.495097	18.859981	5.576643
1	9.102248	17.526338	2.390242
6	9.532605	19.458330	3.228268
1	3.749547	16.212407	0.834799
6	3.701581	14.166587	0.188693
6	3.687375	12.490499	1.935516
1	3.737488	13.220290	3.956909
1	4.763569	18.921364	3.117112
6	3.174249	19.905068	2.072078
6	1.159451	18.613894	1.700160
1	1.170113	16.601380	2.446594
1	9.642547	11.281367	9.647232
1	10.958492	19.987077	8.089254
1	-0.456920	14.403487	10.629264
1	1.659681	22.044142	5.718395
1	6.578762	17.243882	-0.999026
6	6.926004	15.160205	-0.547117
1	7.256098	13.162354	0.202637
1	7.765413	20.962173	5.723953
6	9.152708	20.431050	4.158301
1	10.391102	19.622916	2.583326
6	3.673348	12.824348	0.577998
1	3.686305	14.431886	-0.864442

S60

1	3.656886	11.449106	2.243707
1	3.737824	20.826928	1.958983
6	1.878907	19.806151	1.559520
1	0.155263	18.529337	1.294298
1	6.966867	14.859559	-1.590479
1	9.719292	21.354697	4.238519
1	3.632498	12.040980	-0.174119
1	1.431065	20.653162	1.047110
1	5.074135	17.742879	4.687071

Table S6. Cartesian coordinates for the optimized geometry of **1a**[1].

Atomic Number	X	Y	Z
77	-0.883102	1.181158	-0.126932
1	-1.172342	1.668276	1.339340
15	-2.668939	-0.348047	0.029050
17	-0.368270	0.228581	-2.459959
15	1.085374	2.478569	-0.224207
14	0.522802	-0.544099	0.690796
6	-2.030972	2.622886	-0.788422
6	-2.090057	-1.999206	-0.618270
6	-4.097442	0.078498	-0.995095
6	-3.278714	-0.743613	1.691443
6	0.973187	3.982705	-1.225663
6	1.871159	2.915619	1.353605
6	2.393031	1.465862	-1.090745
15	-0.520212	-2.555407	0.157774
15	2.583969	-0.201545	-0.330933
8	-2.706970	3.473090	-1.141913
1	-2.866452	-2.762174	-0.506050
1	-1.864735	-1.872403	-1.680763
6	-5.180929	0.763428	-0.418933
6	-4.055828	-0.128457	-2.384070
6	-2.522311	-0.420489	2.825842
6	-4.473656	-1.470983	1.837137
6	1.166548	5.255508	-0.667679
6	0.595209	3.851024	-2.574430
6	3.162771	3.474052	1.345042
6	1.220517	2.704589	2.576597
1	3.360806	1.976526	-1.078446
1	2.042749	1.348851	-2.118222
6	0.239758	-3.747698	-0.971451
6	-0.866385	-3.378790	1.728998
6	3.099340	-1.397252	-1.585411
6	3.932662	-0.090528	0.876868
1	-5.212639	0.940846	0.652201
6	-6.224471	1.216021	-1.227485
1	-3.201940	-0.612041	-2.847998
6	-5.106987	0.323412	-3.183099
1	-1.606813	0.152041	2.718191
6	-2.948487	-0.826305	4.092565
1	-5.074428	-1.714799	0.964971

6	-4.901447	-1.864131	3.104427
6	0.995293	6.391581	-1.463197
1	1.444108	5.363468	0.376246
1	0.406232	2.868342	-3.000021
6	0.436075	4.991001	-3.360830
1	3.674317	3.662839	0.405031
6	3.792033	3.804911	2.543096
6	1.852953	3.040182	3.776710
1	0.220085	2.285778	2.588925
6	0.639881	-5.007080	-0.494857
6	0.371146	-3.424852	-2.333292
6	0.168588	-3.486806	2.674801
6	-2.112078	-3.971347	1.986289
6	3.621167	-2.622308	-1.131132
6	3.035912	-1.125035	-2.959259
6	3.688882	0.137175	2.239545
6	5.255534	-0.150564	0.399324
6	-6.191374	0.993039	-2.607481
1	-7.062834	1.741239	-0.778385
1	-5.075830	0.156174	-4.256162
1	-2.358602	-0.571362	4.968727
6	-4.137105	-1.546116	4.233058
1	-5.832714	-2.413600	3.212658
1	1.142948	7.377048	-1.030193
6	0.636051	6.261188	-2.807079
1	0.148644	4.889402	-4.403745
6	3.137936	3.587384	3.761381
1	4.788956	4.236394	2.527375
1	1.337810	2.882865	4.720542
1	0.530365	-5.262028	0.554638
6	1.155940	-5.947127	-1.389161
1	0.084562	-2.443247	-2.699723
6	0.877424	-4.377414	-3.214816
6	-0.045204	-4.177706	3.867152
1	1.138494	-3.034731	2.484909
1	-2.922626	-3.903047	1.270008
6	-2.321599	-4.651552	3.185854
1	3.684941	-2.835004	-0.066923
6	4.095597	-3.555779	-2.049408
6	3.524986	-2.063089	-3.870623
1	2.609905	-0.199600	-3.329288
1	2.676576	0.213483	2.618831
6	4.761086	0.296220	3.118821
6	6.319690	0.014583	1.285100
1	5.453753	-0.335873	-0.652752
1	-7.007042	1.344017	-3.233549
1	-4.474342	-1.851392	5.219917
1	0.506042	7.147387	-3.422142
1	3.627651	3.852546	4.694563
1	1.454045	-6.926234	-1.024644
6	1.266592	-5.637206	-2.746859

1	0.968109	-4.134615	-4.269313
1	0.758230	-4.262263	4.593483
6	-1.292042	-4.756277	4.125396
1	-3.290161	-5.101297	3.383798
6	4.057801	-3.272502	-3.418729
1	4.503203	-4.498336	-1.696080
1	3.491307	-1.842962	-4.933939
1	4.567338	0.472213	4.172914
6	6.074019	0.234551	2.645207
1	7.339711	-0.034629	0.914319
1	1.653854	-6.377630	-3.441600
1	-1.460057	-5.289299	5.057164
1	4.442809	-3.995767	-4.132332
1	6.906378	0.355991	3.333072
1	0.882290	-0.792195	2.106256

Table S7. Cartesian coordinates for the optimized geometry of **1a²**.

Atomic Number	X	Y	Z
77	-0.898771	1.204145	-0.123289
1	-1.191481	1.726210	1.330553
15	-2.673148	-0.337267	0.065846
17	-0.380321	0.208136	-2.432435
15	1.075728	2.491438	-0.249087
32	0.563655	-0.557411	0.791445
6	-2.031454	2.602524	-0.812196
6	-2.099066	-1.997701	-0.567278
6	-4.110849	0.069305	-0.952637
6	-3.264122	-0.714543	1.738783
6	0.957270	3.986114	-1.262270
6	1.873539	2.934915	1.320637
6	2.381583	1.474812	-1.117701
15	-0.547958	-2.597689	0.213364
15	2.634054	-0.179913	-0.347324
8	-2.710334	3.441830	-1.190578
1	-2.890949	-2.745262	-0.457019
1	-1.868499	-1.877794	-1.629319
6	-5.198176	0.748109	-0.376728
6	-4.072185	-0.146319	-2.340471
6	-2.495958	-0.373833	2.860065
6	-4.454065	-1.444799	1.907935
6	1.137445	5.264962	-0.713843
6	0.581944	3.840159	-2.610302
6	3.150820	3.524867	1.298771
6	1.250761	2.686364	2.551108
1	3.338104	2.006919	-1.127087
1	2.018244	1.337901	-2.138042
6	0.200917	-3.785580	-0.925288
6	-0.919341	-3.428252	1.773451
6	3.116726	-1.385630	-1.602582

6	4.018155	-0.035040	0.812719
1	-5.227014	0.933064	0.693177
6	-6.249009	1.185425	-1.184344
1	-3.214801	-0.624032	-2.804176
6	-5.130572	0.290265	-3.138307
1	-1.587144	0.205751	2.734411
6	-2.904229	-0.766831	4.136702
1	-5.064176	-1.701526	1.046030
6	-4.864767	-1.824122	3.185001
6	0.956798	6.393026	-1.518544
1	1.411642	5.383654	0.329810
1	0.401275	2.852463	-3.027933
6	0.413228	4.972371	-3.405855
1	3.640602	3.739970	0.352799
6	3.792385	3.852781	2.491141
6	1.896006	3.017804	3.745556
1	0.261379	2.242417	2.573480
6	0.592000	-5.052006	-0.459196
6	0.346268	-3.447803	-2.282220
6	0.106207	-3.554954	2.727225
6	-2.174409	-4.007070	2.016804
6	3.640344	-2.609113	-1.145375
6	3.026266	-1.128551	-2.977867
6	3.807081	0.210956	2.177511
6	5.328478	-0.096378	0.302350
6	-6.219133	0.953327	-2.562848
1	-7.090329	1.706202	-0.735611
1	-5.101752	0.116633	-4.210420
1	-2.305326	-0.498146	5.002594
6	-4.087712	-1.490280	4.300245
1	-5.792400	-2.375874	3.311293
1	1.094297	7.383245	-1.093114
6	0.600862	6.248618	-2.861901
1	0.127612	4.859941	-4.448142
6	3.165784	3.598875	3.716823
1	4.777776	4.309522	2.465399
1	1.402274	2.831500	4.695542
1	0.472855	-5.317529	0.586683
6	1.110774	-5.984505	-1.359730
1	0.069230	-2.460231	-2.639973
6	0.853687	-4.393578	-3.170317
6	-0.125678	-4.250915	3.913220
1	1.083053	-3.113937	2.547250
1	-2.977314	-3.926104	1.293066
6	-2.401838	-4.692854	3.209966
1	3.722677	-2.810840	-0.080123
6	4.090890	-3.555417	-2.062377
6	3.490838	-2.079934	-3.888330

S64

1	2.599163	-0.204244	-3.349522
1	2.803447	0.285326	2.580583
6	4.899781	0.388485	3.027240
6	6.413558	0.087417	1.158713
1	5.500261	-0.297210	-0.751547
1	-7.040410	1.292525	-3.188075
1	-4.411249	-1.785587	5.294676
1	0.463465	7.128689	-3.484108
1	3.665000	3.861843	4.645580
1	1.401569	-6.968951	-1.003773
6	1.233165	-5.660309	-2.713241
1	0.953575	-4.139739	-4.221314
1	0.670595	-4.349870	4.645590
6	-1.381404	-4.816270	4.157193
1	-3.377055	-5.132970	3.396831
6	4.026250	-3.287276	-3.433845
1	4.500079	-4.496540	-1.706963
1	3.436349	-1.871680	-4.953192
1	4.731917	0.578189	4.083384
6	6.200694	0.326498	2.521192
1	7.424351	0.037486	0.763559
1	1.622148	-6.395086	-3.413006
1	-1.563476	-5.353769	5.083731
1	4.392081	-4.020817	-4.147046
1	7.049452	0.461927	3.186023
1	0.988161	-0.844604	2.244868

Table S8. Cartesian coordinates for the optimized geometry of **1a**[3].

Atomic Number	X	Y	Z
77	-0.847277	1.272888	-0.132263
1	-1.147357	1.955601	1.252305
15	-2.621828	-0.250574	0.206669
17	-0.280585	0.092722	-2.326241
15	1.154215	2.514450	-0.341701
50	0.660155	-0.542790	1.069021
6	-1.941856	2.601344	-0.960073
6	-2.154673	-1.927774	-0.470887
6	-4.143330	0.153566	-0.683476
6	-3.048173	-0.623578	1.932857
6	1.031979	3.961864	-1.420764
6	1.963387	3.024949	1.202839
6	2.463761	1.472017	-1.176335
15	-0.660876	-2.671274	0.319626
15	2.799089	-0.153073	-0.363588
8	-2.605789	3.413493	-1.418307
1	-2.991803	-2.619742	-0.330541
1	-1.958691	-1.801329	-1.537915
6	-5.324386	0.495794	-0.008367

6	-4.086556	0.211873	-2.087789
6	-2.422671	0.033671	3.001051
6	-3.995313	-1.628633	2.201699
6	1.180683	5.266508	-0.927096
6	0.678413	3.749761	-2.765796
6	3.222581	3.649518	1.144672
6	1.376392	2.776697	2.451390
1	3.400543	2.036737	-1.223637
1	2.090130	1.285951	-2.184904
6	0.069244	-3.843339	-0.851601
6	-1.258753	-3.616678	1.743656
6	3.186492	-1.403982	-1.607679
6	4.266678	0.044229	0.679730
1	-5.367212	0.466115	1.076144
6	-6.450473	0.881090	-0.740606
1	-3.160391	-0.014351	-2.611193
6	-5.218791	0.589295	-2.808305
1	-1.703680	0.820654	2.801215
6	-2.733949	-0.308557	4.319545
1	-4.499323	-2.139604	1.385988
6	-4.301802	-1.969802	3.516960
6	0.991724	6.354505	-1.783458
1	1.437379	5.435887	0.114073
1	0.519776	2.741310	-3.141150
6	0.500939	4.842286	-3.613268
1	3.685788	3.862696	0.185052
6	3.881511	4.010796	2.318016
6	2.040095	3.138340	3.627001
1	0.396756	2.313668	2.502010
6	0.584470	-5.059172	-0.367393
6	0.131114	-3.544937	-2.223126
6	-0.841217	-3.329931	3.049689
6	-2.174762	-4.659750	1.511412
6	3.570925	-2.669305	-1.126714
6	3.162621	-1.154281	-2.986507
6	4.138108	0.434495	2.021699
6	5.543240	-0.149988	0.121545
6	-6.400690	0.923283	-2.136408
1	-7.364998	1.148076	-0.218288
1	-5.177860	0.629807	-3.893314
1	-2.251564	0.213457	5.141539
6	-3.670620	-1.310824	4.578250
1	-5.033941	-2.747352	3.715099
1	1.105360	7.364929	-1.400644
6	0.658194	6.144433	-3.123923
1	0.232368	4.678927	-4.653338
6	3.292177	3.753757	3.561311
1	4.853287	4.493386	2.263575

S66

1	1.574116	2.950021	4.590479
1	0.536689	-5.296365	0.691289
6	1.128307	-5.982654	-1.261038
1	-0.228359	-2.593131	-2.600535
6	0.669773	-4.480321	-3.105489
6	-1.340999	-4.076964	4.119189
1	-0.132648	-2.530644	3.242422
1	-2.490165	-4.901784	0.499426
6	-2.667376	-5.401527	2.582909
1	3.597767	-2.869595	-0.057685
6	3.950156	-3.665718	-2.022290
6	3.546415	-2.160004	-3.876751
1	2.855591	-0.191208	-3.378483
1	3.160484	0.602536	2.462778
6	5.279480	0.629257	2.800068
6	6.678595	0.050611	0.906880
1	5.648624	-0.465515	-0.912689
1	-7.279571	1.221378	-2.701409
1	-3.915289	-1.575738	5.603281
1	0.514506	6.993497	-3.786448
1	3.805918	4.040939	4.474810
1	1.510444	-6.928831	-0.887764
6	1.162291	-5.699205	-2.629301
1	0.702927	-4.254817	-4.167395
1	-1.015748	-3.851459	5.130786
6	-2.250972	-5.110278	3.887703
1	-3.370076	-6.209939	2.400669
6	3.944171	-3.410039	-3.397712
1	4.252250	-4.638977	-1.647481
1	3.539559	-1.959852	-4.944535
1	5.176014	0.929221	3.838832
6	6.548049	0.437382	2.245379
1	7.664123	-0.101417	0.475612
1	1.572391	-6.427591	-3.323663
1	-2.634226	-5.693090	4.720872
1	4.248434	-4.186068	-4.094649
1	7.435195	0.584174	2.855416
1	1.284936	-0.945818	2.616866

Table S9. Cartesian coordinates for the optimized geometry of **1a**[4].

Atomic Number	X	Y	Z
77	-0.070304	-1.658150	-0.093046
1	-0.018322	-2.266531	1.359641
15	2.297769	-1.484468	-0.140628
17	-0.174984	-0.567551	-2.380267
15	-2.441003	-1.507940	0.003753
82	-0.043385	0.851827	1.020215
6	-0.085402	-3.420175	-0.747306

6	2.804944	0.050007	-1.067340
6	3.109542	-2.819721	-1.049661
6	3.123765	-1.292121	1.465108
6	-3.290649	-2.850012	-0.862126
6	-3.177338	-1.345407	1.655642
6	-3.028195	0.024344	-0.887657
15	2.205832	1.640674	-0.332367
15	-2.269279	1.619769	-0.330118
8	-0.093622	-4.508034	-1.106579
1	3.898604	0.087468	-1.112093
1	2.403163	-0.041471	-2.078426
6	3.950172	-3.742259	-0.409451
6	2.803070	-2.966288	-2.414689
6	2.414550	-1.361976	2.672330
6	4.504648	-1.024566	1.491709
6	-4.051646	-3.804211	-0.170121
6	-3.084961	-2.977744	-2.247876
6	-4.563490	-1.134892	1.767584
6	-2.391888	-1.385704	2.816225
1	-4.115799	0.094785	-0.782784
1	-2.764721	-0.128604	-1.936347
6	2.161297	2.864439	-1.669759
6	3.507145	2.155598	0.823488
6	-2.016719	2.701690	-1.753308
6	-3.454927	2.435644	0.773260
1	4.178012	-3.638709	0.647116
6	4.494120	-4.801688	-1.140475
1	2.121370	-2.273826	-2.903300
6	3.358021	-4.022489	-3.135719
1	1.354364	-1.591691	2.662289
6	3.070824	-1.157570	3.888821
1	5.073294	-0.981022	0.567199
6	5.156279	-0.820601	2.705893
6	-4.618610	-4.873516	-0.868307
1	-4.201139	-3.718006	0.901768
1	-2.460561	-2.264251	-2.780350
6	-3.661845	-4.044527	-2.935462
1	-5.189463	-1.115396	0.879522
6	-5.147299	-0.958805	3.020651
6	-2.978948	-1.203660	4.071469
1	-1.326474	-1.575049	2.738740
6	2.552488	4.186982	-1.393001
6	1.717750	2.516297	-2.956465
6	3.242443	2.353295	2.185169
6	4.810901	2.347184	0.329788
6	-1.349595	3.914776	-1.504716
6	-2.493553	2.414163	-3.039327
6	-3.494141	2.088304	2.133890
6	-4.340653	3.404386	0.269582
6	4.203487	-4.939742	-2.500310
1	5.144523	-5.517512	-0.645507

1	3.126589	-4.134271	-4.191406
1	2.514855	-1.222327	4.820232
6	4.439860	-0.883867	3.906359
1	6.222372	-0.613260	2.716331
1	-5.207926	-5.612314	-0.332332
6	-4.429277	-4.991873	-2.247663
1	-3.507513	-4.140938	-4.006643
6	-4.355408	-0.988515	4.174230
1	-6.218794	-0.797202	3.097662
1	-2.364107	-1.242735	4.966588
1	2.899066	4.463284	-0.401372
6	2.529202	5.142604	-2.409734
1	1.374429	1.510010	-3.172274
6	1.706901	3.478508	-3.965591
6	4.273797	2.729085	3.049613
1	2.240424	2.221904	2.582224
1	5.022745	2.217573	-0.728805
6	5.834984	2.723808	1.196375
1	-0.976440	4.145541	-0.508743
6	-1.182070	4.839067	-2.532631
6	-2.313246	3.343360	-4.066985
1	-3.011383	1.484218	-3.250095
1	-2.824597	1.333554	2.537279
6	-4.416727	2.701781	2.981155
6	-5.261383	4.011636	1.124866
1	-4.305085	3.687889	-0.778333
1	4.630797	-5.763865	-3.064878
1	4.951325	-0.727181	4.852152
1	-4.874265	-5.823716	-2.786645
1	-4.813337	-0.853250	5.150362
1	2.848677	6.159249	-2.197280
6	2.116047	4.788216	-3.697406
1	1.377050	3.202236	-4.963001
1	4.063129	2.881124	4.104411
6	5.567358	2.913567	2.557698
1	6.839138	2.876299	0.810232
6	-1.664798	4.554615	-3.814380
1	-0.670439	5.775967	-2.335587
1	-2.689737	3.121557	-5.061684
1	-4.443071	2.431224	4.032827
6	-5.299241	3.663277	2.479015
1	-5.944863	4.760370	0.734130
1	2.113009	5.531699	-4.489958
1	6.367116	3.210999	3.230525
1	-1.534186	5.276713	-4.615656
1	-6.012339	4.144708	3.142652
1	-0.068098	1.998965	2.377885

Table S10. Cartesian coordinates for the optimized geometry of *trans*-**1a**.

Atomic Number	X	Y	Z
77	5.261934	16.150126	6.685450
1	5.605606	17.658034	6.410380
15	7.584551	15.711970	6.578045
17	4.741512	13.672524	6.711351
15	2.960582	16.586299	6.561972
6	5.246731	15.819252	4.462296
6	5.259838	16.457242	8.542720
6	7.973564	15.383300	4.783653
6	8.218303	14.257290	7.442560
6	8.663336	17.116641	7.000007
6	1.931954	15.788511	7.819798
6	2.433243	18.325402	6.549978
6	2.404722	15.876899	4.930994
15	6.814349	16.339006	3.749625
15	3.654202	16.053461	3.609833
8	5.239463	16.688839	9.668424
1	9.008580	15.631329	4.533702
1	7.796541	14.321394	4.577880
6	7.629602	13.884548	8.659925
6	9.317530	13.534332	6.947464
6	8.134891	18.317833	7.489221
6	10.053863	16.985572	6.837121
6	1.604956	16.527545	8.971758
6	1.562363	14.436671	7.729993
6	1.058242	18.613463	6.455715
6	3.357117	19.375251	6.613462
1	1.430719	16.255520	4.604563
1	2.329038	14.794963	5.085666
6	7.062061	15.832183	2.039100
6	7.181626	18.078568	3.973471
6	3.401286	14.686598	2.460373
6	3.481927	17.625435	2.762752
1	6.756701	14.407837	9.032355
6	8.149694	12.812071	9.384491
1	9.779214	13.798542	5.999702
6	9.828241	12.457842	7.673602
1	7.065303	18.421565	7.630238
6	8.984520	19.383476	7.795350
1	10.482959	16.046281	6.497260
6	10.897993	18.053415	7.137777
6	0.903755	15.920000	10.013082
1	1.888883	17.572614	9.055489
1	1.847412	13.834129	6.875311
6	0.851117	13.840943	8.772254
1	0.329320	17.806545	6.441716
6	0.623068	19.936659	6.397414
6	2.916205	20.700638	6.564327
1	4.415075	19.157536	6.709989
6	7.575374	16.720655	1.079443

6	6.736297	14.511600	1.680006
6	6.179848	19.007198	4.287624
6	8.520748	18.493452	3.869477
6	2.991117	14.896293	1.135401
6	3.602689	13.379192	2.945244
6	4.300877	17.886813	1.647929
6	2.571567	18.597622	3.204229
6	9.248259	12.099899	8.894766
1	7.687943	12.525714	10.325116
1	10.676526	11.900217	7.286310
1	8.568166	20.309911	8.181560
6	10.363391	19.255919	7.615187
1	11.972098	17.943612	7.015054
1	0.652846	16.496138	10.899303
6	0.521584	14.578666	9.912840
1	0.562584	12.796512	8.694554
6	1.553229	20.982835	6.448168
1	-0.439420	20.153079	6.326957
1	3.635975	21.512314	6.629805
1	7.820902	17.741822	1.354840
6	7.755178	16.286618	-0.234952
1	6.328943	13.819846	2.412137
6	6.918888	14.088636	0.364621
6	6.515973	20.345440	4.486656
1	5.150374	18.692014	4.392590
1	9.308723	17.780132	3.643967
6	8.849142	19.832429	4.073979
1	2.813129	15.900035	0.764001
6	2.808414	13.799613	0.289665
6	3.411198	12.293254	2.093033
1	3.900546	13.204070	3.978992
1	4.982814	17.131320	1.275448
6	4.226184	19.120079	1.005277
6	2.505126	19.831633	2.555038
1	1.921294	18.410299	4.048445
1	9.647204	11.261294	9.458761
1	11.023650	20.083866	7.859113
1	-0.029639	14.109035	10.722869
1	1.211256	22.013824	6.414670
1	8.153746	16.971356	-0.978325
6	7.426863	14.974719	-0.592492
1	6.665165	13.069688	0.087227
1	5.736404	21.062427	4.727812
6	7.847105	20.758844	4.380281
1	9.885316	20.149267	4.003470
6	3.021247	12.502697	0.764008
1	2.492408	13.960995	-0.737103
1	3.560989	11.284280	2.467214
1	4.857344	19.315857	0.142992
6	3.335060	20.097553	1.463119
1	1.798968	20.579601	2.903306

S71

1	7.569725	14.641152	-1.616667
1	8.106611	21.801654	4.541188
1	2.872931	11.652874	0.103211
1	3.278823	21.058772	0.959537
1	5.348138	14.722750	4.441615

Table S11. Cartesian coordinates for the optimized geometry of **1b**.

Atomic Number	X	Y	Z
6	-0.892825	1.537961	4.406163
6	-0.601241	0.192775	4.187922
6	-0.113868	-0.210487	2.947070
7	0.037357	0.686038	1.931076
6	-0.139919	2.013555	2.167913
6	-0.630606	2.459212	3.395242
6	0.321710	2.992426	1.120587
6	0.362026	-1.615473	2.701236
77	0.499946	-0.024918	-0.065698
17	2.870910	0.095053	0.777135
15	0.423038	2.253454	-0.586459
6	1.776853	3.083249	-1.439917
6	2.863815	2.336202	-1.914362
6	3.908699	2.982745	-2.579095
6	3.872587	4.366896	-2.764879
6	2.788924	5.114800	-2.288105
6	1.738967	4.476952	-1.629257
6	-1.119261	2.733613	-1.411398
6	-1.132017	3.145943	-2.750991
6	-2.348354	3.425665	-3.380722
6	-3.549318	3.297352	-2.678750
6	-3.538509	2.882098	-1.341636
6	-2.329088	2.594324	-0.710810
15	0.058501	-2.102366	0.940011
6	1.046892	-3.572468	0.577349
6	0.470932	-4.854497	0.605262
6	1.257161	-5.972160	0.320356
6	2.610504	-5.816367	0.005482
6	3.180695	-4.539509	-0.029541
6	2.404839	-3.414031	0.250102
6	-1.689264	-2.580111	0.824838
6	-2.353263	-2.413663	-0.400850
6	-3.681478	-2.816655	-0.539601
6	-4.360206	-3.379805	0.546253
6	-3.705485	-3.545878	1.769763
6	-2.371836	-3.153243	1.909007
6	0.852073	-0.655105	-1.777970
8	1.065373	-1.051887	-2.837541
1	-1.285595	1.868320	5.363749
1	-0.730458	-0.545110	4.972833
1	-0.783587	3.522231	3.550845
1	-0.282525	3.904512	1.126607
1	1.357456	3.266090	1.366412

1	1.459356	-1.609432	2.779495
1	-0.039888	-2.321270	3.432151
1	-1.045913	-0.002281	-0.401481
1	2.906482	1.267274	-1.736453
1	4.752420	2.403795	-2.944240
1	4.688671	4.866624	-3.280207
1	2.761210	6.191333	-2.433750
1	0.889985	5.057822	-1.276514
1	-0.199695	3.252193	-3.297779
1	-2.354237	3.746116	-4.419069
1	-4.492721	3.519664	-3.170190
1	-4.471675	2.780981	-0.793717
1	-2.329522	2.252312	0.321849
1	-0.582801	-4.979191	0.836471
1	0.810493	-6.962666	0.339465
1	3.218432	-6.688913	-0.219118
1	4.230651	-4.416570	-0.281331
1	2.846142	-2.421714	0.218062
1	-1.833657	-1.959801	-1.239544
1	-4.187451	-2.686796	-1.492485
1	-5.396910	-3.687695	0.439144
1	-4.229332	-3.983837	2.615207
1	-1.871667	-3.303478	2.861455

Table S12. Cartesian coordinates for the optimized geometry of *cis*-**1c**.

Atomic Number	X	Y	Z
6	-2.549113	-0.073643	2.237966
6	-1.345668	-0.802528	2.834812
7	-0.084263	-0.133873	2.375117
77	-0.017744	0.040035	0.159595
6	1.150130	-0.786789	2.922088
6	2.389507	-0.065615	2.389277
6	0.050066	0.289097	-1.675892
1	-0.067604	1.612186	0.375670
17	0.057055	-2.456674	0.160946
8	0.101525	0.459625	-2.814063
1	-0.101524	0.822460	2.731699
15	-2.367120	0.039070	0.381183
6	-3.195233	1.585873	-0.094608
6	-4.301119	1.594468	-0.957304
6	-4.894904	2.808062	-1.317002
6	-4.395417	4.012013	-0.816020
6	-3.290063	4.007203	0.043423
6	-2.687570	2.800936	0.395855
6	-3.308804	-1.314918	-0.355027
6	-2.812041	-1.953848	-1.500011
6	-3.564998	-2.950269	-2.122897
6	-4.809833	-3.316667	-1.603963
6	-5.309331	-2.681543	-0.461854
6	-4.564433	-1.679163	0.160186
15	2.309752	0.086340	0.529005

6	3.197091	1.608974	0.102332
6	4.584812	1.676926	0.323756
6	5.282089	2.845925	0.021673
6	4.604669	3.948086	-0.513477
6	3.228827	3.879687	-0.745605
6	2.523265	2.713283	-0.437305
6	3.281902	-1.263701	-0.172428
6	3.511836	-2.450587	0.537166
6	4.206067	-3.499754	-0.067253
6	4.659611	-3.373860	-1.382939
6	4.421110	-2.194875	-2.097419
6	3.733473	-1.140987	-1.496841
1	-2.609364	0.955439	2.612981
1	-3.479838	-0.582959	2.503812
1	-1.381204	-0.792686	3.931662
1	-1.292565	-1.834578	2.478811
1	1.117308	-0.757282	4.018646
1	1.118634	-1.824466	2.582624
1	2.439416	0.959291	2.776739
1	3.304433	-0.584337	2.692237
1	-4.696213	0.661837	-1.347796
1	-5.748910	2.808546	-1.988953
1	-4.860630	4.953190	-1.096541
1	-2.895088	4.942933	0.430288
1	-1.809913	2.804713	1.038524
1	-1.832202	-1.694994	-1.884330
1	-3.172362	-3.447539	-3.005419
1	-5.390561	-4.098575	-2.086186
1	-6.278126	-2.963194	-0.058200
1	-4.972557	-1.176979	1.033655
1	5.118749	0.814554	0.715362
1	6.353687	2.895194	0.195324
1	5.152097	4.855244	-0.755400
1	2.703997	4.730199	-1.172439
1	1.455176	2.656846	-0.620743
1	3.145381	-2.568269	1.551998
1	4.384746	-4.416938	0.487185
1	5.196859	-4.193582	-1.852346
1	4.772999	-2.094960	-3.120614
1	3.557712	-0.223400	-2.053009

Table S13. Cartesian coordinates for the optimized geometry of *trans*-**1c**.

Atomic Number	X	Y	Z
6	-1.165347	1.116744	2.859330
6	-2.295205	0.671304	1.928237
7	-1.843731	-0.517257	1.140791
77	0.115353	-0.225233	0.174206
6	-2.887540	-1.044026	0.208224
6	-2.333545	-2.265703	-0.528156
6	1.765284	0.025576	-0.643779
17	0.779523	-2.045220	1.766062

1	-0.549933	0.897161	-0.719771
8	2.782897	0.189256	-1.156885
1	-1.616399	-1.264571	1.808127
15	0.362808	1.423165	1.844312
6	1.782676	1.382966	2.962447
6	2.825542	2.310438	2.792245
6	3.960238	2.238194	3.601033
6	4.061725	1.245870	4.580602
6	3.028427	0.318760	4.747368
6	1.893237	0.377977	3.938777
6	0.223299	3.137232	1.258671
6	0.411316	3.458988	-0.092287
6	0.338573	4.789418	-0.513614
6	0.074150	5.802954	0.410632
6	-0.108459	5.488550	1.762407
6	-0.027581	4.162914	2.187417
15	-0.744569	-1.789904	-1.369624
6	0.161268	-3.312222	-1.729886
6	0.266427	-4.324949	-0.760976
6	1.025683	-5.464211	-1.028406
6	1.693197	-5.595561	-2.249987
6	1.601364	-4.583434	-3.210046
6	0.838408	-3.443344	-2.955006
6	-1.233381	-1.094221	-2.975094
6	-2.096398	-1.827486	-3.808762
6	-2.460288	-1.323534	-5.057012
6	-1.955246	-0.091627	-5.489244
6	-1.085487	0.633537	-4.671255
6	-0.726166	0.135535	-3.415984
1	-0.928318	0.323093	3.576149
1	-1.445731	2.016253	3.415289
1	-2.548503	1.457784	1.210203
1	-3.195310	0.409653	2.498820
1	-3.788407	-1.303224	0.778716
1	-3.132025	-0.238584	-0.491610
1	-3.056029	-2.647158	-1.255674
1	-2.099910	-3.064839	0.183625
1	2.749678	3.088900	2.038557
1	4.762189	2.959148	3.467193
1	4.945460	1.193233	5.210933
1	3.108095	-0.458522	5.502415
1	1.117078	-0.370854	4.050755
1	0.614521	2.670844	-0.809376
1	0.489799	5.032479	-1.561967
1	0.014658	6.837042	0.081742
1	-0.306637	6.275984	2.484573
1	-0.144263	3.930719	3.243315
1	-0.213741	-4.216680	0.205182
1	1.101799	-6.245529	-0.277167
1	2.285971	-6.483734	-2.452074
1	2.120387	-4.681204	-4.159711

S75

1	0.764782	-2.664437	-3.708425
1	-2.472504	-2.797422	-3.492198
1	-3.131004	-1.893133	-5.694628
1	-2.236930	0.297831	-6.463935
1	-0.685064	1.585714	-5.008907
1	-0.052879	0.698726	-2.778626

Table S14. Cartesian coordinates for the optimized geometry of **1e**.

Atomic Number	X	Y	Z
77	-1.001168	1.021618	-0.140407
1	-0.958169	0.860049	1.416847
15	-2.561017	-0.737908	-0.205298
17	-0.990229	1.080374	-2.715560
15	0.838902	2.458191	-0.002480
6	0.574513	-0.507382	-0.260443
6	-2.323817	2.362748	-0.033049
6	-1.627405	-2.221802	-0.795576
6	-3.996017	-0.579704	-1.307508
6	-3.259140	-1.171693	1.419577
6	0.629654	4.181747	-0.538986
6	1.650236	2.516017	1.626729
6	2.077282	1.700173	-1.148131
15	0.059629	-2.114941	-0.063045
15	2.155593	-0.094512	-0.759421
8	-3.128575	3.184306	0.049493
1	-2.131467	-3.165311	-0.568872
1	-1.522051	-2.101332	-1.878112
6	-5.244938	-0.221162	-0.772700
6	-3.850453	-0.728565	-2.696551
6	-3.372661	-0.180376	2.404005
6	-3.754860	-2.457963	1.678044
6	1.194427	5.252727	0.172347
6	-0.140384	4.431303	-1.688514
6	3.030460	2.744755	1.738487
6	0.885392	2.363844	2.791728
1	3.065020	2.168047	-1.119175
1	1.640824	1.798552	-2.147796
6	1.092634	-3.387316	-0.832171
6	-0.211145	-2.657653	1.658230
6	2.805375	-0.906431	-2.259655
6	3.484068	-0.247155	0.484603
1	-5.369572	-0.103943	0.299816
6	-6.335801	-0.020989	-1.620138
1	-2.882615	-0.959118	-3.127385
6	-4.947992	-0.533655	-3.535572
1	-2.990572	0.815903	2.208942
6	-3.965623	-0.473061	3.633525
1	-3.697997	-3.233137	0.919274
6	-4.329459	-2.754182	2.914019
6	0.995106	6.562913	-0.269258
1	1.777371	5.069713	1.069690

1	-0.591525	3.606021	-2.233250
6	-0.327810	5.743022	-2.124379
1	3.639868	2.877323	0.850808
6	3.638759	2.790824	2.992845
6	1.493548	2.418464	4.047110
1	-0.185000	2.201136	2.713926
6	2.092588	-4.025175	-0.081694
6	0.949605	-3.680833	-2.197081
6	-0.200721	-1.704494	2.683277
6	-0.515768	-3.995972	1.951491
6	3.910028	-1.768625	-2.224545
6	2.141328	-0.670719	-3.475534
6	3.189040	-0.774083	1.745262
6	4.783271	0.211199	0.209415
6	-6.190304	-0.179551	-3.001147
1	-7.298998	0.254887	-1.199051
1	-4.827830	-0.648883	-4.609508
1	-4.054832	0.304568	4.387730
6	-4.437453	-1.761927	3.893361
1	-4.697477	-3.757748	3.110127
1	1.429322	7.389303	0.287534
6	0.237580	6.809572	-1.417413
1	-0.924159	5.931073	-3.013363
6	2.872082	2.624549	4.149592
1	4.710600	2.952291	3.064632
1	0.890634	2.301196	4.944051
1	2.207365	-3.800739	0.974730
6	2.933584	-4.957876	-0.691368
1	0.197460	-3.173228	-2.793418
6	1.787970	-4.617590	-2.798732
6	-0.498755	-2.084259	3.993285
1	0.028496	-0.670676	2.442898
1	-0.517834	-4.742240	1.160443
6	-0.804334	-4.374258	3.262555
1	4.417806	-1.971670	-1.287932
6	4.355249	-2.379717	-3.398778
6	2.598983	-1.275994	-4.645586
1	1.261415	-0.031932	-3.501759
1	2.179904	-1.109820	1.957106
6	4.179197	-0.842560	2.728205
6	5.770155	0.146846	1.192528
1	5.024977	0.612634	-0.771931
1	-7.041599	-0.025446	-3.659139
1	-4.891056	-1.993372	4.853645
1	0.082492	7.830524	-1.756853
1	3.347160	2.659479	5.126624
1	3.705407	-5.451199	-0.106434
6	2.777604	-5.258828	-2.046761
1	1.673986	-4.841296	-3.855489
1	-0.500073	-1.339298	4.784672
6	-0.800712	-3.416969	4.283436

S77

1	-1.032888	-5.412450	3.489242
6	3.707913	-2.128729	-4.610386
1	5.208138	-3.052452	-3.363495
1	2.088684	-1.080436	-5.585335
1	3.940445	-1.248225	3.707949
6	5.468317	-0.380499	2.454032
1	6.773801	0.504185	0.976396
1	3.428844	-5.989500	-2.519336
1	-1.032567	-3.712198	5.303546
1	4.062415	-2.599162	-5.524166
1	6.238732	-0.428559	3.219441

Table S15. Cartesian coordinates for the optimized geometry of **1e**[1].

Atomic Number	X	Y	Z
77	-0.989676	1.166457	-0.162721
1	-1.212891	1.698408	1.296679
15	-2.669585	-0.414972	0.217252
17	-0.578988	0.188096	-2.517351
15	0.969802	2.421400	-0.348820
14	0.443154	-0.499094	1.075712
6	-2.148736	2.577537	-0.828839
6	-2.112765	-2.036663	-0.476697
6	-4.264302	-0.137078	-0.617168
6	-3.060811	-0.714249	1.969067
6	0.878688	3.875343	-1.438098
6	1.750874	2.987629	1.197820
6	2.275099	1.352614	-1.117370
15	-0.393377	-2.470170	0.055985
15	2.457916	-0.184001	-0.105486
8	-2.822597	3.445566	-1.164833
1	-2.810376	-2.853572	-0.266378
1	-2.092346	-1.852365	-1.553187
6	-4.242778	0.302012	-1.951815
6	-5.489594	-0.351565	0.031426
6	-3.341243	-1.996526	2.463907
6	-3.132100	0.387692	2.836455
6	1.014221	5.180282	-0.942006
6	0.564442	3.669947	-2.792942
6	3.039535	3.547879	1.148490
6	1.111921	2.847478	2.435318
1	3.232933	1.873283	-1.219885
1	1.892300	1.067347	-2.100931
6	0.308420	-3.477721	-1.301154
6	-0.656328	-3.722634	1.371804
6	3.213943	-1.422914	-1.203521
6	3.785489	0.241953	1.080493
1	-3.292765	0.478662	-2.450312
6	-5.442456	0.514721	-2.630779
1	-5.510891	-0.682227	1.065783
6	-6.686720	-0.127163	-0.653826

1	-3.295779	-2.864317	1.815643
6	-3.665684	-2.176163	3.810517
1	-2.921466	1.383954	2.458458
6	-3.468791	0.207629	4.177609
6	0.850592	6.271628	-1.799482
1	1.243468	5.346499	0.106167
1	0.413375	2.662619	-3.172306
6	0.411301	4.764873	-3.643015
1	3.546252	3.668836	0.194998
6	3.676472	3.953411	2.318784
6	1.749118	3.261393	3.608102
1	0.123102	2.405420	2.482038
6	-0.111494	-3.352076	-2.633477
6	1.281486	-4.436466	-0.969809
6	-0.195835	-3.524727	2.678078
6	-1.373417	-4.891184	1.057823
6	4.236101	-2.256783	-0.719734
6	2.775895	-1.551643	-2.531257
6	3.580581	0.183447	2.463115
6	5.033757	0.652058	0.579225
6	-6.664761	0.302984	-1.983179
1	-5.422810	0.855165	-3.662807
1	-7.634775	-0.286029	-0.146468
1	-3.865057	-3.176762	4.184280
6	-3.730137	-1.076247	4.668853
1	-3.524894	1.067652	4.839881
1	0.954191	7.281000	-1.409819
6	0.554572	6.066348	-3.149189
1	0.170772	4.601656	-4.690350
6	3.030692	3.811154	3.552022
1	4.675941	4.376660	2.270245
1	1.243600	3.148194	4.563582
1	-0.814766	-2.580947	-2.925993
6	0.396909	-4.212391	-3.608351
1	1.614771	-4.545067	0.058624
6	1.799263	-5.277825	-1.952961
6	-0.455933	-4.480538	3.665349
1	0.346319	-2.614858	2.924355
1	-1.712529	-5.066497	0.039535
6	-1.642123	-5.835771	2.046793
1	4.578407	-2.164272	0.306589
6	4.839592	-3.183673	-1.570746
6	3.394682	-2.471680	-3.376225
1	1.950371	-0.949037	-2.899184
1	2.613591	-0.127284	2.851074
6	4.611598	0.537944	3.338200
6	6.059430	1.002556	1.454529
1	5.208063	0.683699	-0.493504
1	-7.597733	0.478899	-2.512459
1	-3.984165	-1.216861	5.716333
1	0.429041	6.917173	-3.813803

1	3.528829	4.127270	4.464968
1	0.049958	-4.119407	-4.634234
6	1.346147	-5.179565	-3.271411
1	2.549879	-6.016401	-1.685255
1	-0.094626	-4.319627	4.677781
6	-1.183713	-5.630452	3.354643
1	-2.201177	-6.734223	1.798285
6	4.429184	-3.283345	-2.902222
1	5.637601	-3.818339	-1.194123
1	3.059117	-2.560429	-4.405285
1	4.443267	0.496078	4.411040
6	5.848731	0.946222	2.837608
1	7.022791	1.315560	1.060254
1	1.738546	-5.847863	-4.033484
1	-1.391043	-6.369612	4.124314
1	4.907908	-3.997350	-3.567251
1	6.649347	1.220100	3.520025

Table S16. Cartesian coordinates for the optimized geometry of **1e**^{2}.

Atomic Number	X	Y	Z
77	-0.910265	1.254765	-0.193614
1	-1.192411	1.864345	1.227179
15	-2.631483	-0.291464	0.106314
17	-0.415327	0.217800	-2.504621
15	1.091228	2.454241	-0.303608
32	0.527905	-0.438384	1.208833
6	-2.027708	2.634465	-0.966622
6	-2.103198	-1.938106	-0.567184
6	-4.173289	0.070897	-0.789057
6	-3.110465	-0.685294	1.821063
6	1.049512	3.967419	-1.312420
6	1.910564	2.887369	1.266732
6	2.360411	1.405194	-1.151557
15	-0.545297	-2.468452	0.275311
15	2.509157	-0.223418	-0.287149
8	-2.707344	3.469561	-1.368089
1	-2.886588	-2.695341	-0.456771
1	-1.882546	-1.779693	-1.625805
6	-5.370200	0.366886	-0.121288
6	-4.115738	0.147922	-2.191684
6	-2.578865	0.020610	2.906679
6	-3.999800	-1.747205	2.061750
6	1.353091	5.232123	-0.789869
6	0.622690	3.842617	-2.646363
6	3.239870	3.345406	1.250199
6	1.255628	2.732839	2.494657
1	3.334257	1.901377	-1.208671
1	1.965877	1.238817	-2.155162
6	0.255315	-3.667342	-0.836245
6	-1.139635	-3.478717	1.680061

6	3.087599	-1.421976	-1.533223
6	3.975692	0.014003	0.786732
1	-5.417312	0.323532	0.962635
6	-6.506108	0.723434	-0.853549
1	-3.178244	-0.036156	-2.710669
6	-5.256194	0.496010	-2.914749
1	-1.889677	0.837834	2.726418
6	-2.927782	-0.327423	4.214257
1	-4.425356	-2.301533	1.229957
6	-4.343953	-2.096391	3.365407
6	1.241581	6.364804	-1.601771
1	1.669635	5.335730	0.243626
1	0.348399	2.867022	-3.042229
6	0.524174	4.976295	-3.451902
1	3.761797	3.476298	0.306576
6	3.900912	3.634656	2.441823
6	1.918353	3.026115	3.689509
1	0.230921	2.378209	2.512004
6	0.828691	-4.836147	-0.306480
6	0.318601	-3.422680	-2.217220
6	-0.774901	-3.186147	2.999042
6	-1.984847	-4.572286	1.420663
6	3.761377	-2.566066	-1.071435
6	2.910182	-1.231884	-2.911249
6	3.880964	-0.049949	2.181707
6	5.213215	0.310424	0.188185
6	-6.452696	0.783382	-2.248154
1	-7.430906	0.955077	-0.331508
1	-5.208176	0.552352	-3.999149
1	-2.509995	0.228495	5.049604
6	-3.807074	-1.386305	4.445095
1	-5.026064	-2.923766	3.540089
1	1.472871	7.344574	-1.191908
6	0.833282	6.238471	-2.931615
1	0.195570	4.876269	-4.483104
6	3.240676	3.473346	3.664906
1	4.930770	3.979902	2.417157
1	1.400682	2.902625	4.637205
1	0.786920	-5.031390	0.760863
6	1.425347	-5.766955	-1.157709
1	-0.077277	-2.499593	-2.630400
6	0.907398	-4.364899	-3.059791
6	-1.258613	-3.971557	4.049681
1	-0.122134	-2.342413	3.206738
1	-2.257478	-4.820515	0.397828
6	-2.463395	-5.354061	2.469850
1	3.904504	-2.723000	-0.005233
6	4.278399	-3.487801	-1.979740
6	3.447697	-2.150416	-3.815042
1	2.345273	-0.387372	-3.288918
1	2.927057	-0.274232	2.651650

6	5.008870	0.190170	2.972057
6	6.334623	0.552870	0.979326
1	5.301214	0.340547	-0.895376
1	-7.337981	1.060069	-2.814785
1	-4.074919	-1.660896	5.462119
1	0.748229	7.121078	-3.560205
1	3.757831	3.696410	4.594605
1	1.856370	-6.674536	-0.742940
6	1.455612	-5.538661	-2.535700
1	0.944442	-4.175015	-4.128607
1	-0.975714	-3.734067	5.071759
6	-2.101098	-5.053001	3.788323
1	-3.114115	-6.199258	2.260742
6	4.135798	-3.274395	-3.353996
1	4.799389	-4.368207	-1.613584
1	3.320718	-1.985863	-4.881923
1	4.925720	0.142219	4.054634
6	6.233091	0.494349	2.374901
1	7.288117	0.780774	0.509738
1	1.911310	-6.269530	-3.198636
1	-2.474830	-5.663023	4.606759
1	4.551996	-3.986980	-4.061269
1	7.108936	0.681527	2.991005

Table S17. Cartesian coordinates for the optimized geometry of *cis*-**1f**.

Atomic Number	X	Y	Z
77	0.356271	-1.481411	-0.014788
1	0.430695	-1.595966	1.545580
15	2.563508	-0.759932	-0.007323
17	0.230896	-0.989052	-2.549469
15	-1.941880	-1.821519	0.123778
5	-0.198200	0.715048	0.292445
6	0.818427	-3.352127	-0.203569
6	2.620150	0.848681	-0.915231
6	3.740746	-1.850992	-0.854290
6	3.305771	-0.342299	1.604330
6	-2.574765	-3.393578	-0.540396
6	-2.734960	-1.590355	1.749884
6	-2.720353	-0.523460	-0.939445
15	1.265592	1.906173	-0.266735
15	-1.973365	1.088658	-0.460972
8	1.099969	-4.464827	-0.280599
1	3.599787	1.334205	-0.896585
1	2.339594	0.631528	-1.950188
6	4.445408	-2.818394	-0.119348
6	3.827364	-1.842705	-2.255297
6	2.484793	-0.083635	2.709398
6	4.693523	-0.153013	1.715501
6	-3.416863	-4.239873	0.195253
6	-2.136524	-3.778833	-1.819924
6	-4.117991	-1.350703	1.824697

6	-1.989796	-1.662436	2.933043
1	-3.812517	-0.494479	-0.896005
1	-2.386798	-0.768231	-1.950702
6	1.073747	3.172758	-1.564696
6	1.896630	2.797884	1.189022
6	-2.179546	2.185477	-1.899970
6	-3.137881	1.760624	0.780832
1	4.367833	-2.843929	0.963958
6	5.247389	-3.750442	-0.779052
1	3.245188	-1.136816	-2.838898
6	4.634167	-2.776236	-2.908483
1	1.411086	-0.204496	2.616156
6	3.042786	0.355030	3.911767
1	5.338939	-0.351489	0.864117
6	5.249272	0.275400	2.921187
6	-3.826225	-5.459876	-0.350463
1	-3.745983	-3.956350	1.190185
1	-1.455522	-3.140006	-2.377856
6	-2.558719	-4.992801	-2.360498
1	-4.716391	-1.304968	0.919488
6	-4.738147	-1.170185	3.059688
6	-2.612285	-1.485032	4.171104
1	-0.923409	-1.855639	2.883215
6	1.169621	4.539310	-1.262982
6	0.880363	2.759761	-2.893585
6	0.976787	3.268684	2.138515
6	3.259352	3.085131	1.349025
6	-2.237130	3.571686	-1.680152
6	-2.295474	1.685725	-3.204669
6	-2.817791	1.828372	2.142354
6	-4.420159	2.150136	0.353876
6	5.347373	-3.727691	-2.173513
1	5.791339	-4.494874	-0.203565
1	4.698382	-2.763651	-3.993324
1	2.397277	0.561524	4.761414
6	4.423814	0.531439	4.021287
1	6.325023	0.409011	3.002008
1	-4.473358	-6.116145	0.225768
6	-3.402725	-5.835220	-1.627548
1	-2.218471	-5.287138	-3.349949
6	-3.985042	-1.235033	4.236505
1	-5.806496	-0.976708	3.103375
1	-2.024067	-1.545671	5.083273
1	1.323550	4.865413	-0.238995
6	1.089242	5.485550	-2.287455
1	0.778896	1.703445	-3.131209
6	0.807608	3.711238	-3.909062
6	1.417014	4.004928	3.239497
1	-0.080808	3.052312	2.022186
1	3.987775	2.740064	0.623468
6	3.698499	3.806619	2.459282

1	-2.147924	3.969536	-0.672990
6	-2.430179	4.442569	-2.750353
6	-2.504162	2.562827	-4.271074
1	-2.202757	0.624167	-3.404148
1	-1.845364	1.501181	2.489838
6	-3.763085	2.284624	3.064177
6	-5.362813	2.599903	1.277244
1	-4.677386	2.113184	-0.701551
1	5.973219	-4.453763	-2.685759
1	4.857628	0.867484	4.959617
1	-3.721745	-6.785138	-2.048724
1	-4.468432	-1.093753	5.199853
1	1.173200	6.542879	-2.049867
6	0.916057	5.073249	-3.610065
1	0.661065	3.387446	-4.935584
1	0.696649	4.367736	3.968170
6	2.779513	4.268339	3.405748
1	4.759112	4.006493	2.584161
6	-2.576762	3.938764	-4.046218
1	-2.469985	5.513395	-2.571849
1	-2.604471	2.166157	-5.277898
1	-3.505794	2.326272	4.119114
6	-5.034241	2.670824	2.635631
1	-6.350493	2.899961	0.936854
1	0.862596	5.810264	-4.407238
1	3.124411	4.831438	4.269065
1	-2.738970	4.618897	-4.878337
1	-5.768587	3.024660	3.354727
1	-0.300285	0.973846	1.461552

Table S18. Cartesian coordinates for the optimized geometry of **1f**[1].

Atomic Number	X	Y	Z
77	-0.885806	1.278288	-0.203946
1	-1.128114	1.878129	1.227788
15	-2.612965	-0.248602	0.129384
17	-0.373682	0.163025	-2.469564
15	1.132687	2.432652	-0.331431
13	0.520772	-0.468063	0.929063
6	-2.013856	2.703808	-0.964279
6	-2.162956	-1.928930	-0.539944
6	-4.155595	0.141033	-0.759078
6	-3.098080	-0.625257	1.847908
6	1.087688	3.949511	-1.339735
6	1.982914	2.865586	1.223903
6	2.413723	1.405240	-1.205883
15	-0.634852	-2.554746	0.293044
15	2.630226	-0.216146	-0.343189
8	-2.688958	3.565060	-1.311545
1	-2.986846	-2.639253	-0.419791
1	-1.944120	-1.791243	-1.601931
6	-5.341351	0.475817	-0.090468

6	-4.101773	0.204315	-2.162509
6	-2.527911	0.055063	2.929984
6	-4.033791	-1.645402	2.095393
6	1.360790	5.219489	-0.814112
6	0.673436	3.818749	-2.677044
6	3.288377	3.387513	1.179198
6	1.378747	2.641695	2.466445
1	3.370307	1.931624	-1.274116
1	2.012305	1.230183	-2.205191
6	0.116819	-3.770965	-0.838583
6	-1.250276	-3.520168	1.711041
6	3.172226	-1.430047	-1.592625
6	4.094208	0.039675	0.717183
1	-5.385636	0.444839	0.993987
6	-6.469931	0.857068	-0.822030
1	-3.171267	-0.008959	-2.683192
6	-5.234842	0.576379	-2.885242
1	-1.801116	0.837915	2.744274
6	-2.885075	-0.274976	4.240118
1	-4.490310	-2.179307	1.266666
6	-4.385701	-1.977595	3.401352
6	1.233025	6.350889	-1.625753
1	1.665447	5.328995	0.222315
1	0.418083	2.838927	-3.075326
6	0.558932	4.950727	-3.482845
1	3.770127	3.572369	0.223195
6	3.974071	3.673131	2.357306
6	2.066082	2.931484	3.648424
1	0.375382	2.232069	2.504335
6	0.638555	-4.972063	-0.329579
6	0.225272	-3.488487	-2.209674
6	-0.870401	-3.191844	3.018157
6	-2.125754	-4.597247	1.487450
6	3.812457	-2.591875	-1.127138
6	2.972038	-1.254111	-2.968673
6	3.978748	0.005790	2.112521
6	5.338676	0.316391	0.124775
6	-6.420624	0.902574	-2.217232
1	-7.385770	1.119508	-0.298700
1	-5.189380	0.621396	-3.970322
1	-2.437037	0.261814	5.072321
6	-3.811284	-1.291504	4.477342
1	-5.103875	-2.772854	3.580913
1	1.440505	7.334638	-1.212612
6	0.838686	6.218343	-2.959086
1	0.240423	4.845283	-4.516712
6	3.363096	3.444529	3.595529
1	4.985176	4.068227	2.310994
1	1.587271	2.753230	4.607773
1	0.560250	-5.198054	0.729738
6	1.239280	-5.891475	-1.191468

1	-0.136431	-2.544875	-2.607580
6	0.818499	-4.418426	-3.063306
6	-1.368267	-3.931757	4.094635
1	-0.198692	-2.356423	3.193142
1	-2.412296	-4.866867	0.473823
6	-2.617030	-5.333060	2.563916
1	3.975176	-2.737786	-0.061772
6	4.265752	-3.551518	-2.030634
6	3.441759	-2.213514	-3.868734
1	2.440017	-0.389189	-3.348125
1	3.017352	-0.201915	2.572919
6	5.098913	0.255760	2.910420
6	6.451824	0.566939	0.925320
1	5.437630	0.325070	-0.958263
1	-7.300104	1.198427	-2.783214
1	-4.086190	-1.552180	5.496155
1	0.741083	7.099800	-3.587446
1	3.899740	3.665768	4.514566
1	1.632403	-6.823061	-0.792548
6	1.322648	-5.620408	-2.559432
1	0.892437	-4.197013	-4.124070
1	-1.075860	-3.669162	5.107773
6	-2.238249	-4.999956	3.870133
1	-3.291142	-6.166960	2.385970
6	4.091040	-3.358853	-3.404337
1	4.760072	-4.445980	-1.661516
1	3.293623	-2.062758	-4.934916
1	5.003121	0.232747	3.992666
6	6.332245	0.537573	2.320501
1	7.412820	0.779092	0.463777
1	1.783047	-6.341321	-3.230025
1	-2.622323	-5.574762	4.709001
1	4.453857	-4.103015	-4.108481
1	7.202232	0.731050	2.942889
1	0.937617	-0.674579	2.450416

Table S19. Cartesian coordinates for the optimized geometry of **1f²**.

Atomic Number	X	Y	Z
77	-0.890465	1.286113	-0.209618
1	-1.142324	1.894755	1.216269
15	-2.619603	-0.244340	0.122156
17	-0.382856	0.181438	-2.479883
15	1.136453	2.435407	-0.331070
31	0.516703	-0.469527	0.957728
6	-1.993625	2.685273	-0.978671
6	-2.153071	-1.919839	-0.543607
6	-4.160846	0.140639	-0.766497
6	-3.093650	-0.618761	1.842796
6	1.104048	3.947094	-1.344324
6	1.974122	2.862755	1.230956

6	2.409706	1.389045	-1.191155
15	-0.628858	-2.550304	0.291976
15	2.619560	-0.232963	-0.328241
8	-2.661915	3.537293	-1.363091
1	-2.976290	-2.631349	-0.425272
1	-1.931922	-1.782143	-1.605039
6	-5.343582	0.485690	-0.097461
6	-4.109882	0.192079	-2.170527
6	-2.496458	0.043397	2.921409
6	-4.041530	-1.626197	2.095095
6	1.370527	5.218315	-0.817826
6	0.704632	3.813400	-2.685883
6	3.276273	3.392995	1.196117
6	1.366715	2.620609	2.468296
1	3.369800	1.909785	-1.255278
1	2.012245	1.215119	-2.192232
6	0.116796	-3.764450	-0.842857
6	-1.253153	-3.517570	1.704426
6	3.164187	-1.442579	-1.578404
6	4.082426	0.023377	0.733398
1	-5.384904	0.463975	0.987334
6	-6.472536	0.864569	-0.829414
1	-3.181374	-0.028477	-2.691677
6	-5.243401	0.562562	-2.893384
1	-1.755896	0.811796	2.730834
6	-2.842005	-0.289705	4.233628
1	-4.516222	-2.147575	1.268471
6	-4.381564	-1.961678	3.403506
6	1.251965	6.347907	-1.633131
1	1.663182	5.329825	0.221813
1	0.453508	2.832927	-3.085060
6	0.598644	4.943940	-3.494877
1	3.760430	3.589611	0.243599
6	3.955343	3.671374	2.379984
6	2.047313	2.903175	3.655646
1	0.367488	2.200636	2.497140
6	0.629027	-4.972069	-0.339335
6	0.232339	-3.474373	-2.211879
6	-0.872120	-3.197151	3.012767
6	-2.133791	-4.589683	1.476708
6	3.798571	-2.607513	-1.112281
6	2.971799	-1.263507	-2.955298
6	3.962068	0.008536	2.128283
6	5.331584	0.282654	0.142680
6	-6.426333	0.898256	-2.225133
1	-7.386240	1.134426	-0.306164
1	-5.200384	0.598812	-3.978862
1	-2.373484	0.232902	5.063598
6	-3.782412	-1.291979	4.476162
1	-5.109645	-2.746884	3.587328
1	1.454880	7.332487	-1.219751

S87

6	0.872610	6.212530	-2.970581
1	0.291312	4.836422	-4.531883
6	3.340793	3.426429	3.613134
1	4.964104	4.073261	2.341820
1	1.566360	2.711472	4.611357
1	0.546587	-5.203283	0.718523
6	1.225264	-5.890846	-1.204852
1	-0.120406	-2.525312	-2.605019
6	0.820630	-4.403841	-3.069194
6	-1.372658	-3.939355	4.086346
1	-0.196574	-2.365947	3.190955
1	-2.421326	-4.853962	0.461974
6	-2.628511	-5.327830	2.550032
1	3.952894	-2.757100	-0.046200
6	4.255761	-3.565416	-2.015407
6	3.445420	-2.221246	-3.854972
1	2.443224	-0.397065	-3.336131
1	2.997772	-0.185730	2.587312
6	5.080914	0.259183	2.927611
6	6.443806	0.534273	0.944313
1	5.434713	0.276622	-0.939946
1	-7.306186	1.192399	-2.791414
1	-4.048386	-1.554965	5.496740
1	0.782110	7.092701	-3.601791
1	3.872066	3.642320	4.536544
1	1.610687	-6.827490	-0.810250
6	1.314031	-5.612724	-2.571079
1	0.899997	-4.176516	-4.128303
1	-1.078585	-3.682623	5.100520
6	-2.247713	-5.002459	3.857581
1	-3.306584	-6.157763	2.368570
6	4.090209	-3.368764	-3.389741
1	4.745518	-4.462104	-1.645597
1	3.303621	-2.067648	-4.921624
1	4.980663	0.250496	4.009665
6	6.318884	0.523307	2.339241
1	7.408216	0.732724	0.483771
1	1.770869	-6.333144	-3.244626
1	-2.634090	-5.579209	4.694056
1	4.455979	-4.111752	-4.093587
1	7.188104	0.717164	2.962586
1	0.948961	-0.705392	2.456140

Table S20. Cartesian coordinates for the optimized geometry of **1f^3**.

Atomic Number	X	Y	Z
77	-0.889052	1.271982	-0.183644
1	-1.116988	1.945717	1.219074
15	-2.615673	-0.248840	0.237071
17	-0.423639	0.068299	-2.398831
15	1.141978	2.410538	-0.408763

49	0.609816	-0.502315	1.197204
6	-1.996944	2.624832	-0.986997
6	-2.220309	-1.951189	-0.411595
6	-4.176831	0.150976	-0.609108
6	-3.038611	-0.579599	1.980135
6	1.054247	3.896361	-1.456771
6	2.026223	2.890653	1.112741
6	2.406216	1.370610	-1.292991
15	-0.741158	-2.689927	0.421340
15	2.768315	-0.212945	-0.402156
8	-2.673931	3.463210	-1.387917
1	-3.089099	-2.607062	-0.294001
1	-1.991326	-1.833612	-1.473918
6	-5.327568	0.544866	0.087737
6	-4.170991	0.161350	-2.014896
6	-2.372436	0.070557	3.025533
6	-4.011045	-1.548326	2.284188
6	1.313058	5.184210	-0.968607
6	0.620755	3.722950	-2.782974
6	3.321588	3.430112	1.021370
6	1.461710	2.680150	2.376333
1	3.330743	1.940041	-1.430029
1	1.969362	1.143280	-2.266715
6	-0.059379	-3.924208	-0.731564
6	-1.419460	-3.629186	1.825811
6	3.304430	-1.418862	-1.661292
6	4.268804	0.164787	0.565263
1	-5.333169	0.554882	1.173510
6	-6.470572	0.931401	-0.618007
1	-3.265926	-0.097756	-2.559200
6	-5.318291	0.540039	-2.711220
1	-1.621566	0.818163	2.794562
6	-2.668262	-0.240855	4.355187
1	-4.539618	-2.059340	1.484520
6	-4.304226	-1.860389	3.609626
6	1.151926	6.291331	-1.807126
1	1.632977	5.325891	0.059304
1	0.376799	2.728730	-3.151378
6	0.472252	4.831291	-3.615631
1	3.773213	3.604571	0.049015
6	4.037529	3.742795	2.174679
6	2.179543	2.995058	3.533210
1	0.461450	2.266884	2.449376
6	0.369519	-5.173314	-0.250667
6	0.136649	-3.592892	-2.082453
6	-0.967122	-3.360164	3.123696
6	-2.393993	-4.620457	1.618156
6	4.129206	-2.477203	-1.239595
6	2.877982	-1.365235	-2.996523
6	4.229821	0.105530	1.963975
6	5.455160	0.548480	-0.083597

6	-6.469794	0.924360	-2.014895
1	-7.359596	1.239132	-0.073587
1	-5.310483	0.544470	-3.798102
1	-2.144704	0.271161	5.158349
6	-3.631927	-1.206955	4.648276
1	-5.050759	-2.617363	3.832903
1	1.348939	7.289053	-1.423476
6	0.737924	6.116785	-3.129683
1	0.138658	4.693228	-4.640819
6	3.467761	3.523527	3.433730
1	5.041632	4.149360	2.092250
1	1.731222	2.826159	4.508802
1	0.226249	-5.436823	0.793152
6	0.969589	-6.086412	-1.119917
1	-0.153390	-2.615470	-2.457113
6	0.727610	-4.516819	-2.944269
6	-1.490476	-4.071572	4.207116
1	-0.213999	-2.593785	3.288175
1	-2.737287	-4.845436	0.611177
6	-2.912031	-5.328598	2.701025
1	4.467305	-2.528545	-0.207387
6	4.535647	-3.454395	-2.147718
6	3.302215	-2.339209	-3.902974
1	2.201377	-0.587526	-3.333133
1	3.314985	-0.188996	2.471212
6	5.364869	0.436197	2.709730
6	6.584431	0.878971	0.663843
1	5.496867	0.577642	-1.169987
1	-7.360493	1.224529	-2.560654
1	-3.859777	-1.453681	5.682001
1	0.614384	6.979555	-3.779033
1	4.029016	3.764203	4.332899
1	1.292674	-7.053232	-0.742461
6	1.145059	-5.762770	-2.468076
1	0.870304	-4.255715	-3.988747
1	-1.139726	-3.855667	5.212774
6	-2.460279	-5.053647	3.997659
1	-3.663165	-6.096773	2.535765
6	4.129691	-3.383223	-3.483836
1	5.175947	-4.266094	-1.812492
1	2.977595	-2.280889	-4.938796
1	5.327315	0.391754	3.794925
6	6.539524	0.823883	2.062757
1	7.500658	1.173307	0.158311
1	1.607554	-6.477501	-3.143843
1	-2.864698	-5.607545	4.841044
1	4.454766	-4.140209	-4.192774
1	7.422183	1.079497	2.643519
1	1.233989	-0.905245	2.769208

Table S21. Cartesian coordinates for the optimized geometry of **1f⁴**.

Atomic Number	X	Y	Z
77	-0.816310	1.145904	-0.078078
1	-0.997720	1.859891	1.313780
15	-2.596801	-0.325723	0.400545
17	-0.481025	-0.063322	-2.306949
15	1.181352	2.336101	-0.472182
81	0.745605	-0.602755	1.343319
6	-1.932951	2.477562	-0.843099
6	-2.280856	-2.027579	-0.268301
6	-4.154498	0.151280	-0.410149
6	-2.998686	-0.620028	2.153468
6	0.959241	3.755128	-1.589697
6	2.091314	2.960527	0.978070
6	2.436204	1.297466	-1.361514
15	-0.787613	-2.847162	0.479749
15	2.966759	-0.203147	-0.398377
8	-2.615339	3.314292	-1.237250
1	-3.169666	-2.649241	-0.119446
1	-2.102454	-1.903115	-1.338971
6	-5.271558	0.581515	0.319423
6	-4.185491	0.168168	-1.815439
6	-2.368446	0.093876	3.179879
6	-3.942713	-1.607948	2.483973
6	1.128606	5.077933	-1.157782
6	0.518564	3.495722	-2.899174
6	3.366447	3.524302	0.797469
6	1.562623	2.866128	2.271137
1	3.305650	1.912838	-1.614477
1	1.952533	0.961676	-2.281664
6	-0.283715	-4.104999	-0.744083
6	-1.487220	-3.787495	1.882396
6	3.592794	-1.370145	-1.655439
6	4.448572	0.380245	0.499251
1	-5.249017	0.581563	1.405069
6	-6.417637	1.013889	-0.353799
1	-3.306609	-0.124224	-2.384852
6	-5.335855	0.593454	-2.478962
1	-1.647013	0.864395	2.929984
6	-2.664817	-0.181607	4.517405
1	-4.447670	-2.165315	1.700762
6	-4.236254	-1.883441	3.817455
6	0.870930	6.134666	-2.035696
1	1.457256	5.284547	-0.143704
1	0.345198	2.472761	-3.224507
6	0.271733	4.555667	-3.770924
1	3.788621	3.613638	-0.198894
6	4.101441	3.969391	1.893843
6	2.299691	3.314438	3.370409
1	0.574537	2.442216	2.414809
6	0.115937	-5.382376	-0.314475

6	-0.175242	-3.766562	-2.103304
6	-0.999446	-3.569629	3.177545
6	-2.524535	-4.714215	1.680679
6	4.753796	-2.119516	-1.396748
6	2.858126	-1.615461	-2.827441
6	4.498856	0.282982	1.895969
6	5.532782	0.944993	-0.194286
6	-6.453338	1.016115	-1.750292
1	-7.280794	1.348945	0.215475
1	-5.356977	0.602916	-3.565607
1	-2.169435	0.378744	5.306045
6	-3.595014	-1.172233	4.837326
1	-4.958689	-2.657169	4.060867
1	1.000964	7.158966	-1.696162
6	0.447897	5.875948	-3.341640
1	-0.066638	4.351161	-4.783353
6	3.570169	3.862175	3.183582
1	5.090569	4.392075	1.742927
1	1.879472	3.235947	4.369713
1	0.040643	-5.654678	0.734414
6	0.599525	-6.311727	-1.237527
1	-0.442558	-2.770814	-2.444810
6	0.299982	-4.705281	-3.019933
6	-1.550872	-4.259727	4.261068
1	-0.192271	-2.861616	3.344817
1	-2.895583	-4.904393	0.676321
6	-3.071217	-5.403013	2.762247
1	5.328918	-1.941554	-0.492508
6	5.180257	-3.087177	-2.308383
6	3.297851	-2.577423	-3.737814
1	1.937696	-1.073493	-3.023511
1	3.670789	-0.160264	2.442471
6	5.613666	0.757529	2.593412
6	6.644302	1.415512	0.502983
1	5.511124	1.005419	-1.279868
1	-7.346522	1.351722	-2.270744
1	-3.822229	-1.390866	5.877490
1	0.249657	6.699890	-4.022157
1	4.146407	4.206078	4.038596
1	0.900608	-7.299059	-0.896680
6	0.689045	-5.977817	-2.591940
1	0.370672	-4.437482	-4.070939
1	-1.169973	-4.081643	5.263227
6	-2.585715	-5.173867	4.055551
1	-3.870883	-6.121030	2.598399
6	4.456722	-3.315930	-3.482346
1	6.082430	-3.657423	-2.102119
1	2.728523	-2.752120	-4.647075
1	5.643000	0.682378	3.677217
6	6.684312	1.324443	1.899784
1	7.480839	1.847940	-0.040220

1	1.061171	-6.704976	-3.308966
1	-3.012385	-5.711849	4.898315
1	4.793983	-4.066071	-4.192906
1	7.551822	1.691127	2.442639
1	1.564618	-1.311418	2.724215

Table S22. Cartesian coordinates for the optimized geometry of *trans*-**1f**.

Atomic Number	X	Y	Z
77	-1.150570	0.742021	-0.103871
1	-0.781908	0.257464	1.346118
15	-2.328392	-1.271521	-0.311905
17	-1.380296	1.360587	-2.569274
15	0.311331	2.538845	0.081554
5	0.613605	-0.490722	-0.801407
6	-2.657705	1.775624	0.528994
6	-1.184517	-2.688439	-0.727726
6	-3.618047	-1.368873	-1.588910
6	-3.119007	-1.867556	1.231173
6	-0.348823	4.145224	-0.461493
6	1.028301	2.906530	1.721644
6	1.783016	2.219445	-1.006717
15	0.471989	-2.246278	-0.074368
15	2.287459	0.459172	-0.873758
8	-3.523362	2.386763	0.983448
1	-1.555756	-3.644398	-0.349453
1	-1.081792	-2.738625	-1.816542
6	-4.333126	-0.204301	-1.901609
6	-3.935205	-2.573896	-2.236820
6	-3.008472	-1.147418	2.425848
6	-3.828685	-3.080123	1.222771
6	-0.999712	4.952740	0.486960
6	-0.338289	4.532257	-1.809692
6	1.859375	4.032172	1.865972
6	0.785206	2.087853	2.828863
1	2.605587	2.929024	-0.872890
1	1.396937	2.296106	-2.030188
6	1.664714	-3.472340	-0.691421
6	0.359092	-2.404554	1.723484
6	3.190900	0.094255	-2.409428
6	3.442167	0.248888	0.504652
1	-4.058534	0.738870	-1.443624
6	-5.368594	-0.250848	-2.835797
1	-3.379297	-3.482427	-2.020164
6	-4.967052	-2.614374	-3.175999
1	-2.466716	-0.209216	2.438023
6	-3.583497	-1.639140	3.600339
1	-3.952510	-3.633959	0.295534
6	-4.398548	-3.572341	2.396462
6	-1.619054	6.138396	0.092231
1	-1.023268	4.657984	1.532556
1	0.112020	3.897808	-2.564126

6	-0.952985	5.724807	-2.197044
1	2.025501	4.695696	1.020613
6	2.458954	4.312658	3.092858
6	1.383077	2.372745	4.059949
1	0.126951	1.232533	2.727041
6	2.178549	-4.496773	0.118427
6	2.125404	-3.325020	-2.012233
6	0.933793	-1.419589	2.537331
6	-0.332728	-3.474910	2.310619
6	4.552510	-0.236422	-2.419643
6	2.461061	0.121784	-3.611805
6	3.846747	-1.059505	0.824690
6	3.925948	1.325845	1.258340
6	-5.688156	-1.453464	-3.472054
1	-5.913439	0.657635	-3.077702
1	-5.205313	-3.549436	-3.676427
1	-3.490697	-1.070933	4.522312
6	-4.273511	-2.852686	3.590554
1	-4.948629	-4.509804	2.377916
1	-2.120986	6.755432	0.832852
6	-1.592674	6.528889	-1.250311
1	-0.940491	6.017372	-3.243573
6	2.224568	3.478516	4.193070
1	3.098777	5.185441	3.195105
1	1.182258	1.735116	4.917120
1	1.838511	-4.601319	1.144662
6	3.142284	-5.369651	-0.392827
1	1.751058	-2.515193	-2.632522
6	3.085930	-4.201972	-2.516074
6	0.825005	-1.510186	3.925142
1	1.449190	-0.578347	2.089981
1	-0.801125	-4.233284	1.690433
6	-0.446917	-3.558707	3.698105
1	5.118814	-0.254405	-1.493302
6	5.180529	-0.552717	-3.627684
6	3.098683	-0.186867	-4.813230
1	1.401590	0.372706	-3.605799
1	3.492065	-1.902662	0.239231
6	4.706107	-1.283508	1.898731
6	4.778652	1.095847	2.340457
1	3.628959	2.340432	1.023974
1	-6.490007	-1.485130	-4.205199
1	-4.721868	-3.233782	4.504592
1	-2.073838	7.453804	-1.557579
1	2.686511	3.700758	5.151649
1	3.540567	-6.161071	0.236826
6	3.595677	-5.223789	-1.707466
1	3.442830	-4.079403	-3.535141
1	1.276624	-0.743777	4.548946
6	0.133639	-2.576993	4.506615
1	-0.998083	-4.381173	4.144880

6	4.456170	-0.530301	-4.822106
1	6.235733	-0.813077	-3.633073
1	2.534826	-0.161643	-5.742077
1	5.011510	-2.298133	2.139889
6	5.166225	-0.206522	2.664482
1	5.136181	1.937146	2.927420
1	4.348358	-5.902572	-2.100001
1	0.041074	-2.641066	5.587725
1	4.947707	-0.775114	-5.760214
1	5.828730	-0.383070	3.507848
1	0.416663	-0.741847	-1.968950

Table S23. Cartesian coordinates for the optimized geometry of **1d**.

Atomic Number	X	Y	Z
6	2.520060	2.472098	-0.496915
6	1.786139	2.771974	-1.600489
7	0.747065	1.861933	-1.645677
6	0.804093	0.995861	-0.598088
7	1.899752	1.392183	0.106239
6	2.425823	0.708058	1.290461
6	2.774213	-0.753182	0.973936
6	-0.290833	1.856670	-2.683599
6	-1.675467	2.092233	-2.070947
77	-0.485779	-0.619241	-0.198729
6	-1.673524	-2.045138	0.240617
17	0.334238	-1.548844	-2.406975
1	-0.844305	0.127283	1.149600
15	1.233763	-1.765059	0.944763
6	1.681598	-3.383410	0.271404
6	2.558557	-3.487660	-0.819631
6	2.830998	-4.737758	-1.376246
6	2.218385	-5.884397	-0.863165
6	1.329482	-5.781644	0.211427
6	1.059989	-4.536312	0.779560
6	0.904035	-2.049487	2.716367
6	1.877032	-2.727153	3.475030
6	1.675051	-2.957843	4.834533
6	0.497337	-2.519323	5.451848
6	-0.474522	-1.852306	4.703859
6	-0.273491	-1.617130	3.340159
15	-2.272684	0.597305	-1.155375
6	-3.344016	-0.271010	-2.335263
6	-4.436682	0.421205	-2.891765
6	-5.286278	-0.219567	-3.791434
6	-5.052124	-1.554474	-4.143960
6	-3.966729	-2.241865	-3.597602
6	-3.110774	-1.604401	-2.694751
6	-3.365247	1.244258	0.150692
6	-4.621666	0.674990	0.399311
6	-5.390671	1.122814	1.477796
6	-4.912421	2.137657	2.309608

6	-3.654587	2.702946	2.068664
6	-2.880683	2.252821	0.999854
1	3.318742	1.254310	1.605246
1	1.685673	0.773174	2.096527
1	3.441862	-1.157152	1.741410
1	3.273983	-0.818454	0.002825
1	-0.240213	0.896881	-3.207535
1	-0.045174	2.659678	-3.383671
1	-1.648380	2.944883	-1.384602
1	-2.399010	2.311366	-2.862574
1	3.007725	-2.601098	-1.254055
1	3.512942	-4.812767	-2.218804
1	2.430064	-6.855842	-1.302107
1	0.848655	-6.670498	0.611055
1	0.376321	-4.464332	1.620725
1	2.784044	-3.091615	2.998650
1	2.431240	-3.484205	5.410877
1	0.338896	-2.702860	6.511291
1	-1.393182	-1.515839	5.177037
1	-1.033402	-1.100169	2.765462
1	-4.634771	1.452754	-2.609673
1	-6.130486	0.318552	-4.214295
1	-5.714837	-2.053343	-4.846326
1	-3.775970	-3.274381	-3.877048
1	-2.247533	-2.130785	-2.306115
1	-5.001095	-0.111497	-0.245913
1	-6.364886	0.678202	1.663048
1	-5.514798	2.487779	3.143622
1	-3.277262	3.491167	2.715015
1	-1.893227	2.679006	0.837545
8	-2.388775	-2.887455	0.557135
1	1.910617	3.535748	-2.352735
1	3.413694	2.920399	-0.090563

Table S24. Cartesian coordinates for the optimized geometry of **1g**.

Atomic Number	X	Y	Z
6	-0.768102	1.455417	4.512734
6	-0.642093	0.093597	4.231491
6	-0.220411	-0.331233	2.965308
6	0.048440	0.601230	1.934716
6	0.005142	1.975280	2.272562
6	-0.416959	2.394122	3.540590
6	0.527745	2.987371	1.276383
6	0.060553	-1.796579	2.713558
77	0.497466	-0.039000	-0.051506
17	2.946354	-0.057169	0.684627
15	0.461418	2.249962	-0.419550
6	1.738350	3.074868	-1.413791
6	2.816451	2.330926	-1.910760
6	3.810150	2.964889	-2.662432
6	3.732447	4.336229	-2.917522

6	2.658410	5.082818	-2.418156
6	1.663198	4.455094	-1.668953
6	-1.130975	2.801614	-1.117340
6	-1.271646	3.095955	-2.480306
6	-2.527746	3.415841	-3.002817
6	-3.649031	3.443289	-2.169141
6	-3.512509	3.144996	-0.808783
6	-2.261263	2.819853	-0.284126
15	0.036630	-2.107845	0.889635
6	1.092781	-3.552363	0.577589
6	0.761878	-4.807746	1.116333
6	1.589118	-5.907130	0.886520
6	2.749315	-5.759528	0.116769
6	3.080917	-4.511954	-0.417332
6	2.256461	-3.406354	-0.188631
6	-1.662527	-2.659621	0.522012
6	-1.923621	-3.615505	-0.469137
6	-3.241828	-3.941486	-0.799394
6	-4.305531	-3.315779	-0.143540
6	-4.048016	-2.357480	0.843098
6	-2.733444	-2.025252	1.172184
6	0.817409	-0.611187	-1.852843
8	0.968253	-0.954355	-2.946130
1	-1.108403	1.782925	5.492319
1	-0.859763	-0.643276	5.003033
1	-0.458501	3.457424	3.771439
1	0.005381	3.950658	1.314309
1	1.595115	3.166595	1.466182
1	1.087641	-2.028874	3.027467
1	-0.621810	-2.471689	3.243491
1	-1.056915	0.026039	-0.336638
1	2.889225	1.273117	-1.679031
1	4.647075	2.384565	-3.042673
1	4.507297	4.826101	-3.502727
1	2.596097	6.150518	-2.614789
1	0.821967	5.033023	-1.293523
1	-0.401632	3.077394	-3.130939
1	-2.628408	3.642782	-4.061526
1	-4.625561	3.693033	-2.577028
1	-4.382487	3.160646	-0.156481
1	-2.162985	2.564335	0.768057
1	-0.146525	-4.926284	1.702343
1	1.329249	-6.877122	1.303795
1	3.393061	-6.617476	-0.063076
1	3.985113	-4.393337	-1.009070
1	2.526410	-2.427055	-0.570729
1	-1.099021	-4.105361	-0.979739
1	-3.435828	-4.684151	-1.569660
1	-5.330659	-3.570953	-0.401126
1	-4.872017	-1.864569	1.353654
1	-2.537371	-1.262596	1.921797

Table S25. Cartesian coordinates for the optimized geometry of **1h**.

Atomic Number	X	Y	Z
6	-0.723649	-1.062884	-4.617648
77	0.732737	-0.123611	-1.875938
1	-1.489412	0.875557	-5.346241
15	0.410589	-1.805911	-0.320200
6	-0.905866	-2.784328	-1.155386
6	-0.578391	-2.983266	-2.660408
6	0.006603	-1.663298	-3.332340
6	-1.166980	0.409626	-4.406707
15	0.152420	1.362228	-3.550070
1	0.974551	-1.987097	-3.722208
1	-1.789700	-2.143041	-1.047507
1	-1.119676	-3.737059	-0.654592
1	-2.008466	0.448067	-3.705079
6	-0.681390	2.862212	-2.902151
6	-1.788090	2.709975	-2.050047
6	-0.214567	4.153857	-3.185012
6	-2.422094	3.825000	-1.503640
6	-0.844285	5.270841	-2.626731
6	-1.949338	5.111132	-1.788490
1	-2.143664	1.713606	-1.802118
1	0.642587	4.289948	-3.837334
1	-3.280373	3.690630	-0.849278
1	-0.466971	6.266031	-2.849613
1	-2.437742	5.980669	-1.355342
6	1.328301	2.006818	-4.776007
6	2.678204	2.124201	-4.418569
6	0.901714	2.435001	-6.043213
6	3.594248	2.660824	-5.328025
6	1.819757	2.966919	-6.948640
6	3.168599	3.080056	-6.590862
1	3.011313	1.762449	-3.451093
1	-0.145203	2.353646	-6.323165
1	4.642322	2.738629	-5.050052
1	1.485348	3.292252	-7.930958
1	3.884793	3.490602	-7.298926
6	-0.351083	-1.259231	1.261178
6	-1.083505	-0.062449	1.311285
6	-0.245431	-2.039583	2.424328
6	-1.707564	0.337972	2.494186
6	-0.869531	-1.636136	3.607232
6	-1.604275	-0.447992	3.645459
1	-1.147274	0.563425	0.427699
1	0.334505	-2.957576	2.411588
1	-2.263679	1.272286	2.517869
1	-0.775083	-2.249434	4.500321
1	-2.083961	-0.131521	4.568652
6	1.760659	-2.902669	0.204986
6	1.564282	-4.266756	0.468972
6	3.030519	-2.336303	0.387599

6	2.625844	-5.056128	0.914251
6	4.089380	-3.128074	0.836740
6	3.889785	-4.486122	1.100265
1	0.587069	-4.715996	0.318950
1	2.467585	-6.113735	1.111720
1	5.073848	-2.685182	0.964498
1	4.718279	-5.102354	1.441726
6	-2.010839	-1.812202	-5.064266
1	-2.869221	-1.381367	-4.526971
1	-2.182428	-1.611204	-6.131983
6	-2.076418	-3.329245	-4.806160
6	-1.890709	-3.514830	-3.291537
17	3.073157	-0.747302	-2.588354
1	-0.801803	0.102975	-1.548637
6	1.365764	1.206758	-0.652089
8	1.706386	2.026194	0.087792
1	3.193899	-1.291769	0.143148
1	-2.736461	-2.985100	-2.826609
1	-2.002555	-4.575574	-3.025919
6	-1.077332	-4.118795	-5.665394
1	-0.047256	-3.815175	-5.486130
1	-1.154613	-5.192107	-5.452566
1	-1.297818	-3.959833	-6.729200
6	-3.511796	-3.776421	-5.190444
1	-4.239487	-3.176402	-4.630888
1	-3.669622	-3.571814	-6.256585
15	-3.910303	-5.607993	-4.903383
6	-5.463591	-5.483129	-3.914129
6	-6.562070	-6.326179	-4.160657
6	-5.517579	-4.629232	-2.796920
6	-7.683394	-6.301831	-3.327762
6	-6.639193	-4.604851	-1.965235
6	-7.729343	-5.440156	-2.227656
1	-6.545159	-6.996871	-5.015653
1	-4.675877	-3.978785	-2.571988
1	-8.525425	-6.956197	-3.543240
1	-6.660253	-3.931629	-1.110756
1	-8.603826	-5.420462	-1.581741
6	-4.561570	-6.088597	-6.566011
6	-3.996228	-7.196667	-7.213748
6	-5.585056	-5.375126	-7.214671
6	-4.438180	-7.583761	-8.484419
6	-6.028313	-5.759265	-8.480540
6	-5.453879	-6.865734	-9.119009
1	-3.204912	-7.757275	-6.719907
1	-6.040625	-4.521457	-6.718482
1	-3.989239	-8.444429	-8.974990
1	-6.821969	-5.199083	-8.970317
1	-5.799375	-7.164907	-10.105912
6	0.522127	-4.069077	-2.735306
1	1.455650	-3.694494	-2.305005

S99

1	0.217153	-4.970116	-2.186554
1	0.732722	-4.354807	-3.766291
6	0.309951	-1.048563	-5.770502
1	1.226838	-0.541476	-5.453719
1	0.587895	-2.059270	-6.072450
1	-0.093557	-0.525841	-6.648405

Table S26. Cartesian coordinates for the optimized geometry of **1i**.

Atomic Number	X	Y	Z
15	2.395086	-0.360284	-0.112193
77	0.004076	-0.279640	-0.110703
6	3.070884	1.313789	-0.569900
6	3.136929	-1.561488	-1.246007
6	3.068761	-0.710394	1.535954
15	-2.367307	-0.251376	0.198958
7	0.133583	1.886435	0.036277
6	-0.080695	-2.122063	-0.246020
6	2.098917	2.136173	-1.419998
1	3.329460	1.858688	0.344006
1	3.987088	1.165834	-1.150689
6	2.460944	-1.940341	-2.417408
6	4.405299	-2.099213	-0.956497
6	4.254748	-0.112487	1.994588
6	2.438029	-1.685753	2.326463
6	-2.863647	1.507721	0.483017
6	-2.924648	-1.093132	1.707817
6	-3.374767	-0.885937	-1.150931
7	0.991875	2.681231	-0.606835
7	-0.701604	2.711870	0.669069
1	2.597069	3.009747	-1.844575
1	1.634492	1.544917	-2.218529
1	1.482629	-1.530818	-2.645300
6	3.057996	-2.845638	-3.297089
6	4.990869	-3.002847	-1.842917
1	4.923607	-1.832178	-0.040081
1	4.780435	0.621680	1.390784
6	4.789219	-0.474694	3.233817
6	2.980033	-2.050734	3.558332
1	1.528140	-2.164469	1.978652
6	-1.859372	2.196770	1.421405
1	-2.930277	2.041075	-0.470054
1	-3.852449	1.514784	0.952059
6	-4.306805	-1.095038	1.982536
6	-2.045217	-1.738269	2.589211
6	-3.740103	-2.244245	-1.131195
6	-3.717135	-0.082578	-2.251167
6	0.708816	3.990553	-0.399916
6	-0.396748	4.011666	0.433600
1	2.532581	-3.138680	-4.201769
6	4.319663	-3.375694	-3.012964
1	5.966500	-3.423098	-1.614990

1	5.706197	-0.006781	3.581100
6	4.153637	-1.442220	4.016344
1	2.489317	-2.810635	4.160249
1	-2.300106	3.069005	1.907603
1	-1.480396	1.516606	2.192058
1	-5.004650	-0.626920	1.292223
6	-4.792381	-1.723934	3.127167
6	-2.537989	-2.370729	3.734155
1	-0.980740	-1.754949	2.386010
1	-3.483791	-2.871950	-0.282307
6	-4.453365	-2.785410	-2.200342
6	-4.440755	-0.630346	-3.310289
1	-3.410941	0.957157	-2.299073
6	1.401127	5.198615	-0.934724
6	-1.073280	5.243026	0.933856
1	4.777816	-4.084550	-3.697274
1	4.573632	-1.725207	4.977500
1	-5.859628	-1.724357	3.330358
6	-3.907862	-2.362672	4.005168
1	-1.851424	-2.873387	4.409702
1	-4.738515	-3.833452	-2.180625
6	-4.807303	-1.979419	-3.287339
1	-4.712057	-0.005185	-4.156176
1	1.637905	5.068957	-1.997110
1	2.354047	5.334885	-0.403733
6	0.483547	6.430190	-0.721164
1	-1.317402	5.147750	1.998594
1	-2.021909	5.377391	0.394556
6	-0.138263	6.455240	0.687572
1	-4.289353	-2.857677	4.893944
1	-5.368480	-2.402514	-4.115889
1	1.071648	7.336951	-0.886182
1	-0.312297	6.416317	-1.476449
1	-0.713749	7.374445	0.826186
1	0.657099	6.451569	1.443591
8	-0.142532	-3.264191	-0.331270
1	0.161960	-0.366494	1.460315
17	-0.369130	0.216393	-2.547425

Table S27. Cartesian coordinates for the optimized geometry of *cis*-**1j**.

Atomic Number	X	Y	Z
6	0.476843	-0.035856	-3.818114
77	1.785425	0.691691	-0.809822
1	1.257087	1.642132	-4.980442
15	1.205482	-0.965213	0.776297
6	-0.035649	-2.120595	-0.031271
6	0.037673	-2.068481	-1.569465
15	0.062004	-0.294063	-2.041182
6	0.797400	1.459527	-4.003852
15	1.921056	2.144432	-2.664876
1	-1.026818	-1.799923	0.306971

1	0.138206	-3.139585	0.328076
1	-0.798405	-2.611367	-2.022776
1	0.982214	-2.485833	-1.933559
1	-0.354040	-0.341385	-4.464071
1	1.354899	-0.657662	-4.019389
1	-0.121628	2.053042	-3.946135
1	0.742228	1.633186	-0.094491
17	3.293735	-0.939044	-2.045255
6	3.208007	1.541222	0.167028
6	1.331438	3.842254	-2.389097
6	1.058467	4.317551	-1.100039
6	1.165607	4.696067	-3.493841
6	0.613469	5.629768	-0.915451
6	0.714148	6.002083	-3.306969
6	0.436871	6.470241	-2.017070
1	1.193825	3.662072	-0.245794
1	1.398593	4.346050	-4.496621
1	0.408457	5.993800	0.087918
1	0.584971	6.656583	-4.164819
1	0.089612	7.489995	-1.873324
6	0.327278	-0.311365	2.233698
6	0.650134	0.967436	2.710176
6	-0.622887	-1.083107	2.922070
6	0.035221	1.466512	3.859773
6	-1.241968	-0.578824	4.067187
6	-0.912443	0.695411	4.538885
1	1.375341	1.573713	2.177354
1	-0.887519	-2.076492	2.570481
1	0.294288	2.457634	4.222888
1	-1.979770	-1.181343	4.590409
1	-1.394092	1.085788	5.431412
6	-1.608435	0.366942	-1.796550
6	-2.735530	-0.416222	-2.100849
6	-1.783169	1.689390	-1.360857
6	-4.017922	0.115908	-1.958560
6	-3.067410	2.221107	-1.230154
6	-4.185042	1.435040	-1.524074
1	-2.619926	-1.440030	-2.447592
1	-0.918476	2.299273	-1.120590
1	-4.884896	-0.497853	-2.187795
1	-3.192987	3.246680	-0.893330
1	-5.184617	1.847105	-1.414163
6	2.527621	-2.020772	1.440874
6	2.189736	-3.130367	2.235434
6	3.874681	-1.708672	1.219603
6	3.192345	-3.920051	2.796220
6	4.875722	-2.500477	1.787685
6	4.537644	-3.604313	2.573397
1	1.148418	-3.373641	2.431405
1	4.142308	-0.875541	0.581839
1	2.925358	-4.776801	3.409213

1	5.918935	-2.256848	1.606080
1	5.318573	-4.220432	3.011313
6	3.563752	2.323586	-3.401489
6	4.014827	1.429430	-4.383271
6	4.423665	3.320637	-2.912847
6	5.312680	1.543695	-4.883636
6	5.721537	3.425570	-3.413120
6	6.166338	2.538740	-4.399270
1	3.367975	0.636952	-4.744991
1	4.077925	4.018884	-2.154839
1	5.658395	0.849956	-5.645106
1	6.382630	4.201798	-3.037189
1	7.177209	2.623463	-4.789183
8	4.034670	2.093261	0.742232

Table S28. Cartesian coordinates for the optimized geometry of *trans*-**1j**.

Atomic Number	X	Y	Z
6	0.634961	-0.183731	-3.578103
77	1.441765	0.961507	-0.556096
1	1.502518	1.384389	-4.827810
15	1.142220	-0.791878	1.010751
6	-0.203656	-1.876656	0.313511
6	-0.062587	-1.970513	-1.217437
15	-0.067013	-0.248614	-1.869632
6	0.893194	1.294876	-3.922767
15	1.729684	2.229376	-2.522638
1	-1.162673	-1.421685	0.584460
1	-0.150742	-2.865903	0.779380
1	-0.849998	-2.588883	-1.658880
1	0.905947	-2.408078	-1.489164
1	-0.045626	-0.639924	-4.305764
1	1.571738	-0.752374	-3.557936
1	-0.061247	1.801336	-4.099468
17	-0.308813	2.337769	0.588078
1	2.507264	0.008618	-1.250713
6	2.824723	1.864053	0.440209
6	1.067249	3.910971	-2.592261
6	1.063635	4.681407	-1.419919
6	0.611883	4.469372	-3.799112
6	0.605560	5.999825	-1.456007
6	0.148671	5.785228	-3.826722
6	0.146072	6.550801	-2.655334
1	1.385384	4.244335	-0.481212
1	0.623812	3.888113	-4.717106
1	0.596709	6.589612	-0.543608
1	-0.204502	6.213381	-4.761068
1	-0.216521	7.575169	-2.678917
6	0.646163	-0.389313	2.702455
6	1.601447	-0.394746	3.732771
6	-0.670260	0.020148	2.972460
6	1.235605	-0.011930	5.023824

6	-1.029735	0.392196	4.267818
6	-0.079976	0.376840	5.293599
1	2.623054	-0.703862	3.531149
1	-1.404325	0.079834	2.176185
1	1.977373	-0.021218	5.817937
1	-2.049713	0.706229	4.471866
1	-0.363446	0.671951	6.300458
6	-1.777735	0.318186	-2.002942
6	-2.860446	-0.576187	-2.034727
6	-2.012729	1.698468	-2.128788
6	-4.160746	-0.094592	-2.198811
6	-3.312638	2.171299	-2.306368
6	-4.387119	1.277734	-2.339920
1	-2.704332	-1.646230	-1.935114
1	-1.193828	2.403971	-2.048526
1	-4.994086	-0.791702	-2.218328
1	-3.485388	3.240141	-2.397171
1	-5.400365	1.649711	-2.466885
6	2.577495	-1.903889	1.162429
6	2.424361	-3.114355	1.862828
6	3.831890	-1.570276	0.634180
6	3.505366	-3.981926	2.013446
6	4.915805	-2.438657	0.792791
6	4.753627	-3.645244	1.477034
1	1.465972	-3.372588	2.306538
1	3.963708	-0.635179	0.101453
1	3.376630	-4.915600	2.554429
1	5.885883	-2.168406	0.384029
1	5.596620	-4.320334	1.598520
6	3.485133	2.346696	-2.999142
6	4.233422	1.165960	-3.142115
6	4.104063	3.587652	-3.207208
6	5.579079	1.226544	-3.501520
6	5.457636	3.643401	-3.553557
6	6.194999	2.467203	-3.703986
1	3.769010	0.199960	-2.960947
1	3.535639	4.506178	-3.097829
1	6.149357	0.308424	-3.617291
1	5.932264	4.608947	-3.706578
1	7.246327	2.514186	-3.975020
8	3.668621	2.385932	1.014602

Table S29. Cartesian coordinates for the optimized geometry of **1k**.

Atomic Number	X	Y	Z
77	2.823570	2.294117	9.404679
15	1.803577	0.268428	10.045102
15	3.557242	4.529257	9.658139
6	2.718760	2.554420	11.401839
6	1.459097	0.511414	11.905594
6	0.123606	-0.107215	9.348291
6	2.740140	-1.321398	9.859795

6	4.103810	4.626871	11.474730
6	4.896013	5.306794	8.646411
6	2.143169	5.722619	9.550858
7	2.192153	1.708950	12.318630
6	3.335614	3.539182	12.146287
1	0.387818	0.675225	12.056688
1	1.781565	-0.344149	12.501253
6	-0.735270	1.152644	9.171967
1	0.358920	-0.517355	8.355848
6	-0.635911	-1.175697	10.158014
1	1.979199	-2.111485	9.890045
6	3.391923	-1.320571	8.464156
6	3.764465	-1.579115	10.975608
1	5.180599	4.417450	11.504350
1	3.925415	5.627319	11.884197
1	4.363664	5.587620	7.726923
6	6.025607	4.337606	8.275561
6	5.443925	6.583743	9.309883
1	2.577266	6.718644	9.711331
6	1.516221	5.662654	8.148394
6	1.083813	5.460089	10.630561
7	2.421283	2.072381	13.579430
7	3.128138	3.195529	13.448988
1	-0.281562	1.854276	8.468086
1	-0.881017	1.671442	10.128512
1	-1.723735	0.865437	8.794800
1	-0.050024	-2.083824	10.331147
1	-1.540107	-1.461472	9.608715
1	-0.957435	-0.779539	11.128688
1	2.662907	-1.130250	7.666472
1	3.837864	-2.305035	8.281521
1	4.179225	-0.562919	8.416109
1	3.282987	-1.746752	11.945801
1	4.475479	-0.753205	11.058356
1	4.323937	-2.489095	10.728007
1	5.646140	3.435876	7.789397
1	6.583730	4.019454	9.161197
1	6.714866	4.849971	7.593591
1	4.658648	7.303764	9.565428
1	6.136270	7.074484	8.616241
1	6.006040	6.338002	10.218335
1	2.239835	5.876438	7.354377
1	0.711163	6.403232	8.078779
1	1.089394	4.669462	7.969641
1	1.488563	5.556430	11.643949
1	0.665451	4.454220	10.517114
1	0.270236	6.186392	10.520833
6	3.605243	3.887744	14.647975
1	3.242551	3.345695	15.522249
1	3.218129	4.910918	14.649069
1	4.699253	3.902279	14.638106

S105

6	2.991172	2.051502	7.498919
8	3.082112	1.913583	6.361962
1	1.366752	2.871859	9.218048
17	5.192884	1.511972	9.922505

Table S30. Cartesian coordinates for the optimized geometry of **1l**.

Atomic Number	X	Y	Z
6	2.492407	2.488018	-0.450647
6	1.774881	2.761030	-1.625927
7	0.753631	1.817599	-1.684754
6	0.800746	0.983098	-0.610873
7	1.855347	1.401892	0.144047
6	2.328045	0.733096	1.355571
6	2.737449	-0.717494	1.060079
6	-0.264124	1.767044	-2.737989
6	-1.658048	2.036156	-2.160165
77	-0.485968	-0.630596	-0.208218
6	3.604850	3.245397	-0.079244
6	3.969981	4.289232	-0.929217
6	3.248745	4.565245	-2.107219
6	2.138887	3.806235	-2.477285
6	-1.678532	-2.053506	0.236993
17	0.325759	-1.605350	-2.397852
1	-0.844551	0.125271	1.135764
15	1.227436	-1.769094	0.955212
6	1.731584	-3.359154	0.256433
6	2.655807	-3.418526	-0.797938
6	2.969281	-4.646922	-1.380603
6	2.350539	-5.816420	-0.930601
6	1.414308	-5.758220	0.106516
6	1.103583	-4.534760	0.700310
6	0.850293	-2.102700	2.708921
6	1.795645	-2.817288	3.468738
6	1.563185	-3.076732	4.818168
6	0.383355	-2.628760	5.424518
6	-0.559944	-1.922830	4.675744
6	-0.328856	-1.659609	3.321988
15	-2.266448	0.590098	-1.175360
6	-3.379224	-0.299948	-2.299792
6	-4.500738	0.377656	-2.815466
6	-5.374631	-0.275452	-3.682388
6	-5.135599	-1.607253	-4.043536
6	-4.020639	-2.279174	-3.539117
6	-3.140257	-1.629676	-2.668769
6	-3.317096	1.300451	0.131853
6	-4.553458	0.727006	0.459863
6	-5.286322	1.218271	1.544227
6	-4.791427	2.280397	2.304536
6	-3.553315	2.849738	1.985008
6	-2.815429	2.357272	0.909122
1	3.183985	1.300126	1.726518

1	1.540070	0.776837	2.116559
1	3.375359	-1.104954	1.860737
1	3.288878	-0.765157	0.116308
1	-0.209116	0.785113	-3.217813
1	-0.008524	2.533763	-3.472072
1	-1.640002	2.925767	-1.522333
1	-2.372051	2.209401	-2.971670
1	4.165467	3.039964	0.827311
1	4.830132	4.902343	-0.677179
1	3.565574	5.386352	-2.743368
1	1.592219	4.021492	-3.389797
1	3.112972	-2.513786	-1.184329
1	3.687946	-4.687042	-2.194526
1	2.593992	-6.770897	-1.389805
1	0.928266	-6.664927	0.456684
1	0.382507	-4.497263	1.512007
1	2.704533	-3.186920	3.000093
1	2.297632	-3.632373	5.395164
1	0.201182	-2.834698	6.476004
1	-1.479702	-1.577625	5.140428
1	-1.066564	-1.111769	2.747036
1	-4.700618	1.406960	-2.526728
1	-6.241495	0.250743	-4.073257
1	-5.817681	-2.115664	-4.720054
1	-3.826179	-3.309015	-3.825866
1	-2.255161	-2.143524	-2.313241
1	-4.945778	-0.096466	-0.129158
1	-6.245699	0.770756	1.790111
1	-5.365926	2.664286	3.143345
1	-3.163107	3.674983	2.575029
1	-1.842784	2.789965	0.686236
8	-2.395576	-2.893317	0.554935

Table S31. Cartesian coordinates for the optimized geometry of **1m**.

Atomic Number	X	Y	Z
7	2.461218	0.944932	0.536616
7	1.799019	2.027053	0.190574
6	1.598185	-0.111584	0.583544
6	0.331410	0.323070	0.253717
7	0.493403	1.643239	0.016357
6	-0.617084	2.474344	-0.403862
15	-2.007519	1.274716	-0.908156
6	1.828004	-1.577523	0.802764
15	0.098561	-2.271025	1.087665
77	-1.366167	-0.774279	-0.000183
17	-0.345727	-1.637196	-2.168725
6	-3.522086	2.069911	-0.289484
6	-3.898935	3.343597	-0.749669
6	-5.048064	3.956079	-0.249639
6	-5.831788	3.299814	0.707063
6	-5.462619	2.032108	1.163614

6	-4.308538	1.417723	0.668859
6	-2.074565	1.409628	-2.714739
6	-3.299741	1.384180	-3.397087
6	-0.010068	-2.308142	2.913034
6	-2.936231	-1.867224	-0.226446
8	-3.879817	-2.519851	-0.343129
6	0.414532	-3.428726	3.645992
6	0.415552	-3.397489	5.042047
6	0.008637	-2.243829	5.719178
6	-0.398398	-1.120365	4.994217
6	-0.411150	-1.151883	3.598089
6	-3.320027	1.391649	-4.793016
6	-2.120623	1.418323	-5.511172
6	-0.898701	1.427677	-4.832002
6	-0.871201	1.413770	-3.437449
6	0.026987	-3.997836	0.540847
6	-0.980164	-4.823384	1.070264
6	-1.149556	-6.121966	0.591859
6	-0.320599	-6.606790	-0.425621
6	0.670106	-5.784098	-0.966407
6	0.842213	-4.481430	-0.492069
1	-0.331535	3.111948	-1.245775
1	-0.984296	3.098789	0.419662
1	2.249220	-2.049654	-0.092254
1	2.460642	-1.819980	1.664059
1	-1.904963	-0.235629	1.388281
1	-3.301878	3.846706	-1.506344
1	-5.334972	4.941651	-0.607930
1	-6.729448	3.777104	1.092633
1	-6.071541	1.519024	1.903757
1	-4.007293	0.436606	1.023192
1	-4.233025	1.363663	-2.840982
1	0.737772	-4.326017	3.126494
1	0.737335	-4.273970	5.599396
1	0.010861	-2.220554	6.806297
1	-0.708456	-0.217286	5.514339
1	-0.726260	-0.279225	3.035613
1	-4.272033	1.376264	-5.317962
1	-2.138215	1.423203	-6.598326
1	0.035969	1.428724	-5.386577
1	0.080981	1.380509	-2.916670
1	-1.631759	-4.449250	1.855847
1	-1.931096	-6.752237	1.008956
1	-0.454351	-7.618314	-0.801309
1	1.304908	-6.148764	-1.769906
1	1.585808	-3.840027	-0.950791

Table S32. Cartesian coordinates for the optimized geometry of **1n**.

Atomic Number	X	Y	Z
77	2.664193	0.935536	10.806587
5	2.584962	-1.109653	10.392841
15	4.894839	0.418242	10.388538
15	0.393178	0.451080	10.861167
7	3.704129	-1.974863	10.139428
7	1.434320	-1.965072	10.528236
6	5.053160	-1.465351	10.158397
6	6.119085	0.813169	11.679169
6	5.620845	1.113444	8.861869
6	0.202908	-1.422640	11.055485
6	-0.438609	0.797419	9.273217
6	-0.695116	1.165387	12.130199
6	3.267636	-3.296706	10.208807
6	1.858519	-3.291387	10.458897
1	5.599789	-1.663987	9.226074
1	5.632532	-1.876581	10.996027
6	6.933926	1.951199	11.568431
6	6.163982	0.040726	12.851315
6	4.957177	2.124281	8.156479
6	6.870342	0.660167	8.405392
1	0.084562	-1.637865	12.126684
1	-0.688596	-1.766044	10.513129
6	-1.158226	1.984978	9.081260
6	-0.261322	-0.086805	8.197391
6	-0.152800	1.993324	13.120954
6	-2.071996	0.883426	12.129080
6	3.962872	-4.496708	10.092639
6	1.158489	-4.485869	10.596371
1	6.897643	2.561279	10.670182
6	7.797219	2.299896	12.608744
6	7.031758	0.392536	13.886348
1	5.499584	-0.808624	12.970593
1	3.992379	2.472527	8.511240
6	5.530218	2.670859	7.003960
6	7.438246	1.201659	7.252236
1	7.405606	-0.108093	8.958436
1	-1.296397	2.674131	9.910077
6	-1.702140	2.280933	7.828757
6	-0.810819	0.209975	6.949205
1	0.317670	-0.996698	8.334408
1	0.915993	2.179484	13.134265
6	-0.984789	2.539387	14.102489
6	-2.897578	1.427902	13.112984
1	-2.498549	0.252700	11.352524
1	5.034414	-4.501913	9.908034
6	3.246897	-5.696853	10.231204
1	0.090387	-4.482930	10.799724
6	1.869189	-5.691515	10.479535
1	8.427740	3.180585	12.512381

6	7.850699	1.519144	13.767484
1	7.056440	-0.208885	14.791580
1	5.006995	3.455520	6.462947
6	6.767428	2.209229	6.548981
1	8.403739	0.842193	6.904460
1	-2.260412	3.203571	7.688666
6	-1.531314	1.394479	6.761495
1	-0.672626	-0.482183	6.121962
1	-0.559220	3.178922	14.871650
6	-2.353452	2.258603	14.099877
1	-3.962668	1.208717	13.108589
1	3.773816	-6.644077	10.148391
1	1.339710	-6.634613	10.588686
1	8.523613	1.791503	14.577147
1	7.210847	2.632281	5.650713
1	-1.956370	1.625328	5.787646
1	-2.997953	2.684184	14.865564
6	2.763681	2.866554	11.179291
8	2.829183	4.008592	11.329482
17	2.836695	0.189795	13.252900
1	2.484691	1.209608	9.258343

Table S33. Cartesian coordinates for the optimized geometry of *cis*-**1o**.

Atomic Number	X	Y	Z
6	-3.219086	0.981603	-0.312982
6	-3.108995	-0.546593	-0.215363
6	-1.924143	-0.942893	0.679616
77	-0.046823	0.022281	-0.010907
6	-1.761892	-2.468860	0.763381
6	-0.545194	-2.832372	1.626062
6	1.574626	0.892292	-0.535655
17	-0.307757	-1.265060	-2.180573
1	-0.069233	0.729526	1.407096
8	2.555849	1.440934	-0.809628
1	-2.124847	-0.566616	1.695141
15	-1.541245	1.631473	-0.766898
6	-1.427938	3.304520	-0.042655
6	-0.456758	3.601731	0.921163
6	-0.388658	4.881499	1.480730
6	-1.292178	5.869576	1.082440
6	-2.264004	5.579118	0.117392
6	-2.329051	4.304726	-0.446172
6	-1.562237	1.942316	-2.558436
6	-2.392352	1.199545	-3.408785
6	-2.333066	1.393376	-4.790285
6	-1.437335	2.318796	-5.332048
6	-0.596719	3.051810	-4.487730
6	-0.656868	2.863500	-3.106791
15	0.895947	-1.842712	1.002808
6	1.870605	-2.944588	-0.065907
6	3.232779	-2.677519	-0.271073

6	3.976065	-3.459469	-1.155577
6	3.363943	-4.511604	-1.844833
6	2.005388	-4.774167	-1.650568
6	1.257841	-3.990358	-0.769492
6	1.984985	-1.567928	2.443370
6	2.256884	-0.271516	2.897018
6	3.079150	-0.073253	4.010646
6	3.631107	-1.169063	4.678317
6	3.364667	-2.467726	4.228137
6	2.549832	-2.666614	3.113507
1	-3.977417	1.327119	-1.024982
1	-3.448786	1.409541	0.671024
1	-4.053020	-0.956086	0.180416
1	-2.949434	-0.973880	-1.212581
1	-2.664695	-2.935445	1.190907
1	-1.630477	-2.861383	-0.251998
1	-0.309993	-3.902891	1.632189
1	-0.703690	-2.507679	2.662212
1	0.239007	2.825710	1.225000
1	0.372223	5.105499	2.224679
1	-1.238686	6.864847	1.517417
1	-2.965791	6.347209	-0.199001
1	-3.071727	4.087721	-1.210339
1	-3.068883	0.457555	-2.997450
1	-2.977630	0.810017	-5.443227
1	-1.388424	2.463759	-6.408657
1	0.107103	3.768382	-4.904324
1	-0.000502	3.433749	-2.453961
1	3.711731	-1.859795	0.261909
1	5.031438	-3.246427	-1.307887
1	3.942900	-5.119456	-2.536082
1	1.521391	-5.580951	-2.195492
1	0.196657	-4.180561	-0.646720
1	1.820582	0.572890	2.372409
1	3.289613	0.937191	4.353112
1	4.270724	-1.014552	5.544138
1	3.796618	-3.323094	4.742279
1	2.361025	-3.675328	2.753687

Table S34. Cartesian coordinates for the optimized geometry of *trans*-**1o**.

Atomic Number	X	Y	Z
6	-3.263631	0.906779	-0.178942
6	-3.061796	-0.611552	-0.316308
6	-1.908260	-1.066585	0.590566
77	-0.080141	0.163406	0.352125
6	-1.619846	-2.569027	0.459699
6	-0.469939	-2.957609	1.399672
6	1.510678	1.191248	0.079247
1	-0.057275	-0.411559	-1.122182
17	-0.428397	0.892154	2.764753
8	2.477148	1.785275	-0.152123

1	-2.206868	-0.870427	1.631044
15	-1.619875	1.675940	-0.499459
6	-1.681277	3.404906	0.068743
6	-0.764884	3.867110	1.021473
6	-0.807978	5.202026	1.435538
6	-1.761539	6.073820	0.904472
6	-2.677946	5.613906	-0.049147
6	-2.635853	4.284733	-0.469592
6	-1.475091	1.845547	-2.315227
6	-2.433735	1.350413	-3.208088
6	-2.240248	1.469523	-4.588760
6	-1.090556	2.086378	-5.085830
6	-0.129601	2.584263	-4.197304
6	-0.318433	2.460686	-2.821804
15	0.937361	-1.826567	0.997141
6	1.868705	-2.688336	-0.321428
6	2.209290	-2.034390	-1.511925
6	2.936491	-2.703596	-2.501209
6	3.326505	-4.030903	-2.308788
6	2.993424	-4.689718	-1.119538
6	2.272957	-4.020437	-0.130108
6	2.069140	-1.833699	2.422389
6	3.460629	-1.884728	2.238244
6	4.319115	-1.803268	3.336175
6	3.797068	-1.667732	4.626080
6	2.413190	-1.604719	4.813106
6	1.550035	-1.680376	3.718813
1	-4.047928	1.318904	-0.824607
1	-3.501300	1.157997	0.862077
1	-3.996678	-1.130827	-0.049489
1	-2.836039	-0.866565	-1.361183
1	-2.512936	-3.164473	0.710623
1	-1.349666	-2.811044	-0.578318
1	-0.165328	-4.007076	1.321189
1	-0.753069	-2.749055	2.437881
1	-0.046554	3.177869	1.452672
1	-0.097227	5.555657	2.178371
1	-1.792766	7.111082	1.230152
1	-3.418549	6.291578	-0.467453
1	-3.335086	3.934098	-1.225755
1	-3.329360	0.862944	-2.835392
1	-2.990057	1.078898	-5.272838
1	-0.941372	2.179047	-6.158898
1	0.768194	3.065974	-4.577318
1	0.435298	2.841678	-2.136931
1	1.895966	-1.006570	-1.661704
1	3.195275	-2.185766	-3.421654
1	3.889074	-4.551910	-3.079953
1	3.297721	-5.721863	-0.962727
1	2.032725	-4.531873	0.798908
1	3.873074	-1.991722	1.238937

1	5.394827	-1.846001	3.182569
1	4.466257	-1.604587	5.481001
1	2.001494	-1.482582	5.811892
1	0.480596	-1.583328	3.869573

Table S35. Cartesian coordinates for the optimized geometry of **1p**.

Atomic Number	X	Y	Z
6	-1.693314	-0.016134	2.971599
6	-2.782661	-0.279332	1.926145
7	-2.245217	-1.128318	0.867332
77	-0.480900	-0.349602	-0.056472
6	-3.298177	-1.488898	-0.077115
6	-2.741887	-2.476009	-1.109134
6	1.108816	0.271130	-0.839473
17	-1.910457	1.613805	-0.863769
1	0.266942	-1.618130	0.511946
8	2.071688	0.684649	-1.336286
15	-0.199850	0.591493	2.058561
6	1.243457	-0.051622	2.976593
6	2.251207	0.778362	3.485362
6	3.356663	0.221486	4.137262
6	3.459350	-1.162700	4.289873
6	2.454984	-1.995555	3.781491
6	1.357458	-1.444396	3.122176
6	-0.118217	2.396832	2.239976
6	0.275614	3.183272	1.149428
6	0.397138	4.567255	1.295001
6	0.122148	5.172033	2.524237
6	-0.273920	4.390971	3.615529
6	-0.391109	3.007393	3.474705
15	-1.196333	-1.723562	-1.799893
6	-1.591930	-0.995243	-3.416120
6	-1.008220	0.224223	-3.783728
6	-1.259305	0.765616	-5.046670
6	-2.095952	0.097555	-5.944521
6	-2.683278	-1.119240	-5.580982
6	-2.429940	-1.665450	-4.321829
6	-0.077775	-3.122754	-2.161296
6	0.292731	-3.956196	-1.092639
6	1.168307	-5.020636	-1.300986
6	1.696051	-5.256082	-2.576466
6	1.340404	-4.423356	-3.639428
6	0.453770	-3.360592	-3.435795
1	-2.004577	0.704294	3.734794
1	-1.401526	-0.953388	3.457888
1	-3.629013	-0.795233	2.413284
1	-3.160907	0.686284	1.541032
1	-4.128401	-1.971254	0.468615
1	-3.714423	-0.608048	-0.601486
1	-3.457327	-2.703045	-1.905915
1	-2.441835	-3.407917	-0.617496

1	2.175450	1.855685	3.371355
1	4.136476	0.873083	4.524311
1	4.319184	-1.593512	4.797284
1	2.533047	-3.074647	3.891644
1	0.591613	-2.091599	2.701056
1	0.450343	2.716461	0.187133
1	0.693419	5.172343	0.441966
1	0.210211	6.250588	2.632504
1	-0.490227	4.857843	4.573473
1	-0.686804	2.403883	4.329404
1	-0.391459	0.759572	-3.071410
1	-0.811081	1.717092	-5.321183
1	-2.295977	0.525293	-6.924208
1	-3.336226	-1.641588	-6.276129
1	-2.879001	-2.617513	-4.049772
1	-0.094750	-3.754659	-0.096699
1	1.447101	-5.661783	-0.468004
1	2.385050	-6.081850	-2.736978
1	1.751860	-4.597193	-4.630882
1	0.178953	-2.717494	-4.266599

Table S36. Cartesian coordinates for the optimized geometry of **1q**.

Atomic Number	X	Y	Z
77	5.336188	16.049329	6.849367
1	5.690062	17.569327	6.728209
15	7.592143	15.567966	6.479565
17	4.747135	13.508149	6.776810
15	3.116917	16.617611	6.561833
5	5.155142	16.264281	4.638951
6	5.399846	16.130703	8.771810
6	7.998297	15.508324	4.666867
6	8.247400	13.993856	7.138554
6	8.792851	16.819789	7.092555
6	1.968481	16.261565	7.952030
6	2.834083	18.380632	6.192377
6	2.412424	15.656279	5.147168
15	6.747694	16.615074	3.852833
15	3.605204	15.918064	3.761070
8	5.409792	16.309366	9.918322
1	9.046012	15.768552	4.479366
1	7.789352	14.496464	4.305025
6	7.755521	13.523073	8.363130
6	9.243008	13.266808	6.470350
6	8.350552	18.006336	7.687294
6	10.172206	16.606016	6.935160
6	0.903521	17.114448	8.283268
6	2.182473	15.095676	8.704908
6	1.820864	18.817536	5.325408
6	3.621587	19.338456	6.853379
1	1.380784	15.926579	4.900102
1	2.460124	14.606562	5.457536

6	6.886466	16.359780	2.057254
6	7.453366	18.282493	4.209959
6	3.468617	14.419301	2.685870
6	2.850746	17.227935	2.703264
1	6.950900	14.055124	8.857763
6	8.270936	12.353199	8.921880
1	9.618794	13.609268	5.509788
6	9.753230	12.091671	7.027396
1	7.286845	18.172228	7.815668
6	9.269984	18.974645	8.099233
1	10.530758	15.676716	6.499751
6	11.089992	17.571897	7.347246
6	0.062171	16.803200	9.355155
1	0.738283	18.026268	7.716185
1	3.009744	14.436642	8.451837
6	1.333425	14.786418	9.768793
1	1.194484	18.100266	4.807895
6	1.630647	20.179278	5.085251
6	3.420984	20.699419	6.624060
1	4.401827	19.008463	7.532651
6	7.090357	17.422332	1.164522
6	6.669680	15.064683	1.557748
6	6.583789	19.237737	4.749500
6	8.807915	18.599877	4.034787
6	3.261850	14.494150	1.300126
6	3.749636	13.172310	3.272403
6	3.598839	18.369342	2.405393
6	1.520161	17.143736	2.263927
6	9.270691	11.636258	8.257507
1	7.876937	11.991952	9.868571
1	10.521983	11.532381	6.499153
1	8.912040	19.896495	8.551100
6	10.639095	18.762629	7.927667
1	12.155534	17.394403	7.220263
1	-0.754612	17.474434	9.611211
6	0.274378	15.638625	10.098347
1	1.506408	13.881174	10.346164
6	2.431332	21.125708	5.731147
1	0.860655	20.495996	4.386600
1	4.040109	21.428553	7.142058
1	7.258299	18.424977	1.548043
6	7.069718	17.192447	-0.213871
1	6.473939	14.244244	2.243661
6	6.658939	14.838194	0.180793
6	7.059114	20.503086	5.101612
1	5.543452	18.960725	4.909983
1	9.494054	17.860618	3.627839
6	9.284863	19.862095	4.390760
1	3.067752	15.452324	0.828230
6	3.323703	13.339322	0.512907
6	3.792414	12.021485	2.486395

1	3.966181	13.111276	4.338141
1	4.616203	18.437681	2.783677
6	3.033429	19.417050	1.675506
6	0.941856	18.202184	1.559611
1	0.936127	16.249058	2.469891
1	9.663772	10.719465	8.690821
1	11.353553	19.517586	8.247689
1	-0.378978	15.399814	10.934577
1	2.284138	22.186581	5.543071
1	7.217452	18.021713	-0.901829
6	6.855962	15.901423	-0.706348
1	6.478979	13.835165	-0.196280
1	6.375847	21.236083	5.524253
6	8.409482	20.815565	4.923731
1	10.338250	20.100035	4.263091
6	3.583221	12.100679	1.102016
1	3.172032	13.412970	-0.562008
1	3.999072	11.061478	2.954495
1	3.626960	20.299136	1.445893
6	1.699596	19.340950	1.262562
1	-0.095562	18.137914	1.238257
1	6.838116	15.724823	-1.779377
1	8.785374	21.795900	5.208094
1	3.628529	11.202464	0.489954
1	1.249526	20.165185	0.713721

Table S37. Cartesian coordinates for the optimized geometry of **1q**[1].

Atomic Number	X	Y	Z
77	-0.947303	1.325521	-0.168129
1	-1.085635	1.859123	1.301942
15	-2.575289	-0.257386	0.236307
17	-0.541329	0.302370	-2.516899
15	1.091135	2.407389	-0.302441
13	0.575256	-0.335074	1.386299
6	-2.133954	2.775701	-0.735915
6	-2.091024	-1.917066	-0.429900
6	-4.174995	0.061655	-0.600645
6	-3.031360	-0.639446	1.967967
6	1.150309	3.892629	-1.383203
6	1.792637	2.988792	1.280843
6	2.389798	1.354593	-1.092056
15	-0.515131	-2.438983	0.403102
15	2.499498	-0.343812	-0.339420
8	-2.867356	3.668396	-0.804777
1	-2.886706	-2.664121	-0.325184
1	-1.872787	-1.751192	-1.488458
6	-5.353859	0.351809	0.099953
6	-4.173606	0.119704	-2.005353
6	-2.483436	0.078170	3.037333
6	-3.909164	-1.703439	2.236317

6	1.942878	5.010604	-1.084462
6	0.382949	3.880005	-2.558776
6	3.156176	2.892855	1.590134
6	0.921613	3.589436	2.203829
1	3.365807	1.852459	-1.132117
1	2.012835	1.242752	-2.111523
6	0.217569	-3.660282	-0.747239
6	-1.144626	-3.505643	1.770507
6	3.057935	-1.407071	-1.741271
6	4.086029	-0.226338	0.610048
1	-5.361635	0.327284	1.185544
6	-6.522153	0.680169	-0.594945
1	-3.250056	-0.050983	-2.553317
6	-5.344535	0.437680	-2.693309
1	-1.794645	0.891359	2.836785
6	-2.811225	-0.258138	4.354833
1	-4.338328	-2.271845	1.416035
6	-4.233412	-2.041412	3.548327
6	1.964121	6.107246	-1.951226
1	2.531930	5.031217	-0.171587
1	-0.235858	3.015647	-2.785825
6	0.416589	4.972930	-3.426400
1	3.848922	2.431151	0.895670
6	3.637672	3.365323	2.814301
6	1.405184	4.074245	3.418097
1	-0.137378	3.657983	1.970096
6	0.263487	-3.394684	-2.126751
6	0.819228	-4.831577	-0.253757
6	-0.793484	-3.226970	3.095110
6	-1.992275	-4.592509	1.497321
6	3.821068	-2.550252	-1.438012
6	2.706304	-1.166229	-3.078789
6	4.112262	-0.500428	1.981146
6	5.269987	0.174685	-0.032394
6	-6.522428	0.717472	-1.991057
1	-7.430209	0.908745	-0.041623
1	-5.333692	0.478978	-3.780015
1	-2.373226	0.303097	5.176553
6	-3.682676	-1.317005	4.611727
1	-4.903350	-2.874957	3.741880
1	2.571819	6.975651	-1.706926
6	1.203442	6.089359	-3.123586
1	-0.180864	4.955780	-4.334906
6	2.764900	3.956888	3.729705
1	4.693845	3.260643	3.049602
1	0.720531	4.535685	4.125866
1	-0.137365	-2.463736	-2.518912
6	0.851157	-4.312556	-2.995714
1	0.797791	-5.046245	0.811061
6	1.420897	-5.737496	-1.129685
6	-1.289512	-4.016948	4.137016

S117

1	-0.144013	-2.375974	3.302991
1	-2.254563	-4.827842	0.468480
6	-2.488424	-5.379007	2.535920
1	4.094434	-2.761388	-0.407195
6	4.256521	-3.403470	-2.450499
6	3.161867	-2.013361	-4.091479
1	2.057070	-0.337620	-3.340146
1	3.185826	-0.786423	2.480518
6	5.300418	-0.364056	2.707084
6	6.451454	0.328472	0.693668
1	5.266444	0.358959	-1.104345
1	-7.431955	0.972412	-2.530013
1	-3.928661	-1.585131	5.636623
1	1.218514	6.944427	-3.795601
1	3.139207	4.322348	4.683152
1	0.877485	-4.096013	-4.059800
6	1.427542	-5.487628	-2.504091
1	1.876871	-6.643008	-0.735379
1	-1.016604	-3.786021	5.164064
6	-2.137376	-5.090759	3.860800
1	-3.144879	-6.217675	2.314713
6	3.943551	-3.129630	-3.785133
1	4.844854	-4.281631	-2.195234
1	2.893252	-1.800091	-5.123787
1	5.308342	-0.581194	3.772927
6	6.467616	0.061379	2.068618
1	7.359611	0.650693	0.189048
1	1.892122	-6.194992	-3.186724
1	-2.525856	-5.703131	4.671576
1	4.292329	-3.789338	-4.576086
1	7.388619	0.181097	2.634989

Table S38. Cartesian coordinates for the optimized geometry of **1q²**.

Atomic Number	X	Y	Z
77	-1.019667	1.295185	-0.238847
1	-1.253689	1.926969	1.180918
15	-2.622949	-0.304148	0.231143
17	-0.544090	0.148325	-2.521555
15	1.014729	2.375051	-0.379862
31	0.466079	-0.373747	1.518898
6	-2.154594	2.687493	-0.985688
6	-2.175541	-1.946286	-0.500478
6	-4.257752	0.007824	-0.543562
6	-3.002780	-0.719662	1.974111
6	1.007798	3.848460	-1.474648
6	1.824053	2.952109	1.158804
6	2.330863	1.323296	-1.159414
15	-0.529395	-2.502032	0.160598
15	2.587142	-0.186107	-0.107269
8	-2.830358	3.596821	-1.220873

1	-2.955951	-2.701195	-0.353801
1	-2.067468	-1.736398	-1.566366
6	-4.262379	0.258703	-1.927019
6	-5.460712	0.065121	0.172103
6	-3.741504	-1.873626	2.284301
6	-2.527137	0.082572	3.018387
6	1.244209	5.150087	-1.012508
6	0.648027	3.647466	-2.818927
6	3.128960	3.471519	1.113661
6	1.180349	2.839810	2.396165
1	3.260616	1.877917	-1.333452
1	1.912359	0.998270	-2.115893
6	0.124623	-3.628218	-1.136610
6	-1.055366	-3.714923	1.452773
6	3.328639	-1.413181	-1.248965
6	4.021872	0.310141	0.936949
1	-3.323975	0.256788	-2.478050
6	-5.460428	0.537957	-2.583522
1	-5.466159	-0.111317	1.243595
6	-6.657931	0.360707	-0.489092
1	-4.115132	-2.511311	1.489026
6	-3.995597	-2.219215	3.610610
1	-1.947688	0.968392	2.780827
6	-2.785326	-0.259152	4.348734
6	1.137286	6.237221	-1.886251
1	1.504492	5.319507	0.028018
1	0.411979	2.645851	-3.171321
6	0.554655	4.733672	-3.688557
1	3.643331	3.561707	0.161304
6	3.775131	3.869145	2.281911
6	1.826260	3.240693	3.569647
1	0.177077	2.429647	2.434032
6	1.053558	-4.609764	-0.744745
6	-0.206990	-3.513969	-2.495345
6	-0.676871	-3.523828	2.786335
6	-1.866543	-4.813563	1.121349
6	4.396740	-2.226012	-0.829626
6	2.761785	-1.628396	-2.516820
6	3.925407	0.235334	2.331057
6	5.213970	0.774605	0.355819
6	-6.661708	0.590726	-1.866430
1	-5.454506	0.729278	-3.654064
1	-7.585652	0.412982	0.076361
1	-4.555253	-3.123591	3.834301
6	-3.515444	-1.411542	4.646919
1	-2.404271	0.369875	5.149577
1	1.315947	7.244132	-1.515672
6	0.799746	6.031771	-3.225618
1	0.276734	4.567564	-4.726800
6	3.123259	3.752995	3.514720
1	4.789451	4.256105	2.233131

S119

1	1.316371	3.142473	4.524975
1	1.330481	-4.705230	0.302703
6	1.608960	-5.476837	-1.684211
1	-0.868827	-2.726292	-2.838434
6	0.339556	-4.396351	-3.430455
6	-1.112358	-4.408077	3.778597
1	-0.058225	-2.666099	3.047730
1	-2.147250	-4.982616	0.084108
6	-2.306365	-5.692112	2.110950
1	4.840066	-2.077396	0.151015
6	4.907160	-3.212508	-1.675707
6	3.285748	-2.607290	-3.360759
1	1.899281	-1.049111	-2.835343
1	2.998813	-0.115858	2.783151
6	4.999418	0.629785	3.135149
6	6.284612	1.168847	1.157029
1	5.304962	0.818464	-0.726962
1	-7.593238	0.820201	-2.378655
1	-3.705652	-1.684489	5.682377
1	0.717383	6.877957	-3.903798
1	3.630247	4.054995	4.428242
1	2.326835	-6.227968	-1.363465
6	1.243580	-5.382355	-3.030599
1	0.062238	-4.301057	-4.477925
1	-0.816935	-4.244461	4.812399
6	-1.930626	-5.488617	3.445074
1	-2.937077	-6.537355	1.844160
6	4.359630	-3.400504	-2.947365
1	5.737911	-3.829672	-1.340491
1	2.838059	-2.761739	-4.338603
1	4.909311	0.576238	4.217526
6	6.177756	1.098043	2.551619
1	7.202558	1.528087	0.697029
1	1.672199	-6.062629	-3.762647
1	-2.273918	-6.173635	4.217215
1	4.758462	-4.167496	-3.606955
1	7.011865	1.407817	3.177302

Free ligands

Table S39. Cartesian coordinates for the optimized geometry of the free ligand of **1a**.

Atomic Number	X	Y	Z
15	7.877647	15.228534	6.349021
15	2.451407	17.776146	6.854422
6	5.192981	17.240307	5.009554
6	7.718653	15.703688	4.531171
6	8.468150	13.488362	6.170566
6	9.436885	16.122411	6.782468
6	0.993625	17.270012	7.866583
6	1.703980	18.825343	5.537422

6	2.683972	16.150745	5.901977
15	6.754487	17.246329	4.301359
15	3.891999	16.228737	4.534270
1	8.689529	15.787927	4.028507
1	7.144204	14.906500	4.045913
6	8.412989	12.693453	7.329339
6	8.922229	12.906348	4.977037
6	9.371988	17.124297	7.761444
6	10.667686	15.844604	6.166792
6	-0.158459	18.068546	7.955189
6	1.083002	16.119037	8.670783
6	0.601088	18.419486	4.767911
6	2.279844	20.080264	5.292232
1	1.737555	15.801047	5.473204
1	3.035589	15.396555	6.613334
6	6.684131	17.498791	2.501032
6	7.730965	18.595770	5.002902
6	4.417478	14.510773	4.194910
6	2.995391	16.783127	3.057755
1	8.054677	13.124144	8.262992
6	8.806659	11.354356	7.296128
1	8.973126	13.491436	4.063187
6	9.306928	11.563140	4.940127
1	8.423802	17.342073	8.247975
6	10.515450	17.849418	8.108445
1	10.735753	15.048975	5.427989
6	11.809657	16.567919	6.513043
6	-1.201495	17.713809	8.815539
1	-0.245729	18.965610	7.349189
1	1.975717	15.496978	8.642651
6	0.035914	15.762040	9.521714
1	0.134940	17.455862	4.956504
6	0.089875	19.248636	3.771280
6	1.765291	20.916042	4.295796
1	3.132042	20.404744	5.885839
6	6.648657	18.809757	1.999143
6	6.576642	16.414312	1.619360
6	7.153279	19.560641	5.838954
6	9.094364	18.676321	4.675786
6	4.489390	13.989585	2.894811
6	4.894250	13.744384	5.273784
6	3.304952	18.019369	2.482999
6	1.966074	15.994239	2.517232
6	9.250014	10.783518	6.098429
1	8.761129	10.755458	8.202316
1	9.654705	11.127683	4.006263
1	10.453608	18.626057	8.866475
6	11.733936	17.573665	7.484119
1	12.760302	16.341485	6.035959
1	-2.087247	18.341926	8.870968
6	-1.111169	16.558875	9.596291

S121

1	0.118246	14.864891	10.130375
6	0.671704	20.499605	3.534329
1	-0.761003	18.922332	3.178950
1	2.214908	21.890136	4.119361
1	6.743480	19.653449	2.677923
6	6.495249	19.029378	0.630683
1	6.607789	15.395959	1.992686
6	6.414365	16.639340	0.250203
6	7.941712	20.591703	6.356230
1	6.095859	19.513030	6.079526
1	9.551524	17.931972	4.030657
6	9.873775	19.709156	5.190526
1	4.133924	14.575441	2.053686
6	5.031327	12.718569	2.678437
6	5.428500	12.475908	5.054551
1	4.885813	14.152052	6.281259
1	4.082449	18.630090	2.927760
6	2.604018	18.458743	1.359368
6	1.264478	16.439710	1.397878
1	1.718154	15.033812	2.962748
1	9.550028	9.739193	6.069382
1	12.625350	18.132601	7.757940
1	-1.925233	16.283011	10.261412
1	0.269078	21.147309	2.759514
1	6.475778	20.045866	0.246411
6	6.371062	17.944888	-0.244763
1	6.326757	15.794804	-0.428381
1	7.493445	21.335917	7.009072
6	9.298541	20.666331	6.033065
1	10.930176	19.760228	4.944350
6	5.499682	11.961879	3.755039
1	5.084821	12.322053	1.667622
1	5.811491	11.899546	5.891098
1	2.846894	19.420374	0.916073
6	1.588160	17.670220	0.814632
1	0.468488	15.829020	0.979940
1	6.249122	18.118176	-1.310717
1	9.909705	21.468549	6.438285
1	5.926724	10.977285	3.585634
1	1.041547	18.014768	-0.059531
1	5.123726	17.615403	6.026059

Table S40. Cartesian coordinates for the optimized geometry of the free ligand of **1b.**

Atomic Number	X	Y	Z
6	-0.806300	1.235672	3.133088
6	-0.547003	-0.127254	2.994459
6	0.521366	-0.531446	2.182602
7	1.303384	0.347955	1.534059
6	1.040974	1.658727	1.653079
6	-0.006405	2.146211	2.449470

6	1.854557	2.594904	0.807627
6	0.825813	-1.988526	1.964563
15	1.320295	2.441255	-1.022436
6	1.642648	4.151777	-1.629020
6	2.651802	4.967406	-1.088660
6	2.946148	6.213007	-1.652847
6	2.235724	6.668251	-2.765794
6	1.231743	5.863557	-3.317009
6	0.944038	4.617508	-2.759868
6	-0.514912	2.449639	-0.781856
6	-1.150443	1.197815	-0.743651
6	-2.508169	1.095771	-0.431363
6	-3.253384	2.250184	-0.177421
6	-2.635209	3.504631	-0.232970
6	-1.273173	3.603371	-0.525882
15	0.497741	-2.529636	0.177493
6	0.834565	-4.338540	0.398519
6	-0.155458	-5.333703	0.431972
6	0.194304	-6.680473	0.575097
6	1.535302	-7.053136	0.696285
6	2.530488	-6.069988	0.662592
6	2.183437	-4.727464	0.504203
6	-1.346826	-2.499622	0.070486
6	-1.903654	-2.416674	-1.217247
6	-3.288479	-2.413425	-1.402248
6	-4.141723	-2.470879	-0.296211
6	-3.601207	-2.542222	0.991527
6	-2.215767	-2.564784	1.170677
1	-1.629689	1.581140	3.753935
1	-1.158019	-0.867602	3.502269
1	-0.194532	3.214124	2.505431
1	1.718094	3.631207	1.135648
1	2.916623	2.329869	0.853403
1	1.898053	-2.169816	2.103550
1	0.278219	-2.623976	2.669330
1	3.216850	4.634679	-0.221925
1	3.730225	6.828267	-1.216684
1	2.461634	7.638513	-3.201550
1	0.671507	6.207513	-4.183768
1	0.161269	4.002409	-3.198462
1	-0.573410	0.295890	-0.933901
1	-2.975609	0.116302	-0.388022
1	-4.312174	2.174613	0.060843
1	-3.212424	4.406409	-0.038525
1	-0.794808	4.579096	-0.553923
1	-1.202874	-5.058654	0.345879
1	-0.586016	-7.438377	0.595457
1	1.804863	-8.100488	0.809961
1	3.578086	-6.349946	0.748895
1	2.968573	-3.974108	0.455321
1	-1.244770	-2.348760	-2.081083

S123

1	-3.699658	-2.350782	-2.406947
1	-5.220017	-2.455038	-0.436060
1	-4.258888	-2.586012	1.856951
1	-1.813070	-2.640832	2.175503

Table S41. Cartesian coordinates for the optimized geometry of the free ligand of **1c**.

Atomic Number	X	Y	Z
6	3.279245	0.715998	0.447518
6	2.415458	-0.221297	1.294942
7	1.525282	-1.033971	0.474261
6	0.622122	-1.867915	1.254119
6	-0.259460	-2.750514	0.363407
1	2.058837	-1.598257	-0.181368
15	2.250809	1.755107	-0.755293
6	3.336377	3.237717	-0.936982
6	4.735074	3.176919	-0.811561
6	5.529447	4.299177	-1.070319
6	4.940859	5.505781	-1.454857
6	3.548992	5.579787	-1.586607
6	2.758517	4.457756	-1.338567
6	0.971844	2.376288	0.430850
6	1.236476	3.336671	1.421187
6	0.250864	3.693562	2.344575
6	-1.009557	3.086979	2.295042
6	-1.283395	2.129805	1.313899
6	-0.299486	1.782624	0.383411
15	-1.311975	-1.816364	-0.884432
6	-2.215782	-3.278162	-1.584956
6	-3.392527	-3.814171	-1.036454
6	-3.999970	-4.933439	-1.612314
6	-3.436508	-5.539545	-2.739582
6	-2.265423	-5.014593	-3.294596
6	-1.666243	-3.887136	-2.726772
6	-2.621142	-1.061750	0.179768
6	-2.780947	-1.299801	1.553695
6	-3.793882	-0.663940	2.278543
6	-4.674688	0.210873	1.637625
6	-4.531045	0.453129	0.267002
6	-3.506936	-0.168138	-0.449308
1	3.999238	0.135160	-0.145869
1	3.852127	1.373937	1.113194
1	3.074173	-0.834162	1.944673
1	1.783285	0.379944	1.960780
1	1.160901	-2.524624	1.969740
1	-0.002155	-1.193720	1.855421
1	0.372435	-3.419194	-0.238104
1	-0.891676	-3.397502	0.985275
1	5.215287	2.250304	-0.508145
1	6.610052	4.228438	-0.964572
1	5.557697	6.379554	-1.651072

1	3.078489	6.514544	-1.884101
1	1.678019	4.529834	-1.444758
1	2.215331	3.807995	1.465219
1	0.467921	4.440567	3.105511
1	-1.775263	3.361137	3.017664
1	-2.257145	1.650856	1.269866
1	-0.508675	1.030155	-0.372667
1	-3.838464	-3.350948	-0.159998
1	-4.914035	-5.333471	-1.178430
1	-3.910653	-6.410199	-3.186667
1	-1.824982	-5.474755	-4.176414
1	-0.767388	-3.469604	-3.178356
1	-2.116134	-1.984977	2.070541
1	-3.895008	-0.855767	3.344513
1	-5.462480	0.704981	2.201186
1	-5.207267	1.137224	-0.240352
1	-3.388594	0.044323	-1.510536

Table S42. Cartesian coordinates for the optimized geometry of the free ligand of **1d**.

Atomic Number	X	Y	Z
6	2.484664	0.942622	-1.769864
6	1.594816	1.352772	-2.711679
7	0.425185	1.660994	-2.028514
6	0.529697	1.463271	-0.679183
7	1.815941	1.014453	-0.553972
6	2.404236	0.635873	0.730905
6	3.085175	-0.738505	0.705709
6	-0.781131	2.141522	-2.712102
6	-2.015900	2.161605	-1.812070
15	1.918969	-2.137406	0.217821
6	2.950377	-3.598257	0.680587
6	4.355512	-3.584024	0.670838
6	5.086946	-4.747748	0.932559
6	4.428045	-5.946755	1.211698
6	3.028455	-5.974956	1.222916
6	2.299583	-4.816580	0.955078
6	0.751598	-2.059771	1.649964
6	1.145901	-2.357220	2.966323
6	0.234154	-2.255811	4.017787
6	-1.084055	-1.855173	3.765291
6	-1.484716	-1.554895	2.462200
6	-0.570271	-1.656558	1.408164
15	-2.569341	0.431399	-1.282323
6	-4.146726	0.279183	-2.247450
6	-5.169606	1.243242	-2.202495
6	-6.330058	1.088589	-2.961378
6	-6.487961	-0.037600	-3.779364
6	-5.481850	-1.004472	-3.831123
6	-4.318742	-0.845685	-3.067848
6	-3.212537	0.777985	0.414186
6	-4.421063	0.218514	0.866082

6	-4.831117	0.381902	2.192184
6	-4.042079	1.107865	3.089652
6	-2.833534	1.657565	2.651517
6	-2.414369	1.488241	1.330570
1	3.140058	1.396445	1.028190
1	1.586404	0.648043	1.456366
1	3.506517	-0.935774	1.699622
1	3.917749	-0.729639	-0.008849
1	-0.951497	1.494874	-3.583624
1	-0.586996	3.156585	-3.086817
1	-1.806616	2.747658	-0.914530
1	-2.830346	2.647294	-2.361200
1	4.892637	-2.662522	0.463702
1	6.174323	-4.711738	0.923459
1	4.996669	-6.850092	1.419120
1	2.503415	-6.902195	1.442012
1	1.212294	-4.851779	0.972302
1	2.165085	-2.682666	3.162537
1	0.549239	-2.490537	5.032558
1	-1.795643	-1.774102	4.584079
1	-2.500740	-1.227947	2.263891
1	-0.883218	-1.406317	0.396765
1	-5.058323	2.111875	-1.557400
1	-7.113779	1.841782	-2.914293
1	-7.392997	-0.158875	-4.370275
1	-5.600054	-1.882339	-4.462413
1	-3.536148	-1.601241	-3.106674
1	-5.049134	-0.341617	0.178316
1	-5.771290	-0.055916	2.521034
1	-4.363238	1.237662	4.120627
1	-2.202276	2.207959	3.345881
1	-1.444798	1.865325	1.010859
1	1.690671	1.440243	-3.784885
1	3.503288	0.597566	-1.868072

Table S43. Cartesian coordinates for the optimized geometry of the free ligand of **1e**.

Atomic Number	X	Y	Z
15	7.339191	14.731706	6.278273
15	3.072191	17.055268	7.061160
6	5.375878	16.884992	4.590461
6	7.786915	15.144177	4.501713
6	8.719328	13.565852	6.679030
6	7.892560	16.257262	7.161401
6	1.475607	16.765982	7.948901
6	2.724844	18.672464	6.235785
6	2.868507	15.837796	5.642284
15	6.855072	16.637805	3.911192
15	3.929905	16.219214	4.179957
1	8.866589	15.286920	4.372414
1	7.477521	14.290174	3.890232

6	9.173550	13.461867	8.007403
6	9.243483	12.673358	5.726906
6	6.929392	17.006044	7.851447
6	9.223223	16.703823	7.143844
6	0.920410	17.804291	8.720739
6	0.857365	15.504086	7.990385
6	1.490894	18.987434	5.646233
6	3.763727	19.612331	6.182835
1	1.821438	15.761847	5.325210
1	3.186040	14.855892	6.012389
6	6.951190	16.504409	2.072636
6	7.997403	18.021299	4.286870
6	3.975104	14.605608	3.283663
6	2.847026	17.280574	3.132921
1	8.787807	14.144603	8.760992
6	10.125725	12.507184	8.367176
1	8.915243	12.726486	4.691876
6	10.194498	11.714163	6.088160
1	5.890075	16.687963	7.845253
6	7.292223	18.181289	8.516181
1	9.977397	16.129001	6.612246
6	9.584817	17.878539	7.803023
6	-0.220529	17.590837	9.494857
1	1.377889	18.790899	8.701767
1	1.262760	14.679263	7.410049
6	-0.283390	15.288856	8.770146
1	0.676845	18.268708	5.686258
6	1.302746	20.213342	5.008056
6	3.577772	20.841701	5.544609
1	4.722647	19.367774	6.631486
6	7.060361	17.676600	1.303933
6	6.743426	15.282285	1.413848
6	7.518155	19.122959	5.000687
6	9.328245	18.005420	3.845875
6	3.585242	14.458912	1.945447
6	4.590996	13.522616	3.937287
6	3.392575	18.457731	2.613620
6	1.519350	16.942263	2.830846
6	10.641553	11.627396	7.409074
1	10.468790	12.452618	9.398192
1	10.590282	11.038769	5.332443
1	6.534615	18.754410	9.046497
6	8.618445	18.618905	8.492939
1	10.616013	18.222193	7.770932
1	-0.637737	18.411267	10.074906
6	-0.828984	16.330837	9.523726
1	-0.747027	14.304699	8.783162
6	2.347586	21.142144	4.954534
1	0.347350	20.439124	4.540835
1	4.393767	21.559977	5.503796
1	7.218475	18.630898	1.800115

S127

6	6.973014	17.626381	-0.087783
1	6.616547	14.363894	1.979101
6	6.658225	15.232373	0.020486
6	8.364912	20.197744	5.282591
1	6.482860	19.109638	5.329624
1	9.702197	17.157836	3.275580
6	10.173352	19.080308	4.123395
1	3.127213	15.291583	1.420499
6	3.806775	13.253207	1.271898
6	4.811248	12.320882	3.264847
1	4.931049	13.634458	4.965589
1	4.418541	18.708650	2.872756
6	2.620753	19.293456	1.802803
6	0.747058	17.775516	2.020540
1	1.088018	16.023541	3.222272
1	11.385043	10.885026	7.689332
1	8.900348	19.536713	9.004417
1	-1.718606	16.164843	10.126561
1	2.202300	22.095363	4.451113
1	7.063233	18.542323	-0.667693
6	6.774126	16.401917	-0.735216
1	6.491754	14.276729	-0.470979
1	7.990952	21.046575	5.850624
6	9.691691	20.178735	4.844946
1	11.204639	19.063493	3.778113
6	4.420268	12.183082	1.926119
1	3.508066	13.157043	0.230433
1	5.290017	11.492731	3.783085
1	3.049157	20.212916	1.410508
6	1.298576	18.954526	1.505428
1	-0.281991	17.508032	1.790661
1	6.707581	16.361302	-1.819969
1	10.351309	21.015042	5.065668
1	4.595116	11.247471	1.399908
1	0.695800	19.606464	0.877025

Table S44. Cartesian coordinates for the optimized geometry of the free ligand of **1f**.

Atomic Number	X	Y	Z
15	8.129127	15.188073	6.305233
15	1.979101	17.776000	6.976069
5	5.114000	17.446268	5.431142
6	7.656853	15.796612	4.600465
6	8.810663	13.518248	5.872352
6	9.724376	16.105886	6.558513
6	0.325805	17.304347	7.657745
6	1.470472	18.740865	5.480243
6	2.464145	16.132411	6.192107
15	6.732879	17.405244	4.587308
15	3.814799	16.265903	4.938354
1	8.529265	15.881069	3.940369

1	6.981482	15.043763	4.179958
6	9.152610	12.685344	6.953232
6	8.973064	13.018036	4.571523
6	9.799196	17.033205	7.607009
6	10.853783	15.902480	5.749729
6	-0.650723	18.303418	7.832092
6	0.042744	16.009470	8.125366
6	0.392279	18.369436	4.661035
6	2.220281	19.876711	5.142958
1	1.594025	15.651246	5.728803
1	2.838344	15.486150	6.993711
6	6.746898	17.777943	2.766501
6	7.858826	18.668530	5.267301
6	4.459769	14.558821	4.735532
6	2.857574	16.512072	3.362707
1	9.024257	13.049747	7.971566
6	9.647719	11.398011	6.741316
1	8.710661	13.629565	3.713791
6	9.460105	11.724989	4.355822
1	8.927786	17.202890	8.234832
6	10.975650	17.751913	7.836796
1	10.814388	15.171331	4.945272
6	12.030646	16.616092	5.980128
6	-1.872210	18.013068	8.440329
1	-0.456809	19.312127	7.474367
1	0.775211	15.214791	8.010059
6	-1.180035	15.719610	8.739233
1	-0.198518	17.493470	4.915463
6	0.074597	19.113844	3.526000
6	1.900993	20.626713	4.006696
1	3.065984	20.162111	5.762961
6	6.652645	19.115462	2.339492
6	6.597495	16.758998	1.809934
6	7.493751	19.424807	6.388245
6	9.113558	18.872104	4.673179
6	4.633241	13.971402	3.474006
6	4.916034	13.880344	5.877059
6	3.232201	17.567730	2.528710
6	1.814953	15.657908	2.970086
6	9.799934	10.910273	5.438211
1	9.908182	10.772336	7.592225
1	9.573755	11.356128	3.338459
1	11.014939	18.477950	8.645129
6	12.093501	17.543261	7.026356
1	12.900133	16.446399	5.348355
1	-2.615691	18.798947	8.555065
6	-2.143513	16.718426	8.897551
1	-1.378759	14.708801	9.089153
6	0.829531	20.245255	3.197137
1	-0.752478	18.806251	2.890833
1	2.493716	21.502668	3.752970

S129

1	6.754077	19.917217	3.067838
6	6.420352	19.422535	0.999984
1	6.647923	15.716378	2.112146
6	6.354787	17.066441	0.468756
6	8.367784	20.388807	6.896303
1	6.530948	19.244622	6.857061
1	9.401871	18.288890	3.802667
6	9.991108	19.824182	5.191867
1	4.287640	14.488985	2.584453
6	5.262434	12.726044	3.357460
6	5.518731	12.627316	5.760685
1	4.835587	14.355264	6.851333
1	4.041040	18.221935	2.843899
6	2.574099	17.773797	1.313268
6	1.154012	15.863818	1.759054
1	1.525900	14.823134	3.605500
1	10.178496	9.904705	5.270302
1	13.010153	18.100324	7.206784
1	-3.095880	16.492138	9.371009
1	0.584555	20.822459	2.308400
1	6.360571	20.463553	0.688791
6	6.264914	18.398031	0.055787
1	6.233250	16.262270	-0.254049
1	8.074602	20.979183	7.761451
6	9.616870	20.588980	6.300469
1	10.968116	19.963081	4.736220
6	5.700337	12.051126	4.498514
1	5.410016	12.287318	2.373012
1	5.877824	12.115169	6.648881
1	2.877504	18.597062	0.671252
6	1.536145	16.923882	0.926914
1	0.345542	15.199520	1.460686
1	6.075486	18.637583	-0.987734
1	10.301468	21.331282	6.704610
1	6.199931	11.090425	4.408440
1	1.022264	17.083600	-0.018569
1	4.766456	18.477964	5.930069

Table S45. Cartesian coordinates for the optimized geometry of the free ligand of **1g**.

Atomic Number	X	Y	Z
6	1.952481	1.297237	4.050070
6	1.554927	-0.039382	3.942460
6	0.826677	-0.455697	2.812722
6	0.466809	0.413630	1.763169
6	0.861136	1.760173	1.923931
6	1.606424	2.197295	3.036413
6	0.486445	2.789872	0.873514
6	0.408651	-1.906644	2.683712
15	1.490546	2.675702	-0.734503
6	1.250953	4.432447	-1.314295

6	2.335063	5.320607	-1.213790
6	2.200879	6.668706	-1.564801
6	0.974804	7.152201	-2.030046
6	-0.114242	6.278408	-2.138666
6	0.023600	4.934859	-1.783796
6	0.331759	1.807257	-1.884112
6	0.408925	2.052549	-3.268761
6	-0.416639	1.367081	-4.162260
6	-1.329302	0.417186	-3.686523
6	-1.399149	0.154842	-2.315309
6	-0.572561	0.838484	-1.416847
15	0.186986	-2.330567	0.863622
6	0.150978	-4.203672	1.111875
6	-0.914258	-4.914296	1.695596
6	-0.844653	-6.296768	1.886253
6	0.299694	-7.005086	1.499711
6	1.368906	-6.316275	0.919417
6	1.288710	-4.932506	0.725373
6	-1.619751	-2.085727	0.558914
6	-2.261187	-2.854086	-0.430145
6	-3.592244	-2.614674	-0.782488
6	-4.312677	-1.596226	-0.146955
6	-3.689917	-0.832955	0.845064
6	-2.356763	-1.074298	1.198476
1	2.526781	1.634803	4.912890
1	1.820414	-0.748835	4.731003
1	1.916190	3.243138	3.115734
1	-0.572888	2.703456	0.598618
1	0.661676	3.809732	1.242554
1	1.153826	-2.600412	3.100196
1	-0.540927	-2.112965	3.205266
1	3.293632	4.946381	-0.856990
1	3.055246	7.338450	-1.480245
1	0.867695	8.198957	-2.308843
1	-1.073759	6.646695	-2.498690
1	-0.823295	4.259955	-1.877917
1	1.106239	2.797537	-3.648681
1	-0.349229	1.577202	-5.229053
1	-1.975083	-0.117569	-4.381684
1	-2.093116	-0.588550	-1.931708
1	-0.585099	0.589830	-0.350984
1	-1.809836	-4.375237	1.995268
1	-1.683071	-6.823730	2.340470
1	0.354176	-8.082535	1.646056
1	2.262838	-6.856541	0.610711
1	2.120770	-4.402582	0.262437
1	-1.709852	-3.645531	-0.933947
1	-4.062666	-3.216281	-1.558817
1	-5.346131	-1.398314	-0.426548
1	-4.239502	-0.035842	1.343431
1	-1.852784	-0.445379	1.927322

Table S46. Cartesian coordinates for the optimized geometry of the free ligand of **1h**.

Atomic Number	X	Y	Z
6	-0.112167	1.720223	-1.181233
6	-0.712353	2.246625	0.162014
6	-0.074557	1.504207	1.325389
6	1.435628	1.396709	1.381299
6	1.978062	0.852445	0.022407
6	1.428622	1.526143	-1.261479
6	1.631474	0.563764	-2.466318
6	2.148582	2.845990	-1.600475
6	1.716437	0.336936	2.471271
6	2.180106	2.682141	1.807143
6	-2.216207	1.849551	0.232445
6	-0.641717	3.785407	0.267000
15	-3.370597	2.374962	-1.144416
6	-2.954465	1.109397	-2.439846
6	-2.442882	1.535266	-3.676080
6	-2.000941	0.609926	-4.627357
6	-2.071092	-0.759918	-4.358477
6	-2.593522	-1.197776	-3.133259
6	-3.032330	-0.271398	-2.187264
6	-4.962792	1.634197	-0.536609
6	-6.092291	1.752870	-1.369255
6	-7.328010	1.227801	-0.990339
6	-7.467256	0.579976	0.243901
6	-6.357440	0.461160	1.083115
6	-5.115563	0.979722	0.698015
15	0.645477	0.719722	3.978714
6	1.479319	-0.464941	5.177837
6	0.771460	-1.381461	5.981260
6	1.412364	-2.129481	6.973485
6	2.785619	-1.984541	7.197981
6	3.505807	-1.070517	6.418783
6	2.860326	-0.322328	5.432951
6	-0.929178	-0.193330	3.673936
6	-2.143950	0.432721	4.006359
6	-3.367699	-0.193657	3.773532
6	-3.407011	-1.466643	3.177234
6	-2.208610	-2.103771	2.849235
6	-0.980706	-1.481747	3.108394
15	3.370412	-0.014193	-2.862380
6	3.028852	-1.033301	-4.380840
6	4.108113	-1.759963	-4.920459
6	3.955910	-2.536932	-6.068577
6	2.716794	-2.595873	-6.718792
6	1.638377	-1.876952	-6.199435
6	1.789509	-1.106698	-5.040133
6	3.579636	-1.396416	-1.642894
6	2.687741	-2.480557	-1.583160
6	2.816108	-3.454752	-0.591449

6	3.845943	-3.366549	0.351533
6	4.753852	-2.303738	0.287173
6	4.621183	-1.329788	-0.706197
1	-0.564662	0.734320	-1.338016
1	-0.416596	2.340886	-2.040281
1	-0.471521	0.481676	1.312484
1	1.690724	-0.205514	-0.021549
1	3.079691	0.880763	-0.012368
1	1.005566	-0.326998	-2.325398
1	1.266769	1.076849	-3.368230
1	3.231265	2.683443	-1.678342
1	1.787398	3.224310	-2.567683
1	1.973874	3.621908	-0.856546
1	1.456621	-0.661763	2.097003
1	2.772540	0.313992	2.768245
1	3.260684	2.479960	1.880085
1	2.046908	3.509819	1.111006
1	1.813793	3.009914	2.787385
1	-2.286951	0.757634	0.320806
1	-2.617489	2.271541	1.163776
1	-1.182234	4.258995	-0.565926
1	-1.100752	4.099213	1.213161
1	0.381112	4.162947	0.258149
1	-2.369229	2.601654	-3.881474
1	-1.593330	0.959609	-5.574278
1	-1.718258	-1.482137	-5.091604
1	-2.649513	-2.262516	-2.914289
1	-3.423978	-0.617949	-1.233441
1	-5.995159	2.258147	-2.329488
1	-8.184554	1.326604	-1.655123
1	-8.430872	0.173191	0.544598
1	-6.446874	-0.046081	2.041952
1	-4.269212	0.852427	1.365089
1	-0.294825	-1.516880	5.818663
1	0.835358	-2.836333	7.569020
1	3.286050	-2.570298	7.966869
1	4.575489	-0.940537	6.580280
1	3.439696	0.392491	4.850260
1	-2.117105	1.437213	4.424891
1	-4.294156	0.313692	4.037858
1	-4.360656	-1.948464	2.970518
1	-2.225889	-3.091540	2.390004
1	-0.055958	-1.999152	2.865514
1	5.077381	-1.719495	-4.425210
1	4.804699	-3.095178	-6.459567
1	2.596091	-3.196628	-7.617948
1	0.667341	-1.918824	-6.689975
1	0.925257	-0.579638	-4.648926
1	1.879080	-2.549514	-2.307344
1	2.105204	-4.277665	-0.546178
1	3.935663	-4.115464	1.135241

1	5.554441	-2.225448	1.019724
1	5.312700	-0.489823	-0.739084

Table S47. Cartesian coordinates for the optimized geometry of the free ligand of **1i**.

Atomic Number	X	Y	Z
15	-0.691631	3.589301	6.993483
6	0.878666	2.675950	7.540788
6	-0.200507	5.304185	7.465068
6	-0.415057	3.551457	5.172718
15	-0.656863	3.650899	13.863805
7	-0.718239	3.366458	10.443122
6	1.167062	2.820361	9.038426
1	0.769945	1.619239	7.273314
1	1.750451	3.062109	7.000563
6	1.029936	5.871856	7.090932
6	-1.078113	6.052334	8.263870
6	-0.544725	4.708104	4.386540
6	-0.178184	2.320892	4.533646
6	-2.427444	3.218611	13.336627
6	-0.662425	5.442464	13.422178
6	-0.906754	3.660428	15.689098
7	0.008658	2.429434	9.862731
7	-1.719374	2.713543	11.003811
1	2.005609	2.187186	9.347722
1	1.384295	3.858964	9.297817
1	1.710199	5.315409	6.450337
6	1.376427	7.155766	7.514510
6	-0.734687	7.339913	8.687001
1	-2.034278	5.622874	8.555105
1	-0.732125	5.667995	4.859471
6	-0.424503	4.636052	2.996018
6	-0.050081	2.253328	3.145114
1	-0.095392	1.405313	5.116416
6	-2.682305	3.448252	11.843759
1	-2.617530	2.171821	13.598235
1	-3.147786	3.831052	13.890679
6	-1.680160	6.322205	13.830866
6	0.373380	5.932304	12.612742
6	-0.449816	4.722082	16.487126
6	-1.465645	2.532739	16.317439
6	-0.511110	1.183470	10.038163
6	-1.645770	1.369985	10.797496
1	2.328531	7.586963	7.214821
6	0.493337	7.891066	8.314870
1	-1.422639	7.907817	9.307553
1	-0.524435	5.541041	2.401867
6	-0.172797	3.411778	2.371483
1	0.142050	1.295705	2.667482
1	-3.681390	3.107957	11.551303
1	-2.569449	4.503223	11.583350

1	-2.476489	5.964628	14.479603
6	-1.664407	7.659274	13.431290
6	0.393504	7.272549	12.214610
1	1.166582	5.260137	12.292821
1	-0.010628	5.600508	16.022758
6	-0.564355	4.662081	17.878709
6	-1.586535	2.479184	17.707217
1	-1.807297	1.685822	15.725189
6	-0.015379	-0.130455	9.539297
6	-2.557901	0.287775	11.264253
1	0.762146	8.893118	8.639998
1	-0.075877	3.358897	1.290357
1	-2.453993	8.331871	13.757513
6	-0.626176	8.135793	12.621142
1	1.201381	7.638430	11.586715
1	-0.208494	5.493579	18.482023
6	-1.136053	3.544786	18.492766
1	-2.029194	1.603977	18.176452
1	1.072617	-0.206438	9.654791
1	-0.232386	-0.217683	8.465689
6	-0.736998	-1.255037	10.323972
1	-3.607078	0.585563	11.148328
1	-2.391511	0.106299	12.335168
6	-2.252074	-0.994509	10.449644
1	-0.611918	9.179069	12.315374
1	-1.227518	3.502112	19.574819
1	-0.563517	-2.210036	9.819126
1	-0.295408	-1.329353	11.326206
1	-2.738618	-1.847777	10.931498
1	-2.688301	-0.891438	9.447638

Table S48. Cartesian coordinates for the optimized geometry of the free ligand of **1j**.

Atomic Number	X	Y	Z
6	0.393204	0.919285	-2.821451
1	0.492532	2.295580	-4.490093
15	0.395831	-0.697134	2.054195
6	-0.277845	-1.580292	0.528554
6	0.269085	-1.029240	-0.795695
15	0.160311	0.838624	-0.959504
6	0.348012	2.339889	-3.402282
15	1.651745	3.491448	-2.663396
1	-1.367836	-1.458319	0.552464
1	-0.058983	-2.653469	0.605226
1	-0.256298	-1.509284	-1.633900
1	1.334472	-1.276253	-0.889755
1	-0.372357	0.300032	-3.309125
1	1.368190	0.461413	-3.029753
1	-0.634678	2.791286	-3.211708
6	1.767330	4.780405	-3.976515
6	2.919346	5.588827	-4.027884

6	0.712785	5.068199	-4.859385
6	3.020669	6.635275	-4.944132
6	0.809560	6.125625	-5.770557
6	1.963641	6.910132	-5.820196
1	3.747207	5.387681	-3.350778
1	-0.192135	4.467142	-4.842842
1	3.924771	7.239571	-4.973742
1	-0.018859	6.330275	-6.445457
1	2.040297	7.728903	-6.531631
6	0.108107	-1.997749	3.332025
6	0.974928	-2.101658	4.435784
6	-1.030259	-2.822411	3.297904
6	0.719242	-3.010564	5.463326
6	-1.288088	-3.729893	4.329903
6	-0.414335	-3.829703	5.415531
1	1.862949	-1.475375	4.482524
1	-1.722369	-2.761309	2.461967
1	1.407945	-3.081115	6.302527
1	-2.172453	-4.361705	4.281177
1	-0.613381	-4.537733	6.216433
6	-1.671130	1.084176	-0.844749
6	-2.590321	0.319172	-1.581760
6	-2.161465	2.068134	0.027159
6	-3.964094	0.532196	-1.453868
6	-3.537174	2.287781	0.155785
6	-4.440310	1.520201	-0.583772
1	-2.230373	-0.452195	-2.259954
1	-1.458495	2.659173	0.610337
1	-4.663550	-0.069993	-2.030072
1	-3.901639	3.054909	0.835222
1	-5.510243	1.687717	-0.483296
6	2.213600	-0.884314	1.757816
6	2.833522	-2.136228	1.609596
6	2.995444	0.275547	1.651486
6	4.204266	-2.226301	1.361659
6	4.370318	0.188190	1.408258
6	4.976185	-1.062220	1.262964
1	2.239461	-3.042595	1.701799
1	2.521045	1.248848	1.753971
1	4.672561	-3.201868	1.249767
1	4.964461	1.095525	1.328983
1	6.045481	-1.132137	1.075843
6	3.151094	2.459939	-3.009561
6	3.662975	1.683578	-1.955891
6	3.741520	2.348844	-4.279373
6	4.728484	0.804265	-2.169441
6	4.816886	1.482451	-4.489848
6	5.309967	0.704267	-3.436435
1	3.212044	1.752629	-0.968530
1	3.359427	2.945941	-5.103486
1	5.096122	0.200365	-1.343806

S136

1	5.266119	1.409682	-5.478176
1	6.143124	0.025207	-3.603593

Table S49. Cartesian coordinates for the optimized geometry of the free ligand of **1k**.

Atomic Number	X	Y	Z
15	0.121653	-0.179798	10.913591
15	5.191518	5.242565	10.510692
6	2.552727	2.421122	9.937133
6	1.970754	0.045778	10.546664
6	0.143675	-2.013608	11.373711
6	-0.531646	-0.240373	9.148730
6	3.333029	4.858960	10.482250
6	5.115200	7.131006	10.543784
6	5.625730	4.910847	8.710629
7	2.453521	1.391392	10.842130
6	2.997601	3.440291	10.791225
1	2.535864	-0.663840	11.157979
1	2.181353	-0.133407	9.490012
6	0.743870	-2.188080	12.779109
1	-0.921960	-2.276589	11.428657
6	0.822262	-2.948746	10.362330
1	0.153273	-0.860543	8.553366
6	-1.931854	-0.869939	9.111910
6	-0.545465	1.180203	8.560044
1	2.868232	5.535691	11.212134
1	2.920138	5.095239	9.496618
1	6.158610	7.436414	10.384951
6	4.696126	7.612236	11.943340
6	4.246002	7.777786	9.456507
1	4.832725	5.347342	8.087668
6	6.965158	5.573287	8.352577
6	5.674248	3.396334	8.447817
7	2.771270	1.652414	12.119144
7	3.111176	2.929336	12.062268
1	0.232297	-1.557644	13.516098
1	1.809013	-1.922514	12.792387
1	0.661160	-3.236138	13.097461
1	0.366803	-2.875620	9.368784
1	0.741003	-3.992309	10.697683
1	1.890213	-2.715942	10.266262
1	-1.921081	-1.918154	9.432918
1	-2.332557	-0.830019	8.089962
1	-2.623353	-0.318622	9.763798
1	0.446951	1.648272	8.590326
1	-1.238672	1.819112	9.123865
1	-0.889020	1.144799	7.516494
1	5.331781	7.180133	12.726120
1	3.654290	7.340559	12.159292
1	4.766924	8.706529	12.004952
1	4.567944	7.487203	8.450645

1	4.301906	8.873068	9.528113
1	3.194084	7.490686	9.574140
1	6.919315	6.665848	8.428009
1	7.243196	5.314282	7.322064
1	7.765951	5.216773	9.014844
1	4.703826	2.920138	8.627851
1	6.423993	2.916902	9.091837
1	5.960527	3.214476	7.402307
6	3.523877	3.618642	13.279708
1	3.593701	2.885961	14.085578
1	2.783225	4.384853	13.536314
1	4.494413	4.094507	13.105921

Table S50. Cartesian coordinates for the optimized geometry of the free ligand of **1l**.

Atomic Number	X	Y	Z
6	2.698542	1.688870	-0.817925
6	1.858500	2.182613	-1.832641
7	0.578790	2.199976	-1.285456
6	0.551861	1.746917	0.005858
7	1.861492	1.438593	0.266505
6	2.302432	0.823726	1.514477
6	2.858045	-0.596260	1.327835
6	-0.582789	2.670584	-2.043125
6	-1.901589	2.517886	-1.287903
6	4.074634	1.563552	-1.016302
6	4.580231	1.937180	-2.265798
6	3.737032	2.420814	-3.282290
6	2.359554	2.554885	-3.080321
15	1.646176	-1.772514	0.486220
6	2.633981	-3.328097	0.644004
6	3.932980	-3.370598	0.102267
6	4.678722	-4.550621	0.116209
6	4.135370	-5.720572	0.657357
6	2.840004	-5.696544	1.181017
6	2.096332	-4.512851	1.175667
6	0.399591	-1.949158	1.836985
6	0.745333	-2.252302	3.165593
6	-0.238142	-2.342539	4.151335
6	-1.582483	-2.128883	3.820314
6	-1.936951	-1.826923	2.504674
6	-0.949429	-1.738902	1.518274
15	-2.429695	0.712754	-1.083193
6	-3.849462	0.646578	-2.275080
6	-4.914213	1.565074	-2.255751
6	-5.949565	1.477373	-3.186818
6	-5.937618	0.465320	-4.155247
6	-4.888165	-0.455343	-4.184341
6	-3.851148	-0.364204	-3.248010
6	-3.310096	0.801682	0.538183
6	-4.560689	0.190778	0.736309

6	-5.150758	0.168402	2.003428
6	-4.501755	0.755097	3.093808
6	-3.250681	1.351414	2.908477
6	-2.653074	1.367362	1.647223
1	3.074755	1.459798	1.970122
1	1.431086	0.809998	2.174824
1	3.143216	-0.990479	2.310769
1	3.760201	-0.574054	0.708485
1	-0.613478	2.115657	-2.991722
1	-0.420391	3.729532	-2.291135
1	-1.812679	2.966590	-0.295914
1	-2.676827	3.056914	-1.843609
1	4.731273	1.196978	-0.233229
1	5.647161	1.851933	-2.455275
1	4.165263	2.698507	-4.241916
1	1.708845	2.934764	-3.862720
1	4.365871	-2.476780	-0.343018
1	5.683579	-4.557373	-0.300807
1	4.714444	-6.640927	0.666077
1	2.404748	-6.600998	1.600869
1	1.094083	-4.507881	1.594879
1	1.786230	-2.431225	3.425571
1	0.041234	-2.578406	5.176220
1	-2.348992	-2.189250	4.589789
1	-2.973965	-1.632467	2.246969
1	-1.223760	-1.478690	0.498718
1	-4.936201	2.343541	-1.496418
1	-6.767955	2.193675	-3.157561
1	-6.744998	0.396356	-4.880733
1	-4.874596	-1.244584	-4.932667
1	-3.034492	-1.083495	-3.270131
1	-5.081750	-0.261195	-0.103497
1	-6.122039	-0.304022	2.134799
1	-4.963302	0.741258	4.078522
1	-2.727366	1.792964	3.753846
1	-1.655698	1.783593	1.518713

Table S51. Cartesian coordinates for the optimized geometry of the free ligand of **1m**.

Atomic Number	X	Y	Z
7	1.636278	0.083727	-1.610328
7	1.034634	1.189328	-1.946594
6	1.304021	-0.221906	-0.310786
6	0.432363	0.727496	0.253193
7	0.327645	1.574019	-0.811820
6	-0.590581	2.686132	-0.918907
15	-1.957409	2.507134	0.363090
6	1.810033	-1.474194	0.330475
15	0.959383	-3.044460	-0.300954
6	-3.020018	3.886373	-0.349679
6	-3.878303	3.741156	-1.453938

6	-4.619273	4.823395	-1.936454
6	-4.508955	6.080348	-1.330748
6	-3.655395	6.243181	-0.235383
6	-2.926602	5.153240	0.252093
6	-2.909923	1.046191	-0.253355
6	-4.174468	0.826853	0.322938
6	-0.671987	-3.047091	0.562653
6	-1.496878	-4.173972	0.379935
6	-2.754513	-4.250015	0.980278
6	-3.223977	-3.182749	1.754764
6	-2.424051	-2.050953	1.921635
6	-1.154390	-1.980094	1.339066
6	-4.947387	-0.279828	-0.032136
6	-4.459526	-1.203502	-0.962030
6	-3.203929	-0.999485	-1.537460
6	-2.435068	0.117053	-1.193949
6	1.898124	-4.288966	0.712673
6	3.164606	-4.677806	0.233838
6	3.960075	-5.581171	0.942164
6	3.498930	-6.132586	2.142979
6	2.240482	-5.761706	2.627611
6	1.451677	-4.846325	1.923992
1	-1.006550	2.713162	-1.934064
1	-0.099243	3.653114	-0.727661
1	2.872981	-1.642786	0.109002
1	1.690669	-1.421466	1.419064
1	-3.968332	2.769236	-1.933014
1	-5.280637	4.687123	-2.790879
1	-5.085526	6.923308	-1.707324
1	-3.563153	7.216062	0.245012
1	-2.277283	5.281881	1.117809
1	-4.556871	1.531903	1.060514
1	-1.145231	-5.001747	-0.235463
1	-3.372897	-5.134227	0.832345
1	-4.214796	-3.225536	2.203476
1	-2.791739	-1.200410	2.490736
1	-0.573105	-1.066230	1.447720
1	-5.921361	-0.430553	0.430830
1	-5.043430	-2.084848	-1.218585
1	-2.802521	-1.722150	-2.244222
1	-1.457627	0.241005	-1.645338
1	3.526617	-4.266775	-0.708002
1	4.937584	-5.861206	0.552607
1	4.112677	-6.843742	2.692727
1	1.872150	-6.180630	3.563006
1	0.479899	-4.560073	2.317120

S140

Table S52. Cartesian coordinates for the optimized geometry of the free ligand of **1n**.

Atomic Number	X	Y	Z
5	2.643785	-0.610633	10.450139
15	4.934057	0.674139	9.019382
15	0.353959	0.675690	11.880202
7	3.661341	-1.557882	9.948054
7	1.625930	-1.557269	10.952774
6	4.910573	-1.189353	9.333916
6	5.517999	1.355519	10.633383
6	6.605560	0.608133	8.131769
6	0.376822	-1.187984	11.566710
6	-0.229810	1.356360	10.265837
6	-1.317550	0.610733	12.767885
6	3.284698	-2.877182	10.138037
6	2.002156	-2.876798	10.763559
1	5.039559	-1.678496	8.354654
1	5.777693	-1.471860	9.956421
6	6.083843	2.641402	10.644573
6	5.359245	0.681948	11.855269
6	6.585055	0.609015	6.726049
6	7.857467	0.549832	8.770667
1	0.247680	-1.676536	12.546246
1	-0.490395	-1.470553	10.944368
6	-0.795286	2.642398	10.253956
6	-0.071265	0.682081	9.044314
6	-1.297034	0.612548	14.173603
6	-2.569477	0.552334	12.129034
6	3.925063	-4.078948	9.833778
6	1.361415	-4.078187	11.068516
1	6.220590	3.174705	9.705102
6	6.470646	3.248703	11.844410
6	5.754016	1.284130	13.055942
1	4.899640	-0.301052	11.867646
1	5.625543	0.668256	6.212060
6	7.766499	0.544468	5.980635
6	9.043451	0.501559	8.031120
1	7.901311	0.549426	9.856945
1	-0.931870	3.176249	11.193140
6	-1.181933	3.249158	9.053796
6	-0.465880	1.283726	7.843319
1	0.388058	-0.301058	9.032465
1	-0.337502	0.671877	14.687545
6	-2.478491	0.548813	14.919068
6	-3.755468	0.504866	12.868620
1	-2.613327	0.551218	11.042756
1	4.905979	-4.078356	9.363218
6	3.273929	-5.286835	10.147938
1	0.380499	-4.077017	11.539075
6	2.012171	-5.286460	10.755056
1	6.896900	4.250599	11.831323
6	6.304564	2.569958	13.055943

1	5.613769	0.750616	13.994343
1	7.722370	0.540960	4.892438
6	9.003571	0.495773	6.632561
1	10.001495	0.462135	8.548188
1	-1.607902	4.251183	9.066346
6	-1.016062	2.569709	7.842628
1	-0.325800	0.749662	6.905206
1	-2.434356	0.546022	16.007267
6	-3.715579	0.500006	14.267183
1	-4.713526	0.465348	12.351586
1	3.759360	-6.233109	9.914828
1	1.526443	-6.232447	10.988716
1	6.596418	3.041638	13.992842
1	9.926756	0.457699	6.056942
1	-1.307794	3.040964	6.905478
1	-4.638770	0.462561	14.842834

Table S53. Cartesian coordinates for the optimized geometry of the free ligand of **1o.**

Atomic Number	X	Y	Z
6	-3.017810	1.302521	0.176187
6	-2.995229	-0.232275	0.134423
6	-1.868516	-0.794699	0.956245
6	-1.521786	-2.232290	0.726625
6	-0.558127	-2.778649	1.789270
1	-1.958101	-0.530459	2.017191
15	-1.279964	1.903521	-0.233901
6	-1.606273	3.694917	-0.605513
6	-0.626474	4.439811	-1.299681
6	-0.738433	5.818324	-1.466245
6	-1.827823	6.513311	-0.916775
6	-2.800510	5.797884	-0.212485
6	-2.696622	4.409871	-0.067163
6	-1.125500	1.225297	-1.953635
6	-0.527043	-0.037134	-2.100789
6	-0.417152	-0.635118	-3.357833
6	-0.904825	0.016520	-4.496889
6	-1.508067	1.271683	-4.362979
6	-1.623877	1.866831	-3.103106
15	0.746550	-1.481759	2.227141
6	1.539808	-1.144397	0.610119
6	1.814656	-2.165317	-0.324443
6	2.455588	-1.870608	-1.532334
6	2.839919	-0.560065	-1.826393
6	2.566222	0.464370	-0.905443
6	1.919868	0.172289	0.295586
6	2.015223	-2.634022	2.975305
6	3.395223	-2.466883	2.741786
6	4.345718	-3.236280	3.416235
6	3.946705	-4.197093	4.354004
6	2.581258	-4.374672	4.603494

6	1.632851	-3.605067	3.924595
1	-3.766563	1.738047	-0.503019
1	-3.241315	1.644634	1.197635
1	-4.008024	-0.591475	0.451498
1	-2.892720	-0.552792	-0.913751
1	-2.407684	-2.918548	0.707223
1	-1.050501	-2.362027	-0.267817
1	-0.080355	-3.716272	1.474468
1	-1.105081	-2.984944	2.719592
1	0.232156	3.917070	-1.719560
1	0.026815	6.358123	-2.022892
1	-1.912431	7.591714	-1.036698
1	-3.655235	6.319997	0.216836
1	-3.476896	3.874195	0.467419
1	-0.168969	-0.551199	-1.216290
1	0.058948	-1.609534	-3.440707
1	-0.819780	-0.449693	-5.477482
1	-1.899716	1.786393	-5.239876
1	-2.103342	2.837928	-3.011859
1	1.537028	-3.190730	-0.093191
1	2.653621	-2.668324	-2.247582
1	3.327386	-0.331364	-2.771883
1	2.837270	1.492764	-1.135713
1	1.672809	0.972038	0.988917
1	3.721449	-1.731031	2.009934
1	5.404241	-3.090738	3.203230
1	4.686914	-4.798130	4.879036
1	2.252238	-5.121141	5.325964
1	0.576187	-3.763670	4.131370

Table S54. Cartesian coordinates for the optimized geometry of the free ligand of **1p**.

Atomic Number	X	Y	Z
6	-0.961674	2.239754	1.296767
6	-2.113901	1.376868	0.768087
7	-1.546513	0.340282	-0.030760
6	-2.440809	-0.748696	-0.215044
6	-1.856964	-1.791976	-1.177209
15	0.404801	0.997479	1.693593
6	-0.492189	-0.278225	2.672556
6	-0.408598	-1.622786	2.280699
6	-1.108238	-2.617326	2.965760
6	-1.907799	-2.282219	4.071897
6	-2.010735	-0.946847	4.464092
6	-1.311943	0.049378	3.768731
6	1.251004	1.917353	3.088225
6	1.447489	3.312697	3.033568
6	2.219232	3.980699	3.989367
6	2.816147	3.272280	5.037397
6	2.632041	1.885327	5.110501
6	1.867322	1.222104	4.149317

15	-1.612448	-1.100645	-2.912367
6	-1.727820	-2.706577	-3.863458
6	-2.795507	-2.891193	-4.755530
6	-2.959079	-4.096111	-5.450700
6	-2.049035	-5.139512	-5.264572
6	-0.976270	-4.970131	-4.379635
6	-0.819533	-3.766854	-3.689371
6	0.213529	-0.825144	-3.015171
6	0.903736	-0.282708	-1.915866
6	2.267612	0.010552	-2.016411
6	2.962071	-0.222157	-3.208339
6	2.278187	-0.748646	-4.310797
6	0.915802	-1.045387	-4.215161
1	-0.577172	2.902639	0.509911
1	-1.240393	2.852041	2.165127
1	-2.671427	0.986976	1.657809
1	-2.853595	2.018949	0.224623
1	-2.681446	-1.284128	0.742842
1	-3.436926	-0.435569	-0.622071
1	-2.535133	-2.651243	-1.271075
1	-0.892329	-2.155480	-0.798073
1	0.186185	-1.876541	1.406203
1	-1.033288	-3.653287	2.639484
1	-2.457385	-3.055691	4.605826
1	-2.641475	-0.674265	5.309716
1	-1.384281	1.086075	4.088614
1	0.984650	3.885476	2.232432
1	2.347151	5.060655	3.919825
1	3.411569	3.791048	5.786608
1	3.082909	1.319083	5.924968
1	1.728779	0.145088	4.224262
1	-3.504873	-2.078207	-4.904054
1	-3.794468	-4.216701	-6.138701
1	-2.170709	-6.076795	-5.804690
1	-0.262698	-5.778748	-4.228246
1	0.020503	-3.637156	-3.011367
1	0.347985	-0.063198	-1.002181
1	2.779174	0.425270	-1.149587
1	4.024529	0.005916	-3.281389
1	2.805699	-0.932268	-5.246155
1	0.398437	-1.463818	-5.076457

Table S55. Cartesian coordinates for the optimized geometry of the free ligand of **1q**.

Atomic Number	X	Y	Z
15	7.774498	14.630654	6.441642
15	2.911510	16.588374	6.877741
5	5.315571	16.108083	4.804811
6	8.188509	15.030207	4.658479
6	9.387328	13.850219	6.944569
6	7.968540	16.290037	7.242080

6	1.290667	16.484453	7.795841
6	2.860673	18.363770	6.361071
6	2.386837	15.726461	5.298063
15	6.889967	16.213294	4.002343
15	3.735156	15.964060	4.034063
1	9.208321	15.421529	4.547113
1	8.109507	14.098063	4.087447
6	9.845865	13.963033	8.274237
6	10.095909	12.986173	6.084973
6	6.877513	16.823516	7.944476
6	9.159539	17.028468	7.170227
6	0.846276	17.545762	8.611115
6	0.562086	15.278071	7.846235
6	1.764734	18.926752	5.687548
6	3.956375	19.182919	6.668779
1	1.416145	16.085603	4.933689
1	2.301635	14.655773	5.510632
6	6.993500	15.957154	2.176976
6	7.784719	17.833854	4.224118
6	3.419670	14.572849	2.843687
6	3.054146	17.415943	3.060282
1	9.324629	14.626549	8.960813
6	10.964008	13.256873	8.718548
1	9.777147	12.875763	5.051207
6	11.212117	12.272651	6.530236
1	5.935010	16.281544	7.956052
6	6.987549	18.062950	8.582988
1	10.006948	16.626348	6.621016
6	9.263704	18.277030	7.789603
6	-0.277787	17.411338	9.428085
1	1.382178	18.491908	8.590927
1	0.874360	14.434891	7.234020
6	-0.561962	15.141170	8.663995
1	0.907533	18.305503	5.444113
6	1.772242	20.272935	5.313494
6	3.961788	20.532845	6.308842
1	4.818844	18.749741	7.167222
6	6.910573	17.051962	1.292689
6	6.916868	14.659388	1.635464
6	7.109420	18.861095	4.887483
6	9.075857	18.068892	3.730656
6	3.474033	14.768624	1.452816
6	3.343407	13.251411	3.326997
6	3.896627	18.509307	2.853365
6	1.745413	17.459233	2.558417
6	11.657327	12.404287	7.849862
1	11.300081	13.376414	9.747568
1	11.741877	11.619085	5.838588
1	6.136016	18.464287	9.128719
6	8.178762	18.793910	8.502346
1	10.184313	18.850283	7.701550

1	-0.601772	18.253905	10.037476
6	-0.992457	16.207974	9.460952
1	-1.107564	14.198663	8.673290
6	2.869558	21.080292	5.624246
1	0.928724	20.685183	4.764013
1	4.824438	21.151168	6.548779
1	6.958668	18.062824	1.689083
6	6.761313	16.854870	-0.080528
1	6.932007	13.796588	2.297154
6	6.770640	14.462889	0.261734
6	7.713822	20.107803	5.066010
1	6.109032	18.647175	5.261030
1	9.604910	17.276296	3.204829
6	9.681131	19.317674	3.897014
1	3.564624	15.775588	1.055046
6	3.435725	13.681857	0.574301
6	3.289787	12.167654	2.451789
1	3.354977	13.073924	4.400858
1	4.903841	18.457983	3.264374
6	3.446412	19.635526	2.160299
6	1.286300	18.583647	1.867491
1	1.085287	16.605141	2.699890
1	12.531413	11.855845	8.195131
1	8.255610	19.767992	8.982350
1	-1.871095	16.104303	10.094400
1	2.880165	22.126367	5.323824
1	6.696379	17.716805	-0.743067
6	6.695209	15.557859	-0.607115
1	6.696758	13.449850	-0.128791
1	7.182933	20.895533	5.596829
6	9.000848	20.339707	4.569553
1	10.681718	19.494942	3.505000
6	3.334141	12.377324	1.064280
1	3.498072	13.859436	-0.497988
1	3.219445	11.155882	2.848878
1	4.112075	20.484482	2.014246
6	2.137767	19.677215	1.669276
1	0.266952	18.609989	1.484060
1	6.572857	15.403596	-1.677434
1	9.474309	21.310734	4.706046
1	3.303083	11.531891	0.379384
1	1.779380	20.557232	1.137491

Monodentate complexes in C_s symmetry

Table S56. Cartesian coordinates for the optimized geometry of *trans*-**2a**.

Atomic Number	X	Y	Z
6	0.371466	1.436013	0.000000
1	1.465856	1.280209	0.000000
15	0.182340	2.325719	1.560312
15	0.182340	2.325719	-1.560312
6	0.488025	4.122552	-1.592050
6	1.799774	4.622111	-1.670915
1	2.658521	3.961061	-1.615503
6	2.022376	5.989696	-1.826072
1	3.040387	6.361774	-1.899246
6	0.942671	6.873925	-1.896292
1	1.118767	7.937329	-2.033231
6	-0.362574	6.388351	-1.786258
1	-1.205996	7.071933	-1.827078
6	-0.591236	5.022079	-1.631025
1	-1.611171	4.658753	-1.562012
6	-1.442872	2.142368	-2.324990
6	-2.443315	1.350806	-1.755825
1	-2.219593	0.770050	-0.874764
6	-3.693387	1.244786	-2.368894
1	-4.466965	0.629891	-1.916847
6	-3.938915	1.909479	-3.572308
1	-4.908450	1.823244	-4.055142
6	-2.930618	2.681836	-4.163059
1	-3.114950	3.192635	-5.103886
6	-1.690815	2.808508	-3.540118
1	-0.925356	3.432227	-3.993616
6	1.492231	1.631062	-2.613494
1	2.449709	2.061934	-2.313531
1	1.571798	0.555467	-2.465403
1	1.299223	1.876775	-3.661043
6	1.492231	1.631062	2.613494
1	1.299223	1.876775	3.661043
1	1.571798	0.555467	2.465403
1	2.449709	2.061934	2.313531
6	0.488025	4.122552	1.592050
6	1.799774	4.622111	1.670915
1	2.658521	3.961061	1.615503
6	2.022376	5.989696	1.826072
1	3.040387	6.361774	1.899246
6	0.942671	6.873925	1.896292
1	1.118767	7.937329	2.033231
6	-0.362574	6.388351	1.786258
1	-1.205996	7.071933	1.827079
6	-0.591236	5.022079	1.631025
1	-1.611171	4.658753	1.562012
6	-1.442872	2.142368	2.324990

6	-1.690815	2.808508	3.540118
1	-0.925356	3.432227	3.993616
6	-2.930618	2.681836	4.163059
1	-3.114950	3.192635	5.103886
6	-3.938915	1.909479	3.572308
1	-4.908450	1.823243	4.055143
6	-3.693387	1.244785	2.368894
1	-4.466965	0.629890	1.916847
6	-2.443315	1.350806	1.755825
1	-2.219593	0.770050	0.874764
77	0.141997	-1.025228	0.000000
1	-1.441039	-1.006809	0.000000
6	0.224334	-2.868716	0.000000
8	0.343848	-4.013313	0.000000
17	2.634791	-0.732208	0.000000
15	0.005020	-1.531966	2.434332
6	1.625289	-1.931714	3.163289
6	2.483798	-2.833157	2.511989
6	3.709824	-3.175469	3.078812
6	4.107471	-2.609038	4.293561
6	3.267111	-1.702712	4.943797
6	2.031102	-1.368705	4.386120
15	0.005019	-1.531966	-2.434332
6	1.625288	-1.931714	-3.163289
6	2.031101	-1.368705	-4.386120
6	3.267111	-1.702712	-4.943798
6	4.107470	-2.609038	-4.293562
6	3.709823	-3.175469	-3.078813
6	2.483797	-2.833157	-2.511989
6	-0.845042	-0.561350	3.743995
6	-1.013251	-3.049760	2.569696
6	-2.270763	-3.074940	1.947262
6	-3.102229	-4.184831	2.092239
6	-2.679462	-5.281293	2.851156
6	-1.427512	-5.258690	3.470840
6	-0.594407	-4.144447	3.337059
6	-0.845043	-0.561350	-3.743995
6	-1.013251	-3.049760	-2.569696
6	-2.270763	-3.074939	-1.947262
6	-3.102229	-4.184831	-2.092239
6	-2.679462	-5.281292	-2.851156
6	-1.427512	-5.258690	-3.470841
6	-0.594407	-4.144447	-3.337059
1	-0.799592	-1.184748	4.643256
1	-0.390656	0.405762	3.944958
1	-1.889071	-0.427558	3.462724
1	-1.889072	-0.427558	-3.462724
1	-0.390657	0.405762	-3.944958
1	-0.799593	-1.184748	-4.643256
1	-2.589393	-2.235054	1.335694
1	0.377880	-4.135620	3.819783

S148

1	-4.075526	-4.199427	1.608807
1	-1.094382	-6.109306	4.059124
1	-3.322665	-6.150668	2.956269
1	2.208550	-3.272133	1.562659
1	1.390470	-0.675532	4.920329
1	4.358888	-3.879372	2.565646
1	3.565225	-1.261596	5.891039
1	5.066597	-2.873156	4.730514
1	-2.589394	-2.235054	-1.335694
1	0.377880	-4.135620	-3.819783
1	-4.075526	-4.199427	-1.608807
1	-1.094382	-6.109306	-4.059125
1	-3.322665	-6.150668	-2.956269
1	1.390469	-0.675532	-4.920329
1	2.208549	-3.272133	-1.562659
1	3.565225	-1.261596	-5.891040
1	4.358887	-3.879372	-2.565647
1	5.066597	-2.873156	-4.730515

Table S57. Cartesian coordinates for the optimized geometry of **2b**.

Atomic Number	X	Y	Z
7	-2.552950	-0.781539	0.000000
6	-3.162789	-1.156208	-1.168071
6	-3.052058	-0.238042	-2.355524
1	-4.079264	0.116992	-2.571013
1	-2.688187	-0.718055	-3.278859
1	-2.447644	0.647510	-2.113836
6	-4.055022	-2.242314	-1.198214
1	-4.488585	-2.546959	-2.158008
6	-4.437576	-2.858637	0.000000
1	-5.108996	-3.726189	0.000000
6	-4.055022	-2.242314	1.198214
1	-4.488585	-2.546959	2.158008
6	-3.162789	-1.156208	1.168071
6	-3.052058	-0.238042	2.355524
1	-4.079264	0.116992	2.571013
1	-2.688187	-0.718055	3.278859
1	-2.447644	0.647510	2.113836
77	-0.342139	-0.037250	0.000000
6	1.304754	0.805456	0.000000
8	2.276073	1.427379	0.000000
17	-1.393815	2.234231	-0.000001
15	0.125390	-0.468617	2.357176
6	-0.351765	0.680862	3.692142
6	-0.421295	2.056899	3.389264
6	-0.709617	2.978948	4.409133
6	-0.932459	2.534542	5.723776
6	-0.864260	1.161855	6.023872
6	-0.570459	0.233399	5.012716
15	0.125390	-0.468618	-2.357176
6	-0.351765	0.680861	-3.692142

6	-0.570459	0.233398	-5.012716
6	-0.864260	1.161852	-6.023872
6	-0.932459	2.534540	-5.723778
6	-0.709617	2.978947	-4.409135
6	-0.421295	2.056898	-3.389265
6	-0.375162	-2.184756	2.825601
6	1.961810	-0.576881	2.511636
6	2.690444	0.342293	3.293144
6	4.092086	0.255942	3.351550
6	4.771417	-0.746499	2.640633
6	4.045866	-1.665114	1.860917
6	2.648941	-1.575464	1.788801
6	-0.375162	-2.184757	-2.825601
6	1.961810	-0.576883	-2.511636
6	2.648941	-1.575465	-1.788801
6	4.045866	-1.665115	-1.860917
6	4.771417	-0.746500	-2.640633
6	4.092086	0.255941	-3.351550
6	2.690444	0.342291	-3.293144
1	0.205478	-1.538356	0.000000
1	-0.059858	-2.404342	3.860986
1	-1.456971	-2.348543	2.709796
1	0.158168	-2.865494	2.141381
1	0.158168	-2.865495	-2.141380
1	-1.456971	-2.348544	-2.709796
1	-0.059858	-2.404343	-3.860986
1	2.169921	1.126256	3.853916
1	2.092446	-2.276420	1.155838
1	4.652672	0.976997	3.958904
1	4.570861	-2.450646	1.304352
1	5.865157	-0.812200	2.691533
1	-0.284574	2.403729	2.358361
1	-0.510480	-0.832190	5.262881
1	-0.768526	4.047727	4.169846
1	-1.036414	0.812068	7.049263
1	-1.162616	3.257078	6.516535
1	2.092446	-2.276420	-1.155838
1	2.169921	1.126254	-3.853916
1	4.570861	-2.450647	-1.304352
1	4.652672	0.976995	-3.958904
1	5.865157	-0.812202	-2.691533
1	-0.510480	-0.832191	-5.262881
1	-0.284574	2.403728	-2.358363
1	-1.036414	0.812065	-7.049263
1	-0.768526	4.047726	-4.169848
1	-1.162616	3.257075	-6.516537

S150

Table S58. Cartesian coordinates for the optimized geometry of *cis*-**2c**.

Atomic Number	X	Y	Z
7	-1.642844	-2.125837	0.000000
1	-2.632870	-1.857184	0.000000
6	-1.407801	-2.977579	1.205575
1	-1.742355	-2.461786	2.113939
1	-0.325606	-3.168914	1.278596
1	-1.960410	-3.931717	1.108049
6	-1.407801	-2.977579	-1.205575
1	-0.325606	-3.168914	-1.278596
1	-1.960410	-3.931717	-1.108049
1	-1.742355	-2.461786	-2.113939
77	-0.418470	-0.185701	0.000000
17	1.559440	-1.723797	0.000000
1	-1.745774	0.706696	0.000000
6	0.766423	1.248080	0.000000
8	1.575062	2.069615	-0.000001
15	-0.658686	0.060121	2.391808
6	0.174468	-1.111927	3.506860
6	-0.522870	-1.795229	4.527408
6	0.161264	-2.691100	5.364602
6	1.540672	-2.902681	5.193184
6	2.237176	-2.218952	4.181103
6	1.559631	-1.329026	3.333440
15	-0.658686	0.060121	-2.391808
6	0.174468	-1.111928	-3.506860
6	1.559631	-1.329027	-3.333440
6	2.237176	-2.218952	-4.181103
6	1.540672	-2.902682	-5.193184
6	0.161264	-2.691101	-5.364602
6	-0.522870	-1.795230	-4.527408
6	-2.452088	0.078683	2.842730
6	-0.120613	1.741788	2.897873
6	-0.692654	2.848428	2.231012
6	-0.316320	4.152294	2.581551
6	0.639107	4.360840	3.593317
6	1.210357	3.262053	4.255720
6	0.831455	1.951682	3.914949
6	-2.452088	0.078682	-2.842731
6	-0.120614	1.741788	-2.897874
6	0.831454	1.951681	-3.914950
6	1.210356	3.262052	-4.255721
6	0.639107	4.360839	-3.593319
6	-0.316320	4.152293	-2.581553
6	-0.692654	2.848428	-2.231013
1	-2.956216	-0.863586	-2.566957
1	-2.913888	0.908626	-2.281619
1	-2.570319	0.262985	-3.925563
1	-2.570319	0.262986	3.925562
1	-2.913887	0.908627	2.281618
1	-2.956216	-0.863585	2.566956

1	1.276555	1.099189	-4.439921
1	-1.418259	2.687656	-1.423377
1	1.954970	3.421237	-5.045229
1	-0.763713	5.007958	-2.060868
1	0.938886	5.380968	-3.862807
1	2.101745	-0.821689	-2.528977
1	-1.596583	-1.635426	-4.678523
1	3.312146	-2.385482	-4.041594
1	-0.384575	-3.220041	-6.155472
1	2.072841	-3.602714	-5.849066
1	-1.418259	2.687656	1.423376
1	1.276555	1.099190	4.439920
1	-0.763713	5.007958	2.060866
1	1.954970	3.421238	5.045228
1	0.938886	5.380969	3.862805
1	-1.596583	-1.635425	4.678523
1	2.101745	-0.821689	2.528977
1	-0.384575	-3.220040	6.155472
1	3.312146	-2.385482	4.041594
1	2.072841	-3.602714	5.849066

Table S59. Cartesian coordinates for the optimized geometry of *trans*-**2c**.

Atomic Number	X	Y	Z
7	-2.351196	-1.192343	0.000000
1	-2.743025	-0.233455	0.000000
6	-2.878766	-1.875881	1.205682
1	-3.979049	-1.979648	1.130559
1	-2.436116	-2.883733	1.275877
1	-2.644458	-1.288164	2.104655
6	-2.878766	-1.875881	-1.205682
1	-2.644458	-1.288164	-2.104655
1	-3.979049	-1.979648	-1.130559
1	-2.436116	-2.883733	-1.275877
77	-0.195480	-0.417855	0.000000
17	-1.514743	1.734913	0.000000
1	0.508780	-1.847727	0.000000
6	1.377243	0.577232	0.000000
8	2.279308	1.294742	0.000000
15	0.033758	-0.638729	2.409564
6	-1.138543	0.219137	3.512604
6	-1.337813	1.608640	3.347215
6	-2.221451	2.293192	4.195902
6	-2.917594	1.601488	5.202583
6	-2.724833	0.218685	5.367029
6	-1.835961	-0.473449	4.528934
15	0.033758	-0.638729	-2.409564
6	-1.138543	0.219137	-3.512604
6	-1.835962	-0.473447	-4.528934
6	-2.724834	0.218686	-5.367028
6	-2.917595	1.601489	-5.202582
6	-2.221451	2.293193	-4.195901

6	-1.337813	1.608641	-3.347215
6	0.039672	-2.415137	2.915581
6	1.718261	-0.111745	2.925381
6	1.937867	0.927958	3.849898
6	3.252064	1.287198	4.197192
6	4.345655	0.610336	3.633265
6	4.127507	-0.432500	2.714429
6	2.820169	-0.791039	2.358293
6	0.039672	-2.415136	-2.915581
6	1.718261	-0.111744	-2.925381
6	2.820169	-0.791038	-2.358293
6	4.127507	-0.432499	-2.714429
6	4.345655	0.610337	-3.633265
6	3.252063	1.287199	-4.197192
6	1.937866	0.927959	-3.849898
1	-0.943030	-2.883992	2.755496
1	0.792239	-2.931374	2.296481
1	0.325501	-2.492473	3.979894
1	0.325501	-2.492472	-3.979894
1	0.792239	-2.931374	-2.296481
1	-0.943031	-2.883992	-2.755497
1	1.091323	1.454704	4.303322
1	2.657743	-1.588593	1.621758
1	3.417750	2.099385	4.915528
1	4.978459	-0.964198	2.271113
1	5.368830	0.894601	3.907923
1	-0.817522	2.149355	2.550771
1	-1.691188	-1.549368	4.676877
1	-2.371443	3.371398	4.062282
1	-3.262473	-0.324341	6.153966
1	-3.611656	2.139822	5.859778
1	2.657743	-1.588593	-1.621758
1	1.091322	1.454705	-4.303322
1	4.978459	-0.964197	-2.271113
1	3.417749	2.099386	-4.915528
1	5.368829	0.894602	-3.907923
1	-1.691189	-1.549367	-4.676877
1	-0.817522	2.149356	-2.550771
1	-3.262474	-0.324340	-6.153965
1	-2.371443	3.371399	-4.062281
1	-3.611657	2.139823	-5.859777

Table S60. Cartesian coordinates for the optimized geometry of **2e**.

Atomic Number	X	Y	Z
77	0.225508	-1.002177	0.000000
6	0.859470	-2.766641	0.000000
8	1.371881	-3.798770	0.000000
1	-1.336659	-1.273624	0.000000
17	2.695364	-0.348795	0.000000
15	-0.135329	-1.576875	2.334228

15	-0.135329	-1.576875	-2.334228
6	-1.501385	-0.835904	3.312613
1	-1.729029	-1.523293	4.133179
1	-1.265296	0.149382	3.708360
1	-2.376505	-0.752753	2.666440
6	-1.501385	-0.835904	-3.312613
1	-2.376505	-0.752753	-2.666440
1	-1.265296	0.149382	-3.708360
1	-1.729029	-1.523293	-4.133179
6	-0.780483	-3.305094	2.319636
6	-2.022071	-3.545790	1.713855
6	-0.100308	-4.362431	2.936631
6	-2.585454	-4.820247	1.742300
6	-0.658217	-5.644215	2.945072
6	-1.902465	-5.875170	2.355277
1	-2.545123	-2.736245	1.212120
1	0.863180	-4.193245	3.406165
1	-3.553155	-4.993005	1.279587
1	-0.117759	-6.459915	3.418201
1	-2.337369	-6.871113	2.369700
6	1.290042	-1.671997	3.464372
6	2.544026	-2.039207	2.955906
6	1.145741	-1.434523	4.841493
6	3.638233	-2.165968	3.814081
6	2.244187	-1.555244	5.694144
6	3.492628	-1.922306	5.182170
1	2.679959	-2.197622	1.893287
1	0.182780	-1.155190	5.257696
1	4.606221	-2.446055	3.407289
1	2.122816	-1.366143	6.757664
1	4.347333	-2.015293	5.847250
6	-0.780483	-3.305094	-2.319636
6	-2.022071	-3.545790	-1.713855
6	-0.100308	-4.362431	-2.936631
6	-2.585454	-4.820247	-1.742300
6	-0.658217	-5.644215	-2.945072
6	-1.902465	-5.875170	-2.355277
1	-2.545123	-2.736245	-1.212120
1	0.863180	-4.193245	-3.406165
1	-3.553155	-4.993005	-1.279587
1	-0.117759	-6.459915	-3.418201
1	-2.337369	-6.871113	-2.369700
6	1.290042	-1.671997	-3.464372
6	1.145741	-1.434523	-4.841493
6	2.544026	-2.039207	-2.955906
6	2.244187	-1.555244	-5.694144
6	3.638233	-2.165968	-3.814081
6	3.492628	-1.922306	-5.182170
1	0.182780	-1.155190	-5.257696
1	2.679959	-2.197622	-1.893287
1	2.122816	-1.366143	-6.757664

1	4.606221	-2.446055	-3.407289
1	4.347333	-2.015293	-5.847250
6	-0.098013	1.286185	-0.000000
15	-0.003581	2.155317	1.483460
15	-0.003581	2.155317	-1.483460
6	1.194838	1.430123	2.678373
1	0.680350	0.871018	3.457042
1	1.882215	0.776120	2.137527
1	1.752099	2.233074	3.165164
6	1.194838	1.430123	-2.678373
1	1.752099	2.233074	-3.165164
1	1.882215	0.776120	-2.137527
1	0.680350	0.871018	-3.457042
6	-1.571544	2.238808	-2.443696
6	-2.768104	1.771695	-1.901460
6	-1.567027	2.771157	-3.744053
6	-3.954954	1.829588	-2.638030
6	-2.746671	2.822880	-4.485966
6	-3.945010	2.352922	-3.932587
1	-2.748264	1.328628	-0.913604
1	-0.643382	3.150017	-4.174367
1	-4.882054	1.460627	-2.205833
1	-2.736084	3.234497	-5.492050
1	-4.864354	2.397432	-4.510779
6	0.493624	3.926309	-1.513000
6	1.855682	4.256002	-1.580283
6	-0.462598	4.944651	-1.620159
6	2.252520	5.577437	-1.778756
6	-0.064091	6.268285	-1.813546
6	1.292641	6.586040	-1.903826
1	2.609406	3.479065	-1.482976
1	-1.520455	4.705504	-1.571857
1	3.310685	5.818929	-1.836027
1	-0.815542	7.048888	-1.899472
1	1.602048	7.615101	-2.067383
6	-1.571544	2.238808	2.443696
6	-1.567027	2.771157	3.744053
6	-2.768104	1.771695	1.901460
6	-2.746671	2.822880	4.485966
6	-3.954954	1.829588	2.638030
6	-3.945010	2.352922	3.932587
1	-0.643382	3.150017	4.174367
1	-2.748264	1.328628	0.913604
1	-2.736084	3.234497	5.492050
1	-4.882054	1.460627	2.205833
1	-4.864354	2.397432	4.510779
6	0.493624	3.926309	1.513000
6	1.855682	4.256002	1.580283
6	-0.462598	4.944651	1.620159
6	2.252520	5.577437	1.778756
6	-0.064091	6.268285	1.813546

S155

6	1.292641	6.586040	1.903826
1	2.609406	3.479065	1.482976
1	-1.520455	4.705504	1.571857
1	3.310685	5.818929	1.836027
1	-0.815542	7.048888	1.899472
1	1.602048	7.615101	2.067383

Table S61. Cartesian coordinates for the optimized geometry of **2e** with the $[(Ph_2PH)_2IrCl(CO)H]^+$ fragment.

77	0.261411	-1.025317	-0.000000
6	-0.051515	-2.873932	-0.000000
8	-0.302565	-3.999146	-0.000000
1	-1.277138	-0.695195	-0.000000
17	2.793278	-1.174417	-0.000000
15	0.200000	-1.352414	2.355345
15	0.200000	-1.352414	-2.355345
6	-1.449886	-1.658712	3.049585
6	-1.615706	-1.601430	4.441787
6	-2.535898	-2.004440	2.236958
6	-2.860365	-1.871366	5.009855
6	-3.779123	-2.282546	2.807985
6	-3.943977	-2.212353	4.193990
1	-0.775009	-1.343939	5.080744
1	-2.409459	-2.041719	1.160745
1	-2.984439	-1.816723	6.088176
1	-4.617796	-2.553591	2.171670
1	-4.912550	-2.426413	4.638501
6	1.198887	-2.776134	2.893622
6	2.587214	-2.625965	3.039445
6	0.603148	-4.024434	3.127832
6	3.367905	-3.717407	3.420829
6	1.391276	-5.113726	3.502841
6	2.772980	-4.961816	3.650014
1	3.060871	-1.671497	2.835777
1	-0.471016	-4.145907	3.024196
1	4.442040	-3.595867	3.532306
1	0.924398	-6.078504	3.682933
1	3.384842	-5.810780	3.943906
6	-1.449886	-1.658712	-3.049585
6	-1.615706	-1.601430	-4.441787
6	-2.535898	-2.004440	-2.236958
6	-2.860365	-1.871366	-5.009855
6	-3.779123	-2.282546	-2.807985
6	-3.943977	-2.212353	-4.193990
1	-0.775009	-1.343939	-5.080744
1	-2.409459	-2.041719	-1.160745
1	-2.984439	-1.816723	-6.088176
1	-4.617796	-2.553591	-2.171670
1	-4.912550	-2.426413	-4.638501
6	1.198887	-2.776134	-2.893622
6	0.603148	-4.024434	-3.127832
6	2.587214	-2.625965	-3.039445

6	1.391276	-5.113726	-3.502841
6	3.367905	-3.717407	-3.420829
6	2.772980	-4.961816	-3.650014
1	-0.471016	-4.145907	-3.024196
1	3.060871	-1.671497	-2.835777
1	0.924398	-6.078504	-3.682933
1	4.442040	-3.595867	-3.532306
1	3.384842	-5.810780	-3.943906
6	0.458364	1.259211	0.000000
15	0.742102	2.052771	1.485954
15	0.742102	2.052771	-1.485954
6	2.287803	1.514908	2.313450
1	2.306706	1.759006	3.380374
1	2.414143	0.445119	2.141655
1	3.129136	2.002525	1.813367
6	2.287803	1.514908	-2.313450
1	2.414143	0.445119	-2.141655
1	2.306706	1.759006	-3.380374
1	3.129136	2.002525	-1.813367
6	-0.635896	1.752617	-2.656277
6	-1.887582	1.400471	-2.141358
6	-0.505176	2.031653	-4.025850
6	-3.003444	1.337785	-2.979542
6	-1.616605	1.956320	-4.864228
6	-2.869568	1.615178	-4.339839
1	-1.966813	1.171038	-1.083811
1	0.455794	2.329925	-4.436724
1	-3.970726	1.056722	-2.572733
1	-1.509880	2.173633	-5.923905
1	-3.735019	1.560582	-4.994642
6	0.817994	3.883402	-1.560018
6	2.034453	4.573116	-1.661133
6	-0.383589	4.606031	-1.637972
6	2.048691	5.957241	-1.845283
6	-0.367499	5.987632	-1.817420
6	0.849299	6.666624	-1.928106
1	2.980162	4.045362	-1.600412
1	-1.334276	4.084806	-1.575988
1	2.999236	6.478056	-1.925499
1	-1.305523	6.533235	-1.878255
1	0.861921	7.742985	-2.078690
6	-0.635896	1.752617	2.656277
6	-0.505176	2.031653	4.025850
6	-1.887582	1.400471	2.141358
6	-1.616605	1.956320	4.864228
6	-3.003444	1.337785	2.979542
6	-2.869568	1.615178	4.339839
1	0.455794	2.329925	4.436724
1	-1.966813	1.171038	1.083811
1	-1.509880	2.173633	5.923905
1	-3.970726	1.056722	2.572733

1	-3.735019	1.560582	4.994642
6	0.817994	3.883402	1.560018
6	2.034453	4.573116	1.661133
6	-0.383589	4.606031	1.637972
6	2.048691	5.957241	1.845283
6	-0.367499	5.987632	1.817420
6	0.849299	6.666624	1.928106
1	2.980162	4.045362	1.600412
1	-1.334276	4.084806	1.575988
1	2.999236	6.478056	1.925499
1	-1.305523	6.533235	1.878255
1	0.861921	7.742985	2.078690
1	0.690794	-0.353747	3.207227
1	0.690794	-0.353747	-3.207227

Table S62. Cartesian coordinates for the optimized geometry of *cis*-**2f**.

Atomic Number	X	Y	Z
5	-0.896863	0.990218	0.000000
1	-2.125109	1.008758	0.000000
15	-0.481779	2.162173	-1.598989
6	-0.946325	1.462119	-3.249563
1	-1.981812	1.084184	-3.211054
1	-0.250311	0.683173	-3.588235
1	-0.897189	2.308772	-3.956518
6	1.260372	2.661393	-1.891332
6	2.105820	1.716674	-2.512842
1	1.733785	0.728378	-2.788256
6	3.449056	2.023225	-2.766784
1	4.088027	1.269432	-3.242026
6	3.969647	3.276203	-2.403887
1	5.021211	3.516767	-2.603834
6	3.137162	4.220014	-1.781952
1	3.533031	5.200618	-1.491040
6	1.792107	3.913128	-1.523365
1	1.163201	4.659816	-1.035834
6	-1.589395	3.647030	-1.727221
6	-1.194137	4.889700	-2.268222
1	-0.154284	5.078063	-2.546359
6	-2.146711	5.896682	-2.501996
1	-1.820405	6.861105	-2.910670
6	-3.506222	5.665599	-2.237428
1	-4.247009	6.452352	-2.426272
6	-3.912930	4.412286	-1.751686
1	-4.974692	4.210589	-1.563652
6	-2.962463	3.412654	-1.499931
1	-3.292377	2.437864	-1.125688
15	-0.481779	2.162173	1.598989
6	-0.946325	1.462119	3.249563
1	-1.981812	1.084184	3.211054
1	-0.250311	0.683173	3.588235
6	1.260372	2.661394	1.891332

1	-0.897190	2.308772	3.956518
6	2.105820	1.716674	2.512842
1	1.733785	0.728378	2.788256
6	3.449056	2.023225	2.766784
1	4.088027	1.269432	3.242025
6	3.969646	3.276203	2.403887
1	5.021210	3.516768	2.603834
6	3.137161	4.220014	1.781952
1	3.533030	5.200618	1.491040
6	1.792106	3.913128	1.523365
1	1.163200	4.659817	1.035834
6	-1.589395	3.647030	1.727221
6	-1.194137	4.889700	2.268222
1	-0.154283	5.078063	2.546359
6	-2.146711	5.896682	2.501995
1	-1.820405	6.861105	2.910669
6	-3.506222	5.665599	2.237427
1	-4.247009	6.452352	2.426271
6	-3.912931	4.412286	1.751685
1	-4.974693	4.210589	1.563651
6	-2.962463	3.412654	1.499931
1	-3.292377	2.437864	1.125688
77	-0.140677	1.199074	0.000000
15	-0.538370	1.675513	-2.272319
6	-1.193813	3.398363	-2.374401
6	-2.460208	3.670844	-1.817362
6	-2.969559	4.976953	-1.836007
6	-2.210663	6.022026	-2.394084
6	-0.945772	5.753238	-2.941692
6	-0.436424	4.442794	-2.938688
17	2.232902	0.288332	0.000000
15	-0.538371	1.675513	2.272319
6	0.784817	1.628497	3.532727
6	2.126325	1.785663	3.125342
6	3.147612	1.800155	4.091074
6	2.837386	1.653559	5.453851
6	1.498641	1.498840	5.860403
6	0.471709	1.494222	4.904363
6	0.707505	2.975891	0.000001
8	1.332490	3.945687	0.000001
6	-1.193814	3.398363	2.374403
6	-2.460209	3.670843	1.817363
6	-2.969559	4.976951	1.836008
6	-2.210664	6.022025	2.394087
6	-0.945773	5.753237	2.941695
6	-0.436425	4.442793	2.938690
6	0.784818	1.628499	-3.532725
6	0.471711	1.494224	-4.904362
6	1.498644	1.498843	-5.860401
6	2.837389	1.653562	-5.453849
6	3.147613	1.800158	-4.091072

S159

6	2.126326	1.785665	-3.125340
1	-1.682657	1.587203	0.000000
1	-1.602773	0.988926	2.902673
1	-3.042058	2.862238	1.356475
1	0.549799	4.238374	3.371460
1	-3.959128	5.182105	1.409604
1	-0.349606	6.564935	3.376649
1	-2.606454	7.045168	2.400883
1	2.374282	1.845937	2.059755
1	-0.572956	1.387821	5.224729
1	4.190510	1.918922	3.771985
1	1.254626	1.387682	6.924172
1	3.638623	1.658836	6.203448
1	-3.042057	2.862240	-1.356475
1	0.549799	4.238376	-3.371457
1	-3.959128	5.182106	-1.409603
1	-0.349605	6.564936	-3.376645
1	-2.606453	7.045169	-2.400880
1	-0.572953	1.387823	-5.224727
1	2.374283	1.845940	-2.059753
1	1.254628	1.387685	-6.924170
1	4.190511	1.918925	-3.771982
1	3.638625	1.658840	-6.203445
1	-1.602772	0.988926	-2.902673

Table S63. Cartesian coordinates for the optimized geometry of *trans*-**2f**.

Atomic Number	X	Y	Z
5	0.657200	1.199584	0.000000
1	1.879275	1.308308	0.000000
15	0.374775	2.166618	-1.661924
6	1.782822	1.611716	-2.729075
1	2.612689	2.329595	-2.627457
1	1.481134	1.556986	-3.788727
1	2.139206	0.632695	-2.363230
6	0.478055	4.008890	-1.682825
6	1.727263	4.662869	-1.638815
6	1.795536	6.062201	-1.710851
6	0.619341	6.823206	-1.809566
6	-0.628948	6.179483	-1.823233
6	-0.702179	4.779694	-1.760510
1	2.657090	4.089893	-1.543627
1	2.773313	6.558632	-1.685095
1	0.675452	7.917040	-1.869981
1	-1.552388	6.767864	-1.890031
1	-1.680919	4.287017	-1.790857
6	-1.169607	1.850024	-2.603360
6	-1.280009	2.301797	-3.937522
1	-0.460252	2.866808	-4.399156
6	-2.443639	2.036510	-4.674196
1	-2.523500	2.384693	-5.711412
6	-3.506641	1.326877	-4.083591

1	-4.413285	1.115131	-4.663642
6	-3.404126	0.888403	-2.753753
1	-4.226335	0.327607	-2.293793
6	-2.238075	1.149883	-2.015363
1	-2.130391	0.771283	-0.996607
15	0.374775	2.166618	1.661924
6	0.478055	4.008890	1.682825
6	-0.702179	4.779694	1.760510
1	-1.680919	4.287017	1.790857
6	-0.628948	6.179483	1.823233
1	-1.552388	6.767864	1.890031
6	0.619341	6.823206	1.809566
1	0.675452	7.917040	1.869981
1	2.773313	6.558632	1.685095
6	1.795536	6.062201	1.710851
6	1.727263	4.662869	1.638815
1	2.657090	4.089893	1.543627
6	1.782822	1.611716	2.729075
1	2.612689	2.329595	2.627457
1	1.481134	1.556986	3.788727
1	2.139206	0.632695	2.363230
6	-1.169607	1.850024	2.603360
6	-1.280009	2.301797	3.937522
1	-0.460252	2.866808	4.399156
6	-2.443639	2.036510	4.674196
1	-2.523501	2.384692	5.711412
6	-3.506641	1.326877	4.083591
1	-4.413285	1.115131	4.663642
6	-3.404126	0.888403	2.753753
1	-4.226335	0.327607	2.293793
1	-2.130391	0.771283	0.996607
6	-2.238075	1.149883	2.015363
77	0.312035	-1.105247	0.000000
1	-1.231603	-0.768502	0.000000
6	0.051380	-3.024067	0.000000
8	-0.146015	-4.163585	0.000000
17	2.842224	-1.224720	0.000000
15	0.167483	-1.342893	2.361210
6	1.608471	-2.054340	3.225734
6	2.348438	-3.107416	2.650933
6	3.414869	-3.678539	3.361275
6	3.756192	-3.197092	4.637665
6	3.026321	-2.141175	5.210662
6	1.952311	-1.571730	4.507346
15	0.167483	-1.342893	-2.361210
6	1.608471	-2.054340	-3.225734
6	1.952313	-1.571729	-4.507346
6	3.026323	-2.141175	-5.210662
6	3.756193	-3.197092	-4.637665
6	3.414870	-3.678539	-3.361275
6	2.348438	-3.107415	-2.650933

S161

6	-1.265465	-2.402495	2.854439
6	-2.429761	-2.446036	2.060693
6	-3.533572	-3.214239	2.462325
6	-3.482430	-3.951286	3.657767
6	-2.321470	-3.917414	4.449544
6	-1.216036	-3.147516	4.052434
6	-1.265465	-2.402495	-2.854439
6	-2.429761	-2.446036	-2.060694
6	-3.533572	-3.214239	-2.462326
6	-3.482430	-3.951286	-3.657768
6	-2.321468	-3.917414	-4.449545
6	-1.216035	-3.147516	-4.052434
1	-2.461732	-1.885770	1.121853
1	-0.311034	-3.135919	4.671133
1	-4.432616	-3.245554	1.833647
1	-2.271078	-4.498644	5.378656
1	-4.341880	-4.558859	3.967548
1	2.110265	-3.461103	1.644321
1	1.375701	-0.754641	4.960440
1	3.990889	-4.495009	2.909095
1	3.290783	-1.761783	6.205525
1	4.596197	-3.642510	5.185203
1	-2.461732	-1.885770	-1.121854
1	-0.311033	-3.135919	-4.671133
1	-4.432616	-3.245554	-1.833648
1	-2.271076	-4.498644	-5.378657
1	-4.341879	-4.558859	-3.967549
1	1.375702	-0.754640	-4.960440
1	2.110265	-3.461104	-1.644321
1	3.290785	-1.761783	-6.205525
1	3.990890	-4.495009	-2.909095
1	4.596198	-3.642510	-5.185203
1	-0.066362	-0.215203	-3.181781
1	-0.066363	-0.215203	3.181781

Table S64. Cartesian coordinates for the optimized geometry of **2g**.

Atomic Number	X	Y	Z
6	-2.417102	-0.868846	0.000000
6	-3.141523	-1.177522	-1.191806
6	-3.023195	-0.330105	-2.442070
1	-4.035901	-0.047205	-2.757070
1	-2.562425	-0.825977	-3.304847
1	-2.486729	0.594062	-2.226863
6	-4.173361	-2.131041	-1.187427
1	-4.663404	-2.371837	-2.130808
6	-4.631448	-2.695826	0.000000
1	-5.409786	-3.455706	0.000000
6	-4.173361	-2.131041	1.187427
1	-4.663404	-2.371837	2.130808
6	-3.141523	-1.177522	1.191806
6	-3.023195	-0.330105	2.442070

1	-4.035901	-0.047205	2.757070
1	-2.562425	-0.825977	3.304847
1	-2.486729	0.594062	2.226863
77	-0.380541	-0.014452	0.000000
1	0.203529	-1.494294	0.000000
17	-1.574277	2.208678	0.000000
6	1.262548	0.993058	0.000000
8	2.147920	1.730360	0.000000
15	0.104751	-0.484178	-2.275722
6	-0.300615	0.648468	-3.649962
6	-0.379792	0.225673	-4.984578
6	-0.620053	1.152598	-6.000451
6	-0.771885	2.508680	-5.691161
6	-0.685543	2.932866	-4.362636
6	-0.452371	2.007450	-3.341991
15	0.104751	-0.484178	2.275722
6	-0.300615	0.648468	3.649962
6	-0.452371	2.007450	3.341991
6	-0.685544	2.932866	4.362636
6	-0.771886	2.508680	5.691161
6	-0.620053	1.152599	6.000451
6	-0.379792	0.225673	4.984578
6	-0.387527	-2.193535	-2.745927
6	1.941835	-0.601889	-2.439735
6	2.624498	-1.610114	-1.742756
6	4.012141	-1.715381	-1.817707
6	4.744813	-0.798713	-2.578131
6	4.076179	0.217487	-3.262922
6	2.682942	0.314213	-3.199433
6	-0.387527	-2.193535	2.745927
6	1.941835	-0.601889	2.439735
6	2.682942	0.314214	3.199433
6	4.076179	0.217488	3.262923
6	4.744813	-0.798712	2.578132
6	4.012141	-1.715380	1.817708
6	2.624498	-1.610114	1.742757
1	-0.269748	-2.368653	3.819427
1	-1.410916	-2.395230	2.427992
1	0.280219	-2.870568	2.206867
1	0.280219	-2.870568	-2.206867
1	-1.410916	-2.395230	-2.427992
1	-0.269747	-2.368653	-3.819427
1	2.178017	1.108820	3.738831
1	2.069169	-2.305270	1.120668
1	4.636169	0.940753	3.850748
1	4.522939	-2.506370	1.274827
1	5.828200	-0.874070	2.630436
1	-0.424190	2.333462	2.305705
1	-0.251725	-0.821842	5.241789
1	-0.810754	3.983537	4.113076
1	-0.686602	0.816380	7.032533

1	-0.961205	3.228906	6.483652
1	2.069169	-2.305270	-1.120667
1	2.178017	1.108819	-3.738831
1	4.522939	-2.506371	-1.274825
1	4.636169	0.940752	-3.850747
1	5.828200	-0.874071	-2.630435
1	-0.251725	-0.821842	-5.241789
1	-0.424190	2.333462	-2.305705
1	-0.686602	0.816379	-7.032533
1	-0.810753	3.983537	-4.113076
1	-0.961204	3.228905	-6.483652

Table S65. Cartesian coordinates for the optimized geometry of *cis*-**2h**.

Atomic Number	X	Y	Z
6	2.022570	1.688995	0.000000
1	1.659970	2.740432	0.000000
6	2.930028	1.474659	-1.229425
1	3.206800	0.407908	-1.312855
1	2.478853	1.775468	-2.189436
1	3.867419	2.064044	-1.123825
6	2.930028	1.474659	1.229425
1	3.206800	0.407908	1.312855
1	2.478853	1.775468	2.189436
1	3.867419	2.064044	1.123825
77	0.199664	0.366397	0.000000
1	-0.728574	1.662811	0.000000
6	-1.194458	-0.989180	0.000000
8	-1.914603	-1.894769	0.000000
17	1.820258	-1.599935	0.000000
15	-0.026835	0.676323	2.331615
6	1.105896	-0.128522	3.521884
6	1.376085	-1.501978	3.340809
6	2.219774	-2.172860	4.240473
6	2.804918	-1.481367	5.315337
6	2.543225	-0.111356	5.492633
6	1.694079	0.563713	4.600774
15	-0.026835	0.676323	-2.331615
6	1.105896	-0.128522	-3.521884
6	1.694079	0.563713	-4.600774
6	2.543225	-0.111356	-5.492633
6	2.804918	-1.481367	-5.315337
6	2.219774	-2.172860	-4.240473
6	1.376085	-1.501978	-3.340809
6	-0.077644	2.476453	2.758033
6	-1.710614	0.148671	2.890988
6	-1.919949	-0.671027	4.017467
6	-3.225919	-1.038307	4.388952
6	-4.328706	-0.584280	3.647337
6	-4.124026	0.239292	2.525085
6	-2.822942	0.599276	2.146554
6	-0.077644	2.476453	-2.758033

6	-1.710614	0.148671	-2.890988
6	-2.822942	0.599276	-2.146554
6	-4.124026	0.239292	-2.525085
6	-4.328707	-0.584279	-3.647337
6	-3.225919	-1.038307	-4.388952
6	-1.919949	-0.671027	-4.017467
1	-0.230384	2.628989	3.841654
1	0.843414	2.977005	2.416814
1	-0.935913	2.896322	2.206488
1	-0.935913	2.896322	-2.206488
1	0.843414	2.977005	-2.416814
1	-0.230384	2.628989	-3.841654
1	-1.064276	-1.029411	4.601084
1	-2.657578	1.211990	1.251842
1	-3.378496	-1.684786	5.262727
1	-4.980526	0.591911	1.936052
1	-5.346063	-0.875578	3.938330
1	0.956773	-2.033672	2.479878
1	1.501869	1.632696	4.747058
1	2.431742	-3.238679	4.088642
1	3.001850	0.435330	6.326564
1	3.470976	-2.007460	6.011398
1	-2.657578	1.211990	-1.251842
1	-1.064276	-1.029411	-4.601084
1	-4.980526	0.591911	-1.936051
1	-3.378496	-1.684785	-5.262727
1	-5.346064	-0.875578	-3.938329
1	1.501869	1.632696	-4.747058
1	0.956773	-2.033672	-2.479878
1	3.001850	0.435330	-6.326564
1	2.431743	-3.238679	-4.088641
1	3.470976	-2.007459	-6.011397

Table S66. Cartesian coordinates for the optimized geometry of *trans*-**2h**.

Atomic Number	X	Y	Z
6	-2.360549	-1.065100	0.000000
1	-2.816833	-0.053042	0.000000
6	-2.906339	-1.833681	1.220421
1	-2.707383	-1.352935	2.190834
1	-4.010632	-1.943703	1.144043
1	-2.486218	-2.859454	1.247783
6	-2.906339	-1.833681	-1.220421
1	-4.010632	-1.943703	-1.144043
1	-2.486218	-2.859454	-1.247783
1	-2.707383	-1.352935	-2.190834
77	-0.148431	-0.665409	0.000000
17	-0.475140	1.896252	0.000000
6	1.791330	-0.596022	0.000000
8	2.941036	-0.738490	0.000000
1	-0.117259	-2.250204	0.000000
15	-0.036347	-0.678114	2.375460

6	-1.230847	0.292091	3.394099
6	-2.213176	1.106330	2.798937
6	-3.094815	1.841062	3.609641
6	-3.002231	1.768182	5.009611
6	-2.015440	0.961996	5.605898
6	-1.129030	0.229996	4.801125
15	-0.036347	-0.678114	-2.375460
6	-1.230847	0.292091	-3.394099
6	-1.129030	0.229997	-4.801125
6	-2.015440	0.961997	-5.605898
6	-3.002232	1.768182	-5.009610
6	-3.094816	1.841062	-3.609640
6	-2.213176	1.106330	-2.798937
6	-0.078835	-2.380670	3.087357
6	1.573792	0.007623	2.957977
6	1.847282	1.363976	2.672141
6	3.073639	1.925399	3.055461
6	4.036940	1.144603	3.720648
6	3.768786	-0.204921	4.000546
6	2.540203	-0.774371	3.621040
6	-0.078836	-2.380670	-3.087357
6	1.573792	0.007623	-2.957977
6	2.540203	-0.774370	-3.621040
6	3.768786	-0.204921	-4.000546
6	4.036939	1.144603	-3.720648
6	3.073638	1.925399	-3.055461
6	1.847281	1.363976	-2.672141
1	0.075209	-2.371987	4.181135
1	-1.057366	-2.824745	2.847997
1	0.713229	-2.974059	2.597607
1	0.713229	-2.974059	-2.597607
1	-1.057366	-2.824745	-2.847997
1	0.075209	-2.371987	-4.181135
1	1.109418	1.962898	2.123311
1	2.350716	-1.831108	3.840040
1	3.280869	2.978540	2.826263
1	4.517748	-0.822090	4.513416
1	4.997409	1.586709	4.015418
1	-2.264781	1.178123	1.709056
1	-0.347298	-0.379818	5.272231
1	-3.856017	2.476943	3.139947
1	-1.931543	0.907962	6.698980
1	-3.693900	2.343821	5.638374
1	2.350715	-1.831107	-3.840040
1	1.109417	1.962898	-2.123311
1	4.517748	-0.822090	-4.513416
1	3.280868	2.978540	-2.826263
1	4.997408	1.586709	-4.015418
1	-0.347298	-0.379818	-5.272231
1	-2.264781	1.178123	-1.709056
1	-1.931543	0.907963	-6.698980

1	-3.856017	2.476943	-3.139946
1	-3.693901	2.343821	-5.638373

Table S67. Cartesian coordinates for the optimized geometry of **2j**.

Atomic Number	X	Y	Z
15	-2.248834	0.217539	0.000000
6	-2.847636	1.198526	1.421084
1	-2.707361	0.666799	2.362798
1	-2.265916	2.123125	1.454846
1	-3.911468	1.415776	1.277348
6	-2.847636	1.198526	-1.421084
1	-2.265916	2.123125	-1.454846
1	-2.707361	0.666799	-2.362798
1	-3.911468	1.415776	-1.277348
6	-3.325374	-1.261824	0.000000
6	-3.764021	-1.831045	1.206986
1	-3.509785	-1.367729	2.155166
6	-4.572909	-2.969089	1.207783
1	-4.906120	-3.391511	2.152142
6	-4.968344	-3.550028	0.000000
1	-5.599363	-4.434586	0.000000
6	-4.572909	-2.969089	-1.207783
1	-4.906120	-3.391510	-2.152142
6	-3.764021	-1.831045	-1.206986
1	-3.509785	-1.367729	-2.155166
77	0.160742	0.019368	0.000000
1	0.153537	-1.566608	0.000000
17	0.070831	2.551290	0.000000
6	2.061469	0.281990	0.000000
8	3.166057	0.581577	0.000000
15	0.286245	-0.366996	2.361501
6	-0.357211	0.854660	3.534568
6	0.036313	2.195582	3.393340
6	-0.455250	3.162784	4.271092
6	-1.345836	2.803870	5.287591
6	-1.736637	1.469488	5.434403
6	-1.241965	0.495334	4.564978
15	0.286245	-0.366996	-2.361501
6	-0.357211	0.854660	-3.534568
6	-1.241966	0.495334	-4.564978
6	-1.736639	1.469488	-5.434403
6	-1.345838	2.803870	-5.287591
6	-0.455251	3.162784	-4.271093
6	0.036313	2.195582	-3.393341
6	-0.506220	-1.967314	2.771886
6	2.017017	-0.683676	2.861020
6	2.685786	0.104489	3.805960
6	4.014771	-0.179080	4.136075
6	4.677487	-1.250814	3.534695
6	4.010041	-2.044138	2.594763
6	2.688951	-1.759324	2.255287

6	-0.506221	-1.967314	-2.771886
6	2.017016	-0.683676	-2.861020
6	2.688950	-1.759325	-2.255287
6	4.010040	-2.044138	-2.594764
6	4.677486	-1.250814	-3.534696
6	4.014770	-0.179080	-4.136075
6	2.685786	0.104488	-3.805960
1	-0.365050	-2.204877	3.830949
1	-1.566860	-1.959931	2.519607
1	-0.015241	-2.730837	2.163554
1	-0.015242	-2.730837	-2.163554
1	-1.566861	-1.959931	-2.519607
1	-0.365051	-2.204877	-3.830949
1	2.176880	0.934258	4.285654
1	2.184807	-2.364300	1.505403
1	4.528467	0.439765	4.866920
1	4.520778	-2.880199	2.124094
1	5.709857	-1.468401	3.794973
1	0.703971	2.485556	2.589286
1	-1.552237	-0.537025	4.695011
1	-0.147752	4.198370	4.153521
1	-2.422719	1.184629	6.227730
1	-1.732899	3.560671	5.964824
1	2.184806	-2.364300	-1.505403
1	2.176880	0.934257	-4.285654
1	4.520777	-2.880199	-2.124095
1	4.528467	0.439765	-4.866920
1	5.709856	-1.468401	-3.794974
1	-1.552238	-0.537025	-4.695011
1	0.703971	2.485556	-2.589288
1	-2.422721	1.184629	-6.227730
1	-0.147753	4.198369	-4.153523
1	-1.732901	3.560671	-5.964824

Table S68. Cartesian coordinates for the optimized geometry of **2k**.

Atomic Number	X	Y	Z
6	-0.099767	1.284692	0.000000
15	-0.011382	2.155951	-1.483373
6	-1.580682	2.245614	-2.440447
6	-2.778018	1.781372	-1.897278
6	-3.964811	1.839919	-2.633676
6	-3.954067	2.360615	-3.929343
6	-2.755099	2.827134	-4.483896
6	-1.575308	2.774911	-3.742002
1	-2.758737	1.339782	-0.908953
1	-4.892461	1.473323	-2.200840
1	-4.873358	2.405482	-4.507463
1	-2.743980	3.236527	-5.490806
1	-0.651107	3.150893	-4.173327
6	1.182134	1.431703	-2.684565
1	1.720942	2.238067	-3.186042

1	0.667772	0.857638	-3.451681
1	1.884645	0.793236	-2.144658
15	-0.011382	2.155951	1.483373
6	1.182134	1.431703	2.684565
1	1.720942	2.238067	3.186042
1	0.667772	0.857638	3.451681
1	1.884645	0.793236	2.144658
6	-1.580682	2.245614	2.440447
6	-1.575307	2.774911	3.742002
6	-2.755099	2.827134	4.483896
6	-3.954066	2.360615	3.929343
6	-3.964811	1.839919	2.633676
6	-2.778018	1.781373	1.897278
1	-0.651107	3.150893	4.173327
1	-2.743980	3.236527	5.490806
1	-4.873357	2.405482	4.507463
1	-4.892461	1.473324	2.200840
1	-2.758737	1.339782	0.908953
6	0.495646	3.924156	1.514245
6	1.860751	4.242445	1.580092
6	2.268140	5.560548	1.778343
6	1.316210	6.576694	1.904660
6	-0.043057	6.269917	1.816446
6	-0.452427	4.949345	1.623432
1	2.607633	3.459261	1.481298
1	3.328115	5.794026	1.834102
1	1.633831	7.603307	2.067427
1	-0.787928	7.056591	1.903509
1	-1.512022	4.718047	1.575879
6	0.495646	3.924156	-1.514245
6	1.860751	4.242445	-1.580092
1	2.607633	3.459261	-1.481298
6	2.268139	5.560548	-1.778343
6	1.316210	6.576694	-1.904660
6	-0.043057	6.269917	-1.816446
6	-0.452428	4.949345	-1.623432
1	-1.512023	4.718047	-1.575879
1	-0.787927	7.056591	-1.903509
1	1.633831	7.603307	-2.067428
1	3.328114	5.794026	-1.834101
77	0.230137	-1.002077	0.000000
17	2.696467	-0.335399	0.000000
1	-1.330919	-1.278874	0.000000
6	0.874171	-2.763367	0.000000
8	1.391392	-3.792963	0.000000
15	-0.135784	-1.578291	-2.331540
6	-0.774520	-3.308971	-2.316012
6	-2.017790	-3.553314	-1.714966
6	-2.575542	-4.830239	-1.742222
6	-1.885124	-5.883987	-2.348799
6	-0.639097	-5.649463	-2.933346

6	-0.086870	-4.365263	-2.926388
15	-0.135785	-1.578291	2.331540
6	-0.774520	-3.308971	2.316014
6	-2.017790	-3.553313	1.714968
6	-2.575542	-4.830238	1.742223
6	-1.885125	-5.883987	2.348800
6	-0.639098	-5.649463	2.933347
6	-0.086871	-4.365263	2.926390
6	1.281571	-1.670174	-3.471341
6	1.123042	-1.449807	-4.849588
6	2.215574	-1.570068	-5.709905
6	3.471421	-1.919841	-5.203894
6	3.630678	-2.146867	-3.834423
6	2.542500	-2.020439	-2.968471
6	-1.511850	-0.836980	-3.296170
6	1.281570	-1.670173	3.471341
6	2.542499	-2.020437	2.968472
6	3.630677	-2.146865	3.834424
6	3.471421	-1.919840	5.203895
6	2.215574	-1.570067	5.709905
6	1.123042	-1.449805	4.849588
6	-1.511850	-0.836979	3.296170
1	-1.749291	-1.522521	4.115273
1	-1.279984	0.148943	3.693341
1	-2.379515	-0.753144	2.640398
1	-2.379515	-0.753145	-2.640398
1	-1.279984	0.148942	-3.693341
1	-1.749290	-1.522522	-4.115273
1	-2.546772	-2.744708	1.218099
1	0.877591	-4.193087	3.392709
1	-3.544791	-5.005775	1.283999
1	-0.093006	-6.464193	3.401497
1	-2.315385	-6.881883	2.361939
1	2.687585	-2.165494	1.905075
1	0.153610	-1.184561	5.259962
1	4.604544	-2.413836	3.433024
1	2.084072	-1.394089	6.774396
1	4.321498	-2.012332	5.874836
1	-2.546772	-2.744709	-1.218097
1	0.877592	-4.193087	-3.392707
1	-3.544791	-5.005775	-1.283998
1	-0.093004	-6.464193	-3.401496
1	-2.315383	-6.881884	-2.361938
1	0.153610	-1.184562	-5.259962
1	2.687586	-2.165496	-1.905074
1	2.084072	-1.394090	-6.774396
1	4.604544	-2.413839	-3.433022
1	4.321498	-2.012334	-5.874835

References

(1) Sommer, K. Zur Spaltung Tertiärer Phosphine. *Zeitschrift für Anorg. und Allg. Chemie* **1970**, *376* (1), 37–43.

(2) Rahim, M.; Ahmed, K. J. High-Yield General Synthesis of *trans*-Ir(PR_3)$_2$(CO)Cl (PR_3 = PPh_3, PPh_2Me, $PPhMe_2$, PEt_3, PMe_3). *Inorg. Chem.* **1994**, *33* (13), 3003–3004.

(3) Reitsamer, C.; Stallinger, S.; Schuh, W.; Kopacka, H.; Wurst, K.; Obendorf, D.; Peringer, P. Novel Access to Carbodiphosphoranes in the Coordination Sphere of Group 10 Metals: Template Synthesis and Protonation of PCP Pincer Carbodiphosphorane Complexes of C(Dppm)2. *Dalt. Trans.* **2012**, *41* (12), 3503.

(4) Grätz, M.; Bäcker, A.; Vondung, L.; Maser, L.; Reincke, A.; Langer, R. Donor Ligands Based on Tricoordinate Boron Formed by B–H-Activation of Bis(Phosphine)Boronium Salts. *Chem. Commun.* **2017**, *53* (53), 7230–7233.

(5) Khan, M. M. T.; Rao, E. R. Synthesis and Characterization of Novel Platinum Group Metal Complexes of Bis[2-(Diphenylphosphino)Ethyl]Amine. *Polyhedron* **1987**, *6* (9), 1727–1735.

(6) Wu, Q.; Zhou, F.; Shu, X.; Jian, L.; Xu, B.; Zheng, X.; Yuan, M.; Fu, H.; Li, R.; Chen, H. Synthesis and Application of PNP Pincer Ligands in Rhodium-Catalyzed Hydroformylation of Cycloolefins. *RSC Adv.* **2016**, *6* (109), 107305–107309.

(7) Lee, H. M.; Zeng, J. Y.; Hu, C.-H.; Lee, M.-T. A New Tridentate Pincer Phosphine/ N -Heterocyclic Carbene Ligand: Palladium Complexes, Their Structures, and Catalytic Activities. *Inorg. Chem.* **2004**, *43* (21), 6822–6829.

(8) Li, R.-X.; Li, X.-J.; Wong, N.-B.; Tin, K.-C.; Zhou, Z.-Y.; Mak, T. C. . Syntheses and Characterizations of Iridium Complexes Containing Bidentate Phosphine Ligands and Their Catalytic Hydrogenation Reactions to α,β-Unsaturated Aldehydes. *J. Mol. Catal. A Chem.* **2002**, *178* (1–2), 181–190.

(9) Dolomanov, O. V.; Bourhis, L. J.; Gildea, R. J.; Howard, J. A. K.; Puschmann, H. OLEX2 : A Complete Structure Solution, Refinement and Analysis Program. *J. Appl. Crystallogr.* **2009**, *42* (2), 339–341.

(10) Bourhis, L. J.; Dolomanov, O. V.; Gildea, R. J.; Howard, J. a. K.; Puschmann, H. The Anatomy of a Comprehensive Constrained, Restrained Refinement Program for the Modern Computing Environment – Olex2 Dissected. *Acta Crystallogr. Sect. A Found. Adv.* **2015**, *71* (1), 59–75.

(11) Sheldrick, G. M. A Short History of SHELX. *Acta Crystallogr. Sect. A Found. Crystallogr.* **2007**, *64* (1), 112–122.

(12) Sheldrick, G. M. Crystal Structure Refinement with SHELXL. *Acta Crystallogr. Sect. C Struct. Chem.* **2015**, *71* (1), 3–8.

(13) Grimme, S. Semiempirical GGA-Type Density Functional Constructed with a Long-Range Dispersion Correction. *J. Comput. Chem.* **2006**, *27* (15), 1787–1799.

(14) Weigend, F.; Ahlrichs, R.; Peterson, K. A.; Dunning, T. H.; Pitzer, R. M.; Bergner, A. Balanced Basis Sets of Split Valence, Triple Zeta Valence and Quadruple Zeta Valence Quality for H to Rn: Design and Assessment of Accuracy. *Phys. Chem. Chem. Phys.* **2005**, *7* (18), 3297.

(15) Weigend, F.; Hättig, C.; Patzelt, H.; Ahlrichs, R.; Spencer, S.; Willets, A. Accurate Coulomb-Fitting Basis Sets for H to Rn. *Phys. Chem. Chem. Phys.* **2006**, *8* (9), 1057.

(16) Frisch, M. J.; Trucks, G. W.; Schlegel, H. B.; Scuseria, G. E.; Robb, M. A.; Cheeseman, J. R.; Scalmani, G.; Barone, V.; Petersson, G. A.; Nakatsuji, H.; Li, X.; Caricato, M.; Marenich, A. V.; Bloino, J.; Janesko, B. G.; Gomperts, R.; Mennucci, B.; Hratchian, H. P.; Ortiz, J. V.; Izmaylov, A. F.; Sonnenberg, J. L.; Williams-Young, D.; Ding, F.; Lipparini, F.; Egidi, F.; Goings, J.; Peng, B.; Petrone, A.; Henderson, T.; Ranasinghe, D.; Zakrzewski, V. G.; Gao, J.; Rega, N.; Zheng, G.; Liang, W.; Hada, M.; Ehara, M.; Toyota, K.; Fukuda, R.; Hasegawa, J.; Ishida, M.; Nakajima, T.; Honda, Y.; Kitao, O.; Nakai, H.; Vreven, T.; Throssell, K.; Montgomery, J. A. Jr.; Peralta, J. E.; Ogliaro, F.; Bearpark, M. J.; Heyd, J. J.; Brothers, E. N.; Kudin, K. N.; Staroverov, V. N.; Keith, T. A.; Kobayashi, R.; Normand, J.; Raghavachari, K.; Rendell, A. P.; Burant, J. C.; Iyengar, S. S.; Tomasi, J.; Cossi, M.; Millam, J. M.; Klene, M.; Adamo, C.; Cammi, R.; Ochterski, J. W.; Martin, R. L.; Morokuma, K.; Farkas, O.; Foresman, J. B.; Fox, D. J. Gaussian 16 Revision B.01. Gaussian, Inc.: Wallingford CT 2016.

(17) Van Lenthe, E.; Baerends, E. J. Optimized Slater-Type Basis Sets for the Elements 1-118. *J. Comput. Chem.* **2003**, *24* (9), 1142–1156.

(18) van Lenthe, E.; Baerends, E. J.; Snijders, J. G. Relativistic Regular Two-component Hamiltonians. *J. Chem. Phys.* **1993**, *99* (6), 4597–4610.

(19) Fonseca Guerra, C.; Snijders, J. G.; Te Velde, G.; Baerends, E. J. Towards an Order-N DFT Method. *Theor. Chem. Acc.* **1998**, *99*, 391–403.

(20) te Velde, G.; Bickelhaupt, F. M.; Baerends, E. J.; Fonseca Guerra, C.; van Gisbergen, S. J. A.; Snijders, J. G.; Ziegler, T. Chemistry with ADF. *J. Comput. Chem.* **2001**, *22* (9), 931–967.

(21) Becke, A. D. Density-Functional Exchange-Energy Approximation with Correct Asymptotic Behavior. *Phys. Rev. A* **1988**, *38* (6), 3098–3100.

(22) Perdew, J. P. Density-Functional Approximation for the Correlation Energy of the Inhomogeneous Electron Gas. *Phys. Rev. B* **1986**, *33* (12), 8822–8824.

(23) Baerends, E. J.; Ziegler, T.; Atkins, A. J.; Autschbach, J.; Bashford, D.; Baseggio, O; Bérces, A.; Bickelhaupt, F. M.; Bo, C.; Boerritger, P. M.; Cavallo, L.; Daul, C.; Chong, D. P.; Chulhai, D. V.; Deng, L.; Dickson, R. M.; Dieterich, J. M.; Ellis, D. E.; van Faassen, M.; Ghysels, A.; Giammona, A.; van Gisbergen, S. J. A.; Goez, A.; Götz, A. W.; Gusarov, S.; Harris, F. E.; van den Hoek, P.; Hu, Z.; Jacob, C. R.; Jacobsen, H.; Jensen, L.; Joubert, L.; Kaminski, J. W.; van Kessel, G.; König, C.; Kootstra, F.; Kovalenko, A.; Krykunov, M.; van Lenthe, E.; McCormack, D. A.; Michalak, A.; Mitoraj, M.; Morton, S. M.; Neugebauer, J.; Nicu, V. P.; Noodleman, L.; Osinga, V. P.; Patchkovskii, S.; Pavanello, M.; Peeples, C. A.; Philipsen, P. H. T.; Post, D.; Pye, C. C.; Ramanantoanina, H.; Ramos, P.; Ravenek, W.; Rodríguez, J. I.; Ros, P.; Rüger, R.; Schipper, P. R. T.; Schlüns, D.; van Schoot, H.; Schreckenbach, G.; Seldenthuis, J. S.; Seth, M.; Snijders, J. G.; Solà, M.; Stener, M.; Swart, M.; Swerhone, D.; te Velde, G.; Tognetti, V.; Vernooijs, P.; Versluis, L.; Visscher, L.; Visser, O.; Wang, F.; Wesolowski, T. A.; van Wezenbeek, E. M.; Wiesenekker, G.; Wolff, S. K.; Woo, T. K.; Yakovlev, A. L. ADF2017, SCM, Theoretical Chemistry, Vrije Universiteit, Amsterdam, The Netherlands, Https://Www.Scm.Com.

(24) Marenich, A. V.; Jerome, S. V.; Cramer, C. J.; Truhlar, D. G. Charge Model 5: An Extension of Hirshfeld Population Analysis for the Accurate Description of Molecular Interactions in Gaseous and Condensed Phases. *J. Chem. Theory Comput.* **2012**, *8* (2), 527–541.

(25) Glendening, E. D.; Badenhoop, J. K.; Reed, A. E.; Carpenter, J. . E.; Bohmann, J. A.; Morales, C. M.; Landis, C. R.; Weinhold, F. NBO 6.0. Theoretical Chemistry Institute, University of Wisconsin: Madison 2013.

(26) Lu, T.; Chen, F. Multiwfn: A Multifunctional Wavefunction Analyzer. *J. Comput. Chem.* **2012**, *33* (5), 580–592.

(27) Mayer, H. A.; Fawzi, R.; Steimann, M. Synthesis, X-Ray Structure and Complexation Behavior of the New Tripodal Phosphane Ligandcis, Cis-1,3,5-Tris[(Diphenylphosphanyl)Methyl]1-1,3,5-Trimethylcyclohexane (Tdppmtmcy). Crystal Structure of Ir(Tdppmtmcy)(CO)Cl. *Chem. Ber.* **1993**, *126* (6), 1341–1346.

(28) Morokuma, K. Molecular Orbital Studies of Hydrogen Bonds. III. C=O···H–O Hydrogen Bond in $H_2CO···H_2O$ and $H_2CO···2H_2O$. *J. Chem. Phys.* **1971**, *55* (3), 1236–1244.

(29) Ziegler, T.; Rauk, A. On the Calculation of Bonding Energies by the Hartree Fock Slater Method: I. The Transition State Method. *Theor. Chim. Acta* **1977**, *46* (1), 1–10.

(30) Frenking, G. Towards a Rigorously Defined Quantum Chemical Analysis of the Chemical Bond in Donor–Acceptor Complexes. *Coord. Chem. Rev.* **2003**, *238–239* (22), 55–82.

(31) Bickelhaupt, F. M.; Baerends, E. J. Kohn-Sham Density Functional Theory: Predicting and Understanding Chemistry. In *Reviews in Computational Chemistry, Vol. 15*; Wiley-VCH, New York, 2000; pp 1–86.

(32) Frenking, G.; Matthias Bickelhaupt, F. The EDA Perspective of Chemical Bonding. In *The Chemical Bond*; Wiley-VCH Verlag GmbH & Co. KGaA: Weinheim, Germany, 2014; pp 121–157.

inorganics

MDPI

Article

Comparing the Acidity of $(R_3P)_2BH$-Based Donor Groups in Iridium Pincer Complexes

Leon Maser, Christian Schneider, Lukas Alig and Robert Langer *

Department of Chemistry, Philipps-Universität Marburg, Hans-Meerwein-Str. 4, 35032 Marburg, Germany; leon.maser@chemie.uni-marburg.de (L.M.); c.schneider2013@gmail.com (C.S.); lukas.alig@uni-goettingen.de (L.A.)

* Correspondence: robert.langer@chemie.uni-marburg.de; Tel.: +49-6421-282-5617

Received: 31 March 2019; Accepted: 29 April 2019; Published: 7 May 2019

Abstract: In the current manuscript, we describe the reactivity of a series of iridium(III) pincer complexes with the general formulae $[(PEP)IrCl(CO)(H)]^n$ (n = +1, +2) towards base, where PEP is a pincer-type ligand with different central donor groups, and E is the ligating atom of this group (E = B, C, N). The donor groups encompass a secondary amine, a phosphine-stabilised borylene and a protonated carbodiphosphorane. As all ligating atoms E exhibit an E–H bond, we addressed the question of wether the coordinated donor group can be deprotonated in competition to the reductive elimination of HCl from the iridium(III) centre. Based on experimental and quantum chemical investigations, it is shown that the ability for deprotonation of the coordinated ligand decreases in the order of $(R_3P)_2CH^+ > R_2NH > (R_3P)_2BH$. The initial product of the reductive elimination of HCl from $[(PBP)IrCl(CO)(H)]^n$ (**1c**), the square planar iridium(I) complex, $[(PBP)Ir(CO)]^+$ (**3c**), was found to be unstable and further reacts to $[(PBP)Ir(CO)_2]^+$ (**5c**). Comparing the C–O stretching vibrations of the latter with those of related complexes, it is demonstrated that neutral ligands based on tricoordinate boron are very strong donors.

Keywords: boron; iridium; pincer; carbodiphosphorane

1. Introduction

Tricoordinate boron compounds, BR_3, are typically Lewis acids and stabilise their electron deficiency by π-donating substituents, hyperconjugation or dimerisation and formation of two-electron three-centre bonds. In consequence, they can accept electron donation from electron rich metal centres and serve as Z-type ligands [1,2]. More recently, several groups demonstrated that the introduction of π-accepting substituents allows to stabilise an occupied p_z-orbital and therewith of a trigonal planar Lewis-base with the general formulae L_2BR (**III**) [3–9]. Consequently, such compounds are able to serve as electron-donating or L-type ligands, but the coordination chemistry of such nucleophilic boron compounds is rather unexplored [8–10].

In particular, the similarity to related carbon compounds of the type L_2CH^+ (**II**) and secondary amines (**I**) caught our attention. Pseudo-tetrahedral, secondary amines (**I**) can serve as cooperative ligands in homogeneous catalysts (Figure 1), by providing a proton in concerted proton hydride transfers or simply by pre-coordination of the substrate via hydrogen bridge bonds (e.g., in Figure 1, cycle **A**) [11]. Protonated carbodiphosphoranes of the type $(R_3P)_2CH^+$ (**II**) can be deprotonated by strong bases and easily form their deprotonated analogues when coordinated to a metal centre [12]. For the corresponding boron compounds, $(R_3P)_2BH$ (**III**), previous studies indicated that the boron-bound hydrogen atom in such ligands is not hydridic [13,14]. Due to the π-accepting nature of the cyanido substituents in compounds like $[HB(CN)_3]^-$, they can be deprotonated [15], which stands in contrast to the reactivity of the majority of hydrogen-containing boron compounds.

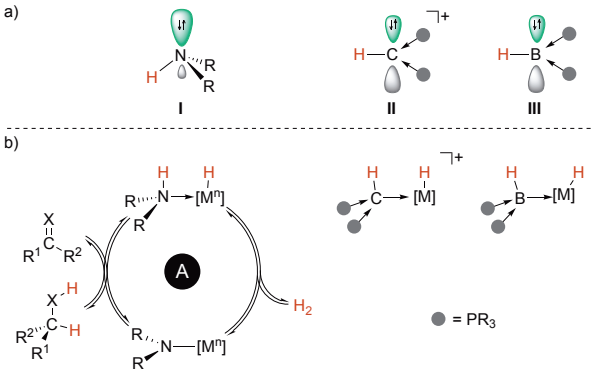

Figure 1. (**a**) Secondary amines (**I**), protonated carbodiphosphoranes (**II**) and phosphine-stabilized borylenes (**III**) in comparison; (**b**) Secondary amine ligands and their role in cooperative catalysis in comparison to the analogous metal complexes with **II** and **III** as ligands.

Motivated by these observations, we began to study a series of isotypical iridium complexes in their reactivity towards base. Herein, we demonstrate that among this series **I**–**III** the carbon-based ligand **II** is the most acidic ligand, while for the other ligands a competitive reductive elimination is observed. In case of the boron-based ligand, this leads to an unique iridium(I) complex. The comparison with related iridium dicarbonyl complexes reveals strong electron donating properties of donor groups akin to **III**.

2. Results and Discussion

As the starting point for our study, we choose the isotypical iridium(III) pincer complexes **1a**–**1c** to investigate. In this context, we compare the amine based pincer-type complex $[\{(PPh_2CH_2CH_2)_2NH\}IrCl(CO)(H)]^+ Cl^-$ (**1a**) with the formally carbon(0)- and boron(I)-based complexes $[\{(dppm)_2CH\}IrCl(CO)(H)]^{2+} 2\,Cl^-$ (**1b**) and $[\{(dppm)_2BH\}IrCl(CO)(H)]^+ Br^-$ (**1c**) [16]. In principle, the deprotonation of **1a**–**1c** can take place at several positions in the complex, but commonly either the central donor group E is deprotonated or the hydrido ligand is abstracted in a reductive elimination (Figure 2).

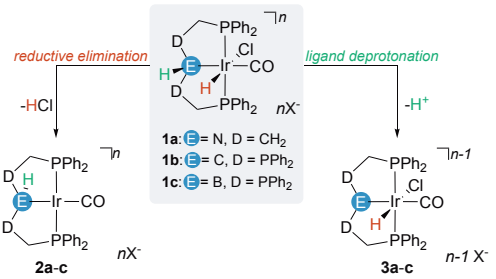

Figure 2. Cooperative ligand site vs. redox reactivity—principle reaction pathways of octahedral iridium(III) complexes **1a**–**1c** towards base (n = +, 2+). X^- = Cl^- (**a**,**b**), Br^- (**c**)

2.1. Deprotonation vs. Reductive Elimination

The reaction of the cationic complex **1a** with one equivalent of $LiN(SiMe_3)_2$ results in the formation of a new complex **2a** (Figure 3), as judged by the observation of a single resonance at 55.5 ppm in the $^{31}P\{^1H\}$ NMR spectrum of the reaction mixture. The resonance at −16.12 ppm in the ^1H NMR spectrum,

corresponding to the hydrido ligand in **1a** disappears and the absence of a resonance in this region (0 to −40 ppm) suggests that no hydrido ligand is present in the newly formed **2a** (Supplementary Materials). By comparison of NMR spectroscopic data with analogues isopropyl-substituted iridium pincer complexes [17], we concluded that the reductive elimination of HCl is the preferred reaction pathway. Addition of a second equivalent of $LiN(SiMe_3)_2$ resulted in the formation of a mixture of complexes and the $^{31}P\{^1H\}$ NMR spectrum displayed several new singlet resonances as well as a new AB spin system (Supplementary Materials). The latter finding either indicates a conformational change to a facially coordinated ligand with different ligands in *trans*-position, but this seems to be unlikely for a square pyramidal iridium(I) complex that is already formed with the first equivalent of base. A second possibility involves a β-hydride elimination from the amide ligands and subsequent tautomerisation, as previously observed for different noble metal complexes with this type of ligand [18].

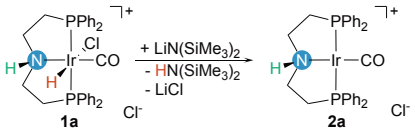

Figure 3. Reactivity of **1a** towards base.

The NMR spectra of the iridium(III) complex **1b** at ambient temperature show the presence of the *cis*- and the *trans*-isomers (ca. 1:1) as well as small quantities of **3b** (ca. 1%) [16]. The ^1H NOESY NMR spectrum of **1b** at ambient temperature displays exchange correlations between the hydride resonances of *cis*- and *trans*-**1b**, as well as between the resonances of *trans*-**1b** and **3b** (Figure 4a). These findings suggests the presence of an equilibrium between the two isomers of **1b** (Figure 4b). Furthermore one of the isomers (*trans*-**1b**) seems to be in an equilibrium with the deprotonated species **1b**, even though no additional base is present in the mixture. A broad resonance at 3.51 ppm in the ^1H NMR spectrum is assigned to HCl [19], which provides further support for reversible (de)protonation equilibrium. To get further insights about the solution behaviour of **1b**, we acquired ^1H and $^1H\{^{31}P\}$ NMR spectra at different temperatures. The ratio of integrals for the hydride resonances enables to estimate the equilibrium constant $K_{cis/trans}$ at different temperatures. The corresponding *Van't Hoff* plot (Figure 4c) displays two regions of linearity between 300 and 270 K (R^2 = 0.995) as well as between 260 and 230 K (R^2 = 0.937), which might be related to the presence of a second equilibrium or solubility issues at low temperatures. However, a reliable quantification of **3b** turned out to be difficult, due to the low concentration at ambient temperature, which decreases even further at lower temperatures. The corresponding exchange rates were accessed by line-shape-analysis of the hydride resonances in the $^1H\{^{31}P\}$ NMR spectra at different temperatures. An *Eyring* analysis (Figure 4d) revealed an *Gibbs* enthalpy of activation $\Delta G^{\ddagger}_{298}$ = 69.23 kJ·mol^{-1} for the *cis*-/*trans*-isomerisation process.

In view of the primary question, these observations suggest that **1b** gets selectively deprotonated at the coordinated donor group. The iridium(III) complex **3b** is indeed observed by NMR spectroscopy in reactions with base. As complex **1b**, in contrast to **1a** and **1c**, is dicationic, one would expect a higher acidity of the coordinated donor group, but the acidity of hydrido ligands was previously demonstrated to be increased by several orders of magnitude with an increasing charge of the complex [20].

Addition of an excess base (DBU) to **1b** results in the formation of the iridium(I) complex **4b** as major product according to the $^{31}P\{^1H\}$ NMR spectrum of the reaction mixture (Figure 5), which displayed new triplet resonances at 23.4 ppm ($^2J_{P,P}$ = 48.5 Hz) and 38.3 ppm ($^2J_{P,P}$ = 49.3 Hz). A broad multiplet resonance at 4.01–4.12 ppm with an integral of four in combination with multiplet resonances between 6.9 and 7.8 ppm with an overall integral of 40 protons are observed in the ^1H NMR spectrum (Supplementary Materials), while the absence of resonances corresponding to a hydrido ligand or a protonated CDP moiety indicate that a deprotonated pincer ligand is coordinated in **4b**. The observation of one band at 1925 cm^{-1} for the C–O stretching vibration of a carbonyl ligand

Inorganics **2019**, *7*, 61

is in line with an electron-rich mono-carbonyl complex. The composition of the cationic complex $[\{(dppm)_2C\}Ir(CO)]^+ Cl^-$ in **4b** was further confirmed by high resolution ESI-MS.

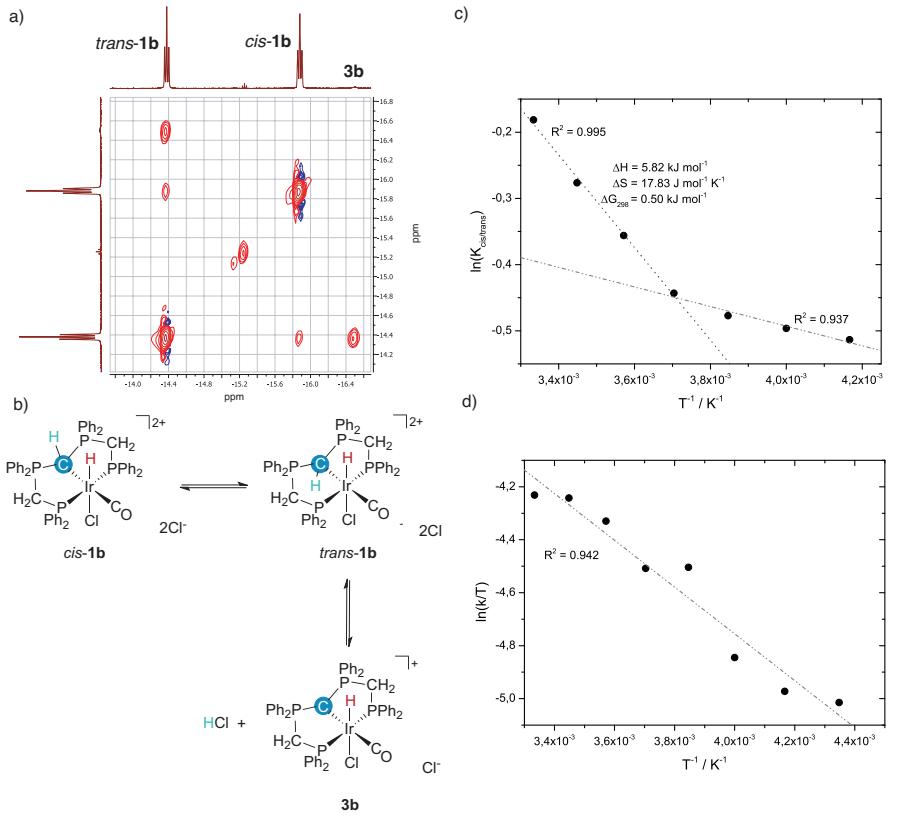

Figure 4. (**a**) Hydride region in the ^{1}H NOESY NMR spectrum at ambient temperature, showing chemical exchange correlations; (**b**) Equilibrium of the complexes in solution; (**c**) *Van't Hoff* plot for the *cis*-/*trans*-isomerisation of **1b**; (**d**) *Eyring* plot for the *cis*-/*trans*-isomerisation of **1b**.

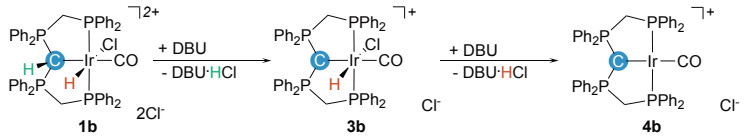

Figure 5. Reactivity of **1b** towards base.

A similar observation to the reaction of **1a** is made for the boron-based iridium pincer complex (**1c**). Treatment of complex **1c** with one equivalent $LiN(SiMe_3)_2$ leads to the formation of two species according to the $^{31}P\{^1H\}$ NMR spectrum of the reaction mixture, broadened resonance at −5.6 ppm, as well as a broad resonance at 24.9 and a multiplet at 2.9 ppm, both assignable to the newly formed complex **5c** (Figure 6). After removal of all volatiles and washing of the residue with *n*-hexane, complex **5c** is obtained in analytically pure form. The ^{1}H NMR spectrum of **5c** shows a complete set of resonances for the dppm arms of the coordinated ligand (Supplementary Materials),

while resonances corresponding to a boron-bound hydrogen atom and potential hydrido ligands are absent (Figure 7b). Upon ^{11}B-decoupling a triplet resonance at 3.20 ppm ($^{2}J_{P,H}$ = 23.2 Hz) is observed in the ^{1}H{^{11}B} NMR spectrum, assignable to a boron-bound hydrogen atom, clearly indicating that a reductive elimination is favoured over of the ligand deprotonation. The ^{11}B{^{1}H} NMR spectrum of **5c** gives rise to a broadened resonance at −35.4 ppm, which is in agreement with previously reported boron-based donor ligands [8–10,13,21]. The identity of **5c** was finally confirmed by single crystal X-Ray diffraction experiments (Figure 7a), which revealed a cationic iridium(I) complex with a trigonal bipyramidal environment (τ_5 = 0.70) [22]. In addition to the facially coordinated PBP-ligand, two carbonyl ligands are observed, one occupying an equatorial and one an axial coordination site. The Ir–B bond in **5c** is with 2.276 Å slightly shorter than in the octahedral iridium(III) complex **1c** (d_{Ir-B} = 2.285 Å) [16].

As the yield of the dicarbonyl complex **5c** was below 50% and no other potential source of carbon monoxide was present in the reaction mixture, we assumed that the formation of **5c** proceeds via a square planar iridium(I) intermediate **2c** that subsequently reacts in carbonyl transfer step to **5c** and unidentified decomposition products (Figure 6). This hypothesis is further verified by an increased yield of 59% in the deprotonation reaction in the presence of carbon monoxide.

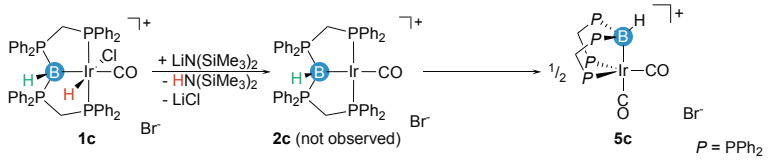

Figure 6. Reactivity of **1c** towards base.

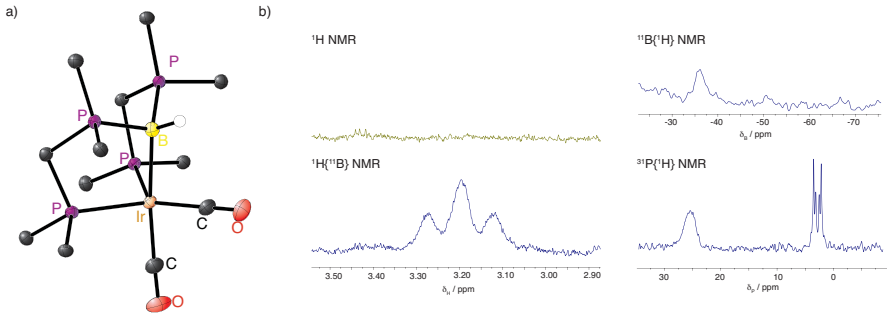

Figure 7. (**a**) Molecular structure of the cationic complex in **5c** in the solid state (ellipsoids are drawn at 50% probability level; carbon atoms of the phenyl rings, carbon-bound hydrogen atoms, co-crystallized solvent molecules and counter ion are omitted for clarity); (**b**) Selected NMR spectra of complex **5c**.

2.2. Proton Affinities and Deprotonation Pathways

Quantum chemical investigations using density functional theory (DFT) were performed to get further insights about the reactivity of the reported iridium complexes towards bases. First we confirmed that deprotonation of the coordinated donor group results in an energetic minimum (**3a**–**3c**) according to the frequency calculation (no imaginary modes) and calculated the proton affinities (PAs) for **3a**–**3c** (Table 1 and Figure 8). In agreement with the experimental results, complex **3b** exhibits the lowest proton affinity (PA, represents the energy difference between complexes calculated without solvation and counter ions; the energy of free proton is not considered) with 864 kJ·mol^{-1}, while the PAs of the neutral complexes **3a** (1129 kJ·mol^{-1}) and **3c** (1257 kJ·mol^{-1}) are significantly higher.

The low PA of the CDP-group in the coordinated pincer-type ligand indicates that it might be less efficient as internal base in a potential catalyst, but in turn it suggests that protonated CDPs might be potential cooperative groups that facilitate an efficient proton-hydride-transfer from or to the catalyst.

In comparison, the value of 1257 kJ·mol^{-1} is too high to expect metal-ligand-cooperativity via proton-hydride-transfer, but it clearly suggests that deprotonation of coordinated $(R_3P)_2BH$ groups should be facile with strong bases in the absence of more acidic sites, which would yield an unprecedented phosphine-stabilized boride.

Table 1. Calculated Proton affinities of complexes **3a**–**3c** and **6a**–**6c** (G16, B97D/def2-TZVPP).

Donor in 1	Reactivity	PA(3)/kJ·mol^{-1}	Reactivity	PA(6)/kJ·mol^{-1}	ΔPA/kJ·mol^{-1}
R_2NH	**1a**→**3a**	1129	**1a**→**6a**	1126	3
$(Ph_2RP)_2CH$	**1b**→**3b**	864	**1b**→**6b**	900	−36
$(Ph_2RP)_2BH$	**1c**→**3c**	1257	**1c**→**6c**	1175	82

To elucidate the reductive elimination pathway, we removed a proton from the metal-coordinated hydrido ligand in **1a**–**1c** in a *gedankenexperiment* and performed geometry optimisations. The resulting complexes (**6a**–**6c**) exhibit elongated iridium chloride distances (Figure 8), but were confirmed as energetic minima by frequency calculations. Although the Ir–Cl distances in **6a**–**6c** are in range between a weak bond (2.737 Å) and non-bonding (4.181 Å), the resulting proton affinities may be used as estimate in comparison to **3a**–**3c**.

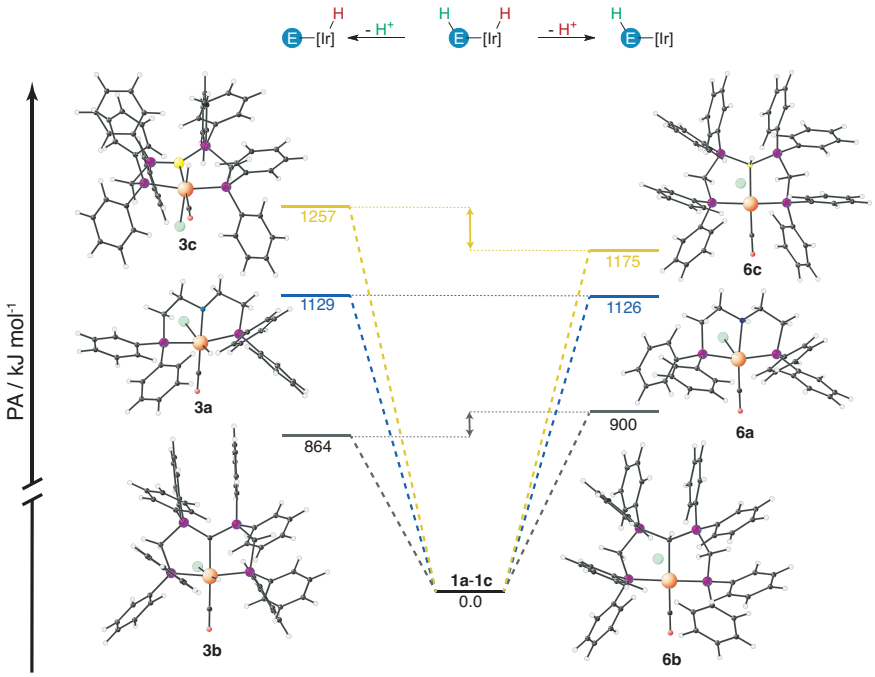

Figure 8. Proton affinities and DFT-optimized structures of **3a**–**3c** and **6a**–**6c** (G16, B97D/def2-TZVPP).

It becomes evident that in case of the amine-based ligand product of ligand- (**3a**) and metal-deprotonation (**6a**) exhibit very similar proton affinities (ΔPA = 3 kJ·mol^{-1}), which suggests that

both pathways are in principle favourable. The experimentally observed selectivity for the reductive elimination might be kinetically favoured. In case of the protonated CDP-based ligand in **1b** the ligand deprotonation is favoured 36 kJ·mol^{-1} over the deprotonation at the metal site, which again is in line with the experimental observations. Notably, both PAs, of **3b** and **6b**, are rather low. For the boron-based pincer-type ligand in **1c** the deprotonation at the metal centre is clearly favoured.

2.3. Comparison with Related Iridium(I) Dicarbonyl Complexes

In comparison to related trigonal bipyramidal iridium(I) dicarbonyl complexes, **5c** exhibits very similar structural features (Table 2). All complexes with two Ph_2RP-groups and one carbonyl ligand in the equatorial plane differ in the ligand or donor group in the apical position, *trans* to the second carbonyl ligand [23–25]. With τ_5-parameters between 0.58 and 0.75, four of the five complexes are best described as trigonal bipyramidal complexes. In the IR spectrum, two bands for the C–O-stretching frequency are observed for each complex, which in principle allow to estimate the net electron donor ability of the specified donor group in comparison. Like for other dicarbonyl-based ligand parameters [26–28], averaging of *cis*- and *trans*-influences on symmetric and asymmetric C–O-stretching modes can provide a rough picture of the net donor strength. For the neutral complexes, all values, respectively, indicate an increasing donor ability in the order $R_3SiCH_2^-$ > Cl^- > Br^-. The cationic complex with a Ph_2RP-group in the apical position gives rise to an increased value of $\tilde{\nu}_{CO}$(av) = 1996 cm^{-1}, confirming that anionic ligands exhibit stronger donor abilities. An unexpected finding in this context is the low value measured for complex **5c** ($\tilde{\nu}_{CO}$(av) = 1958 cm^{-1}), which is significantly lower than those of the anionic donor groups. Despite the fact that donor groups based on $(Ph_3P)_2BH$ are overall neutral, this observation suggests that they are stronger donors than alkyl-ligands, which are known as one of the strongest donors in coordination and organometallic chemistry.

Table 2. Comparison of Iridium(I) dicarbonyl complexes from literature with the new complex **5c**.

Complex	Donor	τ_5	$\tilde{\nu}_{CO}$/cm^{-1}	$\tilde{\nu}_{CO}$(av)/cm^{-1}	Ref.
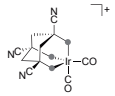	Ph_2RP	0.42	2047, 1944	1996	[23]
	Br^-	0.70	2023, 1950	1987	[24]
	Cl^-	0.58	2017, 1944	1981	[24]
	$R_3SiCH_2^-$	0.75	2001, 1927	1964	[25]
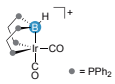	$(R_3P)_2BH$	0.70	2000, 1916	1958	this work

3. Materials and Methods

All experiments were carried out under an atmosphere of purified argon or nitrogen in the MBraun glove boxes LABmaster 130 and UNIlab or using standard Schlenk techniques. THF and diethyl ether were dried over Na/K alloy, n-hexane was dried over $LiAlH_4$, toluene was dried over

sodium, dichloromethane was dried over CaH_2, methanol was dried over magnesium and ethyl acetate was dried over potassium carbonate. After drying, solvents were stored over appropriate molecular sieves. Deuterated solvents were degassed with freeze-pump-thaw cycles and stored over appropriate molecular sieves under argon atmosphere. Complexes **1a**–**1c** synthesised according to previously reported procedures [16].

^1H, ^{13}C, ^{11}B and ^{31}P NMR spectra were recorded using Bruker BioSpin GmbH (Rheinstetten, Germany) Avance HD 250, 300 A, DRX 400, DRX 500 and Avance 500 NMR spectrometers at 300 K. ^1H and $^{13}C\{^1H\}$, ^{13}C-APT (attached proton test) NMR chemical shifts are reported in ppm downfield from tetramethylsilane. The resonance of the residual protons in the deuterated solvent was used as internal standard for ^1H NMR spectra. The solvent peak of the deuterated solvent was used as internal standard for ^{13}C NMR spectra. The assignment of resonances in ^1H and ^{13}C NMR spectra was further supported by ^1H COSY, ^1H NOESY, ^1H,^{13}C HMQC and ^1H,^{13}C HMBC NMR spectra. ^{11}B NMR chemical shifts are reported in ppm downfield from $BF_3 \cdot Et_2O$ and referenced to an external solution of $BF_3 \cdot Et_2O$ in $CDCl_3$. ^{31}P NMR chemical shifts are reported in ppm downfield from H_3PO_4 and referenced to an external 85 % solution of phosphoric acid in D_2O. The following abbreviations are used for the description of NMR data: br (broad), s (singlet), d (doublet), t (triplet), q (quartet), quin (quintet), m (multiplet). FT-IR spectra were recorded by attenuated total reflection of the solid samples on a Bruker Tensor IF37 spectrometer. The intensity of the absorption band is indicated as w (weak), m (medium), s (strong), vs (very strong) and br (broad). HR-ESI mass spectra were acquired with a LTQ-FT mass spectrometer (Thermo Fisher Scientific, Waltham, MA, USA). The resolution was set to 100,000.

Reactivity of [($\{Ph_2PCH_2CH_2\}_2$NH)IrCl(CO)(H)]Cl (1a) towards base 20 mg [($\{Ph_2PCH_2CH_2\}_2$NH)IrCl(CO)(H)]Cl (**1a**, 27.3 µmol, 1.0 eq.) and 4.6 mg LiHMDS (27.5 µmol, 1.0 eq.) were suspended in 0.6 mL THF-d_8. After stirring for 16 h, the resulting light orange suspension was filtered and, after addition of 0.2 ml THF-d_8, the first NMR spectra were recorded. [($\{Ph_2PCH_2CH_2\}_2$NH)Ir(CO)]Cl (**2a**) was identified as the main product, while small amounts of **1a** remained unreacted. Further 4.7 mg of LiHMDS (27.5 µmol, 1.0 eq.) were added, upon which the color changed to a dark orange, and the second set of NMR spectra were recorded.

NMR spectra after addition of 1.0 eq. LiHMDS: ^1H NMR (300 MHz, THF-d_8, 300 K): δ = 2.61–2.86 (m, 4H, CH_2), 3.08–3.46 (m, 4H, CH_2), 7.03–7.24 (m, 4H, H_{arom}), 7.25–7.51 (m, 12H, H_{arom}), 7.73–8.03 (m, 4H, H_{arom}) ppm. Neither N–H nor Ir–H resonances could be identified. $^{31}P\{^1H\}$ NMR (122 MHz, THF-d_8, 300 K) δ = 31.7 (s, **1a**), 55.5 (br s, **2a**) ppm.

NMR spectra after addition of 2.0 eq. LiHMDS: $^{31}P\{^1H\}$ NMR (122 MHz, THF-d_8, 300 K) δ = −3.8 (s), −0.9 (s), 25.0 (s), 31.9 (s, **1a**), 36.1 (s), 39.8 (d, $J_{P,P}$ = 291.7 Hz), 52.6 (d, $J_{P,P}$ = 292.3 Hz), 56.1 (br s, **2a**) ppm. ^1H NMR (300 MHz, THF-d_8, 300 K): Due to the multiple decomposition products visible in the $^{31}P\{^1H\}$ NMR spectrum, no analysis was performed.

Formation of [($\{dppm\}_2$C)Ir(CO)]Cl (4b) 57 mg [($\{dppm\}_2$CH)IrCl(CO)(H)]Cl_2 (**1b**, 51.4 µmol, 1.0 eq.) were dissolved in 2 mL deuterated dichloromethane. After addition of 15.3 µL DBU (103 µmol, 2.0 eq.), the solution changed color from colorless to yellow. After removal of the solvent in vacuo, a yellow solid remained, containing [($\{dppm\}_2$C)Ir(CO)]Cl (**4b**). ^1H NMR (300 MHz, CD_2Cl_2, 300 K): δ = 4.01–4.12 (m, 4H, CH_2), 7.06–7.18 (m, 8H, $H_{arom.}$), 7.25–7.46 (m, 24H, $H_{arom.}$), 7.59–7.78 (m, 8H, $H_{arom.}$) ppm. ^{13}C APT NMR (75 MHz, CD_2Cl_2, 300 K): δ = 129.0–129.3 (m, $C_{arom.}$), 131.4 (br s, $C_{arom.}$), 132.7 (br s, $C_{arom.}$), 132.9 (t, $J_{C,P}$ = 5.1 Hz, $C_{arom.}$), 133.4 (t, $J_{C,P}$ = 7.2 Hz, $C_{arom.}$) ppm. Neither the carbonyl nor the CH_2 resonances were observed. $^{31}P\{^1H\}$ NMR (122 MHz, CD_2Cl_2, 300 K) δ = 23.4 (t, $^2J_{P,P}$ = 48.5 Hz), 38.3 (t, $^2J_{P,P}$ = 49.3 Hz) ppm. FT-IR/cm^{-1}: 3050 (w), 2962 (w), 2932 (m), 2925 (m), 2858 (m), 2855 (w), 2013 (w), 1979 (w), 1925 (s, CO), 1646 (s), 1612 (s), 1586 (s), 1481 (m), 1434 (s), 1323 (s), 1207 (w), 1119 (m), 1103 (m), 1097 (s), 1070 (s), 824 (m), 740 (s), 721 (m), 691 (s), 543 (m), 527 (m), 503 (s), 481 (s). HRMS: (ESI+, MeCN/CH_2Cl_2): 1001.1966 [($\{dppm\}_2$C)Ir(CO)]$^+$ measured, 1001.1972 calculated, Δ = 0.60 ppm.

Synthesis of [({dppm}$_2$BH)Ir(CO)$_2$]Br (5c) Complex **1c** was generated in situ by the reaction of 90.0 mg [IrCl(CO)(PPh$_3$)$_2$] (116 µmol) with 100.0 mg of [(dppm)$_2$BH$_2$]Br (116 µmol, 1.0 eq.) in 5 mL THF. The resulting solution of **1c** was cooled to −74 °C and 20.0 mg LiN(SiMe$_3$)$_2$ (116 µmol, 1.0 eq.) dissolved in 2 mL THF were added drop-wise. The reaction mixture was allowed to warm to ambient temperature, the argon atmosphere was replaced by carbon monoxide and the mixture was stirred for further two hours at ambient temperature. All volatiles were removed in vacuo, the residue was washed with 5 mL toluene and dried under high vacuum to yield 74.0 mg of a colorless solid, containing [({dppm}$_2$BH)Ir(CO)$_2$]Br (**4c**, 68 µmol, 59 %). ^{31}P{^{1}H} NMR (101.3 MHz, CD_2Cl_2, 300 K): δ = 25.4 (br, 2P, P–B–P), 3.5-2.2 (m, 2P, P–Ir–P) ppm. ^{11}B{^{1}H} NMR (96.3 MHz, CD_2Cl_2, 300 K): δ = −35.4 (br, 1B, BH) ppm. Only resonances that are change upon ^{11}B-decoupling are reported in the ^{1}H{^{11}B} NMR spectrum. ^{1}H NMR (300 MHz, CD_2Cl_2, 300 K): δ = 7.51–7.66 (m, 4H, H$_{arom.}$), 7.40–7.49 (m, 8H, H$_{arom.}$), 7.08–7.31 (m, 8H, H$_{arom.}$), 6.82–7.10 (m, 20H, H$_{arom.}$), 5.42–5.61 (m, 2H, CH_2), 4.07–4.16 (m, 2H, CH_2) ppm. ^{1}H{^{11}B} NMR (300 MHz, CD_2Cl_2, 300 K) δ = 3.20 (t, $^2J_{HP}$ = 23.2 Hz, 1H, BH) ppm. ^{13}C{^{1}H} NMR (121.5 MHz, CD_2Cl_2, 300 K) δ = 134.7 (vt, 4C, C$_{arom.}$), 133.5 (s, 4C, C$_{arom.}$), 133.0 (s, 4C, C$_{arom.}$), 132.0 (s, 4C, C$_{arom.}$), 131.3 (s, 4C, C$_{arom.}$), 130.9 (vt, 4C, C$_{arom.}$), 130.2 (s, 4C, C$_{arom.}$), 129.2 (s, 4C, C$_{arom.}$), 129.2 (s, 4C, C$_{arom.}$), 128.9 (s, 4C, C$_{arom.}$), 128.7 (s, 4C, C$_{arom.}$), 128.3 (s, 4C, C$_{arom.}$), 33.5 (vt, 1C, CH_2), 30.3 (vt, 1C, CH_2) ppm. FT-IR: $\tilde{\nu}$/cm^{-1} = 3050 (w), 3017 (w), 2962 (w), 2823 (w), 2724 (w), 2000 (s, CO), 1916 (s, CO), 1586 (w), 1574 (w), 1483 (m), 1434 (s), 1379 (w), 1333 (w), 1306 (w), 1260 (m), 1094 (s), 1024 (s), 869 (w), 797 (s), 778 (s), 731 (vs), 685 (vs), 616 (w), 554 (m), 523 (s), 480 (s). HRMS (ESI+, MeOH) m/z = 969.1884 [({dppm}$_2$BH)Ir(CO)$_2$]$^+$, calc. 969.1887 (Δ = 0.31 ppm).

4. Conclusions

In the current manuscript, we reported the first iridium(I) complex formally containing phosphine-stabilised borylene as a donor group. The comparison to related iridium(I) dicarbonyl complexes suggests strong donor properties of this type of nucleophilic boron compounds. In an internal competition with a hydrido-ligand, the reactivity towards base reveals that analogous carbon compounds and protonated CDPs are easy to deprotonate, while only strong bases contribute to deprotonate phosphine-stabilized borylenes in the coordination sphere of a central metal atom.

Supplementary Materials: The following are available online at http://www.mdpi.com/2304-6740/7/5/61/s1, Figures S1–S12: NMR and IR spectra of compounds **2a**, **4b** and **5c**; Table S1: crystallographic data for compound **5c**; xyz-coordinates.

Author Contributions: L.M., C.S. and L.A. performed the experiments. All calculations were made by L.M., R.L. and L.M. wrote the manuscript. R.L. designed and directed the project.

Funding: This work was supported by the Deutsche Forschungsgemeinschaft (LA 2830/3-2, 2830/5-1 and 2830/6-1).

Acknowledgments: R.L. is grateful to S. Dehnen for her continuous support.

Conflicts of Interest: The authors declare no conflict of interest.

Abbreviations

The following abbreviations are used in this manuscript:

CDP	carbodiphosphorane
DBU	1,8-Diazabicyclo[5.4.0]undec-7-ene
dppm	1,1-bis(diphenylphosphino)methane
DFT	density functional theory
ESI	electro spray ionisation
HMDS	hexamethyldisilazane
NMR	nuclear magnetic resonance
HRMS	high resolution mass spectrometry
THF	tetrahydrofurane

References

1. Bouhadir, G.; Bourissou, D. Complexes of ambiphilic ligands: reactivity and catalytic applications. *Chem. Soc. Rev.* **2016**, *45*, 1065–1079. [CrossRef]
2. Amgoune, A.; Bourissou, D. σ-Acceptor, Z-type ligands for transition metals. *Chem. Commun.* **2011**, *47*, 859–871. [CrossRef]
3. Braunschweig, H.; Dewhurst, R.D.; Hupp, F.; Nutz, M.; Radacki, K.; Tate, C.W.; Vargas, A.; Ye, Q. Multiple complexation of CO and related ligands to a main-group element. *Nature* **2015**, *522*, 327–330. [CrossRef]
4. Landmann, J.; Sprenger, J.A.P.; Bertermann, R.; Ignat'ev, N.; Bernhardt-Pitchougina, V.; Bernhardt, E.; Willner, H.; Finze, M. Convenient access to the tricyanoborate dianion $B(CN)_3^{2-}$ and selected reactions as a boron-centred nucleophile. *Chem. Commun.* **2015**, *51*, 4989–4992. [CrossRef]
5. Bernhardt, E.; Bernhardt-Pitchougina, V.; Willner, H.; Ignatiev, N. "Umpolung" at boron by reduction of $[B(CN)_4]^-$ and formation of the dianion $[B(CN)_3]^{2-}$. *Angew. Chem. Int. Ed.* **2011**, *50*, 12085–12088. [CrossRef]
6. Kinjo, R.; Donnadieu, B.; Celik, M.A.; Frenking, G.; Bertrand, G. Synthesis and characterization of a neutral tricoordinate organoboron isoelectronic with amines. *Science* **2011**, *333*, 610–613. [CrossRef]
7. Ruiz, D.A.; Melaimi, M.; Bertrand, G. An efficient synthetic route to stable bis(carbene)borylenes $[(L_1)(L_2)BH]$. *Chem. Commun.* **2014**, *50*, 7837–7839. [CrossRef]
8. Kong, L.; Li, Y.; Ganguly, R.; Vidovic, D.; Kinjo, R. Isolation of a Bis(oxazol-2-ylidene)-phenylborylene adduct and its reactivity as a boron-centered nucleophile. *Angew. Chem. Int. Ed.* **2014**, *53*, 9280–9283. [CrossRef]
9. Kong, L.; Ganguly, R.; Li, Y.; Kinjo, R. Diverse reactivity of a tricoordinate organoboron L_2PhB: (L = oxazol-2-ylidene) towards alkali metal, group 9 metal, and coinage metal precursors. *Chem. Sci.* **2015**, *6*, 2893–2902. [CrossRef]
10. Ruiz, D.A.; Ung, G.; Melaimi, M.; Bertrand, G. Deprotonation of a Borohydride: Synthesis of a Carbene-Stabilized Boryl Anion. *Angew. Chem. Int. Ed.* **2013**, *52*, 7590–7592. [CrossRef]
11. Dub, P.A.; Gordon, J.C. The mechanism of enantioselective ketone reduction with Noyori and Noyori–Ikariya bifunctional catalysts. *Dalton Trans.* **2016**, *45*, 6756–6781. [CrossRef]
12. Maser, L.; Herritsch, J.; Langer, R. Carbodiphosphorane-based nickel pincer complexes and their (de)protonated analogues: Dimerisation, ligand tautomers and proton affinities. *Dalton Trans.* **2018**, *47*, 10544–10552. [CrossRef]
13. Vondung, L.; Frank, N.; Fritz, M.; Alig, L.; Langer, R. Phosphine-Stabilized Borylenes and Boryl Anions as Ligands? Redox Reactivity in Boron-Based Pincer Complexes. *Angew. Chem. Int. Ed.* **2016**, *55*, 14450–14454. [CrossRef]
14. Vondung, L.; Jerabek, P.; Langer, R. Ligands Based on Phosphine-Stabilized Aluminum(I), Boron(I), and Carbon(0). *Chem. Eur. J.* **2019**, *25*, 3068–3076. [CrossRef]
15. Landmann, J.; Keppner, F.; Hofmann, D.B.; Sprenger, J.A.; Höring, M.; Zottnick, S.H.; Müller-Buschbaum, K.; Ignat'ev, N.V.; Finze, M. Deprotonation of a Hydridoborate Anion. *Angew. Chem. Int. Ed.* **2017**, *56*, 2795–2799. [CrossRef]
16. Maser, L.; Schneider, C.; Vondung, L.; Alig, L.; Langer, R. Quantifying the Donor Strength of Ligand-Stabilized Main Group Fragments. *J. Am. Chem. Soc.* **2019**. [CrossRef]
17. Friedrich, A.; Ghosh, R.; Kolb, R.; Herdtweck, E.; Schneider, S. Iridium olefin complexes bearing dialkylamino/amido PNP pincer ligands: Synthesis, reactivity, and solution dynamics. *Organometallics* **2009**, *28*, 708–718. [CrossRef]
18. Schneider, S.; Meiners, J.; Askevold, B. Cooperative aliphatic PNP amido pincer ligands-versatile building blocks for coordination chemistry and catalysis. *Eur. J. Inorg. Chem.* **2012**, *2012*, 412–429. [CrossRef]
19. Cheng, F.; Yang, X.; Peng, H.; Chen, D.; Jiang, M. Well-controlled formation of polymeric micelles with a nanosized aqueous core and their applications as nanoreactors. *Macromolecules* **2007**, *40*, 8007–8014. [CrossRef]
20. Morris, R.H. Estimating the acidity of transition metal hydride and dihydrogen complexes by adding ligand acidity constants. *J. Am. Chem. Soc.* **2014**, *136*, 1948–1959. [CrossRef]
21. Grätz, M.; Bäcker, A.; Vondung, L.; Maser, L.; Reincke, A.; Langer, R. Donor ligands based on tricoordinate boron formed by B–H-activation of bis(phosphine)boronium salts. *Chem. Commun.* **2017**, *53*, 7230–7233. [CrossRef]

22. Addison, A.W.; Rao, T.N.; Reedijk, J.; van Rijn, J.; Verschoor, G.C.; Trans, D.; Addison, A.W.; Rao, T.N. Synthesis, structure, and spectroscopic properties of copper(II) compounds containing nitrogen–sulphur donor ligands; the crystal and molecular structure of aqua[1,7-bis(*N*-methylbenzimidazol-2′-yl)-2,6-dithiaheptane]copper(II) perchlorate. *Dalton Trans. J. Chem. Soc.* **1984**, 1349–1356. [CrossRef]
23. Heins, W.; Mayer, H.A.; Fawzi, R.; Steimann, M. Stereochemical and Electronic Control of Functionalized Tripodal Phosphines. Reactivity of the Adamantane-Type Ir(tripod)(CO)Cl (tripod = *cis*,*cis*-1,3,5-$(PPh_2)_3$-1,3,5-$X_3C_6H_6$; X = H, COOMe, CN) Complexes toward H^+, H_2, CO, and C_2H_4. *Organometallics* **1996**, *15*, 3393–3403. [CrossRef]
24. Fox, D.J.; Duckett, S.B.; Flaschenriem, C.; Brennessel, W.W.; Schneider, J.; Gunay, A.; Eisenberg, R. A Model Iridium Hydroformylation System with the Large Bite Angle Ligand Xantphos: Reactivity with Parahydrogen and Implications for Hydroformylation Catalysis. *Inorg. Chem.* **2006**, *45*, 7197–7209. [CrossRef]
25. Passarelli, V.; Pérez-Torrente, J.J.; Oro, L.A. Intramolecular C–H Oxidative Addition to Iridium(I) in Complexes Containing a *N*,*N*′-Diphosphanosilanediamine Ligand. *Inorg. Chem.* **2014**, *53*, 972–980. [CrossRef]
26. Chianese, A.R.; Li, X.; Janzen, M.C.; Faller, J.W.; Crabtree, R.H. Rhodium and iridium complexes of *N*-heterocyclic carbenes via transmetalation: Structure and dynamics. *Organometallics* **2003**, *22*, 1663–1667. [CrossRef]
27. Kelly III, R.A.; Clavier, H.; Giudice, S.; Scott, N.M.; Stevens, E.D.; Bordner, J.; Samardjiev, I.; Hoff, C.D.; Cavallo, L.; Nolan, S.P. Determination of *N*-Heterocyclic Carbene (NHC) Steric and Electronic Parameters using the [(NHC)Ir$(CO)_2$Cl] System. *Organometallics* **2008**, *27*, 202–210. [CrossRef]
28. Wolf, S.; Plenio, H. Synthesis of (NHC)Rh(cod)Cl and (NHC)Rh$Cl(CO)_2$ complexes—Translation of the Rh- into the Ir-scale for the electronic properties of NHC ligands. *J. Organomet. Chem.* **2009**, *694*, 1487–1492. [CrossRef]

Inorganics **2019**, *7* S1/S50

Supplementary Materials: Comparing the Acidity of $(R_3P)_2BH$-Based Donor Groups in Iridium Pincer Complexes

Leon Maser, Christian Schneider, Lukas Alig and Robert Langer

Content

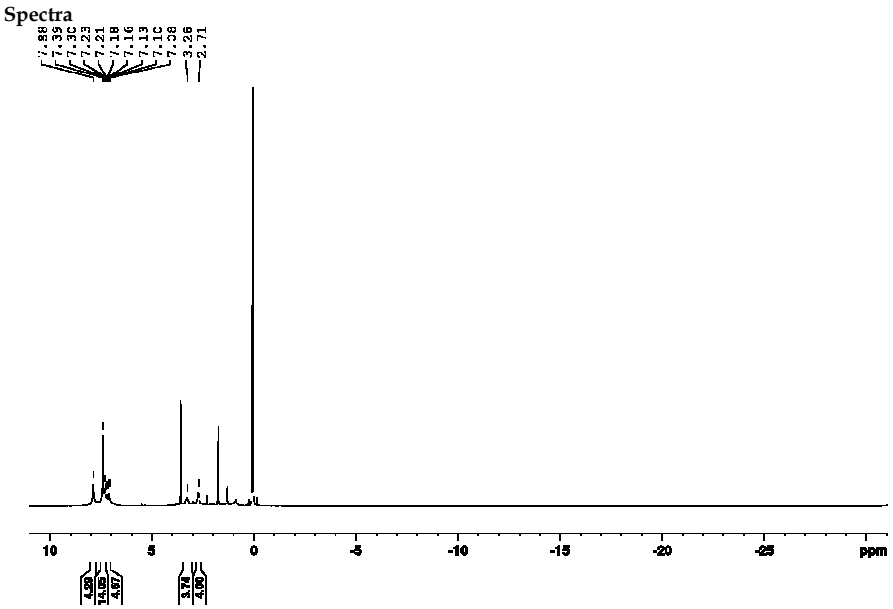

Figure S1. ^{1}H NMR spectrum of [(κ^{3}*P,N,P*-^{Ph}PN^{H}P)Ir(CO)]Cl (**2a**) in THF-d_8 after addition of the first equivalent of LiHMDS.

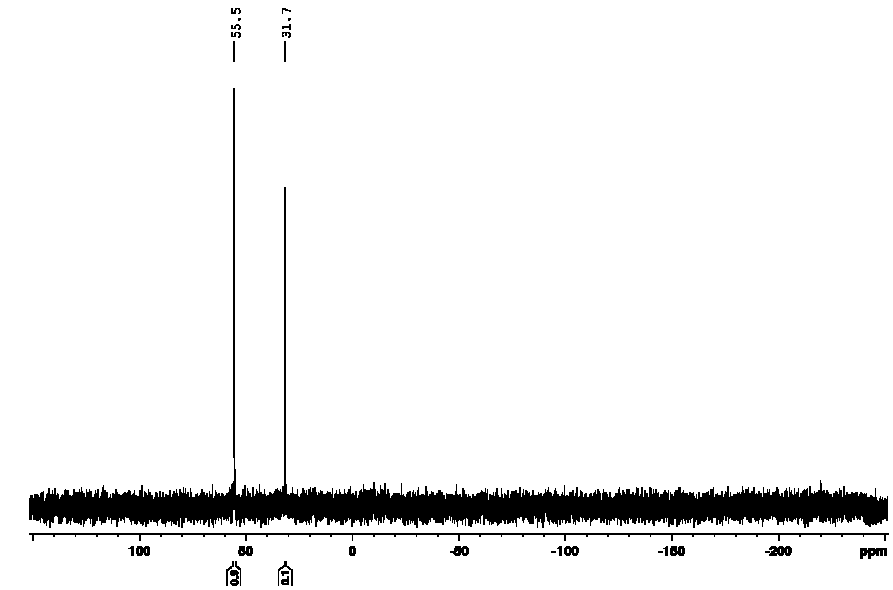

Figure S2. ^{31}P{^{1}H} NMR spectrum of [(κ^{3}*P,N,P*-^{Ph}PN^{H}P)Ir(CO)]Cl (**2a**) in THF-d_8 after addition of the first equivalent of LiHMDS.

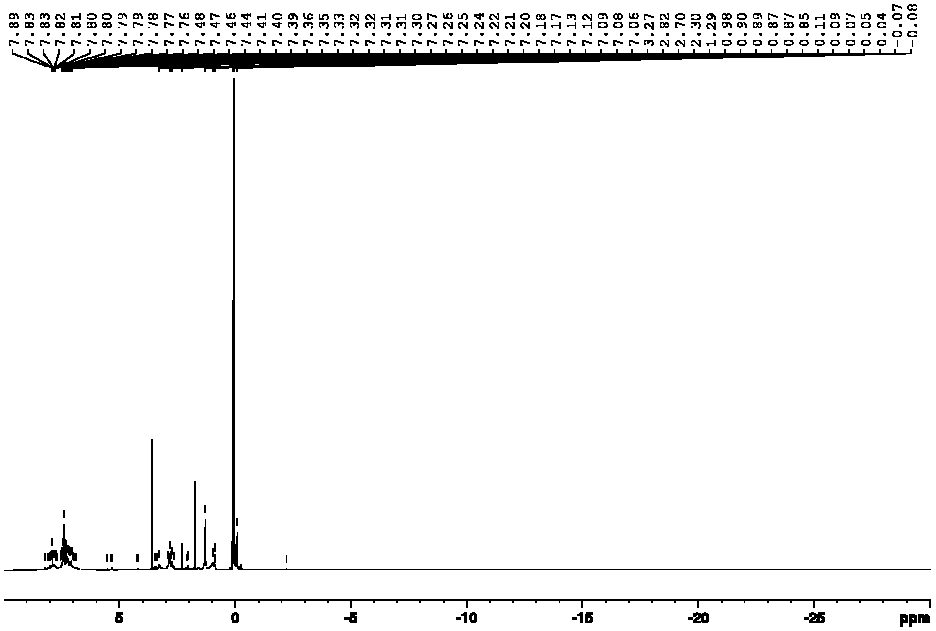

Figure S3. ^{1}H NMR spectrum of [(κ^3*P,N,P*-^{Ph}PN^{H}P)Ir(CO)]Cl in (**2a**) THF-d_8 after addition of the second equivalent of LiHMDS.

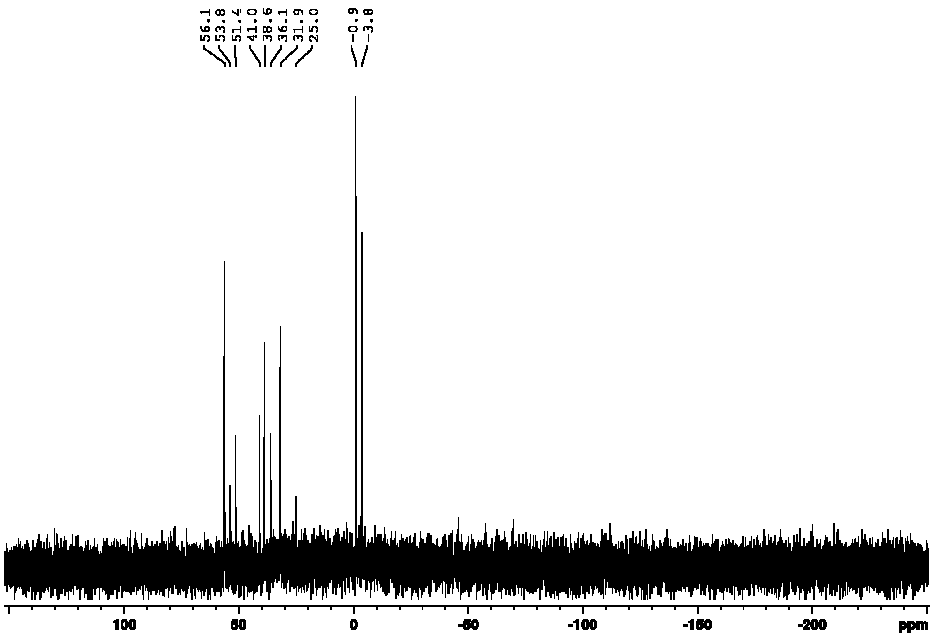

Figure S4. ^{31}P{^{1}H} NMR spectrum of [(κ^3*P,N,P*-^{Ph}PN^{H}P)Ir(CO)]Cl (**2a**) in THF-d_8 after addition of the second equivalent of LiHMDS.

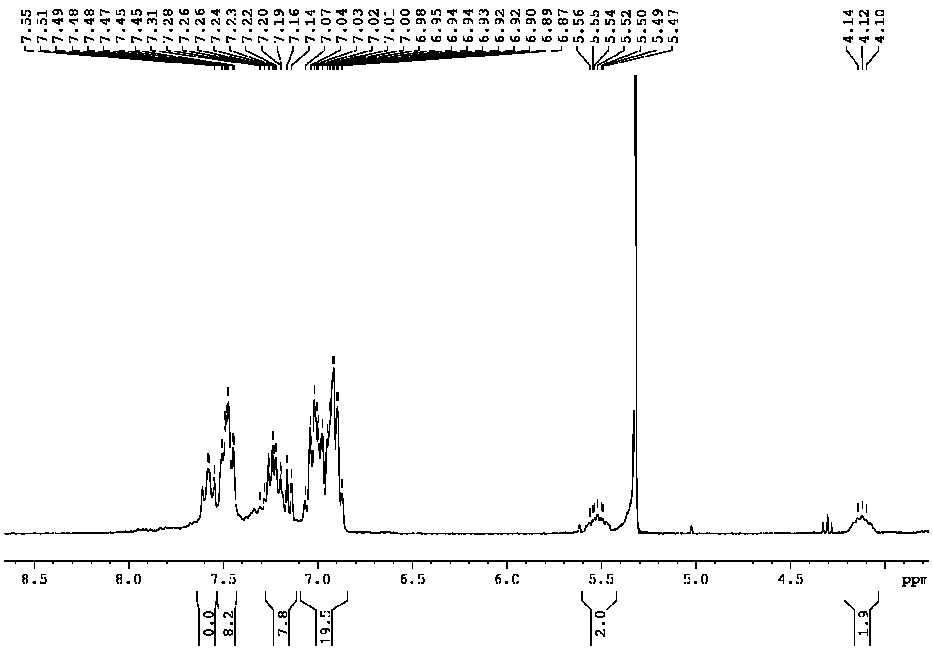

Figure S5. ^{1}H NMR spectrum of [{κ^3*P,C,P*-HB(dppm)$_2$}Ir(CO)$_2$]Br (**5c**) in CD_2Cl_2.

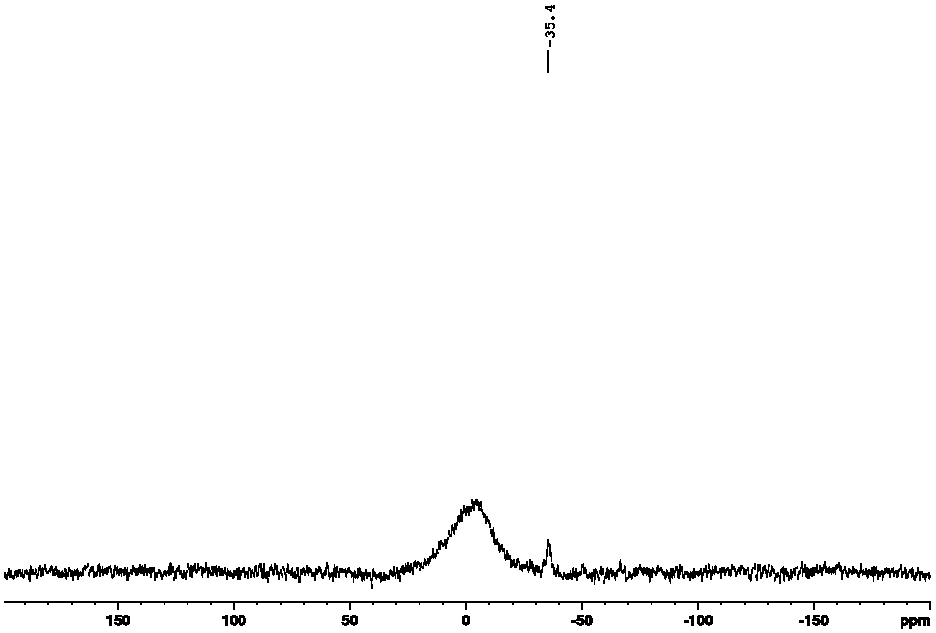

Figure S6. $^{11}B\{^{1}H\}$ NMR spectrum of [{κ^3*P,C,P*-HB(dppm)$_2$}Ir(CO)$_2$]Br (**5c**) with reduced glass peak in CD_2Cl_2.

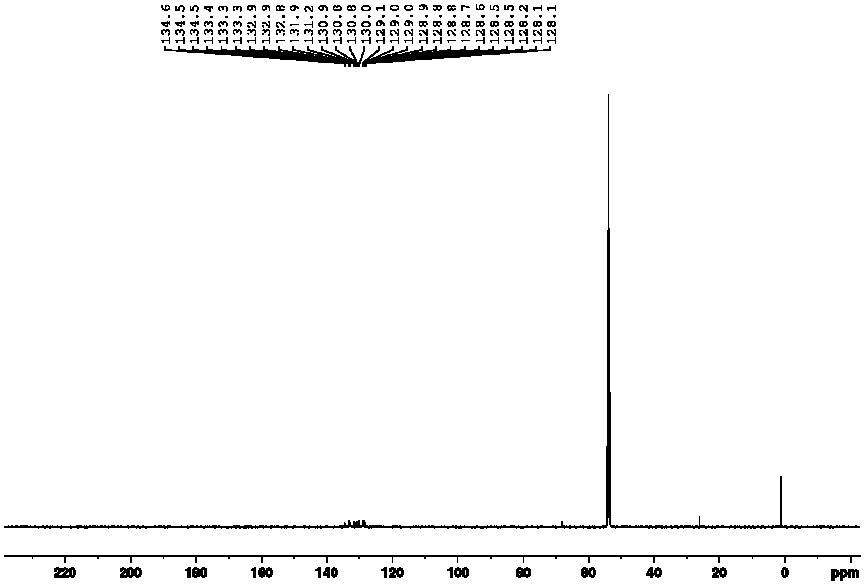

Figure S7. $^{13}C\{^{1}H\}$ NMR spectrum of [{κ³*P,C,P*-HB(dppm)$_2$}Ir(CO)$_2$]Br (**5c**) in CD_2Cl_2.

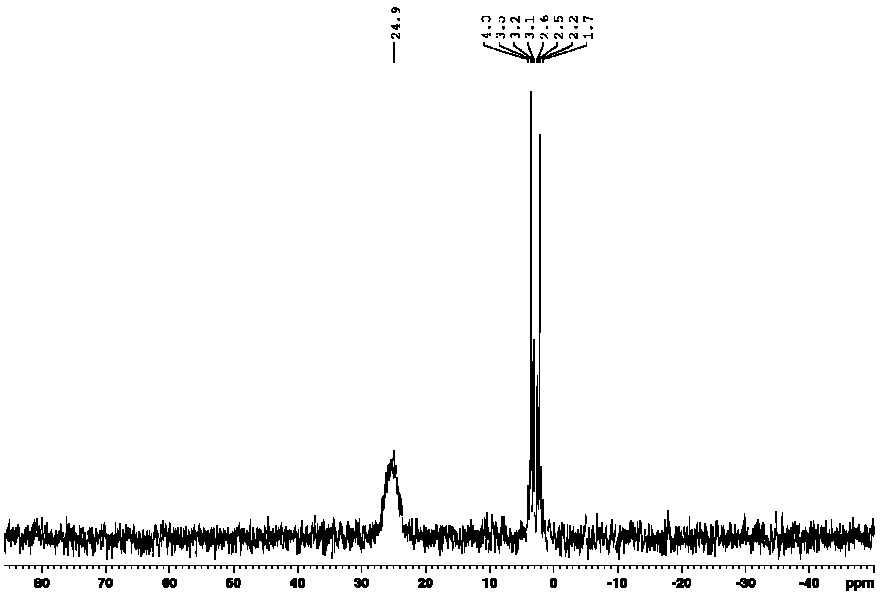

Figure S8. $^{31}P\{^{1}H\}$ NMR spectrum of [{κ³*P,C,P*-HB(dppm)$_2$}Ir(CO)$_2$]Br (**5c**) in CD_2Cl_2.

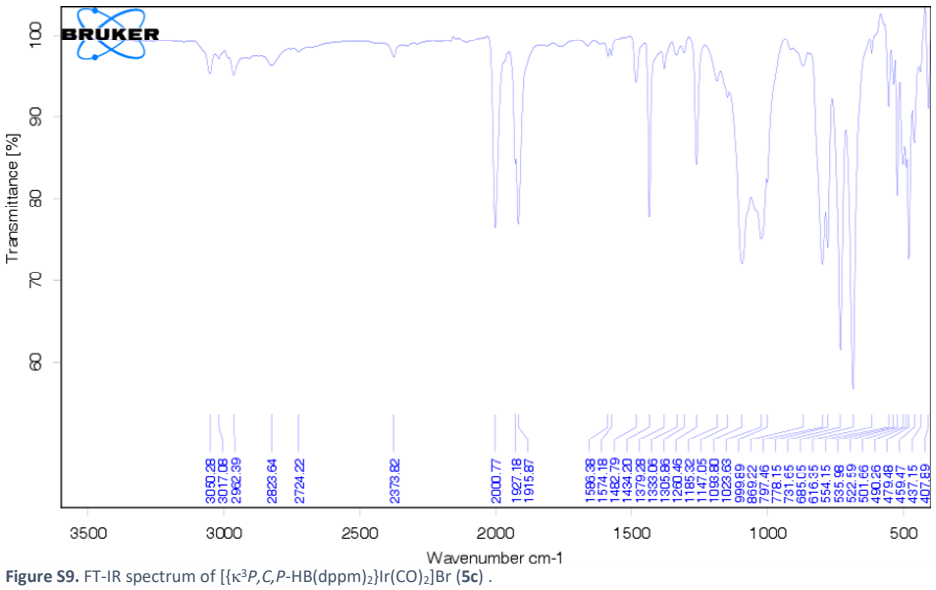

Figure S9. FT-IR spectrum of [{κ³*P,C,P*-HB(dppm)$_2$}Ir(CO)$_2$]Br (**5c**) .

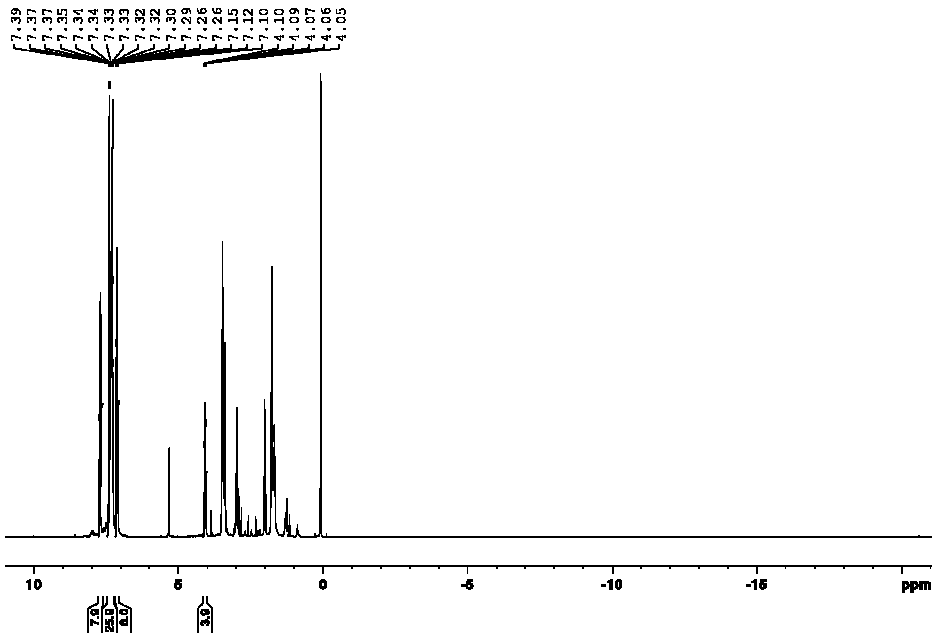

Figure S10. ^{1}H NMR spectrum of [{κ³*P,C,P*-C(dppm)$_2$}Ir(CO)]Cl (**4b**) in CD_2Cl_2.

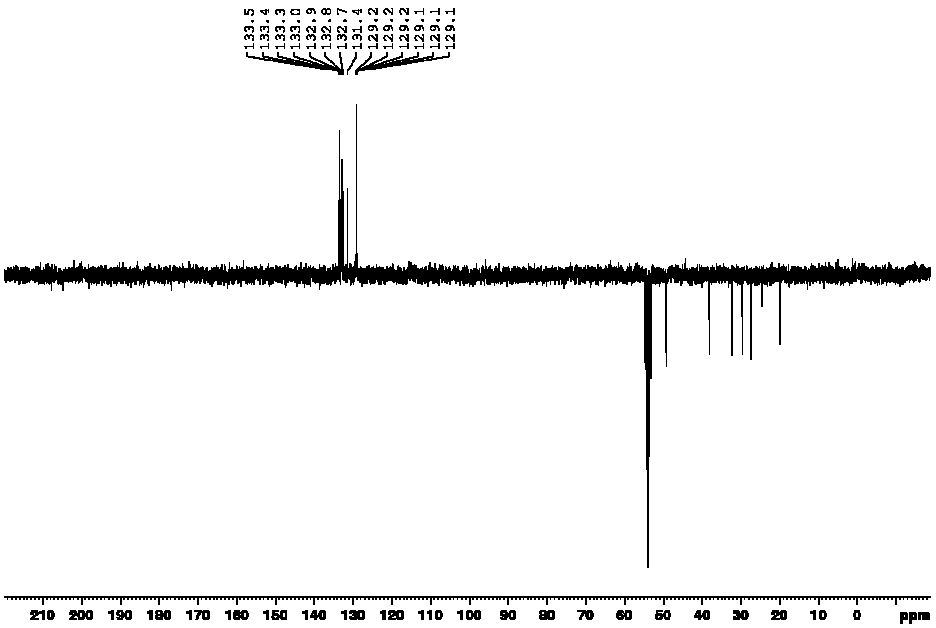

Figure S11. ^{13}C APT NMR spectrum of [{κ^3*P,C,P*-C(dppm)$_2$}Ir(CO)]Cl (**4b**) in CD_2Cl_2.

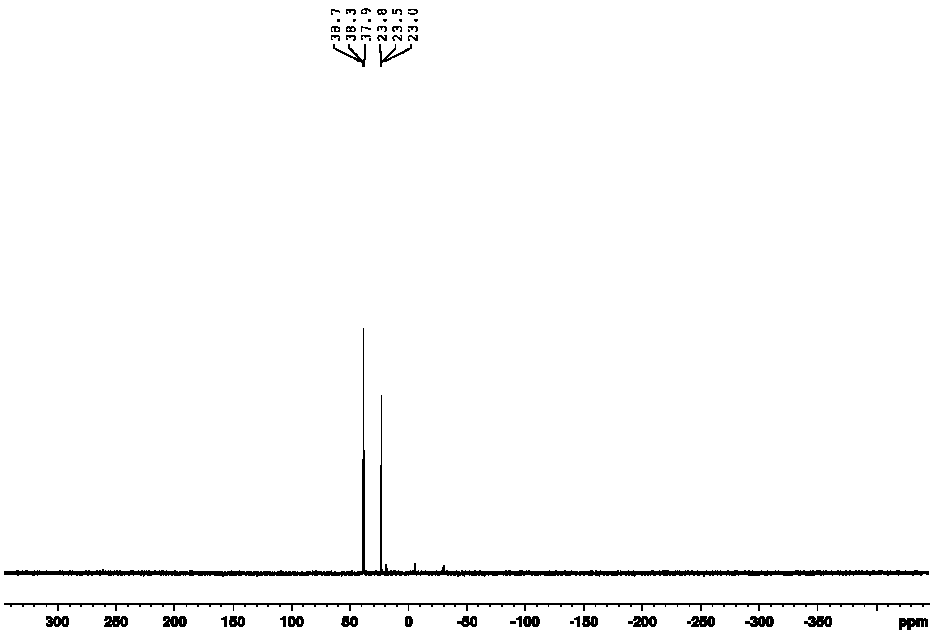

Figure S12. $^{31}P\{^1H\}$ NMR spectrum of [{κ^3*P,C,P*-C(dppm)$_2$}Ir(CO)]Cl (**4b**) in CD_2Cl_2.

X-Ray Crystallography

The single crystal X-ray diffraction data for the structural analysis were collected using graphite-monochromated Mo-K_α-radiation ($\lambda_{MoK\alpha}$= 0.71073) the pixel detector system Bruker Quest D8. The structures were solved with the Olex2 software by direct methods with SHELXT and refined against F^2 by full-matrix-least-square techniques using SHELXL.[8–11] Crystallographic data for **5c** was deposited at Cambridge Crystallographic Data Centre (CCDC 1906827) and can be obtained free of charge via www.ccdc.cam.ac.uk/.

Table S1. Crystallographic data of complex **5c**.

Complex	**5c**
Formula	$C_{52}H_{45}BIrO_2P_4Br{\cdot}C_4H_8O$
M / g·mol^{-1}	1180.79
T/K	110(2)
Crystal System	monoclinic
Space Group	*C*2/*c*
a / Å	40.6382(15)
b / Å	12.2295(5)
c / Å	24.2274(9)
α / °	90
β / °	125,090(1)
γ / °	90
V / Å^3	9852.3(7)
Z	8
$\rho_{calc.}$ / g·cm^{-3}	1.557
μ / mm^{-1}	3.696
F(000)	4624
Θ_{min}/°	2.220
Θ_{max}/°	31.282
Measured Refl.	142905
Independent Refl.	14758 (R_{Int} = 0.0304)
Ind. Refl. (I>2 (I))	13053
Parameters/Restraints	599/0
R_1	0.0277
R_1 (all data)	0.0354
wR_2	0.0695
wR_2 (all data)	0.0728
GooF	1.023
Max. peak + hole / e·Å^{-3}	0.963/-2.678
CCDC	1906827

DFT Calculations
DFT calculations were performed with Grimme's B97D functional including dispersion[2] and the def2TZVPP basis set after a pre-optimization with the def2SVP basis set[3,4] in Gaussian16.[5,10] Crystal structures were used as starting models, where possible. After optimization, a frequency calculation was performed to ascertain that a ground state was found (no imaginary modes). The proton affinities (PA's) were calculated as the difference in Gibbs energy (E) between a protonated complex and it's deprotonated counterpart:

$$PA = E(\text{complex}) - E(\text{complexH}^+)$$

Not included in the calculations were counter ions and implicit or explicit solvation effects.

Cartesian coordinates of all DFT-optimized geometries
2a

Atomic center	X	Y	Z
C	2.468401	0.037735	2.303634
C	1.252147	0.779264	2.860264
N	0.001002	0.113688	2.364581
Ir	0.000446	-0.216336	0.175704
C	-1.252391	0.772813	2.863327
C	-2.466255	0.028582	2.305156
C	-0.000112	-0.589134	-1.622508
O	-0.000668	-0.843453	-2.753197
H	0.003912	-0.835160	2.748519
P	2.294569	-0.047588	0.442908
C	3.337804	-1.425166	-0.109891
C	4.681199	-1.270876	-0.483591
C	5.422915	-2.385269	-0.882340
C	4.830531	-3.651610	-0.909168
C	3.488352	-3.806530	-0.546563
C	2.739898	-2.696147	-0.154548
C	3.011102	1.509476	-0.162325
C	2.352439	2.194722	-1.195991
C	2.880134	3.386998	-1.695509
C	4.063338	3.907087	-1.163187
C	4.721273	3.233501	-0.128598
C	4.198701	2.039504	0.371092

P	-2.293417	-0.050364	0.444280
C	-3.336744	-1.425990	-0.112932
C	-4.681756	-1.269944	-0.480145
C	-5.424720	-2.382163	-0.882463
C	-4.831803	-3.648022	-0.919451
C	-3.488071	-3.804572	-0.563324
C	-2.738407	-2.696305	-0.167534
C	-3.011007	1.507772	-0.157107
C	-4.193844	2.041059	0.383448
C	-4.717831	3.234941	-0.115148
C	-4.066352	3.904908	-1.156093
C	-2.888031	3.381348	-1.695866
C	-2.358704	2.189496	-1.197172
H	2.495273	-0.994308	2.674996
H	3.397841	0.530144	2.604609
H	1.254009	0.786505	3.958095
H	1.226420	1.813000	2.501470
H	-1.253339	0.776353	3.961166
H	-1.231067	1.807918	2.508241
H	-2.488731	-1.005038	2.672416
H	-3.397404	0.515902	2.609068
H	5.141526	-0.287279	-0.480654
H	6.461562	-2.263022	-1.177921
H	5.410641	-4.514962	-1.224222
H	3.022732	-4.787881	-0.583854
H	1.685362	-2.799508	0.096667
H	1.425091	1.794038	-1.594941
H	2.366195	3.910813	-2.497141
H	4.471898	4.836686	-1.550564
H	5.640581	3.636691	0.287880
H	4.723241	1.523084	1.170935
H	-5.142256	-0.286432	-0.469321
H	-6.464640	-2.258643	-1.172996

H	-5.412808	-4.509728	-1.237356
H	-3.022271	-4.785507	-0.608465
H	-1.682942	-2.800541	0.079311
H	-4.713786	1.527458	1.188051
H	-5.633358	3.640736	0.307092
H	-4.476073	4.834312	-1.542701
H	-2.379092	3.902217	-2.502594
H	-1.435058	1.786263	-1.602072

1a

Atomic center	X	Y	Z
C	-2.469296	0.059318	2.319369
C	-1.256470	-0.662388	2.905861
N	-0.002247	-0.027873	2.382531
Ir	-0.003139	0.062266	0.161027
C	1.240848	-0.675936	2.915386
C	2.471388	0.008612	2.317724
C	0.010061	0.241681	-1.683770
H	-0.027542	1.641908	0.319045
Cl	0.042031	-2.433412	0.254304
O	0.027843	0.368886	-2.828613
H	0.003027	0.941256	2.703126
P	-2.344262	0.100207	0.454922
C	-3.168466	1.638820	-0.053120
C	-4.300666	1.629596	-0.880971
C	-4.890990	2.836543	-1.267716
C	-4.361794	4.051756	-0.828193
C	-3.230181	4.064646	-0.003717
C	-2.631296	2.864636	0.375225
C	-3.324559	-1.267948	-0.200233
C	-2.871544	-1.955626	-1.335076
C	-3.655424	-2.964721	-1.896365
C	-4.887644	-3.295218	-1.325786

C	-5.343529	-2.611415	-0.193587
C	-4.567658	-1.596292	0.366881
P	2.335177	0.091994	0.456391
C	3.226714	1.585929	-0.054640
C	4.621402	1.644008	0.121111
C	5.322692	2.791718	-0.246263
C	4.641960	3.881855	-0.801463
C	3.258803	3.822773	-0.988255
C	2.549459	2.677997	-0.614514
C	3.268776	-1.295867	-0.223264
C	3.506735	-2.458313	0.523185
C	4.169182	-3.538288	-0.062347
C	4.582729	-3.467555	-1.395223
C	4.335961	-2.313075	-2.145990
C	3.680040	-1.228612	-1.564676
H	-2.505547	1.102389	2.656956
H	-3.397210	-0.427535	2.632858
H	-1.257492	-0.611116	4.002132
H	-1.226802	-1.707621	2.587599
H	1.242762	-0.605061	4.010538
H	1.186415	-1.725071	2.616464
H	2.545575	1.046539	2.664499
H	3.389139	-0.510313	2.611655
H	-4.718845	0.688258	-1.223599
H	-5.765570	2.823058	-1.912519
H	-4.824369	4.987781	-1.129542
H	-2.812199	5.008946	0.335175
H	-1.733945	2.880977	0.989889
H	-1.901228	-1.724105	-1.758960
H	-3.296570	-3.499688	-2.771190
H	-5.492438	-4.086958	-1.759993
H	-6.302471	-2.865136	0.250128
H	-4.942218	-1.056551	1.232956

H	5.157079	0.789981	0.528317
H	6.399716	2.833466	-0.107763
H	5.192264	4.772128	-1.094240
H	2.730984	4.663515	-1.430480
H	1.475551	2.628676	-0.762627
H	3.170896	-2.533215	1.552565
H	4.354253	-4.436370	0.520533
H	5.095235	-4.311174	-1.849719
H	4.656769	-2.256048	-3.182603
H	3.497835	-0.330228	-2.149389

3c

Atomic center	X	Y	Z
Ir	-0.965866	1.107124	-0.147826
H	-0.850549	0.798465	1.382446
P	-2.556850	-0.596921	-0.298809
Cl	-0.991659	1.407128	-2.739964
P	1.018600	2.276305	0.012485
B	0.573522	-0.501111	-0.241563
C	-2.178355	2.565931	0.181128
C	-1.765449	-2.264448	-0.516589
C	-3.782769	-0.501627	-1.651396
C	-3.592732	-0.865309	1.197665
C	0.967537	4.077576	-0.349646
C	1.821427	2.174255	1.646434
C	2.227909	1.610423	-1.218740
P	-0.086009	-2.109868	0.262603
P	2.223386	-0.215901	-0.941173
O	-2.853508	3.454135	0.500146
H	-2.395782	-3.065741	-0.115103
H	-1.590771	-2.420526	-1.585970
C	-4.256062	0.758634	-2.039857
C	-4.279962	-1.649781	-2.284543
C	-3.378292	-0.118823	2.361286

C	-4.591240	-1.853261	1.192737
C	1.750250	5.007180	0.353534
C	0.103768	4.524526	-1.362589
C	3.215512	2.135549	1.801879
C	1.010955	2.200730	2.794016
H	3.221294	2.065569	-1.152314
H	1.786399	1.817257	-2.199963
C	0.858714	-3.597489	-0.187970
C	-0.502456	-2.265458	2.053737
C	2.681472	-0.975682	-2.564100
C	3.715836	-0.561166	0.087081
H	-3.837720	1.650888	-1.588164
C	-5.231202	0.865413	-3.031906
H	-3.906535	-2.632173	-2.007721
C	-5.251173	-1.541103	-3.282797
H	-2.612364	0.648507	2.366972
C	-4.134237	-0.369069	3.509587
H	-4.787109	-2.421832	0.287142
C	-5.346517	-2.102373	2.338412
C	1.669732	6.368187	0.045534
H	2.410827	4.673234	1.148784
H	-0.506139	3.805721	-1.904880
C	0.034439	5.884129	-1.670885
H	3.864208	2.121139	0.933759
C	3.786319	2.074265	3.074130
C	1.582864	2.154396	4.065167
H	-0.068413	2.239650	2.682076
C	1.468699	-4.415770	0.774264
C	1.066021	-3.857341	-1.552990
C	0.024318	-1.295422	2.914723
C	-1.362576	-3.249107	2.562510
C	3.705389	-1.925769	-2.696645
C	1.852187	-0.700770	-3.666229

C	3.561784	-1.256410	1.288782
C	4.982727	-0.070312	-0.265928
C	-5.731842	-0.282304	-3.654009
H	-5.586067	1.848313	-3.331798
H	-5.627099	-2.437213	-3.771154
H	-3.950462	0.211911	4.410033
C	-5.115875	-1.361638	3.502953
H	-6.117068	-2.869826	2.321838
H	2.272305	7.082809	0.601840
C	0.813541	6.808714	-0.967617
H	-0.637015	6.221273	-2.457162
C	2.972746	2.080651	4.210822
H	4.867062	2.013754	3.172332
H	0.941824	2.173788	4.943784
H	1.310080	-4.217151	1.830664
C	2.283935	-5.478247	0.374547
H	0.626319	-3.204163	-2.302611
C	1.873523	-4.924881	-1.947599
C	-0.295635	-1.312577	4.274267
H	0.662189	-0.519890	2.494646
H	-1.786799	-3.999808	1.899652
C	-1.686777	-3.264286	3.919732
H	4.338984	-2.167218	-1.848874
C	3.905649	-2.583744	-3.914895
C	2.067061	-1.345831	-4.883506
H	1.020159	-0.006144	-3.558350
H	2.567912	-1.598678	1.567835
C	4.655163	-1.465845	2.131856
C	6.072427	-0.251685	0.588747
H	5.118587	0.451727	-1.210905
H	-6.484970	-0.195392	-4.433772
H	-5.702728	-1.556145	4.397712
H	0.749242	7.868626	-1.203489

H	3.417279	2.031520	5.202017
H	2.763292	-6.102897	1.124761
C	2.485447	-5.734499	-0.985121
H	2.037264	-5.110948	-3.005523
H	0.115481	-0.551475	4.933411
C	-1.151907	-2.295741	4.777223
H	-2.362733	-4.022611	4.307759
C	3.092878	-2.293313	-5.012023
H	4.696437	-3.326107	-4.001037
H	1.425848	-1.115218	-5.731505
H	4.524013	-2.012328	3.063109
C	5.909976	-0.952346	1.789529
H	7.047456	0.147536	0.317498
H	3.121917	-6.560472	-1.294268
H	-1.412711	-2.304803	5.833212
H	3.250632	-2.803146	-5.959992
H	6.758574	-1.094046	2.455078

cis-**1b**

Atomic center	X	Y	Z
Ir	-0.967562	1.107539	-0.053154
H	-1.062866	0.993800	1.512120
P	-2.609615	-0.570106	-0.273964
Cl	-0.749647	1.020180	-2.571690
P	0.921039	2.497931	0.161386
C	0.619248	-0.500533	0.108764
C	-2.237381	2.497523	-0.043208
C	-1.650701	-2.000034	-0.971265
C	-3.989662	-0.299105	-1.414457
C	-3.359079	-1.112245	1.284481
C	0.773112	4.220299	-0.356438
C	1.753788	2.443971	1.775831
C	2.145651	1.716360	-1.003978
P	-0.078889	-2.167551	-0.062214

P	2.219142	-0.083635	-0.685854
O	-3.010237	3.345547	-0.014248
H	-2.200106	-2.946427	-0.975012
H	-1.408684	-1.701617	-1.997808
C	-5.217577	0.133969	-0.881917
C	-3.838364	-0.433102	-2.805049
C	-3.502256	-0.186844	2.328255
C	-3.881713	-2.406939	1.425248
C	1.250522	5.272636	0.441666
C	0.124506	4.490255	-1.575892
C	3.128027	2.725672	1.873320
C	1.032503	2.143823	2.940952
H	3.148321	2.146416	-0.932996
H	1.745496	1.868611	-2.010596
C	0.936166	-3.391558	-0.904140
C	-0.442366	-2.787722	1.591731
C	2.718199	-0.917923	-2.207155
C	3.546106	-0.351813	0.517440
H	-5.349049	0.234707	0.191397
C	-6.281212	0.426245	-1.736090
H	-2.889558	-0.731747	-3.235645
C	-4.911941	-0.148381	-3.649275
H	-3.102531	0.816786	2.220383
C	-4.156295	-0.555289	3.505498
H	-3.803874	-3.126962	0.615021
C	-4.515736	-2.777840	2.610659
C	1.085730	6.591866	0.013142
H	1.737990	5.068973	1.390213
H	-0.264276	3.677147	-2.184094
C	-0.025386	5.810983	-1.996127
H	3.703743	2.986917	0.990469
C	3.770390	2.680238	3.110092
C	1.677204	2.102777	4.179024

H	-0.034263	1.954062	2.880900
C	1.930033	-4.068798	-0.175385
C	0.740875	-3.678226	-2.264900
C	-0.603555	-1.917576	2.682290
C	-0.664690	-4.166962	1.755547
C	3.695610	-1.927084	-2.135854
C	2.212436	-0.518134	-3.456140
C	3.361889	-1.041978	1.723317
C	4.818114	0.155159	0.193576
C	-6.131448	0.283065	-3.118532
H	-7.227900	0.758792	-1.319580
H	-4.792418	-0.258192	-4.723542
H	-4.276675	0.169429	4.306245
C	-4.656368	-1.852005	3.650463
H	-4.911196	-3.784023	2.718581
H	1.449783	7.407089	0.632274
C	0.453326	6.861249	-1.203712
H	-0.523610	6.021484	-2.938455
C	3.047492	2.363262	4.264462
H	4.832870	2.897850	3.172702
H	1.107757	1.877433	5.076784
H	2.078006	-3.857470	0.879428
C	2.707629	-5.040192	-0.803669
H	-0.013228	-3.153379	-2.842271
C	1.526467	-4.649025	-2.885015
C	-0.963587	-2.428981	3.928380
H	-0.493304	-0.845093	2.561316
H	-0.544485	-4.848432	0.918254
C	-1.026269	-4.668469	3.005259
H	4.100562	-2.236750	-1.179334
C	4.156002	-2.529808	-3.304464
C	2.681195	-1.130310	-4.618699
H	1.455675	0.255238	-3.523486

H	2.396775	-1.458548	1.993544
C	4.433262	-1.204600	2.605048
C	5.882796	-0.009838	1.076566
H	4.983413	0.668325	-0.750643
H	-6.963333	0.506124	-3.780960
H	-5.162549	-2.140318	4.567807
H	0.326936	7.889108	-1.532679
H	3.548855	2.331365	5.228015
H	3.464886	-5.574127	-0.236391
C	2.501825	-5.334886	-2.155189
H	1.371662	-4.873224	-3.936229
H	-1.094259	-1.752816	4.768012
C	-1.171793	-3.801123	4.092457
H	-1.190195	-5.735086	3.129809
C	3.653392	-2.132394	-4.546803
H	4.914647	-3.304653	-3.242953
H	2.293405	-0.811645	-5.582277
H	4.282270	-1.736433	3.540241
C	5.690634	-0.687143	2.286196
H	6.861604	0.385671	0.820098
H	3.101109	-6.100937	-2.639634
H	-1.452178	-4.194432	5.065734
H	4.023977	-2.596631	-5.456838
H	6.521293	-0.814457	2.974926
H	0.901991	-0.444449	1.164525

trans-**1b**

Atomic center	X	Y	Z
Ir	-1.267291	0.39785	-0.082621
H	-0.853271	0.12866	1.408581
P	-1.879332	-1.88393	-0.212566
Cl	-1.556359	0.67297	-2.582775
P	-0.442835	2.59145	0.017913
C	0.787406	-0.27071	-0.701776

C	-2.974683	0.97329	0.462777
C	-0.341901	-2.81105	-0.718483
C	-3.112680	-2.36684	-1.441699
C	-2.345366	-2.65746	1.368385
C	-1.481175	3.86614	-0.739507
C	0.000770	3.24952	1.652806
C	1.138110	2.57638	-0.968345
P	1.114865	-1.92377	-0.072780
P	2.073044	1.01586	-0.799415
O	-3.996777	1.34443	0.835395
H	-0.350242	-3.84647	-0.367627
H	-0.273161	-2.80060	-1.812324
C	-4.164177	-1.48357	-1.727464
C	-3.066650	-3.62455	-2.067915
C	-2.464675	-1.90064	2.540747
C	-2.596816	-4.04042	1.406525
C	-2.359816	4.58337	0.093371
C	-1.516829	4.06722	-2.128905
C	0.517286	4.55665	1.737145
C	-0.141518	2.48555	2.817223
H	1.778620	3.44212	-0.771294
H	0.834266	2.59437	-2.020767
C	2.582557	-2.70819	-0.761758
C	1.088134	-2.04767	1.714680
C	3.006034	0.79347	-2.327030
C	3.181748	1.07557	0.609675
H	-4.189478	-0.49557	-1.282811
C	-5.170635	-1.86429	-2.615040
H	-2.253232	-4.31780	-1.870498
C	-4.072666	-3.99626	-2.960495
H	-2.285672	-0.83198	2.516338
C	-2.813605	-2.52127	3.742511
H	-2.548323	-4.63480	0.497536

C	-2.938682	-4.65723	2.608985
C	-3.252246	5.50043	-0.461346
H	-2.345301	4.43383	1.169113
H	-0.885590	3.48972	-2.794355
C	-2.405425	4.99521	-2.673254
H	0.598905	5.17197	0.844193
C	0.910743	5.07520	2.969994
C	0.245206	3.01246	4.052651
H	-0.561014	1.48722	2.759339
C	3.495851	-3.39669	0.054134
C	2.794928	-2.62499	-2.149918
C	1.220408	-0.91690	2.532286
C	0.885090	-3.31426	2.289746
C	4.408452	0.81406	-2.350762
C	2.275847	0.62403	-3.519964
C	4.054203	-0.00691	0.830725
C	3.175391	2.16073	1.499167
C	-5.127730	-3.11880	-3.230046
H	-5.980927	-1.17511	-2.835152
H	-4.032152	-4.96835	-3.444153
H	-2.911622	-1.92660	4.646691
C	-3.044897	-3.89790	3.780252
H	-3.137255	-5.72537	2.630448
H	-3.927128	6.05228	0.186940
C	-3.272812	5.71139	-1.843502
H	-2.424271	5.15096	-3.748201
C	0.778166	4.30118	4.129982
H	1.306592	6.08538	3.029418
H	0.118156	2.42140	4.955802
H	3.335551	-3.45562	1.126393
C	4.619213	-3.99351	-0.520501
H	2.100220	-2.08603	-2.788181
C	3.920282	-3.22374	-2.713431

C	1.159643	-1.05532	3.918155
H	1.353433	0.06450	2.097179
H	0.763419	-4.19578	1.666285
C	0.821402	-3.44366	3.676009
H	4.974689	0.96663	-1.437956
C	5.078988	0.63885	-3.563626
C	2.956712	0.45627	-4.724320
H	1.185899	0.62799	-3.515759
H	4.094032	-0.83455	0.132178
C	4.886570	-0.01117	1.947270
C	4.011794	2.14677	2.616701
H	2.524778	3.01009	1.338115
H	-5.910145	-3.40990	-3.925456
H	-3.321794	-4.37845	4.714775
H	-3.964936	6.43052	-2.272873
H	1.074240	4.71148	5.091751
H	5.325837	-4.52806	0.108205
C	4.832249	-3.90663	-1.900274
H	4.085102	-3.15739	-3.784884
H	1.264782	-0.17687	4.548411
C	0.960817	-2.31515	4.490373
H	0.654173	-4.42117	4.118177
C	4.357341	0.45641	-4.746094
H	6.165077	0.65295	-3.582864
H	2.394768	0.33087	-5.645716
H	5.560965	-0.84687	2.111661
C	4.860276	1.06097	2.846707
H	4.000340	2.98966	3.301397
H	5.707572	-4.37388	-2.343104
H	0.908628	-2.41901	5.570734
H	4.883948	0.32545	-5.687574
H	5.511034	1.05498	3.716866
H	0.598283	-0.47403	-1.767572

1c

Atomic center	X	Y	Z
Ir	0.213137	-1.510509	-0.023748
H	0.260533	-1.642447	1.536302
P	2.480829	-1.011548	0.009344
Cl	0.162043	-0.990985	-2.555591
P	-2.108654	-1.621961	0.091296
B	-0.123917	0.727978	0.295365
C	0.489455	-3.416514	-0.222744
C	2.705513	0.589631	-0.885577
C	3.552396	-2.208215	-0.835278
C	3.244981	-0.680511	1.630851
C	-2.887673	-3.118971	-0.590709
C	-2.890834	-1.324307	1.711861
C	-2.744187	-0.245927	-0.968915
P	1.456127	1.771826	-0.241283
P	-1.845841	1.280886	-0.471252
O	0.660082	-4.551102	-0.305792
H	3.728214	0.975473	-0.854283
H	2.414984	0.408387	-1.924686
C	4.150474	-3.245686	-0.101445
C	3.653148	-2.199069	-2.235334
C	2.442879	-0.349197	2.730373
C	4.643503	-0.630541	1.756088
C	-3.816671	-3.882547	0.130706
C	-2.477238	-3.537112	-1.869134
C	-4.243973	-0.949192	1.775946
C	-2.168123	-1.477944	2.901153
H	-3.828476	-0.109073	-0.935182
H	-2.426627	-0.515714	-1.978957
C	1.403490	3.059956	-1.531126
C	2.158119	2.586679	1.226984
C	-1.928184	2.402468	-1.903562

C	-2.950156	2.056598	0.765061
H	4.060128	-3.270740	0.980882
C	4.862572	-4.248183	-0.761001
H	3.149546	-1.434987	-2.818741
C	4.369833	-3.203563	-2.888340
H	1.363446	-0.362347	2.626446
C	3.029776	0.023814	3.941112
H	5.274393	-0.886273	0.909100
C	5.227119	-0.267531	2.970044
C	-4.339550	-5.052214	-0.428102
H	-4.125816	-3.574528	1.124763
H	-1.730839	-2.965205	-2.415909
C	-3.012339	-4.699536	-2.422871
H	-4.825987	-0.838207	0.865715
C	-4.855271	-0.716432	3.006604
C	-2.782081	-1.248072	4.134836
H	-1.125696	-1.775607	2.859531
C	1.631356	4.408188	-1.218022
C	1.183174	2.677184	-2.864864
C	1.280192	3.139937	2.171680
C	3.540964	2.736276	1.401578
C	-1.850261	3.786033	-1.673591
C	-2.080264	1.925526	-3.213077
C	-2.638299	2.083044	2.129919
C	-4.183270	2.574238	0.329485
C	4.977992	-4.226014	-2.154279
H	5.324397	-5.046770	-0.186353
H	4.445617	-3.190060	-3.972424
H	2.399606	0.287546	4.786424
C	4.420347	0.061649	4.064537
H	6.309971	-0.241813	3.061668
H	-5.054156	-5.644959	0.137144
C	-3.942825	-5.459047	-1.704142

H	-2.693246	-5.019456	-3.411429
C	-4.123880	-0.863617	4.189683
H	-5.899564	-0.418260	3.042070
H	-2.211745	-1.372924	5.051819
H	1.806793	4.710474	-0.190193
C	1.655201	5.364652	-2.235854
H	0.979859	1.637772	-3.111541
C	1.215035	3.638043	-3.873592
C	1.780394	3.821419	3.282264
H	0.207553	3.030307	2.044077
H	4.238686	2.325595	0.680032
C	4.038538	3.403120	2.521312
H	-1.731950	4.166244	-0.662622
C	-1.945546	4.678997	-2.738754
C	-2.190531	2.826203	-4.274538
H	-2.091254	0.861382	-3.419887
H	-1.706540	1.658683	2.483693
C	-3.542720	2.624538	3.046603
C	-5.085722	3.109007	1.247688
H	-4.432527	2.570128	-0.728490
H	5.533796	-5.007086	-2.666400
H	4.876103	0.346652	5.009336
H	-4.350267	-6.369770	-2.135515
H	-4.600316	-0.681624	5.149658
H	1.841195	6.406809	-1.989365
C	1.454991	4.980528	-3.563125
H	1.047202	3.337341	-4.903870
H	1.092418	4.248933	4.007136
C	3.160594	3.947278	3.462919
H	5.112462	3.495976	2.657365
C	-2.128617	4.201002	-4.039745
H	-1.880783	5.747258	-2.552365
H	-2.319776	2.448266	-5.285262

H	-3.292929	2.633318	4.104125
C	-4.765080	3.137790	2.609512
H	-6.035417	3.507834	0.900659
H	1.482655	5.724594	-4.355042
H	3.551113	4.467537	4.333653
H	-2.214453	4.899490	-4.868033
H	-5.467764	3.557829	3.324611
H	-0.211315	0.987699	1.465457

6c

Atomic center	X	Y	Z
Ir	-1.089824	0.823382	-0.113372
H	-0.758427	0.326058	1.341282
P	-2.417137	-1.096857	-0.302629
Cl	-1.272914	1.434121	-2.584624
P	0.504294	2.505763	0.055432
B	0.575438	-0.546267	-0.798567
C	-2.513924	1.974352	0.509134
C	-1.384253	-2.600387	-0.704574
C	-3.710963	-1.108198	-1.579075
C	-3.250098	-1.616470	1.245789
C	-0.032263	4.152371	-0.503091
C	1.247744	2.833560	1.692186
C	1.947068	2.065263	-1.029266
P	0.301288	-2.279019	-0.054906
P	2.316523	0.273128	-0.879400
O	-3.330527	2.653718	0.957467
H	-1.826819	-3.521775	-0.317346
H	-1.286061	-2.668578	-1.792829
C	-4.335724	0.104255	-1.903075
C	-4.118909	-2.291785	-2.215596
C	-3.084761	-0.895467	2.433595
C	-4.049753	-2.771708	1.248689
C	-0.619620	5.015938	0.437422

C	0.007082	4.524648	-1.854908
C	2.161903	3.894208	1.826072
C	0.943657	2.046261	2.807063
H	2.821169	2.711612	-0.901924
H	1.567518	2.161264	-2.053547
C	1.397286	-3.597874	-0.659873
C	0.177412	-2.411163	1.744333
C	3.189061	-0.173888	-2.411231
C	3.452485	-0.011059	0.501329
H	-3.990168	1.028181	-1.453994
C	-5.372106	0.127541	-2.837120
H	-3.633467	-3.237782	-1.990123
C	-5.151222	-2.262771	-3.154688
H	-2.473363	-0.001010	2.437022
C	-3.694982	-1.330939	3.612521
H	-4.215616	-3.323344	0.326722
C	-4.654865	-3.208074	2.426822
C	-1.147353	6.241368	0.031227
H	-0.665066	4.733778	1.485767
H	0.407648	3.850708	-2.603123
C	-0.515492	5.756669	-2.253790
H	2.377571	4.535141	0.974494
C	2.781521	4.140040	3.050432
C	1.561908	2.296656	4.035580
H	0.222351	1.242432	2.713166
C	1.832214	-4.650598	0.159854
C	1.867308	-3.498509	-1.981875
C	0.825524	-1.464956	2.548962
C	-0.593410	-3.420298	2.341397
C	4.521646	-0.607025	-2.417850
C	2.462943	-0.102488	-3.614056
C	3.756731	-1.343279	0.833934
C	4.016896	1.033198	1.244897

C	-5.782262	-1.053353	-3.462012
H	-5.846531	1.072410	-3.087836
H	-5.459953	-3.181772	-3.646276
H	-3.558967	-0.762670	4.529077
C	-4.475105	-2.488658	3.614055
H	-5.274511	-4.101222	2.417014
H	-1.600720	6.901733	0.765778
C	-1.091943	6.615946	-1.314961
H	-0.481243	6.037475	-3.303051
C	2.484941	3.336593	4.158453
H	3.485774	4.962683	3.144582
H	1.313616	1.684287	4.898712
H	1.485627	-4.719271	1.186925
C	2.726727	-5.598919	-0.342755
H	1.555255	-2.668545	-2.609964
C	2.758315	-4.450579	-2.477033
C	0.710720	-1.533832	3.937536
H	1.403100	-0.669547	2.093799
H	-1.118253	-4.146803	1.728299
C	-0.713084	-3.481987	3.729579
H	5.085316	-0.659121	-1.491193
C	5.123375	-0.981544	-3.622620
C	3.074831	-0.470051	-4.812280
H	1.425572	0.228159	-3.610787
H	3.338855	-2.162618	0.256406
C	4.597035	-1.621627	1.910341
C	4.850112	0.749455	2.329434
H	3.797668	2.065122	1.000791
H	-6.584492	-1.031047	-4.195087
H	-4.950731	-2.825919	4.531529
H	-1.501649	7.571745	-1.631173
H	2.962794	3.532245	5.115026
H	3.064049	-6.412258	0.294530

C	3.189365	-5.500396	-1.658572
H	3.123087	-4.365146	-3.497102
H	1.219444	-0.798008	4.554170
C	-0.059383	-2.539516	4.528904
H	-1.324901	-4.255967	4.183977
C	4.402337	-0.915583	-4.817440
H	6.155776	-1.321271	-3.625184
H	2.514149	-0.410945	-5.741510
H	4.824653	-2.654163	2.161241
C	5.137859	-0.575430	2.665962
H	5.270686	1.566740	2.908484
H	3.888209	-6.238045	-2.044384
H	-0.156118	-2.586094	5.610545
H	4.873509	-1.205904	-5.753014
H	5.785387	-0.793717	3.511188
H	0.359547	-0.792816	-1.963733

6b

Atomic center	X	Y	Z
Ir	-1.025134	0.998247	-0.145560
H	-1.014310	0.825415	1.411040
P	-2.539616	-0.798014	-0.259847
Cl	-0.955945	1.077687	-2.719252
P	0.775605	2.477876	0.045908
C	0.589783	-0.491096	-0.240011
C	-2.382280	2.306017	-0.059256
C	-1.556606	-2.254102	-0.839069
C	-3.952118	-0.665909	-1.394090
C	-3.264412	-1.261481	1.345031
C	0.536813	4.200055	-0.482624
C	1.547302	2.542426	1.694012
C	2.058354	1.759225	-1.076050
P	0.109881	-2.112183	-0.066550
P	2.171448	-0.036062	-0.698853

O	-3.208562	3.107139	0.010512
H	-2.042591	-3.211325	-0.631164
H	-1.429161	-2.122525	-1.917930
C	-5.221485	-0.342012	-0.885983
C	-3.770803	-0.800168	-2.780412
C	-3.424901	-0.281052	2.333817
C	-3.734424	-2.561404	1.582358
C	1.058617	5.278735	0.249585
C	-0.212238	4.439981	-1.647961
C	2.918566	2.803670	1.839672
C	0.759604	2.362511	2.839668
H	3.033433	2.250667	-1.020575
H	1.642913	1.854922	-2.084888
C	1.191208	-3.352991	-0.820685
C	-0.187382	-2.674944	1.643881
C	2.875468	-0.820055	-2.189437
C	3.474061	-0.166316	0.574714
H	-5.373772	-0.236365	0.184163
C	-6.296975	-0.161630	-1.757180
H	-2.787895	-1.003759	-3.190201
C	-4.853032	-0.625276	-3.643390
H	-3.062843	0.725716	2.155083
C	-4.038878	-0.597778	3.546956
H	-3.641071	-3.328925	0.819432
C	-4.330111	-2.881268	2.802353
C	0.837643	6.587166	-0.186889
H	1.624901	5.102794	1.158931
H	-0.630338	3.608351	-2.209157
C	-0.421495	5.750187	-2.078407
H	3.544966	2.958016	0.967476
C	3.496319	2.854519	3.108207
C	1.336982	2.421896	4.109286
H	-0.304403	2.174519	2.735679

C	2.188779	-3.972352	-0.051770
C	1.087067	-3.639049	-2.190691
C	-0.224006	-1.729978	2.675889
C	-0.465940	-4.022541	1.920073
C	3.999741	-1.655461	-2.134881
C	2.234224	-0.590872	-3.418730
C	3.162850	-0.710231	1.824218
C	4.767711	0.325576	0.333344
C	-6.115676	-0.305652	-3.135544
H	-7.276125	0.087459	-1.356693
H	-4.705230	-0.729030	-4.715045
H	-4.164513	0.171449	4.304581
C	-4.484982	-1.899727	3.786190
H	-4.677953	-3.894987	2.982407
H	1.238521	7.419397	0.385972
C	0.101136	6.824489	-1.350582
H	-1.001492	5.930772	-2.979673
C	2.707325	2.660527	4.245467
H	4.561944	3.041353	3.206207
H	0.716483	2.282929	4.991006
H	2.273521	-3.753590	1.008673
C	3.066212	-4.879519	-0.648484
H	0.336773	-3.145114	-2.800683
C	1.961784	-4.550397	-2.779476
C	-0.542960	-2.127243	3.975741
H	-0.014599	-0.689031	2.448557
H	-0.431440	-4.762339	1.123715
C	-0.775493	-4.418106	3.221213
H	4.490480	-1.853561	-1.188180
C	4.486854	-2.246240	-3.302862
C	2.733525	-1.175567	-4.582198
H	1.339815	0.026580	-3.460800
H	2.157576	-1.072010	2.009944

C	4.131333	-0.762478	2.829497
C	5.732818	0.277371	1.338747
H	5.022222	0.740529	-0.639101
H	-6.955001	-0.167017	-3.812094
H	-4.954933	-2.149717	4.733881
H	-0.070934	7.844042	-1.686020
H	3.158633	2.699212	5.233564
H	3.836089	-5.358608	-0.049326
C	2.949089	-5.173398	-2.009332
H	1.877824	-4.768408	-3.840227
H	-0.580818	-1.388837	4.772350
C	-0.818919	-3.469143	4.248927
H	-0.983813	-5.463301	3.434840
C	3.861839	-2.001414	-4.527382
H	5.354874	-2.898355	-3.252618
H	2.240522	-0.984988	-5.532148
H	3.879915	-1.181576	3.800379
C	5.414791	-0.267133	2.588933
H	6.732177	0.660645	1.148765
H	3.628761	-5.884291	-2.471933
H	-1.067077	-3.777994	5.261138
H	4.248812	-2.455846	-5.436071
H	6.168201	-0.302571	3.371760

3c

Atomic center	X	Y	Z
Ir	0.108846	-1.425129	0.109731
P	2.395399	-1.275351	0.171055
P	-2.110170	-1.043712	-0.338562
B	0.376603	0.822833	0.498066
C	-0.015045	-3.299109	-0.070373
C	2.860501	0.064917	-1.036488
C	3.420287	-2.702038	-0.319833
C	3.140959	-0.722664	1.747013

C	-2.795503	-1.865166	-1.822932
C	-3.283788	-1.432405	1.007048
C	-2.384337	0.759211	-0.731563
P	1.583055	1.396352	-0.874982
P	-1.330083	1.707796	0.429111
O	-0.086636	-4.455424	-0.147187
H	3.866099	0.468366	-0.881736
H	2.796393	-0.352370	-2.046872
C	3.210601	-3.904835	0.373952
C	4.396366	-2.647760	-1.325464
C	2.365090	-0.780982	2.912392
C	4.466257	-0.270039	1.816695
C	-4.173096	-1.846146	-2.092118
C	-1.923611	-2.498208	-2.718894
C	-4.462244	-0.713595	1.253493
C	-2.956851	-2.516991	1.836615
H	-3.434991	1.063259	-0.721341
H	-1.978571	0.912489	-1.738746
C	0.702443	1.501203	-2.457226
C	2.524670	2.929382	-0.610169
C	-1.405610	3.448201	-0.085837
C	-2.109362	1.600870	2.062884
H	2.449818	-3.958411	1.148493
C	3.966950	-5.034805	0.066560
H	4.579541	-1.726610	-1.871342
C	5.147891	-3.784940	-1.636912
H	1.336950	-1.127875	2.841623
C	2.906210	-0.380700	4.135806
H	5.085388	-0.244673	0.922547
C	5.003602	0.139511	3.038263
C	-4.668695	-2.445092	-3.251372
H	-4.860549	-1.384241	-1.387984
H	-0.861151	-2.522336	-2.494586

C	-2.422507	-3.100897	-3.876169
H	-4.731802	0.139588	0.638938
C	-5.297670	-1.070443	2.313206
C	-3.799993	-2.881215	2.886820
H	-2.031642	-3.059979	1.667074
C	0.229181	2.727027	-2.947373
C	0.323714	0.304291	-3.088026
C	2.756610	3.330464	0.714626
C	3.085575	3.661242	-1.668821
C	-0.502017	4.345043	0.507435
C	-2.280023	3.904760	-1.082794
C	-1.720543	0.578226	2.941304
C	-3.134714	2.487333	2.424133
C	4.935469	-4.977687	-0.941865
H	3.795188	-5.961681	0.607375
H	5.899171	-3.735750	-2.421030
H	2.301137	-0.428607	5.037776
C	4.223205	0.085160	4.198659
H	6.030307	0.493313	3.086990
H	-5.737086	-2.433444	-3.451569
C	-3.793616	-3.071837	-4.145675
H	-1.742239	-3.601944	-4.560603
C	-4.970087	-2.156193	3.129884
H	-6.201520	-0.497324	2.502679
H	-3.538040	-3.724817	3.520323
H	0.491248	3.654186	-2.448778
C	-0.603358	2.753372	-4.068928
H	0.637572	-0.650846	-2.672414
C	-0.511395	0.337093	-4.204798
C	3.529713	4.462887	0.976881
H	2.333576	2.753740	1.533261
H	2.921761	3.348616	-2.696259
C	3.849310	4.799077	-1.401545

H	0.179394	3.998651	1.278563
C	-0.463364	5.676807	0.096789
C	-2.241391	5.240725	-1.489517
H	-2.978447	3.221176	-1.555363
H	-0.933539	-0.110753	2.648399
C	-2.367692	0.437845	4.168505
C	-3.773197	2.344863	3.657126
H	-3.425757	3.289608	1.750534
H	5.519900	-5.860977	-1.185745
H	4.644036	0.400209	5.150190
H	-4.182509	-3.546195	-5.043118
H	-5.621822	-2.432277	3.954833
H	-0.966848	3.706566	-4.443259
C	-0.974208	1.561881	-4.698080
H	-0.815062	-0.592982	-4.675648
H	3.708859	4.767758	2.004719
C	4.069932	5.201921	-0.080110
H	4.275194	5.368183	-2.223796
C	-1.330916	6.125773	-0.905536
H	0.246213	6.361133	0.554022
H	-2.920511	5.588091	-2.263843
H	-2.076594	-0.363844	4.841625
C	-3.392865	1.318095	4.526873
H	-4.564234	3.034921	3.938878
H	-1.625558	1.585490	-5.567924
H	4.666557	6.087177	0.124406
H	-1.298777	7.163344	-1.227587
H	-3.894517	1.205749	5.484618
H	0.872370	1.053548	1.572975

4b

Atomic center	X	Y	Z
Ir	-1.039938	1.017908	-0.179121
P	-2.543295	-0.728528	-0.347908

P	0.714589	2.488009	-0.011299
C	0.526554	-0.438256	-0.383928
C	-2.374344	2.309909	-0.069301
C	-1.591907	-2.245923	-0.882167
C	-3.849537	-0.564644	-1.607306
C	-3.377194	-1.193705	1.206550
C	0.501288	4.198339	-0.591524
C	1.472673	2.552469	1.645185
C	2.064548	1.808326	-1.101584
P	0.071507	-2.066059	-0.127868
P	2.130980	0.002368	-0.783589
O	-3.204260	3.123399	-0.011660
H	-2.074655	-3.192198	-0.623117
H	-1.483340	-2.172438	-1.969235
C	-5.078358	-1.234707	-1.515180
C	-3.583510	0.262413	-2.710132
C	-3.622956	-0.170005	2.135477
C	-3.781032	-2.503000	1.507242
C	1.119668	5.299065	0.018887
C	-0.327224	4.392433	-1.708745
C	2.819034	2.890214	1.850798
C	0.673807	2.203404	2.744640
H	3.041754	2.278082	-0.953678
H	1.740639	1.966953	-2.134983
C	1.187200	-3.321370	-0.808625
C	-0.214648	-2.523709	1.615417
C	2.764249	-0.769519	-2.308823
C	3.416606	-0.189275	0.493679
H	-5.298651	-1.854388	-0.650241
C	-6.029661	-1.084510	-2.526790
H	-2.639940	0.803704	-2.749586
C	-4.535623	0.403997	-3.721017
H	-3.288945	0.839779	1.917383

C	-4.267970	-0.451297	3.340118
H	-3.603719	-3.313126	0.806357
C	-4.412603	-2.784995	2.720113
C	0.915853	6.583136	-0.493138
H	1.743000	5.158031	0.897131
H	-0.835594	3.538087	-2.151503
C	-0.519714	5.675259	-2.221326
H	3.453328	3.159210	1.011172
C	3.361044	2.868425	3.136304
C	1.215779	2.189850	4.031093
H	-0.365010	1.929351	2.574267
C	2.250189	-3.800354	-0.026394
C	1.060876	-3.739415	-2.142128
C	-0.403867	-1.507409	2.560304
C	-0.356695	-3.867473	1.994438
C	3.907552	-1.576037	-2.353581
C	2.008658	-0.566267	-3.476818
C	3.049389	-0.666941	1.756392
C	4.740322	0.221177	0.262564
C	-5.758178	-0.269601	-3.630540
H	-6.985056	-1.597158	-2.449461
H	-4.330836	1.049786	-4.571237
H	-4.457322	0.350369	4.049460
C	-4.659490	-1.759849	3.637283
H	-4.711909	-3.805024	2.946788
H	1.388313	7.435994	-0.012563
C	0.102163	6.771708	-1.614025
H	-1.166072	5.822360	-3.082704
C	2.560492	2.517355	4.227681
H	4.407810	3.119496	3.284843
H	0.590637	1.920469	4.878820
H	2.353881	-3.478905	1.005641
C	3.171514	-4.695020	-0.573215

H	0.253100	-3.361950	-2.762202
C	1.981527	-4.636757	-2.682194
C	-0.734109	-1.832835	3.876599
H	-0.307573	-0.469641	2.251145
H	-0.209499	-4.659930	1.264711
C	-0.680404	-4.188649	3.313147
H	4.481431	-1.760575	-1.451793
C	4.299610	-2.163201	-3.559736
C	2.409288	-1.145402	-4.679456
H	1.099465	0.030582	-3.435644
H	2.018462	-0.947194	1.942289
C	3.996612	-0.747815	2.779084
C	5.685039	0.140265	1.285812
H	5.033617	0.601081	-0.713111
H	-6.503219	-0.150722	-4.413096
H	-5.153209	-1.981183	4.580078
H	-0.057026	7.772541	-2.007029
H	2.985138	2.498533	5.228204
H	3.991130	-5.064916	0.037294
C	3.035577	-5.116603	-1.898615
H	1.878633	-4.957696	-3.714951
H	-0.892658	-1.041021	4.603811
C	-0.872345	-3.170894	4.254103
H	-0.785426	-5.230023	3.606432
C	3.558820	-1.943715	-4.722535
H	5.182956	-2.795731	-3.586621
H	1.827079	-0.977115	-5.581884
H	3.701022	-1.111998	3.759454
C	5.313950	-0.346695	2.544747
H	6.708666	0.457246	1.103311
H	3.750396	-5.817490	-2.321871
H	-1.131190	-3.422952	5.279321
H	3.870596	-2.396808	-5.660103

H	6.051321	-0.405807	3.341252

1a

Atomic center	X	Y	Z
C	2.462746	-0.033536	2.284013
C	1.249540	0.682345	2.881989
N	-0.001062	0.066510	2.340398
Ir	0.000261	-0.112881	0.143720
C	-1.250788	0.686289	2.879620
C	-2.464794	-0.027949	2.281527
C	0.002021	-0.258419	-1.709140
Cl	-0.000302	-2.559336	0.693573
H	0.000248	1.466817	0.065465
O	0.003378	-0.337215	-2.857789
H	-0.002644	-0.924430	2.611567
P	2.338588	0.023125	0.429078
C	3.415152	-1.269007	-0.233700
C	4.182908	-1.009819	-1.382663
C	4.957468	-2.024622	-1.945802
C	4.972040	-3.298217	-1.369346
C	4.204441	-3.559724	-0.230286
C	3.420945	-2.553933	0.335841
C	3.081552	1.606898	-0.060955
C	2.419692	2.477435	-0.937351
C	3.027611	3.672251	-1.331942
C	4.296167	4.004553	-0.850543
C	4.964924	3.136221	0.020236
C	4.364756	1.939001	0.408757
P	-2.338961	0.025231	0.426633
C	-3.417983	-1.266670	-0.232523
C	-3.423883	-2.550496	0.339503
C	-4.210619	-3.556203	-0.222198
C	-4.981450	-3.295675	-1.359313
C	-4.966726	-2.023241	-1.938314

C	-4.188806	-1.008525	-1.379617
C	-3.078955	1.609527	-0.066176
C	-4.359863	1.947149	0.405801
C	-4.956768	3.145547	0.015855
C	-4.287130	4.009424	-0.858666
C	-3.020956	3.671496	-1.342462
C	-2.416225	2.475581	-0.946341
H	2.465587	-1.088272	2.579681
H	3.396281	0.425792	2.622176
H	1.237080	1.740250	2.600985
H	1.248155	0.606846	3.976755
H	-1.250731	0.612913	3.974528
H	-1.235631	1.743543	2.596314
H	-3.397708	0.433680	2.618194
H	-2.469986	-1.082227	2.578692
H	4.182506	-0.020444	-1.830928
H	5.551152	-1.818281	-2.832243
H	5.578074	-4.086261	-1.808419
H	4.207489	-4.550770	0.215165
H	2.799202	-2.779925	1.194953
H	1.433779	2.219272	-1.308847
H	2.510711	4.340682	-2.015319
H	4.767010	4.935366	-1.155406
H	5.955025	3.388806	0.390036
H	4.902491	1.258089	1.064235
H	-2.799892	-2.775617	1.197233
H	-4.213801	-4.546370	0.225207
H	-5.590193	-4.083594	-1.794844
H	-5.562969	-1.817703	-2.823219
H	-4.188188	-0.020021	-1.829747
H	-4.898304	1.269869	1.064450
H	-5.945003	3.402556	0.387600
H	-4.755421	4.941209	-1.164484

H	-2.503438	4.336482	-2.028725
H	-1.431961	2.213028	-1.319190

3a

Atomic center	X	Y	Z
C	-2.440215	0.102190	2.342155
C	-1.196042	-0.602406	2.893972
N	-0.000365	-0.017664	2.294689
Ir	-0.000618	-0.044764	0.156490
C	1.200155	-0.592440	2.893946
C	2.438570	0.120075	2.339368
C	-0.001618	0.011489	-1.720324
Cl	0.001377	-2.599834	0.304611
H	-0.002937	1.532117	0.227001
O	-0.002162	0.008247	-2.880036
P	-2.304833	0.075364	0.494390
C	-3.064683	1.632944	-0.085341
C	-4.125941	1.665907	-0.999632
C	-4.632769	2.892217	-1.442810
C	-4.088701	4.089224	-0.972731
C	-3.027064	4.060387	-0.060073
C	-2.512882	2.840121	0.375363
C	-3.379881	-1.246267	-0.135202
C	-2.946602	-2.036656	-1.207787
C	-3.788989	-3.017488	-1.736672
C	-5.061937	-3.217355	-1.196249
C	-5.498050	-2.432100	-0.123390
C	-4.660784	-1.447758	0.403779
P	2.303864	0.081158	0.492100
C	3.378031	-1.245633	-0.128325
C	2.947480	-2.034907	-1.202859
C	3.788143	-3.020129	-1.726114
C	5.056846	-3.225783	-1.177916
C	5.490251	-2.441850	-0.103062

C	4.654687	-1.452962	0.418404
C	3.065184	1.634420	-0.097214
C	2.507737	2.845134	0.347032
C	3.025797	4.062021	-0.093282
C	4.097330	4.083812	-0.994470
C	4.647138	2.883196	-1.448382
C	4.136269	1.660376	-1.000296
H	-3.373005	-0.366008	2.672398
H	-2.440805	1.156547	2.639467
H	-1.161367	-0.462084	3.988904
H	-1.275619	-1.688929	2.701802
H	1.165436	-0.450426	3.988655
H	1.287964	-1.678839	2.703815
H	3.375122	-0.337378	2.673832
H	2.429025	1.176255	2.630203
H	-4.554293	0.738020	-1.366920
H	-5.453107	2.908091	-2.156453
H	-4.484384	5.041340	-1.318112
H	-2.595097	4.989538	0.304275
H	-1.669250	2.816330	1.061258
H	-1.944605	-1.906152	-1.599484
H	-3.442465	-3.633807	-2.562297
H	-5.712638	-3.986887	-1.605109
H	-6.487399	-2.585385	0.301000
H	-5.009620	-0.831819	1.229069
H	1.948479	-1.899985	-1.600580
H	3.443468	-3.635451	-2.553245
H	5.706209	-3.998856	-1.582198
H	6.476214	-2.599691	0.327494
H	5.001894	-0.838441	1.245389
H	1.656829	2.826726	1.023988
H	2.589201	4.993915	0.258304
H	4.496174	5.033208	-1.343681

H	5.475189	2.893517	-2.153166
H	4.569199	0.729716	-1.354947

6c

Atomic center	X	Y	Z
Ir	0.034392	-1.372840	-0.464806
P	-2.163729	-1.347011	0.116934
Cl	0.113102	0.022313	3.475447
P	2.260719	-1.218400	-0.002581
B	-0.015050	0.919901	-0.506608
C	0.073508	-3.229179	-0.795431
C	-2.494818	0.204456	1.086220
C	-2.610142	-2.704843	1.254770
C	-3.466455	-1.372442	-1.168271
C	2.860330	-2.566949	1.075252
C	3.471428	-1.123094	-1.368193
C	2.531743	0.289249	1.041373
P	-1.721829	1.574152	0.149565
P	1.615202	1.655409	0.246341
O	0.094055	-4.350143	-1.107490
H	-3.545737	0.364683	1.348489
H	-1.879957	0.121357	1.999915
C	-3.262793	-3.853371	0.780334
C	-2.151916	-2.662765	2.581253
C	-3.071386	-1.220645	-2.503093
C	-4.828808	-1.503894	-0.859513
C	3.961355	-3.372620	0.756820
C	2.112947	-2.823267	2.237424
C	4.763182	-0.599839	-1.216122
C	3.062774	-1.597379	-2.622604
H	3.581251	0.525195	1.246869
H	1.982379	0.074298	1.976762
C	-1.897746	3.060528	1.200729
C	-2.818958	1.926702	-1.273271

C	1.591354	3.046806	1.416989
C	2.736073	2.226294	-1.089667
H	-3.599609	-3.902977	-0.251137
C	-3.472721	-4.941768	1.629886
H	-1.593864	-1.804007	2.950637
C	-2.372095	-3.752629	3.425843
H	-2.009893	-1.124727	-2.724488
C	-4.029382	-1.183118	-3.519353
H	-5.137489	-1.638539	0.174529
C	-5.784533	-1.476766	-1.875348
C	4.316366	-4.431375	1.599217
H	4.534228	-3.183614	-0.146661
H	1.254690	-2.199882	2.481828
C	2.481747	-3.872813	3.078073
H	5.089523	-0.227951	-0.248640
C	5.630850	-0.540549	-2.307084
C	3.936647	-1.552364	-3.711272
H	2.050174	-1.980973	-2.733086
C	-2.353601	4.273123	0.657615
C	-1.551966	2.989809	2.560221
C	-2.297294	2.412112	-2.479586
C	-4.208814	1.798087	-1.133902
C	1.229598	4.314304	0.931065
C	1.919262	2.886140	2.769441
C	2.574167	1.779704	-2.408307
C	3.832399	3.044160	-0.771350
C	-3.032274	-4.892307	2.955853
H	-3.976138	-5.829009	1.252669
H	-2.013723	-3.708702	4.451683
H	-3.717774	-1.054514	-4.553049
C	-5.385019	-1.311696	-3.206658
H	-6.839239	-1.583308	-1.631479
H	5.166862	-5.059991	1.344975

C	3.579548	-4.681238	2.759693
H	1.904314	-4.061124	3.979980
C	5.219443	-1.019391	-3.555501
H	6.625047	-0.117415	-2.185561
H	3.613532	-1.923921	-4.680998
H	-2.625773	4.336204	-0.391916
C	-2.474755	5.401772	1.470588
H	-1.165031	2.064460	2.987729
C	-1.680310	4.123647	3.363142
C	-3.150388	2.745316	-3.534971
H	-1.224704	2.524976	-2.597112
H	-4.632499	1.431562	-0.205017
C	-5.058998	2.120994	-2.190085
H	0.965417	4.441103	-0.116090
C	1.214600	5.413476	1.785967
C	1.905899	3.994588	3.620827
H	2.136644	1.902441	3.169959
H	1.747793	1.125207	-2.659225
C	3.491416	2.150354	-3.393449
C	4.745313	3.416545	-1.759294
H	3.965965	3.398460	0.247320
H	-3.195671	-5.741274	3.615940
H	-6.130916	-1.285789	-3.997805
H	3.857183	-5.505676	3.412776
H	5.896594	-0.971311	-4.405227
H	-2.834428	6.335299	1.043767
C	-2.143612	5.327760	2.825932
H	-1.406939	4.060014	4.413066
H	-2.732221	3.117596	-4.467160
C	-4.531440	2.595160	-3.394782
H	-6.132017	1.994526	-2.074212
C	1.560656	5.255624	3.132578
H	0.924030	6.389033	1.405410

H	2.153870	3.861837	4.670864
H	3.363170	1.784550	-4.408660
C	4.575662	2.970418	-3.073470
H	5.587158	4.055107	-1.502061
H	-2.241350	6.206685	3.459244
H	-5.194788	2.843160	-4.219962
H	1.545736	6.113695	3.800557
H	5.288818	3.257070	-3.842817
H	0.003539	1.259922	-1.665181

6b

Atomic center	X	Y	Z
Ir	0.387021	-1.251939	0.244220
P	2.532371	-0.551963	-0.242585
Cl	-0.102935	0.193110	-3.107148
P	-1.811682	-1.858684	-0.042953
C	-0.301773	0.926915	0.288616
C	0.923749	-3.002847	0.473659
C	2.334539	1.101445	-1.073983
C	3.378544	-1.587413	-1.477062
C	3.717523	-0.347927	1.122424
C	-2.034593	-3.296845	-1.131889
C	-2.858147	-2.141928	1.415551
C	-2.581153	-0.470149	-1.007824
P	1.067287	2.026247	-0.154305
P	-2.010539	1.110766	-0.310141
O	1.255168	-4.096120	0.676473
H	3.255537	1.688967	-1.145022
H	1.919455	0.875509	-2.068541
C	4.747615	-1.883265	-1.395143
C	2.602787	-2.118715	-2.520778
C	3.576454	-1.207818	2.222564
C	4.768817	0.578728	1.099962
C	-2.739478	-4.438782	-0.728157

C	-1.397804	-3.261922	-2.384565
C	-4.257304	-2.053548	1.375397
C	-2.216452	-2.474022	2.617834
H	-3.675261	-0.497703	-1.029829
H	-2.153777	-0.549148	-2.016267
C	0.698927	3.567004	-1.020972
C	1.885733	2.460141	1.412322
C	-2.458492	2.453879	-1.427890
C	-3.051181	1.332836	1.175426
H	5.348431	-1.489403	-0.580925
C	5.337753	-2.704865	-2.358880
H	1.544851	-1.881039	-2.578667
C	3.203302	-2.930359	-3.482505
H	2.749085	-1.912358	2.246021
C	4.481006	-1.145546	3.283087
H	4.895325	1.246830	0.252754
C	5.662517	0.651080	2.169878
C	-2.811691	-5.544358	-1.580782
H	-3.223007	-4.470547	0.243826
H	-0.841449	-2.377383	-2.689851
C	-1.485282	-4.366070	-3.231277
H	-4.765580	-1.808277	0.446524
C	-5.005126	-2.278891	2.531263
C	-2.967902	-2.714817	3.769759
H	-1.129890	-2.525252	2.640700
C	0.464256	4.747837	-0.294277
C	0.643677	3.578417	-2.424433
C	1.747590	1.660308	2.557504
C	2.802689	3.525405	1.421558
C	-2.589085	3.750354	-0.902422
C	-2.747903	2.208966	-2.778609
C	-2.655225	0.860057	2.436610
C	-4.344366	1.859938	1.015403

C	4.568248	-3.226906	-3.402318
H	6.396905	-2.939288	-2.290102
H	2.602527	-3.334524	-4.293164
H	4.369998	-1.819849	4.128419
C	5.522652	-0.213128	3.259987
H	6.470175	1.378179	2.149924
H	-3.354718	-6.431709	-1.265931
C	-2.188060	-5.508667	-2.830398
H	-0.999861	-4.335859	-4.203450
C	-4.361322	-2.611255	3.728384
H	-6.088573	-2.199526	2.498476
H	-2.467366	-2.978406	4.698041
H	0.496086	4.740811	0.790897
C	0.209159	5.939290	-0.970620
H	0.772642	2.657101	-2.986493
C	0.374050	4.775708	-3.088835
C	2.488090	1.948303	3.704507
H	1.112069	0.779916	2.546800
H	2.938450	4.138181	0.535415
C	3.537422	3.809457	2.571813
H	-2.382675	3.940940	0.146433
C	-3.004420	4.794250	-1.725140
C	-3.171296	3.260744	-3.592888
H	-2.608848	1.221343	-3.200969
H	-1.690460	0.385833	2.579390
C	-3.527021	0.940214	3.522882
C	-5.213209	1.935407	2.104507
H	-4.670550	2.221674	0.044989
H	5.030635	-3.867627	-4.149003
H	6.223553	-0.158862	4.089070
H	-2.246703	-6.370253	-3.490606
H	-4.946902	-2.790665	4.626489
H	0.041212	6.853031	-0.406706

C	0.168739	5.954961	-2.368021
H	0.326287	4.782187	-4.174157
H	2.383605	1.315004	4.580563
C	3.377204	3.024198	3.717066
H	4.237138	4.640840	2.570821
C	-3.300734	4.549311	-3.069905
H	-3.098596	5.796165	-1.316514
H	-3.394165	3.068417	-4.638665
H	-3.210085	0.562012	4.490220
C	-4.804244	1.480753	3.361253
H	-6.207582	2.352457	1.969569
H	-0.028987	6.885443	-2.894040
H	3.954360	3.242581	4.611561
H	-3.631127	5.364470	-3.708682
H	-5.481426	1.540950	4.209152
H	-0.423050	1.173587	1.348210

References

[1] M. M. T. Khan, E. R. Rao, *Polyhedron* **1987**, *6*, 1727–1735.

[2] S. Grimme, *J. Comput. Chem.* **2006**, *27*, 1787–1799.

[3] F. Weigend, R. Ahlrichs, K. A. Peterson, T. H. Dunning, R. M. Pitzer, A. Bergner, *Phys. Chem. Chem. Phys.* **2005**, *7*, 3297.

[4] F. Weigend, C. Hättig, H. Patzelt, R. Ahlrichs, S. Spencer, A. Willets, *Phys. Chem. Chem. Phys.* **2006**, *8*, 1057.

[5] M. J. Frisch, G. W. Trucks, H. B. Schlegel, G. E. Scuseria, M. A. Robb, J. R. Cheeseman, G. Scalmani, V. Barone, G. A. Petersson, H. Nakatsuji, et al., **2016**.

[6] A. V. Marenich, S. V. Jerome, C. J. Cramer, D. G. Truhlar, *J. Chem. Theory Comput.* **2012**, *8*, 527–541.

[7] E. D. Glendening, J. K. Badenhoop, A. E. Reed, J. . E. Carpenter, J. A. Bohmann, C. M. Morales, C. R. Landis, F. Weinhold, **2013**.

[8] T. Lu, F. Chen, *J. Comput. Chem.* **2012**, *33*, 580–592.

[9] *NBO 6.0.* E. D. Glendening, J, K. Badenhoop, A. E. Reed, J. E. Carpenter, J. A. Bohmann, C. M. Morales, C. R. Landis, and F. Weinhold, Theoretical Chemistry Institute, University of Wisconsin, Madison, **2013**.

[10] *Gaussian 16*, Revision A.03, M. J. Frisch, G. W. Trucks, H. B. Schlegel, G. E. Scuseria, M. A. Robb, J. R. Cheeseman, G. Scalmani, V. Barone, G. A. Petersson, H. Nakatsuji, X. Li, M. Caricato, A. V. Marenich, J. Bloino, B. G. Janesko, R. Gomperts, B. Mennucci, H. P. Hratchian, J. V. Ortiz, A. F. Izmaylov, J. L. Sonnenberg, D. Williams-Young, F. Ding, F. Lipparini, F. Egidi, J. Goings, B. Peng, A. Petrone, T. Henderson, D. Ranasinghe, V. G. Zakrzewski, J. Gao, N. Rega, G. Zheng, W. Liang, M. Hada, M. Ehara, K. Toyota, R. Fukuda, J. Hasegawa, M. Ishida, T. Nakajima, Y. Honda, O. Kitao, H. Nakai, T. Vreven, K. Throssell, J. A. Montgomery, Jr., J. E. Peralta, F. Ogliaro, M. J. Bearpark, J. J. Heyd, E. N. Brothers, K. N. Kudin, V. N. Staroverov, T. A. Keith, R. Kobayashi, J. Normand, K. Raghavachari, A. P. Rendell, J. C. Burant, S. S. Iyengar, J. Tomasi, M. Cossi, J. M. Millam, M. Klene, C. Adamo, R. Cammi, J. W. Ochterski, R. L. Martin, K. Morokuma, O. Farkas, J. B. Foresman, D. J. Fox, *Gaussian, Inc.*, Wallingford CT, **2016**.